

2017

New Approaches To Heterocycle Synthesis: A Greener Route To Structurally Complex Protonated Azomethine Imines, And Their Use In 1,3-Dipolar Cycloadditions

Ram Chandra Dhakal
University of Vermont

Follow this and additional works at: <https://scholarworks.uvm.edu/graddis>

 Part of the [Chemistry Commons](#), and the [Medicinal Chemistry and Pharmaceutics Commons](#)

Recommended Citation

Dhakal, Ram Chandra, "New Approaches To Heterocycle Synthesis: A Greener Route To Structurally Complex Protonated Azomethine Imines, And Their Use In 1,3-Dipolar Cycloadditions" (2017). *Graduate College Dissertations and Theses*. 777.
<https://scholarworks.uvm.edu/graddis/777>

This Dissertation is brought to you for free and open access by the Dissertations and Theses at ScholarWorks @ UVM. It has been accepted for inclusion in Graduate College Dissertations and Theses by an authorized administrator of ScholarWorks @ UVM. For more information, please contact donna.omalley@uvm.edu.

NEW APPROACHES TO HETEROCYCLE SYNTHESIS: A GREENER ROUTE TO
STRUCTURALLY COMPLEX PROTONATED AZOMETHINE IMINES, AND
THEIR USE IN 1,3-DIPOLAR CYCLOADDITIONS

A Dissertation Presented

by

Ram Chandra Dhakal

to

The Faculty of the Graduate College

of

The University of Vermont

In Partial Fulfillment of the Requirements
for the Degree of Doctor of Philosophy
Specializing in Chemistry
October, 2017

Defense Date: July 19, 2017
Dissertation Examination Committee:

Matthias Brewer, Ph.D., Advisor
Matthew White, Ph.D., Chairperson
Adam Whalley, Ph.D.
Giuseppe Petrucci, Ph.D.
Cynthia J. Forehand, Ph.D., Dean of the Graduate College

ABSTRACT

1-Aza-2-azoniaallene salts are reactive intermediates that undergo [3+2] cycloaddition with many different types of multiple bonds. For the past several years, the Brewer group has studied the reactivity of these intermediates in intramolecular reactions, and have discovered that these cationic heteroallenes can react through a variety of other, mechanistically distinct, pathways to give different classes of nitrogen heterocycles. For example, prior work in the Brewer group revealed that 1-aza-2-azoniaallene salts could react in an intramolecular [4+2] cycloaddition reaction to give protonated azomethine imine salts containing a 1,2,3,4-tetrahydrocinnoline scaffold. Further study of the scope and limitations of this Diels-Alder-like reaction are described herein. These studies primarily focused on how varying the *N*-aryl ring and alkene substituents affected the reaction. We discovered that in several instances, the metal mediated reaction did not facilitate the cycloaddition very well, so we searched for alternative ways to facilitate the reaction. We discovered that a non-metallic Lewis acid (TMSOTf) provided very clean products with α -chloroazo compounds. I hypothesized that changing the leaving group adjacent to the azo might further improve the reaction. With this in mind, I developed a technique to prepare α -trifluoroacetoxyazo compounds by treating aryl hydrazones with trifluoroacetoxy dimethylsulfonium trifluoroacetate. This technique is compatible with all types of functional groups including nitro aryl compounds, which gave low yields of the corresponding chloroazo derivatives. Importantly, these α -trifluoroacetoxyazo compounds gave even better cycloaddition results when treated with TMSOTf, and this method is more practical, more environmentally friendly, and greener than the metal mediated technique. This process even returned sterically hindered products in high yield, and provide a dearomatized non-protonated azomethine imine salt, which further verified the proposed mechanism of the [4+2] cycloaddition.

Azomethine imines are well known to undergo 1,3-dipolar cycloadditions with alkenes. We wondered if the protonated azomethine imine salts generated by the [4+2] cycloaddition could be used in a subsequent base-mediated [3+2] cycloaddition to generate structurally complex tetra- or pentacyclic products. We were pleased to find that the protonated azomethine imines indeed reacted smoothly with a variety of π -system in the presence of triethylamine to give the corresponding cycloadducts in high yields with moderate to high diastereoselectivities. In an attempt to understand the diastereoselectivity of these [3+2] cycloadditions better, I modeled them computationally.

CITATIONS

Material from this dissertation has been published in the following form:

Dhakal, R.; Brewer, M.. (2016). Intramolecular (4+2) cycloaddition of aryl-1-aza-2-azoniaallene salts: a practical approach to highly sterically-congested polycyclic protonated azomethine imines. *Tetrahedron*, 72 (26), 3718-3728.

Hong, X; Bercovici, D. A.; Yang, Z; Al-Bataineh, N.; Srinivasan, R.; Dhakal, R. C.; Houk, K. N.; Brewer, M.. (2015). Mechanism and Dynamics of Intramolecular C–H Insertion Reactions of 1-Aza-2-azoniaallene Salts. *Journal of the American Chemical Society*, 137 (28), 9100–9107.

DEDICATION

To my wife, Sangita, for her endless love, encouragement, and great support.

ACKNOWLEDGMENTS

I would like to express my heartiest gratitude and sincerity to my advisor, Professor Matthias Brewer, for his kind supervision, encouragement, and providing me such an excellent opportunity to carry out my Ph.D work under his guidance. His guidance helped me in all the time of research and writing of this thesis. He has always been very kind and respectful with me. I shall remain thankful to him for his continuous guidance, valuable direction, suggestions, comments, and inspiration at all times have been of immense value without which this work would not have been accomplished.

I would like to thank my thesis committee members, Professor Adam Whalley and Professor Giuseppe Petrucci for their advices though my graduate study. I would like to sincerely thank Professor Matthew White for being the chair of my dissertation committee.

I would like to acknowledge Dr. Monika Ivancic for her help to solve the NMR problems, Bruce O'Rourke for Mass Spectroscopy, and Professor Rory Waterman for X-ray crystallography.

My special thanks to Dr. Jabre, Dr. Bayir, Dr. Al-Bataineh, Dr. Giampa, and current Brewer group members for their help during my graduate studies. Financial support from the National Science Foundation (CHEM-1362286) is gratefully acknowledged.

I would like to acknowledge Andrea Lucey, Angela Gatesy, Kevin Kolinich, Hollis Robinson, Edward A. Curtiss, Christine Cardillo, and Travis Verret for their help and supports during the entire research work.

Finally, I would like to express my deep sense of gratitude to my parents, sisters, and brother for their help, encouragement, and great support.

TABLE OF CONTENT

	Page
CITATIONS	ii
DEDICATION	iii
ACKNOWLEDGMENTS	iv
TABLE OF CONTENTS	v
LIST OF TABLES	ix
LIST OF FIGURES	x
LIST OF ABBREVIATIONS	xi
CHAPTER 1: INTRAMOLECULAR CYCLOADDITION REACTIONS OF HETEROALLENE SALTS	
1.1 Introduction	1
1.2 Heteroallene salts	3
1.3 Jochims and coworkers' contributions to the chemistry of heteroallene salts	4
1.3.1 [3+2] Cycloaddition of 1-aza-2-azoniaallene salts with a variety of π -systems	4
1.3.2 [3+2] Cycloaddition of 1,3-diaza-2-azoniaallene salts with alkenes	13
1.4 Applications of 1-aza-2-azoniaallene salts in synthesis	13
1.4.1 Synthesis of electrically neutral heterocycles	13
1.4.2 Synthesis of Cinnolinium salt	14
1.4.3 Syntheses of C-nucleosides from 1-aza-2-azoniaallene and 1,3-diaza-2- azoniaallene salts	15
1.4.4 Reaction with azomethines and azirine to form iminium and azolium salts	16
1.4.5 Syntheses of coumarin derivatives	17
1.4.6 Syntheses of 3'-azole derivatives	17
1.4.7 Synthesis of dienes and allylic ethers via [3,3] sigmatropic rearrangement of 1-aza-2-azoniaallene intermediates from N-allylhydrazones	19
1.5 Theoretical studies on the mechanisms for cycloadditions between 1-aza-2- azoniaallene cations and RNCO	20
1.6 Brewer group's contributions to cycloadditions of 1-aza-2-azoniaallene salts	23
1.6.1 [3+2] Cycloaddition reactions	23
1.6.2 [4+2] Cycloaddition reactions	27
1.6.3 Computational study on the role of tether for intramolecular [3+2] and [4+2] cycloadditions between heteroallene and pendent alkenes	28
1.7 Scope of intramolecular [4+2] cycloaddition reaction	31
1.7.1 Scope of the SbCl ₅ mediated intramolecular [4+2] cycloadditions from α -chloroazo precursors	32
1.7.2 Scope of the TMSOTf mediated intramolecular [4+2] cycloadditions from α -chloroazo precursors	34
1.7.3 TMSOTf mediated intramolecular [4+2] cycloadditions from α - trifluoroacetoxyazo precursors	37
1.7.4 Formation of dearomatized non-protonated azomethine imine salt	44
1.8 Conclusions	45
References	46

CHAPTER 2: INTRAMOLECULAR C-H AND ALKENE AMINATION OF 1-AZA-2-AZONIAALLENE SALTS

2.1 Introduction.....	49
2.2 Intramolecular C-H amination of 1-aza-2-azoniaallene salts	49
2.3 Theoretical study of intramolecular C-H amination of 1-aza-2-azoniaallene salt.....	53
2.4 Effect of tether length on intramolecular reactions of 1-aza-2-azoniaallenes	55
2.5 Kinetic isotope effects for intramolecular C-H amination of 1-aza-2-azoniaallene.....	57
2.6 Exploration of the scope of 1-aza-2-azoniaallene salts.....	58
2.6.1 Limitation of C-H insertion on secondary aliphatic center.....	58
2.6.2 Limitation of C-H insertion to synthesize indoline and indole products	59
2.7 C-H Amination and chloro-amination of allylic heteroallene salts	62
2.8 Limitation of intramolecular alkene aminations	65
2.9 New type of C-H amination via nitrenium cation.....	69
2.10 New type of alkene amination via nitrenium cation.....	72
2.11 Conclusions	74
References.....	75

CHAPTER 3: NEW SYNTHETIC ROUTES TO SYNTHESIZE α -SUBSTITUTED AZO COMPOUNDS

3.1 Introduction.....	78
3.2 Preparation of α -chloroazo compounds and their stability	79
3.3 Brewer group's contribution for the formation of α -chloroazo compounds.....	81
3.4 Discovery of a new method with acetyl chloride.....	85
3.5 Effect of aryl ring substitution on α -chloroazo formation	86
3.6 New methods to form α -substituted azo compounds.....	88
3.7 Proposed mechanism for formation of α -trifluoroacetoxyazo compound	96
3.8 Conclusions.....	97
References.....	97

CHAPTER 4: 1,3-DIPOLAR CYCLOADDITION OF PROTONATED AZOMETHINE IMINE SALTS

4.1 Introduction.....	99
4.2 Reactivities of azomethine imines	100
4.2.1 Acyclic azomethine imines	100
4.2.2 <i>C,N</i> -Cyclic azomethine imines	101
4.2.3 <i>N,N'</i> -Cyclic azomethine imines	103
4.3 Cycloaddition of protonated azomethine imine salts (<i>C,N</i> or <i>N,N'</i> -cyclic azomethine imine)	106
4.3.1 Optimization of intermolecular 1,3-dipolar cycloaddition of protonated azomethine imine salts.....	107
4.3.2 Reactions with dipolarophile having activated alkenes	108
4.3.2.1 With diethyl and dimethyl maleates as dipolarophiles.....	108
4.3.2.2 With dimethyl fumarate as dipolarophile	110
4.3.3 Reactions with dimethyl acetylene dicarboxylate as dipolarophile.....	111
4.3.4 Reactions with maleic anhydride and <i>N</i> -methylmaleimide as dipolarophiles	111

4.3.5 Reactions involving unsymmetrical π -systems as dipolarophiles	113
4.4 Summary of 1,3-dipolar cycloaddition of azomethine imines.....	115
4.5 Oxidation of protonated azomethine imine salt	116
4.6 Computational study for 1,3-dipolar cycloadditions of azomethine imine salts	117
4.6.1 Computational methods	117
4.6.2 Calculation of energy barriers of 1,3-dipolar cycloaddition of azomethine imine and MVK.....	118
4.6.3 Calculation of energy barriers of 1,3-dipolar cycloaddition of azomethine imine and maleic anhydride.....	120
4.6.4 Calculation of energy barriers of 1,3-dipolar cycloaddition of azomethine imine and dimethyl maleate and fumarate.....	121
4.6.5 Calculation of energy barriers of 1,3-dipolar cycloaddition of azomethine imine and dimethyl acetylene dicarboxylate	124
4.7 Issues with determining the stereochemistry of the cycloaddition products	125
4.8 Conclusions.....	126
References	126
SUMMARY OF THESIS AND FUTURE GOAL.....	130
CHAPTER 5: EXPERIMENTAL INFORMATION	
5.1 General experimental information	134
5.2 Experimental information for [4+2] cycloaddition (Chapter 1)	135
5.2.1 Representative procedure for SbCl_5 mediated [4+2]-cycloaddition	135
5.2.2 Preparation and characterization data of protonated azomethine imine SbCl_6 salts	136
5.2.3 Representative experimental procedure for TMSOTf mediated [4+ 2] cycloaddition.....	137
5.2.4 Preparation and characterization data of protonated azomethine imine triflate salts	137
5.3 Experimental information for dearomatized non-protonated azomethine imine salt (Chapter 1)	147
5.4 Experimental information for Chapter 2.....	148
5.4.1 Preparation of aryl hydrazones	148
5.4.2 Characterization data of aryl hydrazones.....	148
5.4.3 Preparation of aryl α -chloroazo compounds	149
5.4.4 Characterization data of α -chloroazo compounds	150
5.4.5 Preparation of α -trifluoroacetoxyazo compounds	151
5.4.6 Characterization data of α -trifluoroacetoxyazo compounds	151
5.4.7 Experimental information to prepare starting materials for new type of C-H amination (Chapter 2).....	152
5.4.7.1 Preparation and characterization data of 1-hydroxy-1,3- diphenylurea (2.103)	152
5.4.7.2 Preparation and characterization data of 1,3-diphenyl-1-(3- phenylpropoxy)urea (2.105)	153
5.4.7.3 Preparation and characterization data of N-phenyl-O-(3- phenylpropyl)hydroxylamine (2.106)	153

5.4.7.4 Characterization data of 2,2,2-trifluoro-N-phenyl-N-(3-phenylpropoxy)acetamide (2.108)	154
5.4.7.5 Characterization data of 1-(but-3-en-1-yloxy)-1,3-diphenylurea (2.113)	154
5.4.7.6 Characterization data of O-(but-3-en-1-yl)-N-phenylhydroxylamine (2.114)	154
5.5 Experimental information for Chapter 3	155
5.5.1 Preparation of α -chloroazo using acetyl chloride	155
5.5.2 General experimental procedure for preparation of aryl hydrazones	155
5.5.3 Characterization data for aryl hydrazones	156
5.5.4 Preparation and characterization data of α -chloroazo compounds	164
5.5.5 Representative experimental procedures to prepare of α -trifluoroacetoxyazo compounds	166
5.5.6 Preparation and characterization data of α -trifluoroacetoxyazo compounds	166
5.6 Experimental information for Chapter 4	175
5.6.1 Experimental information of 1,3-dipolar cycloaddition reactions	175
5.6.2 Representative experimental procedure for 1,3-dipolar cycloaddition reactions	175
5.6.3 Characterization data for 1,3-dipolar cycloaddition reactions	176
COMPREHENSIVE BIBLIOGRAPHY	202
APPENDIX	209

LIST OF TABLES

Table	Page
Table 1.1 Optimization of intramolecular [4+2] cycloaddition reaction using α -trifluoroacetoxy azo derivative of dihydro- β -ionone.....	39
Table 2.1 Examples of substrate scope for C-H amination with above conditions	50
Table 3.1 Examples of α -chloroazo compounds prepared by Jochims and coworkers.....	80
Table 3.2 A variety of examples of phenyl- α -chloroazo compounds that form from the corresponding phenyl hydrazones under Swern oxidation condition	83
Table 3.3 Formation of hydrazones and α -chloroazo compounds	87
Table 3.4 Optimization to α -trifluoroacetoxyazo compounds.....	89
Table 3.5 Formation of a variety of hydrazones and α -chloroazo compounds using trifluoroacetoxy dimethylsulfonium trifluoroacetate as an oxidant.....	90
Table 3.6 Scope of reaction with a simple pendent alkene.....	92
Table 3.7 Further experimentation to form α -trifluoroacetoxyazo compound.....	94
Table 4.1 Optimization of 1,3-dipolar cycloaddition of protonated azomethine imine	108
Table 4.2 Calculated energy barriers for all possible transition states generated by the cycloaddition of azomethine imine 4.106 and MVK.....	119
Table 4.3 Calculated energy barriers for all possible transition states generated by the cycloaddition of azomethine imine 4.106 and maleic anhydride.....	121
Table 4.4 Calculated energy barriers for all possible transition states generated by the cycloaddition of azomethine imine 4.106 and dimethyl maleate.....	122
Table 4.5 Calculated energy barriers for all possible transition states generated by the cycloaddition of azomethine imine 4.106 and dimethyl fumarate.....	124
Table 4.6 Calculated energy barriers for all possible transition states generated by the cycloaddition of azomethine imine 4.106 and dimethyl acetylene dicarboxylate	125
Table 5.1 Optimization of 1,3-dipolar cycloaddition of protonated azomethine imine...	175

LIST OF FIGURES

Figure	Page
Figure 1.1. Chemical structures of nitrogen heterocyclic drugs	1
Figure 1.2. Cephalosporin C and its derivative ceftriaxone.....	2
Figure 1.3. General structure of a 1-aza-2-azoniaallene salt	3
Figure 1.4. Three different structures of 1-aza-2-azoniaallene salts.....	3
Figure 1.5. Jochim's mechanistic study of [3+2] cycloadditions of heteroallene cation with carboimide.....	8
Figure 1.6. Mechanistic study of [3+2] cycloadditions of 1-aza-2-azoniaallene salt with alkyne	10
Figure 1.7. Energy profile diagram for cycloadditions between 1-aza-2-azoniaallene cations and RNCO	22
Figure 1.8. Proposed transition states to form ring-fused and bridged diazenium salts	25
Figure 1.9. Location of partial positive charge in diazenium salts	25
Figure 1.10. Proposed conformations leading to diazenium salts	26
Figure 1.11. The Possible transition states and DFT-computed activation enthalpies and free energies (energy in kcal/mol) for the intramolecular [3+2] and [4+2] cycloadditions	29
Figure 1.12. The Possible transition states, products, and DFT-computed energies (in kcal/mol) for intramolecular [3+2] and [4+2] cycloadditions between heteroallene and propene.....	31
Figure 1.13. ¹ HNMR spectrum showing the characteristic peak of the protonated azomethine imine salt	35
Figure 1.14. Crystal structure of protonated azomethine imine 1.170	36
Figure 2.1. Gibbs free energy changes in kcal/mol of single and triplet C-H amination pathways of aryl-1-aza-2-azoniaallene	54
Figure 2.2. Probability vs. timing of N-H and C-N bond formation at 298 K.....	55
Figure 2.3. A Morse potential diagram showing zeropoint energy for C-H and C-D	57
Figure 2.4. Gibbs free energy barrier in kcal/mol for C-H amination and aziridinium pathways for 5-membered ring	64
Figure 2.5. Gibbs free energy barrier in kcal/mol for C-H amination and aziridinium pathways for 6-membered ring.....	65
Figure 2.6. Comparison of traditional approach with new approach to undergo new type of C-H amination.....	70
Figure 3.1. Structure of α -chloroazo compound.....	78
Figure 4.1. Classification of azomethine imines.....	99
Figure 4.2. C,N or N,N'-Cyclic azomethine amine.....	106

LIST OF ABBREVIATIONS

(Ac)₂O = acetic anhydride
¹³C NMR = carbon 13 NMR
¹H NMR = Proton NMR
Ac = acetate
AcOH = acetic acid
ACS = American Chemical Society
Ar = aryl
br = broad
Bu (*n*-Bu) = butyl
CDCl₃ = chloroform-d
d = doublet
D.P. or dec. point = decomposition point
Dec = decomposition
DI = Deionized Water
DMF = dimethylformamide
DMP = Dess-Martin periodinane
DMSO = dimethyl sulfoxide
Dr = diastereomeric
ESI-MS = electrospray ionization mass spectroscopy
Et = ethyl
etc. = et cetera
EtoAc = ethyl acetate
FT-IR = Fourier transform infrared spectroscopy
g = gram
GC = gas chromatography
GC-MS = gas chromatography mass
h = hour (s)
hrs = hours
Hz = Hertz
i-Pr = isopropyl
IR = infrared
IUPAC = International Union of Pure and Applied Chemistry
KJ = kilojoules
LC-MS = liquid chromatography mass spectrometry
lit = literature
m = multiplet
Me = methyl
mg = milligram
MHz = megahertz
min = minute
mL = milliliter
mmol = millimole

mol-equiv = mole equivalent
mp = melting point
MS = Mass Spectroscopy
N.R. = No Reaction
n-Hep = heptyl
n-Hex = hexyl
NMR = nuclear magnetic resonance
n-Pr = normal propyl
Ph = phenyl
ppm = parts per million
PTP = protein tyrosine phosphates
q = quartet
rt = room temperature
s = singlet
spectrometry
t = triplet
TBAB = tetra-*n*-butylammonium bromide
t-Bu = *tert*-butyl
temp. = temperature
Tf = triflate
TFA = trifluoroacetate
TFAA = trifluoroacetic anhydride
THF = tetrahydrofuran
TLC = thin layer chromatography
TMS = trimethylsilyl
TMSOTf = trimethylsilyl trifluoromethanesulfonate
TsOH = *p*-toluenesulfonic acid or tosylic acid
VO(acac)₂ = vanadyl acetylacetonate
μl = microliter
B3LYP = Becke, 3-parameter, Lee-Yang-Parr
AM1 = a semiempirical molecular orbital technique in computational chemistry
DNA = deoxyribonucleic acid
RNA = ribonucleic acid
HOMO = highest occupied molecular orbital
LUMO = lowest unoccupied molecular orbital
FMO = frontier molecular orbital
DFT = density functional theory

CHAPTER 1: INTRAMOLECULAR CYCLOADDITION REACTIONS OF HETEROALLENE SALTS

1.1 Introduction

The chemistry of heterocycles, cyclic compounds that contain at least one non-carbon atom (typically, oxygen, nitrogen, or sulfur) within the ring, is an important branch of organic chemistry. Heterocycles are present in a wide variety of natural products, pharmaceuticals, agrochemicals, biomolecules, biologically active molecules, polymers, nanoparticles, and dyes. Heterocyclic compounds containing nitrogen make up the greatest class of biologically active compounds,^{1,2} and nitrogen heterocycles play a major role in living things. For example, genetic material (DNA) is composed of nitrogen containing heterocyclic bases purines and pyrimidines, and most drugs, such as penicillin, erlotinib (cancer), nevirapine (HIV), penciclovir (herpes), and imatinib (cancer), are nitrogen heterocycles (Figure 1.1).

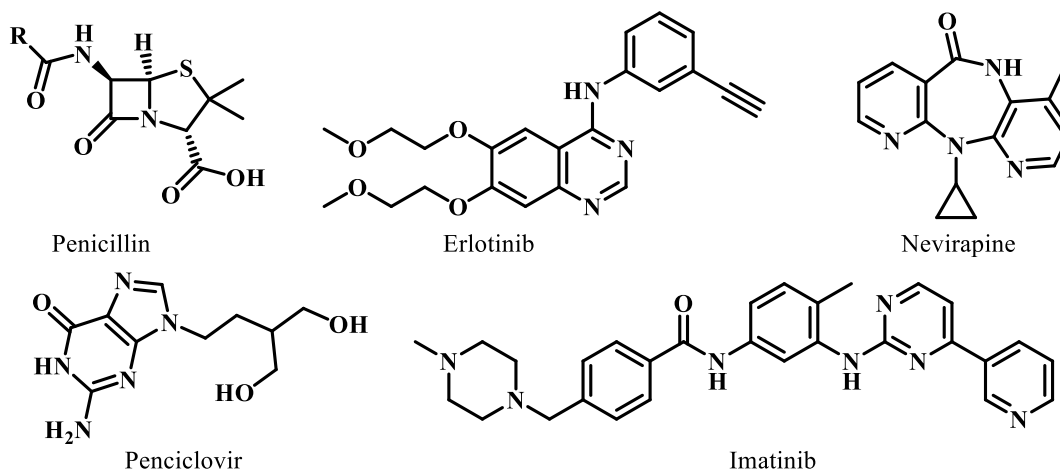


Figure 1.1. Chemical structures of nitrogen heterocyclic drugs.

Many heterocyclic natural products have been isolated from various sources including plants, animals, marine organisms, and microbial metabolites. Nitrogen containing

natural products (alkaloids) and their synthetic analogs play a significant role in drug discovery. For example, ceftriaxone is an antibiotic useful for the treatment of many bacterial infections. It is derived from cephalosporin C, which is a natural product that can be isolated from *Cephalosporium acremonium* (Figure 1.2).^{3,4,5}

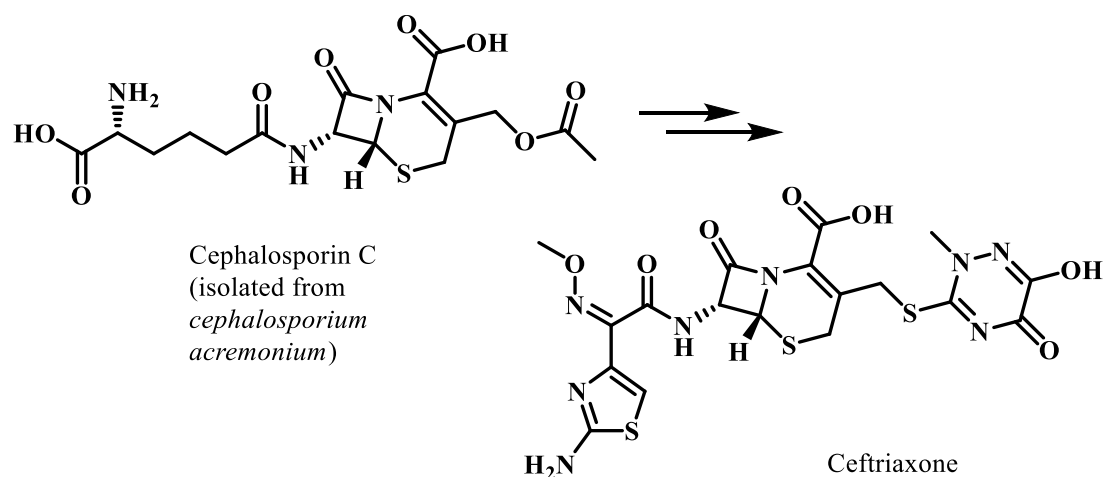


Figure 1.2. Cephalosporin C and its derivative ceftriaxone.

Over the past decades, a lot of synthetic strategies have been developed to prepare biologically active compounds, natural products, and their derivatives. However, developing new green and concise synthetic routes to novel nitrogen heterocycles, particularly structurally complex ones, is still very significant. With this in mind, my research has focused on developing new strategies to synthesize structurally complex tri- and tetracyclic nitrogen heterocycles, such as protonated azomethine imines, via a green approach. The methodology I developed takes advantage of the reactivity of 1-aza-2-azoniallene salts, which are highly reactive species that will be discussed in depth in the next several sections of this thesis. In addition, I have developed a method to take advantage of the protonated azomethine imine products in a subsequent 1,3-dipolar cycloaddition, which give structurally complex tetra- and pentacyclic nitrogen

heterocycles. Overall, this methodology provides access to structurally unique heterocycles that may find use in biological studies.

1.2 Heteroallene salts

A 1-aza-2-azoniaallene salt (e.g. **1.1**, Figure 1.3) is a cationic heteroallene that has a central nitrogen which has double bonds to both a nitrogen and a carbon atom. These heteroallene salts are only stable in solution at low temperatures.^{6,7} All attempts so far to isolate these salts have failed.^{8,9}

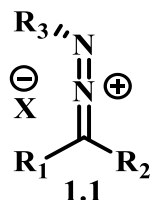


Figure 1.3. General structure of a 1-aza-2-azoniaallene salt.

Due to the presence of a +1 formal charge on 1-aza-2-azoniaallenes, they can be represented by three different structures (Figure 1.4) which result in diverse reactivities that lead to various *N*-heterocyclic products.¹⁰

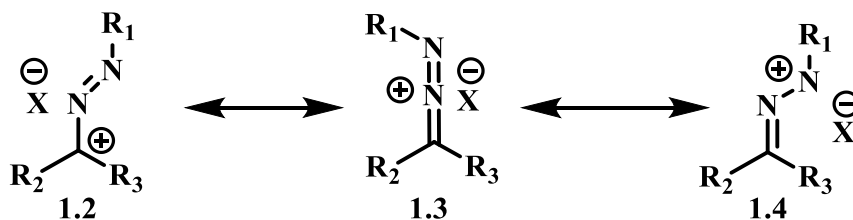
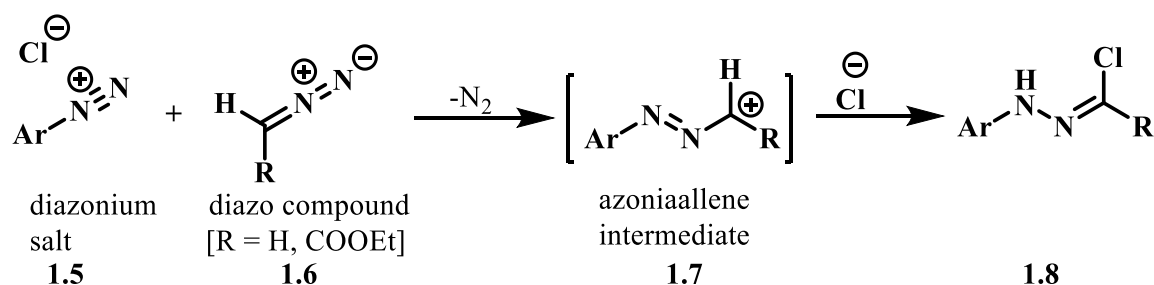


Figure 1.4. Three different structures of 1-aza-2-azoniaallene salts.

These salts were first reported as intermediates by Huisgen and Koch in 1955. They treated a diazonium salt (**1.5**) with a diazo species (**1.6**) to produce an azoniaallene intermediate (**1.7**), which was then trapped by the chloride counter ion (Scheme 1.1).¹¹

Many other methods, such as electrochemical oxidations of various hydrazones,^{10,12,13} chemical oxidation of aryl hydrazones in the presence of lead tetraacetate,^{14,15} solvolysis of α,α' -dichloroazoalkenes,¹⁷ and treating α -chloroazos with Lewis acid,^{7,8} have been reported to produce 1-aza-2-azoniaallene salt intermediates.



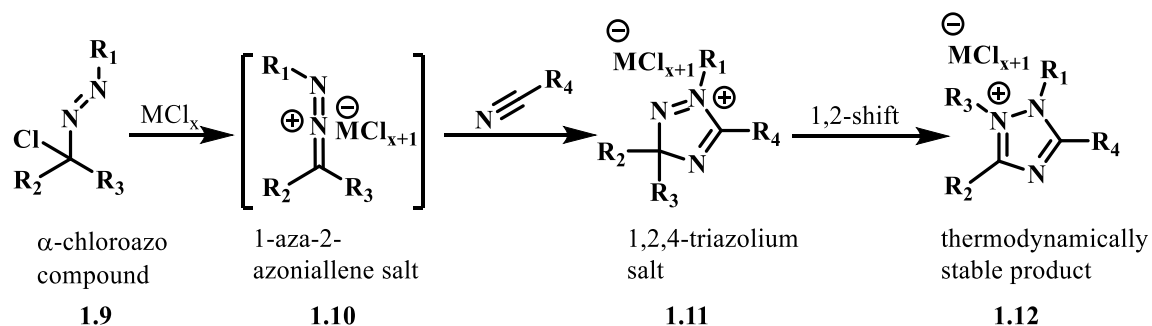
Scheme 1.1. Trapping of azoniaallene intermediate starting from the reaction of diazonium salt with diazo compound.

1.3 Jochims and coworkers' contributions to the chemistry of heteroallene salts

1-Aza-2-azoniaallene salts behave as cationic four-electron three-center components that can undergo cycloaddition to many different types of multiple bonds. Jochims and coworkers reported a variety of [3+2] cycloaddition reactions with multiple bonds.

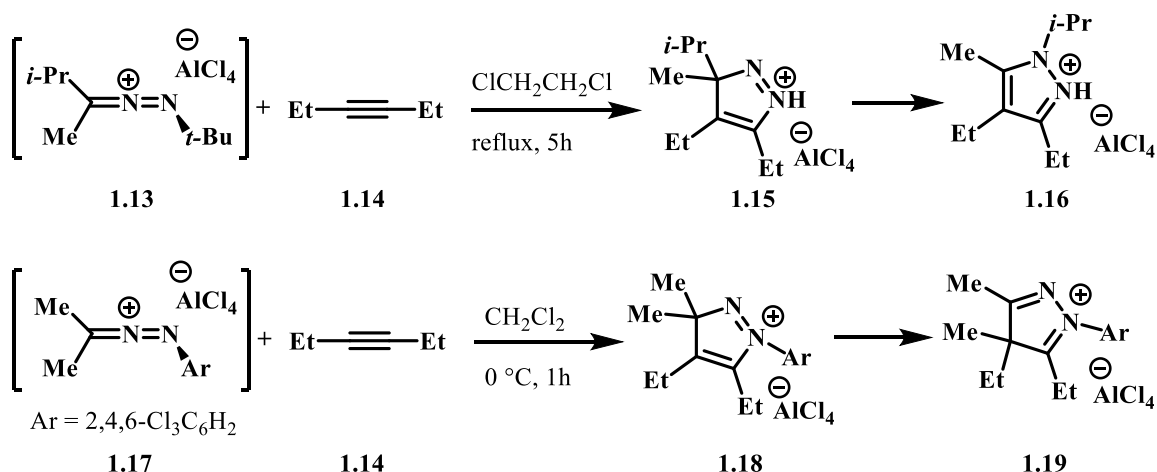
1.3.1 [3+2] Cycloaddition of 1-aza-2-azoniaallene salts with a variety of π -systems

Jochims and coworkers reported that an α -chloroazo compound (e.g. **1.9**, Scheme 1.2) generated from the reaction of a hydrazone with *t*-butyl hypochlorite, reacted with a halophilic Lewis acid (SbCl_5 or AlCl_3) in the presence of nitriles to afford a substituted 1,2,4-triazolium salt (e.g. **1.11**) which may rearrange to give a thermodynamically stable product (e.g. **1.12**, Scheme 2).^{6, 11} In many cases, they could not isolate the initial cyclization product **1.11** due to fast rearrangement to **1.12**.



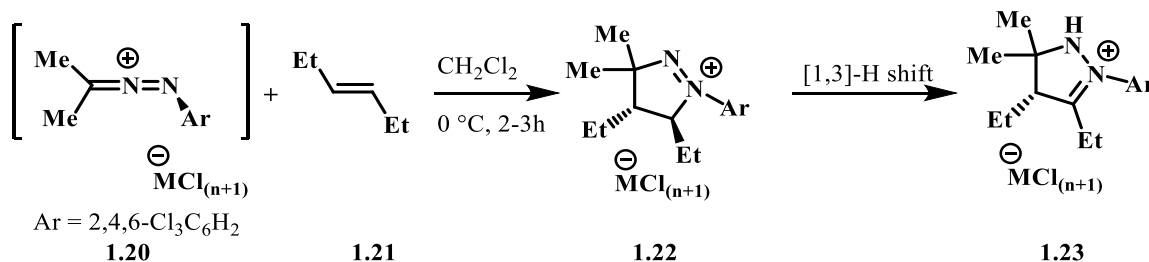
Scheme 1.2. Polar [3+2] cycloadditions between 1-aza-2-azoniaallene salts and nitriles.

They further reported that [3+2] cycloadditions of 1-aza-2-azoniaallene cations occur with multiple π systems. For example, 1-aza-2-azoniaallene salt **1.13** (Scheme 1.3) reacts with 3-hexyne to give 1*H*-pyrazolium salt **1.16**.⁸ In this reaction, the isopropyl group is solely migrated to the adjacent nitrogen atom due to the formation of more stable carbocation intermediate. However, when they replaced the isopropyl group by methyl group, the methyl group was solely migrated to the adjacent carbon atom to afford the product **1.19**.⁸



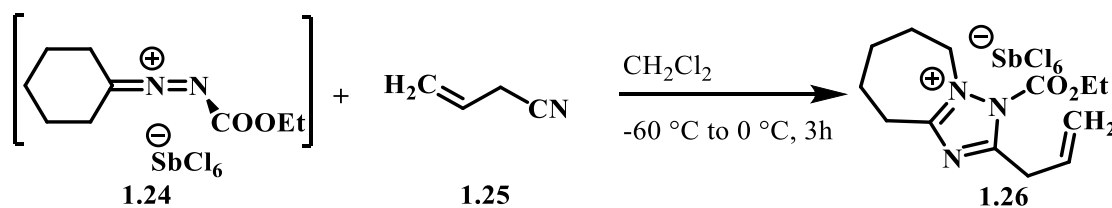
Scheme 1.3. Polar [3+2] cycloadditions between 1-aza-2-azoniaallene salts and 3-hexyne.

To understand the stereoselectivity of [3+2] cycloadditions, they treated 1-aza-2-azoniaallene salt **1.20** (Scheme 1.4) with *trans* 3-hexene which gave a *trans* form of a single stereoisomer (**1.22**).⁸ They did not observe any trace of a second stereoisomer. From this observation, they concluded that this cycloaddition reaction occurs via a concerted mechanism.



Scheme 1.4. Polar [3+2] cycloadditions between 1-aza-2-azoniaallene salts and 3-hexene.

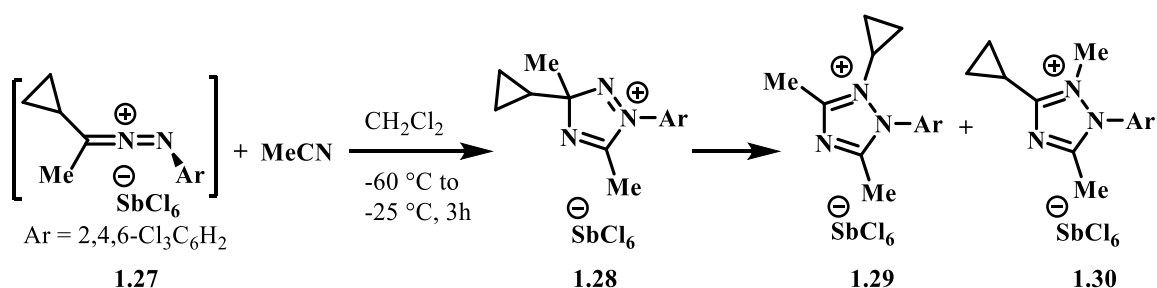
In a competition experiment, they treated 1-aza-2-azoniaallene salt **1.24** with homoallylic nitrile **1.25** (Scheme 1.5).⁸ The nitrile group reacted exclusively in favor of the alkene with cation **1.24** to give triazole **1.26** as the only product. This result shows that a nitrile group undergoes [3+2] cycloaddition with a heteroallene salt more rapidly than an olefin.



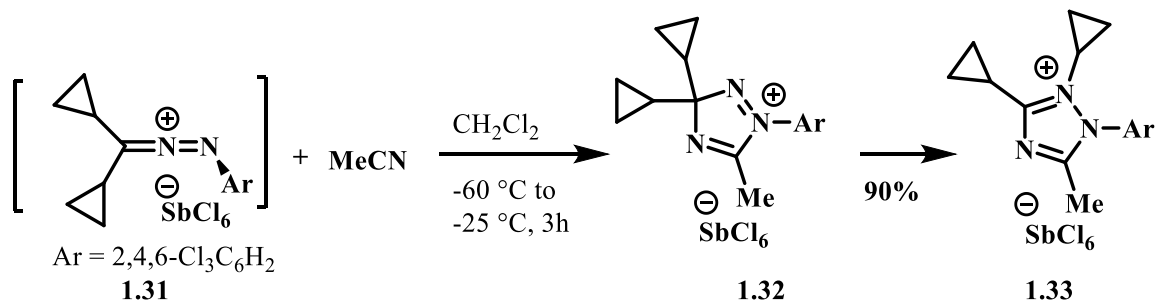
Scheme 1.5. Competitive experiment of allylic cyanide.

To understand the mechanism of migratory aptitudes for [3+2] cycloadditions, they treated 1-aza-2-azoniaallene salt **1.27** containing methyl and cyclopropyl group with acetonitrile (Scheme 1.6).⁸ This salt gave an equimolecular mixture of the triazolium salt **1.29** and **1.30** which shows that the migratory aptitudes of methyl and cyclopropyl are

comparable. However, when they took 1-aza-2-azoniaallene salt **1.31** (Scheme 1.7) containing two cyclopropyl groups, they isolated only **1.33** in 90% yield.⁸ They did not observe any trace of an allylic compound which could be obtained from ring opening of the cyclopropane. Based on this observation, the intermediate in which a cation was directly adjacent to the cyclopropane was ruled out. Thus, they concluded that the rearrangement occurs via a concerted [1,5]-sigmatropic migration of the cyclopropyl group.

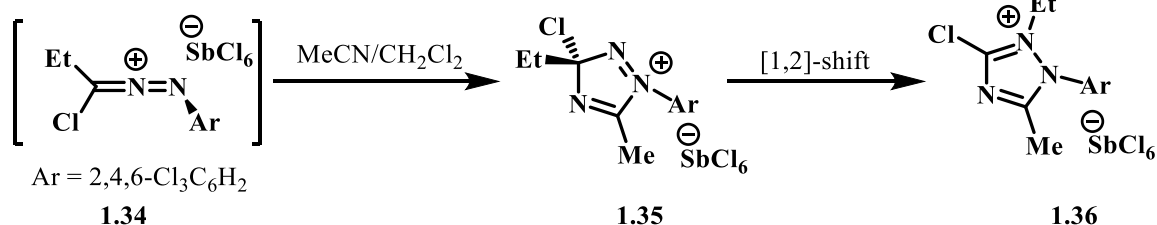


Scheme 1.6. [3+2] Cycloaddition reaction with cyclopropyl and methyl substituents.



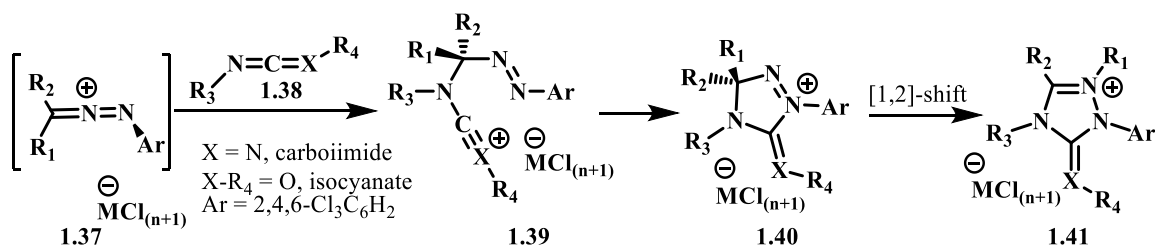
Scheme 1.7. [3+2] Cycloaddition reaction with dicyclopropyl substituents on 1-aza-2-azoniaallene salt.

To examine the migratory aptitudes with respect to electron withdrawing and electron releasing groups, they treated the heteroallene **1.34** (Scheme 1.8) with acetonitrile. The ethyl group preferentially migrated to the nitrogen atom to provide the thermodynamically stable product **1.36**.¹⁷



Scheme 1.8. [3+2] Cycloaddition reaction of 1-aza-2-azoniaallene salt containing an electron-withdrawing and releasing groups.

In a study of the scope of the reaction of 1-aza-2-azoniaallene cations with different π -systems, they reported that carbodiimides and isocyanates react to give five-membered heterocycles (Scheme 1.9).^{9,18} Although there were a number of possibilities for the migration of the R₁ group, they confirmed via X-ray structural analysis that migration occurs to the adjacent nitrogen to give product **1.41**. To determine if the cycloaddition occurs via a concerted or a two-step process, they performed AM1 calculations. Reactions proceeding through a concerted cycloaddition, were higher energy than the two-step pathway (Figure 1.5).¹⁸



Scheme 1.9. [3+2] cycloadditions of heteroallene salt with carbodiimide and isocyanate.

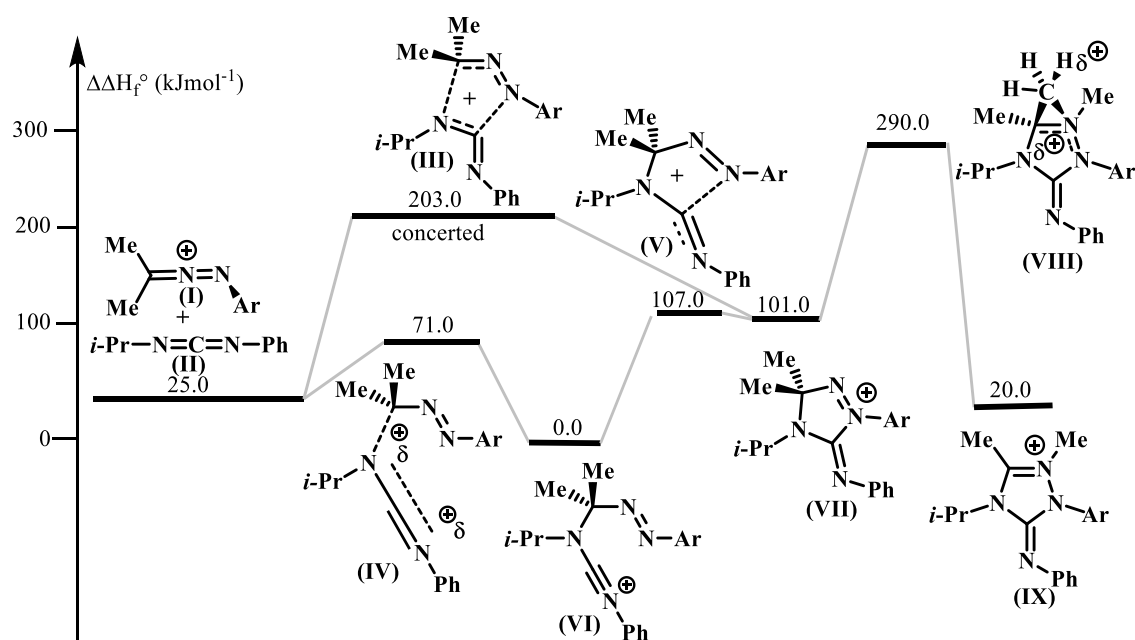
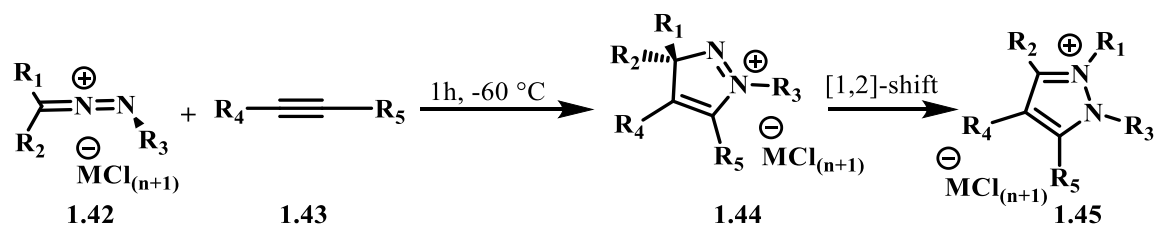


Figure 1.5. Jochim's mechanistic study of [3+2] cycloadditions of heteroallene cation with carboiimide.

These authors also investigated the mechanism of the cycloaddition of acetylenes (Scheme 1.10) with 1-aza-2-azoniaallene cations using AM1 computational methods. The formation of intermediate **XIII** from the heteroallene **X** and 2-butyne (**XI**) was calculated to be exothermic by 92 kJ/mol (Figure 1.6).¹⁹ This reaction does not give a low energy intermediate as compared to carbodiimides and isocyanates, and this reaction occurs via an asynchronous concerted mechanism. In this reaction, 1-aza-2-azoniaallene cation **1.42** and the acetylene **1.43** are acting as the 1,3-dipole and dipolarophile respectively (Scheme 1.10). This cycloaddition is electronically similar to a 1,3-dipolar cycloaddition with inverse electron demand. The cycloaddition that forms the intermediate **XIII** is followed by a [1,2] alkyl shift via intermediate **XIV** to provide final product **XV**. The Tao group also reported a computational study on the heteroallene/acetylene

cycloaddition using a higher-level computation.²⁰ This study agreed with the earlier AM1 study.



Scheme 1.10. [3+2] cycloadditions of 1-aza-2-azoniaallene salt with alkyne.

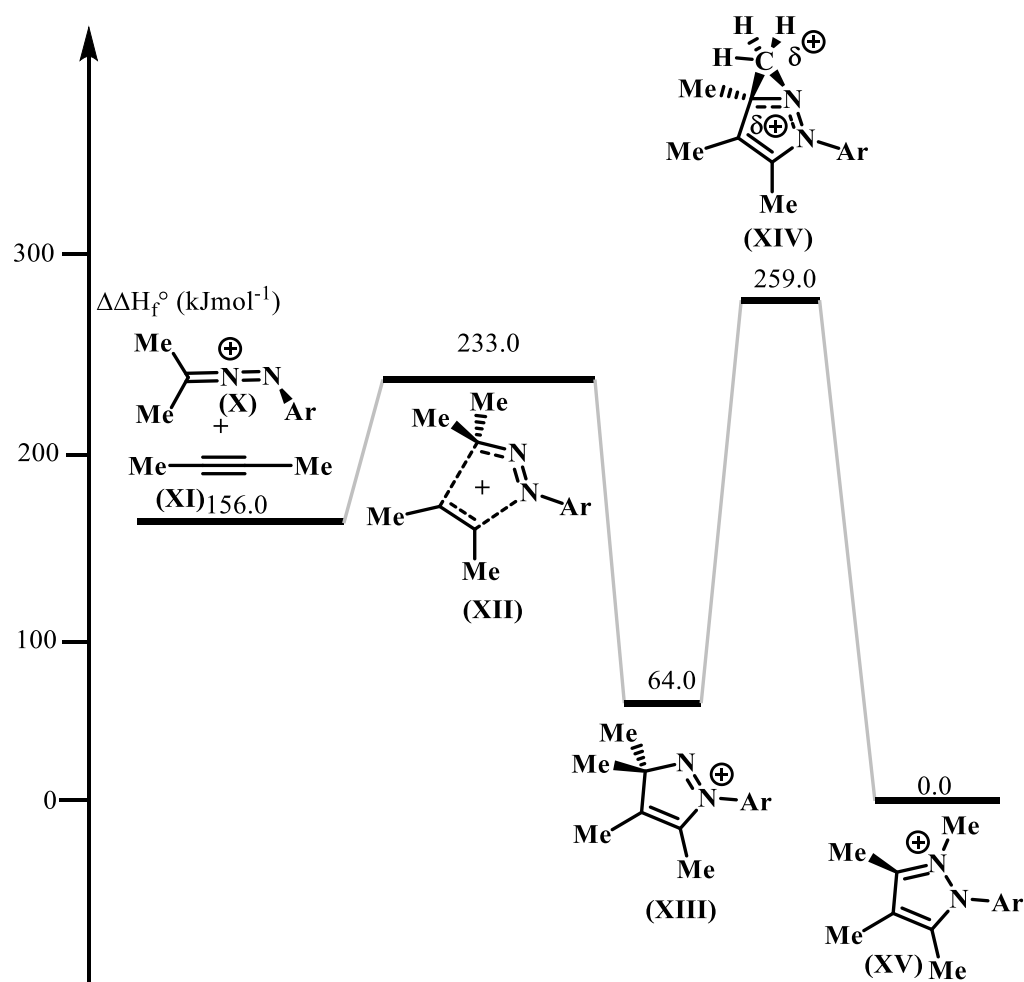
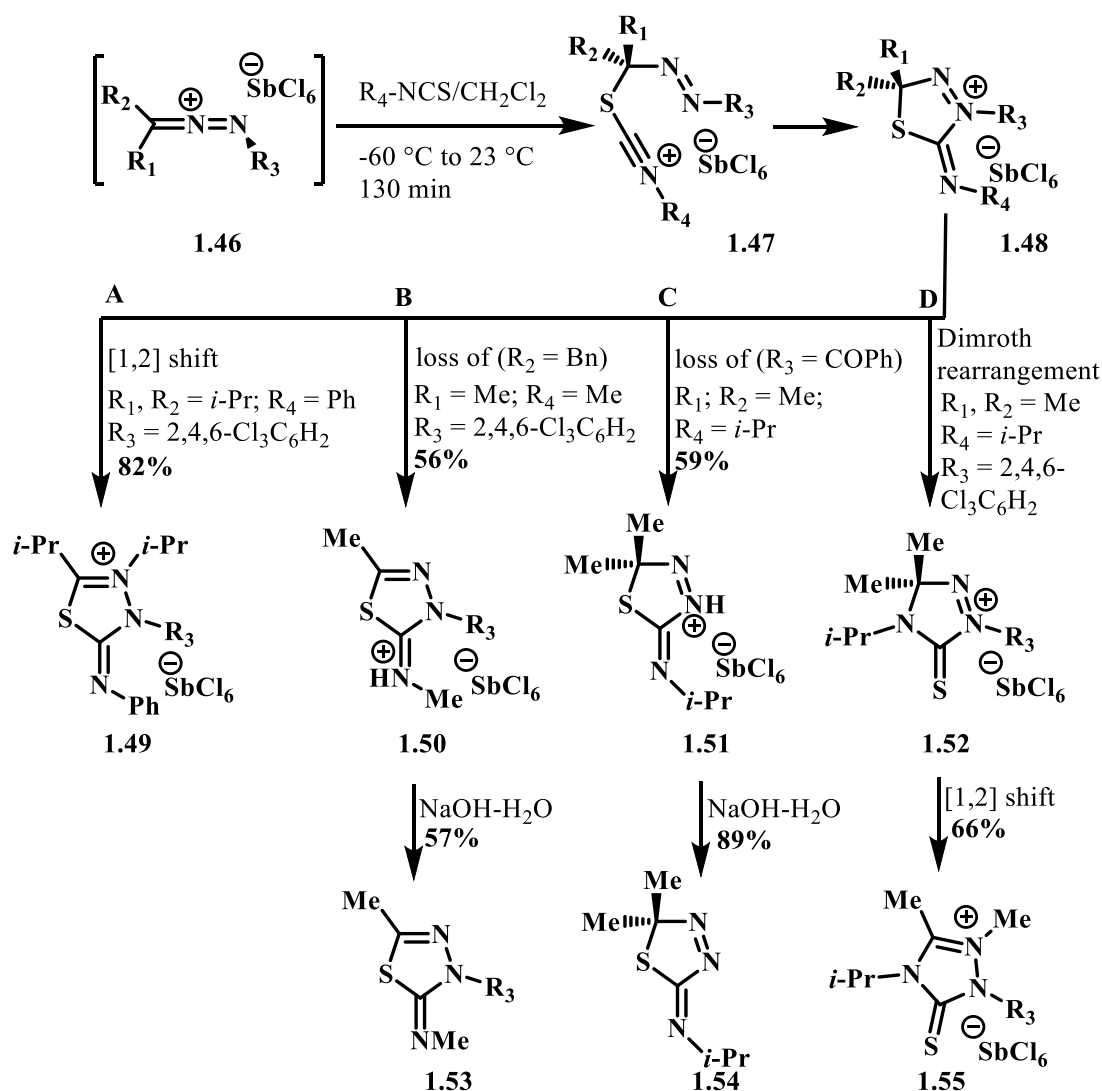


Figure 1.6. Mechanistic study of [3+2] cycloadditions of 1-aza-2-azoniaallene salt with alkyne.

Jochim went on to study reactions of 1-aza-2-azoniaallene salt **1.46** with isothiocyanates (R-NCS) which gave a single heterocycle product in good yield (Scheme 1.11).²¹ According to AM1 calculations, the cycloaddition of heteroallenes to isothiocyanates occurs via a two-step reaction pathway. To understand the migratory aptitude, they used a variety of substituents to carry out this reaction. When R₁, R₂ = *i*-Pr; R₃ = 2,4,6-Cl₃C₆H₂, and R₄ = Ph, intermediate **1.48** follows path **A** (Scheme 1.11) to give product **1.49** in 82% yield, in which isopropyl group preferentially migrates. When R₁, R₄ = Me; R₂ = Bn; and R₃ = 2,4,6-Cl₃C₆H₂, intermediate **1.48** follows path **B** to give product **1.50** in 56% yield followed by hydrolysis in the presence of aqueous sodium hydroxide to provide electrically neutral product **1.53** in 57% yield. In path **B**, instead of 1,2-shift, intermediate **1.48** loses the benzyl group to give product **1.50** because of the presence of traces of water in the reaction trap the free benzyl cation as benzyl alcohol. When R₁, R₂ = Me; R₃ = C₆H₅; and R₄ = *i*-Pr, intermediate **1.48** follows path **C** to give product **1.51** in 59% yield followed by hydrolysis in the presence of aqueous base to give electrically neutral product **1.54** in 89% yield. In path **C**, intermediate **1.48** loses the benzoyl group, which is a good leaving group, to afford the moderately stable iminium salt **1.51**. Again, the presence of traces of moisture in the reaction mixture is responsible for this result. When R₁, R₂ = Me; R₃ = 2,4,6-Cl₃C₆H₂; and R₄ = *i*-Pr, intermediate **1.48** undergoes Dimroth rearrangement to give intermediate **1.52** followed by 1,2-shift to afford triazolium salt **1.55** in 66% yield. Therefore, the substituents on both the heteroallene and the isothiocyanate play a significant role in determining the reaction outcome.



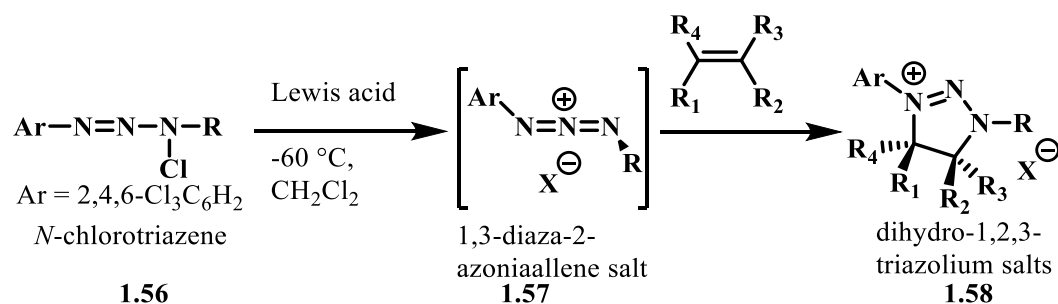
Scheme 1.11. [3+2] Cycloadditions of 1-aza-2-azoniaallene salt with isothiocyanate.

After conducting a systematic study of the reactions of 1-aza-2-azoniaallene salts with a variety of π -systems, Jochims and coworkers concluded that the rate of the reaction of heteroallene salts with π systems follows the following decreasing order:²²

Nitriles \approx carbodiimides \approx strained alkenes \gg unstrained alkenes, alkynes, isocyanates, isothiocyanates.

1.3.2 [3+2] Cycloaddition of 1,3-diaza-2-azoniaallene salts with alkenes

1,3-Diaza-2-azoniaallene salt²³ **1.57** is another reactive heteroallene species. This salt is stable below -50 °C and can be prepared *in situ* by the reaction of *N*-chlorotriazenes with Lewis acids. This species undergoes smooth cycloadditions with electron-rich and electron-deficient olefins to give dihydro-1,2,3-triazolium salts (**1.58**) with complete conservation of the configuration of the alkenes via a concerted process (Scheme 1.12). However, this reactive intermediate neither reacts with nitriles or with isocyanates.²³



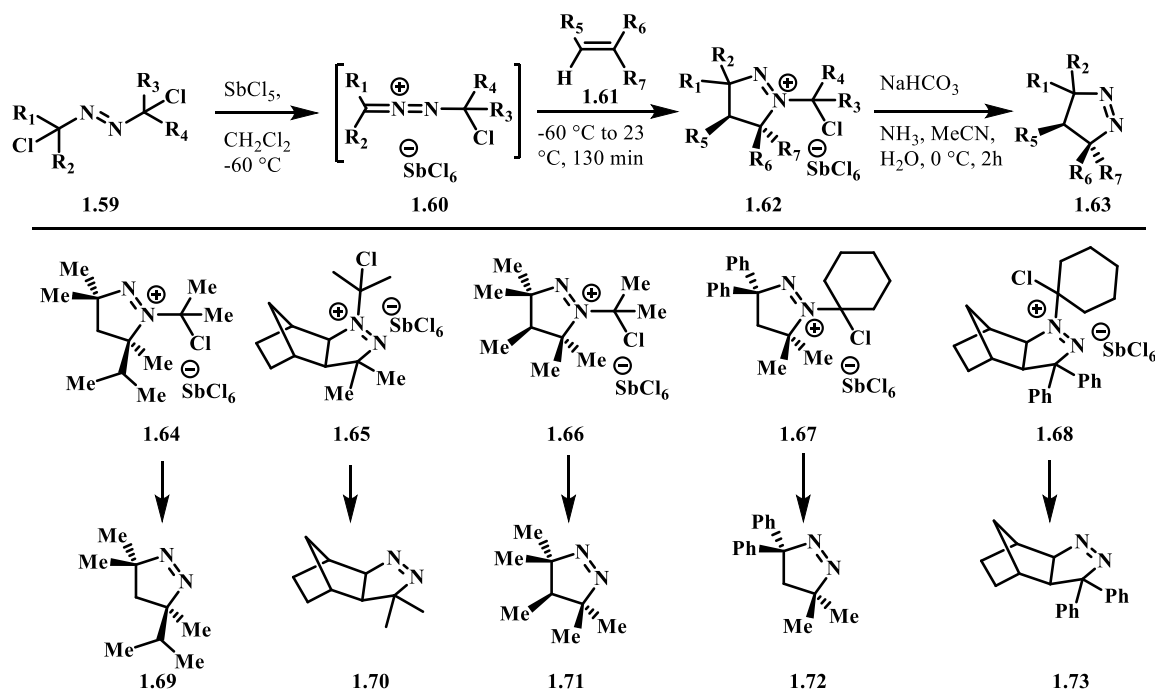
Scheme 1.12. [3+2] Cycloaddition of 1,3-diaza-2-azoniaallene salts with alkenes.

1.4 Applications of 1-aza-2-azoniaallene salts in synthesis

1.4.1 Synthesis of electrically neutral heterocycles

The major drawback of the cycloaddition of cationic heteroallene is that the reaction products end up as salts.⁸⁻¹⁸ Jochims and coworkers were interested in preparing electrically neutral heterocycles using the heteroallene salts, which are achieved by incorporating a cleavable group on nitrogen. In search for 1-aza-2-azoniaallene salts with an appropriate leaving group, they discovered α,α' -dichloroazo compound **1.59** (Scheme 1.13).²⁴ Treating **1.59** with SbCl₅ in the presence of electron-rich alkenes gave 4,5-dihydro-3*H*-pyrazolium salts (**1.62**) which could be hydrolyzed to give a charge neutral

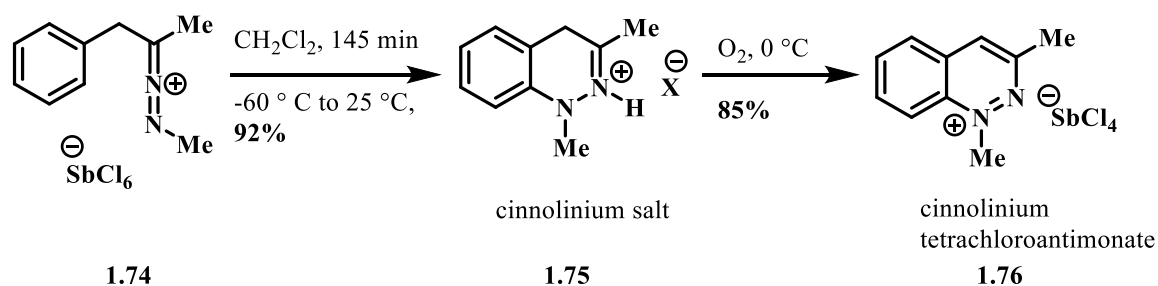
product. They assumed that the intermediate 1-aza-2-azoniaallene salt (**1.60**) formed during the reaction underwent cycloaddition with alkene (**1.61**). The pyrazolium salts (**1.64** – **1.68**) were hydrolyzed with aqueous sodium hydrogen carbonate in the presence of a small amount of ammonia to give the corresponding 3*H*-4,5-dihydropyrazoles (**1.69** – **1.73**).



Scheme 1.13. Formation of electrically neutral heterocycles via [3+2] cycloaddition.

1.4.2 Synthesis of Cinnolinium salt

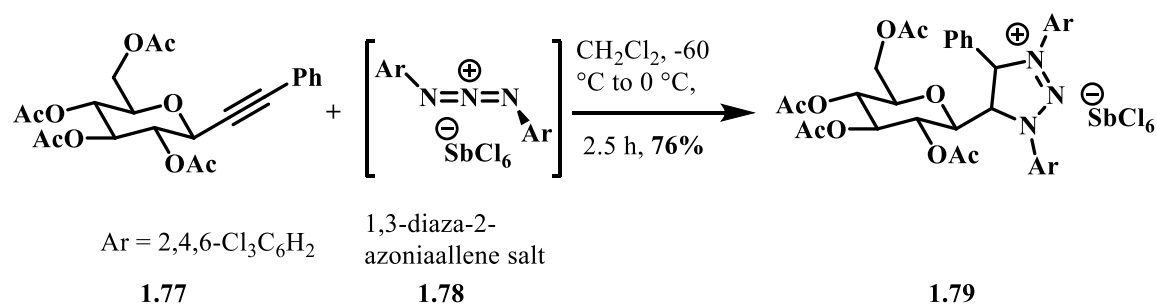
In the synthesis of cinnolinium salts,¹⁸ Jochims and coworkers employed 1-aza-2-azoniaallene **1.74**, which was derived from phenylacetone. In the presence of oxygen, the cinnolinium salt **1.75** was readily dehydrogenated to the cinnolium tetrachloroantimonate **1.76** (Scheme 1.14).



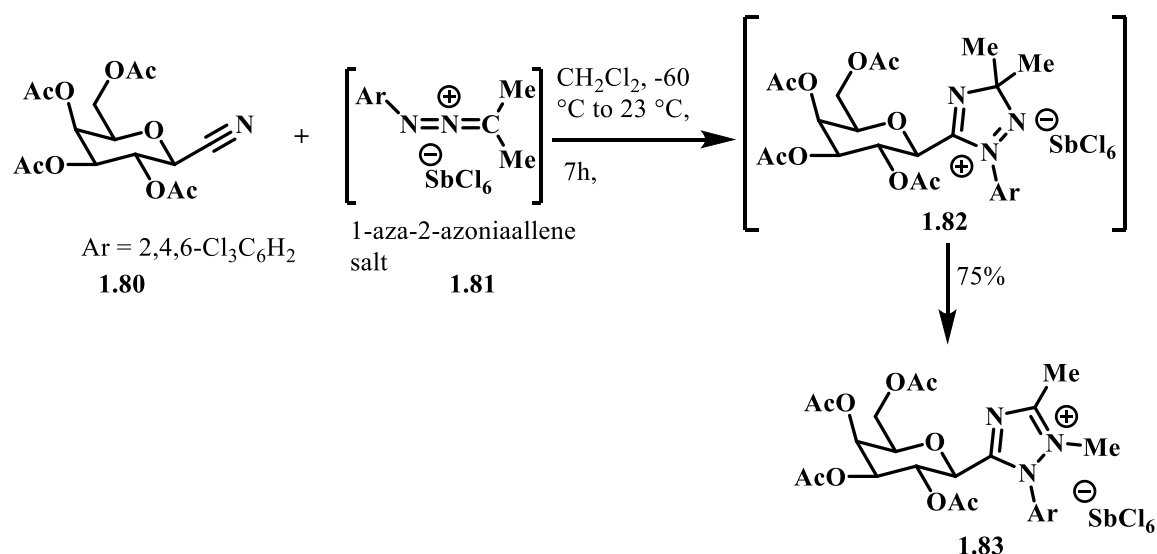
Scheme 1.14. Synthesis of cinnolinium salts via [3+2] cycloaddition.

1.4.3 Syntheses of *C*-nucleosides from 1-aza-2-azoniaallene and 1,3-diaza-2-azoniaallene salts

Nucleosides are the molecular building blocks of the nucleic acids, DNA and RNA. Jochims and coworkers applied 1,3-diaza-2-azoniaallene and 1-aza-2-azoniaallene salts in the synthesis of *C*-nucleosides.²³ The reactive salts (**1.78** and **1.81**) underwent cycloaddition reactions with the triple bonds of glycosylalkyne **1.77** and glycosyl cyanide **1.80** to afford the 4-glucosyl-1,2,3-triazolium salt **1.79** and glycosyl-1,2,4-triazole **1.83** respectively (Scheme 1.15 and 1.16).



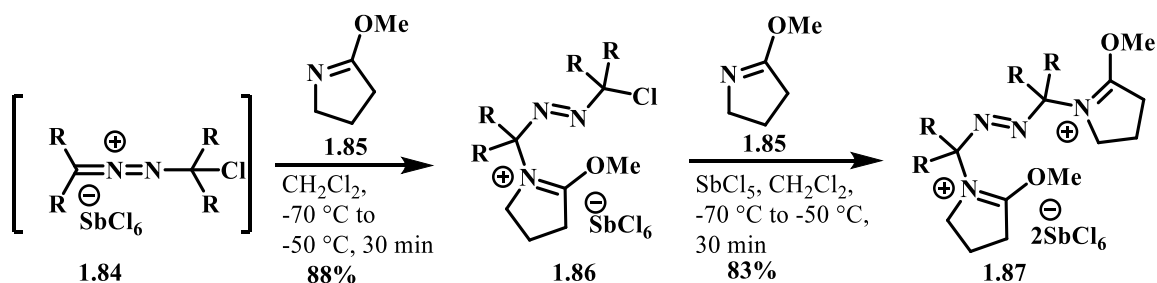
Scheme 1.15. Synthesis of 4-glucosyl-1,2,3-triazolium salt via [3+2] cycloaddition.



Scheme 1.16. Synthesis of glycosyl-1,2,4-triazole via [3+2] cycloaddition.

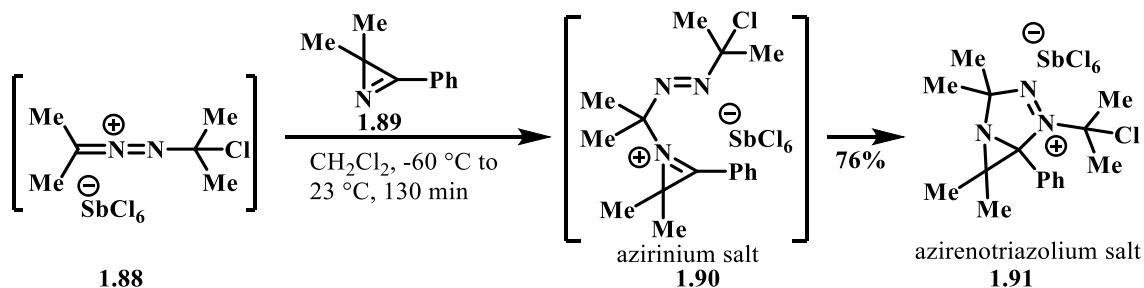
1.4.4 Reaction with azomethines and azirine to form iminium and azolium salts

Azomethines (**1.85**) undergo nucleophilic addition to the heteroallene **1.84** to give the *N*-(azoalkyl)iminium salt **1.86** in 88% yield (Scheme 1.17).²³ When two equivalents of isoamide (**1.85**) and two equivalents of SbCl_5 are used, the product **1.87** can be isolated in 83% yield.



Scheme 1.17. Formation of iminium salt via [3+2] cycloaddition.

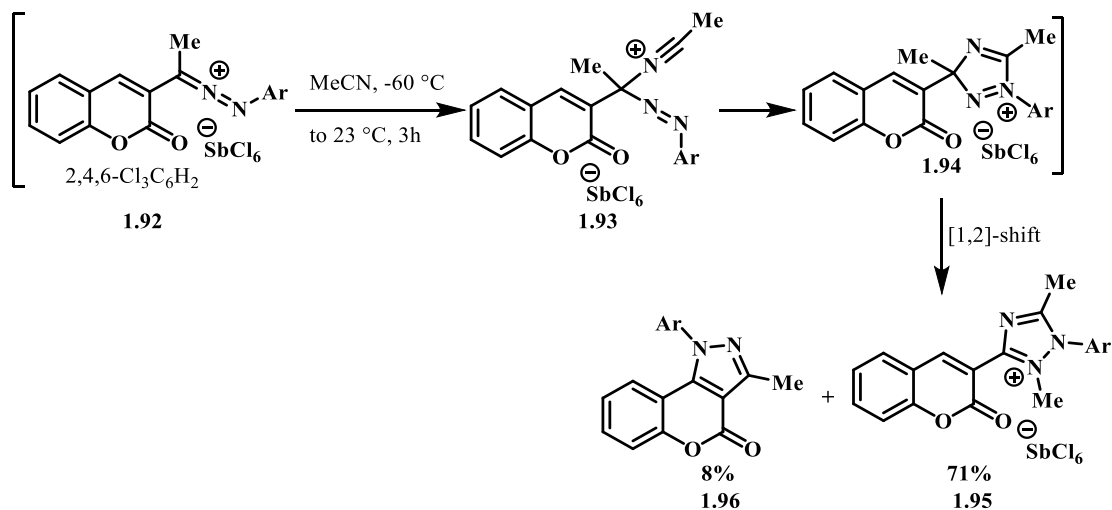
The heteroallene **1.88** undergoes cycloaddition across the $\text{C}=\text{N}$ of the azirine **1.89** to give the azirinium salt **1.90** which is electrophilic enough to close the ring by attack on an azo nitrogen atom to afford the azirenotriazolium salt **1.91** in 76% yield (Scheme 1.18).²³



Scheme 1.18. Formation of azolium salt via [3+2] cycloaddition.

1.4.5 Syntheses of coumarin derivatives

The heteroallene salt **1.92**, containing a coumarin scaffold, reacts with acetonitrile to give intermediate **1.93**, which then cyclizes to provide the 3*H*-triazolium salt **1.94** that undergoes Wagner-Meerwein type [1,2] shift of a methyl group to afford the 1*H*-triazolium salt **1.95** in 71% yield. In addition, a small amount (8% yield) of pyrazole **1.96** was isolated as by product (Scheme 1.19).²² Without acetonitrile, this reaction gives electrically neutral pyrazole **1.96** in 86% yield.

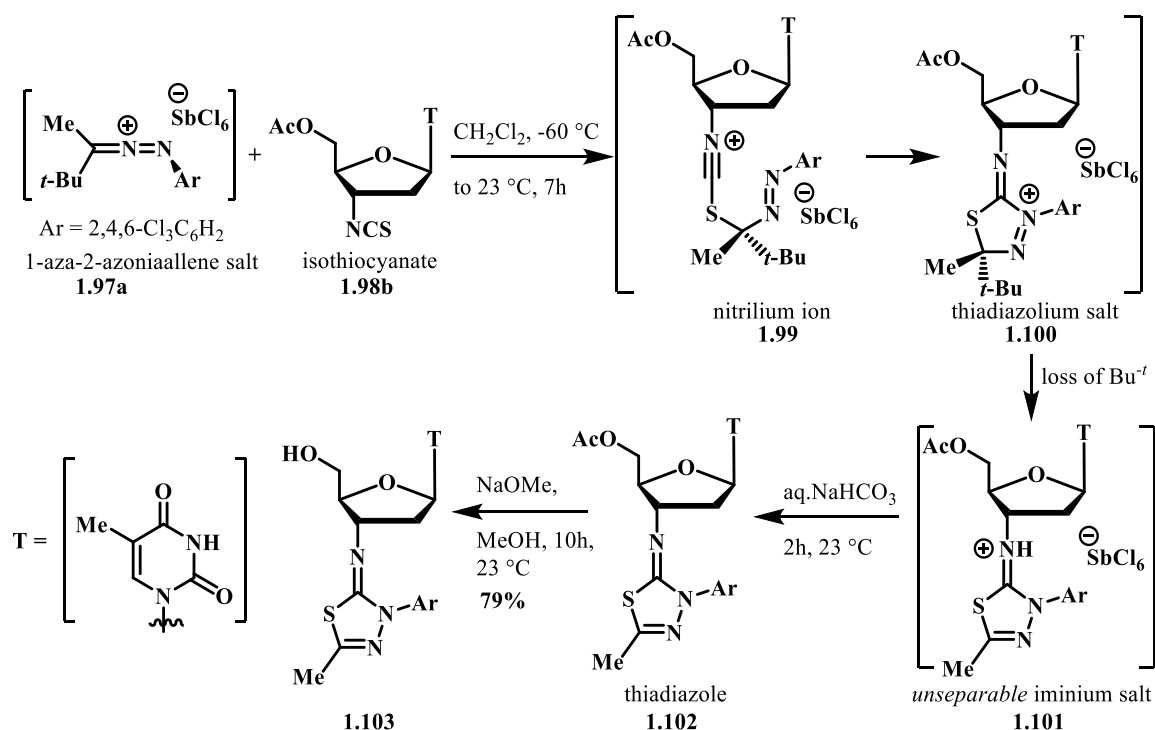


Scheme 1.19. Synthesis of coumarin derivatives from 1-aza-2-azoniallene salt.

1.4.6 Syntheses of 3'-azole derivatives

In the development of new 3'-azole derivatives²⁶ that exhibit anti-AIDS activity,^{27,28} Al-Soud and Al-Masoudi explored a new technique, in which 5'-acetyl-3'-dexo-3'-

isothiocyanatothymidine **1.98a** (Scheme 1.20) and sugar nitrile **1.98b** (Scheme 1.21) undergo cycloadditions with 1-aza-2-azoniaallene salts to afford 3'-azole derivatives. As shown in Scheme 1.20, the heteroallene **1.97a** undergoes a nucleophilic addition reaction with the isothiocyanate **1.98a** to give the nitrilium ion **1.99** as an intermediate followed by cyclization to afford the thiadiazolium salt **1.100**, which loses the *tert*-butyl group as an isobutane to give the iminium salt **1.101**. This salt is deprotonated with added sodium bicarbonate to afford the thiadiazole **1.102**, which is subsequently deacetylated by NaOMe in MeOH to give the product **1.103** in 79% yield.

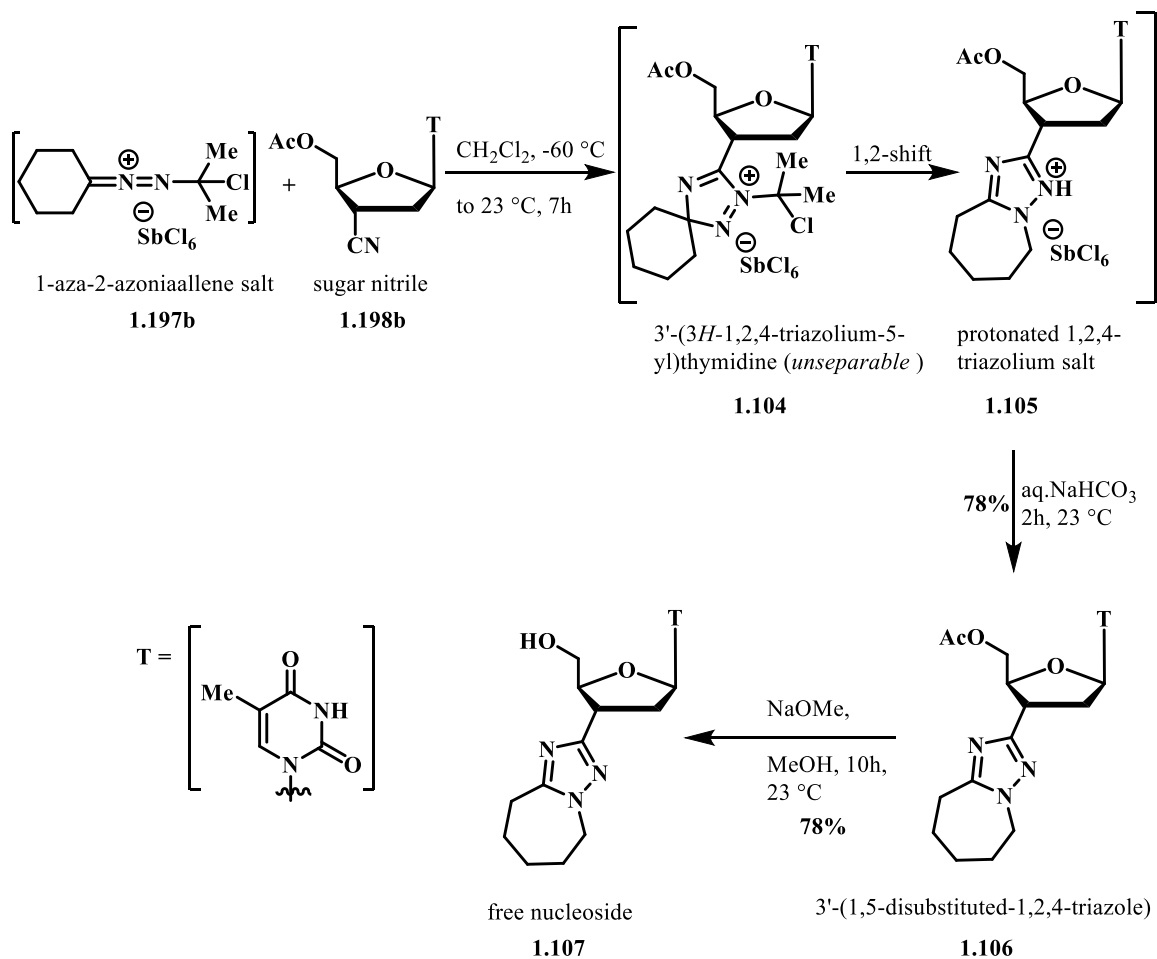


Scheme 1.20. Synthesis of thiadiazole derivative from 1-aza-2-azoniaallene salt.

As shown in Scheme 1.21, heteroallene **1.97a** undergoes cycloaddition with the sugar nitrile **1.98b** to give the unseparable 3'-(3*H*-1,2,4-triazolium5-yl)thymidine **1.104**.

Migration of an alkyl group via a 1,2-shift and elimination of the CClMe₂ group at -30 °C

afforded the protonated 1,2,4-triazolium salt **1.105**.²³ This salt was deprotonated with sodium bicarbonate to afford the 3'-(1,5-disubstituted-1,2,4-triazole **1.106** in 78% yield, which was deacylated by NaOMe in MeOH to give the free nucleoside **1.107** in 78% yield.

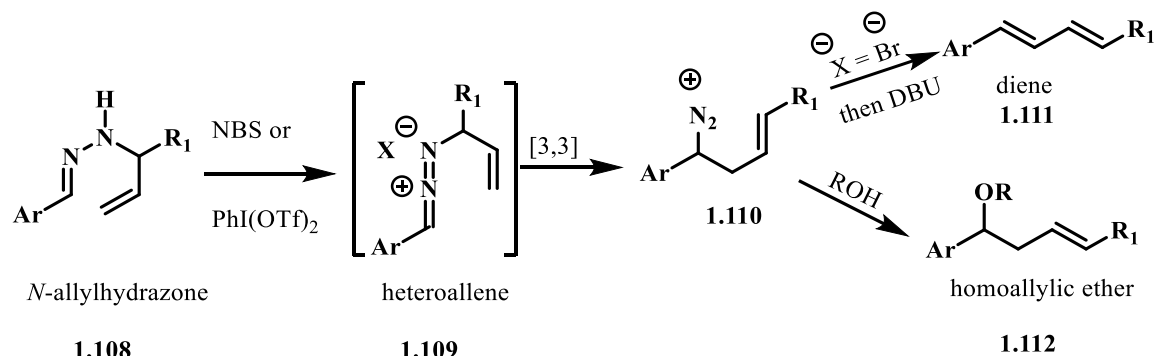


Scheme 1.21. Synthesis of triazole derivative from 1-aza-2-azoniaallene salt.

1.4.7 Synthesis of dienes and allylic ethers via [3,3] sigmatropic rearrangement of 1-aza-2-azoniaallene intermediates from *N*-allylhydrazones

Thomson and coworkers utilized 1-aza-2-azoniaallene salts (**1.109**, Scheme 1.22) to synthesize dienes (**1.111**) and homoallylic ethers (**1.112**).^{29,30} The reactive heteroallene

was generated by reacting *N*-allylhydrazones (**1.108**) with either *N*-bromosuccinimide (NBS) or a hypervalent iodine species. The heteroallene undergoes a subsequent [3,3] sigmatropic rearrangement and nucleophilic substitution or loss of proton to provide the desired products.

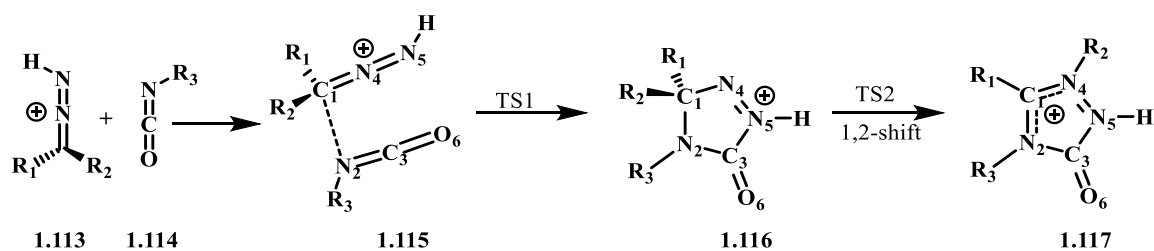


Scheme 1.22. [3,3] Sigmatropic rearrangement of 1-aza-2-azoniaallene intermediates from *N*-allylhydrazones

1.5 Theoretical studies on the mechanisms for cycloadditions between 1-aza-2-azoniaallene cations and RNCO

Although Jochims and coworkers studied the mechanism of cycloaddition reaction between 1-aza-2-azoniaallene cations and isocyanate computationally,¹⁸ a high-level calculation for this study is still very significant. The Fang group reported these studies.³¹ The Fang group used the reaction shown in Scheme 1.23 as a model. In this model reaction, when R₁, R₂, and R₃ are hydrogen atoms, the bond length of the C₁-N₂ bond in structure **1.115** is 2.734 Å at the B3LYP/6-31++G** level. When the two reactants come more closely, 4,5-dihydro-5-oxo-3*H*-1,2,4-triazolum ion (**1.116**) is obtained via transition state TS1, in which the N₂-C₁-N₄ angle becomes 140.0° from the original 167.1°, and the N₂-C₁ and N₅-C₃ distances are 2.092 and 3.371 Å respectively. Therefore, this step (the formation of product **1.116**) is an asynchronous but concerted pathway. This

differs from Jochims and coworkers' AM1 results, which favored a two-step reaction proceeding via acylium ion intermediates. Although the Fang group was able to locate the two-step-process intermediate in model reaction (a, Figure 1.7) by the AM1 method, they failed to find a similar intermediate at the B3LYP/6-31 ++ G** level. Based on the B3LYP/6-31++G** results, they concluded that the cycloaddition reaction occurs by an asynchronous but concerted pathway. During the theoretical study of the 1,2-hydrogen shift, they observed some ring distortion in product **1.117**, in which the N₂-C₁, N₄-C₁, and N₅-C₃ bond lengths are all shortened by about 0.1 Å, whereas N₅-N₄ and C₃-N₂ bond lengths are longer than their counterparts in the product **1.116** by 0.143 and 0.087 Å respectively. The bond distances of N₂-C₁ and N₄-C₁ in the product **1.117** are shorter than a normal carbon and nitrogen single bond, which shows that those bonds have some double bond characteristics. When they studied the effect of the solvent for the model of reaction, they found that cycloaddition products **1.116** and **1.117** are more stable in the solution phase than their in gas phase.



Scheme 1.23. Model reaction for theoretical study.

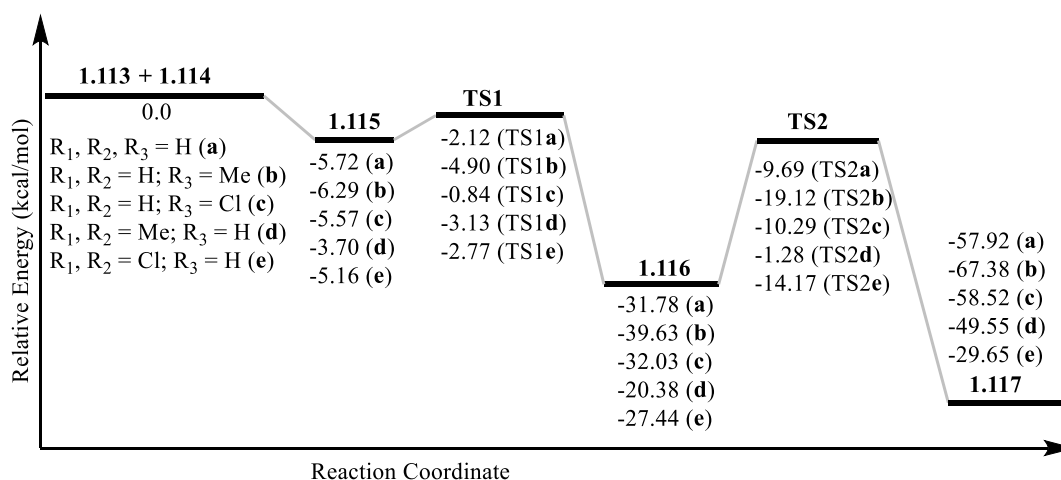


Figure 1.7. Energy profile diagram for cycloadditions between 1-aza-2-azoniaallene cations and RNCO.

The Fang group also studied the effect a variety of substituents, such as electron-withdrawing and electron-releasing groups have on the nitrogen atom of the isocyanates and on the carbon atom of the 1-aza-2-azoniaallene cation at the B3LYP/6-31++G^{**} level.³¹ When R₁, R₂ = H and R₃ = CH₃ (Figure 1.7, **b**), they observed longer bond distances for C₁-N₂ and C₃-N₅ in TS1 than the transition state of an isocyanate without a methyl group because the methyl group on the nitrogen atom has a larger steric effect. The cycloaddition product **1.116b** of this reaction is more stable than without methyl derivative by 9 kcal/mol. Therefore, the methyl substituent favors the rearrangement reaction to give the final product **1.117b**. When the methyl group is replaced by an electron-withdrawing chlorine atom (Figure 1.7, **c**), the stabilization energy of **1.115c** is lower by 0.15 kcal/mol than that of the isocyanate without a chlorine atom. The activation barrier for the cycloaddition reaction to form the product **1.116c** is thus higher. In regard to the rearrangement reaction, the activation barrier and stabilization energy to

form the product **1.117c** from the intermediated **1.116c** are very similar to that reaction, in which the isocyanate is without a chlorine atom.

When two methyl groups are present at the C₁ of the 1-aza-2-azoniaallene cation (Figure 1.7, **d**), they make the C₁-N₂ bond distance of structure **1.115d** longer than those in other complexes due to a larger steric effect. Therefore, methyl substituents on the 1-aza-2-azoniaallene cation disfavors the cycloaddition reaction. The presence of an electron-withdrawing chlorine atom at C1 of the heteroallene cation (Figure 1.7, **e**), makes the bond distance of the C₁-N₄ bond of structure **1.115e** larger than that of structure **1.115a**, and smaller than that of structure **1.115d**. The presence of chloride substituents on the heteroallene cation also lowers the activation energy for the [1,2]-shift reaction.

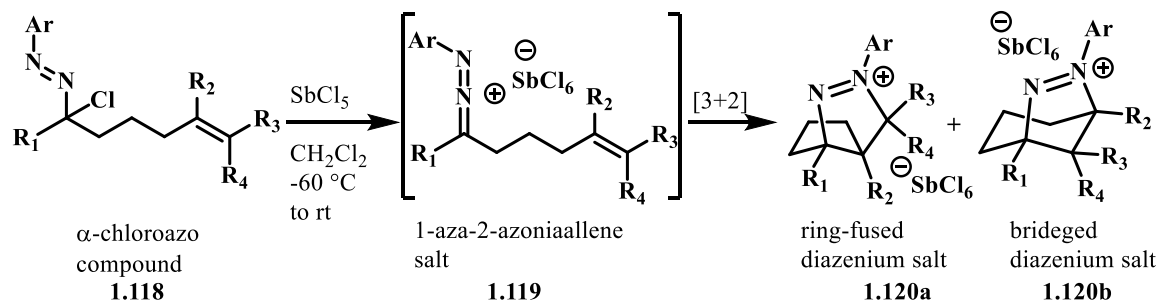
1.6 Brewer group's contributions to cycloadditions of 1-aza-2-azoniaallene salts

For the past several years, the Brewer group has studied the reactivity of 1-aza-2-azoniaallene species in intramolecular reactions. When constrained to intramolecular reactions, cationic heteroallenes can react through a variety of mechanistically distinct pathways to give different classes of nitrogen heterocycles.

1.6.1 [3+2] Cycloaddition reactions

In order to undergo various [3+2] cycloaddition reactions with a variety of π -system, heteroallenes act as 1,3-dipoles to afford the corresponding five membered-ring heterocycles. Using this concept, in 2009, the Brewer group reported that heteroallene salts (e.g. **1.119**, Scheme 1.24) obtained by the reaction of α -chloroazo compounds (e.g. **1.118**) with halophilic Lewis acids, such as aluminum trichloride and antimony pentachloride, can also react with a pendant alkene to give structurally complex bicyclic

diazenium salts **1.120a** and **1.120b** via intramolecular 1,3-dipolar [3+2] cycloaddition reactions.³² No such type of intramolecular [3+2] cycloaddition reactions had been previously reported.



Scheme 1.24. [3+2] cycloaddition to form bicyclic diazenium salts.

The reactivities of intramolecular [3+2] cycloaddition reactions depend on the length of the tether, substituents on alkene as well as on the electronics of the *N*-aryl substituent.³² The pendent alkenes of heteroallenes having electron-withdrawing or -releasing substituents give only ring-fused diazenium salts as single diastereomers, whereas alkenes without any substituents provide a mixture of ring-fused and bridged diazenium salts. In the first case, the diastereoselectivity suggests that the reaction occurs via asynchronous concerted process.³² In latter case, the ratio of the mixture of diazenium salts depends on the length of the tether between the alkene and the 1-aza-2-azoniaallene group. As shown in Figure 1.8, the Brewer group proposed the possible transition states to form the ring-fused diazenium salt **1.121a** and bridged diazenium salt **1.121b**.

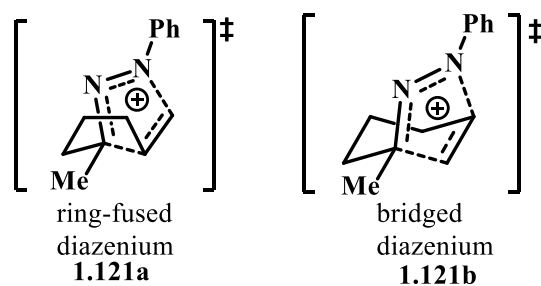


Figure 1.8. Proposed transition states to form ring-fused and bridged diazenium salts.

After a more systematic study of the intramolecular [3+2] cycloaddition, the Brewer group reported in 2010 that the partial positive charge develops on the carbon atom that forms a new C-N bond in the asynchronous cycloaddition mechanism.³³ The proposed transition state **1.121b**, in which a partial positive charge develops on a secondary carbon atom, gives the 6,5-bridged product **1.123b**, whereas the proposed transition state **1.121a**, in which a partial positive charge develops on a primary carbon atom, provides the 5,5-fused product **1.123a** (Figure 1.9). Although the energy of the ring-fused diazenium transition state is higher than that of the bridged diazenium transition state, the ring-fused transition state is entropically favored. Therefore, the fused diazenium salt is always dominant over the bridged diazenium salt.

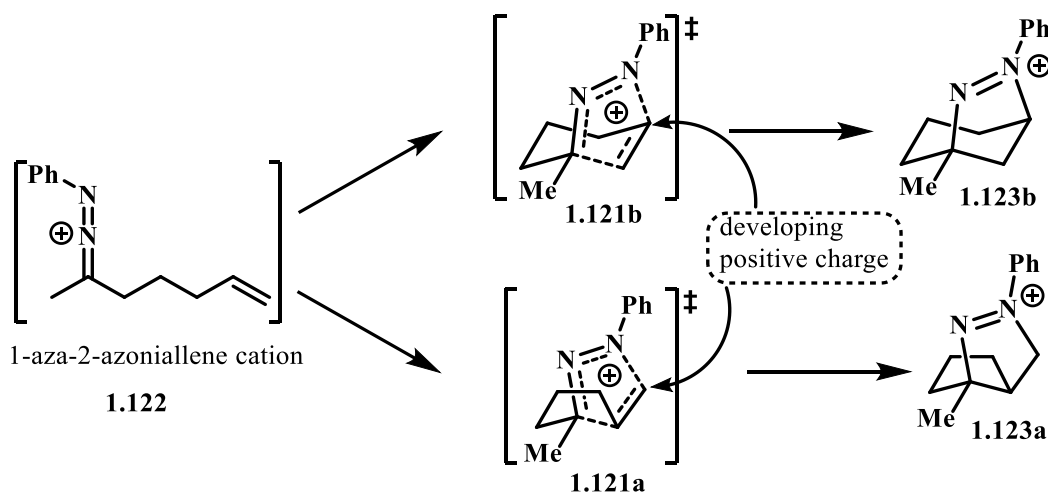
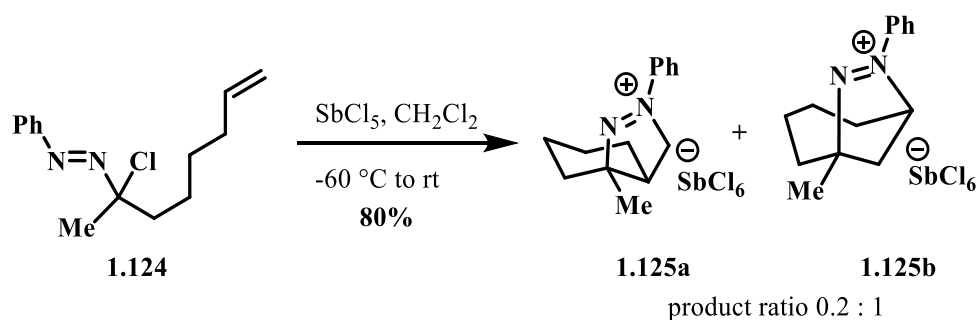


Figure 1.9. Location of partial positive charge in diazenium salts.

To describe the effect of the length of the tether on the formation of fused and bridged bicyclic diazenium salts, the Brewer group reported that the seven-membered carbocyclic ring (diazenium salt **1.125b**, Scheme 1.25) forms in preference to the six-membered bicyclic diazenium salt (**1.125a**).³³ To identify the conformation leading to the 7,5-bridged bicyclic product, the Brewer group described the reactive orbital alignments between the heteroallene and the alkene. When the reactive orbitals are in a chair-like conformation (**1.126**, Figure. 1.10), they do not effectively overlap to give a 6-membered ring. Although the orientation of the reactive orbitals in the boat structure (**1.127**) gives more effective overlap, the boat-like conformation is high in energy and thus the 6,5-fused bicyclic diazenium salt is unfavorable. Conformation **1.128** leading to the 7,5-bridged bicyclic product is favored because the longer tether length lends enough flexibility to provide a good orbital alignment. I have discussed a computational study about the effect of the tether length in the next section.



Scheme 1.25. [3+2] cycloaddition to form seven-membered ring diazenium salts.

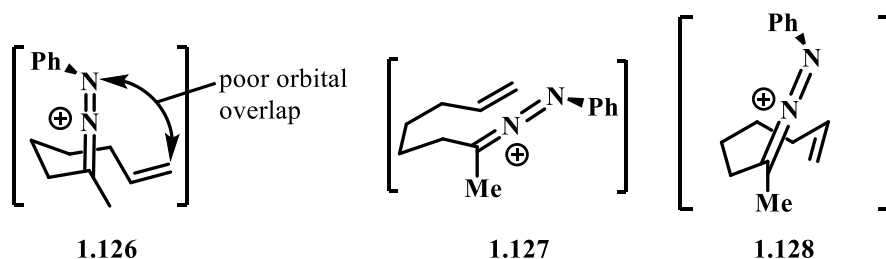
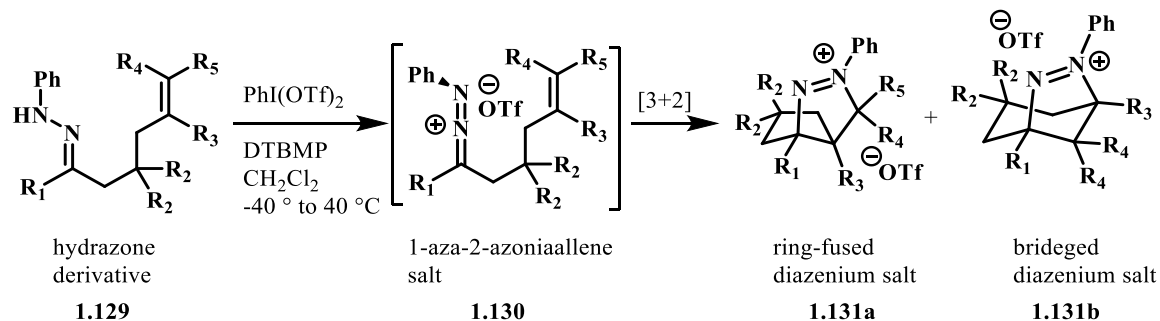


Figure 1.10. Proposed conformations leading to diazenium salts.

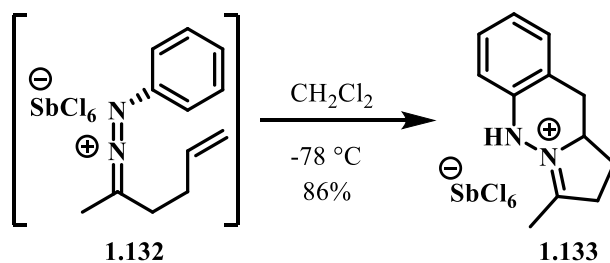
While studying the intramolecular [3+2] cycloaddition reaction of 1-aza-2-azoniaallene salts with pendent alkenes, the Brewer group discovered a new method by which hydrazones can be directly converted into the corresponding diazenium salts (e.g. **1.131a**, **1.132b**, Scheme 1.26) via oxidation with either $\text{Me}_2\text{S}(\text{OTf})_2$ or a hypervalent iodine (III) reagent $[\text{PhI}(\text{OTf})_2]$.³¹



Scheme 1.26. [3+2] Cycloaddition reaction via hypervalent iodine (III) reagent.

1.6.2 [4+2] Cycloaddition reactions

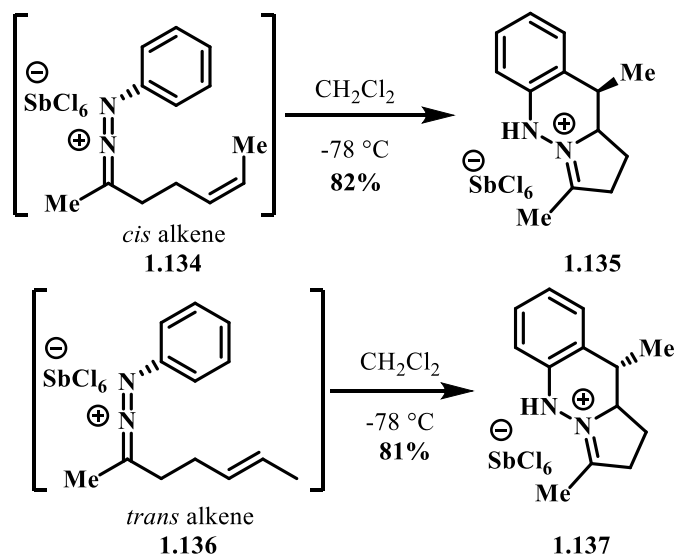
While studying the scope of the intramolecular [3+2] cycloaddition reactions, the Brewer group became interested to see how the length of the tether connecting the reacting groups affected the outcome of the reaction. Brewer found that a heteroallene salt with a shortened tether (**1.132**, Scheme 1.27) reacted by an unprecedented intramolecular [4+2] cycloaddition to provide a tricyclic protonated azomethine imine containing a 1,2,3,4-tetrahydrocinnoline scaffold (e. g. **1.133**) in high yield.³⁵



Scheme 1.27. Intramolecular [4+2] cycloaddition of 1-aza-2-azoniaallene salt.

The derivatives of tetrahydrocinnoline show diverse biological activity.³⁶ An initial exploration of the scope of this reaction has shown the reaction is quite general and gives the corresponding protonated azomethine in high yield.

To determine if this [4+2] cycloaddition occurs by a concerted or stepwise pathway, the Brewer group prepared heteroallenes **1.134** and **1.136** (Scheme 1.28) containing *cis* and *trans* alkenes respectively. The subsequent [4+2] cycloadditions provided unique diastereomers of the corresponding product (**1.135** and **1.137**). This result suggests that the cycloaddition reaction occurs via a concerted pathway.³⁵



Scheme 1.28. Comparison of [4+2] cycloaddition reaction for *cis* and *trans* alkenes.

1.6.3 Computational study on the role of tether for intramolecular [3+2] and [4+2] cycloadditions between heteroallene and pendent alkenes

In light of these surprising experimental results, the Brewer group was interested to study computationally how the length of the tether controls whether the heteroallene undergoes a [3+2] or a [4+2] cycloaddition reaction.³²⁻³⁵ The Brewer group undertook these studies in collaboration with the Houk group from UCLA.³⁵ These studies showed

that when the shortest tether ($n = 0$, in Figure 1.11) is present, it preferentially undergoes intramolecular [4+2] cycloaddition via TS **1.140**, which was already demonstrated experimentally by the Brewer group.³² When $n = 1$ (in Figure 1.11), it gives two regioisomeric [3+2] (e.g. **1.141** and **1.142**) and one [4+2] (e.g. **1.143**) transition states. However, the [4+2] cycloaddition is energetically disfavorable. Therefore, these results correspond to the experimental finding that only [3+2] cycloaddition products **1.141** and **1.142** were observed.^{32,33} When $n = 2$ (in Figure 1.11), the 1,5-substituted [3+2] cycloaddition product **1.145** is more favorable with less TS ΔG which is also consistent with the experimental observation. The latter result is very similar to the intramolecular [3+2] cycloaddition reaction.^{32,33} In conclusion, the shortest tether ($n = 0$) preferentially gives the intramolecular [4+2] cycloaddition product, whereas the longest tether ($n = 2$) gives the [3+2] product and the tether effects are very low.

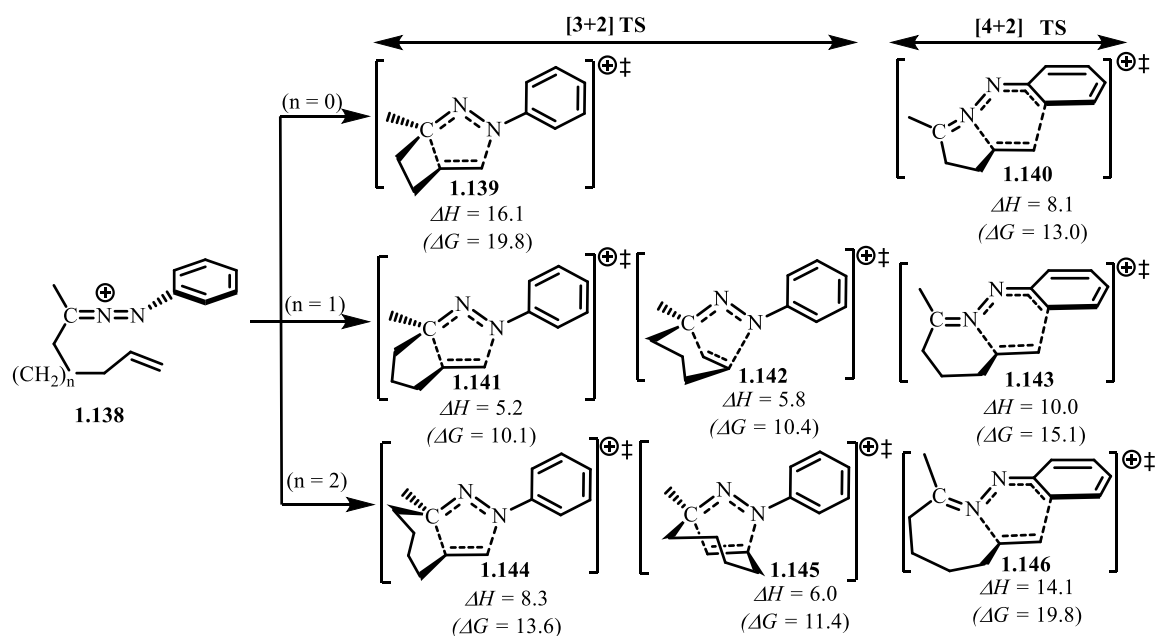


Figure 1.11. The possible transition states and DFT-computed activation enthalpies and free energies (energy in kcal/mol) for the intramolecular [3+2] and [4+2] cycloadditions.

To understand the regioselectivity of intermolecular [3+2] cycloadditions, these group also studied the intermolecular reaction between heteroallene **1.147** and propene (**1.148**) with three possible transition states that correspond to concerted pathway.³⁷ In the transition state **TS-1.149**, the methyl group of propene is proximal to the nitrogen attached to the phenyl ring, whereas in the transition state **TS-1.151**, the methyl group is distal to this nitrogen (Figure 1.11). The free energy barriers for [3+2] cycloaddition via **TS-1.149** is lower by 4.9 kcal/mol than that of cycloaddition via **TS-1.151**. Therefore, the **TS-1.149** provides the more stable five-membered ring product **1.150**. Importantly, the terminal carbon of the heteroallene **1.147** has much a larger LUMO+1 orbital coefficient than the terminal nitrogen, which makes it more electrophilic. Therefore, the terminal carbon of methyl propene (**1.148**) reacts via nucleophilic attack on the electrophilic carbon of the heteroallene **1.147** to provide the more stable product **1.150**. The transition state **TS-1.153**, obtained via [4+2] cycloaddition, has a higher activation barrier than the transition states **TS-1.149** and **TS-1.151**.

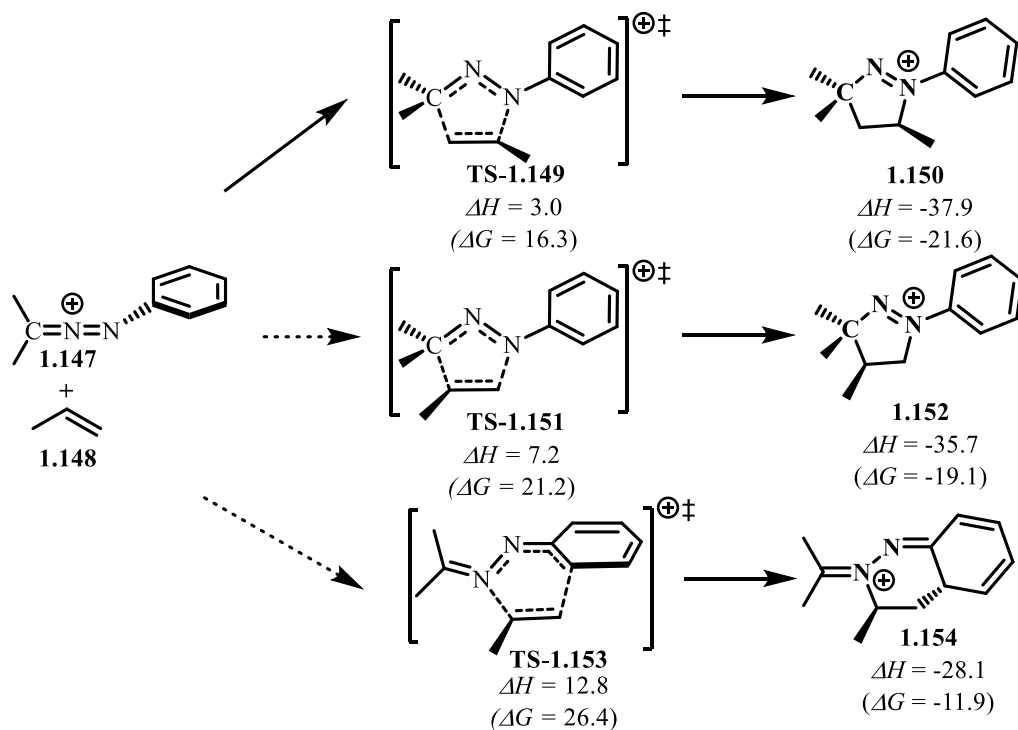


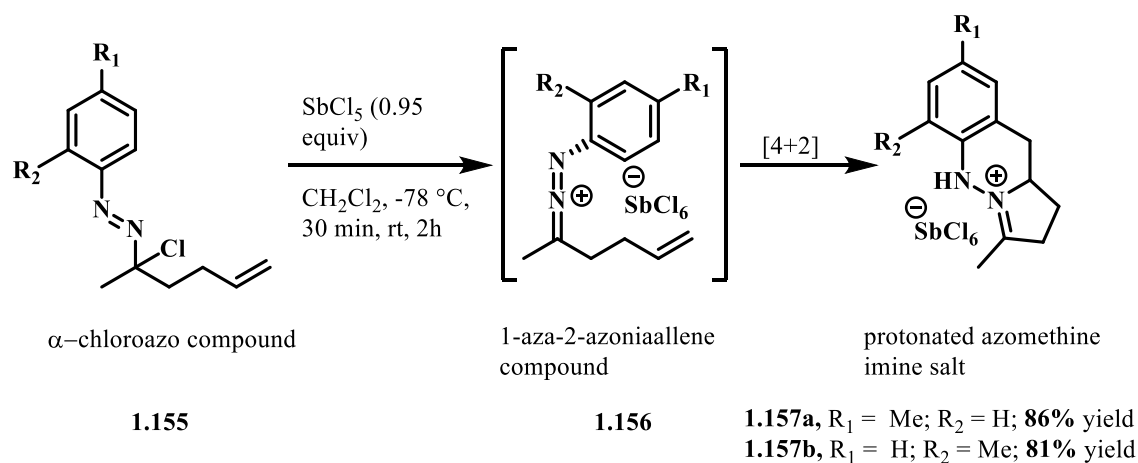
Figure 1.12. The possible transition states, products, and DFT-computed energies (in kcal/mol) for intramolecular [3+2] and [4+2] cycloadditions between heteroallene and propene.

1.7 Scope of intramolecular [4+2] cycloaddition reaction

In prior work, the Brewer group showed that the intramolecular cycloaddition reaction proceeded in high yield.³²⁻³⁵ With a better understanding of the mechanism of this [4+2] cycloaddition in hand, we were interested to determine how changes to the electronics of the *N*-aryl ring or substituent of the alkene would affect the cycloaddition process.

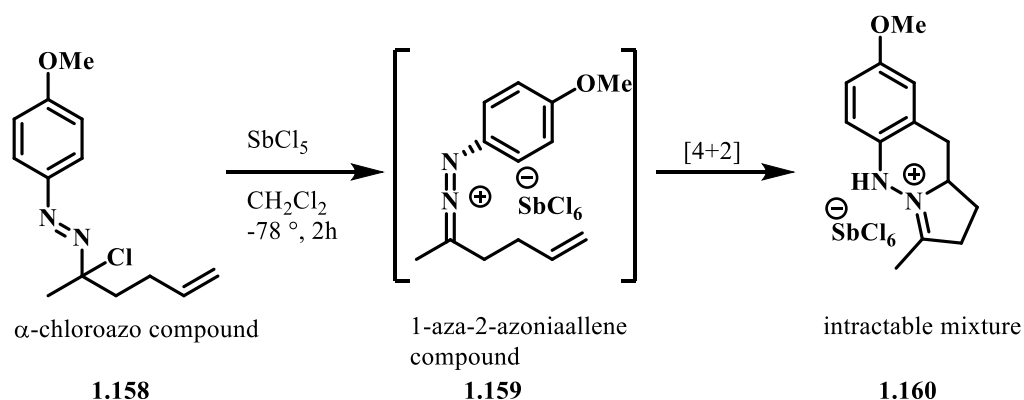
1.7.1 Scope of the SbCl₅ mediated intramolecular [4+2] cycloadditions from α -chloroazo precursors

To determine what affect substitution on the aromatic ring would have on the result of the cycloaddition process. I first prepared α -chloroazo compounds (**1.155**) from toluene hydrazone derivatives. A dichloromethane solution of α -chloroazo compounds were treated with 0.95 equiv of antimony pentachloride at -78 °C to form the protonated azomethine amine salts (**1.157**) in high yields (Scheme 1.29).



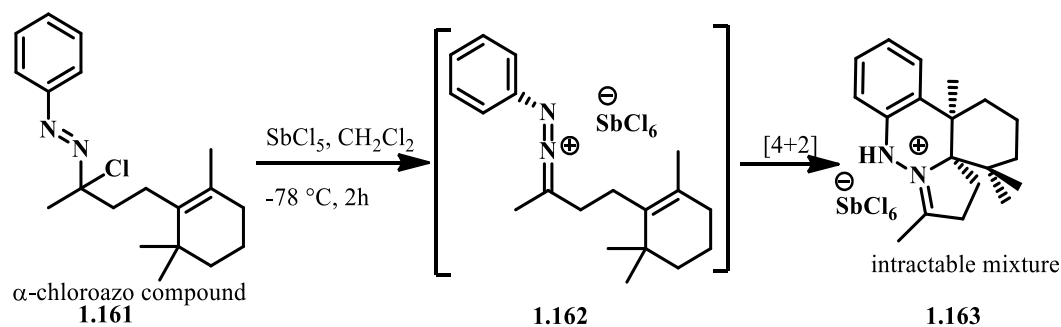
Scheme 1.29. SbCl₅ mediated intramolecular [4+2] cycloaddition reactions.

After these results, I carried out this reaction with a methoxy substituent at the *para*-position. However, this substrate failed to provide a clean cycloaddition product (Scheme 1.30) and due to the presence of SbCl₆, all my attempts to purify the desired product failed.



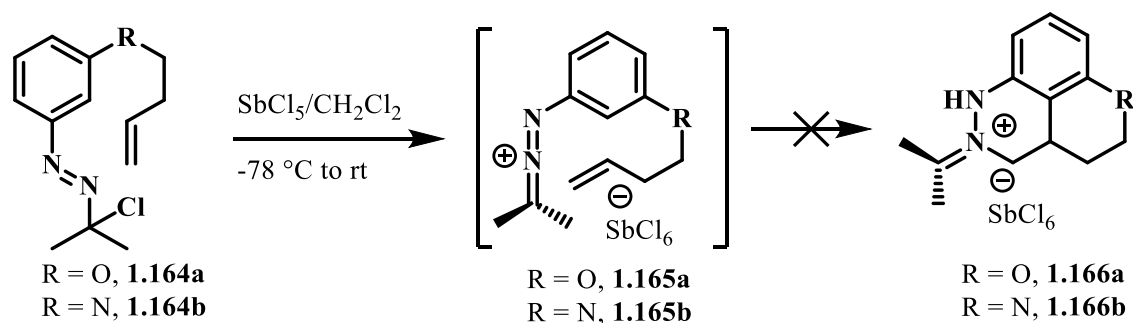
Scheme 1.30. Limitation of SbCl_5 mediated intramolecular [4+2] cycloaddition for methoxy substituent on *N*-aryl ring.

The Brewer group had previously reported that the intramolecular [4+2] cycloaddition reaction with mono-, di-, and tri-substituted alkenes proceeded in high yield.³³ So, we were interested to see if a more highly hindered tetra-substituted alkene would also be a suitable reaction partner for [4+2] cycloaddition. With this in mind, I prepared α -chloro-azo compound **1.161** (Scheme 1.31) from the phenyl hydrazone of dihydro- β -ionone. However, this substrate also did not give clean cycloaddition product under standard SbCl_5 mediated cycloaddition conditions, and all efforts to purify the desired product **1.163** failed.



Scheme 1.31. Limitation of SbCl_5 mediated intramolecular [4+2] cycloaddition of α -chloroazo compound of dihydro- β -ionone derivative.

To expand the scope of this cycloaddition, we were interested to see if a heteroallene salt with an alkene group attached via an *N*-aryl ring would react productively. So, I prepared the α -chloroazo compound **1.164a** and **1.164b** (Scheme 1.32) from the corresponding hydrazone derivatives. However, these systems failed to give any of the expected cycloaddition products. We presume that the reaction failed because of poor orbital alignment between heteroallene and alkene in the transition state of the cycloaddition step.



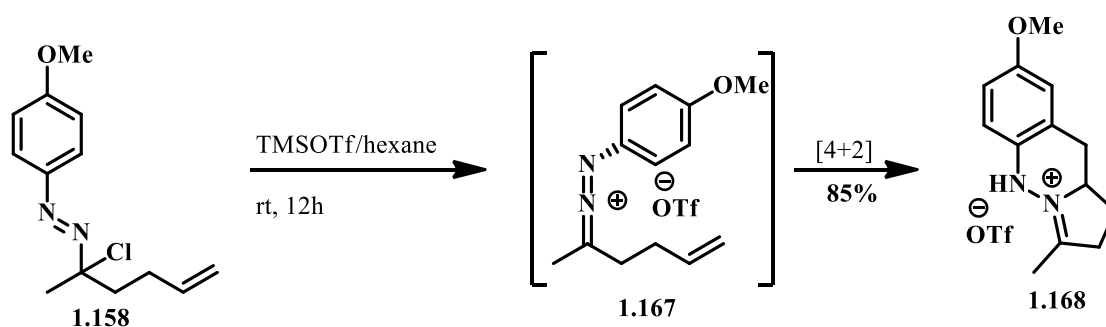
Scheme 1.32. Limitation of SbCl_5 mediated [4+2] cycloadditions of α -chloroazo compound, in which an alkene group is attached via an *N*-aryl ring.

1.7.2 Scope of the TMSOTf mediated intramolecular [4+2] cycloadditions from α -chloroazo precursors

The use of antimony pentachloride as Lewis acid was not ideal from a purification, environmental, and practical standpoint. With these limitations in mind, we sought to develop a greener, more general, and higher yielding alternative. Our initial goal was to find a Lewis acid that could give the desired cycloaddition products more cleanly and in higher yield from an α -chloroazo starting material. Dr. Tsvetkov had established that TMSOTf could be used in place of SbCl_5 to facilitate diazenium salt formation.

Therefore, I reacted a hexane solution of α -chloroazo **1.158** derived from the 4-methoxy

phenyl hydrazone of hex-5-en-2-one, with trimethylsilyltrifluoromethanesulfonate (TMSOTf) at room temperature for 12 hours. These conditions provided the desired product **1.168** in 85% yield (Scheme 1.33). Importantly, this reaction occurred very cleanly. Figure 1.13 shows the ^1H NMR peaks of the protonated azomethine imine salt **1.168**, in which the chemical shift δ 4.53 represents the characteristic ^1H NMR peak for the proton adjacent to the imine nitrogen.



Scheme 1.33. TMSOTf mediated intramolecular [4+2] cycloaddition from α -chloroazo compound containing methoxy substituent on *N*-aryl ring.

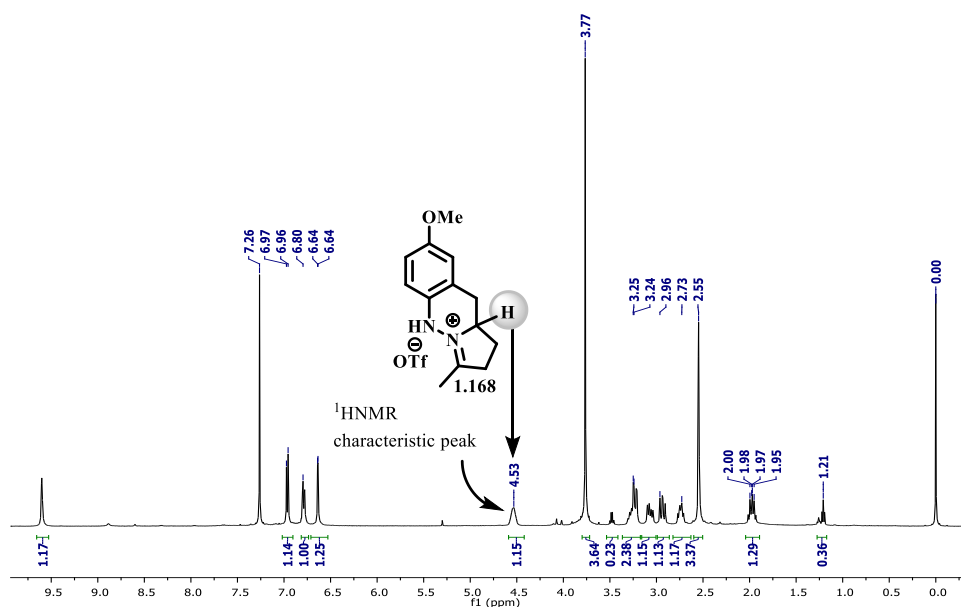
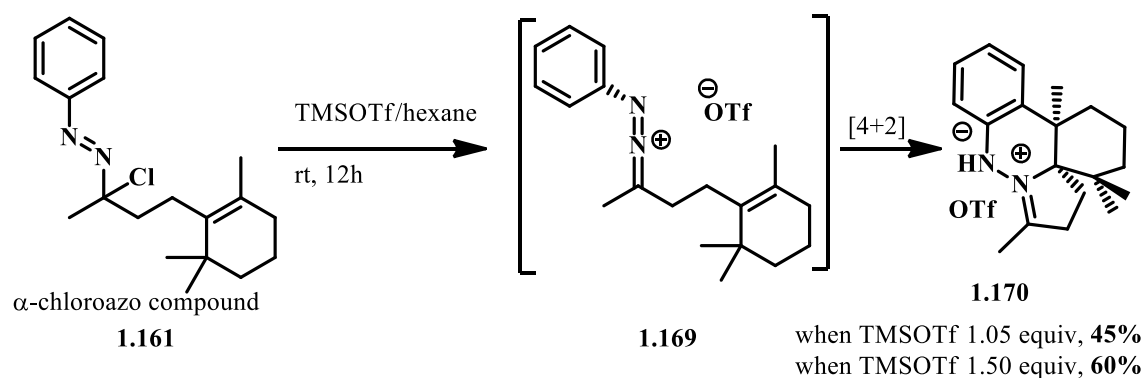


Figure 1.13. ^1H NMR spectrum showing the characteristic peak of the protonated azomethine imine salt.

With this result in hand, I treated a hexane solution of α -chloro-azo **1.161** under the same reaction conditions, which gave the desired product **1.170** in 45% yield after purification by recrystallization from methanol and diethyl ether (Scheme 1.34). When I increased the equivalents of TMSOTf from 1.05 to 1.5, the yield increased to 60%. Crystals of this salt suitable for X-ray diffraction were prepared from a mixture of methanol and diethyl ether. X-ray crystallography provided the crystal structure shown in Fig.1.12, which confirmed the structure of this sterically congested product.



Scheme 1.34. TMSOTf mediated intramolecular [4+2] cycloaddition of α -chloroazo compound of dihydro- β -ionone derivative.

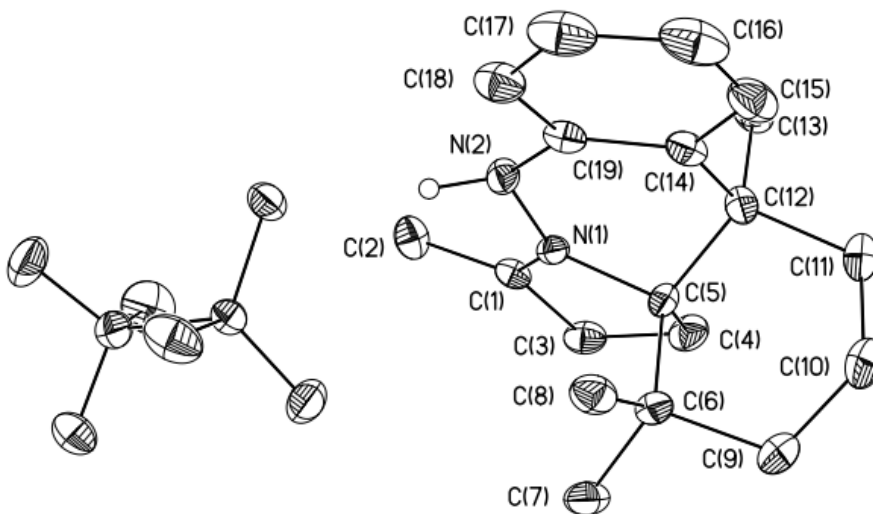
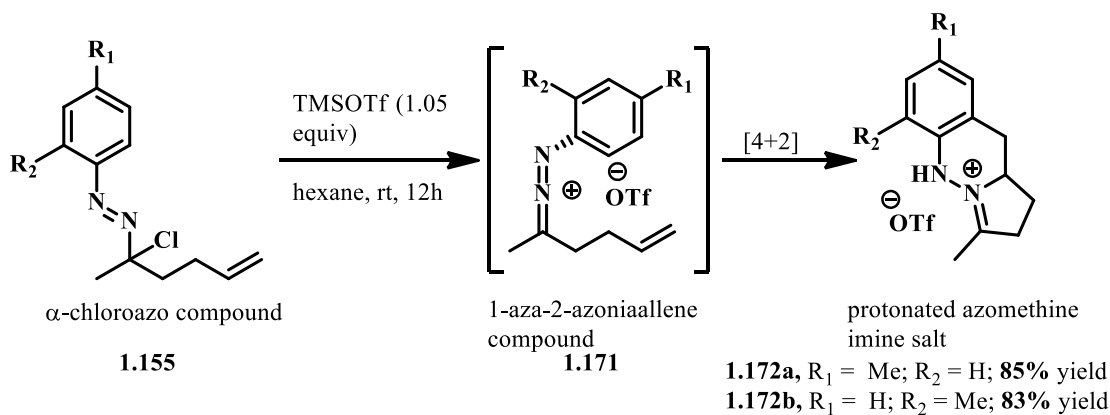


Figure 1.14. Crystal structure of protonated azomethine imine **1.170**.

When the new reaction conditions were also applied to the toluene derived hydrazones (Scheme 1.35), the yield of the desired products were almost identical to the SbCl_5 mediated reactions. However, the TMSOTf mediated reactions provided cleaner cycloaddition products than the SbCl_5 mediated reactions.

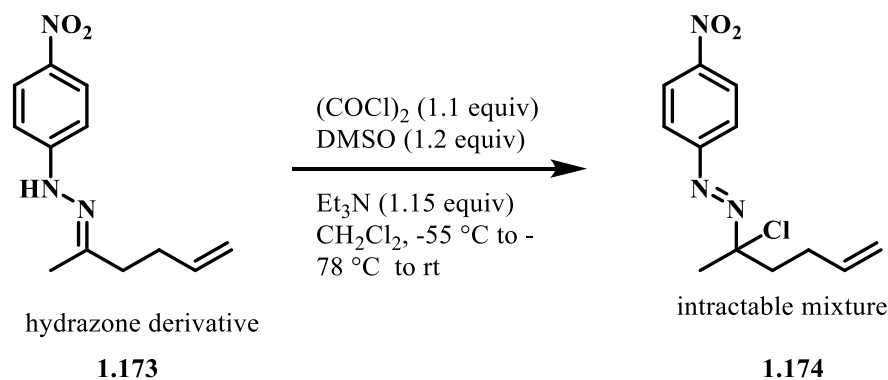


Scheme 1.35. TMSOTf mediated intramolecular [4+2] cycloaddition of α -chloroazo precursors.

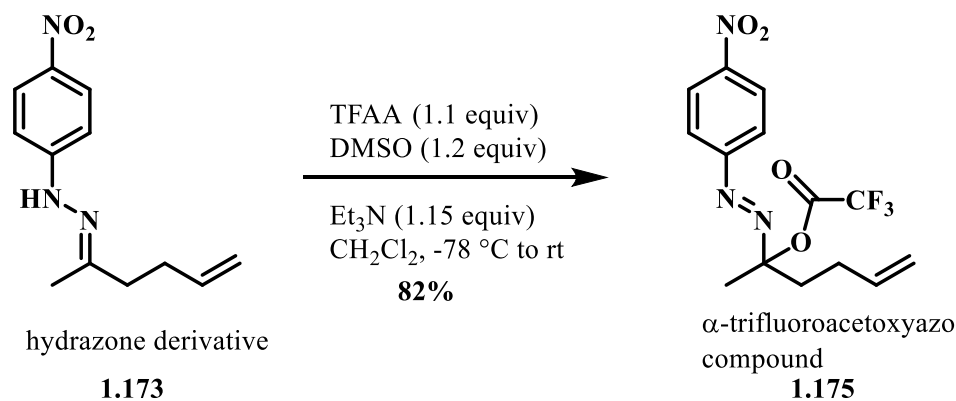
1.7.3 TMSOTf mediated intramolecular [4+2] cycloadditions from α -trifluoroacetoxyazo precursors

We were interested to see how a nitro substituted aryl group would affect the cycloadditions. However, I was not able to form the requisite α -chloroazo compound (**1.174**) under Swern conditions (Scheme 1.36a). To overcome this limitation, I sought to identify an alternate technique to form a different α -substituted azo species that could serve as a heteroallene precursor. To achieve this, I replaced the oxalyl chloride with trifluoroacetic anhydride (TFAA) in Swern reaction, which gave the corresponding α -trifluoroacetoxyazo compound **1.175** in 82% yield (Scheme 1.36b). More details about this method for the preparation of α -trifluoroacetoxyazo derivatives have been discussed

in Chapter 3. However, it is worth noting at this point that this method has proven to be quite general.



Scheme 1.36a. A method to form α -chloroazo compound from a hydrazone derivative.

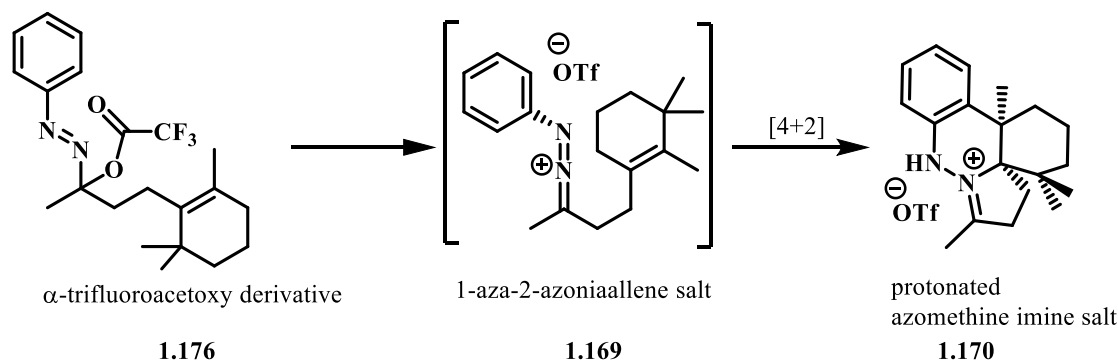


Scheme 1.36b. A new method to prepare α -substituted azo compound.

With a new and general route to prepare α -substituted azo compounds in hand, I needed to establish if these could serve as heteroallene precursors. I began these studies by reacting $\text{BF}_3 \cdot \text{Et}_2\text{O}$ with a hexane solution of α -trifluoroacetoxy **1.176** (Entry 1, Table 1.1) at room temperature for 12 hours. However, this did not give clean cycloaddition product (**1.170**). Therefore, I replaced the $\text{BF}_3 \cdot \text{Et}_2\text{O}$ with TMSOTf. Under identical reaction conditions, this latter Lewis acid gave the protonated azomethine imine salt **1.170** in 55% yield (Entry 2, Table 1.1) which is a slight improvement over the result

obtained from the corresponding α -chloroazo precursor (Scheme 1.32). When I changed the solvent to dichloromethane (Entry 3, Table 1.1), it gave comparable yield, whereas THF polymerized under the reaction conditions (Entry 4, Table 1.1) giving no desired product. When I raised the temperature to 40 °C with 1.5 equivalent of TMSOTf (Entry 5, Table 1.1), the desired product was formed in 47% yield in shorter time (45 mins). Increasing the time to 4 hours with 1.04 equivalent of TMSOTf (Entry 6, Table 1.1) gave substantially improved product yield (67%). Finally, increasing the equivalent of TMSOTf to 1.5 at 40 °C for 4 hours (Entry 7, Table 1.1) provided high product yield (72%) which became the conditions of choice to carry out the reaction scope studies.

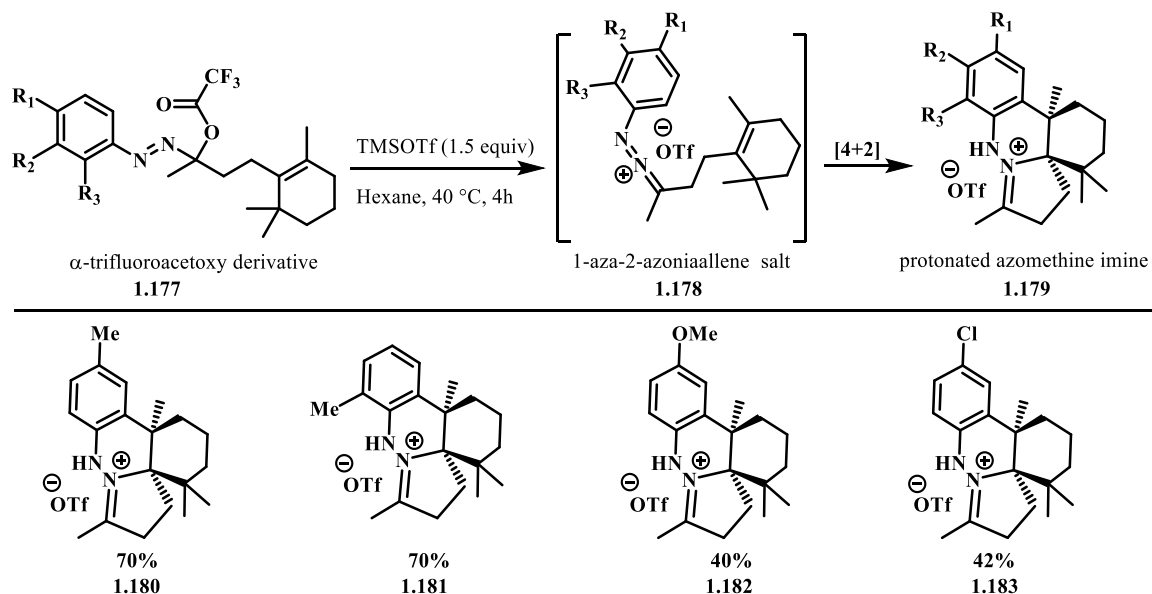
Table 1.1. Optimization of intramolecular [4+2] cycloaddition reaction using α -trifluoroacetoxy azo derivative of dihydro- β -ionone



entry	solvent	reagent (equiv)	time	temperature	yield
1	hexane	BF ₃ ·Et ₂ O (1.05)	12 hrs	rt	-
2	hexane	TMSOTf (1.05)	12 hrs	rt	55%
3	CH ₂ Cl ₂	TMSOTf (1.04)	12 hrs	rt	58%
4	THF	TMSOTf (1.05)	3 hrs	rt	-
5	hexane	TMSOTf (1.5)	45 mins	40 °C	47%
6	hexane	TMSOTf (1.04)	4 hrs	40 °C	67%
7	hexane	TMSOTf (1.5)	4 hrs	40 °C	72%

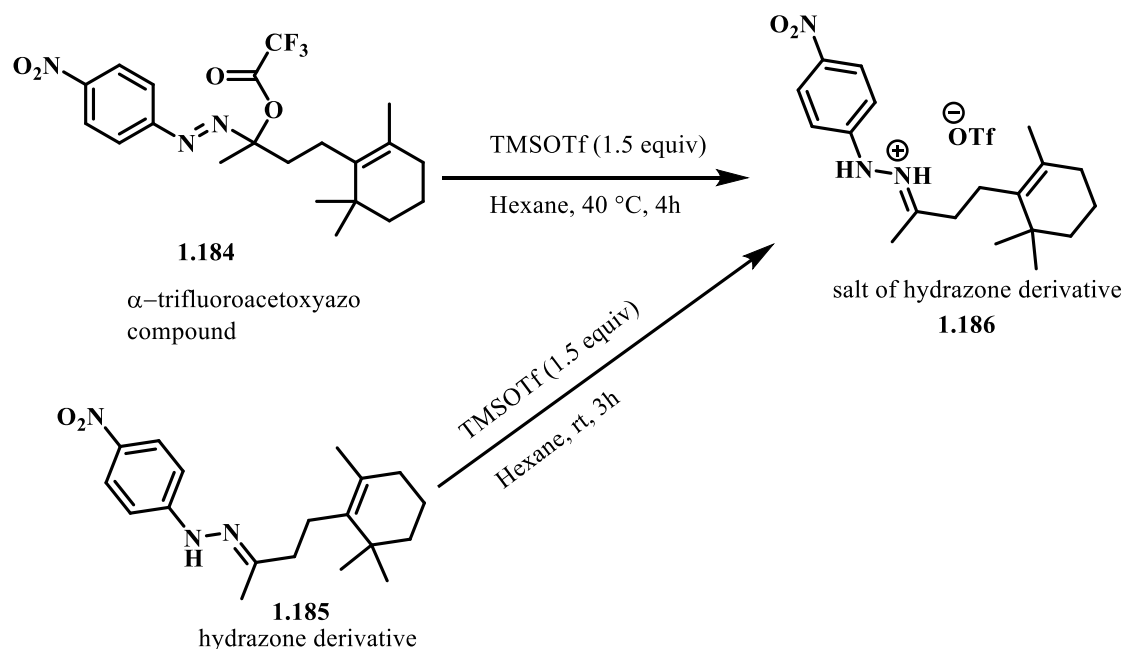
We began these scope studies by evaluating the effect of *N*-aryl substituents on the cycloaddition with a sterically hindered alkene. The methyl substituent either on *ortho*- or

para-position on the *N*-aryl group of **1.177** gave good yield, whereas the methoxy and chloride substituents at the *para*-position gave low yields (Scheme 1.37). The latter reactions were repeated several times, but the yields were consistently low each time. Interestingly, compound **1.182**, containing a methoxy substituent, gave very nice golden crystals, which were not observed for any other substituents.



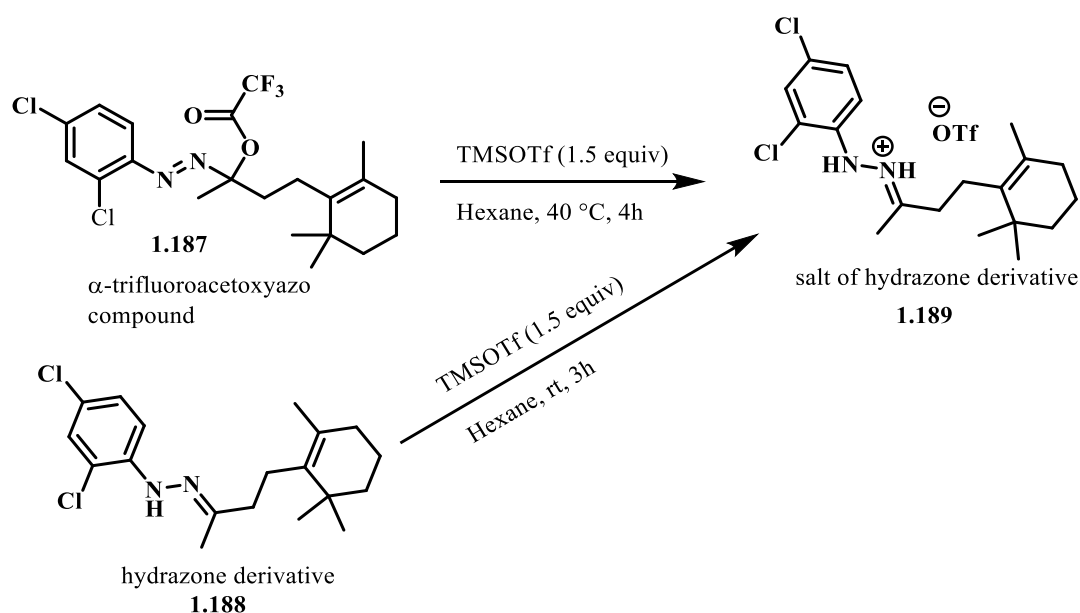
Scheme 1.37. Scope of TMSOTf mediated [4+2] cycloaddition of α -trifluoroacetoxyazo derivatives containing sterically hindered alkene.

When the nitro substituted α -trifluoroacetoxy **1.184** was treated with optimized condition, it did not give a cycloaddition product, but it gave a very small amount of the triflate salt of hydrazone **1.187** (Scheme 1.38). To confirm this product, I treated nitro-substituted hydrazone derivative **1.185** with TMSOTf at room temperature and it gave identical material. Therefore, an electron-withdrawing nitro group seems to prevent the intramolecular [4+2] cycloaddition reaction with a sterically hindered alkene.



Scheme 1.38. Formation of the salt of hydrazone derivative of nitro substituent on *N*-aryl ring from α-trifluoroacetoxyazo compound and hydrazone derivative of dihydro-β-ionone.

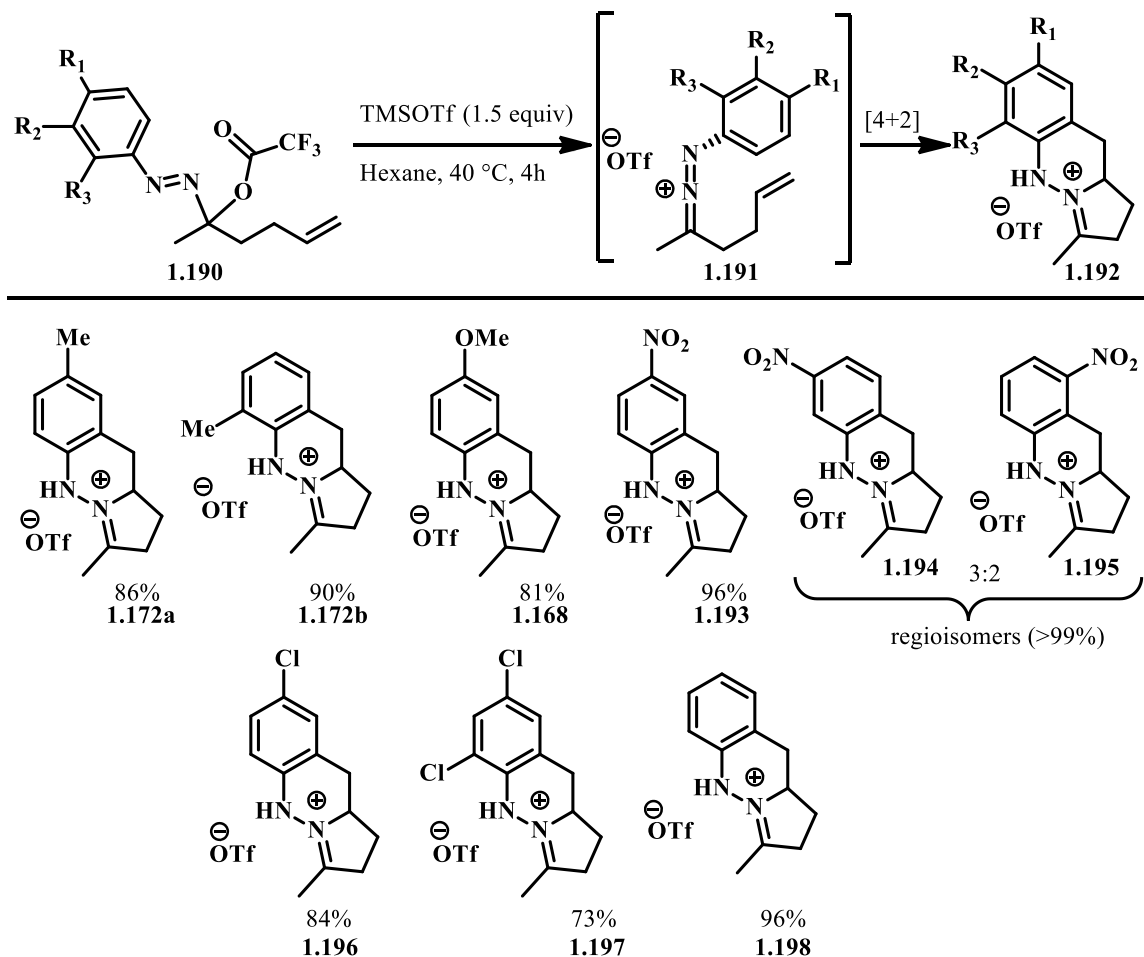
Although the chloride substitution product **1.183** (Scheme 1.37) was formed in low yield, I was still interested to try the cycloaddition reaction with a dichloro-substituted aryl ring. α-Trifluoroacetoxyazo **1.187** was treated with the optimized conditions, it also failed to undergo the cycloaddition reaction, but it gave a very small amount of the hydrazone salt (Scheme 1.39). Therefore, I have concluded that the presence of nitro or dichloride electron-withdrawing groups on the *N*-aryl ring, generally prevents the cycloaddition from occurring with sterically hindered alkenes.



Scheme 1.39. Formation of the salt of hydrazone derivative of dichloro substituents on *N*-aryl ring from α -trifluoroacetoxyazo compound and hydrazone derivative of dihydro- β -ionone.

With a better understanding of the substrate scope, we continued to study the cycloaddition reaction with simple alkenes. The toluene hydrazone gave very good yields (Scheme 1.40), as did an anisol derivative (product **1.168**; 81% yield). This latter result is better than the result obtained from the α -trifluoroacetoxyazo precursor of sterically hindered alkene. Interestingly, an electron withdrawing nitro aryl derivative underwent cycloaddition in excellent yield. (**1.193** in 96% yield). As might be expected, the *meta*-substituted nitro group gave a mixture of regioisomeric cycloaddition products in a 3:2 ratio based on ¹HNMR, but the total yield for both regioisomeric products (**1.194** and **1.195**) was quantitative. These regioisomers were separated based on the solubility. The isomer **1.194** was sparingly soluble in chloroform, whereas the isomer **1.195** was completely soluble in chloroform. Both were soluble in acetonitrile. A chloride

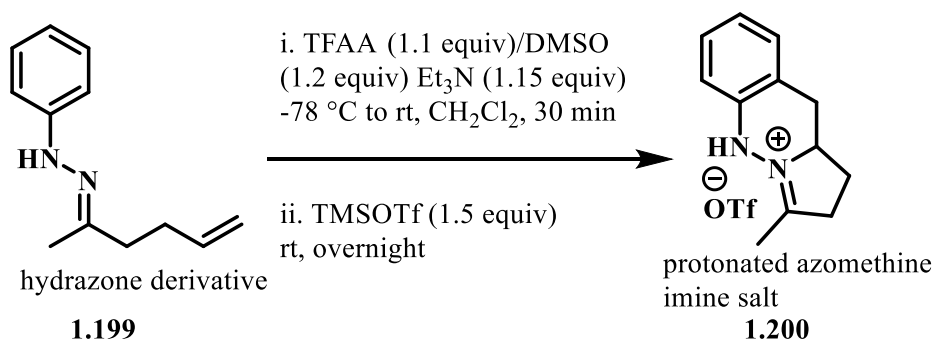
substituent at the *para*-position (**1.196**) also gave good yield, but dichloride substituents at *ortho*- and *para*-positions (**1.197**) gave comparatively lower yield than the mono-substitution. Without any substitution on the aryl group, the cycloaddition reaction occurred very smoothly under the standard condition to afford the desired product **1.198** in 96% yield.



Scheme 1.40. Scope of TMSOTf mediated [4+2] cycloaddition reaction using simple alkene.

I also attempted a one pot synthesis of protonated azomethine imine salts starting directly from hydrazone derivatives. In this case, hydrazone **1.199** (Scheme 1.41) was

treated with trifluoroacetic anhydride in the presence of DMSO and triethyl amine at -78 °C for 30 minutes to form the α -trifluoroacetoxy azo compound. After 30 minutes, without any work-up, TMSOTf was added into the reaction mixture which was then left overnight at room temperature to form the desired product **1.200**. I was only able to recover **1.200** in 19% yield. The actual yield was slightly higher, but the triethylammonium salt generated during the oxidation step, made it impossible to isolate all the product from the mixture.



Scheme 1.41. One pot reaction to form a protonated azomethine imine salt starting from a hydrazone derivative.

1.7.4 Formation of dearomatized non-protonated azomethine imine salt

The Brewer group has already reported that the intramolecular [4+2] cycloaddition reactions occur via concerted pathway, in which the *N*-aryl group is first dearomatized reaction and subsequently aromatized via 1,3-hydride shift to give the protonated azomethine imine salts.³² To further verify this mechanism, we were interested to isolate the dearomatized product. This could be achieved by starting with a substrate that has both ortho positions of the *N*-aryl ring blocked. Several attempts to prepare the desired dearomatized product from α -chloroazo compound of **1.201** failed. Therefore, I prepared α -trifluoroacetoxyazo compound **1.201** from the corresponding hydrazone derivative.

With a better understanding of the mechanism of the intramolecular [4+2] cycloaddition in hand, we used a variety of substituents on the *N*-aryl ring and a more highly hindered tetra-substituted alkene to give structurally complex protonated azomethine imine salts. The metal mediated reaction did not facilitate the cycloadditions very well, so we replaced the antimony pentachloride with TMSOTf. Although the non-metallic Lewis acid provided very clean products with α -chloroazo compounds, the novel α -trifluoroacetoxyazo compounds prepared from the corresponding hydrazone derivatives and trifluoroacetic anhydride, underwent [4+2] cycloadditions more cleanly and in higher yield with TMSOTf as the Lewis acid.

Finally, to further verify the proposed mechanism of the [4+2] cycloaddition, I was also able to synthesize a dearomatized non-protonated azomethine imine salt.

References

1. Ghose, A. K.; Viswanadhan, V. N.; Wendoloski, J. J. *J. Combi. Chem.* **1999**, *1*, 55.
2. Bur, S. K.; Padwa, A. *Chem. Rev.* **2004**, *104*, 2401.
3. Nikolov, A.; Danielsson, B. *Enzyme Microb. Technol.* **1994**, *16*, 1037.
4. Abraham, E. P. *Biochem. J.* **1956**, *62*, 651.
5. Szychowski, J.; Truchon, J-F.; Bennani, Y. L. *J. Med. Chem.* **2014**, *57*, 9292.
6. Moor, M. W. *J. Org. Chem.* **1972**, *37*, 386.
7. Wang, Q. R.; Jochims, J. C.; Kohlbrandt, S.; Dahlenburg, L.; Altalib, M.; Hamed, A.; Ismail, A. E. H. *Synthesis* **1992**, 710.
8. Wang, Q. R.; Amer, A.; Mohr, S.; Ertel, E.; Jochims, J. C. *Tetrahedron* **1993**, *49*, 9973.
9. Wang, Q. R.; Amer, A.; Troll, C.; Fischer, H.; Jochims, J. C. *Chem. Ber.* **1993**, *126*, 2519.
10. Gunic, E.; Tabakovic, I. *J. Org. Chem.* **1988**, *53*, 5081.

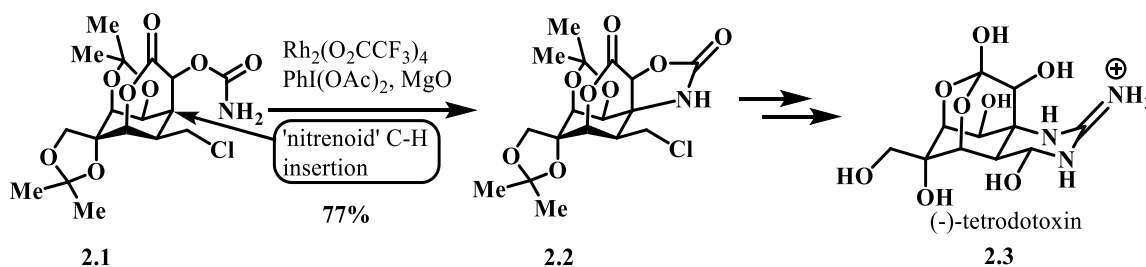
11. Huisgen, R.; Koch, H.-J, *Justus Liebigs Ann. Chem.* **1955**, 591, 200.
12. Okimoto, M.; Chiba, T. *J. Org. Chem.* **1990**, 55, 1070.
13. Hammerich, O.; Paker, V. D. *J. Chem. Soc., Perkin Trans. I* **1997**, 2, 1781.
14. Butler, R. N. *Chem. Rev.* **1984**, 84, 249.
15. Warkentin, J. *Synthesis* **1970**, 279.
16. Hegarty, A. F.; Kearney J. A. *J. Org. Chem.* **1975**, 40, 3529.
17. Guo, Y. P.; Wang, Q., R.; Jochims, J. C. *Synth.* **1996**, 274.
18. Wang, Q.; Mohr, S.; Jochims, J. C. *Chem. Ber.* **1994**, 127, 947.
19. Wang, Q.; Al-Talib, M.; Jochims, J. C. *Chem. Ber.* **1994**, 127, 541.
20. Wang, J-m.; Li, Z-m.; Wang, Q-R.; Tao, F-g. *J. Mol. Model* **2013**, 19, 83.
21. El-Gazzar, A-R. B. A.; Scholten, K.; Guo, Y.; Weibenbach, K.; Hitzler, M.; Roth, G.; Fischer, H.; Jochims, J. C. *J. Chem. Soc., Perkin Trans. I* **1999**, 1999.
22. Hassan, N. A.; Mohamed, T. K.; Abdel Hafez, O. M.; Lutz, M.; Karl, C. C.; Wirschun, W.; Al-Soud, Y. A.; Jochims, J. *J. Prakt. Chem.* **1998**, 340, 151.
23. Al-Masoudi, N.; Hassan, N. A.; Al-Soud, Y. A.; Schmidt, P.; Gaafar, A. E-D. M.; Weng, M.; Marino, S.; Schoch, A.; Amer, A.; Jochims, J. *J. Chem. Soc., Perkin Trans. I* **1998**, 947.
24. Al-Soud, Y. A.; Wirschun, W.; Hassan, N. A.; Maier, G. M.; Jochims, J. C. *Synthesis* **1998**, 721
25. Al-Soud, Y. A.; Shrestha-Dawadi, P. B.; Winkler, M.; Wirschun, W.; Jochims, J. C. *J. Chem. Soc., Perkin Trans.* **1998**, 1, 3759.
26. Al-Soud, Y. A.; Al-Masoudi, N. A. *Heteroatom Chemistry* **2003**, 14, 298.
27. Mitsuya, H.; Yarchoan, R.; Broder, S. *Science* **1990**, 249, 1553.
28. Fleet, G. W.; Son, J. C.; Derome, A. E. *Tetrahedron* **1988**, 44, 625.
29. Mundal, D. A.; Lutz, K. E.; Thomson, R. J. *Org. Lett.* **2008**, 11, 465.
30. Lutz, K. E.; Thomson, R. J. *Angew. Chem. Int. Ed.* **2011**, 50, 4437.
31. Wei, M-J.; Fang, D-C.; Liu, R-Z. *Eur. J. Org. Chem.* **2004**, 4070.

- 32. Javed, M. I.; Wyman, J. M.; Brewer, M. *Org. Lett.* **2009**, *11*, 2189.
- 33. Wyman, J.; Javed, M. I.; Al-Bataineh, N.; Brewer, M. *J. Org. Chem.* **2010**, *75*, 8078.
- 34. Al-Bataineh, N. Q.; Brewer, M. *Tetrahedron Lett.* **2012**, *53*, 5411.
- 35. Bercovici, D. A.; Ogilvie, J. M.; Tsvetkov, N.; Brewer, M. *Angew. Chem. Int. Ed.* **2013**, *52*, 13338.
- 36. Lewgowd, W.; Stanczak, A. *Arch. Pharm.* **2007**, *340*, 65.
- 37. Hong, X.; Liang, Y.; Brewer, M.; Houk, K. N. *Org. Lett.* **2014**, *16*, 4260.

CHAPTER 2: INTRAMOLECULAR C-H AND ALKENE AMINATION OF 1-AZA-2-AZONIAALLENE SALTS

2.1 Introduction

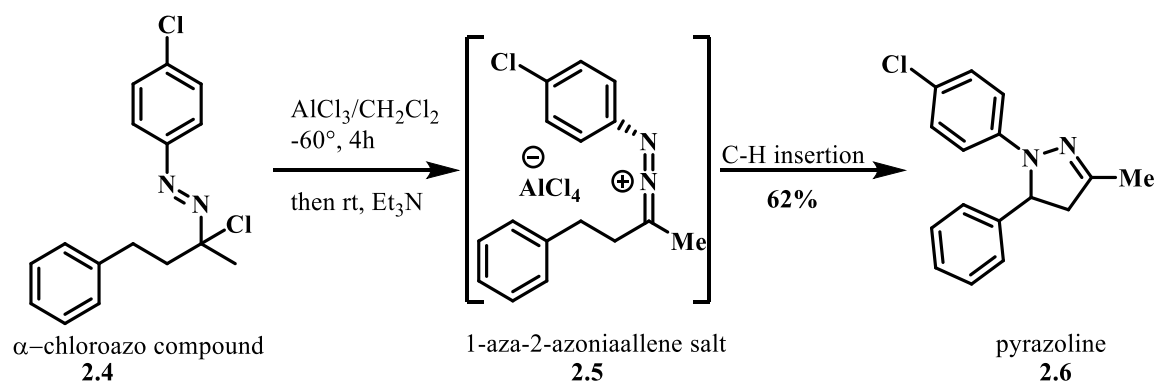
Selective and direct functionalization of unactivated carbon-hydrogen bonds is a powerful tool in synthetic organic chemistry. This approach has a broader potential in the synthesis of complex molecules compared to the traditional approaches of conducting transformation on pre-existing functional groups because C–H bonds are ubiquitous in organic substances.¹⁻¹⁰ In recent years, metal nitrenoid complexes have been extensively used for C-H functionalization, which is referred to as C-H amination. Highlighting the power of C-H amination, DuBois and colleagues have reported a number of syntheses of complex natural products, such as manzacidin,¹² (+)-saxitoxin,¹³ and (-)-tetrodotoxin¹⁴ (2.3, Scheme 2.1) via C-H amination.



Scheme 2.1. Synthesis of (-)-tetrodotoxin (2.3) via nitrenoid C-H insertion reaction.

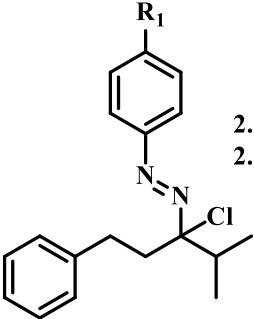
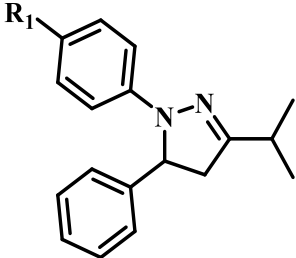
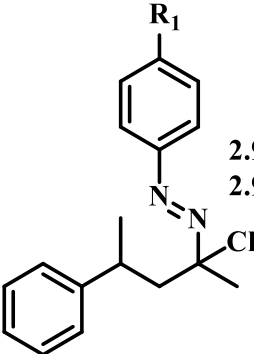
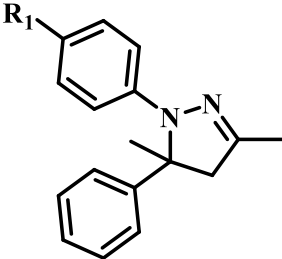
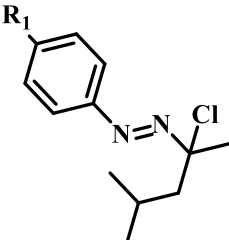
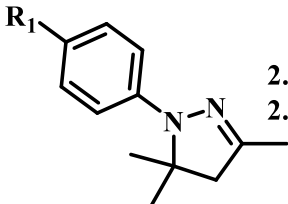
2.2 Intramolecular C-H amination of 1-aza-2-azoniaallene salts

The Brewer group discovered that 1-aza-2-azoniaallene salts (e.g. 2.5, Scheme 2.2) without a pendent alkene, undergo unprecedented C-H amination at benzylic and tertiary aliphatic centers to afford pyrazoline products (e. g. 2.6) without the formation of a metal nitrenoid intermediate.¹⁴

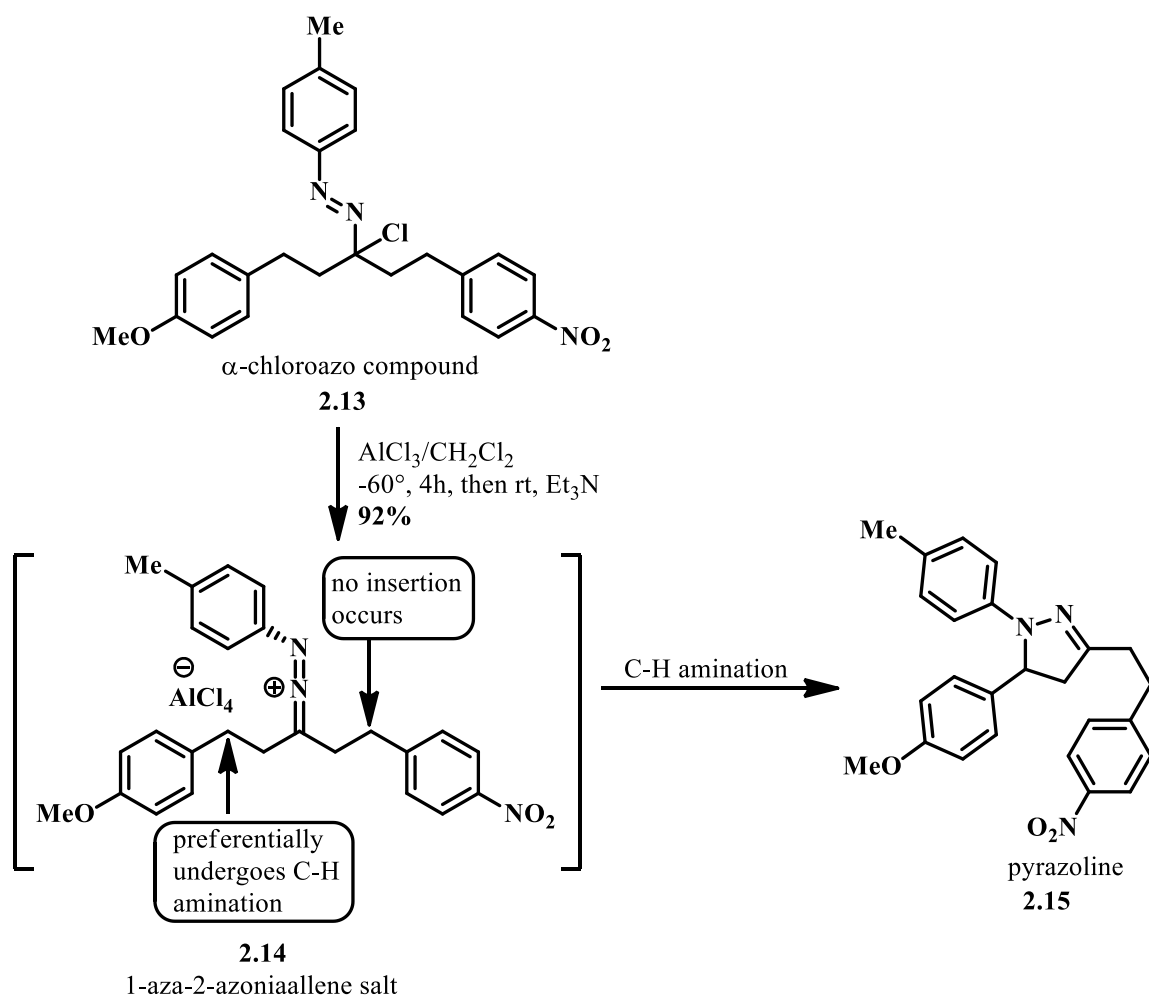


Scheme 2.2. Intramolecular C-H insertion reaction to prepare pyrazoline.

Table 2.1. Examples of substrate scope for C-H amination with above conditions

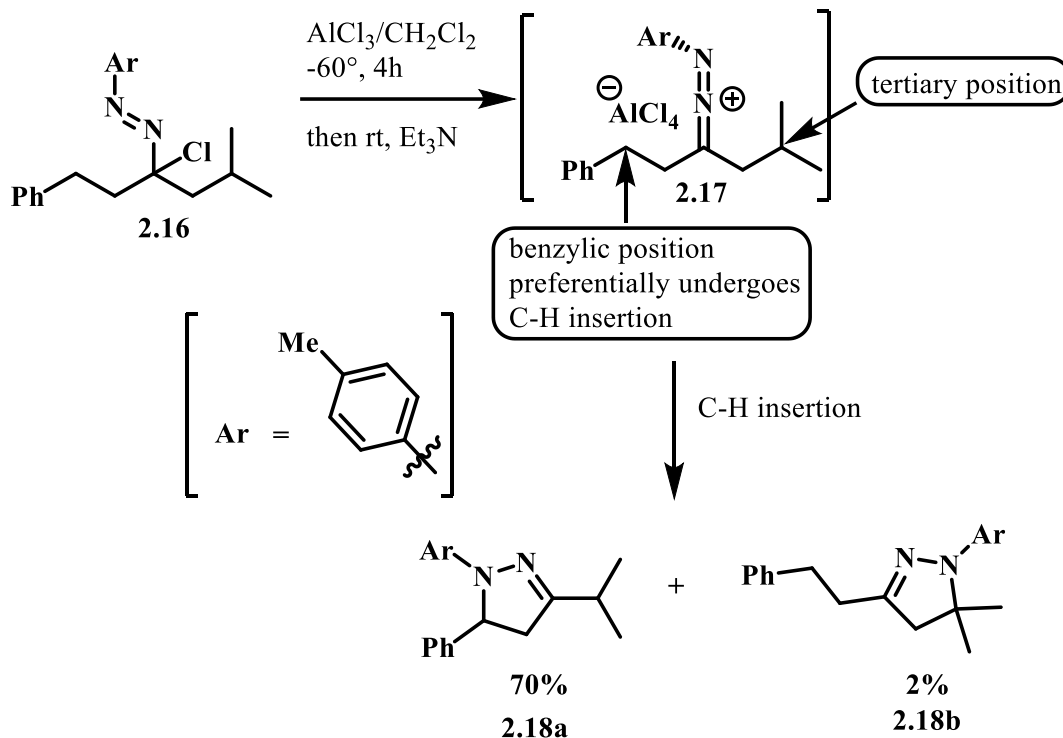
entry	α -chloroazo	product	yield
1	 <p>2.7a 2.7b</p>	 <p>2.8a; R₁ = Cl 64% 2.8b; R₁ = Me 79%</p>	
2	 <p>2.9a 2.9b</p>	 <p>2.10a; R₁ = Cl ~6% 2.10b; R₁ = Me 66%</p>	
3	 <p>2.11a 2.11b</p>	 <p>2.12a; R₁ = Cl 59% 2.12b; R₁ = Me 62%</p>	

To understand how this reactivity is affected by electronic environment of the benzylic position, the Brewer group carried out a competition experiment in which the reactive heteroallene intermediate **2.14** has equal chance to react at a benzylic position of 4-methoxybenzene or 4-nitrobenzene.¹⁴ The experimental result showed that the benzylic position of 4-methoxybenzene reacted exclusively, giving the pyrazoline product **2.15** in 92% yield (Scheme 2.3). This was interpreted to indicate that the electron donating methoxy group stabilizes a benzylic cation that is generated during the reaction, which allows this C-N bond to form more quickly.



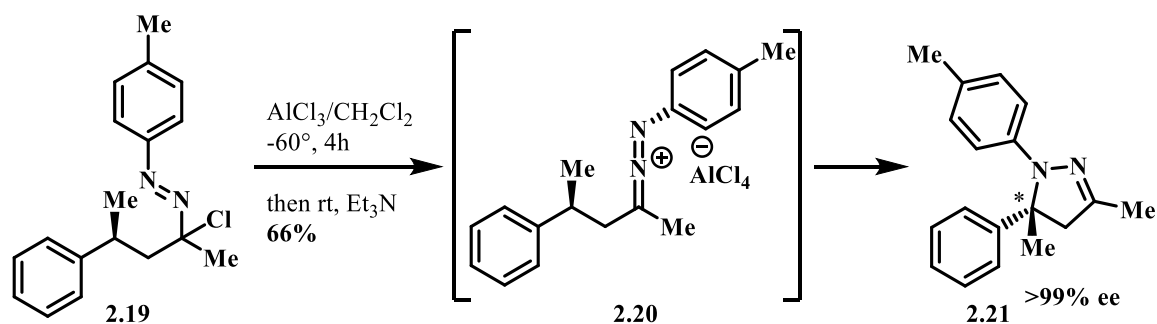
Scheme 2.3. Competition experiment at benzylic positions.

To compare the reactivity between benzylic and tertiary positions, the Brewer group performed another competition reaction, in which the reactive heteroallene **2.17** derived from the α -chloroazo compound **2.16**, has equal chance to undergo C-H insertion at a benzylic or a tertiary position. In this case, the insertion reaction occurred preferentially at the benzylic position (Scheme 2.4).¹⁵



Scheme 2.4. Competition experiment between benzylic and tertiary positions.

To study the stereochemistry, the Brewer group performed the insertion shown in Scheme 2.5 at a tertiary benzylic position. This reaction occurred without loss of enantiomeric excess.¹⁴ Although this result supports the notion that the amination reaction occurs via a concerted process, later computational studies did not support that assertion. I have discussed the theoretical study for this mechanism in the next section.



Scheme 2.5. To study stereochemistry for C-H insertion reaction.

2.3 Theoretical study of intramolecular C-H amination of 1-aza-2-azoniaallene salt

We in collaboration with the Houk group (UCLA) reported computational results that describe the mechanism of intramolecular C-H insertion reactions of 1-aza-2-azoniaallene salts.¹⁴ First, the structures of transition states and the free energy changes of single and triplet C-H amination pathways of aryl-1-aza-2-azoniaallene were calculated.

In the singlet pathway (Figure 2.1), the heteroallene cation **2.22** gives the singlet transition state **2.23** in which the HOMO of the benzylic C-H bond interacts with the LUMO of the 1,3-monopolar heterocumulene fragment. This interaction suggests that a hydride migration occurs initially to form the N-H bond and a benzyl carbocation. Finally, the benzyl carbocation forms a C-N bond with the lone pair of electrons on nitrogen to provide the amination product. In the case of a triplet pathway (Figure 2.1), the triplet diradical heterocumulene species **2.25** could be generated from spin transition of the heteroallene cation **2.22**. This species could then undergo C-H amination via a radical pathway to give diradical species **2.27**. However, the triplet state aryl-1-aza-2-azoniaallene **2.25** is less stable than the singlet **2.22** by 23.9 kcal/mol. Therefore, the singlet C-H amination pathway is more favorable than the triplet C-H pathway. It is also worth noting that literature data,^{16,17,18} indicates that C-H insertion of singlet nitrenes

proceeds with retention of configuration while triplet nitrenes react via H-abstraction/radical recombination resulting in stereochemical erosion, which again support a singlet pathway.

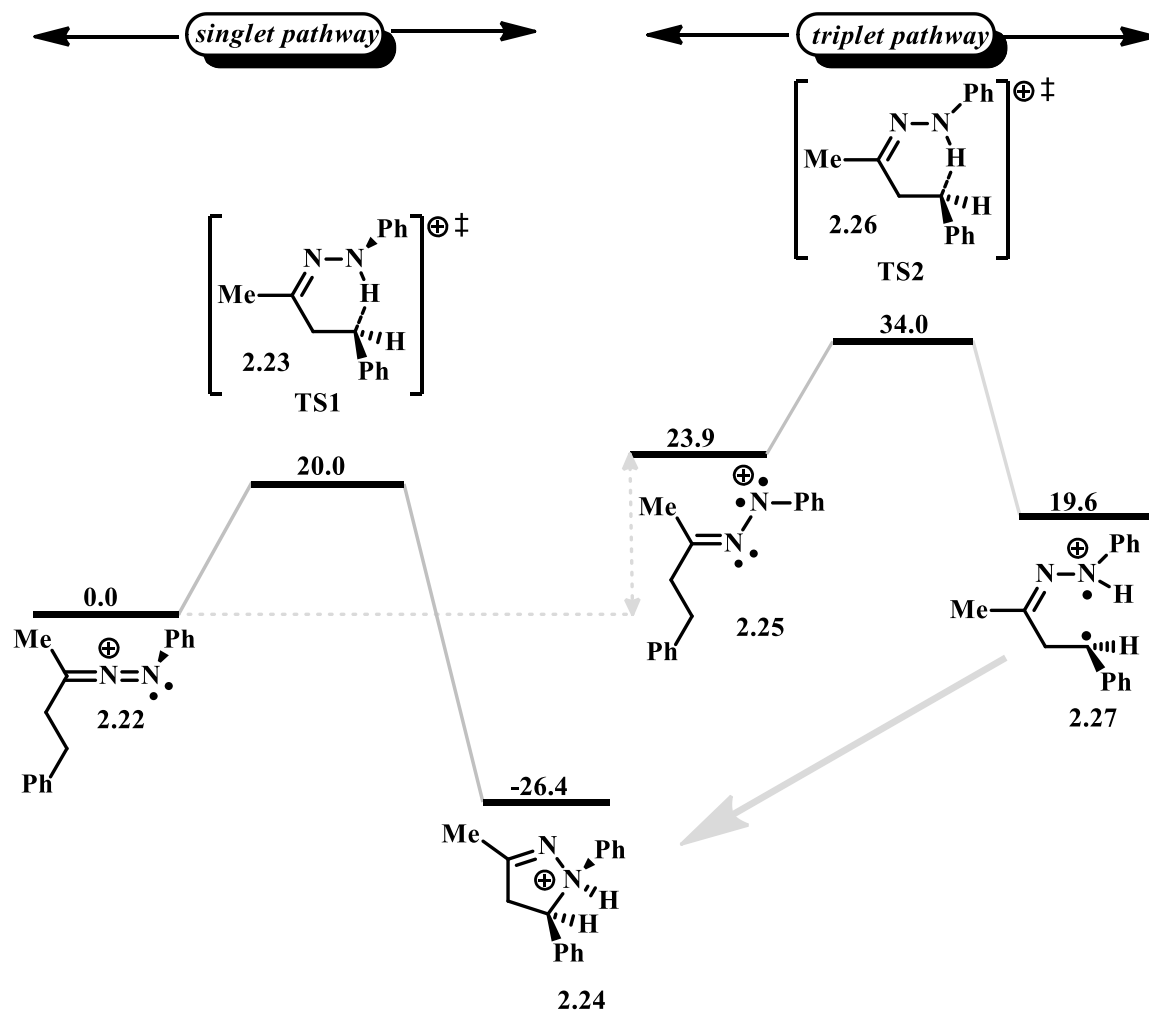


Figure 2.1. Gibbs free energy changes in kcal/mol of singlet and triplet C-H amination pathways of aryl-1-aza-2-azoniaallene.

Based on intrinsic reaction coordinate (IRC),¹⁴ the Houk and the Brewer groups also reported that the benzylic hydride gradually migrates to the electron-deficient terminal nitrogen to form a N-H bond and a benzyl carbocation. The benzyl carbocation subsequently undergoes C-N bond formation to give the heterocyclic product. To support

these facts, these groups report the quasi-classical molecular dynamic trajectories (Figure 2.2) for the singlet C-H amination of an ary-1-aza-2-azoniaallene. This study showed that N-H bond formation takes place much faster than C-N bond formation and that C-C bond rotation occurs much slower than the C-N bond formation, which accounts for the stereospecificity observed for the C-H insertion reaction (Scheme 2.4).

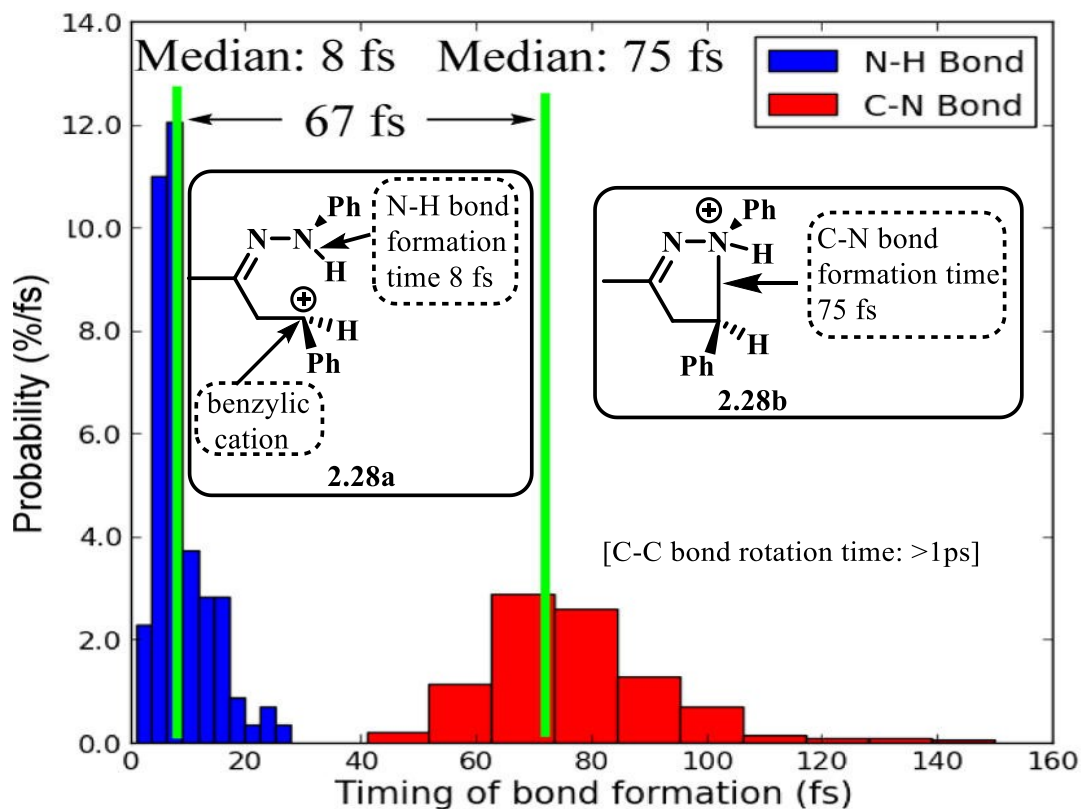
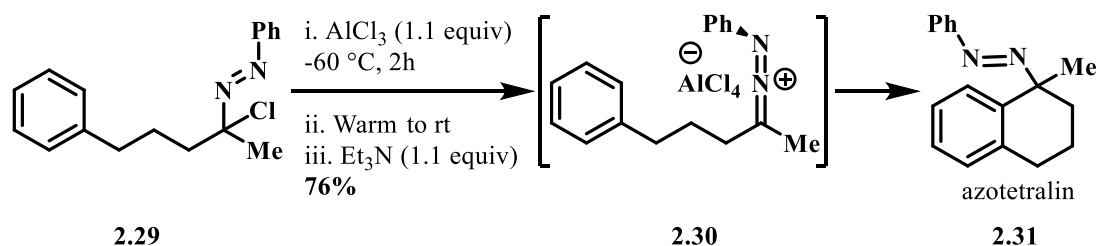


Figure 2.2. Probability vs. timing of N-H and C-N bond formation at 298 K (Figure courtesy of *J. Am. Chem. Soc.* **2015**, 137, 9100-9107).

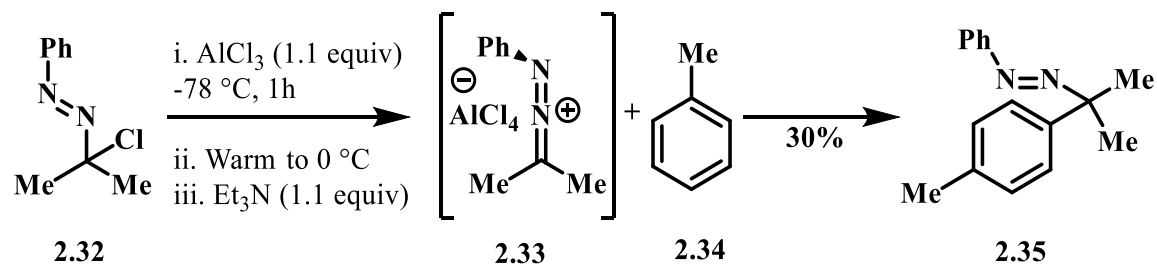
2.4 Effect of tether length on intramolecular reactions of 1-aza-2-azoniaallenes

To understand the effect of the tether length on intramolecular C-H aminations, the Brewer group prepared a heteroallene salt (e.g. **2.30**, Scheme 2.6a), in which the tether is one methylene unit longer than **2.5** (Scheme 2.2). This heteroallene unexpectedly

underwent an electrophilic aromatic substitution reaction to give azotetralin **2.31** in 76% yield instead of a C-H insertion product.¹⁴ This result showed that the tether length plays a vital role in determining the result of these reactions. To investigate the reactivity of this Friedel-Crafts type reaction, the Brewer group also prepared the heteroallene salt **2.33** from the α -chloroazo compound **2.32** and treated it with toluene (**2.34**) to give the azo-cymene **2.35** in 30% yield (Scheme 2.6b).¹⁴ Therefore, this type of reaction is not limited to intramolecular reactions. When the Brewer group, in collaboration with the Houk group, studied the tether effect on the competition between C-H amination and electrophilic aromatic substitution, they found that the longer tether made the transition state leading to electrophilic aromatic substitution more stable than the transition state for C-H amination.¹⁴



Scheme 2.6a. Effect of tether length on intramolecular reactions of 1-aza-2-azoniaallenes.



Scheme 2.6b. Test reaction of 1-aza-2-azoniaallene for Friedel-Crafts type reactivity.

2.5 Kinetic isotope effects for intramolecular C-H amination of 1-aza-2-azoniaallene

Kinetic isotope effects (KIEs) give useful information about relative rates which can be used to determine the mechanism of reactions. In this method, a hydrogen atom is replaced by a deuterium atom, and the relative rates of reaction are compared. The zero-point energy of deuterium is lower than the zero-point energy of hydrogen because deuterium is heavier than hydrogen (Figure 2.3). Due to this, the bond dissociation energy for a C-D is greater than the bond dissociation energy for a C-H. Therefore, the reaction rate for the conversion of C-D is typically slower than the reaction rate for the conversion of C-H. However, the degree to which the different in rate is observed depends on how fully the bond is broken at the transition state. Reactions that have highly developed bond cleavage at the transition state show large KIEs (more than 3). A minimal bond cleavage at the transition state shows the KIEs in between 1 and 2. A KIEs of 1 shows that there is no difference between C-H and C-D bonds and the isotope effect is too small to be detected.^{19,20,21}

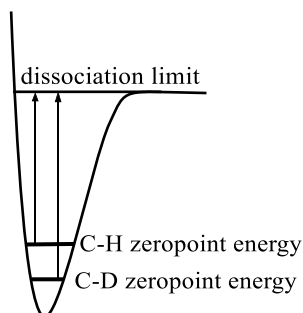
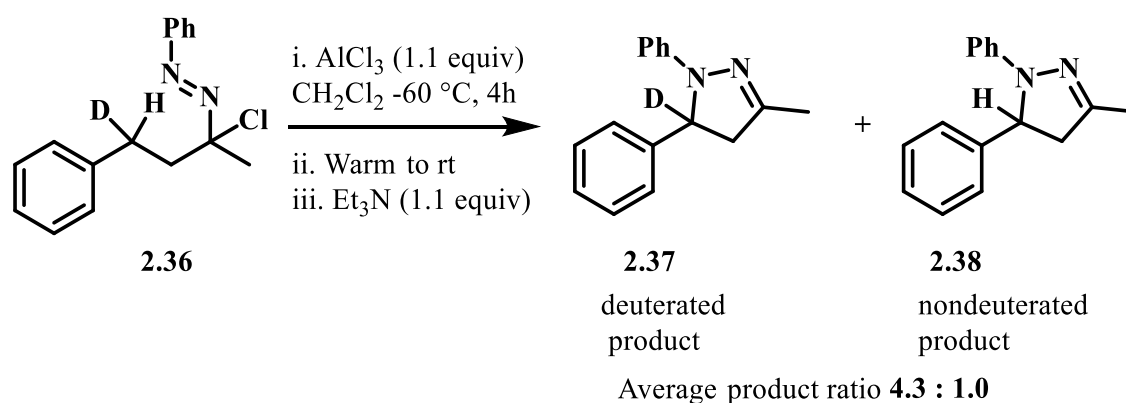


Figure 2.3. A Morse potential diagram showing zero-point energy for C-H and C-D.

The determination of the KIEs for C-H amination could provide crucial information to better understand the mechanism of heteroallene insertion. To complete these experimental studies, I prepared α -chloroazo compound **2.36** (Scheme 2.7) from the

corresponding hydrazone derivative. After subjecting this compound to the insertion reaction under the standard conditions, we observed an average 4.3:1 ratio of deuterated to nondeuterated amination product. This ratio was calculated by integration of the ^1H NMR spectrum of the crude reaction mixture. Based on the literature, KIEs between 3 and 6 generally indicates a rapid radical rebound mechanism,^{24,25} or a highly asynchronous concerted insertion.^{17,22,23} The observed KIEs (4.3) and the computational results are both consistent with the latter mechanism. Therefore, we finally concluded that the mechanism of the C-H amination of 1-aza-2-azoniaallene salts occurs through an asynchronous concerted pathway.



Scheme 2.7. Experimental kinetic isotope effect.

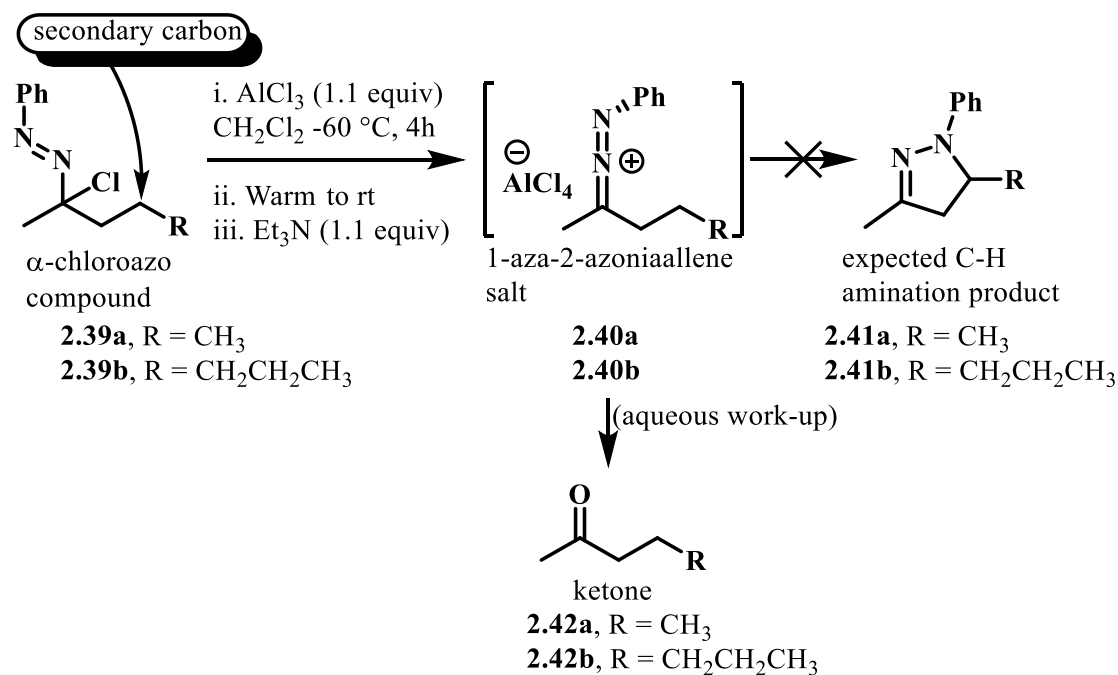
2.6 Exploration of the scope of 1-aza-2-azoniaallene salts

After discovering that 1-aza-2-azoniaallene salts can participate in the intramolecular C-H amination reactions,^{14,15} we were interested to explore the scope of this insertion reaction. The results of these studies are described in the sections that follow.

2.6.1 Limitation of C-H insertion on secondary aliphatic center

As described in section 2.2, table 2.1, 1-aza-2-azoniaallene salt easily undergo intramolecular C-H insertion reaction at tertiary aliphatic and benzylic centers.^{14,15} We

were interested in exploring the C-H amination reaction at a secondary aliphatic center. Therefore, I prepared the α -chloroazo compounds **2.39a** and **2.39b** (Scheme 2.8) from the corresponding hydrazone derivatives. The reactive heteroallene intermediate **2.40a** and **2.40b**, generated by treating the α -chloroazo compounds with AlCl_3 under the standard conditions, did not undergo C-H amination reaction to provide the expected products (**2.41a** and **2.41b**), but instead were hydrolyzed giving the starting ketones **2.42a** and **2.42b**. After several attempts, we concluded that the C-H insertion reaction does not occur at a secondary aliphatic center.¹⁵

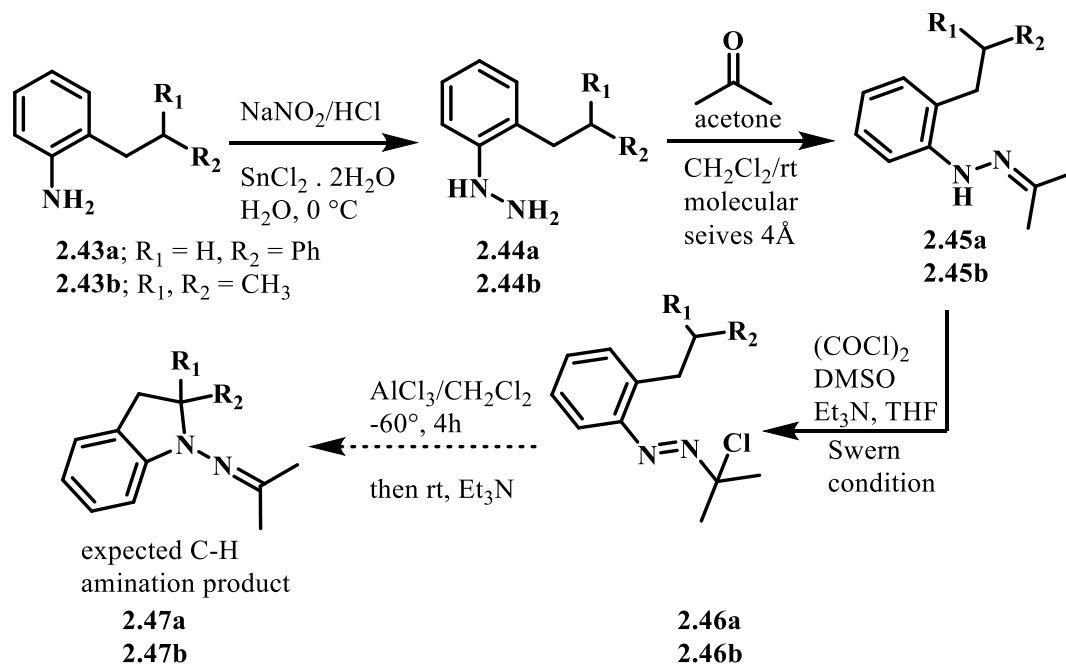


Scheme 2.8. Limitation of C-H insertion reactions at secondary aliphatic centers.

2.6.2 Limitation of C-H insertion to synthesize indoline and indole products

The C-H insertion reaction might not be limited to just pendent groups that are attached to the heteroallene. To extend the scope of the C-H insertion reaction, we proposed that insertion at a position tethered through the *N*-aryl ring could yield indole

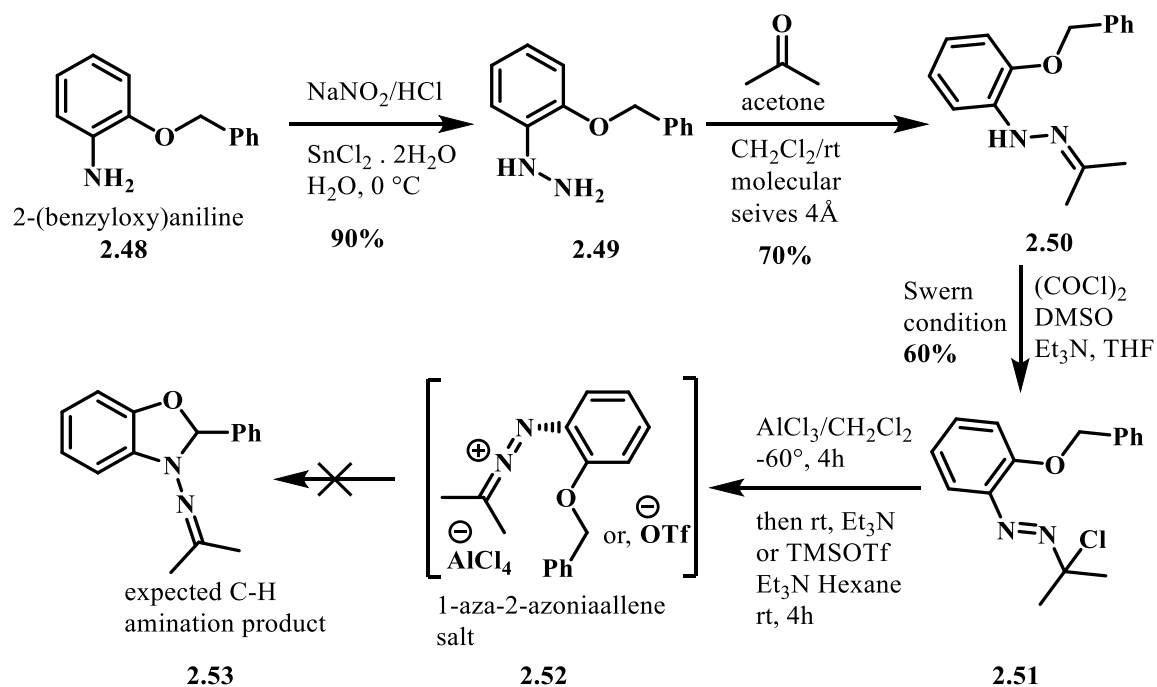
and indoline products (Scheme 2.9). To test this, I prepared hydrazine derivatives **2.44a** and **2.44b** by treating the corresponding aniline derivatives (**2.43a** and **2.43b**) with sodium nitrite, tin (II) chloride, and hydrochloric acid at 0 °C.²⁶ The hydrazones were then reacted with acetone to provide hydrazones **2.45a** and **2.45b**. This reaction did not provide very pure hydrazone derivatives; due to the instability, I was unable to fully purify these derivatives. I took these impure materials to prepare the corresponding α -chloroazo compounds **2.46a** and **2.46b**, but they were impure as well. Previously, I had prepared an *o*-tolylhydrazone and its corresponding α -chloroazo compound without issue. However, in these more functionalized cases, purity was always an issue and I was not able to generate expected products **2.47a** and **2.47b**.



Scheme 2.9. Synthetic approach to form indoles via C-H amination.

We were also interested to synthesize hemiaminal **2.53** (Scheme 2.10 and 2.11) via C-H amination. In this case, we expected the oxygen atom to activate the benzylic

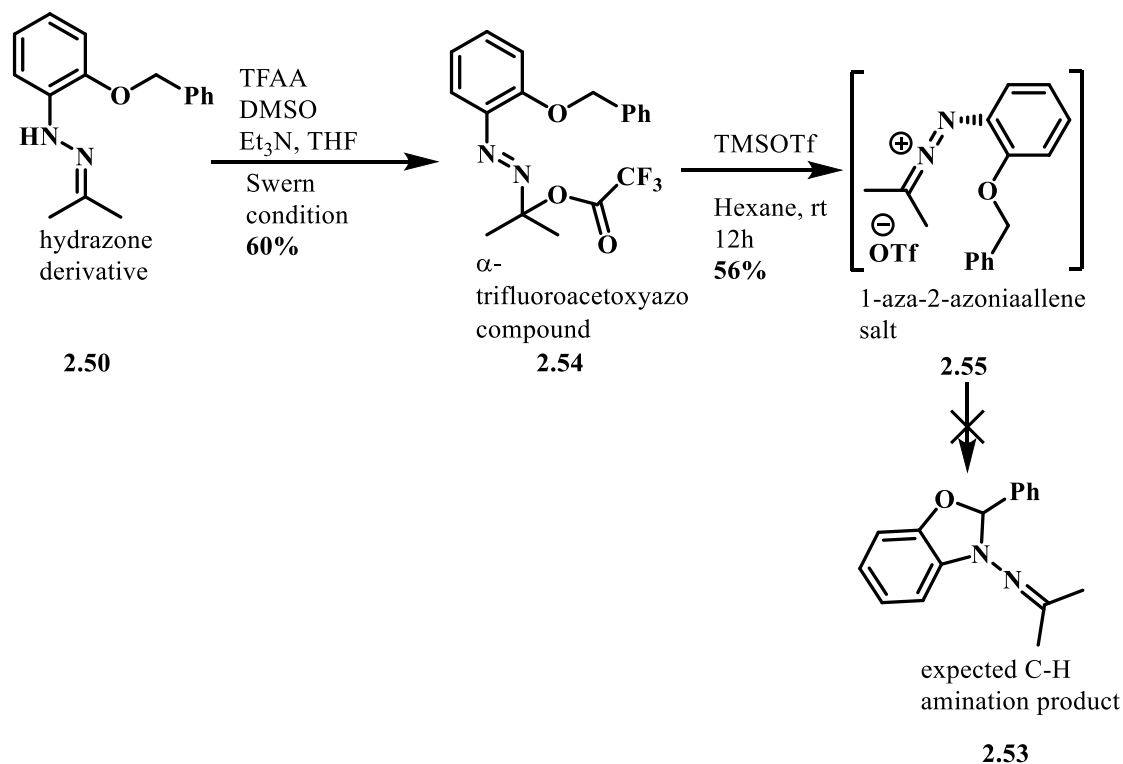
position toward C-H insertion. To test this, I prepared hydrazine **2.49** (Scheme 2.10) by reacting 2-(benzyloxy)aniline (**2.48**) with aqueous sodium nitrate, tin chloride, and hydrochloric acid at 0 °C.²⁷ The hydrazine **2.49** was then treated with acetone to give hydrazone **2.50**, which was then oxidized under Swern conditions to give α -chloroazo compound **2.51** in 60% yield. When this α -chloroazo compound was treated with anhydrous AlCl_3 in the presence of triethylamine at -60 °C, it did not undergo a C-H amination reaction. Replacing the Lewis acid with TMSOTf, did not help the situation, and after aqueous work-up, the starting hydrazone **2.50** was isolated.



Scheme 2.10. Limitation of C-H amination from α -chloroazo compound.

As described in Chapter 1, α -trifluoroacetoxyazo compounds also give heteroallene salts upon treatment with TMSOTf. So, we were interested to try the C-H amination reaction starting from the α -trifluoroacetoxyazo compound. I prepared α -trifluoroacetoxyazo **2.54** (Scheme 2.10) from the hydrazone **2.50**, and treated it with

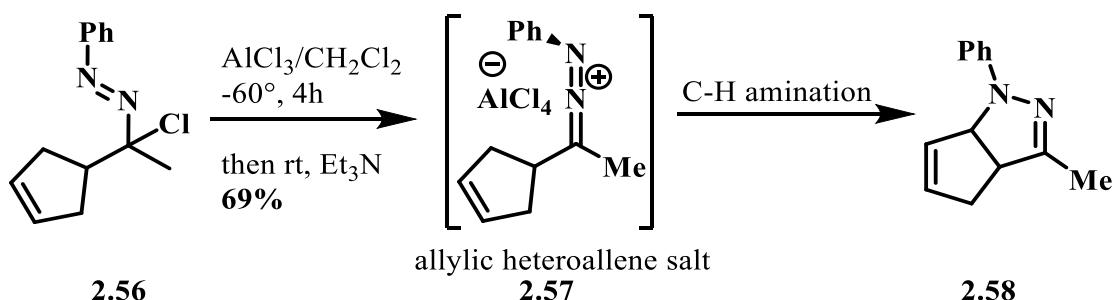
TMSOTf at room temperature for 12 hours. This reaction also failed to give the desired product, and after aqueous work-up, the starting hydrazone **2.50** was isolated.



Scheme 2.11. Limitation of C-H amination from α-trifluoroacetoxyazo compound.

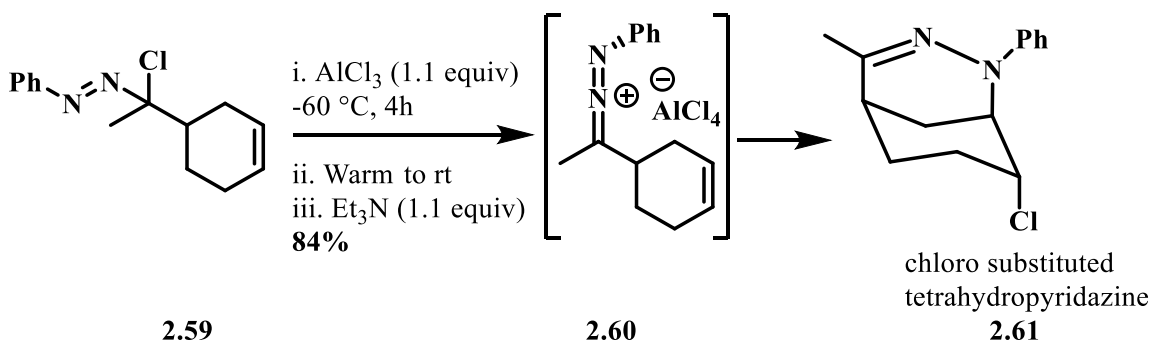
2.7 C-H Amination and chloro-amination of allylic heteroallene salts

The Brewer group had reported that heteroallenes having pendent alkenes undergo either [3+2]^{28,29} or [4+2]³⁰ cycloaddition reactions depending on the length of the connecting the reacting partners.³¹ While studying the substrate scope for the C-H amination, Dr. Al-Batainech prepared heteroallene salt of cyclopentene derivative, which underwent a C-H insertion reaction to give pyrazole **2.58** (Scheme 2.12). In this case, the cycloaddition reaction is unfavorable because of conformational constraints.¹⁵



Scheme 2.12. C-H amination for allylic heteroallene salt.

However, we were surprised to find the seemingly analogous heteroallene **2.60** underwent an alkene addition reaction instead of allylic C-H amination to provide the chloro-substituted tetrahydropyridazine **2.61** in 84% yield (Scheme 2.13).³²



Scheme 2.13. Intramolecular chloro-amination reaction of heteroallene.

In collaboration with Prof. Houk (UCLA) and Dr. Hong (Zhejiang University, China), the Brewer group modeled the reaction of allylic heteroallene salts using DFT calculations.³² These studies compared possible C-H amination and nitrenium [2+1] cycloaddition addition pathways (Figure 2.4). The heteroallene of cyclopentene derivative **2.62** undergoes a C-H amination reaction via transition state **TS-2.63** with an energy barrier of 15.3 kcal/mol. The competing [2+1] cycloaddition pathway proceeds by transition state **TS-2.65**, which has an energy barrier of 16.2 kcal/mol that is 0.9 kcal/mol higher than the C-H amination. Therefore, the C-H amination pathway is more favorable

than the nitrenium (2+1) addition pathway, which is consistent with the experimental result (Scheme 2.12).

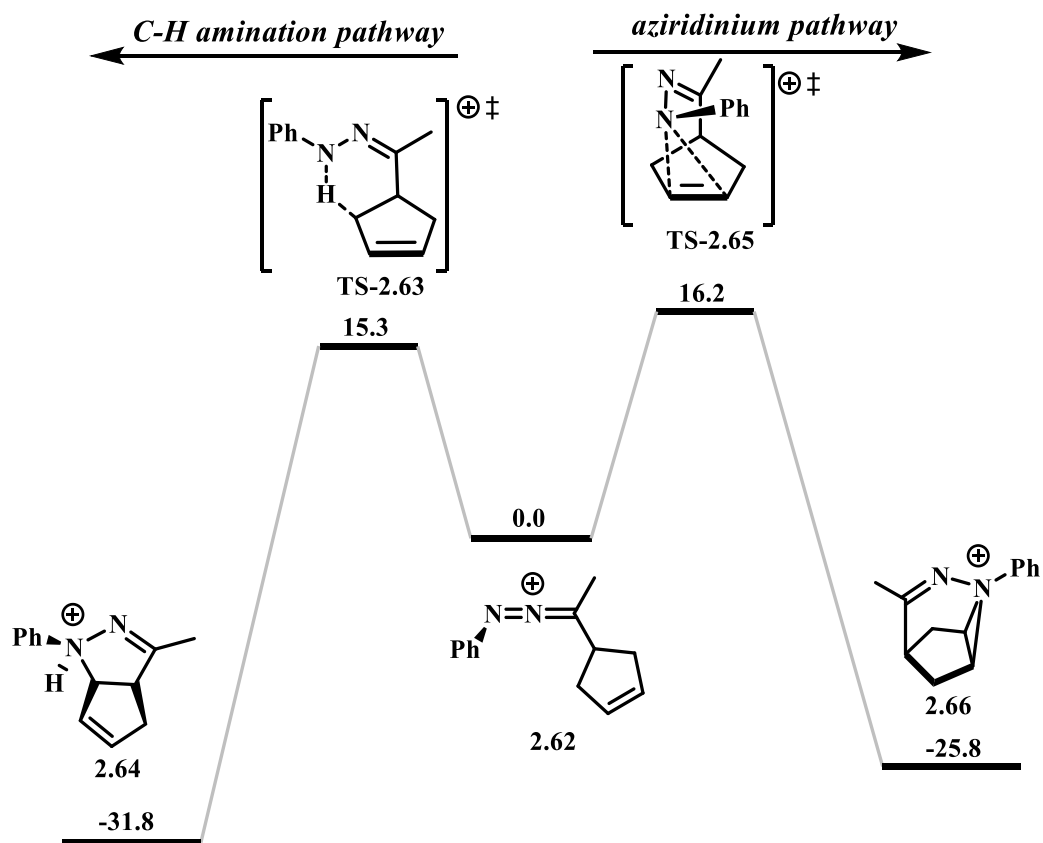


Figure 2.4. Gibbs free energy barrier in kcal/mol for C-H amination and aziridinium pathways for 5-membered ring.

On the other hand, the cyclohexene derivative (**2.67**) undergoes C-H amination via transition state **TS-2.68** with an energy barrier of 20.4 kcal/mol and nitrenium (2+1) addition via transition state **TS-2.70** with an energy barrier of 16.4 kcal/mol. In this case, the cycloaddition pathway is 4.0 kcal/mol lower in energy. Therefore, the nitrenium (2+1) addition pathway is more favorable than C-H amination pathway, which is also consistent with the experimental result (Scheme 2.12) because of the formation of pyrazole **2.58**.

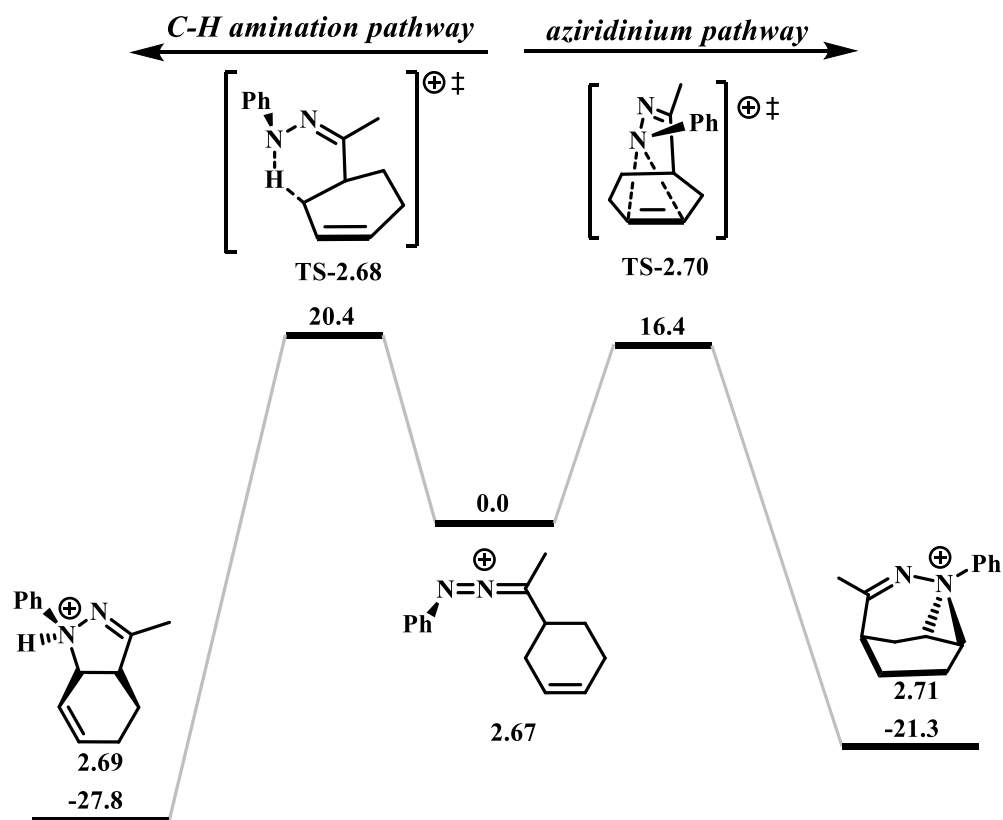
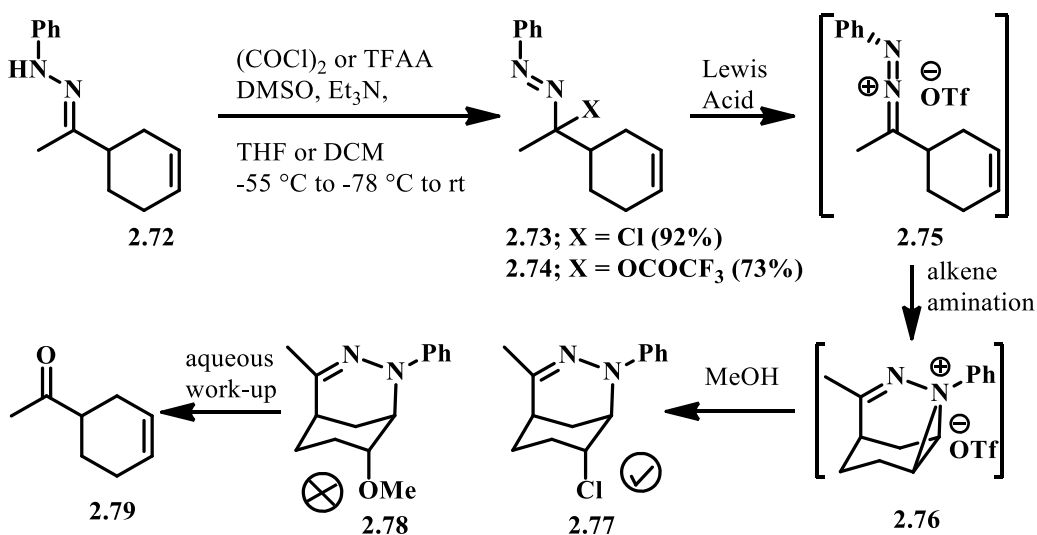


Figure 3.5. Gibbs free energy barrier in kcal/mol for C-H amination and aziridinium pathways for 6-membered ring.

2.8 Limitation of intramolecular alkene aminations

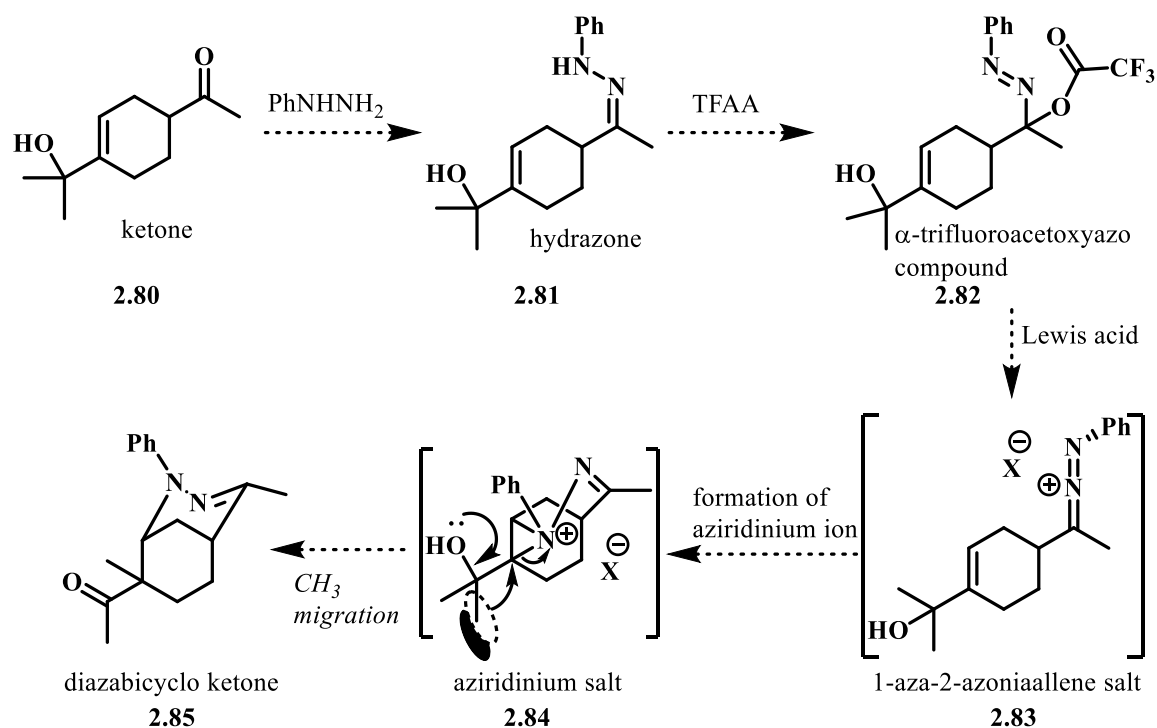
As described in section 2.7, the chloroamination path proceeds through an aziridinium ion intermediate. We hypothesized that it might be possible to trap this intermediate ion by a variety of external nucleophiles. To examine this, I prepared α -substituted azo compounds **2.73** and **2.74** from hydrazone **2.72** (Scheme 2.14). After treating Lewis acid such as, TMSOTf and AgOTf, with a hexane solution of these azo compounds at $-78\text{ }^{\circ}\text{C}$, the reaction mixture was stirred for 10 minutes. Then, an external nucleophile, such as MeOH, was added and stirred for additional 20 minutes at $-78\text{ }^{\circ}\text{C}$ and warmed up to room temperature. After aqueous work-up, I was unable to get the

expected product **2.78**. When I used α -chloroazo compound **2.73** as a starting material, I observed a small amount of chloro-substituted product (**2.77**). The aqueous work-up of the TMSOTf mediated product was oxidized to give starting ketone **2.79**.



Scheme 2.14. Limitation of alkene amination.

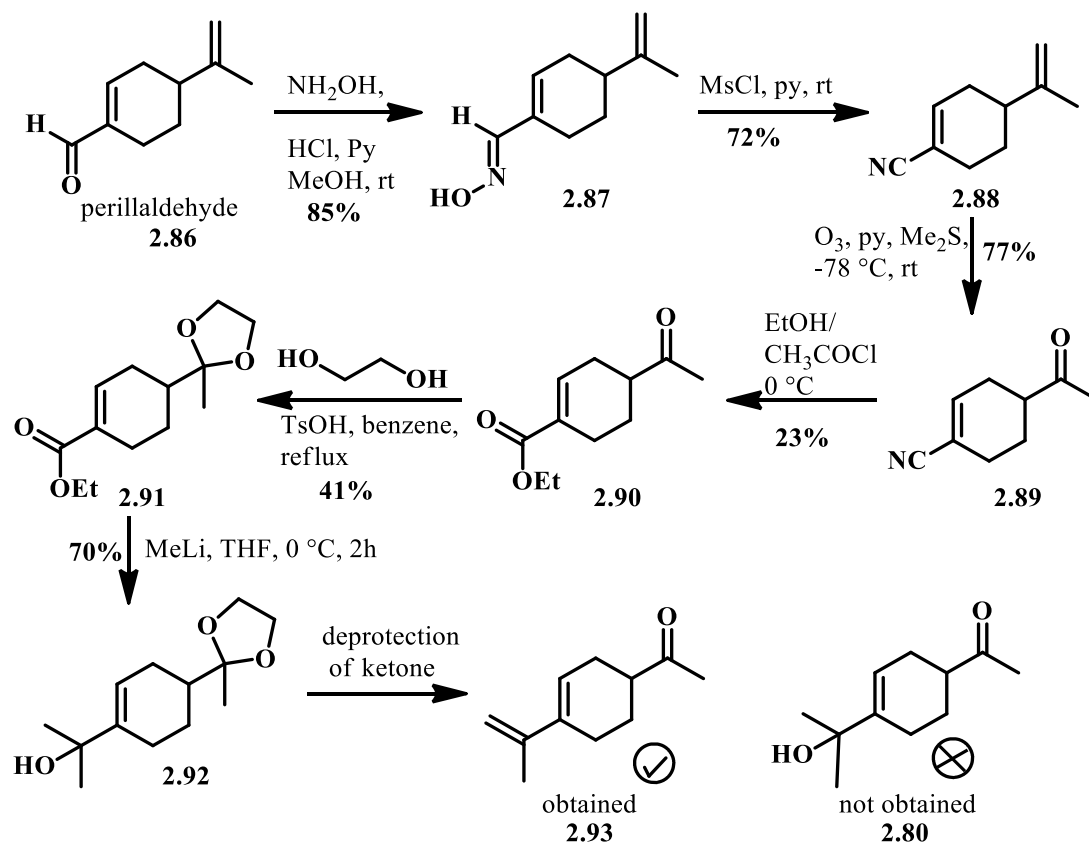
We also thought it might be possible to trap aziridinium ion by migration of a methyl group. For example, as shown in Scheme 2.15, heteroallene **2.83** would be expected to react with the attached alkene to give aziridinium ion **2.84**. In this case, pinacol-type migration of an adjacent methyl group would provide the diazabicyclo ketone **2.85**.



Scheme 2.15. Purposed reaction path to form diazabicyclo ketone (**2.85**) via alkene amination.

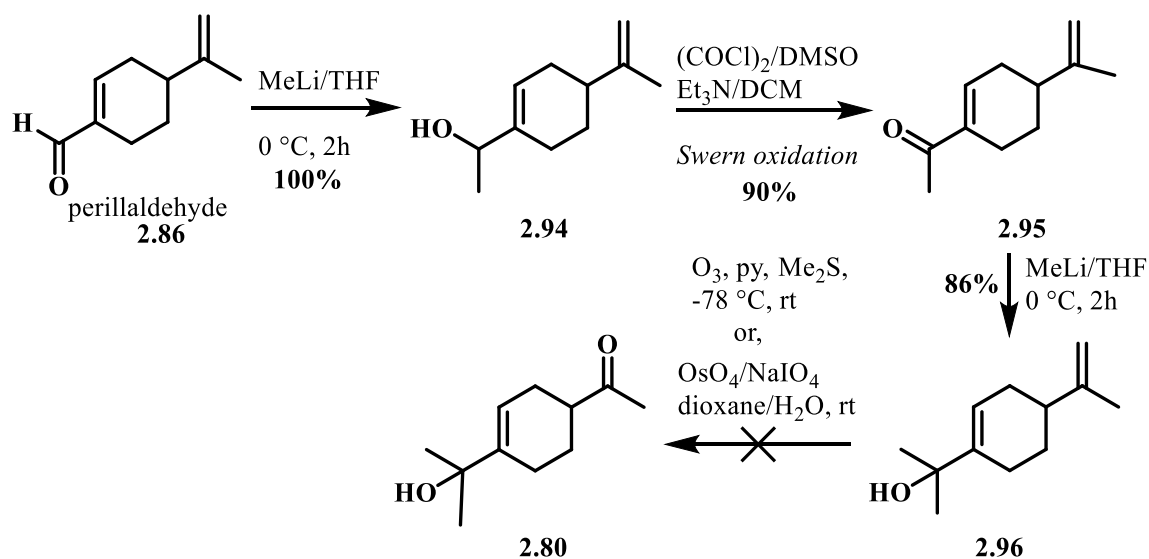
The required ketone **2.80** (Scheme 2.15) was not commercially available and our first goal was to synthesize this ketone. To achieve this, perillaldehyde (**2.86**) was reacted with hydroxyl amine to give the hydroxyl imine **2.87**,³³ which was then converted into the nitrile group³⁴ (**2.88**) by reaction with MsCl and pyridine (Scheme 2.16). The alkene group of **2.88** underwent selective ozonolysis of the uncojugated alkene to form ketone **2.89**, which was then treated with ethanol and acetyl chloride to afford the ester **2.90**. The ketone group of **2.90** was protected as the acetal (**2.91**), which was then treated with methyl lithium to form 3° alcohol **2.92**.³⁵ All that is required is hydrolysis of the acetal to afford ketone. To achieve this, acetal **2.91** was treated under different conditions, including 1M of HCl, THF, 0 to 25 °C, 13h; 6N of HCl, EtOH (95%), 4h, rt; AcOH (20%), EtOH, reflux, 2h; and CAN, CH₃CN, H₂O, 70 °C. Under all of these conditions,

the desired deprotection occurred, but so did elimination of the tertiary alcohol to give the undesired diene **2.93**.



Scheme 2.16. First attempt to prepare the desired ketone **2.80**.

As an alternative strategy to prepare ketone **2.80** (Scheme 2.15), I treated perillaldehyde (**2.96**) with MeLi to form the 2° alcohol (**2.94**, Scheme 2.17), and subsequent Swern oxidation gave the ketone **2.95**, and this ketone was converted into the 3° alcohol with MeLi .³⁵ But, I was not able to selectively oxidize the less substituted alkene to give ketone **2.80**.



Scheme 2.17. Second attempt to prepare the desired ketone **2.80**.

In view of the difficulties, we faced in preparing **2.80**, we determined that this methodology would not be generally useful, and we set this project aside.

2.9 New type of C-H amination via nitrenium cation

The Brewer group has discovered many different reactivities of 1-aza-2-azoniaallene salts,^{14,15,29-32} and we recognized that this reactivity can be ascribed to the aza-substituted nitrenium cation **1.4** (Figure 2.6). We recognized that if we replaced the nitrogen atom of the aza group in structure **1.2** by an oxygen atom, it would give the oxonium cation **2.97** (Figure 2.6). This oxonium cation is a resonance form of nitrenium cation **2.98**, which is analogous to the aza-nitrenium cation **1.4**. Therefore, we hypothesized that the reactivity of **2.98** should be similar to the reactivity of 1-aza-2-azoniaallene cations.

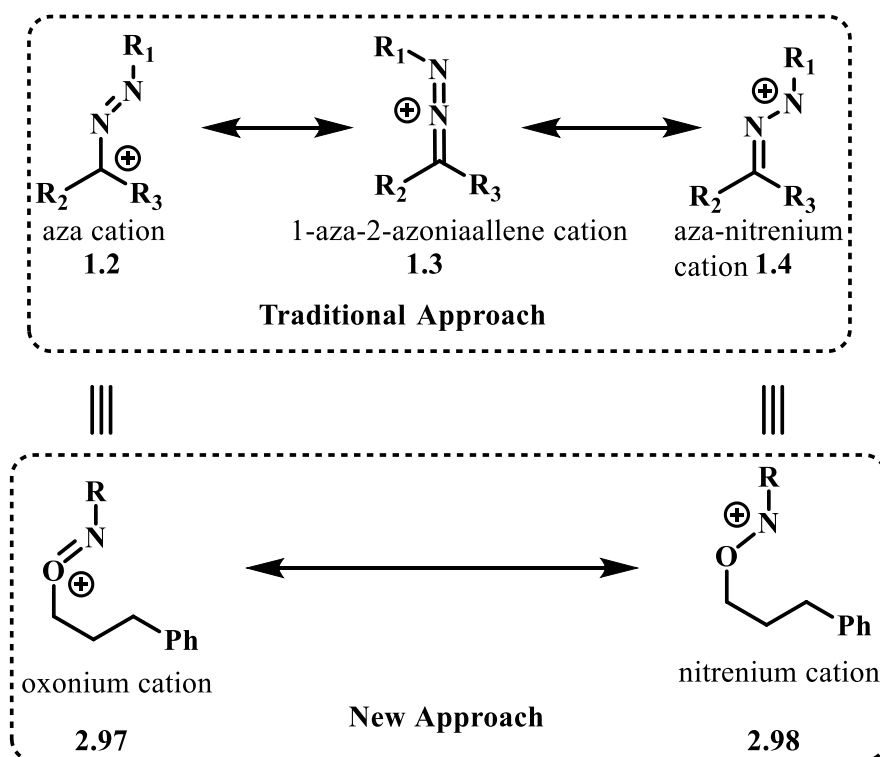
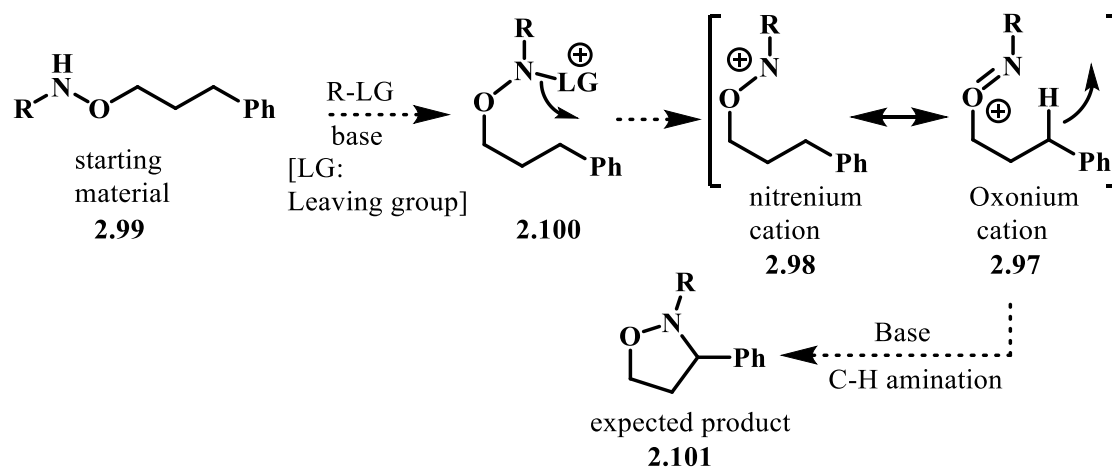


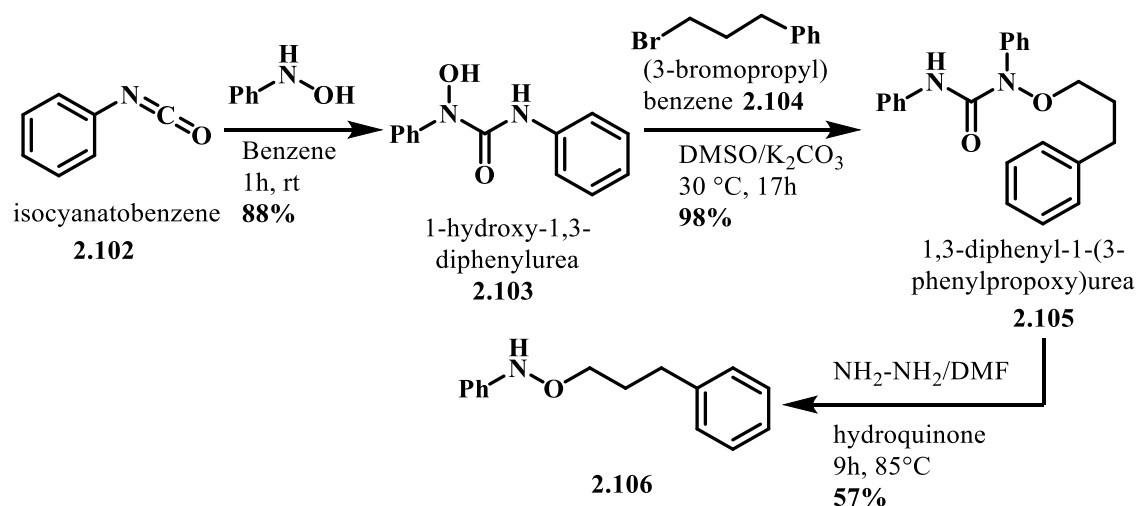
Figure 2.6. Comparison of traditional approach with new approach to undergo new type of C-H amination.

Our major goal was to develop a new synthetic strategy, in which structures, such as **2.98** (Figure 2.6), react via C-H insertion to give a heterocycle containing an O-N bond. This would be useful because O-N bonds are easy to cleave. We thought it might be possible to generate **2.98** from a hydroxyl amine precursor with a good leaving group on nitrogen (Scheme 2.18). After releasing the leaving group, we expected to form the intermediate oxonium cation **2.98** or nitrenium cation **2.97**, which could undergo C-H insertion in the presence of a suitable base to provide the desired product **2.101**.



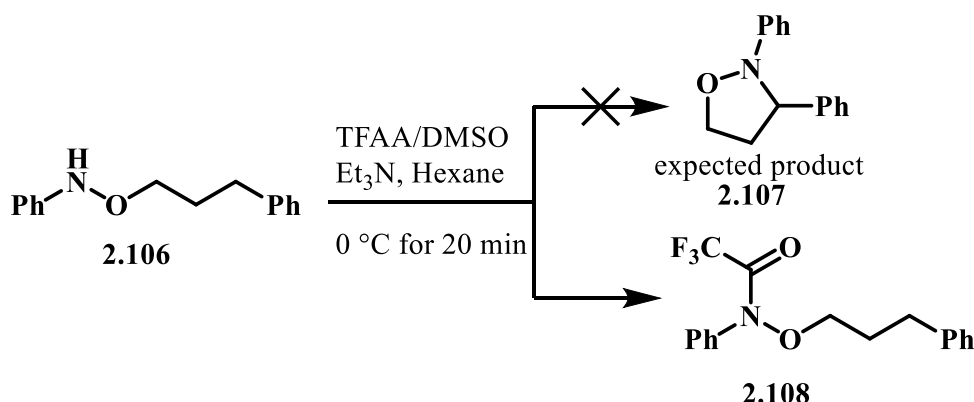
Scheme 2.18. A synthetic strategy to form O-N bond in a ring system via C-H amination.

To this end, I first prepared 1-hydroxy-1,3-diphenylurea³⁶ (**2.103**, Scheme 2.19) from the reaction of isocyanatobenzene (**2.102**) and *N*-phenylhydroxyl amine. This urea derivative underwent nucleophilic substitution with 3-bromopropyl benzene (**2.104**) to give the desired product **2.105**^{36,37} in 98% yield. The nitrogen of the structure **2.105** was deprotected in the presence of hydrazine and hydroquinone to require hydroxyl amine **2.106** in 57% yield.^{36,37}



Scheme 2.19. Formation of a starting material for new type of C-H amination reaction.

Treating **2.106** (Scheme 2.20) with trifluoroacetoxydimethylsulfonium trifluoroacetate generated from trifluoroacetic anhydride (TFAA) and DMSO in the presence of triethyl amine at 0 °C for 20 minutes did not give the desired product **2.107**, but instead gave **2.108**, in which the nitrogen atom is protected by a trifluoroacetyl group. To confirm this result, I treated a small amount of starting material with TFAA in a NMR tube, and it also provided **2.108**.



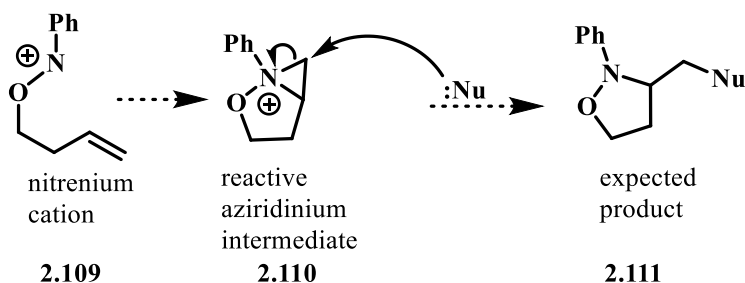
Scheme 2.20. Reaction for C-H amination.

Other potential oxidants, including triflic anhydride, PhI(OTf)₂, and PITFA, also failed to give desired insertion product **2.107**. In all cases, the starting materials were consumed, and in some cases, I isolated *N*-phenylhydroxyl amine which must have formed by breaking the C-O bond of the starting material, but insertion never occurred.

2.10 New type of alkene amination via nitrenium cation

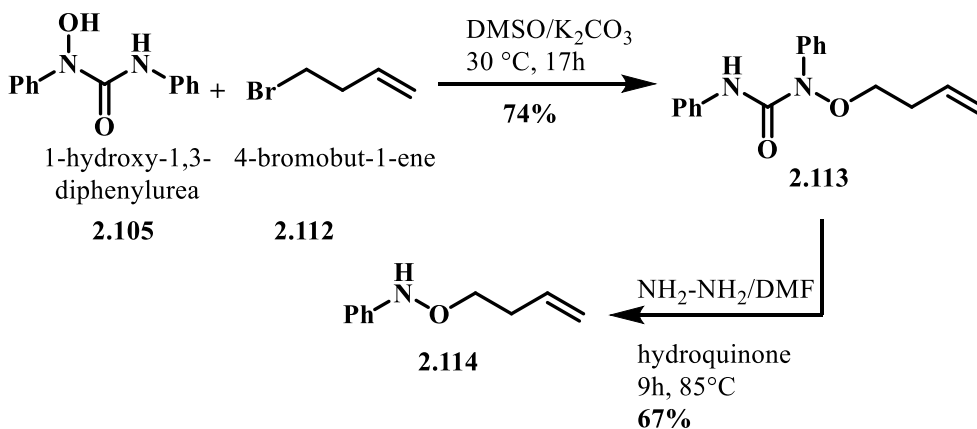
Although the C-H amination of an oxygen stabilized a nitrenium cation failed to provide the desired product, we thought it might be possible to take advantages of that species in an alkene amination reaction³² (Scheme 2.21). Our hypothesis was that the nitrenium cation **2.109** (Scheme 2.20) could form a reactive aziridinium intermediate

(**2.110**) by engaging a pendent alkene. Aziridinium opening by a subsequent nucleophilic attack would provide heterocycle **2.111**.



Scheme 2.21. A synthetic strategy to form O-N bond in a ring system via alkene amination.

To obtain the starting material **2.114** (Scheme 2.22), I treated 1-hydroxyl-1,3-diphenylurea (**2.105**) with 4-bromobut-1-ene (**2.112**) which gave the *O*-alkylated product **2.113** in 74% yield. Subsequent deprotection of nitrogen gave the desired *N*-aryl-*O*-alkyl hydroxyl amine **2.114** in 67% yield.^{36,37}



Scheme 2.22. Formation of starting material for alkene amination via nitrenium cation.

To test the alkene amination reaction, hydroxyl amine **2.114** (Scheme 2.22) was treated with triflic dimethylsulfonium triflate and DTBMP at -78 °C. After few minutes, a few drops of methanol were added into the reaction mixture to open the aziridinium ring.

However, this reaction did not provide the desired product. After changing the oxidant PITFA, I still did not obtain the expected product. These preliminary studies led us to conclude that neither C-H amination nor alkene addition of oxygen-stabilized nitrenium cation would occur under the applied conditions.

2.11 Conclusions

C-H amination has proven to be an important tool to construct C-N bonds as highlighted by its application in natural product synthesis, such as manzacidin,¹² (+)-saxitoxin,¹³ and (-)-tetrodotoxin¹⁴. Developing new methods to effect C-H amination could further increase the scope and utility of this useful reactivity. With this in mind, the Brewer group has developed unprecedented intramolecular C-H amination of heteroallene salts. We have also studied the mechanism of this insertion computationally and experimentally. These studies showed that benzylic position of 4-methoxybenzene are more favorable for C-H amination reaction than benzylic position of 4-nitrobenzene. In the competition reaction between benzylic and aliphatic tertiary positions, the benzylic position preferentially underwent insertion. Computational studies show that heteroallene salts energetically favor the singlet state, and that C-H insertion proceeds via an asynchronous concerted pathway. However, insertion is not always the most favorable process, and a longer tether follows a Friedel-Craft type electrophilic aromatic substitution reaction to provide an azotetralin derivative. Insertion does not occur at secondary aliphatic center. Finally, our efforts to develop a synthesis of indoles and indolines via C-H amination failed.

The intramolecular alkene amination of heteroallene salts provides a new way to synthesize a variety of bicyclic compounds. The Brewer group's studies show that the

heteroallene salt of a cyclohexene derivative (**2.75**, Scheme 2.13) preferentially undergoes alkene amination. Computational studies indicate that this intramolecular reaction occurs via the formation of an aziridinium ion, which is trapped by the chloride counter ion. However, my all attempts to trap the aziridinium ion by an external nucleophile failed.

We purposed a new strategy to affect C-H amination and alkene addition reactions via a nitrenium cation intermediate, but these efforts did not lead to a productive reaction.

References

1. Davis, H. M. L. *Angew. Chem. Int. Ed.* **2006**, *45*, 6422.
2. Davies, H. M. L.; Manning, J. *Nature* **2008**, *451*, 417.
3. MacCross, M.; Baillie, T. *Science* **2004**, *303*, 1810.
4. Godula, K; Sames, D. *Science* **2006**, *312*, 67.
5. Loewenthal, H. J. E. *Tetrahedron* **1959**, *6*, 269.
6. King, S. M.; Herzon, S. *J. Org. Chem.* **2014**, *97*, 8937.
7. Davies, H. M. L.; Beckwith, R. E. J. *Chem. Rev.* **2003**, *103*, 2861.
8. Ellman, J. A. *Science* **2007**, *316*, 1131.
9. Bergman, R. G. *Nature* **2007**, *446*, 391.
10. Sun, C. L; Li, H.; Yu, D. G.; Yu, M.; Zhou, X.; Lu, X. Y.; Huang, K.; Zheng, S.; Li, B. J.; Shi, Z. J. *Nat. Chem.* **2010**, *2*, 1046.
11. Davies, H. M. L.; Manning, J. *Nature* **2008**, *451*, 417.
12. Wehn, P. M.; DuBois, J. *J. Am. Chem. Soc.* **2002**, *124*, 12950.
13. Hinman, A.; Du Bois, J. *J. Am. Chem. Soc.* **2003**, *125*, 11510.
14. Bercovici, D. A.; Brewer, M. *J. Am. Chem. Soc.* **2012**, *134*, 9890.
15. Hong, X.; Bercovici, D.; Yang, Z.; Al-Bataineh, N.; Srinivasan, R.; Dhakal, R.; Houk, K. N.; Brewer, M. *J. Am. Chem. Soc.* **2015**, *137*, 9100.

16. Smolinsky, G.; Feuer, B. I. *J. Am. Chem.* **1984**, *86*, 3085.
17. Nägeli, I.; Baud, C.; Bernardinelli, G.; Jacquier, Y.; Moran, M.; Muller, P. *Helv. Chim. Acta* **1997**, *80*, 1087.
18. Breslow, R.; Gellman, S. H. *J. Am. Chem. Soc.* **1983**, *105*, 6728.
19. Gómez-Gallego, M.; Sierra, M. A. *Chem. Rev.* **2011**, *111*, 4857.
20. Simmons, E. M.; Hartwig, J. F. *Angew. Chem. Int. Ed.* **2012**, *51*, 3066.
21. Jones, W. D. *Acc. Chem. Res.* **2003**, *36*, 140.
22. Harvey, M. E.; Musaev, D. G.; Du Bois, J. *J. Am. Chem. Soc.* **2011**, *133*, 17207.
23. Fiori, K. W.; Espino, C. G.; Brodsky, B. H.; Du Bois, J. *Tetrahedron* **2009**, *65*, 3042.
24. Alderson, J. M.; Phelps, A. M.; Scamp, R. J.; Dolan, N. S.; Schomaker, J. M. *J. Am. Chem. Soc.* **2014**, *136*, 16720.
25. Badiei, Y. M.; Dinescu, A.; Dai, X.; Palomino, R. M.; Heinemann, F. W.; Cundari, T. R.; Warren, T. H. *Angew. Chem. Int. Ed.* **2008**, *47*, 9961.
26. Wang, X-N.; Shao, P-L.; Lv, H.; Ye, S. *Org. Lett.* **2009**, *11*, 4029.
27. Roullier, C.; Chollet-Krugler, M.; Weghe, P.; Devehat, F. L.; Boustie, J. *Bioorg. Med. Chem. Lett.* **2010**, *20*, 4582.
28. Javed, M. I.; Wyman, J. M.; Brewer, M. *Org. Lett.* **2009**, *11*, 2189.
29. Wyman, J.; Javed, M. I.; Al-Bataineh, N.; Brewer, M. *J. Org. Chem.* **2010**, *75*, 8078.
30. Bercovici, D. A.; Ogilvie, J. M.; Tsvetkov, N.; Brewer, M. *Angew. Chem. Int. Ed.* **2013**, *52*, 13338.
31. Hong, X.; Liang, Y.; Brewer, M.; Houk, K. N. *Org. Lett.* **2014**, *16*, 4260.
32. Al-Bataineh, N.; Houk, K. N.; Brewer, M.; Hong, X. *J. Org. Chem.* **2017**, *82*, 4001.
33. Baumann, S. O.; Bendova, M.; Puchberger, M.; Schubert, U. *Eur. J. Inorg. Chem.* **2011**, 573.
34. Hendrickson, J.; Hussoin, M. S. *J. Org. Chem.* **1987**, *52*, 4139.
35. Gamba, D.; Pisoni, D. S.; da Costa, J. S.; Petzhold, C. L.; Borges, A. C. A.; Ceschi, M. A. *J. Braz. Chem. Soc.* **2008**, *19*, 1270.
36. Perronnet, J.; Girault, P.; Demoute, J. P. *J. Heterocycl. Chem.* **1980**, *17*, 727.

37. Fountain, K. R.; White, R. D.; Patel K. D.; New, D. G.; Xu, Y.; Cassely A. J. *J. Org. Chem.* **1996**, *61*, 9434.

CHAPTER 3: NEW SYNTHETIC ROUTES TO SYNTHESIZE α - SUBSTITUTED AZO COMPOUNDS

3.1 Introduction

α -Chloroazo compounds (e.g. **3.1**, Figure 3.1) are useful synthetic precursors to a variety of cyclic and acyclic compounds. Jochims and coworkers used these precursors to synthesize 1,2,4-triazolium salts,¹⁻³ 4,5-dihydro-1,2,3-triazolium salts,^{4,5} 1,3,4-thiadiazolium salts,² 4,5-dihydro-3*H*-pyrazolium salts,⁵⁻⁷ 3*H*-4-,5-dihydropyrazoles,⁸ and 1*H*, or 4*H*-pyrazolium salts⁹ via 1-aza-2-azoniaallene salt intermediates. Al-Soud also synthesized pyrazole, 1,2,4-thiadiazole, 1,2,4-triazole, and 1,3,4-thiadiazoliminothymidine derivatives using α -chloroazo precursors.¹⁰ Finally, Rai and coworkers employed these precursors to prepare azoalkenes, which were used to synthesize tetrahydropyridazine derivatives.¹¹

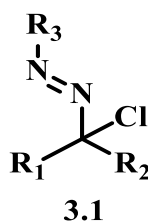
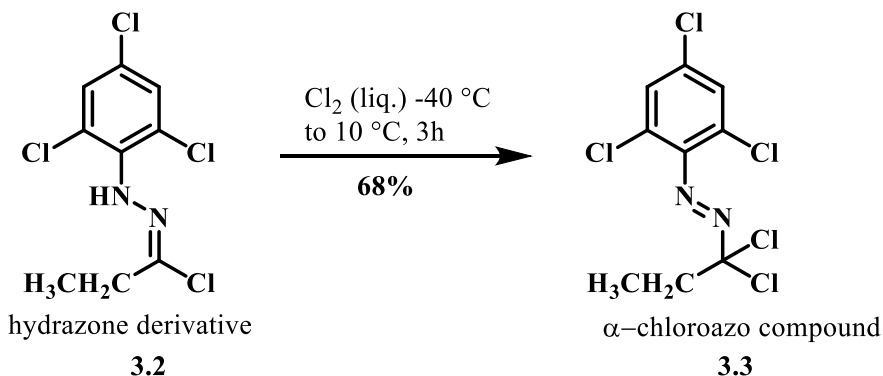


Figure 3.1. Structure of α -chloroazo compound.

The Brewer group also utilized the α -chloroazo compounds to synthesize structurally complex bicyclic diazonium salts,¹²⁻¹⁴ pyrazoline products,^{15,16} protonated azomethine imines salts,^{17,18} azotetralin derivatives,¹⁶ tetrahydropyridazine derivatives,¹⁶ and bicyclo[2.2.2]oct-2-ene via [3+2] and [4+2] cycloadditions,¹⁹ C-H insertions, and alkene aminations of 1-aza-2-azoniaallene salts. These reactions were discussed in detail in Chapters 1 and 2.

3.2 Preparation of α -chloroazo compounds and their stability

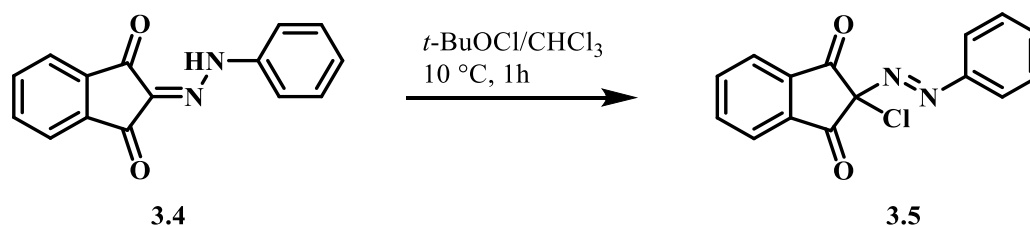
The first synthesis of α -chloroazo compounds was reported by Moon in 1972. In this procedure, hydrazone derivatives were treated with either chlorine or *tert*-butyl hypochlorite.²⁰⁻²² He reported that the stability of these azo compounds depended on the substituents attached to the α -position. Several azo compounds were prepared by chlorination of ketone phenylhydrazone derivatives, and these were not very stable; chromatography on silica gel led to decomposition. Although these azo compounds were not stable at room temperature for prolonged periods, some of the azo compounds were stable in ethanolic solutions of hydrochloric acid or sodium hydroxide at ambient temperature.²⁰ Hydrazone derivatives containing electron-withdrawing groups on the carbon of the C-N double bond gave more stable α -chloroazo products that could be purified using silica gel chromatography. For an example, compound **3.3** (Scheme 3.1) was thermally stable up to 250 °C, at which point it decomposed to release nitrogen gas.²⁰



Scheme 3.1. Formation of α -chloroazo compound from hydrazone and chlorine.

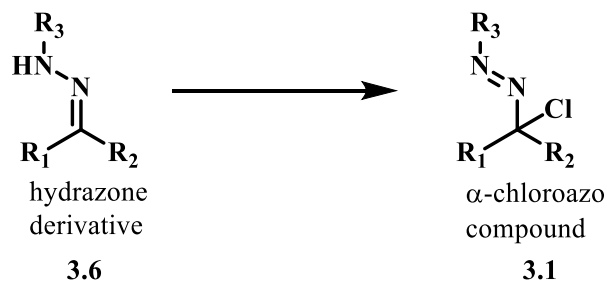
When Moon used electron rich aromatic substituents on the hydrazone derivatives, the aryl ring underwent chlorination before the carbon-nitrogen double bond. To solve

this problem, he replaced chlorine with the less powerful chlorinating agent *tert*-butyl hypochlorite (Scheme 3.2).²¹



Scheme 3.2. Formation of α -chloroazo compound from hydrazone and *tert*-butyl hypochlorite.

Jochims and coworkers used Moon's methods to synthesize a variety of α -chloroazo compounds (3.1, Scheme 3.3).¹⁻⁹ Table 3.1 shows examples of α -chloroazo compounds (3.1) synthesized by Jochims and coworkers starting from the corresponding hydrazone derivatives (3.6).

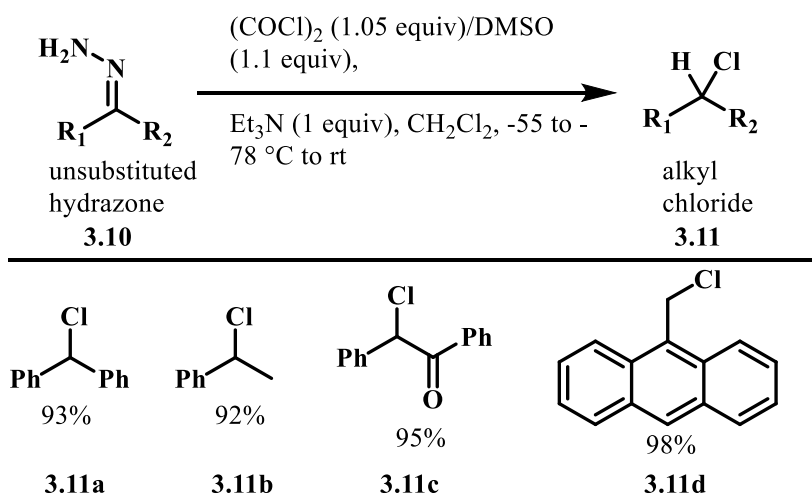


Scheme 3.3. Formation of α -chloroazo compounds from the corresponding hydrazone derivatives.

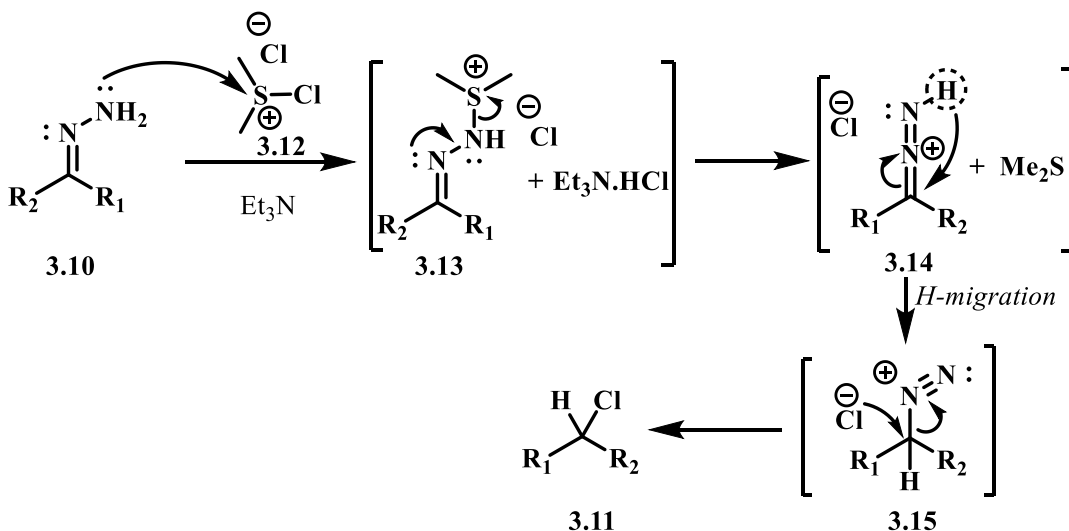
Table 3.1. Examples of α -chloroazo compounds prepared by Jochims and coworkers

entry	R ₁	R ₂	R ₃	reagent	conditions	yield
1	Me	Me	2,4,6-Cl ₃ C ₆ H ₂	<i>t</i> -BuOCl	CH ₂ Cl ₂ , -50 to 0 °C, 3h	99%
2	H	Me	<i>t</i> -Bu	<i>t</i> -BuOCl	CH ₂ Cl ₂ , -50 to 0 °C, 3h	80%
3	(CH ₂) ₅	-	2,4,6-Cl ₃ C ₆ H ₂	<i>t</i> -BuOCl	CH ₂ Cl ₂ , -50 to 0 °C, 3h	78%
4	Et	H	2,4,6-Cl ₃ C ₆ H ₂	<i>t</i> -BuOCl	CH ₂ Cl ₂ , -50 to 0 °C, 3h	92%
5	Me	Me	<i>t</i> -Bu	<i>t</i> -BuOCl	CH ₂ Cl ₂ , -50 to 0 °C, 3h	94%

reaction, hydrazone **3.10** reacts with the dimethylchlorosulfonium ion (**3.12**, Scheme 3.6) generated from DMSO and oxalyl chloride to provide diazosulfonium ion **3.13**. Loss of dimethyl sulfide gives *N*-protonated diazonium ion **3.14**, which tautomerizes to give the diazonium ion **3.15**. Loss of nitrogen and attack by chloride give the final product (**3.11**).

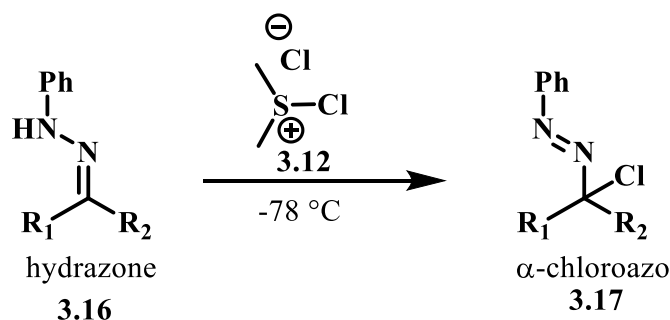


Scheme 3.5. Formation alkyl chloride from unsubstituted hydrazone.



Scheme 3.6. Proposed mechanism for the formation of alkyl chlorides from hydrazones and dimethylchlorosulfonium ion.

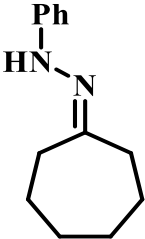
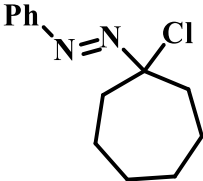
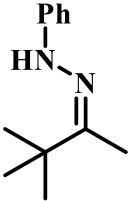
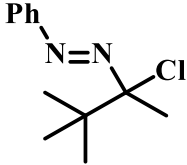
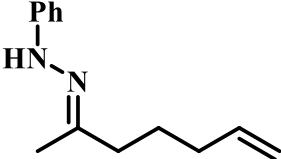
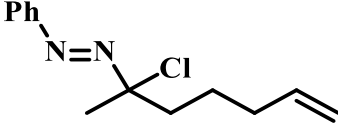
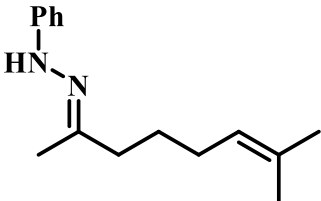
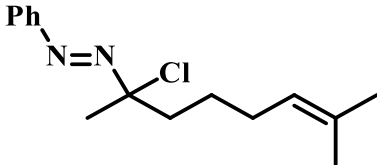
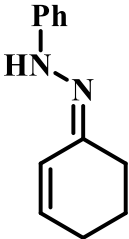
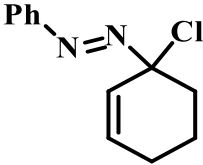
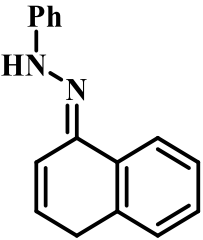
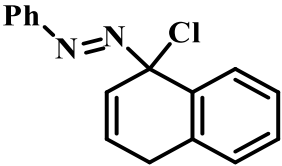
With these results in hand, the Brewer group was interested to carry out this reaction with hydrazones bearing a substituent on the terminal nitrogen. In doing so, the Brewer group surprisingly obtained phenyl- α -chloroazo compounds (**3.17**) in good yield without chlorination of the phenyl ring (Scheme 3.7).²⁴ In exploring of the scope of this reaction, they discovered that hydrazones containing pendent alkenes underwent this reaction very smoothly to give the desired products without chlorination of the alkene (e.g. entries 5 and 6, Table 3.2). However, this method failed to provide the desired α -chloroazo products of allylic and benzylic hydrazones (e.g. entries 7 and 8, Table 3.2).



Scheme 3.7. Formation of phenyl- α -chloroazo compound from phenyl hydrazones.

Table 3.2. A variety of examples of phenyl- α -chloroazo compounds that form from the corresponding phenyl hydrazones under Swern oxidation condition

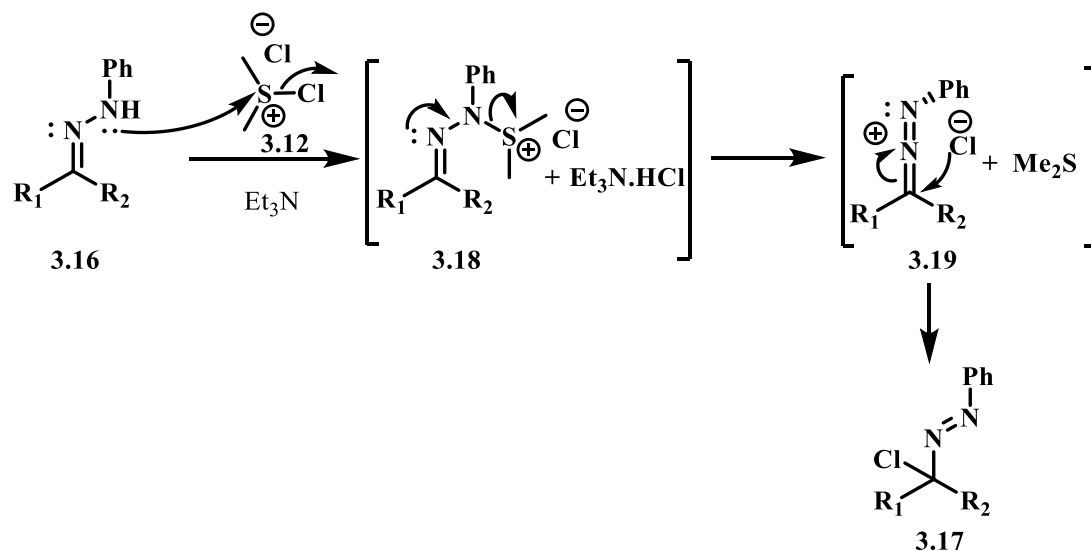
entry	substrate (hydrazone)	product (α -chloroazo)	yield
1			81%
2			78%

3			54%
4			59%
5			83%
6			94%
7			0
8			0

The Brewer group also purposed a mechanism for this reaction, which is shown in Scheme 3.8. The lone pair of electrons on the aryl amine is thought to attack the sulfonium ion (**3.12**) to give aza sulfonium salt **3.18**. Elimination of dimethyl sulfide would give the phenyl-1-aza-2-azoniaallene salt **3.19**, which would then react with a

chloride counter ion at the heteroallene carbon to form phenyl- α -chloroazo compound

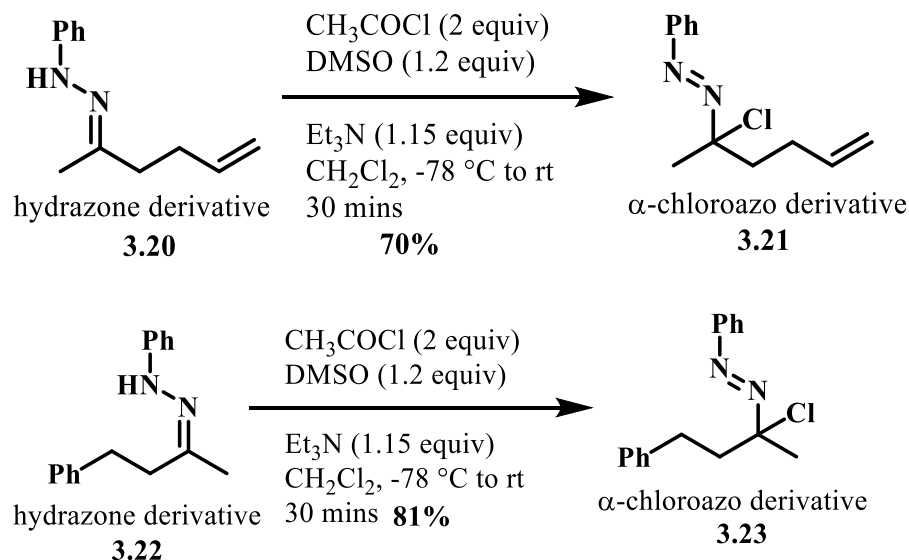
3.17.



Scheme 3.8. Proposed mechanism for formation of α -chloroazo compounds under Swern oxidation conditions.

3.4 Discovery of a new method with acetyl chloride

It is known that acetyl chloride can also activate DMSO for Swern-type oxidations,²⁶ and we were interested to know how this reagent combination would affect hydrazone oxidation. So, I treated acetyl chloride with DMSO at -55 °C to generate the DMSO activated species, and then added a dichloromethane solution of hydrazone and Et₃N at -78 °C, which gave the expected α -chloroazo product in yields similar to the original procedure that used oxalyl chloride as activating agent. Using acetyl chloride, hydrazones **3.20** and **3.22** gave the desired products **3.21** and **3.23** in 70% and 84% yields respectively (Scheme 3.9), while using oxalyl chloride¹⁷ gave the same products in 84% and 97% yields. We concluded that while acetyl chloride is effective for this conversion, it is not optimal.

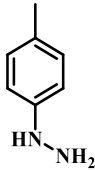
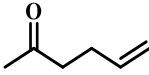
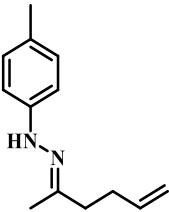
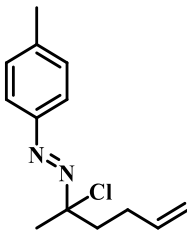
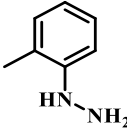
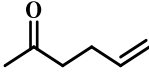
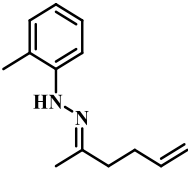
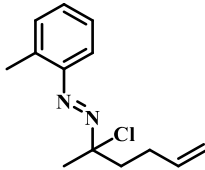
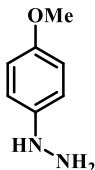
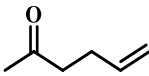
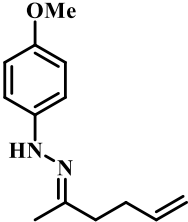
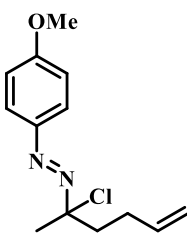
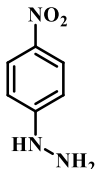
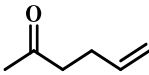
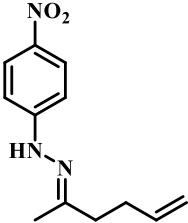
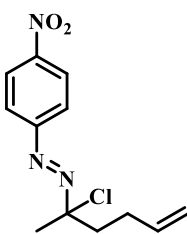
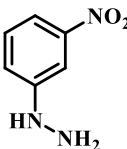
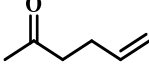
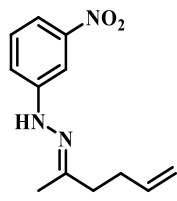
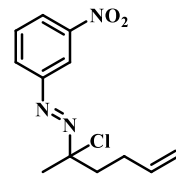
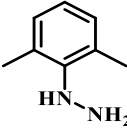
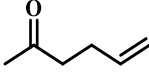
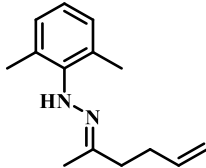
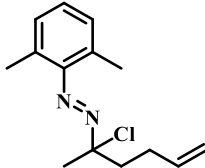


Scheme 3.9. Test reactions to form α -chloroazo compounds using acetyl chloride as activating agent.

3.5 Effect of aryl ring substitution on α -chloroazo formation

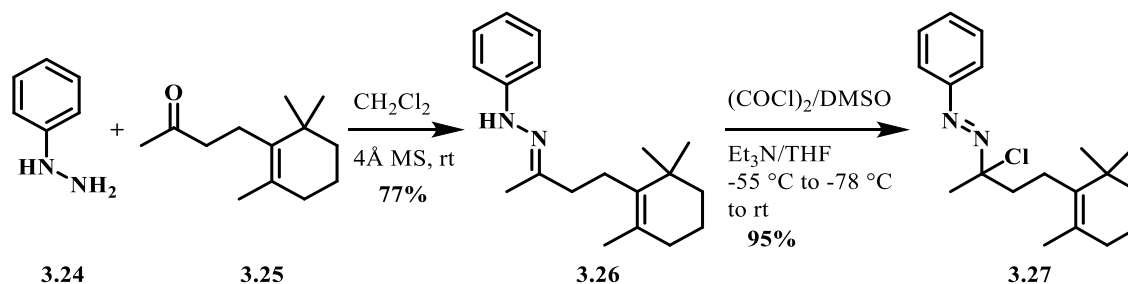
In order to assess the effect of aryl ring substitution on the [4+2] cycloaddition, I had to prepare a variety of α -chloroazo compounds. To do this, I first prepared the corresponding hydrazone derivatives shown in Table 3.3 from *N*-aryl hydrazines and 5-hexen-2-one. These hydrazone derivatives were then treated with chlorodimethylsulfonium chloride (generated *in situ* by reacting oxalyl chloride, DMSO, and triethylamine at -55°C) at -78°C to give the corresponding α -chloroazo compounds.^{23,24} Methyl (Entries 1 and 2, Table 3.3), dimethyl (Entry 6), and methoxy (Entry 3), substituents provided excellent product yields, whereas nitro aryl substituents (Entries 4 and 5) provided intractable mixtures. Due to the instability of the azo products, we were unable to purify these nitro derivatives.

Table 3.3. Formation of hydrazones and α -chloroazo compounds

entry	hydrazine	ketone	hydrazone	yield ^a	α -chloroazo	yield ^b
1				75%		94%
2				83%		95%
3				64%		95%
4				65%		Not pure
5				78%		Not pure
6				92%		93%

a = yield of hydrazones, *b* = yield of α -chloroazo compounds

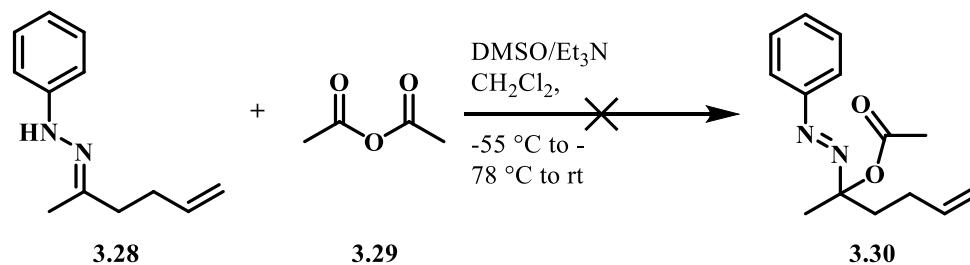
The phenyl hydrazone of dihydro- β -ionone (**3.26**) (Scheme 3.10) also reacted cleanly with chlorodimethylsulfonium chloride to give the desired α -chloroazo compound **3.27** in an excellent yield.



Scheme 3.10. Formation of an α -chloroazo compound of sterically hindered alkene.

3.6 New methods to form α -substituted azo compounds

With unsuccessful attempts to form α -chloroazo derivatives from nitro aryl compounds in mind, we were interested to develop new methods to form α -substituted azo products. Our first goal was to replace chlorodimethylsulfonium chloride by a suitable reagent. I first attempted to prepare α -acetoxyazo compounds (**3.30**) by treating the phenyl hydrazone and acetoxydimethylsulfonium acetate, but this reaction failed (Scheme 3.11). In this reaction, I recovered all the starting material **3.28**.

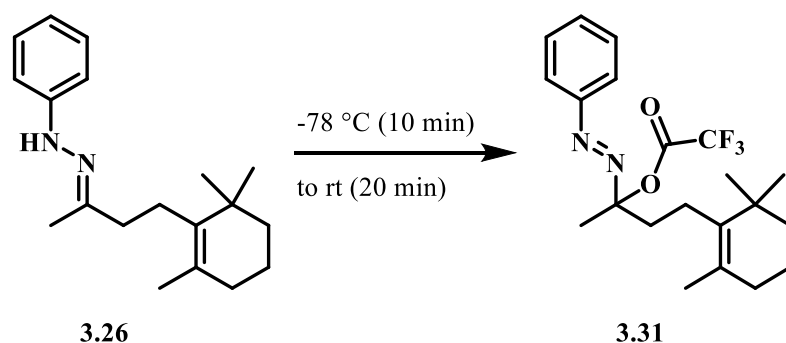


Scheme 3.11. Unsuccessful attempt to prepare α -acetoxyazo compound.

In a second attempt, I used trifluoroacetic anhydride (TFAA) as DMSO activating agent, which surprisingly provided the desired product with high purity. With this result

in hand, I optimized this method by changing a variety of conditions (Table 3.4). When I used 2.2 equivalents of TFAA, 2.5 equivalents of DMSO, and 2.5 equivalents of triethyl amine in DCM at -78 °C, the product **3.31** was isolated in 89% yield (Entry 1, Table 3.4). However, this material contained some triethyl ammonium salt. Changing to 1.1 equivalents of TFAA, 1.2 equivalents of DMSO, and 1.5 equivalents of Et₃N in DCM provided the desired product in 89% yield (Entry 2). Changing the solvent to THF gave the product in 84% yield (Entry 3). Therefore, the conditions described in entry 2 were determined to be the best choice.

Table 3.4. Optimization to α -trifluoroacetoxyazo compounds

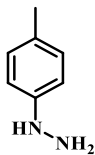
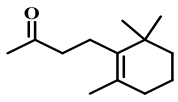
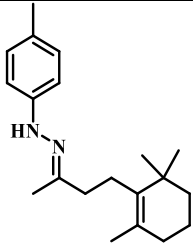
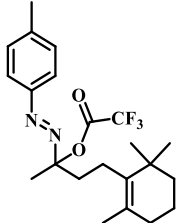
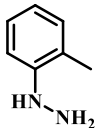
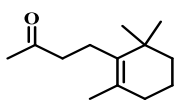
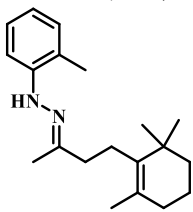
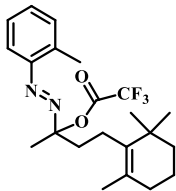
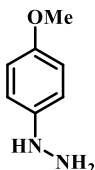
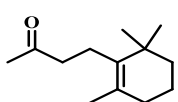
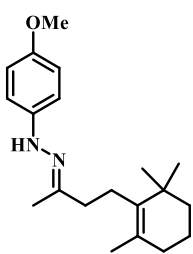
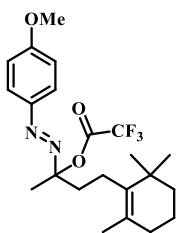
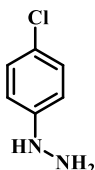
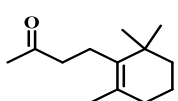
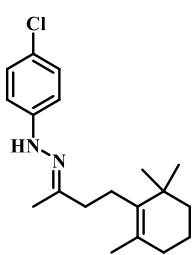
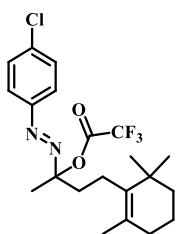
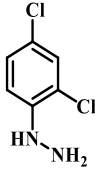
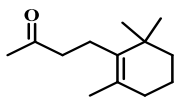
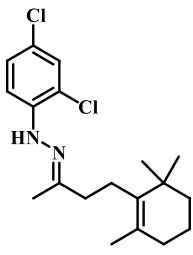
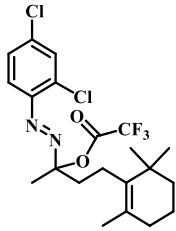


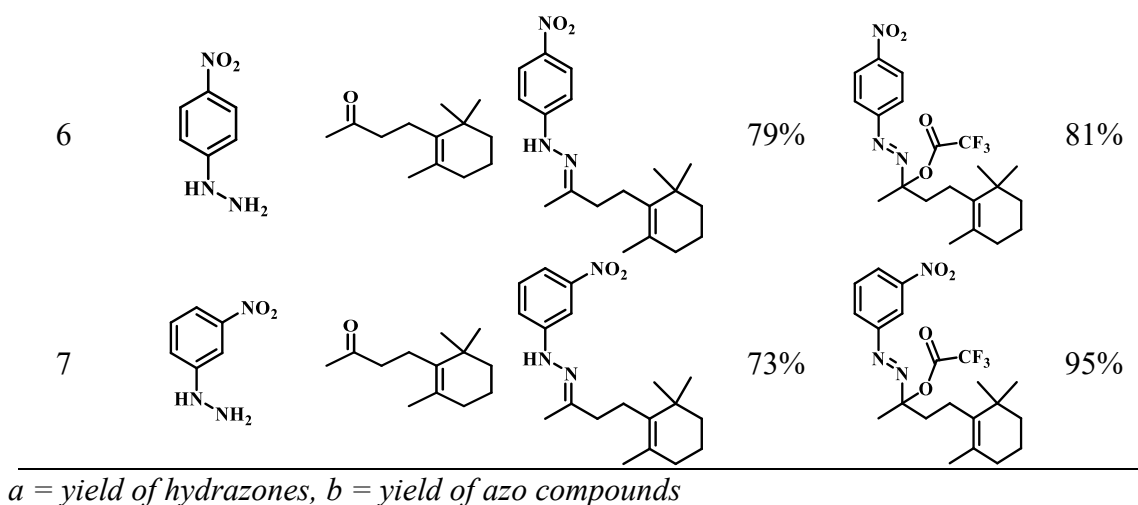
entry	solvent	TFAA	DMSO	Et ₃ N	yield	note
1	CH ₂ Cl ₂	2.0 equiv	2.5 equiv	2.5 equiv	89%	Observed peaks of Et ₃ NH ⁺
2	CH ₂ Cl ₂	1.1 equiv	1.2 equiv	1.15 equiv	87%	Pure (best)
3	THF	1.1 equiv	1.2 equiv	1.15 equiv	84%	Pure (lower) yield)

I next carried out this reaction with substrates that contain a sterically hindered pendent alkene. We were pleased to observe that the reaction was successful for all substituted *N*-aryl hydrazones. Methyl (Entries 1 and 2, Table 3.5), methoxy (Entry 3), chloride (Entry 4), dichloride (Entry 5), and nitro (Entries 6 and 7) substituted aryl

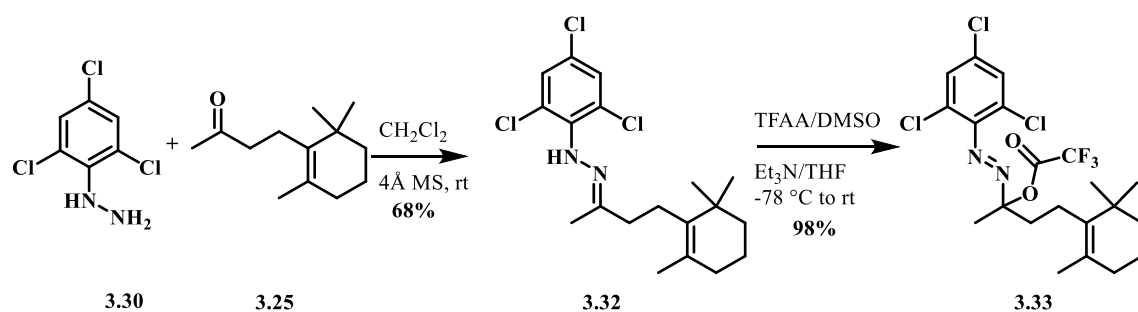
hydrazones underwent this reaction very smoothly to provide the desired products in good yields.

Table 3.5. Formation of a variety of hydrazones and α -chloroazo compounds using trifluoroacetoxy dimethylsulfonium trifluoroacetate as an oxidant

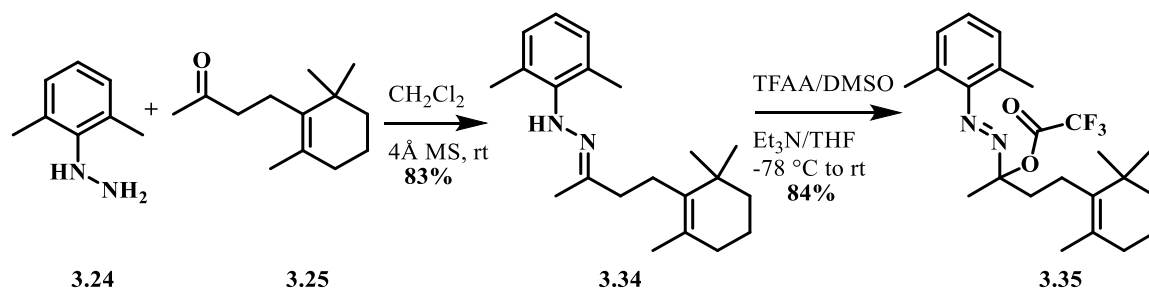
entry	hydrazine	ketone	hydrazone	yield ^a	azo-product	yield ^b
1				76%		76%
2				85%		83%
3				57%		76%
4				55%		86%
5				53%		90%



We were also interested to see if hydrazones with poly-substituted *N*-aryl rings would react productively. We were pleased to see that hydrazone **3.32** (Scheme 3.12a) provided the desired azo product **3.33** in 98% yield. In additions, the dimethyl substituted compound **3.34** (Scheme 3.12b) also gave the desired product **3.35** in very good yield.



Scheme 3.12a. Formation of azo product from trichloro-substituted compound.

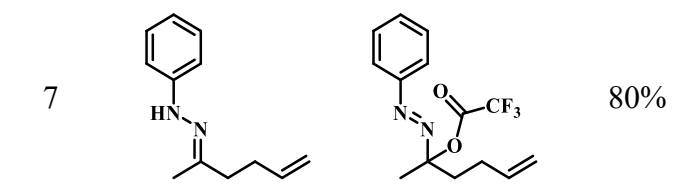


Scheme 3.12b. Formation of azo product from dimethyl-substituted compound.

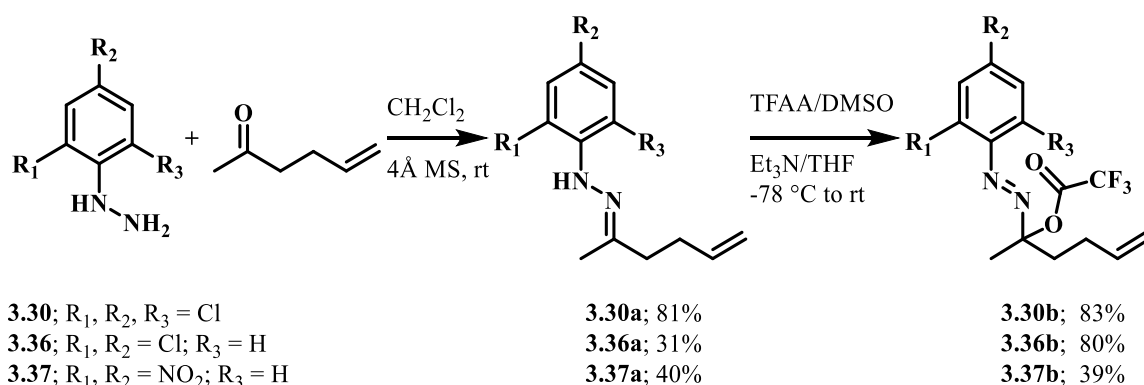
Predictably, hydrazones derived from 5-hexene-2-one also gave the desired azo products in very good yields (Table 3.6).

Table 3.6. Scope of reaction with a simple pendent alkene

entry	hydrazone	azo-compound	yield
1			69%
2			65%
3			74%
4			82%
5			88%
6			80%



To understand the electronic effects of the *N*-aryl ring, I carried out this reaction with hydrazones containing two or three electron withdrawing groups. Tri- and di-chlorosubstituted compounds (**3.30a** and **3.36b**, Scheme 3.13) provided the desired products (**3.30b** and **3.36b**) in very good yields, while di-nitrosubstituted compound (**3.37a**) gave the desired product **3.37b** in low yield.

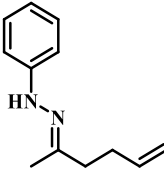
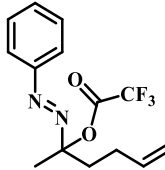
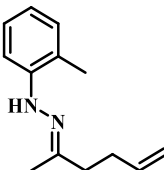
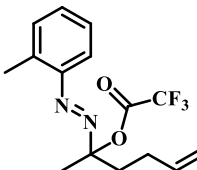
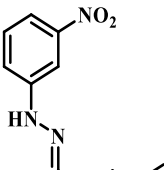
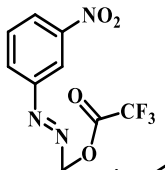
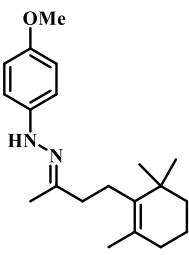
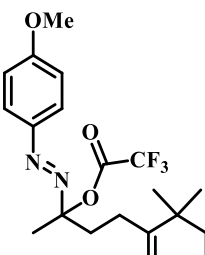
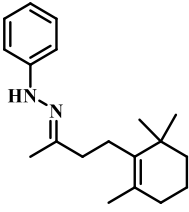
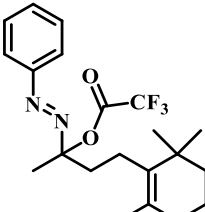


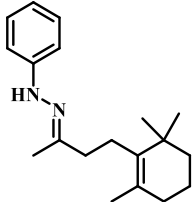
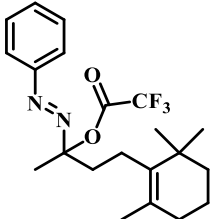
Scheme 3.13. Formation of azo product with dimethyl-substituted *N*-aryl ring.

With further experimentation, we discovered that a hexane solution of hydrazone, DMSO, and Et₃N can be treated with TFAA at 0 °C to provide the desired product in good yield. Although hydrazones that contain the unhindered pendent alkene (entries 1, 2, and 3; table 3.7) and sterically hindered pendent alkenes (entry 5) gave the desired product in very good yields, a methoxy substituent on the aryl ring (entry 4) resulted in comparatively low yield. Although this reaction afforded the desired product in good yield at room temperature (entry 6, table 3.7), this condition was not practically feasible because of the exothermic nature of the reaction. The 0 °C procedure, which is effectively

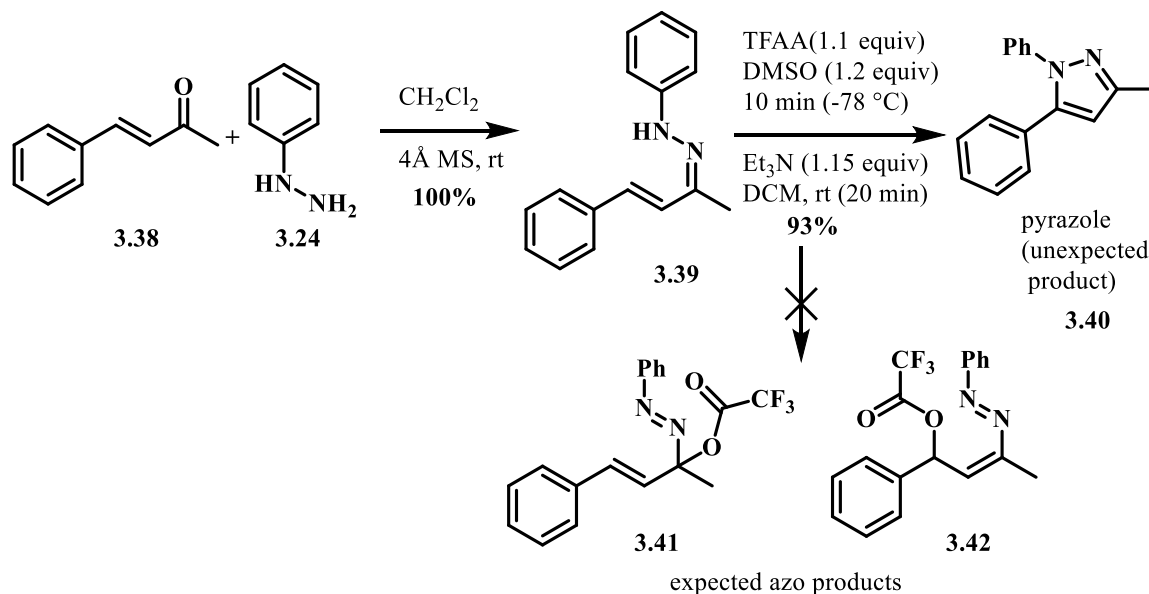
simpler than low-temperature conditions, is remarkable because the trifluoroacetoxy dimethylsulfonium trifluoroacetate generated by the activation of DMSO with TFAA is known to decompose above -30 °C.²³⁻²⁵ In this case, the low polarity of the solvent likely slows the decomposition of the activated DMSO species, allowing the hydrazone to react with the *in situ* generated oxidant.

Table 3.7. Further experimentation to form α -trifluoroacetoxyazo compound

entry	hydrazone	condition	azo-product	yield
1		TFAA (1.1 equiv), DMSO (1.1 equiv), Et ₃ N (1.15 equiv), hexane, 0 °C to rt		87%
2				62%
3				79%
4				57%
5				82%

6		TFAA (1.1 equiv), DMSO (1.1 equiv), Et ₃ N (1.15 equiv), hexane , rt		80%
---	---	---	---	-----

In continuing to explore the scope of this reaction, we were interested to see if allylic hydrazones could react productively because previously²⁴ these hydrazones did not give the corresponding α -chloroazo compounds when treated with chlorodimethylsulfonium chloride. Treating hydrazone **3.39** with trifluoroacetoxy dimethylsulfonium trifluoroacetate at -78 °C, surprisingly gave pyrazole product **3.40** in 93% yield instead of an α - or β -substituted azo product (**3.41** or **3.42**, Scheme 3.14).

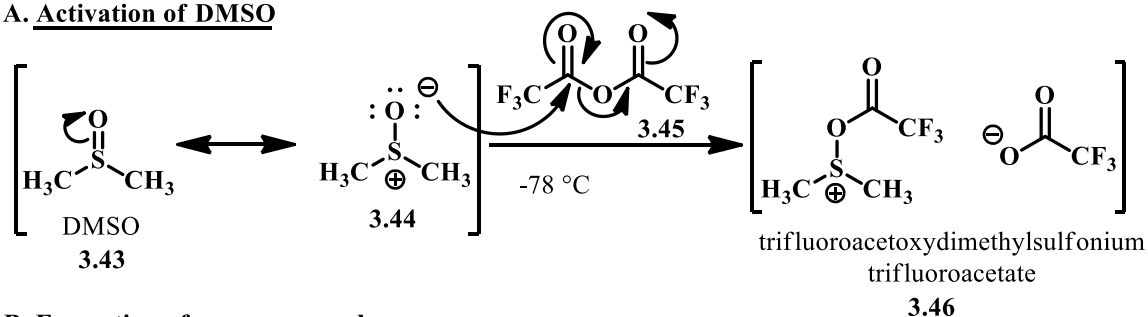


Scheme 3.14. Unexpected result during the attempted formation of an azo product from an allylic hydrazone.

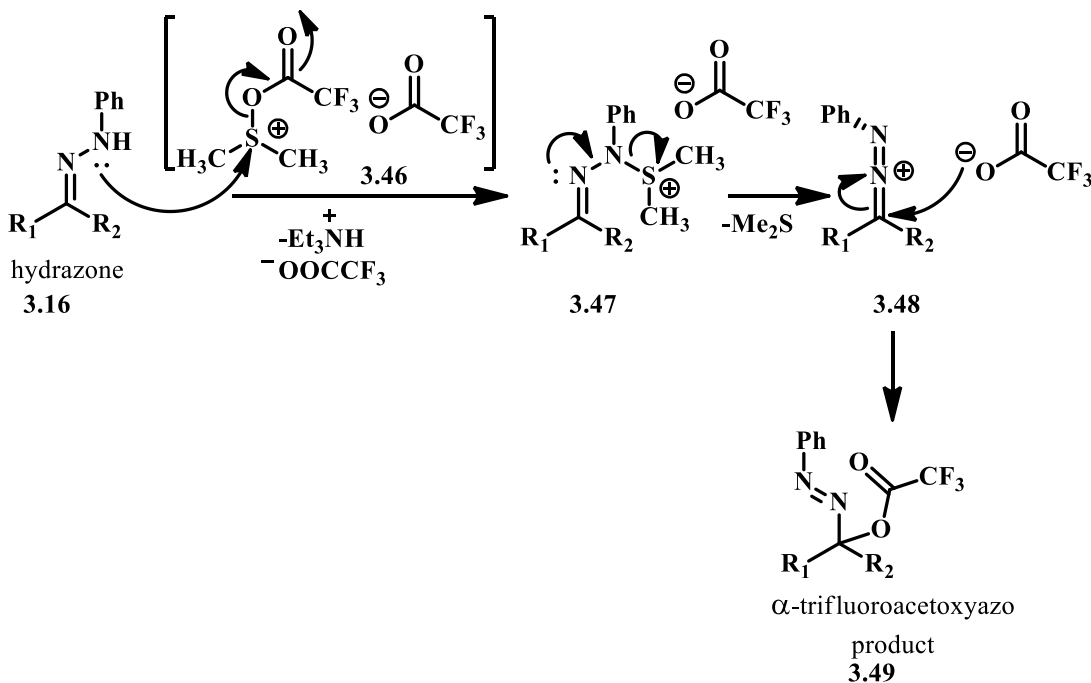
3.7 Proposed mechanism for formation of α -trifluoroacetoxyazo compound

We propose that mechanism of α -trifluoroacetoxyazo formation is analogous to that of α -chloroazo formation. In this case, DMSO is activated by TFAA to give trifluoroacetoxydimethylsulfonium trifluoroacetate (**3.46**, Scheme 3.15, A), which reacts with the aryl hydrazone to give aza sulfonium **3.47** (Scheme 3.15, B). Loss of dimethylsulfide gives aryl-1-aza-2-azoniaallene salt **3.48**, which reacts with trifluoroacetate to provide the desired product **3.49**.

A. Activation of DMSO



B. Formation of azo compound



Scheme 3.15. Proposed mechanism for the formation of α -trifluoroacetoxyazo products.

3.8 Conclusions

α -Chloroazo compounds serve as precursors to 1-aza-2-azaniaallene salts, which can lead to monocyclic, bicyclic, tricyclic, and tetracyclic compounds via cycloaddition reactions, C-H aminations, or alkene additions. The Brewer group developed a new strategy to prepare this precursor based on the Swern oxidation of hydrazones. The strategy developed by the Brewer group was not compatible with aryl hydrazones bearing electron withdrawing functional groups. For example, nitro aryl compounds did not undergo this reaction very smoothly. So, I developed a new method to prepare α -substituted azo compounds, in which trifluoroacetic anhydride activates the DMSO to give trifluoroacetoxy dimethylsulfonium trifluoroacetate, which further reacts with arylhydrazones to give α -trifluoroacetoxyazo compounds. This technique is compatible with all types of functional groups. Notably, aryl-nitro hydrazones are easily converted into the corresponding azo products. For reasons that are not clear, this method converts allylic hydrazones into the corresponding pyrazole derivatives.

References

1. Wang, Q. R.; Jochims, J. C.; Kohlbrandt, S.; Dahlenburg, L.; Altalib, M.; Hamed, A.; Ismail, A. E. H. *Synthesis* **1992**, 710.
2. El-Gazzar, A-R. B. A.; Scholten, K.; Guo, Y.; Weibenbach, K.; Hitzler, M.; Roth, G.; Fischer, H.; Jochims, J. C. *J. Chem. Soc., Perkin Trans. 1* **1999**, 1999.
3. Hassan, N. A.; Mohamed, T. K.; Abdel Hafez, O. M.; Lutz, M.; Karl, C. C.; Wirschun, W.; Al-Soud, Y. A.; Jochims, J. *J. Prakt. Chem.* **1998**, 340, 151.
4. Wang, Q. R.; Amer, A.; Troll, C.; Fischer, H.; Jochims, J. C. *Chem. Ber.* **1993**, 126, 2519.
5. Wang, Q.; Mohr, S.; Jochims, J. C. *Chem. Ber.* **1994**, 127, 947.
6. Wirschun, W.; Jochims, J. *Synthesis*, **1997**, 233.

7. Wirschun, W. G.; Al-Soud, Y. A.; Nusser, K. A.; Orama, O.; Mailer, G-M.; Jochims, J. *J. Chem. Soc., Perkin Trans. 1* **2000**, 4356.
8. Al-Soud, Y. A.; Wirschun, W.; Hassan, N. A.; Maier, G. M.; Jochims, J. C. *Synthesis* **1998**, 721
9. Wang, Q. R.; Amer, A.; Mohr, S.; Ertel, E.; Jochims, J. C. *Tetrahedron* **1993**, 49, 9973.
10. Al-Soud, Y. A.; Al-Masoudi, N. A. *Heteroatom Chemistry* **2003**, 14, 298.
11. Gaonkar, S. L.; Rai, K. M. L. *Tetrahedron Lett.* **2005**, 46, 5969.
12. Javed, M. I.; Wyman, J. M.; Brewer, M. *Org. Lett.* **2009**, 11, 2189.
13. Wyman, J.; Javed, M. I.; Al-Bataineh, N.; Brewer, M. *J. Org. Chem.* **2010**, 75, 8078.
14. Al-Bataineh, N. Q.; Brewer, M. *Tetrahedron Lett.* **2012**, 53, 5411.
15. Bercovici, D. A.; Brewer, M. *J. Am. Chem. Soc.* **2012**, 134, 9890.
16. Hong, X.; Bercovici, D.; Yang, Z.; Al-Bataineh, N.; Srinivasan, R.; Dhakal, R.; Houk, K. N.; Brewer, M. *J. Am. Chem. Soc.* **2015**, 137, 9100.
17. Bercovici, D. A.; Ogilvie, J. M.; Tsvetkov, N.; Brewer, M. *Angew. Chem., Int. Ed.* **2013**, 52, 13338.
18. Dhakal, R. C.; Brewer, M. *Tetrahedron* **2016**, 72, 3718.
19. Al-Bataineh, N.; Houk, K. N.; Brewer, M.; Hong, X. *J. Org. Chem.* **2017**, 82, 4001.
20. Moon, M. W. *J. Org. Chem.* **1972**, 37, 383.
21. Moon, M. W. *J. Org. Chem.* **1972**, 37, 386.
22. Moon, M. W. *J. Org. Chem.* **1972**, 37, 2005.
23. Brewer, M. *Tetrahedron Lett.* **2006**, 47, 7731.
24. Wyman, J. M.; Jochum, S.; Brewer, M. *Synth. Comm.* **2008**, 38, 3623.
25. Javed, M.I., Brewer, M. *Org. Lett.* **2007**, 9, 1789.
26. Omura, K.; Swern, D. *Tetrahedron* **1978**, 34, 1651.

CHAPTER 4: 1,3-DIPOLAR CYCLOADDITION OF PROTONATED AZOMETHINE IMINE SALTS

4.1 Introduction

Azomethine imines (e.g. **4.1**, Figure 4.1), are synthetically useful 1,3-dipoles, that have been used to synthesize a variety of heterocyclic compounds, including tetrazepine derivatives,¹ spiro[pyrazolidine-3,3'-oxindoles],² 2-acryloyl-3-pyrazolidinone,³ five-membered nitrogen heterocycles,^{4,5,6} and (+)-manzacidin C.⁷ They react with a variety of π -systems via [3+2],⁸⁻¹⁰ [3+3],^{2,11,12} [4+3],^{1,13,14} [3+2+3],¹⁴ [5+1],¹⁵ and [5+3]¹⁶ cycloadditions to form pharmaceuticals, and biologically active compounds. These reactive intermediates can be classified into three groups based on their structure: acyclic, *C,N*-cyclic, and *N,N'*-cyclic azomethine imines (Figure 4.1).¹⁶⁻²³ These three types of azomethine imines have difference reactivities, which will be described in the following sections.

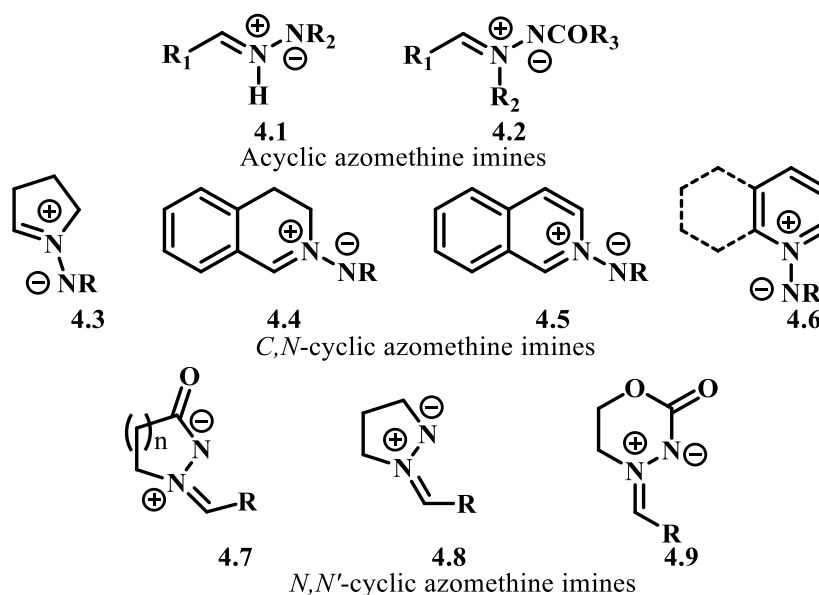
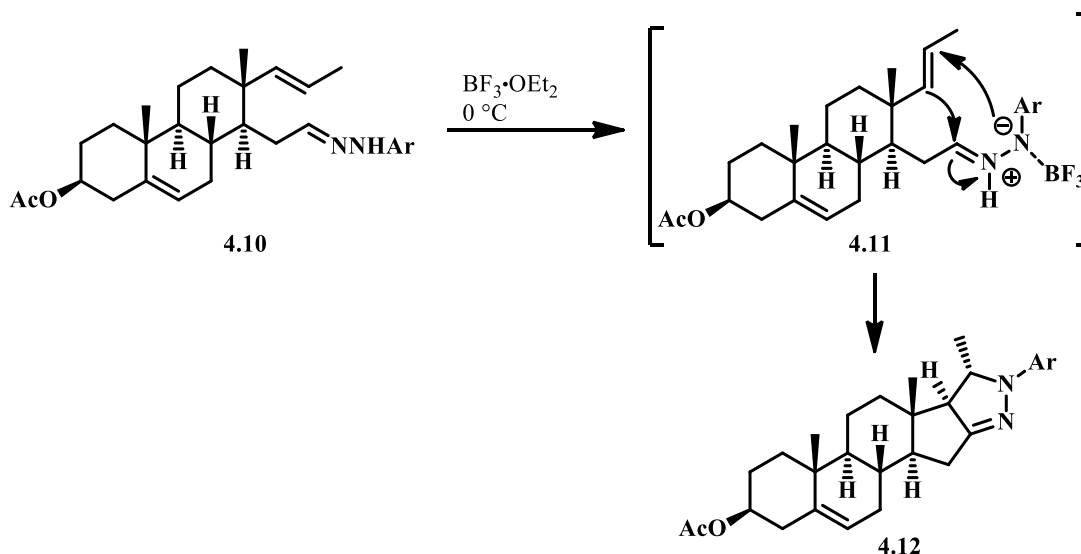


Figure 4.1. Classification of azomethine imines.

4.2 Reactivities of azomethine imines

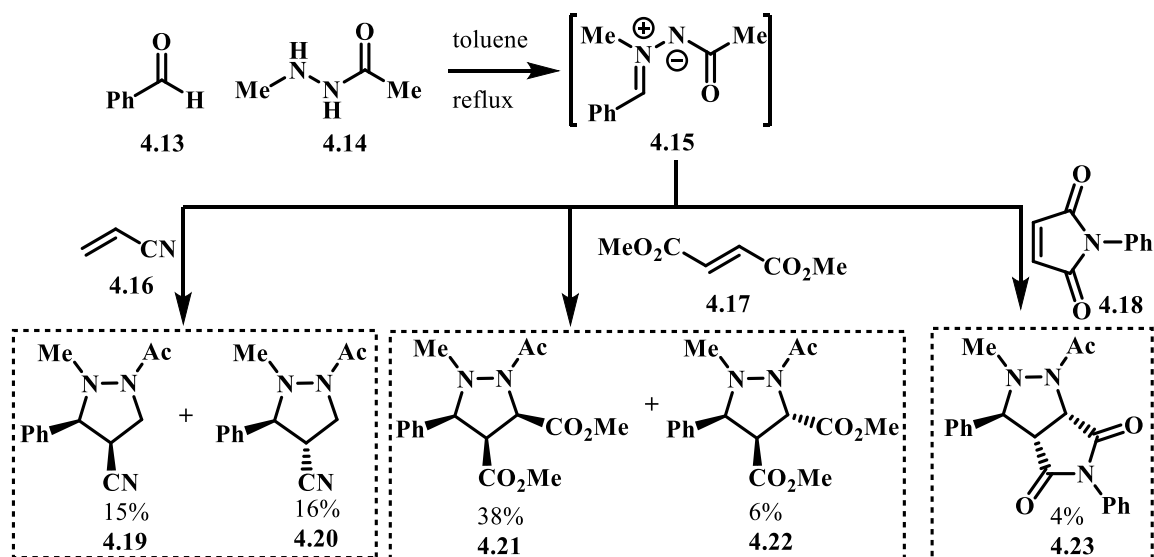
4.2.1 Acyclic azomethine imines

Acyclic azomethine imines are often generated under harsh reaction conditions, and have been used to prepare five-membered heterocycles through intra- and intermolecular cycloadditions.¹⁹ Nájera, Sansano, and Yus described a more mild procedure to facilitate an intramolecular cycloaddition that gives androstenoarylpyrazoline **4.12** (Scheme 4.1). This cycloaddition involves acyclic azomethine imine **4.11** which is formed in the presence of BF_3 and react via an intramolecular [3+2] cycloaddition with a pendent olefin.¹⁹



Scheme 4.1. An intramolecular [3+2] a cycloaddition of acyclic azomethine imine.

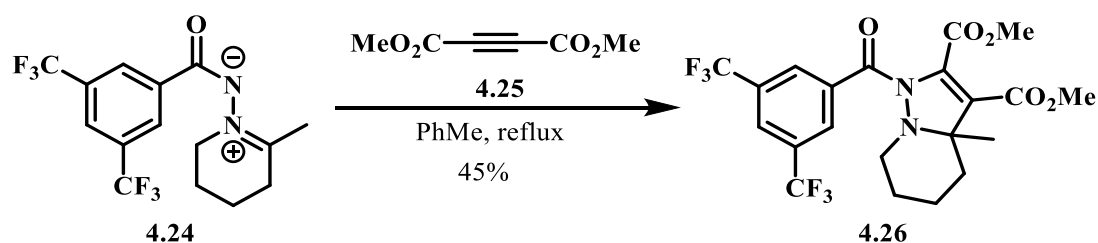
The Iley group reported that azomethine imine **4.15** (Scheme 4.2), generated *in situ* from benzaldehyde (**4.13**) and *N*-alkyl-*N*-acyl hydrazine (**4.14**), undergoes intermolecular cycloaddition reactions with electron-deficient dipolarophiles to give the corresponding 3,4-disubstituted pyrazolidenes as mixtures of *cis/trans* diastereomers in low yields.²⁴



Scheme 4.2. Intermolecular [3+2] cycloaddition of acyclic azomethine imine.

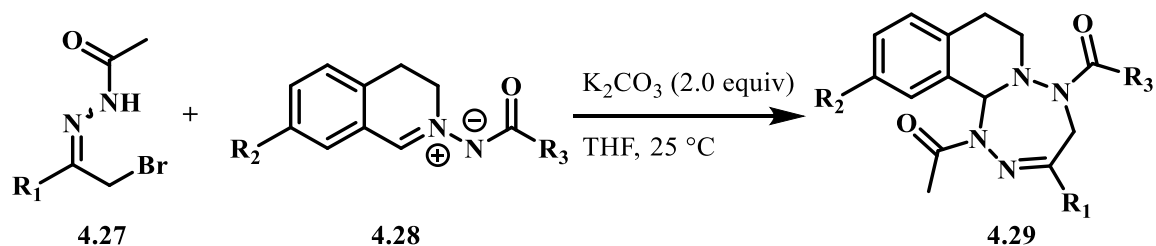
4.2.2 *C,N*-Cyclic azomethine imines

Heterocyclic compounds in which C-N double bond is incorporated into a ring are another class of azomethine imines. These types of compounds have been widely applied to synthesize a variety of ring-fused pyrazolines, pyrazoles, and pyrazolines.¹⁹ For example, azomethine imine **4.24** reacts with methyl acetylenedicarboxylate (**4.25**) to give fused pyrazoline **4.26** in 45% yield (Scheme 4.3).²⁵



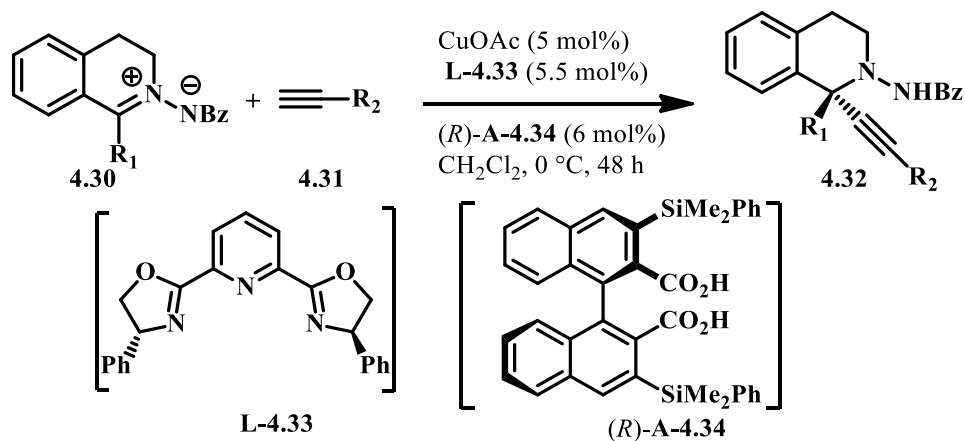
Scheme 4.3. Reaction of *C,N*-cyclic azomethine imine with acetylenedicarboxylate.

The Xiao group reported the synthesis of biologically important and highly functionalized 1,2,4,5-tetrazepine derivatives (**4.29**) via a [4+3] cycloaddition between a *C,N*-cyclic azomethine imine (**4.28**) and an azoalkene (**4.27**, Scheme 4.4).¹



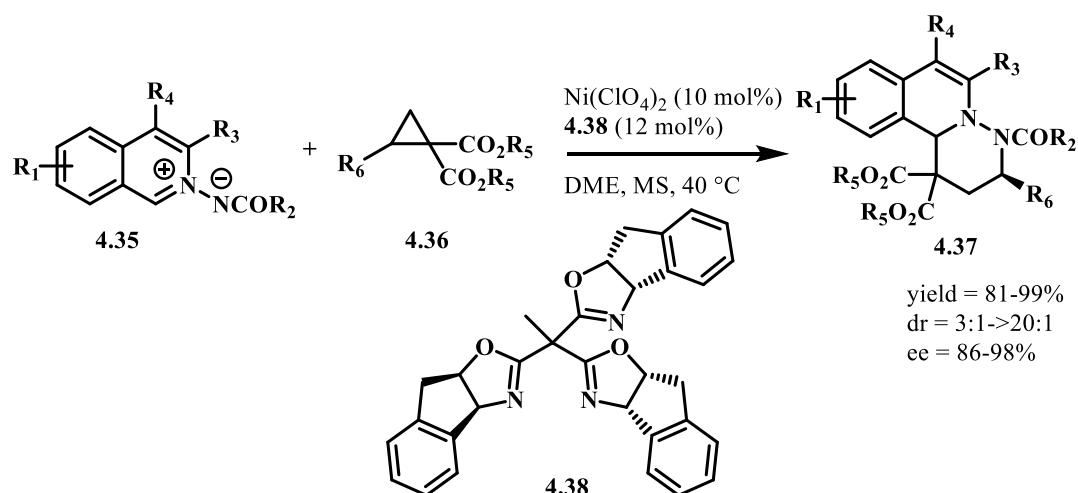
Scheme 4.4. Formation of 1,2,4,5-tetrazepine derivatives using *C,N*-cyclic azomethine imines with azoalkene via [4+3] cycloaddition.

A direct catalytic asymmetric alkynylation of *C,N*-cyclic azomethine imines (4.30) to provide chiral tetrahydroisoquinoline derivatives (4.32, Scheme 4.5) was described by Maruoka and coworkers.²⁶ This was the first catalytic asymmetric reaction wherein alkynes directly add to the carbon nitrogen double bond to give a chiral tetra-substituted carbon center with high enantioselectivity.



Scheme 4.5. Catalytic asymmetric alkynylation of *C,N*-cyclic azomethine imines.

The Tang group developed a highly enantioselective asymmetric [3+3] cycloaddition of cyclopropane diesters (4.36) with aromatic azomethine imines (4.35) catalyzed by $Ni(ClO_4)_2$ complex with trisoxazoline derivative (4.38) as a chiral ligand to afford a variety of 6,6,6-tricyclic dihydroisoquinoline derivatives (4.37) in high yields with excellent diastereo- and enantioselectivities (Scheme 4.6).²⁷

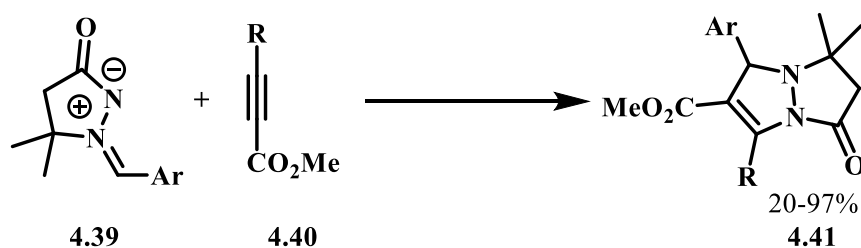


Scheme 4.6. Enantioselective [3+3] cycloaddition of azomethine imine and cyclopropane diesters.

4.2.3 *N,N'*-Cyclic azomethine imines

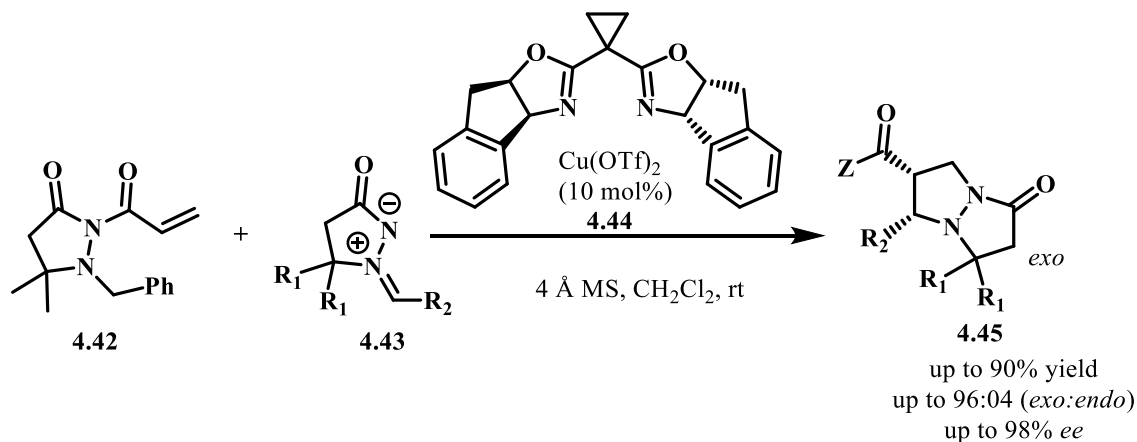
Azomethine imines, in which the N-N bond is incorporated in a ring are called *N,N'*-cyclic azomethine imines. They are more stable and more readily accessible than other types of azomethine imines. These heterocycles have been increasingly applied in preparing pyrazolones and related dinitrogen fused compounds, such as tetrahydropyrazolo-pyrazolones,²⁸ -pyridazinones,¹⁴ -diazepinones,¹⁴ and -diazocinones,¹⁴ which are important products or intermediates to synthesize a variety of biological active molecules.

Over the past years, a number of 1,3-dipolar cycloaddition reactions of *N,N'*-cyclic azomethine imines have been reported. For example, Svete and coworker described the [3+2] cycloaddition of azomethine imines (**4.39**) with dimethyl acetylenedicarboxylates **4.40** to provide 2,3-dihydro-1*H*-,5*H*-pyrazolo[1,2-*a*]-pyrazol-1-ones **4.41** (Scheme 4.7).²⁹



Scheme 4.7. [3+2] Cycloaddition of azomethine imines with alkyne.

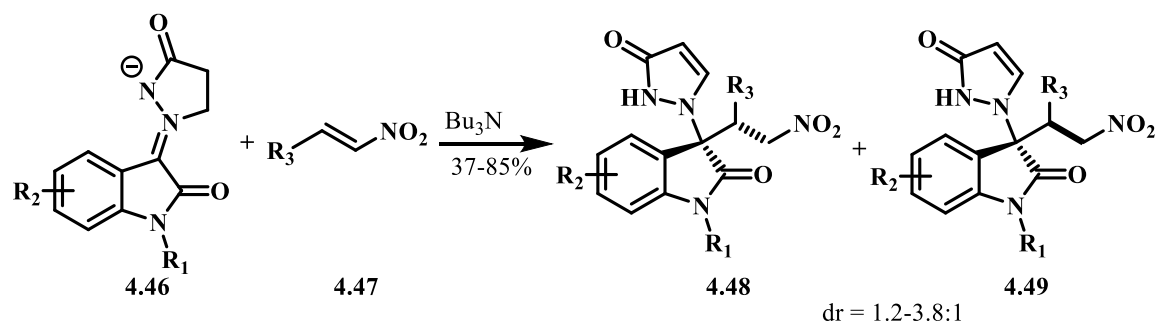
In an investigation of the catalytic and enantioselective cycloaddition of 1,3-dipoles with olefins, the Sibi group explored the first general strategy for copper (II)-catalyzed diastereoselective and enantioselective cycloadditions of azomethine imines (**4.43**) with pyrazolidinone acrylates (**4.42**) to give the cycloadduct **4.45** in good to high yields (Scheme 4.8).³⁰



Scheme 4.8. Copper-catalyzed diastereoselective and enantioselective cycloadditions of azomethine imines.

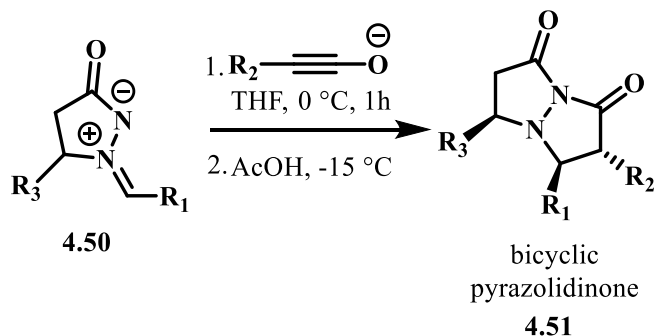
The Wang group reported that an isatin *N,N'*-cyclic azomethine imine **4.46** undergoes an uncommon Michael reaction with β -nitrostyrenes (**4.47**) catalyzed by tributylamine to afford 3-aminoxindoles **4.48** and **4.49** in good yields with moderate to good diastereoselectivities (Scheme 4.9).³¹ The 3-aminoxindole scaffold is found in variety of

biologically active species, such as AG-041R, SSR-149415, HIV protease inhibitors, and anticancer agents.³¹



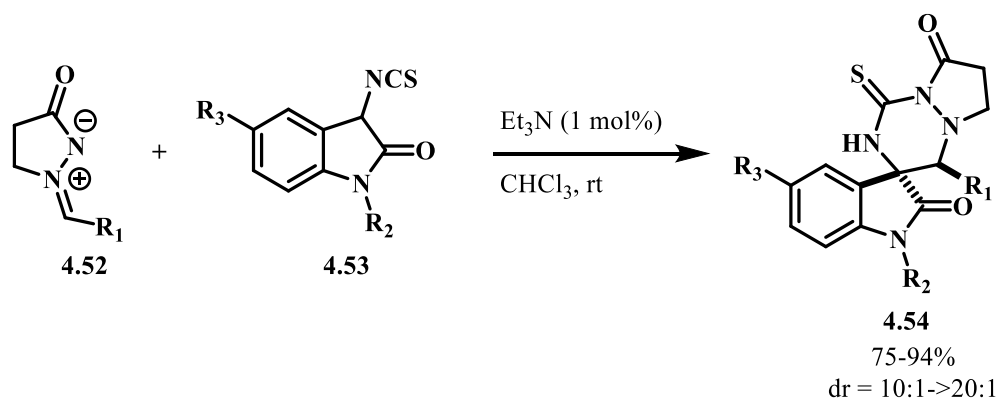
Scheme 4.9. Michael addition with isatin *N,N'*-cyclic azomethine imine.

The Ready group reported the synthesis of bicyclic pyrazolidinones (4.51) in high yields with good diastereoselectivities via a [3+2] cycloaddition of azomethine imines (4.50) with lithium ynolates (Scheme 4.10).⁸



Scheme 4.10. [3+2] Cycloaddition of azomethine imines with ynolates to form bicyclic pyrazolidinones.

The Wang group explored base-catalyzed [3+3] cycloadditions between azomethine imine 4.52 and 3-isothiocyanatooxindoles 4.53 to afford 3,3'-triazinyl spirooxindoles 4.54 in high yields and high diastereoselectivities (Scheme 4.11).³²



Scheme 4.11. Based-catalyzed [3+3] cycloaddition of azomethine imines.

4.3 Cycloaddition of protonated azomethine imine salts (*C,N* and *N,N'*-cyclic azomethine imines)

We derived a number of protonated azomethine imine salts (**4.0**) via the [4+2] cycloaddition of α -substituted azo compounds.^{33,34} This type of azomethine falls into both the *C,N*, and *N,N'*-cyclic azomethine imine classes (e.g. **4.0**, Figure 4.2) because the C-N-N bonds are incorporated in two different rings. These compounds are much more stable than cyclic azomethine imines. Although 1,3-dipolar cycloadditions of azomethine imines are very common, cycloadditions of protonated azomethine imine salts that have a C-N double bond and a N-N bond incorporated in two different rings is not common. Therefore, we were interested to see how the *C,N*, and *N,N'*-cyclic azomethine imines will react with a variety of π system.

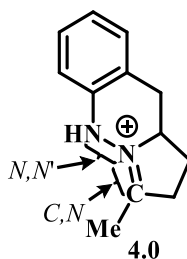
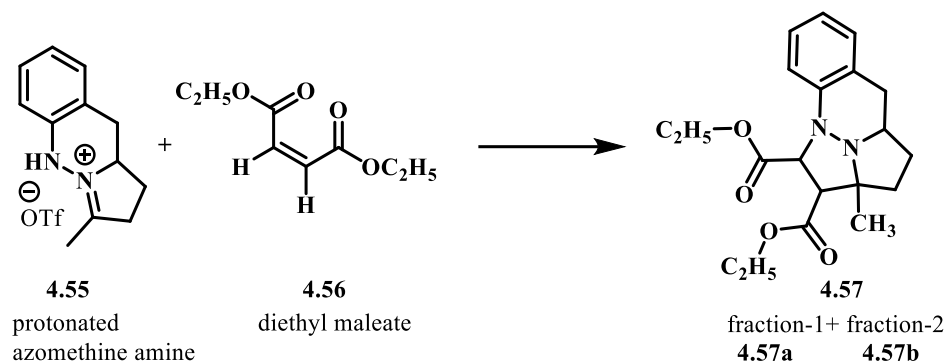


Figure 4.2. *C,N* or *N,N'*-Cyclic azomethine amine.

4.3.1 Optimization of intermolecular 1,3-dipolar cycloaddition of protonated azomethine imine salts

In order to establish that the protonated azomethine imine salt could serve as azomethine imine precursors for 1,3-dipolar cycloadditions, I selected diethyl maleate as cycloaddition partner because this is a doubly activated symmetrical dipolarophiles, which reacts stereospecifically with a variety of dienes in the Diels-Alder reaction,^{43,44} and triethylamine was taken as a base to form azomethine imine (Table 4.1). When the reaction was run at low temperature (-78 °C) in CH₂Cl₂ solvent, the desired cycloaddition occurred in 23% yield and returned two distereoisomers in a 1:22 diastereomeric ratio (Entry 1, Table 4.1). When the reaction temperature was raised to room temperature and the reaction time was extended to two hours, yield increased to 75% with 1:2.8 diastereoisomeric ratio (Entry 3). Changing the solvent to acetonitrile caused the yield to decrease slightly (70%) and gave 1:6.0 diastereoisomeric ratio (Entry 3). Extending the time to 16 hours under the same condition did not improve in yield (Entry 4). Changing the solvent to THF resulted in lower yields (Entries 5 and 6). Increasing the reaction temperature to 30 °C with dichloromethane as a solvent gave similar yield as the room temperature result (1:2.4 diastereoisomeric ratio; Entry 7). When the temperature was increased to 55 °C in acetonitrile for 1 hour, the reaction yield increased to 76% (1:4.8 diastereoisomer ratio; Entry 8), and extending the reaction time to 2 hours gave comparable yield with the same diastereoisomeric ratio (Entry 9). Ultimately, we discovered that lowering the equivalents of triethylamine to 1.3 significantly increased the yield while giving the same diastereoisomeric ratio (Entry 10), and these became the conditions of choice.

Table 4.1. Optimization of 1,3-dipolar cycloaddition of protonated azomethine imine

entry	reagent (equiv)	Et ₃ N (equiv)	solvent	time (hrs.)	temp.	yield	dr. ratio 4.57a: 5.57b
1	1.2	2.0	DCM	1	-78 °C	23%	1:22
2	1.2	2.0	DCM	2	rt	75%	1:2.8
3	1.2	2.0	CH ₃ CN	2	rt	70%	1:6.0
4	1.2	2.0	CH ₃ CN	16	rt	70%	1:5.3
5	1.2	2.0	THF	2	rt	65%	1:3.3
6	1.2	2.0	THF	16	rt	66%	1:3.4
7	1.2	2.0	DCM	2	30 °C	72%	1:2.4
8	1.2	2.0	CH ₃ CN	1	55 °C	76%	1:4.8
9	1.2	2.0	CH ₃ CN	2	55 °C	80%	1:5.1
10	1.2	1.3	CH ₃ CN	2	55 °C	90%	1:4.6

dr = diastereomeric

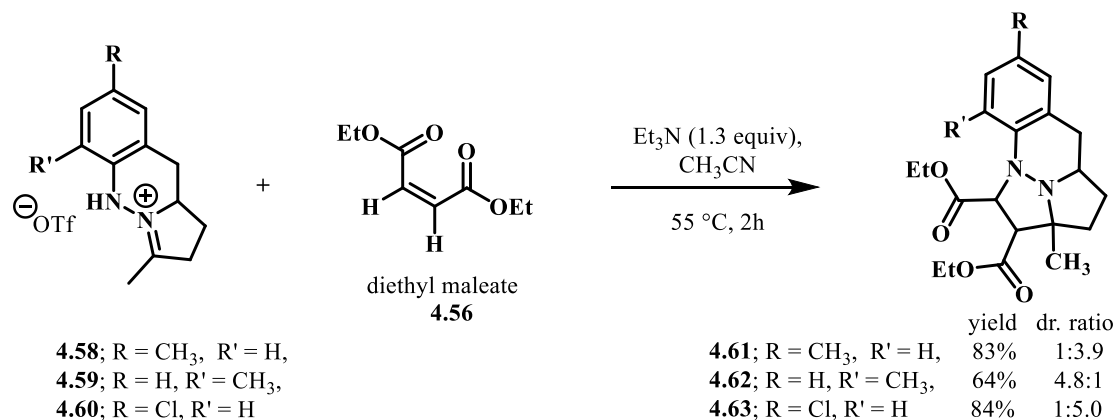
4.3.2 Reactions with dipolarophiles having activated alkenes

Both dialkyl maleate and fumarate are doubly activated symmetrical dipolarophiles, which generally react via a stereospecific intermolecular reaction in the Diels-Alder reaction.^{43,44} Our goal was to understand how the azomethine imines react with these reagents via 1,3-dipolar cycloadditions. These *cis* and *trans* reagents might also provide noteworthy information about the 1,3-dipolar reactions.

4.3.2.1 With diethyl and dimethyl maleates as dipolarophiles

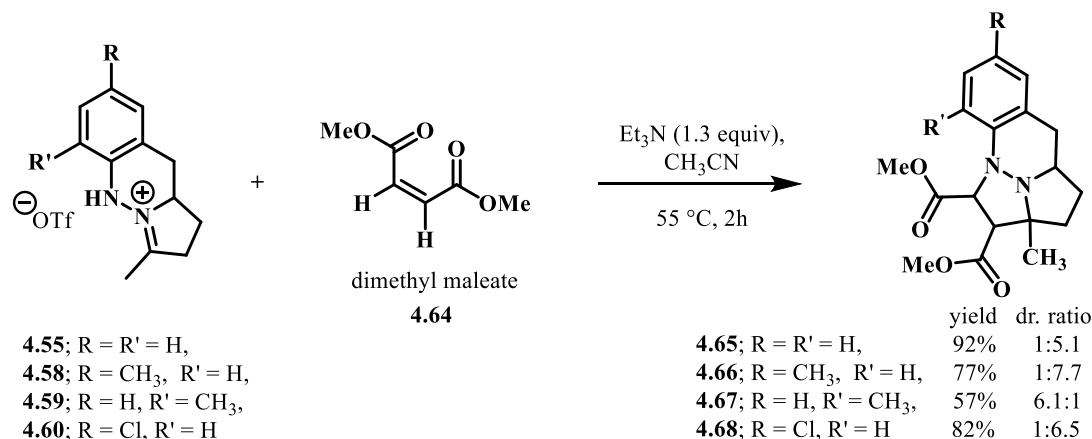
Using the optimized conditions, 1,3-dipolar cycloaddition between diethyl maleate and protonated azomethine imines (Scheme 4.12, **4.58** and **4.60**) that contain a methyl or chloride substituent at the *para*-position of the *N*-aryl ring provided the desired

tetracyclic products (**4.61** and **4.63**) in good yields (83% and 84%) and moderate diastereoselectivities (1:3.9 and 1:5.0). Changing the *N*-aryl methyl group to the *ortho*-position gave the cycloadduct **4.63** in lower yield (64%), but comparable diastereoselectivity (4.8:1).



Scheme 4.12. 1,3-Dipolar cycloaddition between protonated azomethine imines and diethyl maleate.

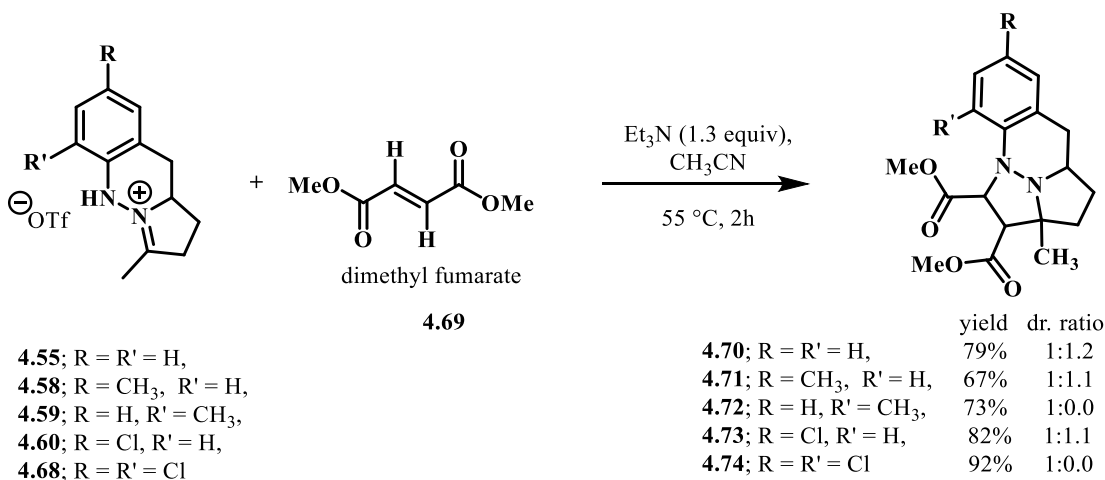
Replacing the diethyl maleate with dimethyl maleate, gave the corresponding products in comparable yields, but these reactions were somewhat more diastereoselective (Scheme 4.13).



Scheme 4.13. 1,3-Dipolar cycloaddition between azomethine imines and dimethyl maleate.

4.3.2.2 With dimethyl fumarate as dipolarophile

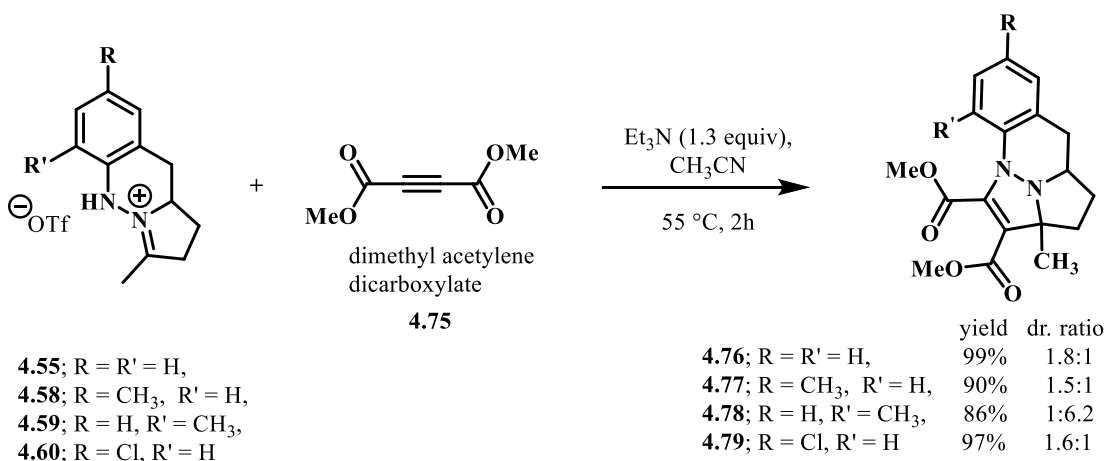
Changing the dipolarophile to dimethyl fumarate (**4.69**, Scheme 4.14), which is a *trans* form of dimethyl maleate (**4.64**, Scheme 4.13), provided the cycloadducts in good to excellent yields. However, the stereochemical outcome of these reactions were different than the cycloadducts formed from dimethyl maleate. *Cis* and *trans* alkenes provided unique diastereomers, so the 1,3-dipolar cycloaddition of azomethine imine occurs via concerted mechanism. In general, reactions involving dimethyl fumarate were less diastereoselective than those involving the maleate reagents. However, azomethine imines that had a methyl or chloride substituent at the *ortho*-position gave only one product diastereomer (**4.72** and **4.74**, Scheme 4.14) in 73% and 99% yield respectively. All other azomethine imines assessed the desired cycloadducts (**4.70**, **4.71** and **4.73**) in moderate to good yields with no diastereoselectivity.



Scheme 4.14. 1,3-Dipolar cycloaddition between protonated azomethine imines and dimethyl fumarate.

4.3.3 Reactions with dimethyl acetylene dicarboxylate as dipolarophile

To extend the scope of this cycloaddition reaction, we were interested to carry out this reaction with alkyne dipolarophiles. For example, dimethyl acetylene dicarboxylate (**4.75**, Scheme 4.15) is also a doubly activated symmetrical dipolarophile, which could also give important information for this 1,3-dipolar cycloaddition. After reacting this reagent with azomethine imines shown in Scheme 4.5 under optimized conditions, in each cases, the desired cycloaddition products were formed in excellent yields (86-99%). In most cases, diastereoselectivities were low, but the substitution at the *ortho*-position of the azomethine imine (**4.78**) increased the diastereomeric ratio to 1:6.2.

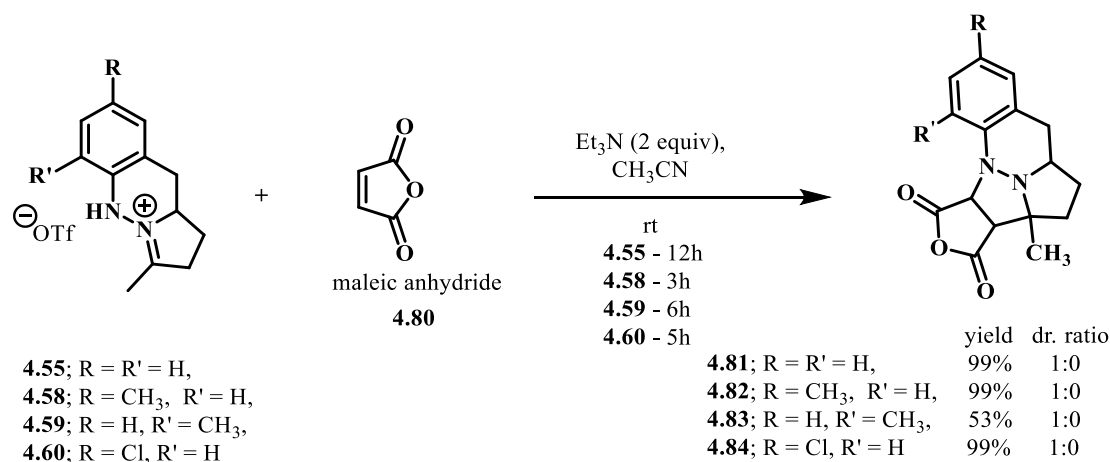


Scheme 4.15. 1,3-Dipolar cycloaddition between protonated azomethine imines and dimethyl acetylene dicarboxylate.

4.3.4 Reactions with maleic anhydride and *N*-methylmaleimide as dipolarophiles

To increase the structural complexity of the products formed by this cycloaddition reaction, we used conjugated cyclic esters as dipolarophiles. Maleic anhydride reacted with protonated azomethine imine salts shown in Scheme 16, very smoothly to provide the corresponding cycloadducts in excellent yields. Interestingly, incorporating a methyl

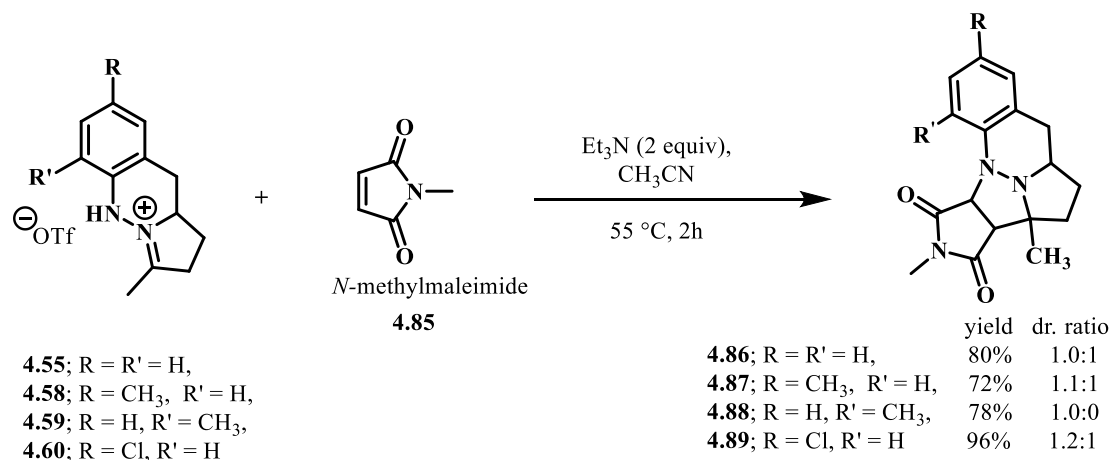
substituent at the *ortho*-position gave only low yields of the desired product. It is noteworthy that all of the reactions were diastereospecific. Due to the instability of the products, this reaction had to be run at room temperature, and these products were not stable in solution for prolonged time. Interestingly, compound **4.81** was soluble in several organic solvents, whereas compounds **4.82** and **4.83** were insoluble in chloroform, slightly soluble in acetonitrile, and completely soluble in dichloromethane, methanol and DMSO. Compound **4.84** was insoluble in acetonitrile and chloroform, and soluble in dichloromethane, methanol, and DMSO.



Scheme 4.16. 1,3-Dipolar cycloaddition between protonated azomethine imines and maleic anhydride.

N-methylmaleimide was also a productive electrophile, giving the cycloaddition products shown in Scheme 4.17 in good yields. Again, diastereoselectivity was low (**4.55**, **4.58** and **4.60**) unless a substituent was present at the *ortho* position of the *N*-aryl ring (**4.59**). Based on the ¹HNMR, compound **4.55** gave an equimolar mixture of two diastereomers, but these had identical R_f values with many different solvents system and thus were inseparably by chromatography. The diastereomers derived from compound

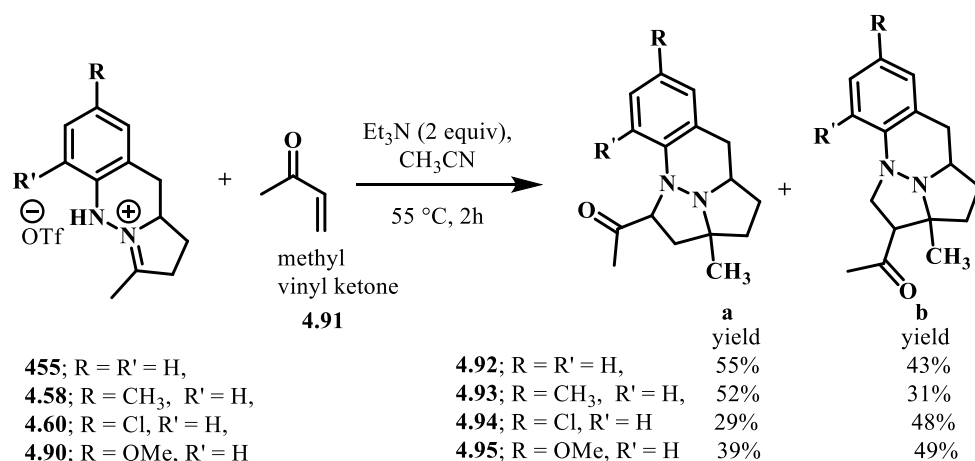
4.58 and **4.60**, on the other hand, were separated based on solubility as one of the diastereomers was insoluble in almost all organic solvent except dichloromethane.



Scheme 4.17. 1,3-Dipolar cycloaddition between protonated azomethine imines and dimethyl acetylene dicarboxylate.

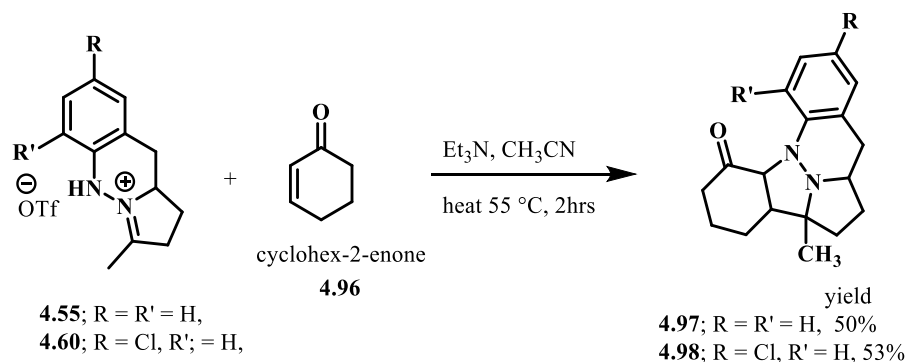
4.3.5 Reactions involving unsymmetrical π -systems as dipolarophiles

In the previous sections, we used a variety of symmetrical acyclic and cyclic reagents as dipolarophiles for the 1,3-dipolar cycloaddition of azomethine amines. These reagents provided diastereoselective, non-diastereoselective as well as diastereospecific products. We were also interested with a variety of unsymmetrical conjugated π -systems as dipolarophiles, which could provide regioisomers including diastereomers. When I treated the azomethine imines shown in Scheme 4.18 with methyl vinyl ketone (MVK), I was able to isolate two different regioisomeric cycloaddition products. Interestingly, these reactions were diastereospecific as only one diastereomer of each product was isolated. All substituents provided the desired cycloadducts in good to excellent yields.



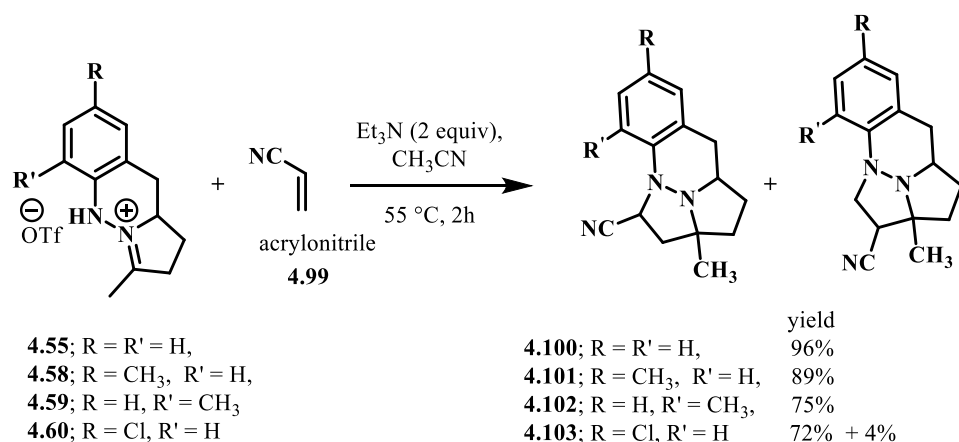
Scheme 4.18. 1,3-Dipolar cycloaddition between protonated azomethine imines and MVK.

Changing the dipolarophile to 2-cyclohexen-1-one gave a single diastereomer in moderate yield. No other regio- or diastereomers were isolated from this reaction.



Scheme 4.19. 1,3-dipolar cycloaddition between protonated azomethine imines and cyclohex-2-enone.

Our interest was not limited to conjugated carbonyl systems, and acrylonitrile was treated with azomethine imines to provide the cycloaddition products in good to excellent yields as mixtures of diastereomers (Scheme 4.20). But, these diastereomers could not be separated by chromatography. In the case of a chloride substituent (**4.103**), I was able to isolate one diastereomer in very low yield (4%).



Scheme 4.20. 1,3-Dipolar cycloaddition between protonated azomethine imines and acrylonitrile.

4.4 Summary of 1,3-dipolar cycloaddition of azomethine imines

Azomethine imines underwent 1,3-dipolar cycloaddition reactions with doubly activated symmetrical alkenes as dipolarophiles to provide the corresponding cycloadducts in high yields with moderate to high diastereoselectivities. Although both dimethyl maleate and diethyl maleate gave the corresponding cycloadducts in comparable yields, the cycloadditions with dimethyl maleate were somewhat more diastereoselective than diethyl maleate. Dimethyl fumarate which is a *trans* form of dimethyl maleate, also provided good to excellent yields. However, the stereochemical outcome of these reactions were different than the cycloadducts formed from dimethyl maleate. So, *Cis* and *trans* alkenes provided unique diastereomers. These results indicate that the 1,3-dipolar cycloaddition reactions of azomethine occurs via concerted mechanism. Also, the reactions involving dimethyl fumarate was less diastereoselective than those involving the maleate reagents. Cycloaddition of dimethyl acetylene dicarboxylate provided excellent yield, but in most cases, the diastereoselectivities were very low.

Activated symmetrical cyclic alkenes, such as maleic anhydride and *N*-methylmaleimide as dipolarophiles, actively involved in the 1,3-dipolar cycloadditions of azomethine imines to provide the corresponding cycloadducts in good to excellent yields. Although the cycloaddition reactions involving maleic anhydride were diastereospecific, the diastereoselectivities of the reactions involving *N*-methylmaleimide were very low.

The 1,3-dipolar cycloaddition reactions of azomethine imines with unsymmetrical alkenes, such as MVK, gave the corresponding two different regioisomeric cycloaddition products in comparable yields. Interestingly, these reactions were diastereospecific. The cycloaddition reactions with 2-cyclohexen-1-one gave a single diastereomer in low yield. In the case of acrylonitrile, it provided the desired cycloadducts in good yields as mixtures of regio- or diastereomers.

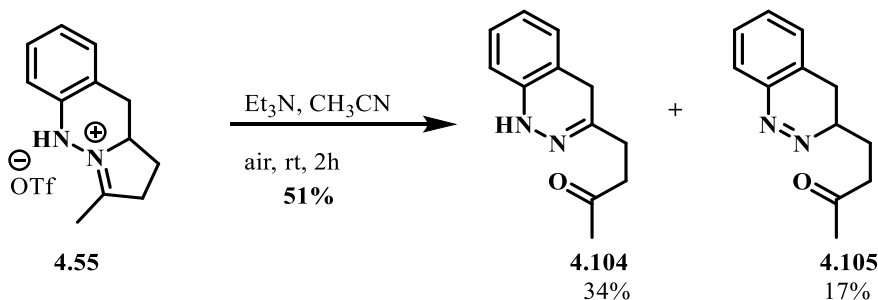
In terms of substituents on the *N*-aryl ring of the azomethine imine salt, an electron withdrawing chloride substituent generally underwent 1,3-dipolar cycloaddition with a variety of π -systems to give the corresponding cycloadducts in higher yields than an electron donating methyl substituent.

In several cases, we observed more than one diastereomers and regioisomers. Due to the lower energy gap between HOMO and LUMO of dipoles and dipolarophiles, the interaction of frontier molecular orbitals became very stronger, which affects the diastereoselectivity and regioselectivity.

4.5 Oxidation of protonated azomethine imine salt

The cycloaddition reactions described above, were run under a nitrogen atmosphere. When I ran this reaction in open air, I isolated ketones **4.104** and **4.105** in addition to the expected cycloadducts. These ketone products are the result of an oxidation reaction, and

when I reacted an acetonitrile solution of azomethine imine salt **4.55** with triethyl amine at room temperature in open air for two hours, I was able to isolate ketones **4.104** in 34 % yield and **4.105** in 17% yield (Scheme 4.21). Base on this result, protonated azomethine imine salts in the presence of base are air sensitive. Therefore, to carry out the cycloaddition reaction of these salts, an inert atmosphere is required.



Scheme 4.21. Oxidation of protonated azomethine imines.

4.6 Computational study for 1,3-dipolar cycloadditions of azomethine imine salts

Although there were a number of possibilities of diastereomers, in most of the cases, I isolated two diastereomers from the cycloaddition of azomethine imine salts with a variety of π -system. To understand why certain diastereomers were more favorable than others, I calculated the energy barrier for these cycloadditions using computational methods.

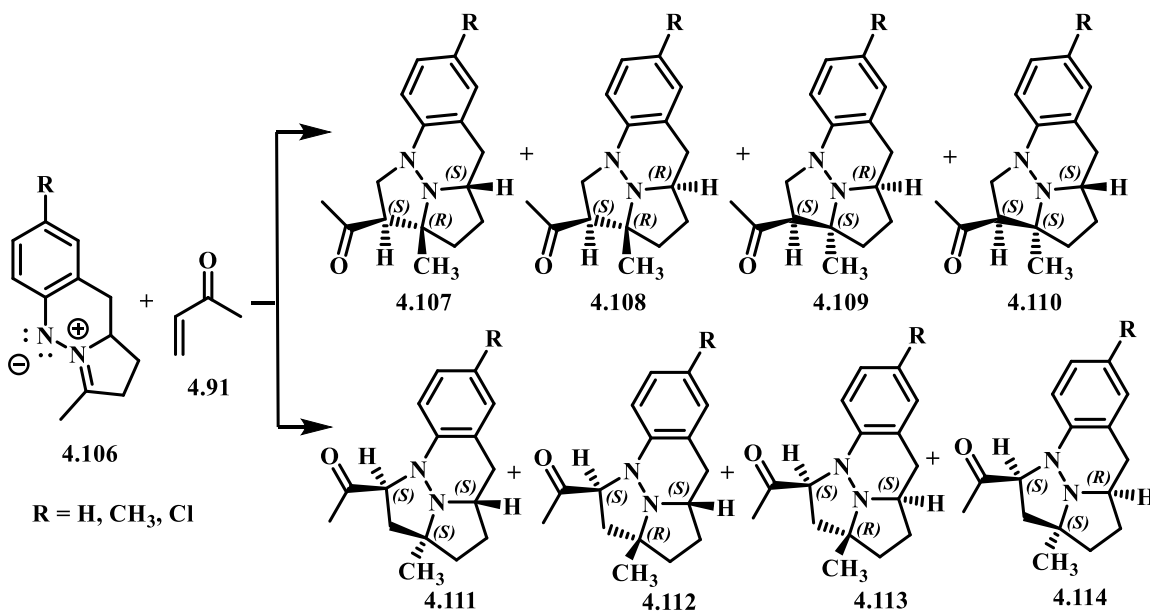
4.6.1 Computational methods

All density functional theory (DFT) calculations were performed with Gaussian 09.³⁵ Geometry optimizations were carried out at the B3LYP level^{36,37,38} with the 6-31G(d) basis set.³⁹ The vibrational frequencies were computed at the same level to check whether each optimized structure is an energy minimum or a transition state and to evaluate its zero-point vibrational energy (ZPVE) and thermal energies at 298 K. The single-point energies and solvation effects in acetonitrile were computed at the M06-2X/6-311+(d,p)

level,^{40,41} based on B3LYP/6-31G(d)-optimized geometries. Solvation energy corrections for acetonitrile were evaluated by a self-consistent reaction field (SCRF) using the SMD⁴² model under the same level of theory as the single-point energy calculation (M06-2X/6-311+(d,p)).

4.6.2 Calculation of energy barriers of 1,3-dipolar cycloaddition of azomethine imine and MVK

The cycloaddition reaction of azomethine imine **4.106** with MVK could provide eight different products including regio- and diastereomers (Scheme 4.22). These, of course, would be formed via eight different transition states. Compounds **4.107**, **4.108**, **4.109**, and **4.110** are diastereomers of one regioisomer, while compounds **4.111**, **4.112**, **4.113**, and **4.114** are diastereomers of another regioisomer.



Scheme 4.22. Possible regio- and diastereomers generated by the cycloaddition of azomethine imine **4.106** with MVK. (*Enantiomers are not shown.*)

In reality, these reactions are fairly diastereoselective, and to understand this selectivity, I calculated the energy barriers for each transition states leading to the products shown above. **TS-4.107**, **TS-4.108**, **TS-4.109**, and **TS-4.110** (Entries 1-4, Table 4.2) are the transition states leading to products **4.107**, **4.108**, **4.109**, and **4.110**, while **TS-4.111**, **TS-4.112**, **TS-4.113**, and **TS-4.114** (Entries 5-8) are the transition states leading to the regioisomeric products **4.111**, **4.112**, **4.113**, and **4.114**.

Table 4.2. Calculated energy barriers for all possible transition states generated by the cycloaddition of azomethine imine **4.106** and MVK

entry	transition state (TS)	ΔG^\ddagger for R = H (kcal/mol)	ΔG^\ddagger for R = CH ₃ (kcal/mol)	ΔG^\ddagger for R = Cl (kcal/mol)
1	TS-4.107	22.61	21.91	23.72
2	TS-4.108	19.15	18.99	20.26
3	TS-4.109	23.38	22.72	24.67
4	TS-4.110	19.18	18.53	19.82
5	TS-4.111	19.87	18.92	20.15
6	TS-4.112	21.47	20.74	22.31
7	TS-4.113	20.61	20.07	21.45
8	TS-4.114	21.30	20.20	21.92

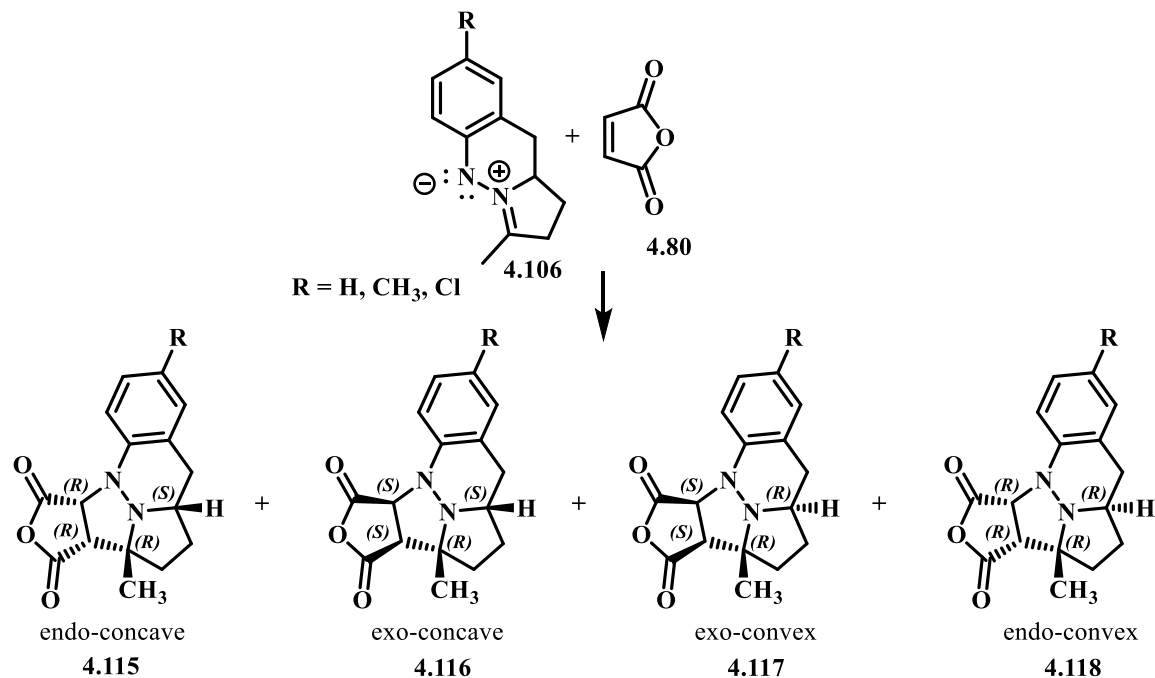
In all cases, the azomethine imine with an electron withdrawing chloride substituent had comparatively higher energy barriers than the azomethine imine containing an electron donating methyl substituent. Experimentally (Scheme 4.18), an electron donating methyl substituent (**4.58**) provided the cycloadduct **4.93** in higher yield than the azomethine imine containing an electron withdrawing chloride substituent (**4.60**). Therefore, the computational results in term of substituents are consistent with the experimental results. When considering the two sets of regioisomers separately, the energy barriers of transition states **TS-4.108** and **TS-4.110** (entries 2 and 4, table 4.2) are similar to each other and lower than those of transition states **TS-4.107** and **TS-4.109** (Entries 1 and 3, Table 4.2). In the case of another regioisomer, transition state **TS-4.111**

(Entry 5, Table 4.2) has the lowest energy barrier. In all cases, the activation barriers of the transition states leading to the diastereomers, in which the methyl group and hydrogen atom adjacent to the central nitrogen are in the opposite faces, have lower than those of the transition states leading to the diastereomers, in which both methyl group and hydrogen atom are on the same face. In this cycloaddition reaction, the regioselectivity might be affected by the equal interactions of frontier molecular orbitals. Therefore, these reactions gave the regioisomeric product in 1:1 ratio.

4.6.3 Calculation of energy barriers of 1,3-dipolar cycloaddition of azomethine imine and maleic anhydride

The cycloaddition of azomethine imine **4.106** with maleic anhydride (**4.80**) could provide four different diastereomeric products (**4.115** – **4.118**, Scheme 4.23).

Experimentally, this reaction was diastereospecific.



Scheme 4.23. Possible diastereomers generated by the cycloaddition of azomethine **4.106**

imine with maleic anhydride. (*Enantiomers are not shown.*)

Computational studies show that an electron withdrawing chloride substituent has higher energy barrier than an electron donating methyl substituent (Table 4.3). In term of diastereomers, transition state **TS-4.117** (Entry 3, Table 4.3) leading to exo-convex diastereomeric product (**4.117**), gave the lowest energy barrier for all substituents, whereas the transition state **TS-4.116** leading to exo-concave diastereomeric product (**4.116**) gave than highest energy barrier for all substituents. Again, the transition state leading to the diastereomeric product, in which the methyl group and hydrogen atom adjacent to the central nitrogen, are on opposite faces, have lowest activation barrier.

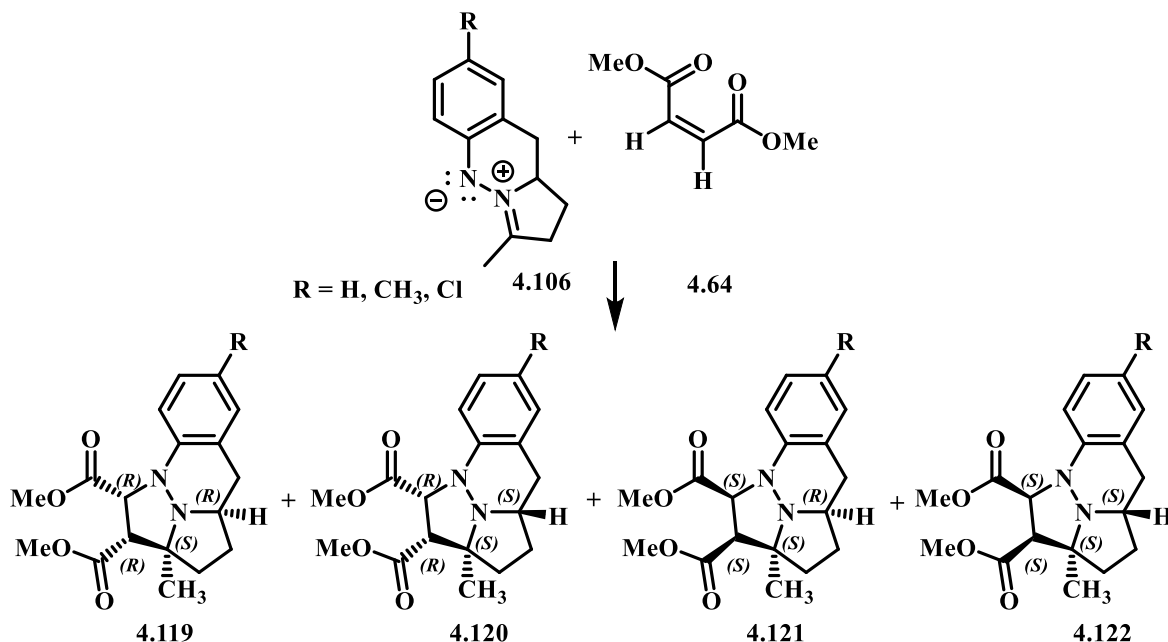
Table 4.3. Calculated energy barriers for all possible transition states generated by the cycloaddition of azomethine imine **4.106** and maleic anhydride

entry	transition state (TS)	ΔG^\ddagger for R = H (kcal/mol)	ΔG^\ddagger for R = CH ₃ (kcal/mol)	ΔG^\ddagger for R = Cl (kcal/mol)
1	TS-4.115	13.54	12.11	14.45
2	TS-4.116	15.23	14.20	16.15
3	TS-4.117	12.26	11.51	13.36
4	TS-4.118	13.00	11.75	13.82

4.6.4 Calculation of energy barriers of 1,3-dipolar cycloaddition of azomethine imine and dimethyl maleate and fumarate

The cycloaddition of an azomethine imine salt with dimethyl maleate could lead to four diastereomeric products (**4.119**, **4.120**, **4.121**, and **4.122**, Scheme 4.24). Experimentally, I isolated only two diastereomers from these reactions, and these products differed from those isolated from the reaction with dimethyl fumarate, so alkene was not isomerized over the course of the reaction. The computational studies (Table 4.4) show that an electron withdrawing chloride substituent has higher activation barrier than an electron donating methyl substituent. Transition states **TS-4.120** and **TS-4.122**

(Entries 2 and 4, Table 4.4) have lower energy barriers than transition states **TS-4.119** and **TS-4.121** (entries 1 and 3, table 4.4). The energy barriers of transition states **TS-4.120** and **TS-4.122** are comparable.



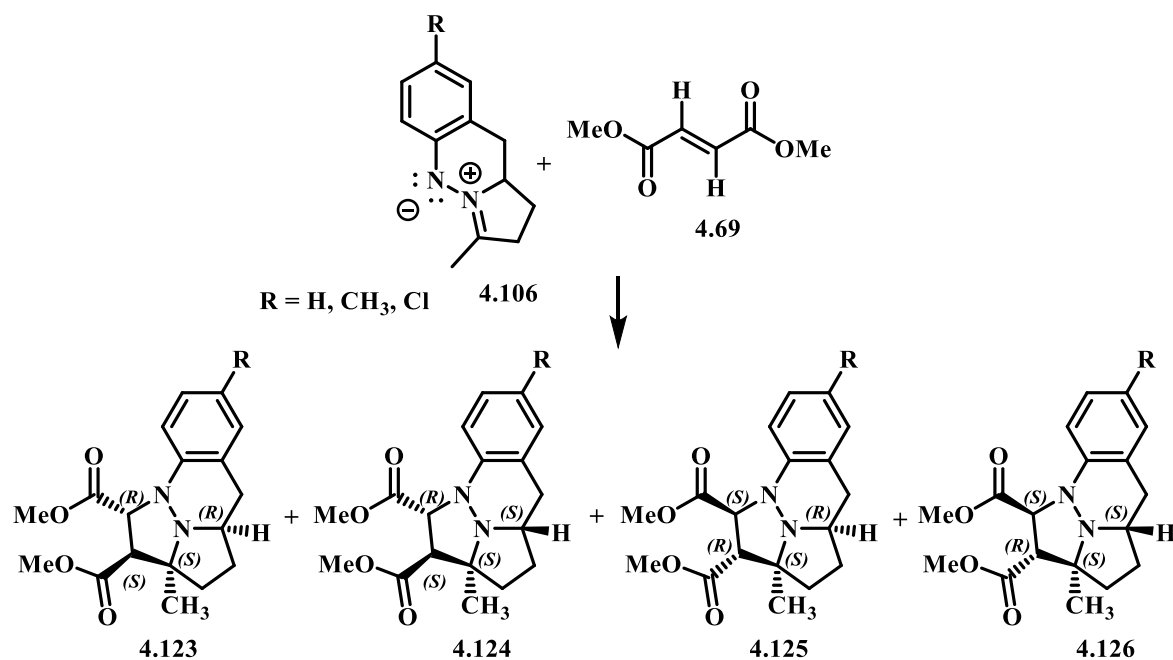
Scheme 4.24. Possible diastereomers generated by the cycloaddition of azomethine imine **4.106** with dimethyl maleate. (*Enantiomers are not shown.*)

Table 4.4. Calculated energy barriers for all possible transition states generated by the cycloaddition of azomethine imine **4.106** and dimethyl maleate

entry	transition State (TS)	ΔG^\ddagger for R = H (kcal/mol)	ΔG^\ddagger for R = CH ₃ (kcal/mol)	ΔG^\ddagger for R = Cl (kcal/mol)
1	TS-4.119	21.92	20.97	22.68
2	TS-4.120	19.82	19.54	21.00
3	TS-4.121	21.64	20.95	22.46
4	TS-4.122	19.31	19.65	19.94

Dimethyl fumarate (*E*-alkene) could also provide four different cycloaddition diastereomers (Scheme 4.25). Experimentally, only two of these diastereomers were isolated. Once again, the isolated products did not correspond to the product that were

isolated from the *Z*-alkene, products showing that the alkene was not isomerized during the reaction. In term of substituents, the computational results (Table 4.5) have the same trend as those of the *Z*-alkene (Table 4.4). In term of diastereomers, transition states **TS-4.124** and **TS-4.126** (Entries 2 and 4, Table 4.5) have lower activation barriers than transition states **TS-4.123** and **TS-4.125** (Entries 1 and 3, Table 4.5). The energy barriers of transition states **TS-4.124** and **TS-4.126** are comparable, which is consistent with the experimental results (Scheme 4.14) because the yields of both diastereomeric products are were similar.



Scheme 4.25. Possible diastereomers generated by the cycloaddition of azomethine imine **4.106** with dimethyl fumarate. (*Enantiomers are not shown.*)

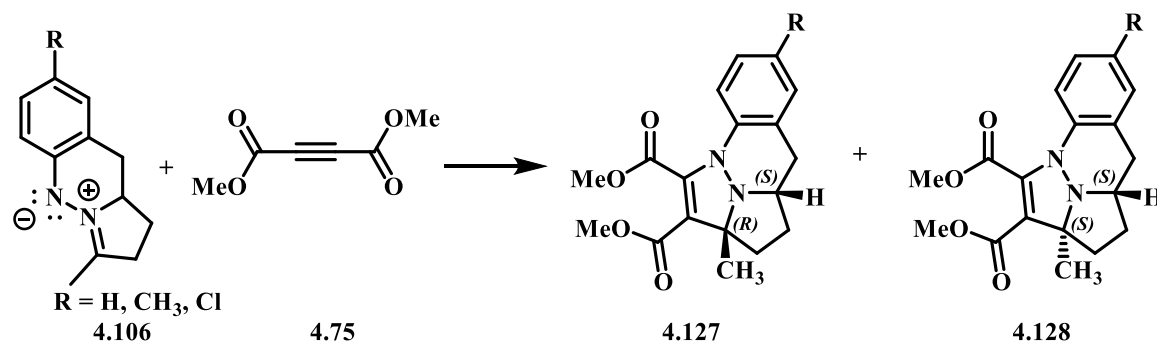
Table 4.5. Calculated energy barriers for all possible transition states generated by the cycloaddition of azomethine imine **4.106** and dimethyl fumarate

entry	transition state (TS)	ΔG^\ddagger for R = H (kcal/mol)	ΔG^\ddagger for R = CH ₃ (kcal/mol)	ΔG^\ddagger for R = Cl (kcal/mol)
1	TS-4.123	17.75	17.12	18.73
2	TS-4.124	16.73	16.11	17.62
3	TS-4.125	19.25	18.46	20.13
4	TS-4.126	16.76	15.82	17.50

In both cases (dimethyl maleate and fumarate), the methyl group and hydrogen atom adjacent to the central nitrogen that are either on opposite faces or on same face, is also following the previous trends regarding the activation barriers.

4.6.5 Calculation of energy barriers of 1,3-dipolar cycloaddition of azomethine imine and dimethyl acetylene dicarboxylate

Both theoretically and experimentally, the cycloaddition reaction of azomethine imine **4.106** with dimethyl acetylene dicarboxylate provides two diastereomers **4.127** and **4.128** (Scheme 4.26). Computational results in term of substituent, show that an electron withdrawing chloride substituent again has a higher activation barrier than an electron donating methyl substituent (Table 4.6). In term of diastereomers, the energy barriers of transition states **TS-127** and **TS-128** (Entries 1 and 2, Table 4.6) are similar, which is consistent with the experimental results (Scheme 4.15) because experimental results also provided two diastereomeric products. In regard to the methyl and hydrogen atom adjacent to the central nitrogen, the trend of the activation barriers of this cycloaddition are also similar to the previous cycloaddition reactions.



Scheme 4.26. Two diastereomers generated by the cycloaddition of azomethine imine **4.106** with dimethyl acetylene dicarboxylate. (*Enantiomers are not shown.*)

Table 4.6. Calculated energy barriers for all possible transition states generated by the cycloaddition of azomethine imine **4.106** and dimethyl acetylene dicarboxylate

entry	transition State (TS)	ΔG^\ddagger for R = H (kcal/mol)	ΔG^\ddagger for R = CH ₃ (kcal/mol)	ΔG^\ddagger for R = Cl (kcal/mol)
1	TS-4.127	13.93	13.44	15.08
2	TS-4.128	12.97	12.54	14.01

4.7 Issues with determining the stereochemistry of the cycloaddition products

Many of the cycloadditions described above provided two diastereomeric products and were attempted to determine the relative configuration of these materials. However, 2D NOSTs of the diastereomers **4.76a** and **4.76b** (Scheme 4.15), did not show significant differences of the spectra, and could not be used to establish configuration. I made many attempts to grow X-ray quality crystals of these compounds without success. I had hoped that the computational studies described above might shed light on this issue, but the energy barriers of the corresponding diastereomers were not different enough to make a reasonable prediction. Therefore, we were unable to determine the configuration of the diastereomeric products.

4.8 Conclusions

Azomethine imines have been used to synthesize a variety of heterocycle compounds via 1,3-dipolar cycloadditions. Although these reactions are common, the cycloadditions described here that have a C-N double bond and a N-N bond incorporated in two different rings have little procedure. We were pleased to find that the azomethine imines generated under basic conditions from the protonated azomethine imines, react smoothly with a variety of π -system to give the corresponding cycloadducts. *Cis* and *trans* alkenes provided unique diastereomers, so 1,3-dipolar cycloaddition reaction of azomethine occurs via concerted mechanism. These 1,3-dipolar cycloadditions typically gave the products as a mixture of two diastereomers. But, efforts to determine the diastereomeric configuration of these products have not been successful.

I also determined the energy barriers of transition states of the corresponding diastereomers. An electron withdrawing chloride substituent on the aryl ring consistently raised energy barrier compared to an electron donating methyl substituent. In all 1,3-dipolar cycloaddition reactions, the transition states leading to the diastereomeric products in which the methyl group and hydrogen atom adjacent to the central nitrogen are on the difference faces have the lowest activation barriers than others. The energy barriers of the transition states leading to the corresponding diastereomers were not very different. Therefore, based on these results, we were unable to determine the stereochemistry of the corresponding diastereomers.

References

1. Hu, X.-Q.; Chen, J.-R.; Gao, S.; Feng, B.; Lu, L.-Q.; Xiao, W.-J. *Chem. Commun.* **2013**, 49, 7905.
2. Yuvaraj, P.; Reddy, B. S. R. *Tetrahedron Lett.* **2014**, 55, 806.

3. Sibi, M. P.; Rane, D.; Stanley, L. M.; Soeta, T. *Org. Lett.* **2008**, *10*, 2971.
4. Grigg, R.; Kemp, J.; Thompson, N. *Tetrahedron Lett.* **1978**, *19*, 2827.
5. Frank, E.; Kardos, Z.; Wölfling, J.; Schneider, G. *Synlet* **2007**, 1311.
6. Arrieta, A.; Carrillo, J. R.; Cossío, F. P.; Díaz-Ortiz, A.; Gómez-Escalonilla, M. J.; de la Hoz, A.; Langa, F.; Moreno, A. *Tetrahedron* **1998**, *54*, 13167.
7. Thi Tong, T. M.; Soeta, T.; Suga, T.; Kawamoto, K.; Hayashi, Y.; Ukaji, Y. *J. Org. Chem.* **2017**, *82*, 1969.
8. Winterton, S. E.; Ready, J. M. *Org. Lett.* **2016**, *18*, 2608.
9. Belskaya, N.P.; Bakulev, V.A.; Fan, Z. *Chem. Heterocycl. Comp.* **2016**, *52*, 627.
10. Jia, Q.; Chen, L.; Yang, G.; Wang, J.; Wei, J.; Du, Z. *Tetrahedron Lett.* **2015**, *56*, 7150.
11. Perreault, C.; Goudreau, S. R.; Zimmer, L. E.; Charette, A. B. *Org. Lett.* **2008**, *10*, 689.
12. Tong, M.-C.; Chen, X.; Tao, H.-Y.; Wang, C.-J. *Angew. Chem. Int. Ed.* **2013**, *52*, 12377.
13. Dorn, H.; Otto, A. *Angew. Chem. Int. Ed.* **1968**, *7*, 214.
14. Na, R.; Jing, C.; Xu, Q.; Jiang, H.; Wu, X.; Shi, J.; Zhong, J.; Wang, M.; Benitez, D.; Tkatchouk, E.; Goddard, III, W. A.; Guo, H.; Kwon, O. *J. Am. Chem. Soc.* **2011**, *133*, 13337.
15. Soeta, T.; Tamura, K.; Ukaji, Y. *Org. Lett.* **2012**, *14*, 1226.
16. Meng, W.; Zhao, H.-T.; Mie, J.; Zheng, Y.; Fu, A.; Ma, J.-A. *Chem. Sci.* **2012**, *3*, 3053.
17. Ochi, M.; Kawasaki, K.; Kataoka, H.; Uchio, Y.; Nishi, H. *Biochem. Biophys. Res. Commun.* **2001**, *283*, 1118.
18. Ghosh, A. K.; Schiltz, G.; Perali, R. S.; Leshchenko, S.; Kay, S.; Walters, D. E.; Koh, Y.; Maeda, K.; Mitsuya, H. *Bioorg. Med. Chem. Lett.* **2006**, *16*, 1869.
19. Nájera, C.; Sansano, J. M.; Yus, M. *Org. Biomol. Chem.* **2015**, *13*, 8596.
20. Hong, L.; Kai, M.; Wu, C.; Sun, W.; Zhu, G.; Li, G.; Yao, X.; Wang, R. *Chem. Commun.* **2013**, *49*, 6713.
21. Belskaya, N. P.; Bakulev, V. A.; Fan, Z. *Chem. of Heterocycl. Compounds* **2016**, *52*, 627.
22. Hashimoto, T.; Kimura, H.; Kawamata, Y.; Maruoka, K. *Nat. Chem.* **2011**, *3*, 642.

23. Hashimoto, T.; Maeda, Y.; Omote, M.; Nakatsu, H.; Maruoka, K. *J. Am. Chem. Soc.* **2010**, *132*, 4076.
24. Jones, R. C. F.; Hollis, S. J.; Iley, J. N. *ARKIVOC* **2007**, 152.
25. Hunt, A. D.; Dion, I.; das Neves, N.; Taing, S.; Beauchemin, A. M. *J. Org. Chem.* **2013**, *78*, 8847.
26. Hashimoto, T.; Omote, M.; Maruoka, K. *Angew. Chem. Int. Ed.* **2011**, *50*, 8952.
27. Zhou, Y.-Y.; Li, J.; Ling, L.; Liao, S.-H.; Sun, X.-L.; Li, Y.-X.; Wang, L.-J.; Tang, Y. *Angew. Chem. Int. Ed.* **2013**, *52*, 1452.
28. Pezdirc, L.; Jovanovski, V.; Bevk, D.; Jakše, R.; Pirc, S.; Meden, A.; Stanovnik, B.; Svete, J.; *Tetrahedron* **2005**, *61*, 3977.
29. Turk, C.; Svete, J.; Stanovnik, B.; Golič, L.; Golič-Grdadolnik, S.; Golobič, A.; Selič, L.; *Helv. Chim. Acta* **2001**, *84*, 146.
30. Sibi, M.; Rane, D.; Stanley, L. M.; Soeta, T.; *Org. Lett.* **2008**, *10*, 2971.
31. Wang, X.; Wu, L.; Yang, P.; Song, X.-J.; Ren, H.-X.; Peng, L.; Wang, L. *Org. Lett.* **2017**, *19*, 3051.
32. Zhu, G.; Sun, W.; Wu, C.; Li, G.; Hong, L.; Wang, R.; *Org. Lett.* **2013**, *15*, 4988.
33. Bercovici, D. A.; Ogilvie, J. M.; Tsvetkov, N.; Brewer, M. *Angew. Chem. Int. Ed.* **2013**, *52*, 13338.
34. Dhakal, R.; Brewer, M. *Tetrahedron* **2016**, *37*, 3718.
35. Frisch, M. J.; Trucks, G. W.; Schlegel, H. B.; Scuseria, G. E.; Robb, M. A.; Cheeseman, J. R.; Scalmani, G.; Barone, V.; Mennucci, B.; Petersson, G. A.; Nakatsuji, H.; Caricato, M.; Li, X.; Hratchian, H. P.; Izmaylov, A. F.; Bloino, J.; Zheng, G.; Sonnenberg, J. L.; Hada, M.; Ehara, M.; Toyota, K.; Fukuda, R.; Hasegawa, J.; Ishida, M.; Nakajima, T.; Honda, Y.; Kitao, O.; Nakai, H.; Vreven, T.; Montgomery, J. A., Jr.; Peralta, J. E.; Ogliaro, F.; Bearpark, M.; Heyd, J. J.; Brothers, E.; Kudin, K. N.; Staroverov, V. N.; Kobayashi, R.; Normand, J.; Raghavachari, K.; Rendell, A.; Burant, J. C.; Iyengar, S. S.; Tomasi, J.; Cossi, M.; Rega, N.; Millam, J. M.; Klene, M.; Knox, J. E.; Cross, J. B.; Bakken, V.; Adamo, C.; Jaramillo, J.; Gomperts, R.; Stratmann, R. E.; Yazyev, O.; Austin, A. J.; Cammi, R.; Pomelli, C.; Ochterski, J. W.; Martin, R. L.; Morokuma, K.; Zakrzewski, V. G.; Voth, G. A.; Salvador, P.; Dannenberg, J. J.; Dapprich, S.; Daniels, A. D.; Farkas, O.; Foresman, J. B.; Ortiz, J. V.; Cioslowski, J.; Fox, D. J. Gaussian 09, revision D.01; Gaussian, Inc.: Wallingford, CT, **2013**.
36. Becke, A. D. *Phys. Rev. A* **1988**, *38*, 3098.

37. Becke, A. D. *J. Chem. Phys.* **1993**, *98*, 5648.
38. Lee, C.; Yang, W.; Parr, R. G. *Phys. Rev. B* **1988**, *37*, 785.
39. Hehre, W. J.; Radom, L.; Schleyer, P. V. R.; Pople, J. A. *Ab Initio Molecular Orbital Theory*, Wiley: New York, 1986.
40. Zhao, Y.; Truhlar, D. *Theor. Chem. Acc.* **2008**, *120*, 215.
41. Zhao, Y.; Truhlar, D. G. *Acc. Chem. Res.* **2008**, *41*, 157.
42. Marenich, A. V.; Cramer, C. J.; Truhlar, D. G. *J. Phys. Chem. B* **2009**, *113*, 6378.
43. Visnick, M.; Battiste, M. *J. Chem. Soc. Chem. Commun.* **1985**, 1621.
44. Winkler, J. *Chem. Rev.* **1996**, *96*, 167.

SUMMARY OF THESIS AND FUTURE GOAL

Summary of thesis

The Brewer group has studied the reactivity of 1-aza-2-azoniaallene salt intermediates in intramolecular reaction, and we have discovered that these cationic heteroallenes can react through a variety of mechanistically distinct pathways to give different classes of nitrogen heterocycles. Throughout Chapter 1 and 2, I have discussed in several of these reactivities including intramolecular [4+2] cycloaddition reactions, intramolecular C-H amination, and alkene amination. My initial studies focused on evaluating the scope of the intramolecular [4+2] cycloaddition reaction, which gives protonated azomethine imine salts containing 1,2,3,4-tetrahydrocinnoline scaffold. I first evaluated what affect substituents on the *N*-aryl ring had on the reaction and whether highly hindered tetra-substituted alkene could give structurally complex protonated azomethine imine salts. The metal mediated reaction did not facilitate the cycloadditions very well, so I replaced the antimony pentachloride with TMSOTf. Although the non-metallic Lewis acid provided very clean products from α -chloroazo starting materials, the novel α -trifluoroacetoxyazo compounds prepared from the corresponding hydrazone derivatives and trifluoroacetic anhydride, underwent [4+2] cycloadditions even more cleanly and in higher yield with TMSOTf as the Lewis acid. To further verify the proposed mechanism of the [4+2] cycloaddition, I synthesized a dearomatized non-protonated azomethine imine salt.

In the case of C-H amination, the Brewer group has explored the unprecedented intramolecular C-H insertion of heteroallene salts. We have also studied the mechanism of this insertion computationally and experimentally. As part of these mechanistic

studies, I carried out kinetic isotope effect experiments. My results were consistent with an asynchronous concerted mechanism. Although the insertion reaction occurs readily at benzylic and tertiary centers, secondary centers do not undergo C-H amination. My attempts to synthesize indoles and indolines via C-H insertion also failed.

The intramolecular alkene amination of heteroallene salts provides a new way to synthesize a variety of bicyclic compounds. The Brewer group studies show that the heteroallene salt of a cyclohexene derivative preferentially undergoes alkene amination via an aziridinium ion intermediate that is trapped by the chloride counter ion. However, my efforts to trap the aziridinium ion by an external nucleophile failed.

I also attempted to develop a new strategy to affect C-H amination and alkene addition reactions via a nitrenium cation intermediate. But, these efforts did not lead to a productive reaction.

In Chapter 3, I discussed the α -chloroazo compounds as precursors to 1-aza-2-azaniaallene salts, which can lead to monocyclic, bicyclic, tricyclic, and tetracyclic compounds via cycloaddition reactions, C-H aminations, or alkene additions. The method developed by the Brewer group to prepare α -chloroazo compounds was not compatible with aryl hydrazones bearing electron withdrawing functional groups. For example, nitro aryl compounds did not undergo this reaction very smoothly. So, I developed a new method to prepare α -substituted azo compounds, in which trifluoroacetic anhydride activates DMSO to give trifluoroacetoxy dimethylsulfonium trifluoroacetate, which further reacts with arylhydrazones to give α -trifluoroacetoxyazo compounds. This technique is more general than the original Swern procedure and is compatible with all

types of functional groups. Notably, aryl-nitro hydrazones are easily converted into the corresponding azo products.

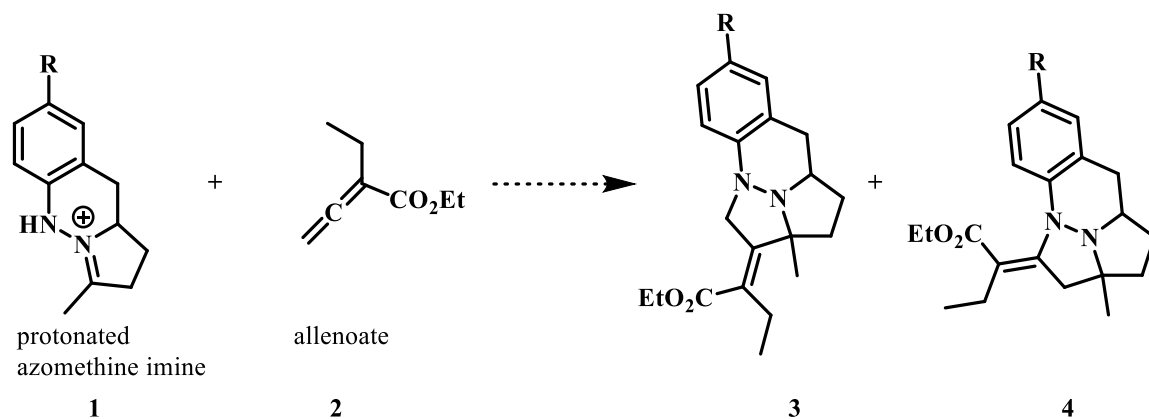
In Chapter 4, I described the work I have done to develop an intermolecular 1,3-dipolar cycloaddition reaction of azomethine imines with a variety of doubly or singly activated π -systems to give structurally complex tetra- or pentacyclic products. These 1,3-dipolar cycloadditions typically gave the products as a mixture of two diastereomers. Cis and trans alkenes provided unique diastereomers, so 1,3-dipolar cycloaddition of azomethine imine occurs via concerted mechanism. Unsymmetrical alkenes (singly activated) provided two different regioisomeric cycloaddition products. But, efforts to determine the diastereomeric configuration of these products have not been successful. And I have determined the energy barriers of transition states for the corresponding diastereomers. Interestingly, an electron withdrawing chloride substituent on the aryl ring consistently raised the energy barrier compared to an electron donating methyl substituent. However, the energy barriers of the transition states leading to diastereomers were not very different. Therefore, we were unable to determine the stereochemistry of the corresponding diastereomers based on these computational results.

Future goal

Intramolecular C-H amination of heteroallene salts is a good strategy to form five-membered *N*-heterocycles. However, this metal mediated and low temperature reaction is not very practical, environmentally friendly, or green. It would be beneficial to develop a new greener strategy to affect the insertion. A good starting point would be to replace the metallic Lewis acid with a suitable alternative. At one point, I used the non-metallic

Lewis acid TMSOTf for the C-H amination reaction. I observed a small amount of the desired product, but I did not optimize the conditions.

I have shown that the base mediated 1,3-dipolar cycloaddition of protonated azomethine imines with π -systems is a good strategy to form structurally complex polycyclic heterocycles. However, this reaction is not very regio- or diastereoselective. To make this reaction more regio- and diastereoselective, polar dipolarophiles, such as lithium ynolates, should be assessed as reaction partners. In addition, allenolate reagents (e.g. **2**, Scheme 1) might be interesting dipolarophiles for this reaction as they would provide an exo double bond. In any events, the configuration of the diastereomers formed in the cycloaddition reaction achieve to date need to be assigned, at which point, meaningful trends may become apparent.



Scheme 1. 1,3-Dipolar cycloaddition of azomethine imine with allenolate.

CHAPTER 5: EXPERIMENTAL INFORMATION

5.1 General experimental information

All reactions were performed under an atmosphere of nitrogen in flame-dried glassware. All solvents were removed *in vacuo* using a rotary evaporator attached to a self-cleaning dry vacuum pump, and further dried under reduced pressure on a high vacuum line. Tetrahydrofuran (THF), acetonitrile (CH₃CN), and dichloromethane (CH₂Cl₂) were dried via a solvent dispensing system. Triethylamine was freshly distilled from CaH₂ before use. Oxalyl chloride, trimethylsilyl trifluoromethanesulfonate and antimony(V)chloride, purchased from Acros Organics, were freshly distilled before use. Anhydrous aluminum(III)chloride (98.5%), purchased from Acros Organics, was used as received and stored in a dry glovebox under an atmosphere of nitrogen. Extra dry DMSO stored over molecular sieves was purchased from Acros Organics and was used as received. All hydrazones were freshly prepared before use as these materials could not be stored and underwent facile auto oxidation on standing in air. Molecular sieves (4 Å) were activated by heating overnight at 120 °C in a vacuum oven.

Reactions were cooled to –78 °C by immersion in dry-ice acetone baths and were maintained at -60 °C with the aid of an immersion cooler. Silica gel flash column chromatography was performed using silica gel (230-400 mesh) and TLC analysis was carried out using silica on glass plates. Visualization of TLC plates was achieved using ultraviolet light, polyphosphomolybdic acid and cerium sulfate in EtOH with H₂SO₄, ceric ammonium molybdate, or iodine.

¹H and ¹³C NMR data was collected at room temperature on a 500 MHz spectrometer in CDCl₃ or CD₃CN. ¹H NMR chemical shifts are reported in ppm (δ units)

downfield from tetramethylsilane. Solvent peaks were used as internal references for all ^{13}C NMR. Accurate mass data was acquired in ESI mode using an orbitrap mass analyzer. X-Ray diffraction data were collected on a Bruker APEX 2 CCD platform ($\text{MoK}\alpha$, $\lambda = 0.71073 \text{ \AA}$) at set temperature of 135 K. A suitable crystal was mounted in a nylon loop under Paratone-N cryoprotectant oil. Direct methods and standard difference map techniques were used for solution structure followed by refinement using full-matrix least squares procedures on F2 via SHELXTL (version 6.14; Sheldrick, G. M., *Acta Cryst.* **2008**, *A64*, 112-122). Non-hydrogen atoms were refined anisotropically. The hydrogen atom on N(2), H(1), was located in the Fourier difference map and refined semi-freely using a distance restraint.

5.2 Experimental information for [4+2] cycloaddition (Chapter 1)

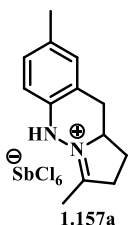
5.2.1 Representative procedure for SbCl_5 mediated [4+2]-cycloaddition

SbCl_5 (0.95 equiv) was added in a dropwise manner to a solution of an α -chloroazo compound (1 equiv) in CH_2Cl_2 under a nitrogen atmosphere at -78°C . The mixture was stirred for 30 min at -78°C and then warmed to room temperature. The solvent was removed *in vacuo* to give a thick foam that was triturated with petroleum ether 3 times and dried under high vacuum to give the cycloaddition product as a powder. To determine yields, the solid material was fully dissolved in CD_3CN , 1,3,5-trimethoxybenzene (0.95 equiv) was added as an internal standard, and an aliquot of this homogeneous mixture was analyzed by ^1H NMR.

5.2.2 Preparation and characterization data of protonated azomethine imine SbCl₆ salts

3,8-dimethyl-2,5,10,10a-tetrahydro-1H-pyrrolo[1,2-b]cinnolin-4-ium

hexachlorostibate(V) (1.157a): The title [4+2] cycloaddition product **1.157a** was



prepared in 86% yield as determined by ¹H NMR (crude product 95%, 444

mg) as described in representative experimental procedure 5.2.1 by reacting

α-chloroazo **1.155a** (206 mg, 0.87 mmol), SbCl₅ (2 M in CH₂Cl₂, 0.42 mL,

0.83 mmol), and CH₂Cl₂ (15 mL). Mp 92.6 °C. ¹H NMR (500 MHz, Acetone-*d*₆) δ = 7.05

(d, *J* = 7.1, 1H), 7.05 (s, 1H), 7.01 (d, *J* = 8.9, 1H), 4.81 – 4.59 (m, 1H), 3.42 – 3.25 (m,

3H), 3.05 (dt, *J* = 17.2, 8.6, 1H), 2.86 – 2.73 (m, 1H), 2.63 (s, 3H), 2.27 (s, 3H), 2.16

(ddd, *J* = 18.9, 12.9, 9.2, 1H). ¹³C NMR (126 MHz, Acetone-*d*₆) δ 168.9, 135.9, 132.7,

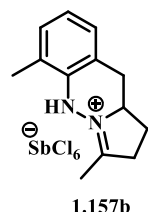
130.2, 129.5, 119.4, 114.9, 67.6, 36.4, 33.4, 25.9, 20.6, 16.3; IR (film) ν_{max}: 3200, 3003,

2970, 2947, 1738, 1724, 1504, 1423, 1366, 1275, 1227, 1217, 1157, 1032, 816 cm⁻¹. MS

(ESI) calcd for [C₁₃H₁₇N₂]⁺: 201.1392, found: 201.1387.

3,6-dimethyl-2,5,10,10a-tetrahydro-1H-pyrrolo[1,2-b]cinnolin-4-ium

hexachlorostibate(V) (1.157b): The title [4⁺+2] cycloaddition product **1.157b** was



prepared in 80% yield as determined by ¹H NMR (crude product 89%, 341

mg) as described in representative experimental procedure 5.2.1 by reacting

α-chloroazo **1.155b** (170 mg, 0.72 mmol), SbCl₅ (2 M in CH₂Cl₂, 0.34 mL,

0.68 mmol), and CH₂Cl₂ (15 mL). Mp 96.8 °C. ¹H NMR (500 MHz, Acetone-*d*₆) δ = 7.11

(dd, *J* = 17.7, 7.5, 2H), 6.97 (t, *J* = 7.5, 1H), 4.72 (d, *J* = 6.1, 1H), 3.50 – 3.31 (m, 3H),

3.11 (dd, *J* = 15.6, 12.6, 1H), 2.90 – 2.77 (m, 1H), 2.73 (s, 3H), 2.32 (s, 3H). ¹³C NMR

(126 MHz, Acetone-*d*₆) δ 176.6, 136.5, 130.4, 127.8, 125.0, 123.6, 120.1, 66.6, 36.6,

34.0, 25.4, 17.3, 17.0; IR (film) ν_{max} : 3200, 3014, 2970, 2941, 1738, 1724, 1474, 1435, 1366, 1269, 1229, 1217, 1206, 1090, 1032 cm^{-1} . MS (ESI) calcd for $[\text{C}_{13}\text{H}_{17}\text{N}_2]^+$: 201.1392, found: 201.1386.

5.2.3 Representative experimental procedure for TMSOTf mediated [4+ 2]

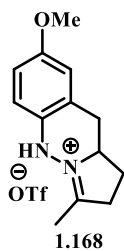
cycloaddition

Freshly distilled trimethylsilyl trifluoromethanesulfonate (1.05 equiv or 1.5 equiv) was added dropwise *via* syringe to a stirred solution of α -chloroazo or α -trifluoroacetoxyazo compound (1.0 equiv) in hexane or CH_2Cl_2 under a nitrogen atmosphere at room temperature. The resulting mixture was stirred at room temperature for 12h or at 40 °C for 4h at which point a light-brown precipitate was collected by filtration, and washed with diethyl ether to give a solid product. In some cases, the product was recrystallized using a very small amount of methanol with diethyl ether to provide very fine crystals.

5.2.4 Preparation and characterization data of protonated azomethine imine triflate

salts

8-methoxy-3-methyl-2,5,10,10a-tetrahydro-1*H*-pyrrolo[1,2-*b*]cinnolin-4-ium



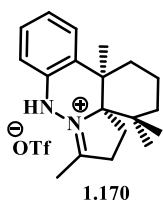
trifluoromethanesulfonate (1.168): The title [4+2] cycloaddition product

1.168 was prepared in 85% yield (137 mg) as described in representative experimental procedure 5.2.3 by reacting α -chloroazo **1.158** (1 equiv, 111 mg, 0.44 mmol), TMSOTf (1.05 equiv, 0.08 mL, 0.46 mmol), and hexane

(5 mL) for 12h at room temperature. Alternatively, the title [4+2] cycloaddition product was prepared in 81% yield (267 mg) as described in representative experimental procedure 5.2.3 by reacting the corresponding α -trifluoroacetoxyazo **1.190** (1 equiv, 300

mg, 0.9 mmol), TMSOTf (1.05 equiv, 0.17 mL, 0.95 mmol), and hexane (20 mL) for 12h at room temperature. Mp 146.2 °C (recrystallized from MeOH/Et₂O). ¹H NMR (500 MHz, CD₃CN) δ = 8.95 (s, 1H), 6.94 (d, *J* = 8.8, 1H), 6.88 – 6.82 (m, 1H), 6.79 (d, *J* = 2.5, 1H), 4.53 – 4.44 (m, 1H), 3.76 (s, 3H), 3.25 (dd, *J* = 16.1, 4.3, 1H), 3.17 – 2.99 (m, 2H), 2.93 (dd, *J* = 16.0, 12.5, 1H), 2.63 (dtd, *J* = 12.2, 8.1, 3.9, 1H), 2.37 (s, 3H), 2.02 – 1.95 (m, 1H). ¹³C NMR (126 MHz, CD₃CN) δ 168.3, 156.4, 131.7, 121.1, 116.1, 115.1, 114.9, 67.5, 56.2, 36.2, 33.3, 25.6, 15.8; IR (film) ν_{max}: 3229, 3015, 2970, 1740, 1503, 1435, 1369, 1277, 1227, 1217, 1155, 1029 cm⁻¹. MS (ESI) calcd for [C₁₃H₁₇N₂O]⁺: 217.1341, found: 217.1337.

(4a*R*,13b*R*)-4,4,7,13b-tetramethyl-1,2,3,4,5,6,9,13b-octahydrobenzo[*c*]pyrrolo[1,2-*b*]cinnolin-8-ium trifluoromethanesulfonate (170): The title [4+2] cycloaddition



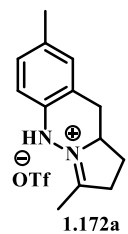
product **170** was prepared in 45% yield (519 mg) as described in representative experimental procedure 5.2.3 by reacting α-chloroazo **1.161** (1 equiv, 851 mg, 2.66 mmol), TMSOTf (1.05 equiv, 0.51 mL, 2.8 mmol), and hexane (20 mL) for 12h at room temperature. Alternatively, treating α-trifluoroacetoxyazo compound **1.176** (1 equiv, 595 mg, 1.5 mmol) with TMSOTf (1.5 equiv, 0.41 mL, 2.25 mmol) in hexane (12 mL) for 4h at 40 °C provided 467 mg of **1.170** (72% yield). Mp 189.4 °C (recrystallized from MeOH/Et₂O). ¹H NMR (500 MHz, CD₃CN) δ = 9.30 (s, 1H), 7.34 (d, *J* = 7.8, 1H), 7.26 (t, *J* = 7.1, 1H), 7.10 (t, *J* = 7.1, 1H), 6.89 (d, *J* = 8.1, 1H), 3.21 – 3.01 (m, 1H), 2.54 (s, 3H), 2.53 – 2.43 (m, 3H), 1.72 – 1.43 (m, 4H), 1.35 – 1.27 (m, 1H), 1.06 (s, 3H), 0.95 (s, 3H), 0.62 (s, 3H). ¹³C NMR (126 MHz, CD₃CN) δ 171.6, 137.6, 128.7, 128.2, 124.8, 124.3, 114.4, 85.4, 42.3, 41.5, 39.4, 36.4, 32.2, 29.8, 27.2, 25.6, 24.9, 18.6, 16.6; IR (film) ν_{max}: 3188, 3003, 1591, 1497,

1445, 1344, 1285, 1242, 1225, 1151, 1028 cm^{-1} . MS (ESI) calcd for $[\text{C}_{19}\text{H}_{27}\text{N}_2]^+$:

283.2174, found: 283.2173.

3,8-dimethyl-2,5,10,10a-tetrahydro-1*H*-pyrrolo[1,2-*b*]cinnolin-4-ium

trifluoromethanesulfonate (1.172a): The title $[4^{\oplus}+2]$ cycloaddition product **1.172a** was

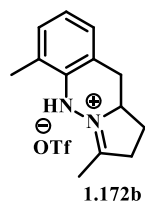


prepared in 85% yield (113 mg) as described in representative experimental procedure 5.2.3 by reacting α -chloroazo **1.155a** (1 equiv, 89 mg, 0.38 mmol), TMSOTf (1.05 equiv, 0.07 mL, 0.39 mmol), and hexane (10 mL) for 12h at room temperature. Alternatively, this product was prepared in 86% yield (325

mg) as described in representative experimental procedure 5.2.3 by reacting the

corresponding α -trifluoroacetoxyazo **1.190** (1 equiv, 340 mg, 1.1 mmol), TMSOTf (1.05 equiv, 0.21 mL, 1.15 mmol), and hexane (7 mL) for 4h at 40 $^{\circ}\text{C}$

(recrystallized from MeOH/Et₂O). ^1H NMR (500 MHz, CD_3CN) δ = 9.08 (s, 1H), 7.08 (d, J = 8.2, 1H), 7.03 (s, 1H), 6.90 (d, J = 8.2, 1H), 4.48 (qd, J = 12.3, 10.4, 1H), 3.24 (dd, J = 16.0, 4.3, 1H), 3.16 – 3.00 (m, 2H), 2.92 (dd, J = 15.8, 12.6, 1H), 2.63 (dtd, J = 12.1, 8.1, 3.9, 1H), 2.38 (s, 3H), 2.28 (s, 3H), 2.01 – 1.95 (m, 1H). ^{13}C NMR (126 MHz, CD_3CN) δ 168.4, 135.7, 133.4, 130.4, 129.8, 119.5, 114.7, 67.6, 36.2, 33.2, 25.7, 20.6, 15.9; IR (film) ν_{max} : 3198, 3024, 2970, 1740, 1728, 1501, 1427, 1366, 1294, 1233, 1217, 1148, 1030, 833 cm^{-1} . MS (ESI) calcd for $[\text{C}_{13}\text{H}_{17}\text{N}_2]^+$: 201.1392, found: 201.1387.



3,6-dimethyl-2,5,10,10a-tetrahydro-1*H*-pyrrolo[1,2-*b*]cinnolin-4-ium

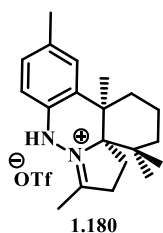
trifluoromethanesulfonate (1.172b): The title $[4+2]$ cycloaddition product

1.172b was prepared in 83% yield (40 mg) as described in representative experimental procedure 5.2.3 by reacting α -chloroazo **1.155b** (1 equiv, 33

mg, 0.14 mmol), TMSOTf (1.05 equiv, 0.03 mL, 0.15 mmol), and 6 mL hexane (6 mL)

for 12h at room temperature. Alternatively, this product was also prepared in 90% yield (181 mg) as described in representative experimental procedure 5.2.3 by reacting the corresponding α -trifluoroacetoxyazo **1.190** (1 equiv, 180 mg, 0.57 mmol), TMSOTf (1.5 equiv, 0.16 mL, 0.86 mmol), and hexane (12 mL) for 4h at 40 °C. Mp 149.1 °C (recrystallized from MeOH/Et₂O). ¹H MR (500 MHz, CD₃CN) δ = 8.22 (s, 1H), 7.13 (d, J = 7.4, 1H), 7.06 (d, J = 7.6, 1H), 6.97 (t, J = 7.5, 1H), 4.54 – 4.36 (m, 1H), 3.30 (dd, J = 16.0, 4.4, 1H), 3.23 – 3.05 (m, 2H), 2.97 (dd, J = 15.9, 12.5, 1H), 2.72 – 2.62 (m, 1H), 2.50 (s, 3H), 2.27 (s, 3H), 1.98 (ddd, J = 9.7, 8.9, 4.9, 1H). ¹³C NMR (126 MHz, CD₃CN) δ 176.1, 136.4, 130.6, 128.0, 124.9, 123.8, 120.0, 66.6, 36.4, 33.8, 25.3, 16.9, 16.6; IR (film) ν_{max} : 3219, 2995, 1713, 1668, 1601, 1479, 1425, 1391, 1362, 1281, 1254, 1234, 1223, 1148, 1030 cm⁻¹. MS (ESI) calcd for [C₁₃H₁₇N₂]⁺: 201.1392, found: 201.1386.

(4aR,13bR)-4,4,7,12,13b-pentamethyl-1,2,3,4,5,6,9,13b-



octahydrobenzo[c]pyrrolo[1,2-b]cinnolin-8-ium

trifluoromethanesulfonate (1.180): The title [4+2] cycloaddition

product **1.180** was prepared in 25% yield (46 mg) as described in

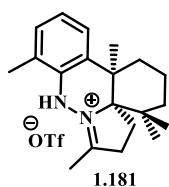
representative experimental procedure 5.2.3 by reacting the corresponding

α -trifluoroacetoxyazo **1.177** (1 equiv, 173 mg, 0.42 mmol), TMSOTf (1.05 equiv, 0.08 mL, 0.44 mmol), and hexane (10 mL) for 12h at room temperature. Alternatively, this product was prepared in 70% yield (531 mg) as described in representative experimental procedure 5.2.3 by reacting the corresponding α -trifluoroacetoxyazo **1.177** (1 equiv, 697 mg, 1.7 mmol), TMSOTf (1.5 equiv, 0.46 mL, 2.54 mmol), and hexane (15 mL) for 4h at 40 °C. Mp 211.5 °C (recrystallized from MeOH/Et₂O). ¹H NMR (500 MHz, Acetone-*d*₆) δ = 10.36 (s, 1H), 7.24 (s, 1H), 7.07 (dd, J = 8.1, 1.0, 1H), 6.89 (d, J = 8.2, 1H), 3.49 – 3.20

(m, 2H), 2.72 (s, 3H), 2.70 – 2.57 (m, 3H), 2.33 (s, 3H), 1.76 (td, $J = 13.1, 4.1$, 1H), 1.69 – 1.54 (m, 2H), 1.50 (ddd, $J = 10.9, 6.5, 3.4$, 1H), 1.40 – 1.31 (m, 1H), 1.13 (s, 3H), 1.04 (s, 3H), 0.72 (s, 3H). ^{13}C NMR (126 MHz, CD_3CN) δ 171.0, 135.3, 134.0, 129.2, 128.1, 125.2, 114.5, 85.4, 42.3, 41.5, 39.4, 36.43, 32.2, 29.9, 27.2, 25.6, 24.9, 20.9, 18.6, 16.5; IR (film) ν_{max} : 3204, 2978, 2870, 1713, 1645, 1614, 1506, 1279, 1242, 1223, 1155, 1028, 827 cm^{-1} . MS (ESI) calcd for $[\text{C}_{20}\text{H}_{29}\text{N}_2]^+$: 297.2331, found: 2297.2332.

(4aR,13bR)-4,4,7,10,13b-pentamethyl-1,2,3,4,5,6,9,13b-

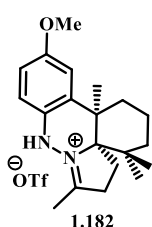
octahydrobenzo[*c*]pyrrolo[1,2-*b*]cinnolin-8-ium trifluoromethanesulfonate (1.181):



The title [4+2] cycloaddition product **1.181** was prepared in 33% yield (111 mg) as described in representative experimental procedure 5.2.3 by reacting the corresponding α -trifluoroacetoxyazo **1.177** (1 equiv, 307 mg, 0.75 mmol), TMSOTf (1.05 equiv, 0.14 mL, 0.79 mmol), and hexane (12 mL) for 12 h at room temperature. Alternatively, this product was prepared in 70% yield (262 mg) as described in representative experimental procedure 6 by reacting the corresponding α -trifluoroacetoxyazo **1.177** (1 equiv, 343 mg, 0.84 mmol), TMSOTf (1.5 equiv, 0.23 mL, 1.3 mmol), and hexane (12 mL) for 4 h at 40 °C. Mp 216.4 °C (recrystallized from MeOH/Et₂O). ^1H NMR (500 MHz, Acetone-*d*₆) δ = 9.38 (s, 1H), 7.28 (d, $J = 7.8$, 1H), 7.14 (dd, $J = 7.4, 0.4$, 1H), 7.05 (t, $J = 7.6$, 1H), 3.43 – 3.33 (m, 2H), 2.82 (s, 3H), 2.76 – 2.54 (m, 3H), 2.31 (s, 3H), 1.80 – 1.45 (m, 4H), 1.35 (ddd, $J = 13.6, 4.9, 3.1$, 1H), 1.12 (s, 3H), 1.07 (s, 3H). ^{13}C NMR (126 MHz, CD_3CN) δ 177.3, 135.8, 130.1, 128.4, 124.3, 123.9, 122.5, 84.1, 42.2, 41.6, 39.5, 36.4, 32.3, 30.0, 26.9, 25.5, 24.7, 18.6, 17.2, 17.1; IR (film) ν_{max} : 3208, 3015, 2970, 2941, 2870, 1740, 1728, 1464, 1423, 1369, 1283, 1254,

1225, 1217, 1150, 1032 cm^{-1} . MS (ESI) calcd for $[\text{C}_{20}\text{H}_{29}\text{N}_2]^+$: 297.2331, found: 2297.2328.

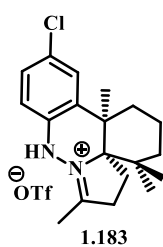
(4a*R*,13b*R*)-12-methoxy-4,4,7,13b-tetramethyl-1,2,3,4,5,6,9,13b-octahydrobenzo[*c*]pyrrolo[1,2-*b*]cinnolin-8-ium trifluoromethanesulfonate (1.182):



The title [4+2] cycloaddition product **1.182** was prepared in 53% yield (330 mg) as described in representative experimental procedure 5.2.3 by reacting the corresponding α -trifluoroacetoxyazo **1.177** (1 equiv, 578 mg, 1.35 mmol), TMSOTf (1.05 equiv, 0.26 mL, 1.42 mmol), and hexane (20 mL) for 12h at room temperature. Alternatively, this product was prepared in 40% yield (143 mg) as described in representative experimental procedure 5.2.3 by reacting the corresponding α -trifluoroacetoxyazo **1.177** (1 equiv, 326 mg, 0.76 mmol), TMSOTf (1.5 equiv, 0.21 mL, 1.15 mmol), and hexane (15 mL) for 4h at 40 °C. The final product was recrystallized using the smallest amount of methanol with diethyl ether to provide golden crystals. Mp 191.5 °C (recrystallized from MeOH/Et₂O). ¹H NMR (500 MHz, CD₃CN) δ = 9.24 (s, 1H), 6.87 (s, 1H), 6.84 (d, J = 2.1, 2H), 3.78 (s, 3H), 3.20 – 2.98 (m, 2H), 2.52 (s, 3H), 2.51 – 2.42 (m, 3H), 1.70 – 1.42 (m, 4H), 1.35 – 1.28 (m, 1H), 1.12 (t, J = 7.0, 1H), 1.06 (s, 3H), 0.95 (s, 3H), 0.64 (s, 3H). ¹³C NMR (126 MHz, CD₃CN) δ 170.6, 157.2, 131.3, 129.7, 115.8, 114.1, 110.3, 85.3, 56.3, 42.4, 41.7, 39.3, 36.4, 32.2, 29.6, 27.1, 25.6, 25.0, 18.7, 16.5; IR (film) ν_{max} : 3196, 3005, 2874, 1713, 1645, 1592, 1501, 1423, 1362, 1277, 1246, 1223, 1155, 1030, 872, 816 cm^{-1} . MS (ESI) calcd for $[\text{C}_{20}\text{H}_{29}\text{N}_2\text{O}]^+$: 313.228, found: 313.2277.

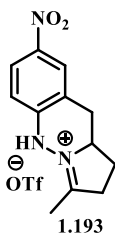
(4aR,13bR)-12-chloro-4,4,7,13b-tetramethyl-1,2,3,4,5,6,9,13b-

octahydrobenzo[c]pyrrolo[1,2-b]cinnolin-8-ium trifluoromethanesulfonate (1.183):



The title [4+2] cycloaddition product **1.183** was prepared in 35% yield (160 mg) as described in representative experimental procedure 5.2.3 by reacting the corresponding α -trifluoroacetoxyazo **1.177** (1 equiv, 422 mg, 0.98 mmol), TMSOTf (1.05 equiv, 0.19 mL, 1.03 mmol), and hexane (20 mL) for 12h at room temperature. Alternatively, this product was prepared in 42% yield (71 mg) as described in representative experimental procedure 5.2.3 by reacting the corresponding α -trifluoroacetoxyazo **1.177** (1 equiv, 157 mg, 0.36 mmol), TMSOTf (1.5 equiv, 0.10 mL, 0.55 mmol), and hexane (15 mL) for 4 h at 40 °C. Mp 230.0 °C (recrystallized from MeOH/Et₂O). ¹H NMR (500 MHz, CD₃CN) δ = 9.73 (s, 1H), 7.28 (dd, J = 26.5, 24.9, 2H), 6.91 (d, J = 8.6, 1H), 3.26 – 2.93 (m, 2H), 2.56 (s, 3H), 2.53 – 2.37 (m, 3H), 1.72 – 1.23 (m, 5H), 1.06 (s, 3H), 0.96 (s, 3H), 0.66 (s, 3H). ¹³C NMR (126 MHz, CD₃CN) δ 172.7, 136.5, 130.1, 128.7, 128.6, 124.8, 116.0, 84.9, 42.3, 41.7, 39.2, 36.5, 32.0, 29.6, 27.0, 25.5, 24.8, 18.5, 16.7; IR (film) ν_{max} : 3177, 3015, 2970, 2947, 1740, 1728, 1493, 1435, 1366, 1279, 1225, 1217, 1161, 1028, 824 cm⁻¹. MS (ESI) calcd for [C₁₉H₂₆ClN₂]⁺: 317.1785, found: 317.1781.

3-methyl-8-nitro-2,5,10,10a-tetrahydro-1H-pyrrolo[1,2-b]cinnolin-4-ium

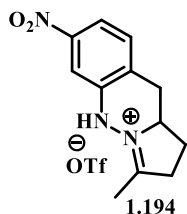


trifluoromethanesulfonate (1.193): The title [4+2] cycloaddition product **1.193** was prepared in 86% yield (324 mg) as described in representative experimental procedure 5.2.3 by reacting α -trifluoroacetoxyazo **1.175** (1 equiv, 298 mg, 0.99 mmol), TMSOTf (1.05 equiv, 0.19 mL, 1.04 mmol), and hexane (20 mL) for 12h at room temperature. Alternatively, this product was prepared in

96% yield (268 mg) as described in representative experimental procedure 5.2.3 by reacting α -trifluoroacetoxyazo **1.175** (1 equiv, 253 mg, 0.732 mmol), TMSOTf (1.5 equiv, 0.20 mL, 1.1 mmol), and hexane (15 mL) for 4h at 40 °C. Mp 209.6 °C (recrystallized from MeOH/Et₂O). ¹H NMR (500 MHz, CD₃CN) δ = 10.05 (s, 1H), 8.27 – 7.83 (m, 2H), 7.16 (d, *J* = 8.7, 1H), 4.64 – 4.33 (m, 1H), 3.45 (dd, *J* = 16.2, 4.3, 1H), 3.23 – 3.07 (m, 2H), 3.03 (dd, *J* = 16.2, 12.5, 1H), 2.73 – 2.62 (m, 1H), 2.45 (s, 3H), 2.05 – 1.96 (m, 1H). ¹³C NMR (126 MHz, Acetone-*d*₆) δ 172.1, 143.4, 143.0, 125.8, 124.9, 119.9, 114.6, 67.0, 36.7, 33.2, 25.7, 16.0; IR (film) ν_{max} : 3186, 3003, 1618, 1593, 1504, 1344, 1287, 1240, 1223, 1153, 1030, 937, 826 cm⁻¹. MS (ESI) calcd for [C₁₂H₁₄N₃O₂]⁺: 232.1086, found: 232.1084.

3-methyl-7-nitro-2,5,10,10a-tetrahydro-1H-pyrrolo[1,2-*b*]cinnolin-4-ium trifluoromethanesulfonate and 3-methyl-9-nitro-2,5,10,10a-tetrahydro-1H-pyrrolo[1,2-*b*]cinnolin-4-ium trifluoromethanesulfonate (1.194 & 1.195): The title [4+2] cycloaddition products was prepared as a 6:4 mixture in 87% yield (200 mg) as described in representative experimental procedure 5.2.3 by reacting the corresponding α -trifluoroacetoxyazo **1.190** (1 equiv, 209 mg, 0.61 mmol), TMSOTf (1.5 equiv, 0.16 mL, 0.91 mmol), and hexane (15 mL) for 12h at room temperature. Alternatively, this mixture was prepared in quantitative yield (467 mg) as described in representative experimental procedure 5.2.3 by reacting the corresponding α -trifluoroacetoxyazo **1.190** (1 equiv, 468 mg, 1.23 mmol), TMSOTf (1.5 equiv, 0.33 mL, 1.85 mmol), and hexane (15 mL) for 4h at 40 °C. The minor isomer (**1.195**) was less soluble in chloroform than the major isomer (**1.194**) and filtration of a chloroform solution provided pure minor isomer in 20% yield (15 mg from 75 mg of the mixture).

3-methyl-7-nitro-2,5,10,10a-tetrahydro-1*H*-pyrrolo[1,2-*b*]cinnolin-4-ium



trifluoromethanesulfonate (1.194): ^1H NMR (500 MHz, CD_3CN) δ =

9.74 (s, 1H), 7.85 (s, 1H), 7.86 – 7.81 (m, 1H), 7.43 (d, J = 8.3, 1H),

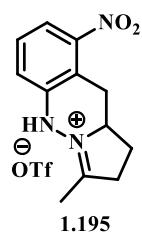
4.58 – 4.47 (m, 1H), 3.45 (dd, J = 16.6, 4.3, 1H), 3.18 – 2.99 (m, 3H),

2.73 – 2.61 (m, 1H), 2.45 (s, 3H), 2.08 – 1.95 (m, 1H). ^{13}C NMR (126 MHz, CD_3CN) δ

171.4, 148.8, 138.8, 131.4, 126.6, 117.8, 109.5, 66.7, 36.5, 33.2, 25.5, 16.1.

3-methyl-9-nitro-2,5,10,10a-tetrahydro-1*H*-pyrrolo[1,2-*b*]cinnolin-4-ium

trifluoromethanesulfonate (1.195): \square Mp 191.7 $^\circ\text{C}$ (recrystallized from MeOH/Et₂O).



^1H NMR (500 MHz, CD_3CN) δ = z (d, J = 21.2, 1H), 7.66 (d, J = 8.1, 1H),

7.47 (t, J = 8.2, 1H), 7.34 (d, J = 8.2, 1H), 4.47 – 4.36 (m, 1H), 3.66 (dd, J =

17.2, 4.3, 1H), 3.21 – 3.00 (m, 3H), 2.66 (dtd, J = 12.5, 8.3, 4.0, 1H), 2.43 (s,

3H), 2.04 (ddd, J = 18.4, 13.2, 9.1, 1H). ^{13}C NMR (126 MHz, CD_3CN) δ

171.2, 150.2, 139.8, 129.7, 119.7, 119.3, 114.7, 65.7, 36.4, 30.5, 25.4, 16.0; IR (film)

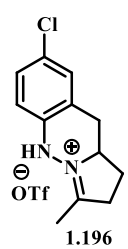
ν_{max} : 3144, 2994, 2947, 1713, 1678, 1618, 1584, 1533, 1358, 1277, 1238, 1225, 1177,

1153, 1177, 1153, 1030, 853, 804 cm^{-1} . MS (ESI) calcd for $[\text{C}_{12}\text{H}_{14}\text{N}_3\text{O}_2]^+$: 232.1086,

found: 232.1082.

8-chloro-3-methyl-2,5,10,10a-tetrahydro-1*H*-pyrrolo[1,2-*b*]cinnolin-4-ium

trifluoromethanesulfonate (1.196): The title [4+2] cycloaddition product **1.196** was



prepared in 72% yield (106 mg) as described in representative experimental

procedure 5.2.3 by reacting the corresponding α -trifluoroacetoxyazo **1.190** (1

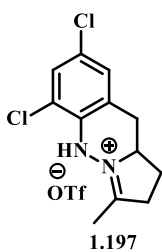
equiv, 134 mg, 0.4 mmol), TMSOTf (1.05 equiv, 0.07 mL, 0.42 mmol), and

hexane (12 mL) for 12h at room temperature. Alternatively, this product was

prepared in 84% yield (361 mg) as described in representative experimental procedure

5.2.3 by reacting the corresponding α -trifluoroacetoxyazo **1.190** (1 equiv, 427 mg, 1.16 mmol), TMSOTf (1.5 equiv, 0.31 mL, 1.73 mmol), and hexane (15 mL) for 4h at 40 °C. Mp 142.0 °C (recrystallized from MeOH/Et₂O). ¹H NMR (500 MHz, CD₃CN) δ = 9.35 (s, 1H), 7.26 (d, J = 8.1, 2H), 7.00 (d, J = 8.4, 1H), 4.48 (dd, J = 4.5, 2.0, 1H), 3.29 (dd, J = 16.1, 4.2, 1H), 3.18 – 3.03 (m, 2H), 2.94 (dd, J = 15.9, 12.6, 1H), 2.69 – 2.57 (m, 1H), 2.40 (s, 3H), 2.05 – 1.95 (m, 1H). ¹³C NMR (126 MHz, CD₃CN) δ 169.8, 136.9, 129.7, 129.0, 127.8, 121.5, 116.2, 67.0, 36.3, 32.9, 25.5, 15.9; IR (film) ν_{max} : 3204, 3003, 1713, 1678, 1610, 1491, 1433, 1420, 1283, 1237, 1223, 1152, 1026, 864, 804 cm⁻¹. MS (ESI) calcd for [C₁₂H₁₄ClN₂]⁺: 221.0846, found: 221.0842.

6,8-dichloro-3-methyl-2,5,10,10a-tetrahydro-1H-pyrrolo[1,2-*b*]cinnolin-4-ium



trifluoromethanesulfonate (1.197): The title [4+2] cycloaddition product

1.197 was prepared in 59% yield (120 mg) as described in representative experimental procedure 5.2.3 by reacting the corresponding α -trifluoroacetoxyazo **1.190** (1 equiv, 186 mg, 0.5 mmol), TMSOTf (1.05

equiv, 0.10 mL, 0.53 mmol), and hexane (15 mL) for 12h at room temperature.

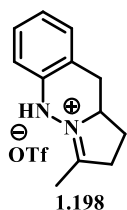
Alternatively, this product was prepared in 73% yield (178 mg) as described in representative experimental procedure 5.2.3 by reacting the corresponding α -

trifluoroacetoxyazo **1.190** (1 equiv, 233 mg, 0.6 mmol), TMSOTf (1.5 equiv, 0.16 mL, 0.86 mmol), and hexane (15 mL) for 4h at 40 °C. Mp 169.9 °C (recrystallized from MeOH/Et₂O). ¹H NMR (500 MHz, CD₃CN) δ = 8.60 (s, 1H), 7.46 (dd, J = 2.2, 0.9, 1H), 7.26 (s, 1H), 4.46 (ddd, J = 8.1, 3.8, 1.9, 1H), 3.34 (dd, J = 16.3, 4.4, 1H), 3.29 – 3.09 (m, 2H), 2.99 (dd, J = 16.3, 12.4, 1H), 2.69 (dddd, J = 13.3, 9.9, 8.3, 3.5, 1H), 2.51 (s, 3H), 2.06 – 1.96 (m, 1H). ¹³C NMR (126 MHz, CD₃CN) δ 178.9, 133.9, 129.0, 128.9, 128.3,

123.8, 121.0, 66.0, 36.7, 33.4, 24.9, 17.0; IR (film) ν_{max} : 3208, 2974, 1713, 1678, 1576, 1479, 1414, 1277, 1244, 1223, 1148, 1028, 856 cm^{-1} . MS (ESI) calcd for $[\text{C}_{12}\text{H}_{13}\text{Cl}_2\text{N}_2]^+$: 255.0456, found: 255.0453.

3-methyl-2,5,10,10a-tetrahydro-1*H*-pyrrolo[1,2-*b*]cinnolin-4-ium

trifluoromethanesulfonate (1.198): The title [4+2] product **1.198** was prepared in 96%



yield (258 mg) as described in representative experimental procedure 5.2.3

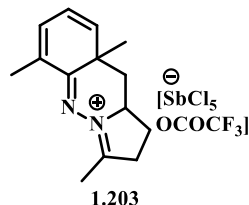
by reacting □ the corresponding α -trifluoroacetoxyazo **1.190** (1 equiv, 240 mg, 0.8 mmol), TMSOTf (1.5 equiv, 0.22 mL, 1.2 mmol), and hexane (15

mL) for 4h at 40 °C. Mp 136.0 °C (recrystallized from MeOH/Et₂O). ¹H

NMR (500 MHz, CDCl₃) δ = 9.83 (s, 1H), 7.19 (t, J = 7.7, 1H), 7.08 (d, J = 7.6, 1H), 7.02 (d, J = 7.9, 1H), 6.97 (td, J = 7.5, 0.9, 1H), 4.47 (dd, J = 5.0, 2.2, 1H), 3.28 – 3.14 (m, 2H), 3.08 (dd, J = 19.5, 9.7, 1H), 2.94 (dd, J = 15.8, 12.6, 1H), 2.75 – 2.64 (m, 1H), 2.50 (s, 3H), 1.98 (dq, J = 13.1, 9.4, 1H). ¹³C NMR (126 MHz, CDCl₃) δ 169.3, 137.0, 129.0, 128.7, 123.0, 117.3, 114.8, 66.1, 35.4, 33.3, 25.2, 16.0. MS (ESI) calcd for $[\text{C}_{19}\text{H}_{27}\text{N}_2]^+$: 187.1235, found: 187.1231.

5.3 Experimental information for dearomatized non-protonated azomethine imine salt (Chapter 1)

3,6,9a-trimethyl-2,9a,10,10a-tetrahydro-1*H*-pyrrolo[1,2-*b*]cinnolin-4-ium



pentachloro(2,2,2-trifluoroacetoxy)stibate(V) (1.203): The title

[4+2] cycloaddition product **1.203** was prepared in 66% yield as

determined by ¹HNMR as described in representative experimental

procedure 5.2.1 by reacting α -trifluoroacetoxyazo compound **1.201** (114 mg, 0.35

mmol), SbCl₅ (2 M in CH₂Cl₂, 0.17 mL, 0.33 mmol), and CH₂Cl₂ (5 mL). ¹H NMR (500

MHz, CD₃CN) δ 6.82 (d, J = 1.9 Hz, 1H), 6.33 – 6.18 (m, 2H), 4.09 (dd, J = 11.3, 4.9 Hz, 1H), 3.19 (d, J = 7.3 Hz, 2H), 2.78 – 2.66 (m, 1H), 2.54 (d, J = 1.3 Hz, 3H), 2.47 (dd, J = 13.6, 9.8 Hz, 1H), 2.24 (dd, J = 13.7, 6.5 Hz, 1H), 2.08 (s, 3H), 2.04 – 1.96 (m, 1H), 1.14 (s, 3H). ¹³C NMR (126 MHz, CD₃CN) δ 182.3, 143.2, 137.8, 130.3, 120.7, 61.8, 37.6, 37.0, 29.2, 26.8, 16.9, 16.5.

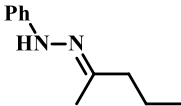
5.4 Experimental information for Chapter 2

5.4.1 Preparation of aryl hydrazones

A ketone (1.0 equiv, 1.0 mmol) was added to a room temperature solution of aryl hydrazine (1.2 equiv, 1.2 mmol) in CH₂Cl₂ (8 mL) containing 4Å molecular sieves under a nitrogen atmosphere. After stirring at room temperature for three hours, the solution was filtered and the filtrate was concentrated. The residue was dissolved in hexane (12 mL), was passed through a plug of basic alumina and was concentrated *in vacuo* to provide a diastereomeric mixture of the hydrazone as a yellow oil.

5.4.2 Characterization data of aryl hydrazones

(E)-1-(pentan-2-ylidene)-2-phenylhydrazine: Yield = 100%; *E/Z* 1:0.18; major


 diastereomer: ¹H NMR (500 MHz, CDCl₃) δ 7.24 – 7.19 (m, 2H), 7.04 (dd, J = 8.6, 1.0 Hz, 2H), 6.86 – 6.78 (m, 2H), 2.30 – 2.25 (m, 2H), 1.85 (s, 3H), 1.61 (dd, J = 15.0, 7.5 Hz, 2H), 0.96 (t, J = 7.4 Hz, 3H). ¹³C NMR (126 MHz, CDCl₃) δ 147.1, 146.1, 129.3, 119.6, 113.1, 113.0, 41.1, 20.1, 14.4, 13.9. Observable resonances for minor diastereomer: ¹H NMR (500 MHz, CDCl₃) δ 2.25 – 2.20 (m, 2H), 2.02 (s, 3H), 1.02 (t, J = 7.4 Hz, 3H). ¹³C NMR (126 MHz, CDCl₃) δ 31.5, 23.4, 18.7.

(E)-1-(hexan-2-ylidene)-2-phenylhydrazine: Yield = 90%; *E/Z* 1:0.19; major

diastereomer: ¹H NMR (500 MHz, CDCl₃) δ 7.25 – 7.19 (m, 2H), 7.08 – 6.98 (m, 2H),

6.82 (tt, $J = 7.4, 1.1$ Hz, 1H), 2.40 – 2.28 (m, 2H), 1.86 (s, 3H), 1.63 – 1.52 (m, 2H), 1.42 – 1.25 (m, 5H), 0.92 (dt, $J = 11.2, 7.0$ Hz, 3H). ^{13}C NMR (126 MHz, CDCl_3) δ 146.1, 129.3, 119.6, 113.1, 39.0, 31.6, 26.5, 22.6, 14.4, 14.1.

Observable resonances for minor diastereomer: ^1H NMR (500 MHz, CDCl_3) δ 2.27 – 2.22 (m, 2H), 2.02 (s, 3H). ^{13}C NMR (126 MHz, CDCl_3) δ 129.3, 77.4, 77.1, 76.9, 32.1, 25.0, 23.4, 22.6.

1-(2-(benzyloxy)phenyl)-2-(propan-2-ylidene)hydrazine (2.50): Yield = 70%. ^1H NMR

(500 MHz, CDCl_3) δ 7.46 – 7.28 (m, 8H), 6.97 – 6.91 (m, 1H), 6.88 (dd, $J = 8.0, 1.1$ Hz, 1H), 6.75 (td, $J = 7.7, 1.6$ Hz, 1H), 5.11 (s, 3H), 2.05 (s, 3H), 1.83 (s, 3H).

(E)-1-(1-(cyclohex-3-en-1-yl)ethylidene)-2-phenylhydrazine (2.72): Yield = 78%. ^1H

NMR (500 MHz, CDCl_3) δ 7.26 – 7.18 (m, 2H), 7.05 (dd, $J = 8.5, 0.9$ Hz, 2H), 6.89 (s, 1H), 6.84 – 6.75 (m, 1H), 5.76 – 5.61 (m, 2H), 2.53 – 2.42 (m, 1H), 2.25 – 2.09 (m, 4H), 1.98 – 1.89 (m, 1H), 1.86 (s, 3H), 1.66 – 1.51 (m, 1H). ^{13}C NMR (126 MHz, CDCl_3) δ 149.4, 146.1, 129.3, 126.8, 126.4, 119.6, 113.1, 53.5, 42.9, 28.9, 26.6, 25.6, 13.0.

5.4.3 Preparation of aryl α -chloroazo compounds

A solution of DMSO (2.5 equiv) in THF (10 mL) was stirred and cooled to $-55\text{ }^\circ\text{C}$ in a flame-dried flask under a nitrogen atmosphere at which point oxalyl chloride (2.0 equiv) was added in a dropwise manner. The reaction was maintained at $-55\text{ }^\circ\text{C}$ until gas evolution ceased (~ 20 min) at which point the reaction was cooled further to $-78\text{ }^\circ\text{C}$. A mixture of Et_3N (2.5 equiv) and hydrazone (1 equiv) in THF (3 mL) was added in a dropwise manner *via* cannula to give a white precipitate. The reaction mixture was

maintained at -78 °C for 30 min and was then allowed to warm to room temperature at which point the solid was removed by filtration through a medium porosity sintered-glass funnel. The filtrate was concentrated by rotary evaporation and the residue was dissolved in pentane (~15 mL). The pentane solution was filtered through a plug of cotton in a pasteur pipette to remove insoluble solids. The pentane was removed *in vacuo* to provide the clean α -chloroazo product as a yellow oil.

5.4.4 Characterization data of α -chloroazo compounds

(E)-1-(2-chloropentan-2-yl)-2-phenyldiazene (2.39a): Yield = 81%. ^1H NMR (500

MHz, CDCl_3) δ 7.83 – 7.65 (m, 2H), 7.47 (d, J = 1.8 Hz, 3H), 2.27 (ddd, J = 14.0, 11.7, 4.7 Hz, 1H), 2.16 (ddd, J = 14.0, 11.8, 4.7 Hz, 1H), 1.90 (s, 3H), 1.57 (dddd, J = 10.9, 9.3, 7.0, 3.2 Hz, 1H), 1.49 – 1.38 (m, 1H),

0.95 (t, J = 7.4 Hz, 3H). ^{13}C NMR (126 MHz, CDCl_3) δ 151.2, 131.3, 129.2, 123.0, 96.8, 45.1, 28.8, 17.7, 14.1.

(E)-1-(2-chloroheptan-2-yl)-2-phenyldiazene (2.39b): Yield = 91%. ^1H NMR (500

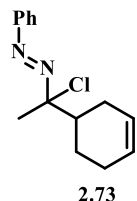
MHz, CDCl_3) δ 7.86 – 7.66 (m, 2H), 7.57 – 7.40 (m, 3H), 2.24 (dddd, J = 54.8, 14.0, 11.7, 4.5 Hz, 2H), 1.93 (s, 3H), 1.68 – 1.51 (m, 1H), 1.48 – 1.20 (m, 5H), 0.90 (dd, J = 8.9, 5.1 Hz, 3H). ^{13}C NMR (126 MHz, CDCl_3) δ 151.2, 131.3, 129.2, 123.0, 97.0, 43.0, 31.8, 28.8, 24.0, 22.5, 14.1.

(E)-1-(2-(benzyloxy)phenyl)-2-(2-chloropropan-2-yl)diazene (2.51): Yield = 60%. ^1H

NMR (500 MHz, CDCl_3) δ 7.50 – 7.47 (m, 2H), 7.45 (dt, J = 3.5, 1.8 Hz, 1H), 7.41 – 7.33 (m, 3H), 7.30 (ddd, J = 8.6, 4.4, 1.2 Hz, 1H), 7.10 (dd, J = 8.3, 1.1 Hz, 1H), 7.00 (ddd, J = 8.0, 7.4, 1.2 Hz, 1H), 5.29 (s, 2H), 1.95

(s, 6H). ^{13}C NMR (126 MHz, CDCl_3) δ 155.6, 141.4, 137.0, 132.4, 128.4, 127.7, 126.9, 121.4, 118.0, 115.9, 93.5, 71.8, 30.3.

(E)-1-(1-chloro-1-(cyclohex-3-en-1-yl)ethyl)-2-phenyldiazene (2.73): Yield = 92%. ^1H



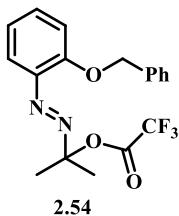
NMR (500 MHz, CDCl_3) δ 7.83 – 7.69 (m, 2H), 7.48 (ddd, J = 7.5, 4.4, 2.3 Hz, 3H), 5.75 – 5.58 (m, 2H), 2.52 (dddd, J = 20.4, 12.8, 5.0, 2.3 Hz, 1H), 2.24 – 2.04 (m, 4H), 1.98 (s, 3H), 1.58 – 1.44 (m, 2H). ^{13}C NMR (126 MHz, CDCl_3) δ 131.2, 129.0, 126.9, 126.7, 125.8, 125.7, 122.9, 45.3, 44.8, 26.7, 26.5, 25.6, 23.8.

5.4.5 Preparation of α -trifluoroacetoxyazo compounds

A solution of DMSO (1.2 equiv) in CH_2Cl_2 (1 mL) was added in a dropwise manner to a -78°C solution of trifluoroacetic anhydride (TFAA) (1.1 or 1.2 equiv) in 10 mL of CH_2Cl_2 under a nitrogen atmosphere. The mixture was stirred for 10 min at -78°C at which point a solution of hydrazone (1 equiv) in CH_2Cl_2 (5 mL) was added dropwise to the mixture via cannula. After 1 min, TEA (1.15 equiv) was added in a dropwise manner. The mixture was stirred for 10 min at -78°C and was then allowed to warm to room temperature (~20 min) at which point the mixture was concentrated. The residue was dissolved in hexane (~15 mL), filtered through a plug of basic alumina to remove triethylammonium salt, and the hexane was removed *in vacuo* to provide the α -trifluoroacetoxyazo product as a yellow oil.

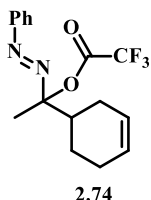
5.4.6 Characterization data of α -trifluoroacetoxyazo compounds

(E)-2-((2-(benzyloxy)phenyl)diazenyl)propan-2-yl 2,2,2-trifluoroacetate (2.54): Yield = 56%. ^1H NMR (500 MHz, CDCl_3) δ 7.46 – 7.42 (m, 2H), 7.42 – 7.33 (m, 4H), 7.30 (t, J



= 7.3 Hz, 1H), 7.07 (d, J = 8.3 Hz, 1H), 7.00 – 6.95 (m, 1H), 5.23 (s, 2H), 1.81 (s, 6H). ^{13}C NMR (126 MHz, CDCl_3) δ 155.6, 141.1, 136.8, 132.6, 128.5, 127.8, 127.0, 121.1, 117.7, 115.1, 106.0, 71.2, 24.4.

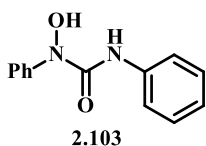
(E)-1-(cyclohex-3-en-1-yl)-1-(phenyldiazenyl)ethyl 2,2,2-



trifluoroacetate (2.74): Yield = 73%. ^1H NMR (500 MHz, CDCl_3) δ 7.75 – 7.66 (m, 2H), 7.53 – 7.45 (m, 3H), 5.80 – 5.51 (m, 2H), 2.38 – 2.27 (m, 1H), 2.27 – 2.04 (m, 4H), 1.97 (d, J = 3.2 Hz, 3H), 1.81 – 1.71 (m, 1H), 1.54 – 1.40 (m, 1H). ^{13}C NMR (126 MHz, CDCl_3) δ 149.4, 146.1, 129.3, 126.8, 126.4, 119.6, 113.1, 53.5, 42.9, 28.9, 26.6, 25.6, 13.0.

5.4.7 Experimental information to prepare starting materials for new type of C-H amination (Chapter 2)

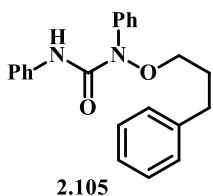
5.4.7.1 Preparation and characterization data of 1-hydroxy-1,3-diphenylurea (2.103)



A solution of phenylisocyanate (1.0 equiv, 0.1191g, 1.0 mmol) in CHCl_3 (4 mL) was transferred into a solution of phenylhydroxyl amine (1.0 equiv, 0.1091g, 1.0 mmol) CHCl_3 (4 mL) under a nitrogen

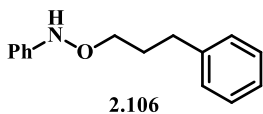
atmosphere. The mixture was stirred for an hour to give a white precipitate of 1-hydroxy-1,3-diphenylurea (**2.103**), which was separated by filtration. Yield = 88%. ^1H NMR (500 MHz, CDCl_3) δ 8.23 (s, 1H), 7.84 (s, 1H), 7.37 (ddd, J = 3.4, 2.9, 1.4 Hz, 2H), 7.24 – 7.21 (m, 4H), 7.18 – 7.12 (m, 2H), 7.10 – 7.00 (m, 2H).

5.4.7.2 Preparation and characterization data of 1,3-diphenyl-1-(3-phenylpropoxy)urea (**2.105**)



A mixture of 1-hydroxy-1,3-diphenylurea (**2.103**) (1 equiv, 0.7614g, 3.34 mmol), 1-bromo-3-phenyl propane (**2.104**) (2 equiv, 1.33g, 6.67 mmol), K₂CO₃, (2.8 equiv, 1.292g, 9.35 mmol) and DMSO (18 equiv, 4.74 g, 60.7 mmol) was stirred at 30 °C for 17h. After that, the reaction mixture was mixed with water (10 mL) and extracted with CH₂Cl₂ (15 mL × 3). It was dried with sodium sulfate and concentrated *in vacuo*. The residue was purified by column chromatography to yield **2.105** in 98% (1.482g) yield. R_f = 0.66, 9:1 Hexane: EtOAc. ¹H NMR (500 MHz, CDCl₃) δ 7.88 (s, 1H), 7.50 (d, *J* = 16.8 Hz, 4H), 7.39 (d, *J* = 0.8 Hz, 2H), 7.32 (s, 4H), 7.21 (tt, *J* = 6.7, 1.2 Hz, 2H), 7.16 (s, 2H), 7.12 – 7.04 (m, 1H), 4.00 (s, 2H), 2.76 (s, 2H), 2.09 (s, 2H). ¹³C NMR (126 MHz, CDCl₃) δ 153.9, 140.6, 140.3, 137.8, 129.0, 128.6, 128.6, 128.3, 126.2, 125.9, 123.7, 122.5, 119.5, 74.3, 32.3, 29.7.

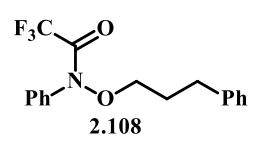
5.4.7.3 Preparation and characterization data of *N*-phenyl-*O*-(3-phenylpropyl)hydroxylamine (**2.106**)



A mixture of **2.105** (1 equiv, 1.184 g, 3.42 mmol), hydroquinone (0.01 equiv, 4mg, 0.03mmol), DMF (1.5mL) refluxed for 5 hours under a nitrogen atmosphere. Then, hydrazine (0.4 mL) was added and refluxed for additional 12 hrs. The reaction mixture was cooled to a room temperature and the reaction was quenched by water and extracted by CH₂Cl₂. The DCM solution was concentrated *in vacuo*. The residue was purified by column chromatography to yield **2.106** in 71% (0.553g) yield. R_f = 0.66, 9:1 Hexane: EtOAc. ¹H NMR (500 MHz, CDCl₃) δ 7.32 – 7.14 (m, 7H), 6.94 (dt, *J* = 9.0, 7.9 Hz, 4H), 3.93 (t, *J* = 6.5 Hz, 2H),

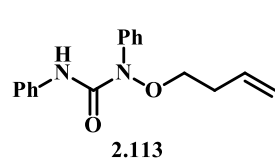
2.76 (t, 2H), 2.18 – 1.85 (m, 2H). ^{13}C NMR (126 MHz, CDCl_3) δ 148.8, 141.8, 129.1, 128.5, 128.5, 126.0, 122.0, 114.2, 74.7, 32.5, 30.3.

5.4.7.4 Characterization data of 2,2,2-trifluoro-*N*-phenyl-*N*-(3-phenylpropoxy)acetamide (2.108)


2.108

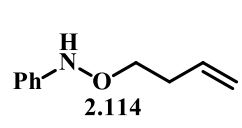
^1H NMR (500 MHz, cdcl_3) δ 10.50 (d, J = 6.2 Hz, 1H), 7.62 – 6.93 (m, 9H), 3.94 (t, J = 5.9 Hz, 2H), 2.70 (d, J = 6.5 Hz, 2H), 2.00 (dd, J = 14.2, 6.9 Hz, 2H).

5.4.7.5 Characterization data of 1-(but-3-en-1-yloxy)-1,3-diphenylurea (2.113)


2.113

The procedure used was the same mentioned in section 5.4.7.2. Yield = 74%. ^1H NMR (500 MHz, CDCl_3) δ 8.02 (s, 1H), 7.51 (ddd, J = 10.3, 6.2, 1.1 Hz, 4H), 7.41 – 7.36 (m, 2H), 7.35 – 7.29 (m, 2H), 7.21 (dd, J = 10.5, 4.3 Hz, 1H), 7.12 – 7.02 (m, 1H), 5.94 (ddt, J = 17.1, 10.4, 6.7 Hz, 1H), 5.29 (td, J = 8.7, 1.1 Hz, 2H), 4.03 (t, J = 6.0 Hz, 2H), 2.57 – 2.42 (m, 2H). ^{13}C NMR (126 MHz, CDCl_3) δ 153.9, 140.2, 138.0, 134.5, 129.0, 128.6, 125.8, 123.5, 122.4, 119.3, 118.4, 73.4, 32.2.

5.4.7.6 Characterization data of *O*-(but-3-en-1-yl)-*N*-phenylhydroxylamine (2.114)

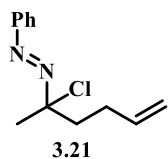

2.114

The procedure used was the same mentioned in section 5.4.7.3. Yield = 67%. ^1H NMR (500 MHz, CDCl_3) δ 7.32 – 7.16 (m, 3H), 7.02 – 6.81 (m, 3H), 5.95 – 5.79 (m, 1H), 5.23 – 4.93 (m, 2H), 3.96 (t, J = 6.7 Hz, 2H), 2.47 (qt, J = 6.7, 1.4 Hz, 2H). ^{13}C NMR (126 MHz, CDCl_3) δ 148.7, 134.9, 128.9, 121.9, 116.8, 114.1, 74.4, 33.1.

5.5 Experimental information for Chapter 3

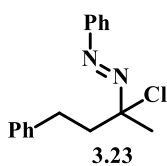
5.5.1 Preparation of α -chloroazo using acetyl chloride

(E)-1-(2-chlorohex-5-en-2-yl)-2-phenyldiazene (3.21): A solution of DMSO (2.5 equiv)



in THF (10 mL) was stirred and cooled to -55 °C in a flame-dried flask under a nitrogen atmosphere at which point acetyl chloride (2.0 equiv) was added in a dropwise manner. The reaction was maintained at -55

°C until gas evolution ceased (~20 min) at which point the reaction was cooled further to -78 °C. A mixture of Et₃N (2.5 equiv) and hydrazone **3.20** (1 equiv) in THF (3 mL) was added in a dropwise manner *via* cannula to give a white precipitate. The reaction mixture was maintained at -78 °C for 30 min and was then allowed to warm to room temperature at which point the solid was removed by filtration through a medium porosity sintered-glass funnel. The filtrate was concentrated by rotary evaporation and the residue was dissolved in hexane (~15 mL). The hexane solution was filtered through a plug of cotton in a pasteur pipette to remove insoluble solids. The hexane was removed *in vacuo* to provide clean α -chloroazo product **3.21** (227mg, 70%) as a yellow oil.



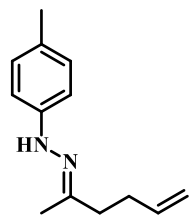
(E)-1-(2-chloro-4-phenylbutan-2-yl)-2-phenyldiazene (3.23): The procedure used was the same mentioned in the preparation of **3.21** (section 5.5.1). Yield = 81%.

5.5.2 General experimental procedure for preparation of aryl hydrazones

The hydrazones prepared in this section were prepared with the same method used to prepare the hydrazone in the section 5.4.1.

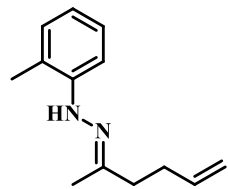
5.5.3 Characterization data for aryl hydrazones

(E)-1-(hex-5-en-2-ylidene)-2-(p-tolyl)hydrazine: Yield = 75% (152 mg); *E/Z* 1:0.14;



major diastereomer: ^1H NMR (500 MHz, CDCl_3) δ = 7.04 (d, J = 8.1, 2H), 6.97 – 6.92 (m, 2H), 6.78 (s, broad, 1H), 6.01 – 5.78 (m, 1H), 5.10 (dd, J = 26.6, 16.4, 1H), 4.98 (d, J = 12.1, 1H), 2.45 – 2.30 (m, 4H), 2.27 (s, 3H), 1.85 (s, 3H). ^{13}C NMR (125 MHz, CDCl_3) δ 145.4, 143.7, 138.1, 129.6, 128.7, 114.8, 113.0, 38.2, 30.8, 20.5, 14.5. Observable resonances for minor diastereomer: ^1H NMR (500 MHz, CDCl_3) δ = 5.12 (dd, J = 17.1, 1.4, 1H), 2.02 (s, 3H). ^{13}C NMR (126 MHz, CDCl_3) δ 137.1, 115.9, 29.1, 28.7, 23.2. MS (ESI) calcd for $[\text{C}_{13}\text{H}_{18}\text{N}_2\text{H}]^+$: 203.1548, found: 203.1552.

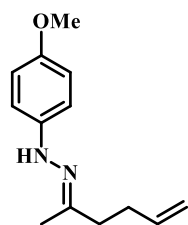
(E)-1-(hex-5-en-2-ylidene)-2-(o-tolyl)hydrazine: Yield = 83% (168 mg); *E/Z* 1:0.18;



major diastereomer: ^1H NMR (500 MHz, CDCl_3) δ = 7.46 (d, J = 8.1, 1H), 7.18 (t, J = 7.7, 1H), 7.06 (d, J = 7.4, 1H), 6.77 (t, J = 7.4, 1H), 6.7-6.9 (s, broad, 1H), 5.98 – 5.77 (m, 1H), 5.08 (dq, J = 5.9, 1.5, 1H), 4.99 (ddt, J = 10.2, 1.9, 1.1, 1H), 2.47 – 2.36 (m, 4H), 2.19 (s, 3H), 1.89 (s, 3H). ^{13}C NMR (126 MHz, CDCl_3) δ 143.5, 138.0, 130.1, 127.2, 120.2, 119.1, 116.2, 114.9, 112.5, 38.2, 30.7, 16.9, 14.5. Observable resonances for minor diastereomer: ^1H NMR (500 MHz, CDCl_3) δ = 7.42 (d, J = 8.1, 2H), 5.14 (dd, J = 17.1, 1.5, 1H), 2.17 (s, 3H), 2.07 (s, 3H). ^{13}C NMR (126 MHz, CDCl_3) δ 34.7. MS (ESI) calcd for $[\text{C}_{13}\text{H}_{18}\text{N}_2\text{H}]^+$: 203.1548, found: 203.1548.

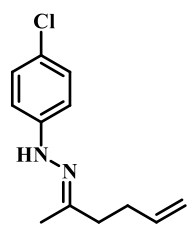
(E)-1-(hex-5-en-2-ylidene)-2-(4-methoxyphenyl)hydrazine: Yield = 64% (140 mg);

E/Z 1:0.18; major diastereomer: ^1H NMR (500 MHz, CDCl_3) δ = 7.00 (d, J = 8.9, 2H), 6.83 (d, J = 8.9, 2H), 6.68 (s, broad, 1H), 5.93 – 5.80 (m, 1H), 5.07 (dd, J = 17.1, 1.5,



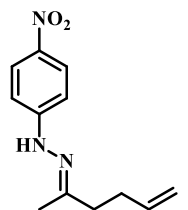
1H), 4.98 (dd, $J = 10.2, 0.8$, 1H), 3.77 (s, 3H), 2.55 – 2.23 (m, 4H), 1.85 (s, 3H). ^{13}C NMR (126 MHz, CDCl_3) δ 153.5, 145.7, 140.2, 138.1, 124.4, 114.6, 114.3, 55.7, 38.2, 30.8, 14.5. Observable resonances for minor diastereomer: ^1H NMR (500 MHz, CDCl_3) δ = 5.12 (d, $J = 17.2$, 1H), 3.88 (s, 3H), 2.02 – 1.99 (m, 3H). ^{13}C NMR (126 MHz, CDCl_3) δ 137.1, 115.9, 55.6, 34.7, 23.1, 19.5. MS (ESI) calcd for $[\text{C}_{13}\text{H}_{18}\text{N}_2\text{OH}]^+$: 219.1497, found: 219.1503.

(E)-1-(4-chlorophenyl)-2-(hex-5-en-2-ylidene)hydrazine: Yield = 68% (152 mg); *E/Z*



1:0.17; major diastereomer: ^1H NMR (500 MHz, CDCl_3) δ = 7.18 (d, $J = 8.8$, 2H), 6.98 (d, $J = 8.8$, 2H), 6.87 (s, broad, 1H), 5.88 (ddt, $J = 16.4$, 10.2, 6.3, 1H), 5.07 (dd, $J = 17.1, 1.5$, 1H), 4.98 (d, $J = 10.0$, 1H), 2.46 – 2.25 (m, 4H), 1.85 (s, 3H). ^{13}C NMR (126 MHz, CDCl_3) δ 146.6, 144.5, 137.9, 129.0, 124.0, 114.9, 114.0, 38.1, 30.6, 14.6. Observable resonances for minor diastereomer: ^1H NMR (500 MHz, CDCl_3) δ = 5.14 (d, $J = 17.2$, 1H), 2.04 (s, 3H). ^{13}C NMR (126 MHz, CDCl_3) δ 136.9, 129.4, 123.8, 116.0, 114.0, 25.2, 15.5. MS (ESI) calcd for $[\text{C}_{12}\text{H}_{15}\text{ClN}_2\text{H}]^+$: 223.1002, found: 223.1008.

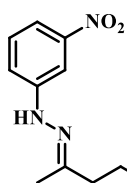
(E)-1-(hex-5-en-2-ylidene)-2-(4-nitrophenyl)hydrazine: Yield = 65% (151 mg); *E/Z*



1:0.13; major diastereomer: ^1H NMR (500 MHz, CDCl_3) δ = 8.14 (d, $J = 9.3$, 2H), 7.44 (s, broad, 1H), 7.05 (d, $J = 9.2$, 2H), 5.88 (ddt, $J = 16.6$, 10.1, 6.4, 1H), 5.09 (dd, $J = 17.1, 1.7$, 1H), 5.01 (dd, $J = 10.2, 1.8$, 1H), 2.54 – 2.19 (m, 4H), 1.92 (s, 3H). ^{13}C NMR (126 MHz, CDCl_3) δ 150.3, 149.7, 139.97, 137.5, 126.1, 115.2, 111.6, 38.2, 30.4, 14.79. ^{13}C NMR (126 MHz, CDCl_3) δ 144.6, 136.5, 129.0, 129.0, 127.6, 123.9, 114.0, 39.8, 39.5, 35.0, 32.7, 28.6, 25.5, 19.8, 19.5,

14.7. Observable resonances for minor diastereomer: ^1H NMR (500 MHz, CDCl_3) δ = 5.15 (dd, J = 17.1, 1.5, 1H), 2.07 (s, 3H).

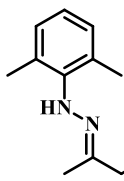
(*E*)-1-(hex-5-en-2-ylidene)-2-(3-nitrophenyl)hydrazine: Yield = 78 % (182 mg); *E/Z*



1:0.19; major diastereomer: ^1H NMR (500 MHz, CDCl_3) δ = 7.88 (dd, J = 4.8, 2.7, 1H), 7.69 – 7.61 (m, 1H), 7.36 – 7.29 (m, 2H), 7.12 (s, broad, 1H), 5.88 (ddt, J = 16.5, 10.1, 6.3, 1H), 5.09 (dd, J = 17.1, 1.7, 1H), 5.01 (dd, J = 10.1, 1.6, 1H), 2.48 – 2.32 (m, 4H), 1.90 (s, 3H). ^{13}C NMR (126 MHz, CDCl_3) δ 149.3, 148.1, 146.7, 137.7, 129.7, 118.5, 115.1, 114.0, 107.4, 38.1, 30.6, 14.7.

Observable resonances for minor diastereomer: ^1H NMR (500 MHz, CDCl_3) δ = 5.15 (dd, J = 17.1, 1.4, 1H), 2.06 (s, 3H). MS (ESI) calcd for $[\text{C}_{12}\text{H}_{15}\text{N}_3\text{O}_2\text{H}]^+$: 234.1243, found: 234.1246.

(*E*)-1-(2,6-dimethylphenyl)-2-(hex-5-en-2-ylidene)hydrazine: Yield = 92 %; *E/Z*

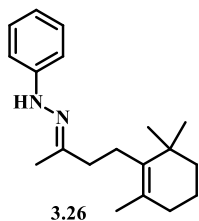


1:0.27; major diastereomer: ^1H NMR (500 MHz, CDCl_3) δ 7.00 (d, J = 7.5 Hz, 2H), 6.86 (t, J = 7.5 Hz, 1H), 5.90 – 5.80 (m, 1H), 5.04 (dd, J = 17.1, 1.4 Hz, 1H), 4.96 (dd, J = 10.2, 1.1 Hz, 1H), 2.45 – 2.29 (m, 10H), 1.91 (s, 3H). ^{13}C NMR (126 MHz, CDCl_3) δ 138.2, 129.1, 129.0, 123.0, 114.9, 87.6, 86.8, 85.16, 38.2, 31.0, 18.9, 14.4.

Observable resonances for minor diastereomer: ^1H NMR (500 MHz, CDCl_3) δ 5.96 – 5.89 (m, 1H), 5.18 – 5.08 (m, 2H), 2.48 – 2.42 (m, 4H).

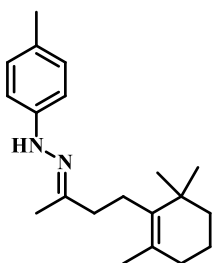
(*E*)-1-phenyl-2-(4-(2,6,6-trimethylcyclohex-1-en-1-yl)butan-2-ylidene)hydrazine

(3.26): Yield = 72% (204 mg); *E/Z* 1:0.25; major diastereomer: ^1H NMR (500 MHz, CDCl_3) δ = 7.24 (dd, J = 8.6, 7.4, 2H), 7.06 (dd, J = 8.6, 1.1, 2H), 6.88 (s, broad, 1H), 6.86 – 6.75 (m, 1H), 2.36 (ddd, J = 7.3, 6.5, 2.9, 2H), 2.31 – 2.25 (m, 2H), 1.94 (dd, J =



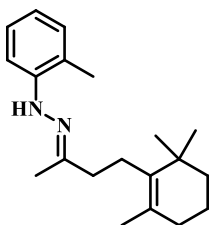
14.1, 7.7, 2H), 1.89 (s, 3H), 1.64 (s, 3H), 1.62 – 1.53 (m, 2H), 1.47 – 1.42 (m, 2H), 1.03 (s, 6H). ^{13}C NMR (126 MHz, CDCl_3) δ 146.8, 146.0, 136.6, 129.1, 127.5, 119.5, 112.9, 39.8, 39.5, 35.0, 32.8, 28.6, 25.6, 19.8, 19.5, 14.6. Observable resonances for minor diastereomer: ^1H NMR (500 MHz, CDCl_3) δ = 7.01 (d, J = 7.5, 2H), 1.70 (s, 3H), 1.05 (s, 6H). ^{13}C NMR (126 MHz, CDCl_3) δ 136.2, 131.2, 128.5, 122.5, 112.8, 35.6, 30.2, 23.6, 23.2, 21.8, 20.0, 19.4. MS (ESI) calcd for $[\text{C}_{19}\text{H}_{28}\text{N}_2\text{H}]^+$: 285.2331, found: 285.2335.

(E)-1-(p-tolyl)-2-(4-(2,6,6-trimethylcyclohex-1-en-1-yl)butan-2-ylidene)hydrazine:



Yield = 76% (227 mg); E/Z 1:0.24; major diastereomer: ^1H NMR (500 MHz, CDCl_3) δ = 7.04 (d, J = 8.4, 2H), 6.97 (d, J = 8.4, 2H), 6.78 (s, broad, 1H), 2.37 – 2.24 (m, 7H), 1.98 – 1.82 (m, 5H), 1.66 – 1.53 (m, 5H), 1.48 – 1.38 (m, 2H), 1.03 (s, 6H). ^{13}C NMR (126 MHz, CDCl_3) δ 143.8, 136.7, 129.6, 128.7, 127.5, 113.0, 39.8, 39.5, 35.0, 32.8, 28.6, 25.6, 20.5, 19.8, 19.5, 14.6. Observable resonances for minor diastereomer: ^1H NMR (500 MHz, CDCl_3) δ = 6.91 (d, J = 8.4, 2H), 2.42 (s, 3H), 2.05 (s, 3H), 1.69 (s, 3H), 1.05 (s, 6H). ^{13}C NMR (126 MHz, CDCl_3) δ 31.6. MS (ESI) calcd for $[\text{C}_{20}\text{H}_{30}\text{N}_2\text{H}]^+$: 299.2487, found: 299.2491.

(E)-1-(o-tolyl)-2-(4-(2,6,6-trimethylcyclohex-1-en-1-yl)butan-2-ylidene)hydrazine:

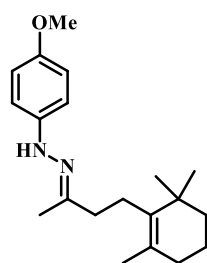


Yield = 85% (254 mg); E/Z 1:0.18; major diastereomer: ^1H NMR (500 MHz, CDCl_3) δ = 7.49 (d, J = 8.1, 1H), 7.18 (t, J = 7.4, 1H), 7.06 (d, J = 7.2, 1H), 6.76 (t, J = 7.4, 1H), 6.71 (s, broad, 1H), 2.41 – 2.27 (m, 4H), 2.19 (d, J = 5.3, 3H), 1.97 – 1.84 (m, 5H), 1.65 (s, 3H), 1.59 (ddd, J = 9.0, 7.3, 2.5, 2H), 1.48 – 1.40 (m, 2H), 1.04 (s, 6H). ^{13}C NMR (126 MHz, CDCl_3) δ

147.6, 143.7, 136.6, 130.1, 127.5, 127.2, 120.23, 119.0, 112.5, 39.8, 39.6, 35.0, 32.8, 28.6, 25.6, 19.8, 19.5, 17.0, 14.5. Observable resonances for minor diastereomer: ^1H NMR (500 MHz, CDCl_3) δ = 7.46 (d, J = 8.0, 1H), 2.08 (s, 3H), 1.71 (s, 3H), 1.06 (s, 6H). ^{13}C NMR (126 MHz, CDCl_3) δ 136.0, 112.4, 39.6, 35.8, 30.3, 28.4, 25.3, 17.2, 15.4. MS (ESI) calcd for $[\text{C}_{20}\text{H}_{30}\text{N}_2\text{H}]^+$: 299.2487, found: 299.2481.

(*E*)-1-(4-methoxyphenyl)-2-(4-(2,6,6-trimethylcyclohex-1-en-1-yl)butan-2-

ylidene)hydrazine: Yield = 57% (180 mg); *E/Z* 1:0.19; major diastereomer: ^1H NMR



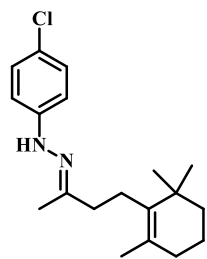
(500 MHz, CDCl_3) δ = 7.02 (d, J = 9.0, 2H), 6.83 (d, J = 9.0, 2H), 6.67 (s, broad, 1H), 3.77 (s, 3H), 2.38 – 2.20 (m, 4H), 1.93 (dd, J = 13.6, 7.0, 2H), 1.87 (s, 3H), 1.64 (s, 3H), 1.62 – 1.52 (m, 2H), 1.47 – 1.39 (m, 2H), 1.03 (s, 6H). ^{13}C NMR (126 MHz, CDCl_3) δ 153.4, 146.7, 140.4,

136.7, 127.5, 114.6, 114.2, 55.7, 39.8, 39.5, 35.0, 32.8, 28.6, 25.7, 19.8, 19.5, 14.6.

Observable resonances for minor diastereomer: ^1H NMR (500 MHz, CDCl_3) δ = 6.99 (d, J = 5.5, 2H), 3.81 (s, 3H), 1.69 (s, 3H), 1.05 (s, 6H). ^{13}C NMR (126 MHz, CDCl_3) δ 124.4, 44.5, 39.7, 28.4, 22.3. MS (ESI) calcd for $[\text{C}_{20}\text{H}_{30}\text{N}_2\text{OH}]^+$: 315.2436, found: 315.2431.

(*E*)-1-(4-chlorophenyl)-2-(4-(2,6,6-trimethylcyclohex-1-en-1-yl)butan-2-

ylidene)hydrazine: Yield = 55% (175 mg); *E/Z* 1:0.25; major diastereomer: ^1H NMR



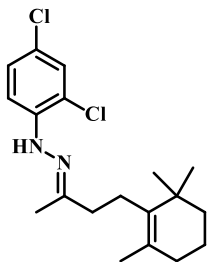
(500 MHz, CDCl_3) δ = 7.21 (d, J = 8.5, 2H), 7.02 (d, J = 8.6, 2H), 6.88 (s, 1H), 2.41 – 2.22 (m, 4H), 2.01 – 1.85 (m, 5H), 1.68 – 1.54 (m, 5H), 1.49 – 1.44 (m, 2H), 1.05 (s, 6H). ^{13}C NMR (126 MHz, CDCl_3) δ 144.6, 136.5, 129.0, 129.0, 127.6, 123.9, 114.0, 39.8, 39.5, 35.0, 32.7, 28.6,

25.5, 19.8, 19.5, 14.7. Observable resonances for minor diastereomer: ^1H NMR (500

MHz, CDCl₃) δ = 6.96 (d, J = 8.2, 2H) δ = 1.71 (s, 3H), 1.10 (s, 6H). ¹³C NMR (126 MHz, CDCl₃) δ 129.42, 113.90. MS (ESI) calcd for [C₁₉H₂₇ClN₂H]⁺: 319.1941, found: 319.1937.

(*E*)-1-(2,4-dichlorophenyl)-2-(4-(2,6,6-trimethylcyclohex-1-en-1-yl)butan-2-

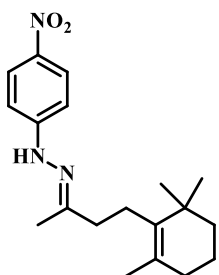
ylidene)hydrazine: Yield = 53%. *E/Z* 1:0.17; major diastereomer: ¹H NMR (500 MHz,



CDCl₃) δ 7.44 (t, J = 9.5 Hz, 1H), 7.26 – 7.24 (m, 1H), 7.18 – 7.14 (m, 1H), 2.40 – 2.20 (m, 4H), 1.97 – 1.88 (m, 5H), 1.67 – 1.56 (m, 4H), 1.45 (dt, J = 6.1, 4.9 Hz, 2H), 1.04 (d, J = 12.6 Hz, 6H), 0.87 (ddd, J = 11.0, 10.4, 5.8 Hz, 1H). ¹³C NMR (126 MHz, CDCl₃) δ 149.8, 140.6,

136.6, 128.5, 128.1, 127.8, 123.4, 117.5, 115.0, 39.9, 39.6, 35.2, 32.9, 28.7, 25.6, 20.0, 19.6, 15.0. Observable resonances for minor diastereomer: ¹H NMR (500 MHz, CDCl₃) δ 2.06 (d, J = 12.9 Hz, 1H), 1.70 (s, 3H), 1.06 (s, 6H), 0.98 – 0.85 (m, 1H). ¹³C NMR (126 MHz, CDCl₃) δ 150.9, 135.9, 135.2, 128.8, 114.9, 39.8, 31.7, 30.7, 28.7, 23.6, 23.5, 20.1, 19.5, 14.2.

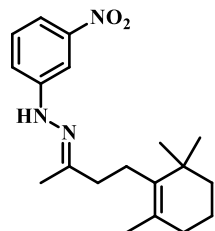
(*E*)-1-(4-nitrophenyl)-2-(4-(2,6,6-trimethylcyclohex-1-en-1-yl)butan-2-



ylidene)hydrazine: Yield = 79%. *E/Z* 1:0.24; major diastereomer: ¹H NMR (500 MHz, CDCl₃) δ 8.16 (d, J = 9.1 Hz, 2H), 7.07 (d, J = 9.0 Hz, 2H), 2.45 – 2.21 (m, 3H), 2.01 – 1.89 (m, 5H), 1.71 – 1.36 (m, 7H), 1.17 – 0.83 (m, 7H). ¹³C NMR (126 MHz, CDCl₃) δ 150.80,

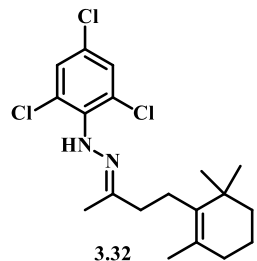
150.49, 139.87, 136.27, 127.92, 126.21, 126.17, 111.65, 39.81, 39.59, 35.07, 32.80, 28.63, 28.43, 25.39, 19.88, 19.50, 14.89. Observable resonances for minor diastereomer: ¹H NMR (500 MHz, CDCl₃) δ 2.52 – 2.47 (m, 2H), 1.70 (s, 2H), 1.05 (s, 6H). ¹³C NMR (126 MHz, CDCl₃) δ 135.97, 111.43, 44.54, 29.80, 22.30, 19.72.

(E)-1-(3-nitrophenyl)-2-(4-(2,6,6-trimethylcyclohex-1-en-1-yl)butan-2-



ylidene)hydrazine: Yield = 73%. *E/Z* 1:0.19; major diastereomer: ^1H NMR (500 MHz, CDCl_3) δ 7.84 (d, J = 16.1 Hz, 1H), 7.65 (d, J = 4.6 Hz, 1H), 7.34 (dd, J = 10.8, 6.5 Hz, 2H), 2.44 – 2.36 (m, 2H), 2.31 – 2.21 (m, 2H), 1.94 (dd, J = 31.5, 21.4 Hz, 6H), 1.67 (d, J = 17.3 Hz, 2H), 1.59 (dd, J = 12.5, 6.5 Hz, 2H), 1.48 – 1.39 (m, 2H), 1.04 (s, 6H). ^{13}C NMR (126 MHz, CDCl_3) δ 149.2, 146.8, 136.4, 129.7, 127.8, 118.5, 113.9, 107.4, 39.8, 39.5, 35.0, 32.8, 28.6, 25.5, 19.9, 19.5, 14.8. Observable resonances for minor diastereomer: ^1H NMR (500 MHz, CDCl_3) δ 1.70 (s, 3H), 1.05 (s, 6H). ^{13}C NMR (126 MHz, CDCl_3) δ 39.6, 35.1, 30.4, 23.1, 8.4.

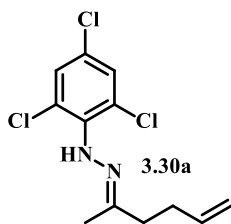
(E)-1-(2,4,6-trichlorophenyl)-2-(4-(2,6,6-trimethylcyclohex-1-en-1-yl)butan-2-



ylidene)hydrazine (3.32): Yield = 68%. *E/Z* 1:0.22; major diastereomer: ^1H NMR (500 MHz, CDCl_3) δ 7.28 (t, J = 9.1 Hz, 2H), 2.37 – 2.30 (m, 2H), 2.26 (dt, J = 8.2, 5.8 Hz, 2H), 1.97 (s, 3H), 1.65 – 1.53 (m, 4H), 1.48 – 1.38 (m, 2H), 1.35 – 1.21 (m, 3H), 1.01 (s, 6H). ^{13}C NMR (126 MHz, CDCl_3) δ 153.9, 139.3, 136.6, 128.8, 127.8, 127.2, 126.6, 39.9, 39.4, 35.1, 32.9, 28.7, 25.5, 22.4, 20.0, 19.6, 15.2, 14.2. Observable resonances for minor diastereomer: ^1H NMR (500 MHz, CDCl_3) δ 2.44 – 2.38 (m, 2H), 1.70 (s, 3H), 1.48 – 1.44 (m, 2H), 1.06 (s, 6H). ^{13}C NMR (126 MHz, CDCl_3) δ 39.8, 34.2, 31.1, 23.7, 23.1, 20.1, 19.5.

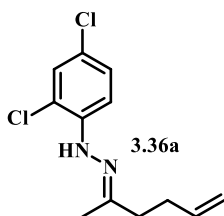
(E)-1-(hex-5-en-2-ylidene)-2-(2,4,6-trichlorophenyl)hydrazine (3.30): Yield = 81%.

E/Z 1:0.17; major diastereomer: ^1H NMR (500 MHz, CDCl_3) δ 7.30 (d, J = 1.7 Hz, 2H), 5.86 (ddt, J = 16.5, 10.1, 6.4 Hz, 1H), 5.10 – 4.92 (m, 2H), 2.45 – 2.29 (m, 4H), 1.95 (s,



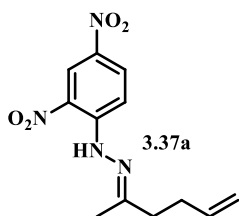
3H). ^{13}C NMR (126 MHz, CDCl_3) δ 152.9, 139.1, 137.7, 128.7, 128.6, 126.9, 115.0, 38.0, 30.6, 15.0. Observable resonances for minor diastereomer: ^1H NMR (500 MHz, CDCl_3) δ 5.17 – 5.09 (m, 2H), 2.48 (d, J = 8.1 Hz, 2H), 2.01 (d, J = 0.6 Hz, 3H). ^{13}C NMR (126 MHz, CDCl_3) δ 136.7, 116.2, 29.5, 29.1, 22.9.

(E)-1-(2,4-dichlorophenyl)-2-(hex-5-en-2-ylidene)hydrazine (3.36a): Yield = 31%;



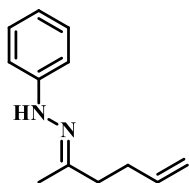
E/Z 1:0.13; major diastereomer: ^1H NMR (500 MHz, CDCl_3) δ = 7.43 (d, J = 8.8, 1H), 7.33 (s, broad, 1H), 7.25 (d, J = 2.3, 1H), 7.18 – 7.13 (m, 1H), 5.88 (ddt, J = 16.4, 10.2, 6.3, 1H), 5.08 (ddd, J = 17.1, 3.3, 1.6, 1H), 4.99 (ddd, J = 10.2, 3.0, 1.2, 1H), 2.45 – 2.40 (m, 2H), 2.40 – 2.34 (m, 2H), 1.90 (s, 3H). ^{13}C NMR (126 MHz, CDCl_3) δ 148.7, 140.4, 137.7, 128.4, 127.9, 123.3, 117.3, 115.0, 114.8, 38.1, 30.5, 14.7. Observable resonances for minor diastereomer: ^1H NMR (500 MHz, CDCl_3) δ = 5.14 (dd, J = 17.1, 1.5, 1H), 2.04 (s, 3H). MS (ESI) calcd for $[\text{C}_{12}\text{H}_{14}\text{Cl}_2\text{N}_2\text{H}]^+$: 257.0612, found: 257.0616.

(E)-1-(2,4-dinitrophenyl)-2-(hex-5-en-2-ylidene)hydrazine (3.37a): Yield = 40%; ^1H



NMR (500 MHz, CDCl_3) δ 9.21 – 9.02 (m, 1H), 8.30 (ddd, J = 9.6, 4.8, 2.6 Hz, 1H), 7.96 (dd, J = 9.6, 2.7 Hz, 1H), 5.87 (ddd, J = 17.0, 10.2, 6.9 Hz, 1H), 5.22 – 4.97 (m, 2H), 2.53 (ddd, J = 14.8, 8.4, 6.5 Hz, 2H), 2.48 – 2.33 (m, 2H), 2.11 (d, J = 42.1 Hz, 3H).

(E)-1-(hex-5-en-2-ylidene)-2-phenylhydrazine: Yield = 71% (133 mg); E/Z 1:0.14;

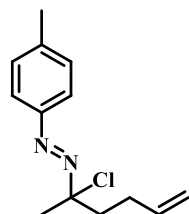


major diastereomer: ^1H NMR (500 MHz, CDCl_3) δ = 7.26 – 7.20 (m, 2H), 7.04 (dt, J = 3.2, 1.7, 2H), 6.87 (s, broad, 1H), 6.84 – 6.79 (m, 1H), 6.05 – 5.77 (m, 1H), 5.07 (d, J = 17.1, 1H), 4.98 (d, J = 10.2, 1H), 2.46 –

2.25 (m, 4H), 1.85 (s, 3H). ^{13}C NMR (126 MHz, CDCl_3) δ 145.9, 138.0, 129.1, 119.6, 114.8, 112.9, 112.9, 38.2, 30.7, 14.5. Observable resonances for minor diastereomer: ^1H NMR (500 MHz, CDCl_3) δ = 5.13 (dd, J = 17.1, 1.3, 1H), 2.03 (s, 3H). ^{13}C NMR (126 MHz, CDCl_3) δ 122.5, 115.9, 29.1, 23.2.

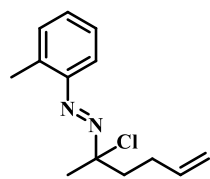
5.5.4 Preparation and characterization data of α -chloroazo compounds

(*E*)-1-(2-chlorohex-5-en-2-yl)-2-(*p*-tolyl)diazene: The title α -chloroazo compound was



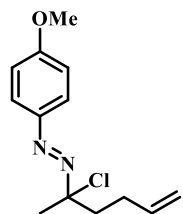
prepared in 94% yield (206 mg) as described in the experimental procedure 5.5.1 using the corresponding hydrazone (1 equiv, 188 mg, 0.93 mmol), oxalyl chloride (2.0 equiv, 0.16 mL, 1.86 mmol), DMSO (2.5 equiv, 0.17 mL, 2.33 mmol), and TEA (2.5 equiv, 0.32 mL, 2.33 mmol). ^1H NMR (500 MHz, CDCl_3) δ = 7.68 (d, J = 8.3, 2H), 7.27 (d, J = 8.0, 2H), 5.86 – 5.75 (m, 1H), 5.04 (dd, J = 17.1, 1.7, 1H), 4.97 (dd, J = 10.2, 1.7, 1H), 2.42 (s, 3H), 2.38 (d, J = 12.9, 1H), 2.35 – 2.22 (m, 2H), 2.20 – 2.09 (m, 1H), 1.90 (s, 3H). ^{13}C NMR (126 MHz, CDCl_3) δ 149.0, 141.9, 137.4, 129.6, 122.9, 115.0, 96.1, 42.0, 28.8, 28.5, 21.4.

(*E*)-1-(2-chlorohex-5-en-2-yl)-2-(*o*-tolyl)diazene: The title α -chloroazo compound was



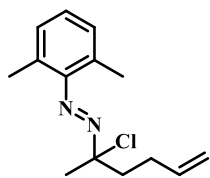
prepared in 95% yield (169 mg) as described in the experimental procedure 5.5.1 using the corresponding hydrazone (1 equiv, 152 mg, 0.75 mmol), oxalyl chloride (2.0 equiv, 0.13 mL, 1.5 mmol), DMSO (2.5 equiv, 0.13 mL, 1.87 mmol), and TEA (2.5 equiv, 0.26 mL, 1.87 mmol). ^1H NMR (500 MHz, CDCl_3) δ = 7.40 – 7.27 (m, 3H), 7.22 (t, J = 7.4, 1H), 5.82 (ddt, J = 16.5, 10.2, 6.2, 1H), 5.01 (dd, J = 34.8, 13.7, 2H), 2.64 (s, 3H), 2.48 – 2.03 (m, 4H), 1.91 (s, 3H). ^{13}C NMR (126 MHz, CDCl_3) δ 149.2, 137.6, 137.4, 131.2, 131.0, 126.3, 116.2, 115.1, 96.7, 41.9, 28.8, 28.5, 17.2.

(*E*)-1-(2-chlorohex-5-en-2-yl)-2-(4-methoxyphenyl)diazene: The title α -chloroazo



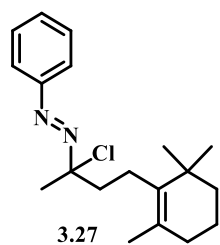
compound was prepared in 95% yield (134 mg) as described in the experimental procedure 5.5.2 using the corresponding hydrazone (1 equiv, 122 mg, 0.56 mmol), oxalyl chloride (2.0 equiv, 0.10 mL, 1.12 mmol), DMSO (2.5 equiv, 0.10 mL, 1.4 mmol), and TEA (2.5 equiv, 0.20 mL, 1.4 mmol). ^1H NMR (500 MHz, CDCl_3) δ = 7.78 (d, J = 9.0, 2H), 6.97 (d, J = 9.0, 2H), 5.88 – 5.70 (m, 1H), 5.04 (dd, J = 17.1, 1.6, 1H), 4.97 (d, J = 10.1, 1H), 3.87 (s, 3H), 2.43 – 2.09 (m, 4H), 1.90 (s, 3H). ^{13}C NMR (126 MHz, CDCl_3) δ 162.2, 145.1, 137.5, 124.9, 115.0, 114.12, 96.0, 55.5, 42.1, 28.9, 28.6.

(*E*)-1-(2-chlorohex-5-en-2-yl)-2-(2,6-dimethylphenyl)diazene: Yield = 93%. ^1H NMR



(500 MHz, CDCl_3) δ 7.13 (dd, J = 8.6, 6.2 Hz, 1H), 7.09 – 7.05 (m, 2H), 5.89 – 5.77 (m, 1H), 5.11 – 4.97 (m, 2H), 2.43 – 2.27 (m, 4H), 2.24 (s, 6H), 1.94 (s, 3H).

(*E*)-1-(2-chloro-4-(2,6,6-trimethylcyclohex-1-en-1-yl)butan-2-yl)-2-phenyldiazene



(3.27): The title α -chloroazo compound **(3.27)** was prepared in 95% yield (209 mg) as described in the experimental procedure 5.5.2 using the corresponding hydrazone (1 equiv, 196 mg, 0.69 mmol), oxalyl chloride (2.0 equiv, 0.12 mL, 1.38 mmol), DMSO (2.5 equiv, 0.12 mL, 1.72 mmol), and TEA (2.5 equiv, 0.24 mL, 0.17 mmol). ^1H NMR (500 MHz, CDCl_3) δ = 7.84 – 7.72 (m, 2H), 7.59 – 7.37 (m, 3H), 2.42 – 2.30 (m, 1H), 2.24 (ddd, J = 12.6, 7.7, 3.7, 2H), 2.04 (d, J = 4.1, 1H), 1.94 – 1.84 (m, 5H), 1.61 – 1.51 (m, 5H), 1.44 – 1.36 (m, 2H), 0.99 (s, 6H). ^{13}C NMR (126 MHz, CDCl_3) δ 151.0, 135.7, 131.2, 129.0, 128.1, 122.8, 96.9, 42.7, 39.7, 35.1, 32.7, 28.7, 28.6, 28.5, 23.1, 19.8, 19.4.

5.5.5 Representative experimental procedures to prepare of α -trifluoroacetoxyazo compounds

a. At low temperature (-78 °C)

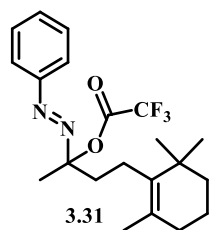
The α -trifluoroacetoxyazo prepared in this section were prepared with the same method used to prepare the α -trifluoroacetoxyazo in the section 5.4.5.

b. At high temperature (0 °C)

TFAA (1.1 or 1.2 equiv) was added dropwise to a 0 °C solution of hydrazone (1.0 equiv), DMSO (1.2 equiv), TEA (1.15 equiv), and hexane under a nitrogen atmosphere. The mixture was stirred for 5 min at 0 °C and for 15 min at room temperature at which point it was filtered through a plug of basic alumina to remove triethylammonium salt. The hexane was removed *in vacuo* to provide the α -trifluoroacetoxyazo product as a yellow oil.

5.5.6 Preparation and characterization data of α -trifluoroacetoxyazo compounds

(*E*)-2-(phenyldiazenyl)-4-(2,6,6-trimethylcyclohex-1-en-1-yl)butan-2-yl 2,2,2-



trifluoroacetate (3.31): The title α -trifluoroacetoxyazo **3.31** was

prepared in 87% (595 mg) yield as described in representative

experimental procedure 5.5.5 (a) using hydrazone **3.26** (1 equiv, 490

mg, 1.72 mmol), TFAA (1.1 equiv, 0.27 mL, 1.89 mmol), DMSO (1.2

equiv, 0.15 mL, 2.06 mmol), and TEA (1.15 equiv, 0.28 mL, 1.98 mmol). Alternatively,

the title α -trifluoroacetoxyazo **3.31** was prepared in 82% yield (267 mg) as described in

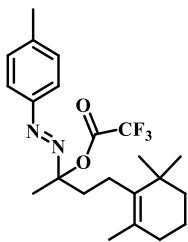
the representative experimental procedure 5.5.5 (b) using hydrazone **3.26** (1 equiv, 233

mg, 0.82 mmol), TFAA (1.2 equiv, 0.14 mL, 0.98 mmol), DMSO (1.2 equiv, 0.07 mL,

0.98 mmol), and TEA (1.2 equiv, 0.13 mL, 0.94 mmol). ¹H NMR (500 MHz, CDCl₃) δ =

7.74 – 7.64 (m, 2H), 7.52 – 7.45 (m, 3H), 2.29 – 1.97 (m, 4H), 1.94 – 1.86 (m, 5H), 1.60 – 1.49 (m, 5H), 1.42 – 1.37 (m, 2H), 0.96 (d, $J = 2.6$, 6H). ^{13}C NMR (126 MHz, CDCl_3) δ 150.7, 135.4, 131.5, 129.1, 128.3, 122.8, 107.6, 39.7, 38.6, 35.0, 32.7, 28.5, 28.4, 21.7, 21.4, 19.6, 19.4.

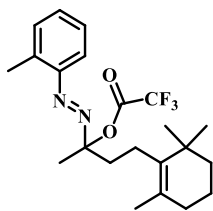
(E)-2-(*p*-tolylidiazenyl)-4-(2,6,6-trimethylcyclohex-1-en-1-yl)butan-2-yl 2,2,2-



trifluoroacetate: The title α -trifluoroacetoxyazo was prepared in 76% yield (204 mg) as described in representative experimental procedure 5.5.5 (a) using hydrazone (1 equiv, 193 mg, 0.65 mmol), TFAA (1.1 equiv, 0.10 mL, 0.71 mmol), DMSO (1.2 equiv, 0.06 mL, 0.78 mmol), and TEA (1.15 equiv, 0.10 mL, 0.75 mmol). ^1H NMR (500 MHz, CDCl_3) δ = 7.61 (d, J =

8.3, 2H), 7.26 (d, J = 8.0, 2H), 2.41 (s, 3H), 2.29 – 2.15 (m, 1H), 2.15 – 2.08 (m, 2H), 2.07 – 1.96 (m, 1H), 1.90 (s, 3H), 1.92 – 1.83 (m, 2H), 1.55 (s, 3H), 1.58 – 1.51 (m, 2H), 1.43 – 1.37 (m, 2H), 0.99 – 0.94 (m, 6H). ^{13}C NMR (126 MHz, CDCl_3) δ 148.8, 142.0, 135.5, 129.6, 128.3, 122.8, 107.5, 39.7, 38.7, 35.0, 32.7, 28.5, 28.4, 28.4, 21.7, 21.4, 19.6, 19.4.

(E)-2-(*o*-tolylidiazenyl)-4-(2,6,6-trimethylcyclohex-1-en-1-yl)butan-2-yl 2,2,2-



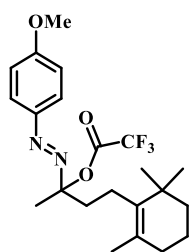
trifluoroacetate: The title α -trifluoroacetoxyazo was prepared in 83% yield (344 mg) as described in representative experimental procedure 5.5.5 (a) using hydrazone (1 equiv, 303 mg, 1.01 mmol), TFAA (1.1 equiv, 0.16 mL, 1.12 mmol), DMSO (1.2 equiv, 0.09

mL, 1.21 mmol), and TEA (1.15 equiv, 0.16 mL, 1.2 mmol). ^1H NMR (500 MHz, CDCl_3) δ = 7.35 (dd, J = 11.6, 7.6, 2H), 7.30 (d, J = 7.4, 1H), 7.22 (t, J = 7.6, 1H), 2.55 (s, 3H), 2.28 – 2.17 (m, 1H), 2.17 – 2.11 (m, 2H), 2.04 – 1.94 (m, 4H), 1.92 – 1.85 (m,

2H), 1.59 – 1.54 (m, 5H), 1.43 – 1.36 (m, 2H), 0.97 (d, $J = 3.5$, 6H). ^{13}C NMR (126 MHz, CDCl_3) δ 149.0, 137.6, 135.4, 131.3, 131.2, 128.3, 126.4, 115.9, 107.4, 39.7, 38.8, 35.0, 32.7, 28.5, 28.4, 28.4, 21.96, 21.3, 19.6, 19.4, 17.2.

(*E*)-2-((4-methoxyphenyl)diazenyl)-4-(2,6,6-trimethylcyclohex-1-en-1-yl)butan-2-yl

2,2,2-trifluoroacetate: The title α -trifluoroacetoxyazo was prepared in 76% yield (287



mg) as described in representative experimental procedure 5.5.5 (a)

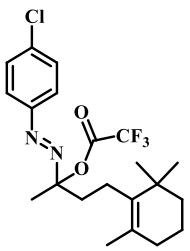
using hydrazone (1 equiv, 281 mg, 0.89 mmol), TFAA (1.2 equiv,

0.15 mL, 1.07 mmol), DMSO (1.2 equiv, 0.08 mL, 1.07 mmol), and

TEA (1.15 equiv, 0.14 mL, 1.02 mmol). Alternatively, the title α -

trifluoroacetoxyazo was prepared in 57% yield (360 mg) as described in representative experimental procedure 5.5.5 (b) using hydrazone (1 equiv, 465 mg, 1.48 mmol), TFAA (1.2 equiv, 0.31 mL, 2.2 mmol), DMSO (1.2 equiv, 0.16 mL, 2.2 mmol), and TEA (1.15 equiv, 0.24 mL, 1.7 mmol). ^1H NMR (500 MHz, CDCl_3) δ = 7.71 (d, $J = 9.1$, 2H), 6.95 (d, $J = 9.0$, 2H), 3.87 (s, 3H), 2.31 – 2.17 (m, 1H), 2.17 – 2.07 (m, 2H), 2.07 – 1.96 (m, 1H), 1.97 – 1.83 (m, 5H), 1.63 – 1.49 (m, 5H), 1.44 – 1.35 (m, 2H), 0.96 (d, $J = 2.3$, 6H). ^{13}C NMR (126 MHz, CDCl_3) δ 162.3, 144.93, 135.5, 128.26, 124.7, 114.1, 107.4, 55.58, 39.7, 38.7, 35.0, 32.7, 28.5, 28.4, 21.8, 21.4, 19.6, 19.4.

(*E*)-2-((4-chlorophenyl)diazenyl)-4-(2,6,6-trimethylcyclohex-1-en-1-yl)butan-2-yl



2,2,2-trifluoroacetate: The title α -trifluoroacetoxyazo was prepared in

86% yield (422 mg) as described in representative experimental

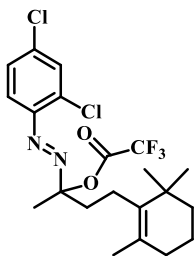
procedure 5.5.5 (a) using hydrazone (1 equiv, 363 mg, 1.14 mmol),

TFAA (1.1 equiv, 0.18 mL, 1.25 mmol), DMSO (1.2 equiv, 0.10 mL,

1.37 mmol), and TEA (1.15 equiv, 0.18 mL, 1.13 mmol). ^1H NMR (500 MHz, CDCl_3) δ

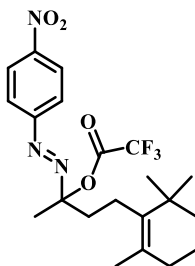
= 7.66 (d, J = 8.8, 2H), 7.45 (d, J = 8.8, 2H), 2.29 – 2.17 (m, 1H), 2.16 – 2.07 (m, 2H), 2.07 – 1.95 (m, 1H), 1.92 – 1.85 (m, 5H), 1.60 – 1.49 (m, 5H), 1.45 – 1.35 (m, 2H), 0.96 (d, J = 3.1, 6H). ^{13}C NMR (126 MHz, CDCl_3) δ 149.03, 137.61, 135.34, 129.38, 128.44, 124.12, 107.52, 39.68, 38.65, 34.99, 32.75, 28.52, 28.45, 21.68, 21.39, 19.61, 19.41.

(*E*)-2-((2,4-dichlorophenyl)diazenyl)-4-(2,6,6-trimethylcyclohex-1-en-1-yl)butan-2-yl



2,2,2-trifluoroacetate: Yield = 90%. ^1H NMR (500 MHz, CDCl_3) δ 7.55 (d, J = 2.1 Hz, 1H), 7.39 (d, J = 8.7 Hz, 1H), 7.29 (d, J = 2.2 Hz, 1H), 2.30 – 2.18 (m, 1H), 2.13 (ddd, J = 10.3, 7.0, 4.8 Hz, 2H), 1.94 (s, 3H), 1.90 (dt, J = 8.6, 6.5 Hz, 2H), 1.58 – 1.54 (m, 4H), 1.44 – 1.37 (m, 2H), 1.32 – 1.24 (m, 2H), 0.99 – 0.94 (m, 6H). ^{13}C NMR (126 MHz, CDCl_3) δ 145.6, 137.8, 135.8, 135.3, 130.4, 128.5, 127.7, 118.8, 107.7, 39.7, 38.7, 35.0, 32.7, 31.6, 28.5, 28.4, 22.6, 21.8, 21.3, 19.6, 14.1.

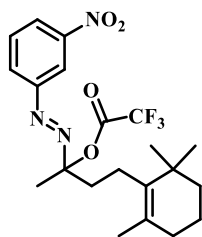
(*E*)-2-((4-nitrophenyl)diazenyl)-4-(2,6,6-trimethylcyclohex-1-en-1-yl)butan-2-yl



2,2,2-trifluoroacetate: Yield = 81%. ^1H NMR (500 MHz, CDCl_3) δ 8.56 – 8.13 (m, 2H), 8.13 – 7.54 (m, 2H), 2.25 (ddd, J = 17.1, 13.3, 12.7 Hz, 1H), 2.14 (ddd, J = 12.8, 12.0, 5.0 Hz, 1H), 2.06 – 1.95 (m, 1H), 1.95 (s, 3H), 1.88 (dd, J = 12.6, 6.3 Hz, 1H), 1.60 – 1.52 (m, 4H), 1.45 – 1.35 (m, 2H), 1.34 – 1.20 (m, 2H), 1.00 – 0.94 (m, 6H), 0.91 – 0.83 (m, 1H). ^{13}C NMR (126 MHz, CDCl_3) δ 153.8, 149.2, 135.1, 128.6, 124.7, 123.4, 107.7, 39.6, 38.5, 35.0, 32.7, 31.6, 28.5, 22.6, 21.6, 21.4, 19.6, 19.3, 14.1.

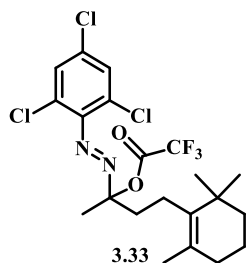
(*E*)-2-((3-nitrophenyl)diazenyl)-4-(2,6,6-trimethylcyclohex-1-en-1-yl)butan-2-yl

2,2,2-trifluoroacetate: Yield = 95%. ^1H NMR (500 MHz, CDCl_3) δ 8.54 (t, J = 2.0 Hz,



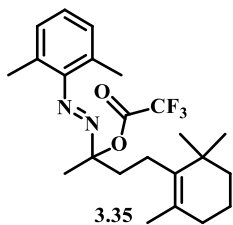
1H), 8.35 (ddd, $J = 8.2, 2.3, 1.1$ Hz, 1H), 8.06 (ddd, $J = 7.9, 1.8, 1.1$ Hz, 1H), 7.69 (t, $J = 8.1$ Hz, 1H), 2.13 (ddd, $J = 18.3, 8.8, 5.5$ Hz, 1H), 2.08 – 1.98 (m, 1H), 1.95 (s, 3H), 1.90 (dd, $J = 10.3, 4.1$ Hz, 2H), 1.59 – 1.51 (m, 5H), 1.41 (dt, $J = 5.8, 3.2$ Hz, 2H), 1.33 – 1.25 (m, 2H), 0.96 (dd, $J = 6.4, 2.8$ Hz, 6H). ^{13}C NMR (126 MHz, CDCl_3) δ 151.0, 148.9, 135.1, 130.1, 128.9, 128.6, 125.7, 117.3, 107.5, 39.6, 38.5, 35.0, 32.7, 31.6, 28.5, 22.6, 21.6, 21.4, 19.6, 19.4, 14.1.

(E)-2-((2,4,6-trichlorophenyl)diazenyl)-4-(2,6,6-trimethylcyclohex-1-en-1-yl)butan-2-



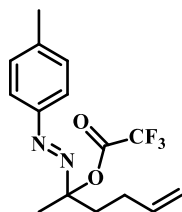
yl 2,2,2-trifluoroacetate (3.33): Yield = 95%. ^1H NMR (500 MHz, CDCl_3) δ 7.40 (s, 2H), 2.30 – 2.20 (m, 1H), 2.19 – 2.10 (m, 1H), 2.00 (s, 3H), 1.91 (t, $J = 6.2$ Hz, 2H), 1.61 – 1.52 (m, 6H), 1.46 – 1.38 (m, 2H), 1.02 – 0.93 (m, 7H). ^{13}C NMR (126 MHz, CDCl_3) δ 145.1, 135.3, 134.2, 129.2, 128.8, 127.6, 108.2, 77.1, 39.8, 38.4, 35.2, 32.9, 28.7, 28.6, 28.6, 22.1, 21.6, 19.7, 19.5.

(E)-2-((2,6-dimethylphenyl)diazenyl)-4-(2,6,6-trimethylcyclohex-1-en-1-yl)butan-2-



yl 2,2,2-trifluoroacetate (3.35): Yield = 84%. ^1H NMR (500 MHz, CDCl_3) δ 7.00 (d, $J = 7.5$ Hz, 2H), 6.84 (t, $J = 7.5$ Hz, 1H), 2.36 – 2.28 (m, 8H), 2.24 (dd, $J = 16.1, 6.6$ Hz, 2H), 1.92 (d, $J = 8.9$ Hz, 5H), 1.62 – 1.52 (m, 5H), 1.50 – 1.38 (m, 2H), 0.99 (d, $J = 13.0$ Hz, 6H).

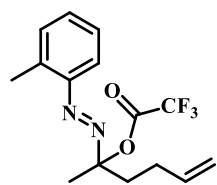
(E)-2-(p-tolyldiazenyl)hex-5-en-2-yl 2,2,2-trifluoroacetate : The title α -



trifluoroacetoxazo was prepared in 69% yield (340 mg) as described in representative experimental procedure 5.5.5 (a) using hydrazone (1 equiv, 318 mg, 1.58 mmol), TFAA (1.1 equiv, 0.24 mL, 1.73 mmol),

DMSO (1.2 equiv, 0.13 mL, 1.88 mmol), and TEA (1.15 equiv, 0.25 mL, 1.81 mmol). ^1H NMR (500 MHz, CDCl_3) δ = 7.61 (d, J = 8.3, 2H), 7.26 (d, J = 6.7, 2H), 5.85 – 5.72 (m, 1H), 5.04 (dd, J = 17.1, 1.5, 1H), 4.98 (dd, J = 10.2, 1.5, 1H), 2.41 (s, 3H), 2.36 – 2.04 (m, 4H), 1.88 (s, 3H). ^{13}C NMR (126 MHz, CDCl_3) δ 148.6, 142.2, 137.0, 129.7, 122.8, 115.3, 107.0, 37.6, 27.0, 22.09, 21.4.

(*E*)-2-(*o*-tolyldiazenyl)hex-5-en-2-yl 2,2,2-trifluoroacetate: The title α -

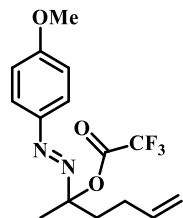


trifluoroacetoxyl was prepared in 65% yield (137 mg) as described in representative experimental procedure 5.5.5 (a) using hydrazone (1 equiv, 136 mg, 0.67 mmol), TFAA (1.1 equiv, 0.10 mL, 0.74 mmol),

DMSO (1.2 equiv, 0.06 mL, 0.80 mmol), and TEA (1.15 equiv, 0.10 mL, 0.77 mmol).

Alternatively, the title α -trifluoroacetoxyl was prepared in 62% yield (180 mg) as described in representative experimental procedure 5.5.5 (b) using hydrazone (1 equiv, 186 mg, 0.92 mmol), TFAA (1.1 equiv, 0.14 mL, 1.01 mmol), DMSO (1.2 equiv, 0.08 mL, 1.10 mmol), and TEA (1.15 equiv, 0.15 mL, 1.06 mmol). ^1H NMR (500 MHz, CDCl_3) δ = 7.36 (t, J = 7.7, 2H), 7.30 (d, J = 7.4, 1H), 7.22 (t, J = 7.6, 1H), 5.79 (dd, J = 17.1, 10.2, 1H), 5.05 (dd, J = 17.1, 1.6, 1H), 4.99 (dd, J = 10.3, 1.6, 1H), 2.54 (s, 3H), 2.34 – 2.03 (m, 4H), 1.93 (s, 3H). ^{13}C NMR (126 MHz, CDCl_3) δ 148.9, 137.7, 136.9, 131.4, 131.3, 126.4, 116.0, 115.4, 107.0, 37.6, 26.9, 22.2, 17.2.

(*E*)-2-((4-methoxyphenyl)diazenyl)hex-5-en-2-yl 2,2,2-trifluoroacetate: The title α -

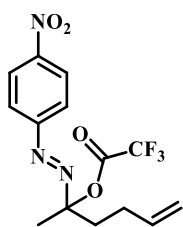


trifluoroacetoxyl was prepared in 74% yield (143 mg) as described in representative experimental procedure 5.5.5 (a) using hydrazone (1 equiv, 130 mg, 0.59 mmol), TFAA (1.1 equiv, 0.09 mL, 0.66 mmol), DMSO

(1.2 equiv, 0.05 mL, 0.72 mmol), and TEA (1.15 equiv, 0.10 mL, 0.09 mmol). ^1H NMR

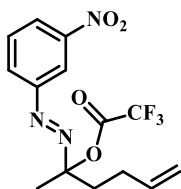
(500 MHz, CDCl₃) δ = 7.71 (d, J = 9.1, 2H), 6.96 (d, J = 9.1, 2H), 5.85 – 5.72 (m, 1H), 5.04 (dd, J = 17.1, 1.6, 1H), 4.98 (dd, J = 10.2, 1.6, 1H), 3.87 (s, 3H), 2.35 – 2.02 (m, 4H), 1.87 (s, 3H). ¹³C NMR (126 MHz, CDCl₃) δ 162.45, 144.81, 137.10, 124.85, 115.33, 114.14, 106.96, 55.61, 37.68, 27.07, 22.14.

(E)-2-((4-nitrophenyl)diazenyl)hex-5-en-2-yl 2,2,2-trifluoroacetate: The title α -



trifluoroacetoxazone was prepared in 82% yield (298 mg) as described in representative experimental procedure 5.5.5 (a) using hydrazone (1 equiv, 244 mg, 1.05 mmol), TFAA (1.1 equiv, 0.16 mL, 1.15 mmol), DMSO (1.2 equiv, 0.09 mL, 1.26 mmol), and TEA (1.15 equiv, 0.17 mL, 1.21 mmol). ¹H NMR (500 MHz, CDCl₃) δ = 8.35 (d, J = 9.0, 2H), 7.83 (d, J = 9.1, 2H), 5.78 (dd, J = 17.1, 10.2, 1H), 5.03 (ddd, J = 13.7, 11.7, 1.5, 2H), 2.33 – 2.08 (m, 4H), 1.92 (s, 3H). ¹³C NMR (126 MHz, CDCl₃) δ 153.6, 149.3, 136.5, 124.7, 123.5, 115.7, 107.2, 37.4, 26.9, 21.9.

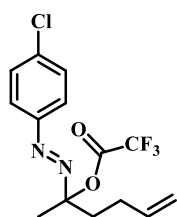
(E)-2-((3-nitrophenyl)diazenyl)hex-5-en-2-yl 2,2,2-trifluoroacetate: The title α -



trifluoroacetoxazone was prepared in 88% yield (207 mg) as described in representative experimental procedure 5.5.5 (a) using hydrazone (1 equiv, 159 mg, 0.68 mmol), TFAA (1.1 equiv, 0.11 mL, 0.75 mmol), DMSO (1.2 equiv, 0.06 mL, 0.82 mmol), and TEA (1.15 equiv, 0.11 mL, 0.78 mmol). Alternatively, the title α -trifluoroacetoxazone was prepared in 79% yield (209 mg) as described in representative experimental procedure 5.5.5 (b) using hydrazone (1 equiv, 180 mg, 0.77 mmol), TFAA (1.2 equiv, 0.13 mL, 0.92 mmol), DMSO (1.2 equiv, 0.07 mL, 0.92 mmol), and TEA (1.15 equiv, 0.89 mL, 0.12 mmol). ¹H NMR (500 MHz, CDCl₃) δ = 8.53 (t, J = 2.0, 1H), 8.36 (ddd, J = 8.2, 2.3, 1.1, 1H), 8.06 (ddd, J = 7.9, 1.9, 1.1,

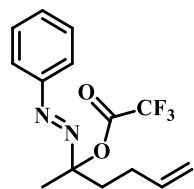
1H), 7.69 (t, $J = 8.1$, 1H), 5.78 (ddt, $J = 16.5$, 10.2, 6.3, 1H), 5.03 (ddq, $J = 21.4$, 10.1, 1.3, 2H), 2.39 – 2.04 (m, 4H), 1.94 (s, 3H). ^{13}C NMR (126 MHz, CDCl_3) δ 150.9, 148.9, 136.5, 130.1, 129.1, 125.8, 117.3, 115.7, 107.0, 37.5, 26.9, 22.0.

(E)-2-((4-chlorophenyl)diazenyl)hex-5-en-2-yl 2,2,2-trifluoroacetate: The title α -



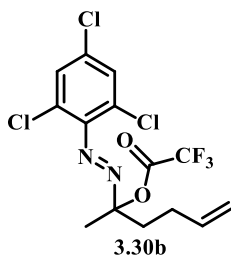
trifluoroacetoxazo was prepared in 80% yield (428 mg) as described in representative experimental procedure 5.5.5 (a) using hydrazone (1 equiv, 353 mg, 1.59 mmol), TFAA (1.1 equiv, 0.25 mL, 1.75 mmol), DMSO (1.2 equiv, 0.14 mL, 1.91 mmol), and TEA (1.15 equiv, 0.25 mL, 1.83 mmol). ^1H NMR (500 MHz, CDCl_3) δ = 7.66 (d, $J = 8.8$, 2H), 7.45 (d, $J = 8.8$, 2H), 5.77 (ddt, $J = 13.4$, 10.2, 6.2, 1H), 5.04 (dd, $J = 17.1$, 1.6, 1H), 4.99 (dd, $J = 10.2$, 1.5, 1H), 2.33 – 2.03 (m, 4H), 1.89 (s, 3H). ^{13}C NMR (126 MHz, CDCl_3) δ 148.9, 137.7, 136.8, 129.3, 124.1, 115.5, 107.0, 37.5, 27.0, 22.0.

(E)-2-(phenyldiazenyl)hex-5-en-2-yl 2,2,2-trifluoroacetate: The title α -



trifluoroacetoxazo was prepared in 80% yield (171 mg) as described in representative experimental procedure 5.5.5 (a) using hydrazone (1 equiv, 336 mg, 0.71 mmol), TFAA (1.1 equiv, 0.11 mL, 0.78 mmol), DMSO (1.2 equiv, 0.06 mL, 0.85 mmol), and TEA (1.15 equiv, 0.11 mL, 0.82 mmol). Alternatively, the title α -trifluoroacetoxazo was prepared in 87% yield (391 mg) as described in representative experimental procedure 5.5.5 (a) using hydrazone (1 equiv, 281 mg, 1.5 mmol), TFAA (1.1 equiv, 0.23 mL, 1.65 mmol), DMSO (1.2 equiv, 0.13 mL, 1.65 mmol), and TEA (1.15 equiv, 0.24 mL, 1.71 mmol). ^1H NMR (500 MHz, CDCl_3) δ = 7.73 – 7.66 (m, 2H), 7.50 – 7.43 (m, 3H), 5.90 – 5.62 (m, 1H), 5.11 – 4.90 (m, 2H),

2.31 – 2.02 (m, 4H), 1.90 (s, 3H). ^{13}C NMR (126 MHz, CDCl_3) δ 150.6, 136.9, 131.6, 129.1, 122.8, 115.4, 107.0, 37.58, 2.02, 22.0.

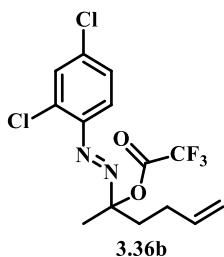


(E)-2-((2,4,6-trichlorophenyl)diazenyl)hex-5-en-2-yl 2,2,2-

trifluoroacetate (3.30b): Yield = 83%. ^1H NMR (500 MHz, CDCl_3)

δ 7.30 (s, 1H), 7.26 (s, 1H), 5.94 – 5.74 (m, 1H), 5.18 – 4.81 (m, 2H), 2.43 – 2.17 (m, 4H), 1.96 (d, J = 6.0 Hz, 3H).

(E)-2-((2,4-dichlorophenyl)diazenyl)hex-5-en-2-yl 2,2,2-trifluoroacetate (3.36b): The



title α -trifluoroacetoxyazo **3.36b** was prepared in 80% yield (186 mg)

as described in representative experimental procedure 5.5.5 (a) using

hydrazone (1 equiv, 161 mg, 0.63 mmol), TFAA (1.1 equiv, 0.10 mL,

0.69 mmol), DMSO (1.2 equiv, 0.06 mL, 0.76 mmol), and TEA (1.15

equiv, 0.10 mL, 0.72 mmol). ^1H NMR (500 MHz, CDCl_3) δ = 7.55 (d, J = 2.1, 1H), 7.39

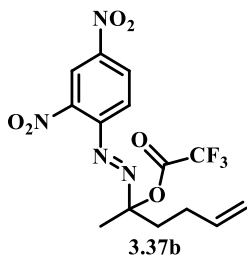
(d, J = 8.6, 1H), 7.28 (dd, J = 8.7, 2.2, 1H), 5.78 (ddt, J = 16.4, 10.2, 6.3, 1H), 5.05 (dd, J

= 17.1, 1.6, 1H), 5.00 (dd, J = 10.3, 1.5, 1H), 2.46 – 2.05 (m, 4H), 1.91 (s, 3H). ^{13}C NMR

(126 MHz, CDCl_3) δ 145.4, 137.9, 136.7, 135.9, 130.4, 127.7, 118.8, 115.6, 107.2, 37.5,

26.9, 22.1.

(E)-2-((2,4-dinitrophenyl)diazenyl)hex-5-en-2-yl 2,2,2-trifluoroacetate (3.37b): Yield



= 39%. ^1H NMR (500 MHz, CDCl_3) δ 9.11 (dt, J = 22.4, 2.3 Hz,

1H), 8.59 (dd, J = 8.2, 2.2 Hz, 1H), 7.96 (dd, J = 9.6, 2.7 Hz, 1H),

5.87 (tdd, J = 10.1, 8.5, 4.9 Hz, 1H), 5.31 – 4.79 (m, 2H), 2.62 –

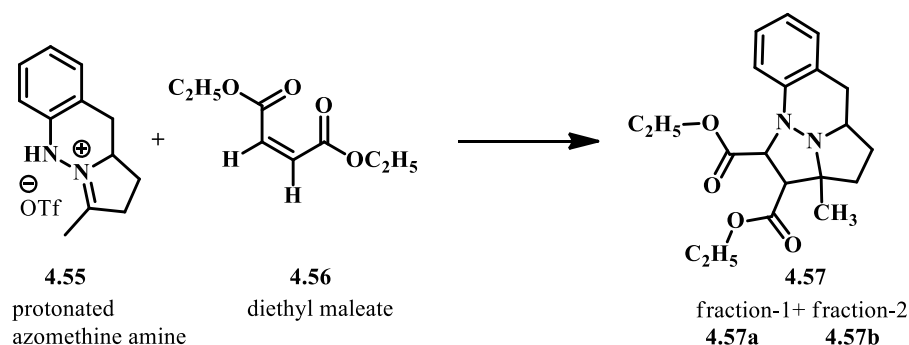
2.27 (m, 4H), 2.13 (dd, J = 43.9, 11.0 Hz, 3H).

5.6 Experimental information for Chapter 4

5.6.1 Experimental information of 1,3-dipolar cycloaddition reactions

A solution of a protonated azomethine amine salt **4.55** (1 equiv, 0.178 mmol) in an organic solvent (7 mL) was brought to the desired temperature (Table 5.1) in a flame-dried flask under a nitrogen atmosphere. Dimethyl maleate **4.56** (1.2 equiv, 0.21 mmol) and triethylamine (1.3 – 2.0 equiv) were added successively in a dropwise manner. The reaction was stirred for the amount of time shown in the Table 5.1 and concentrated in vacuo. The residue was purified by silica gel flash chromatography.

Table 5.1. Optimization of 1,3-dipolar cycloaddition of protonated azomethine imine



entry	reagent (equiv)	Et ₃ N (equiv)	solvent	time (h)	temp	diastereoisomers (yield)		total yield
						fraction-1	fraction-2	
1	1.2	2.0	DCM	1	-78 °C	1% (1 mg)	22% (15 mg)	23%
2	1.2	2.0	DCM	2	rt	20% (12.5 mg)	55% (35 mg)	75%
3	1.2	2.0	CH ₃ CN	2	rt	10 % (6.5 mg)	60% (38 mg)	70%
4	1.2	2.0	CH ₃ CN	16	rt	11% (6.5 mg)	59% (37.5 mg)	70%
5	1.2	2.0	THF	2	rt	15% (10 mg)	50% (32 mg)	65%
6	1.2	2.0	THF	16	rt	15% (9.5 mg)	51% (32.5 mg)	66%
7	1.2	2.0	DCM	2	30 °C	21% (16.5 mg)	51% (35 mg)	72%
8	1.2	2.0	CH ₃ CN	1	55 °C	13% (13 mg)	63% (40 mg)	76%
9	1.2	2.0	CH ₃ CN	2	55 °C	13% (8 mg)	67% (43 mg)	80%
10	1.2	1.3	CH ₃ CN	2	55 °C	16% (10 mg)	74% (47 mg)	90%

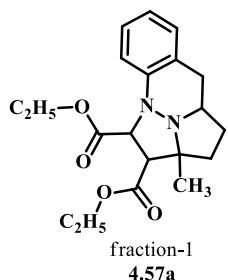
5.6.2 Representative experimental procedure for 1,3-dipolar cycloaddition reactions

A solution of a protonated azomethine amine salt (1 equiv, 0.178 mmol) in acetonitrile (7 mL) was heated to 55 °C in a flame-dried flask under a nitrogen

atmosphere. Dimethyl maleate (1.2 equiv, 0.21 mmol) and triethylamine (1.3 equiv, 0.22 mmol) were added successively in a dropwise manner. The reaction was stirred at 55 °C for 2 hours and concentrated *in vacuo*. The residue was purified by silica gel flash chromatography.

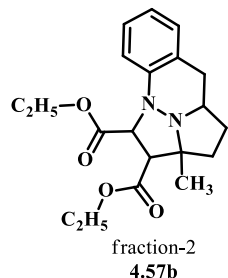
5.6.3 Characterization data for 1,3-dipolar cycloaddition reactions

Diethyl 2a-methyl-2,2a,3,4,4a,5-hexahydro-1*H*-2a¹,9b-diazapentaleno[1,6-



***ab*]naphthalene-1,2-dicarboxylate (4.57a, fraction-1):** R_f = 0.53 in Hexane/EtOAc = 3:1. Yield 16% (10 mg). ^1H NMR (500 MHz, CDCl_3) δ = 7.05 (t, J =7.8, 2H), 6.87 (d, J =7.8, 1H), 6.81 (tt, J =5.9, 2.9, 1H), 4.96 (d, J =9.3, 1H), 4.22 – 4.10 (m, 2H), 4.02 – 3.82 (m, 2H), 3.62 (dd, J =9.1, 4.7, 1H), 3.45 (ddt, J =11.5, 9.1, 4.5, 1H), 2.85 – 2.72 (m, 2H), 2.39 (td, J =12.3, 6.9, 1H), 2.01 (ddd, J =11.3, 6.7, 4.5, 1H), 1.88 (dd, J =12.9, 6.6, 1H), 1.64 – 1.45 (m, 4H), 1.26 (t, J =7.1, 3H), 0.97 (t, J =7.1, 3H). ^{13}C NMR (126 MHz, CDCl_3) δ 171.1, 170.2, 143.5, 141.8, 130.0, 126.4, 125.8, 121.0, 119.5, 69.0, 68.0, 60.9, 60.2, 55.9, 35.7, 35.4, 32.5, 29.1, 14.3, 13.8. MS (ESI) calcd for $[\text{C}_{20}\text{H}_{26}\text{N}_2\text{O}_4\text{H}]^+$: 359.1971, found: 359.1956.

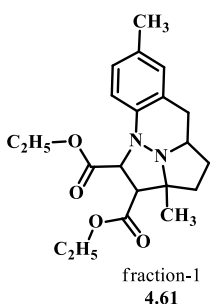
Diethyl 2a-methyl-2,2a,3,4,4a,5-hexahydro-1*H*-2a¹,9b-diazapentaleno[1,6-



***ab*]naphthalene-1,2-dicarboxylate (4.57b, fraction-2):** R_f = 0.45 in Hexane/EtOAc = 3:1. Yield 74% (47 mg). ^1H NMR (500 MHz, CDCl_3) δ 7.08 (dd, J = 16.0, 7.7 Hz, 2H), 6.88 (td, J = 7.5, 1.1 Hz, 1H), 6.78 (dd, J = 8.1, 0.7 Hz, 1H), 4.40 (dq, J = 10.8, 7.2 Hz, 1H), 4.34 – 4.26 (m, 2H), 4.24 – 4.11 (m, 2H), 3.65 (d, J = 11.3 Hz, 1H), 2.90 – 2.76 (m, 2H), 2.61 (ddd, J = 10.2, 7.9, 4.5 Hz, 1H), 2.37 (dt, J = 13.6, 9.4 Hz, 1H), 2.16 (dddd, J = 10.9, 9.3, 5.4, 1.3 Hz, 1H), 1.92 (ddd, J = 13.4, 10.5, 1.3 Hz, 1H), 1.69 (dt, J = 21.8, 10.9 Hz,

1H), 1.52 (s, 3H), 1.35 (t, $J = 7.2$ Hz, 3H), 1.28 (t, $J = 7.1$ Hz, 3H). ^{13}C NMR (126 MHz, CDCl_3) δ 171.6, 169.3, 146.1, 129.7, 126.8, 124.7, 121.7, 118.9, 70.9, 69.5, 61.5, 61.0, 56.9, 56.0, 35.4, 35.4, 28.7, 23.3, 14.3, 14.1. MS (ESI) calcd for $[\text{C}_{20}\text{H}_{26}\text{N}_2\text{O}_4\text{H}]^+$: 359.1971, found: 359.1955.

Diethyl 2a,7-dimethyl-2,2a,3,4,4a,5-hexahydro-1H-2a¹,9b-diazapentaleno[1,6-

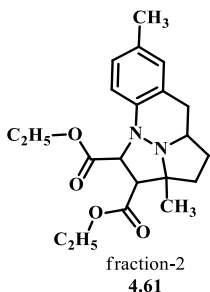


***ab*]naphthalene-1,2-dicarboxylate (4.61, fraction-1):** $R_f = 0.44$ in

Hexane/EtOAc = 3:1. Yield 17% (11 mg). ^1H NMR (500 MHz, CDCl_3) δ 6.86 (d, $J = 7.7$ Hz, 2H), 6.77 (d, $J = 8.2$ Hz, 1H), 4.92 (d, $J = 9.3$ Hz, 1H), 4.16 (dt, $J = 10.8, 7.2, 3.7$ Hz, 2H), 3.97 (dq, $J = 10.8, 7.1$ Hz, 1H), 3.89 (dq, $J = 10.8, 7.1$ Hz, 1H), 3.61 (d, $J = 9.3$ Hz, 1H),

3.45 (ddt, $J = 11.5, 9.1, 4.5$ Hz, 1H), 2.75 – 2.72 (m, 2H), 2.36 (td, $J = 12.3, 6.9$ Hz, 1H), 2.23 (s, 3H), 1.99 (ddd, $J = 11.3, 6.8, 4.5$ Hz, 1H), 1.87 (dd, $J = 13.0, 6.7$ Hz, 1H), 1.57 – 1.49 (m, 4H), 1.26 (t, $J = 7.1$ Hz, 3H), 0.99 (t, $J = 7.1$ Hz, 3H). ^{13}C NMR (126 MHz, CDCl_3) δ 171.0, 170.1, 140.8, 130.3, 130.1, 126.5, 126.1, 119.2, 68.8, 68.0, 60.7, 60.7, 60.1, 55.8, 35.5, 35.1, 32.4, 28.9, 20.7, 14.1, 13.7. MS (ESI) calcd for $[\text{C}_{21}\text{H}_{28}\text{N}_2\text{O}_4\text{H}]^+$: 373.2127, found: 373.2107.

Diethyl 2a,7-dimethyl-2,2a,3,4,4a,5-hexahydro-1H-2a¹,9b-diazapentaleno[1,6-



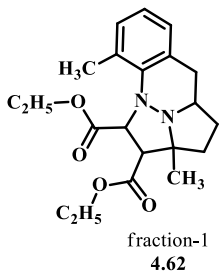
***ab*]naphthalene-1,2-dicarboxylate (4.61, fraction-2):** $R_f = 0.23$ in

Hexane/EtOAc = 3:1. Yield 66% (43.5 mg). ^1H NMR (500 MHz, CDCl_3) δ 6.94 – 6.82 (m, 2H), 6.70 (d, $J = 8.2$ Hz, 1H), 4.39 (dq, $J = 10.6, 7.1$ Hz, 1H), 4.30 (ddd, $J = 14.3, 10.8, 7.2$ Hz, 1H), 4.25 – 4.11 (m, 3H), 3.65 (d, $J = 11.4$ Hz, 1H), 2.79 (qd, $J = 15.0, 6.9$ Hz, 2H),

2.67 – 2.55 (m, 1H), 2.36 (dt, $J = 13.5, 9.3$ Hz, 1H), 2.25 (s, 3H), 2.19 – 2.09 (m, 1H),

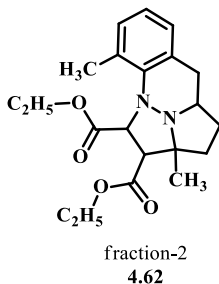
1.91 (dd, $J = 12.7, 11.4$ Hz, 1H), 1.74 – 1.59 (m, 1H), 1.50 (s, 3H), 1.35 (t, $J = 7.2$ Hz, 3H), 1.28 (t, $J = 7.1$ Hz, 3H). ^{13}C NMR (126 MHz, CDCl_3) δ 171.7, 169.4, 143.9, 131.2, 130.1, 127.6, 124.7, 119.1, 70.9, 69.6, 61.5, 61.0, 57.0, 55.8, 35.3, 28.6, 23.3, 20.7, 20.7, 14.3, 14.2. MS (ESI) calcd for $[\text{C}_{21}\text{H}_{28}\text{N}_2\text{O}_4\text{H}]^+$: 373.2127, found: 373.2114.

Diethyl 2a,9-dimethyl-2,2a,3,4,4a,5-hexahydro-1H-2a¹,9b-diazapentaleno[1,6-



***ab*]naphthalene-1,2-dicarboxylate (4.62, fraction-1):** $R_f = 0.63$ in Hexane/EtOAc = 3:1. Yield 53% (35 mg). ^1H NMR (500 MHz, cdcl_3) δ = 6.93 (dd, $J=11.6, 7.4$, 2H), 6.84 (t, $J=7.4$, 1H), 4.99 (d, $J=9.8$, 1H), 4.17 (q, $J=7.1$, 2H), 3.92 (dq, $J=10.8, 7.1$, 1H), 3.83 (dq, $J=10.8, 7.1$, 1H), 3.61 (d, $J=9.8$, 1H), 3.45 – 3.33 (m, 1H), 2.92 (dd, $J=15.3, 3.4$, 1H), 2.75 (dd, $J=15.2, 11.1$, 1H), 2.36 – 2.25 (m, 1H), 2.23 (s, 3H), 2.05 – 1.94 (m, 1H), 1.89 (dd, $J=13.4, 7.9$, 1H), 1.56 – 1.43 (m, 4H), 1.27 (t, $J=7.1$, 3H), 0.91 (t, $J=7.1$, 3H). ^{13}C NMR (126 MHz, CDCl_3) δ 171.2, 170.9, 142.2, 128.7, 128.2, 127.5, 127.4, 122.3, 68.6, 66.2, 60.9, 60.8, 60.7, 55.6, 35.5, 34.4, 31.8, 29.1, 19.5, 14.3, 13.7. MS (ESI) calcd for $[\text{C}_{21}\text{H}_{28}\text{N}_2\text{O}_4\text{H}]^+$: 373.2127, found: 373.2118.

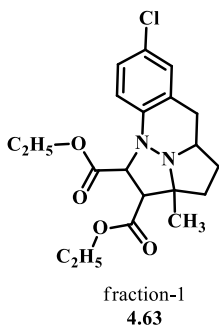
Diethyl 2a,9-dimethyl-2,2a,3,4,4a,5-hexahydro-1H-2a¹,9b-diazapentaleno[1,6-



***ab*]naphthalene-1,2-dicarboxylate (4.62, fraction-2):** $R_f = 0.44$ in Hexane/EtOAc = 3:1. Yield 11% (7 mg). ^1H NMR (500 MHz, CDCl_3) δ = 7.02 – 6.77 (m, 3H), 4.35 – 4.05 (m, 5H), 3.73 (d, $J=11.0$, 1H), 3.02 – 2.91 (m, 1H), 2.85 – 2.71 (m, 2H), 2.41 (ddd, $J=13.5, 9.7, 8.8$, 1H), 2.23 (s, 3H), 2.20 – 2.08 (m, 1H), 1.87 (ddd, $J=13.3, 11.0, 2.0$, 1H), 1.72 – 1.59 (m, 4H), 1.30 (dt, $J=16.8, 7.2$, 6H). ^{13}C NMR (126 MHz, CDCl_3) δ 171.9, 169.4, 144.9,

131.0, 130.1, 127.6, 126.7, 122.9, 70.7, 68.3, 61.20, 61.0, 56.5, 56.5, 35.9, 34.4, 28.2, 22.6, 19.9, 14.3, 13.9. MS (ESI) calcd for $[C_{21}H_{28}N_2O_4H]^+$: 373.2127, found: 373.2122.

Diethyl 7-chloro-2a-methyl-2,2a,3,4,4a,5-hexahydro-1*H*-2a¹,9b-diazapentaleno[1,6-



ab]naphthalene-1,2-dicarboxylate (4.63, fraction-1): $R_f = 0.51$ in

Hexane/EtOAc = 3:1. Yield 14% (10 mg). 1H NMR (500 MHz,

$CDCl_3$) δ 7.06 (d, $J = 2.3$ Hz, 1H), 7.02 (dd, $J = 8.6, 2.4$ Hz, 1H), 6.79

(d, $J = 8.6$ Hz, 1H), 4.93 (d, $J = 9.4$ Hz, 1H), 4.20 – 4.13 (m, 2H), 4.02

– 3.87 (m, 2H), 3.62 (d, $J = 9.4$ Hz, 1H), 3.41 (ddt, $J = 11.4, 9.1, 4.4$

Hz, 1H), 2.82 – 2.71 (m, 2H), 2.40 – 2.30 (m, 1H), 2.02 (ddd, $J = 11.4, 6.8, 4.5$ Hz, 1H),

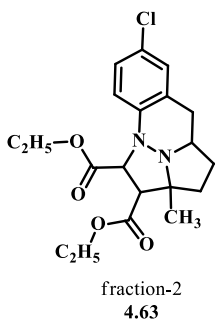
1.88 (dd, $J = 13.0, 6.7$ Hz, 1H), 1.57 – 1.48 (m, 4H), 1.27 (t, $J = 7.1$ Hz, 3H), 1.02 (t, $J =$

7.1 Hz, 3H). ^{13}C NMR (126 MHz, $CDCl_3$) δ 170.8, 170.1, 142.2, 129.7, 128.2, 125.9,

125.9, 120.5, 69.1, 68.0, 61.1, 61.0, 60.2, 55.6, 35.6, 35.4, 32.4, 29.0, 14.3, 13.9. MS

(ESI) calcd for $[C_{20}H_{25}ClN_2O_4H]^+$: 393.1581, found: 393.1578.

Diethyl 7-chloro-2a-methyl-2,2a,3,4,4a,5-hexahydro-1*H*-2a¹,9b-diazapentaleno[1,6-



ab]naphthalene-1,2-dicarboxylate (4.63, fraction-2): $R_f = 0.36$ in

Hexane/EtOAc = 3:1. Yield 70% (49 mg). 1H NMR (500 MHz, $CDCl_3$)

δ 7.06 – 7.00 (m, 2H), 6.73 – 6.68 (m, 1H), 4.38 (dq, $J = 10.8, 7.2$ Hz,

1H), 4.29 (dq, $J = 10.8, 7.2$ Hz, 1H), 4.25 – 4.08 (m, 3H), 3.64 (d, $J =$

11.3 Hz, 1H), 2.80 (qd, $J = 15.3, 6.8$ Hz, 2H), 2.62 – 2.53 (m, 1H),

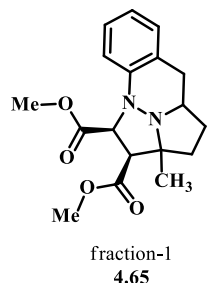
2.37 (dt, $J = 13.7, 9.3$ Hz, 1H), 2.37 (dt, $J = 13.7, 9.3$ Hz, 1H), 2.20 – 2.12 (m, 1H), 1.96

– 1.88 (m, 1H), 1.73 – 1.61 (m, 1H), 1.50 (s, $J = 7.1$ Hz, 3H), 1.34 (t, $J = 7.2$ Hz, 3H),

1.28 (t, $J = 7.1$ Hz, 3H). ^{13}C NMR (126 MHz, $CDCl_3$) δ 171.3, 169.1, 144.8, 129.3,

126.9, 126.7, 126.5, 120.0, 70.9, 69.4, 61.6, 61.1, 56.9, 55.7, 35.5, 35.3, 28.5, 23.2, 14.3, 14.1. MS (ESI) calcd for $[C_{20}H_{25}ClN_2O_4H]^+$: 393.1581, found: 393.1578.

(1*S*,2*S*)-Dimethyl 2a-methyl-2,2a,3,4,4a,5-hexahydro-1*H*-2a¹,9b-diazapentaleno[1,6-



***ab*]naphthalene-1,2-dicarboxylate (6.65, fraction-1):** R_f = 0.41 in

Hexane/EtOAc = 3:1. Yield 15% (9 mg). 1H NMR (500 MHz, $CDCl_3$)

δ 7.06 (dd, J = 15.2, 7.5 Hz, 2H), 6.85 – 6.80 (m, 2H), 5.00 (d, J = 9.7

Hz, 1H), 3.71 (s, 3H), 3.68 (d, J = 9.7 Hz, 1H), 3.55 – 3.46 (m, 4H),

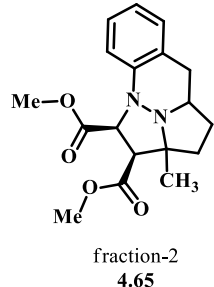
2.81 (qd, J = 14.9, 7.0 Hz, 2H), 2.28 – 2.19 (m, 1H), 2.03 (ddd, J = 11.4, 6.8, 4.4 Hz,

1H), 1.86 (dd, J = 13.0, 6.7 Hz, 1H), 1.59 – 1.48 (m, 4H). ^{13}C NMR (126 MHz, $CDCl_3$) δ

171.3, 170.8, 143.5, 130.1, 126.3, 126.0, 121.1, 118.9, 69.3, 68.0, 60.5, 55.9, 52.1, 52.0,

35.6, 35.4, 32.4, 29.2. MS (ESI) calcd for $[C_{18}H_{22}N_2O_4H]^+$: 331.1658, found: 331.1656.

(1*S*,2*S*)-Dimethyl 2a-methyl-2,2a,3,4,4a,5-hexahydro-1*H*-2a¹,9b-diazapentaleno[1,6-



***ab*]naphthalene-1,2-dicarboxylate (6.65, fraction-2):** R_f = 0.22 in

Hexane/EtOAc = 3:1. Yield 77% (45 mg). 1H NMR (500 MHz, $CDCl_3$)

δ 7.07 (dd, J = 15.3, 7.4 Hz, 2H), 6.89 (td, J = 7.5, 1.1 Hz, 1H), 6.77 –

6.70 (m, 1H), 4.31 (d, J = 11.3 Hz, 1H), 3.89 (s, 3H), 3.72 (s, 3H), 3.67

(d, J = 11.3 Hz, 1H), 2.83 (qd, J = 15.1, 6.9 Hz, 2H), 2.65 – 2.54 (m, 1H), 2.36 (dt, J =

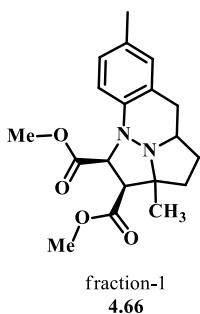
13.6, 9.3 Hz, 1H), 2.20 – 2.09 (m, 1H), 1.92 (ddd, J = 13.5, 10.5, 1.4 Hz, 1H), 1.69 (dt, J =

27.6, 10.7 Hz, 1H), 1.48 (s, 3H). ^{13}C NMR (126 MHz, $CDCl_3$) δ 172.1, 169.9, 146.0,

129.7, 126.8, 124.7, 121.8, 118.9, 71.0, 69.3, 56.9, 56.0, 52.6, 52.1, 35.4, 35.3, 28.6, 23.3.

MS (ESI) calcd for $[C_{18}H_{22}N_2O_4H]^+$: 331.1658, found: 331.1653.

(1*S*,2*S*)-dimethyl 2a,7-dimethyl-2,2a,3,4,4a,5-hexahydro-1*H*-2a¹,9b-



diazapentaleno[1,6-*ab*]naphthalene-1,2-dicarboxylate (4.66,

fraction-1): $R_f = 0.43$ in Hexane/EtOAc = 3:1. Yield 9% (5 mg). ^1H

NMR (500 MHz, CDCl_3) δ 6.93 – 6.79 (m, 2H), 6.72 (d, $J = 8.1$ Hz,

1H), 4.96 (d, $J = 9.7$ Hz, 1H), 3.71 (s, 3H), 3.66 (d, $J = 9.7$ Hz, 1H),

3.56 – 3.40 (m, 4H), 2.76 (qd, $J = 14.9, 7.0$ Hz, 2H), 2.29 – 2.15 (m,

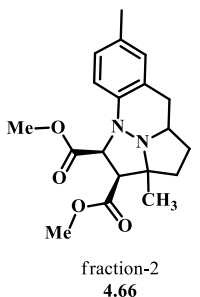
4H), 2.01 (ddd, $J = 11.4, 9.2, 5.7$ Hz, 1H), 1.84 (dd, $J = 13.0, 6.8$ Hz, 1H), 1.62 – 1.44

(m, 4H). ^{13}C NMR (126 MHz, CDCl_3) δ 171.5, 170.9, 141.0, 130.5, 130.2, 126.8, 126.2,

118.8, 69.3, 68.0, 60.6, 55.9, 52.0, 52.0, 35.5, 35.3, 32.4, 29.1, 20.9. MS (ESI) calcd for

$[\text{C}_{19}\text{H}_{24}\text{N}_2\text{O}_4\text{H}]^+$: 345.1814, found: 345.1798.

(1*S*,2*S*)-dimethyl 2a,7-dimethyl-2,2a,3,4,4a,5-hexahydro-1*H*-2a¹,9b-



diazapentaleno[1,6-*ab*]naphthalene-1,2-dicarboxylate (4.66, fraction-

2): $R_f = 0.23$ in Hexane/EtOAc = 3:1. Yield 69% (42 mg). ^1H NMR

(500 MHz, CDCl_3) δ 6.93 – 6.85 (m, 2H), 6.66 (d, $J = 8.1$ Hz, 1H), 4.25

(d, $J = 11.4$ Hz, 1H), 3.88 (s, 3H), 3.72 (s, 3H), 3.67 (d, $J = 11.4$ Hz,

1H), 2.79 (qd, $J = 15.1, 6.9$ Hz, 2H), 2.65 – 2.54 (m, 1H), 2.35 (dt, $J =$

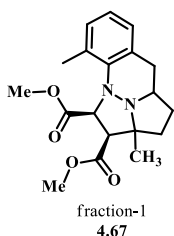
13.7, 9.3 Hz, 1H), 2.24 (s, 3H), 2.18 – 2.09 (m, 1H), 1.91 (ddd, $J = 13.5, 10.6, 1.4$ Hz,

1H), 1.72 – 1.60 (m, 1H), 1.47 (s, 3H). ^{13}C NMR (126 MHz, CDCl_3) δ 172.2, 170.0,

143.8, 131.3, 130.1, 127.6, 124.7, 119.0, 71.0, 69.4, 57.0, 55.9, 52.6, 52.1, 35.3, 35.3,

28.5, 23.3, 20.7. MS (ESI) calcd for $[\text{C}_{19}\text{H}_{24}\text{N}_2\text{O}_4\text{H}]^+$: 345.1814, found: 345.1796.

(1*S*,2*S*)-dimethyl 2a,9-dimethyl-2,2a,3,4,4a,5-hexahydro-1*H*-2a¹,9b-



diazapentaleno[1,6-*ab*]naphthalene-1,2-dicarboxylate (4.67, fraction-

1): $R_f = 0.40$ in Hexane/EtOAc = 3:1. Yield 49% (30 mg). ^1H NMR (500

MHz, CDCl_3) $\delta = 6.96$ (d, $J=7.4$, 1H), 6.91 (d, $J=7.0$, 1H), 6.85 (t, $J=7.4$,

1H), 5.01 (d, $J=10.2$, 1H), 3.71 (s, 3H), 3.66 (d, $J=10.2$, 1H), 3.44 (s, 3H),

3.44 – 3.36 (m, 1H), 2.97 (dd, $J=15.3$, 3.5, 1H), 2.75 (dd, $J=15.3$, 11.0, 1H), 2.20 (s, 3H),

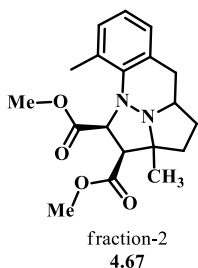
2.14 (ddd, $J=13.4$, 10.3, 8.2, 1H), 2.06 – 1.96 (m, 1H), 1.88 (dd, $J=13.4$, 8.4, 1H), 1.54 (s,

3H), 1.50 (dt, $J=19.9$, 6.8, 1H). ^{13}C NMR (126 MHz, CDCl_3) δ 171.5, 171.4, 142.0,

128.4, 128.2, 127.5, 127.4, 122.4, 77.1, 69.0, 66.1, 61.1, 55.5, 52.0, 35.4, 34.3, 31.6, 29.2,

19.4. MS (ESI) calcd for $[\text{C}_{19}\text{H}_{24}\text{N}_2\text{O}_4\text{H}]^+$: 345.1814, found: 345.1811.

(1*S*,2*S*)-dimethyl 2a,9-dimethyl-2,2a,3,4,4a,5-hexahydro-1*H*-2a¹,9b-



diazapentaleno[1,6-*ab*]naphthalene-1,2-dicarboxylate (4.67, fraction-

2): $R_f = 0.23$ in Hexane/EtOAc = 3:1. Yield 8% (5 mg). ^1H NMR (500

MHz, CDCl_3) $\delta = 6.97$ (d, $J=7.2$, 1H), 6.93 (d, $J=7.2$, 1H), 6.88 (t,

$J=7.3$, 1H), 4.25 (d, $J=11.0$, 1H), 3.79 (s, 3H), 3.76 – 3.69 (m, 4H), 2.99

– 2.91 (m, 1H), 2.84 – 2.69 (m, 2H), 2.43 – 2.33 (m, 1H), 2.20 (s, 3H), 2.18 – 2.10 (m,

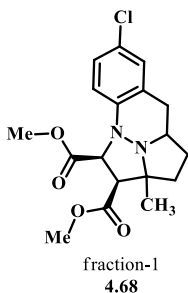
1H), 1.87 (ddd, $J=13.3$, 11.0, 2.0, 1H), 1.67 (dd, $J=12.7$, 10.6, 1H), 1.64 (s, 3H). ^{13}C

NMR (126 MHz, CDCl_3) δ 172.4, 170.0, 144.9, 130.9, 130.1, 127.6, 126.7, 123.0, 77.1,

70.8, 68.0, 56.5, 52.1, 52.0, 35.8, 34.3, 28.1, 22.6, 19.8. MS (ESI) calcd for $[\text{C}_{19}\text{H}_{24}$

$\text{N}_2\text{O}_4\text{H}]^+$: 345.1814, found: 345.1808.

(1*S*,2*S*)-dimethyl 7-chloro-2a-methyl-2,2a,3,4,4a,5-hexahydro-1*H*-2a¹,9b-



diazapentaleno[1,6-*ab*]naphthalene-1,2-dicarboxylate (4.68, fraction-

1): $R_f = 0.48$ in Hexane/EtOAc = 3:1. Yield 11% (7 mg). ^1H NMR (500

MHz, CDCl_3) δ 7.06 (dd, $J = 5.9, 2.6$ Hz, 2H), 6.72 – 6.64 (m, 1H), 4.28

(d, $J = 11.3$ Hz, 1H), 3.90 (s, 3H), 3.74 (s, 3H), 3.69 (d, $J = 11.3$ Hz,

1H), 2.83 (qd, $J = 15.3, 6.9$ Hz, 2H), 2.64 – 2.52 (m, 1H), 2.38 (dt, $J = 13.7, 9.3$ Hz, 1H),

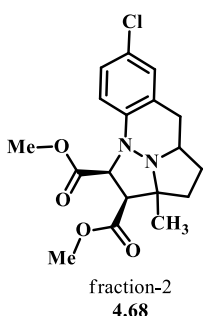
2.22 – 2.11 (m, 1H), 1.95 (ddd, $J = 13.6, 10.5, 1.4$ Hz, 1H), 1.76 – 1.59 (m, 1H), 1.49 (s,

3H). ^{13}C NMR (126 MHz, CDCl_3) δ 171.8, 169.7, 144.7, 129.4, 126.9, 126.6, 120.1,

77.4, 71.0, 69.2, 56.9, 55.7, 52.7, 52.2, 35.4, 35.2, 28.5, 23.3. MS (ESI) calcd for

$[\text{C}_{18}\text{H}_{21}\text{ClN}_2\text{O}_4\text{H}]^+$: 365.1268, found: 365.1267.

(1*S*,2*S*)-dimethyl 7-chloro-2a-methyl-2,2a,3,4,4a,5-hexahydro-1*H*-2a¹,9b-



diazapentaleno[1,6-*ab*]naphthalene-1,2-dicarboxylate (4.68,

fraction-2): $R_f = 0.26$ in Hexane/EtOAc = 3:1. Yield 71% (46 mg). ^1H

NMR (500 MHz, CDCl_3) δ = 7.06 (dd, $J = 5.9, 2.6$, 3H), 6.74 – 6.55 (m,

1H), 4.28 (d, $J = 11.3$, 1H), 3.90 (s, 2H), 3.74 (s, 3H), 3.69 (d, $J = 11.3$,

1H), 2.83 (qd, $J = 15.3, 6.9$, 2H), 2.65 – 2.52 (m, 1H), 2.38 (dt, $J = 13.7$,

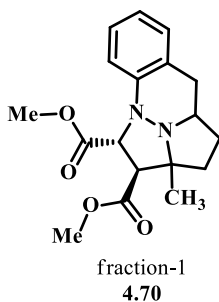
9.3, 1H), 2.22 – 2.09 (m, 1H), 1.95 (ddd, $J = 13.6, 10.5, 1.4$, 1H), 1.76 – 1.62 (m, 1H),

1.49 (s, 3H). ^{13}C NMR (126 MHz, CDCl_3) δ 171.8, 169.7, 144.7, 129.4, 126.9, 126.9,

126.6, 120.1, 71.0, 69.2, 56.9, 55.7, 52.7, 52.2, 35.4, 35.2, 28.5, 23.3. MS (ESI) calcd for

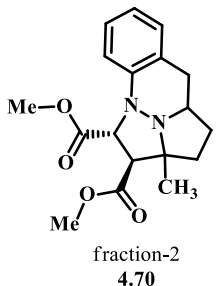
$[\text{C}_{18}\text{H}_{21}\text{ClN}_2\text{O}_4\text{H}]^+$: 365.1268, found: 365.1261.

(1*R*,2*S*)-dimethyl 2*a*-methyl-2,2*a*,3,4,4*a*,5-hexahydro-1*H*-2*a*¹,9*b*-diazapentaleno[1,6-*ab*]naphthalene-1,2-dicarboxylate (4.70, fraction-1): $R_f = 0.56$ in Hexane/EtOAc = 3:1.



Yield 43% (25.5 mg). ^1H NMR (500 MHz, CDCl_3) δ 7.04 (dd, $J = 12.7, 4.6$ Hz, 2H), 6.83 (td, $J = 7.4, 1.1$ Hz, 1H), 6.77 (d, $J = 8.1$ Hz, 1H), 5.12 (d, $J = 8.9$ Hz, 1H), 3.77 (s, 3H), 3.63 (d, $J = 9.0$ Hz, 1H), 3.47 (s, 3H), 3.24 – 3.14 (m, 1H), 2.92 (dd, $J = 15.2, 3.2$ Hz, 1H), 2.74 (dd, $J = 15.2, 10.8$ Hz, 1H), 2.43 (dt, $J = 13.6, 9.3$ Hz, 1H), 2.23 – 2.14 (m, 1H), 1.92 (ddd, $J = 13.5, 10.4, 1.2$ Hz, 1H), 1.62 (dq, $J = 11.7, 10.6$ Hz, 1H), 1.32 (s, 3H). ^{13}C NMR (126 MHz, CDCl_3) δ 172.7, 171.1, 143.3, 129.9, 125.9, 125.4, 121.5, 119.0, 70.5, 69.6, 59.8, 55.3, 52.3, 52.3, 35.1, 34.8, 28.8, 22.8. MS (ESI) calcd for $[\text{C}_{18}\text{H}_{22}\text{N}_2\text{O}_4\text{H}]^+$: 331.1658, found: 331.1651.

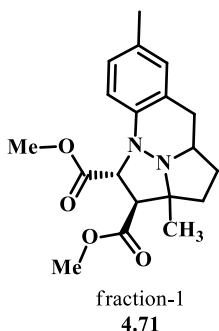
(1*R*,2*S*)-dimethyl 2*a*-methyl-2,2*a*,3,4,4*a*,5-hexahydro-1*H*-2*a*¹,9*b*-diazapentaleno[1,6-*ab*]naphthalene-1,2-dicarboxylate (4.70, fraction-2): $R_f = 0.41$ in Hexane/EtOAc = 3:1. Yield 36% (21 mg).



^1H NMR (500 MHz, CDCl_3) δ 7.08 (dd, $J = 12.0, 7.7$ Hz, 2H), 6.96 (td, $J = 7.4, 1.1$ Hz, 1H), 6.84 (d, $J = 8.1$ Hz, 1H), 4.59 (d, $J = 8.0$ Hz, 1H), 3.84 (s, 3H), 3.75 (s, 3H), 3.36 (d, $J = 8.0$ Hz, 1H), 3.04 (tdd, $J = 11.1, 4.8, 3.4$ Hz, 1H), 2.86 (dd, $J = 15.3, 3.2$ Hz, 1H), 2.76 (dd, $J = 15.3, 10.9$ Hz, 1H), 2.03 – 1.94 (m, 1H), 1.86 (dt, $J = 9.7, 4.8$ Hz, 2H), 1.61 (s, 3H), 1.55 (ddd, $J = 21.1, 11.4, 9.7$ Hz, 1H). ^{13}C NMR (126 MHz, CDCl_3) δ 172.7, 172.6, 145.5, 130.0, 126.6, 126.4, 123.2, 121.1, 70.7, 70.2, 63.7, 53.7, 52.7, 52.3, 35.1, 33.7, 30.9, 28.4. MS (ESI) calcd for $[\text{C}_{18}\text{H}_{22}\text{N}_2\text{O}_4\text{H}]^+$: 331.1658, found: 331.1649.

(1*R*,2*S*)-dimethyl 2*a*,7-dimethyl-2,2*a*,3,4,4*a*,5-hexahydro-1*H*-2*a*¹,9*b*-

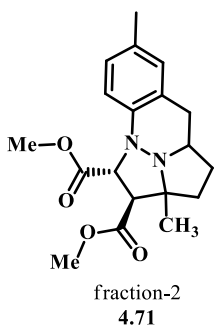
diazapentaleno[1,6-*ab*]naphthalene-1,2-dicarboxylate (4.71, fraction-1): R_f = 0.49 in



Hexane/EtOAc = 3:1. Yield 35% (21.5 mg). ¹H NMR (500 MHz, CDCl₃) δ 6.84 (d, J = 9.5 Hz, 2H), 6.67 (d, J = 8.0 Hz, 1H), 5.09 (d, J = 8.9 Hz, 1H), 3.76 (s, 3H), 3.62 (d, J = 8.9 Hz, 1H), 3.48 (s, 3H), 3.19 (tdd, J = 11.1, 5.3, 3.4 Hz, 1H), 2.86 (dd, J = 15.2, 3.2 Hz, 1H), 2.69 (dd, J = 15.2, 10.8 Hz, 1H), 2.42 (dt, J = 13.6, 9.3 Hz, 1H), 2.22

(s, 3H), 2.20 – 2.14 (m, 1H), 1.91 (ddd, J = 13.5, 10.4, 1.3 Hz, 1H), 1.66 – 1.55 (m, 1H), 1.31 (s, 3H). ¹³C NMR (126 MHz, CDCl₃) δ 172.8, 171.2, 140.9, 130.7, 130.3, 126.7, 125.2, 118.9, 70.5, 69.6, 59.8, 55.3, 52.3, 52.3, 35.0, 34.8, 28.8, 22.8, 20.8. MS (ESI) calcd for [C₁₉H₂₄N₂O₄H]⁺: 345.1814, found: 345.1808.

(1*R*,2*S*)-dimethyl 2*a*,7-dimethyl-2,2*a*,3,4,4*a*,5-hexahydro-1*H*-2*a*¹,9*b*-

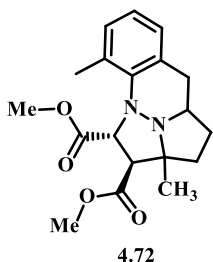


diazapentaleno[1,6-*ab*]naphthalene-1,2-dicarboxylate (4.71,

fraction-2): R_f = 0.35 in Hexane/EtOAc = 3:1. Yield 32% (20 mg). ¹H NMR (500 MHz, CDCl₃) δ 6.93 – 6.82 (m, 2H), 6.73 (d, J = 8.1 Hz, 1H), 4.53 (d, J = 8.3 Hz, 1H), 3.82 (s, 3H), 3.74 (s, 3H), 3.36 (d, J = 8.3 Hz, 1H), 3.04 (tdd, J = 11.1, 4.8, 3.5 Hz, 1H), 2.81 (dd, J = 15.3,

3.3 Hz, 1H), 2.71 (dd, J = 15.2, 10.9 Hz, 1H), 2.25 (s, 3H), 2.01 – 1.94 (m, 1H), 1.89 – 1.78 (m, 2H), 1.60 (s, 3H), 1.58 – 1.48 (m, 1H). ¹³C NMR (126 MHz, CDCl₃) δ 172.7, 172.6, 143.0, 132.7, 130.4, 127.2, 126.5, 121.2, 70.6, 70.3, 63.8, 53.6, 52.6, 52.3, 34.9, 33.7, 30.9, 28.3, 20.8. MS (ESI) calcd for [C₁₉H₂₄N₂O₄H]⁺: 345.1814, found: 345.1805.

(1*R*,2*S*)-dimethyl 2a,9-dimethyl-2,2a,3,4,4a,5-hexahydro-1*H*-2a¹,9b-

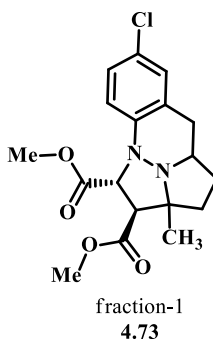


diazapentaleno[1,6-*ab*]naphthalene-1,2-dicarboxylate (4.72): $R_f =$

0.5 in Hexane/EtOAc = 3:1. Yield 73% (45 mg). ^1H NMR (500 MHz, CDCl_3) δ 6.94 – 6.90 (m, 2H), 6.87 – 6.81 (m, 1H), 5.09 (d, $J = 8.3$ Hz, 1H), 3.78 (s, 3H), 3.69 (d, $J = 8.3$ Hz, 1H), 3.39 (s, 3H), 3.38 – 3.31

(m, 1H), 3.00 (dd, $J = 15.5, 3.6$ Hz, 1H), 2.73 (s, 1H), 2.42 (dt, $J = 13.6, 9.3$ Hz, 1H), 2.30 (s, 3H), 2.22 – 2.12 (m, 1H), 1.94 – 1.87 (m, 1H), 1.67 – 1.51 (m, 1H), 1.34 (s, 3H). ^{13}C NMR (126 MHz, CDCl_3) δ 172.9, 171.4, 141.7, 129.8, 128.3, 127.2, 126.7, 122.9, 70.3, 68.1, 60.1, 54.9, 52.3, 52.3, 35.0, 34.6, 28.6, 22.5, 18.9. MS (ESI) calcd for $[\text{C}_{19}\text{H}_{24}\text{N}_2\text{O}_4\text{H}]^+$: 345.1814, found: 345.1798.

(1*R*,2*S*)-dimethyl 7-chloro-2a-methyl-2,2a,3,4,4a,5-hexahydro-1*H*-2a¹,9b-

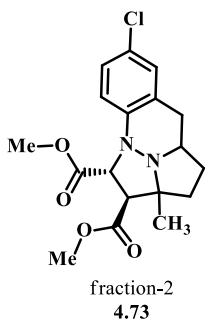


diazapentaleno[1,6-*ab*]naphthalene-1,2-dicarboxylate (4.73,

fraction-1): $R_f = 0.37$ in Hexane/EtOAc = 3:1. Yield 43% (28 mg). ^1H NMR (500 MHz, CDCl_3) δ 7.10 – 6.96 (m, 2H), 6.70 (d, $J = 8.6$ Hz, 1H), 5.09 (d, $J = 8.9$ Hz, 1H), 3.77 (s, 3H), 3.62 (d, $J = 8.9$ Hz, 1H), 3.51 (s, 3H), 3.16 (tdd, $J = 11.1, 5.3, 3.3$ Hz, 1H), 2.89 (dd, $J = 15.4,$

3.2 Hz, 1H), 2.71 (dd, $J = 15.4, 10.8$ Hz, 1H), 2.43 (dt, $J = 13.7, 9.3$ Hz, 1H), 2.19 (s, 1H), 1.93 (ddd, $J = 13.6, 10.4, 1.2$ Hz, 1H), 1.68 – 1.50 (m, 1H), 1.30 (s, 3H). ^{13}C NMR (126 MHz, CDCl_3) δ 172.4, 170.9, 142.0, 129.6, 127.2, 126.4, 126.1, 120.0, 70.5, 69.6, 59.9, 54.9, 52.4, 52.4, 35.0, 34.9, 28.7, 22.8. MS (ESI) calcd for $[\text{C}_{18}\text{H}_{21}\text{ClN}_2\text{O}_4\text{H}]^+$: 365.1268, found: 365.1266.

(1*R*,2*S*)-dimethyl 7-chloro-2a-methyl-2,2a,3,4,4a,5-hexahydro-1*H*-2a¹,9b-



diazapentaleno[1,6-*ab*]naphthalene-1,2-dicarboxylate (4.73,

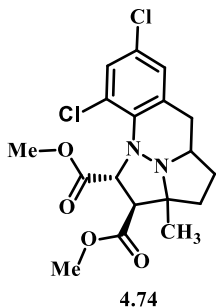
fraction-2): $R_f = 0.32$ in Hexane/EtOAc = 3:1. Yield 39% (19 mg). ^1H

NMR (500 MHz, CDCl_3) δ 7.10 – 6.99 (m, 2H), 6.80 (d, $J = 8.7$ Hz, 1H), 4.55 (d, $J = 7.9$ Hz, 1H), 3.83 (s, 3H), 3.76 (s, 3H), 3.35 (d, $J = 7.9$ Hz, 1H), 3.01 (tdd, $J = 11.1, 4.9, 3.4$ Hz, 1H), 2.83 (dd, $J = 15.5, 3.2$

Hz, 1H), 2.73 (dd, $J = 15.4, 10.9$ Hz, 1H), 2.03 – 1.95 (m, 1H), 1.91 – 1.80 (m, 2H), 1.62 – 1.47 (m, 4H). ^{13}C NMR (126 MHz, CDCl_3) δ 172.6, 172.4, 144.2, 129.6, 128.5, 128.3, 126.6, 122.2, 70.7, 70.3, 63.6, 53.4, 52.8, 52.4, 35.0, 33.6, 30.8, 28.2. MS (ESI) calcd for $[\text{C}_{18}\text{H}_{21}\text{ClN}_2\text{O}_4\text{H}]^+$: 365.1268, found: 365.1248.

(1*R*,2*S*)-dimethyl 7,9-dichloro-2a-methyl-2,2a,3,4,4a,5-hexahydro-1*H*-2a¹,9b-

diazapentaleno[1,6-*ab*]naphthalene-1,2-dicarboxylate (4.74): $R_f = 0.45$ in



Hexane/EtOAc = 3:1. Yield 99% (70 mg). ^1H NMR (500 MHz,

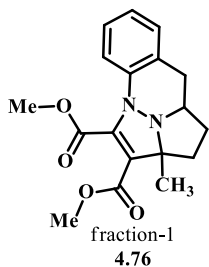
CDCl_3) δ = 7.13 (d, $J = 2.1$, 1H), 7.06 – 6.97 (m, 1H), 5.46 (d, $J = 9.0$, 1H), 3.79 (s, 3H), 3.54 (s, 3H), 3.50 (d, $J = 8.9$, 1H), 3.15 (tdd, $J = 11.1, 5.5, 3.6$, 1H), 3.00 (dd, $J = 15.7, 3.5$, 1H), 2.75 (dd, $J = 15.7, 10.8$, 1H), 2.41 (dt, $J = 13.7, 9.3$, 1H), 2.25 – 2.11 (m, 1H), 1.96 – 1.87 (m, 1H),

1.67 – 1.49 (m, 1H), 1.32 (s, 3H). ^{13}C NMR (126 MHz, CDCl_3) δ 172.9, 170.6, 140.1, 130.1, 128.0, 127.2, 127.0, 125.4, 69.9, 67.8, 60.0, 55.3, 52.6, 52.4, 35.4, 34.7, 28.5, 22.5. MS (ESI) calcd for $[\text{C}_{18}\text{H}_{20}\text{Cl}_2\text{N}_2\text{O}_4\text{H}]^+$: 399.0878, found: 399.0877.

Dimethyl 2a-methyl-3,4,4a,5-tetrahydro-2a*H*-2a¹,9b-diazapentaleno[1,6-

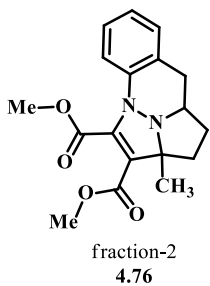
***ab*]naphthalene-1,2-dicarboxylate (4.76, fraction-1):** $R_f = 0.60$ in Hexane/EtOAc = 3:1.

Yield 63% (37 mg). ^1H NMR (500 MHz, CDCl_3) δ 7.15 (d, $J = 7.6$ Hz, 1H), 7.11 (td, $J =$



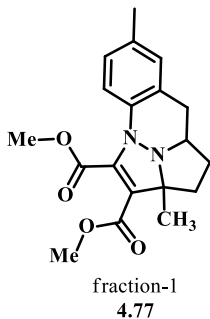
8.0, 1.4 Hz, 1H), 7.04 (td, $J = 7.4, 1.2$ Hz, 1H), 6.97 (dd, $J = 8.1, 0.9$ Hz, 1H), 3.86 (s, 3H), 3.72 (s, 3H), 3.12 – 3.04 (m, 1H), 2.97 – 2.89 (m, 2H), 2.49 (ddd, $J = 13.4, 11.4, 8.4$ Hz, 1H), 2.11 (dd, $J = 13.4, 8.3$ Hz, 1H), 1.97 (ddd, $J = 12.3, 8.2, 4.5$ Hz, 1H), 1.65 – 1.48 (m, 1H), 1.43 (s, 3H). ^{13}C NMR (126 MHz, CDCl_3) δ 164.7, 163.0, 145.3, 138.1, 130.2, 127.6, 126.7, 124.5, 119.1, 110.4, 71.0, 62.6, 53.2, 51.4, 37.6, 34.0, 27.7, 26.1. MS (ESI) calcd for $[\text{C}_{18}\text{H}_{20}\text{N}_2\text{O}_4\text{H}]^+$: 329.1501, found: 329.1501.

Dimethyl 2a-methyl-3,4,4a,5-tetrahydro-2aH-2a¹,9b-diazapentaleno[1,6-



ab]naphthalene-1,2-dicarboxylate (4.76, fraction-2): $R_f = 0.38$ in Hexane/EtOAc = 3:1. Yield 36% (21 mg). ^1H NMR (500 MHz, CDCl_3) δ 7.10 (dddd, $J = 18.6, 12.0, 8.9, 4.4$ Hz, 4H), 3.84 (s, 3H), 3.77 – 3.67 (m, 4H), 3.19 (dd, $J = 16.2, 7.8$ Hz, 1H), 2.71 (dd, $J = 16.2, 6.3$ Hz, 1H), 2.47 (ddd, $J = 12.9, 7.1, 2.5$ Hz, 1H), 2.19 – 2.08 (m, 1H), 1.91 (ddd, $J = 12.9, 11.2, 6.5$ Hz, 1H), 1.79 – 1.69 (m, 1H), 1.60 (s, 3H). ^{13}C NMR (126 MHz, CDCl_3) δ 164.4, 162.7, 144.0, 137.4, 129.8, 128.4, 126.8, 125.8, 119.4, 104.4, 76.0, 65.3, 53.2, 51.0, 39.5, 32.8, 30.7, 27.2. MS (ESI) calcd for $[\text{C}_{18}\text{H}_{20}\text{N}_2\text{O}_4\text{H}]^+$: 329.1501, found: 329.1504.

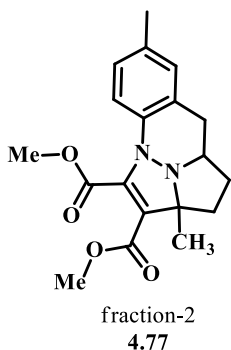
Dimethyl 2a,7-dimethyl-3,4,4a,5-tetrahydro-2aH-2a¹,9b-diazapentaleno[1,6-



ab]naphthalene-1,2-dicarboxylate (4.77, fraction-1): $R_f = 0.33$ in Hexane/EtOAc = 3:1. Yield 54% (33 mg). ^1H NMR (500 MHz, CDCl_3) δ 6.95 (s, 1H), 6.91 (dd, $J = 8.3, 1.4$ Hz, 1H), 6.86 (d, $J = 8.3$ Hz, 1H), 3.85 (s, 3H), 3.71 (s, 3H), 3.12 – 3.04 (m, 1H), 2.88 (d, $J = 6.9$ Hz, 2H), 2.49 (ddd, $J = 13.4, 11.4, 8.4$ Hz, 1H), 2.27 (s, 3H), 2.09 (dd, $J = 13.4, 8.1$ Hz, 1H), 1.95 (ddd, $J = 12.3, 8.1, 4.5$ Hz, 1H), 1.64 – 1.51 (m, 1H),

1.42 (s, 3H). ^{13}C NMR (126 MHz, CDCl_3) δ 164.8, 163.1, 145.5, 135.6, 134.1, 130.7, 127.4, 127.4, 118.9, 110.0, 70.9, 62.7, 53.2, 51.3, 37.6, 33.9, 27.7, 26.1, 20.9. MS (ESI) calcd for $[\text{C}_{19}\text{H}_{22}\text{N}_2\text{O}_4\text{H}]^+$: 343.1658, found: 343.1653.

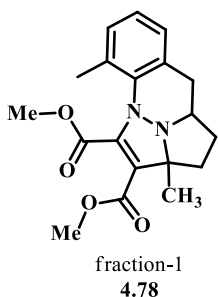
Dimethyl 2a,7-dimethyl-3,4,4a,5-tetrahydro-2aH-2a¹,9b-diazapentaleno[1,6-



ab]naphthalene-1,2-dicarboxylate (4.77, fraction-2): R_f = 0.18 in Hexane/EtOAc = 3:1. Yield 36% (22 mg). ^1H NMR (500 MHz, CDCl_3) δ 6.98 – 6.91 (m, 3H), 3.82 (s, 3H), 3.75 – 3.66 (m, 4H), 3.12 (dd, J = 16.1, 7.6 Hz, 1H), 2.67 (dd, J = 16.0, 6.7 Hz, 1H), 2.47 (ddd, J = 12.9, 7.1, 2.6 Hz, 1H), 2.29 (s, 3H), 2.17 – 2.09 (m, 1H), 1.91

(ddd, J = 12.9, 11.1, 6.5 Hz, 1H), 1.77 – 1.67 (m, 1H), 1.58 (s, 3H). ^{13}C NMR (126 MHz, CDCl_3) δ 164.3, 162.6, 144.3, 135.7, 134.8, 129.9, 128.7, 127.3, 119.4, 103.8, 75.8, 65.3, 53.0, 50.8, 39.1, 32.7, 30.8, 26.9, 21.0. MS (ESI) calcd for $[\text{C}_{19}\text{H}_{22}\text{N}_2\text{O}_4\text{H}]^+$: 343.1658, found: 343.1653.

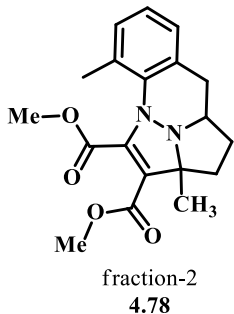
Dimethyl 2a,9-dimethyl-3,4,4a,5-tetrahydro-2aH-2a¹,9b-diazapentaleno[1,6-



ab]naphthalene-1,2-dicarboxylate (4.78, fraction-1): R_f = 0.41 in Hexane/EtOAc = 3:1. Yield 12% (7 mg). ^1H NMR (500 MHz, CDCl_3) δ 7.06 – 6.89 (m, 3H), 3.78 (s, 3H), 3.73 (s, 3H), 3.25 – 3.14 (m, 1H), 3.03 (dd, J = 16.0, 3.7 Hz, 1H), 2.86 (dd, J = 16.0, 11.6 Hz, 1H), 2.48 (ddd, J = 13.6, 10.6, 9.1 Hz, 1H), 2.18 (s, 3H), 2.06 – 1.99 (m, 1H),

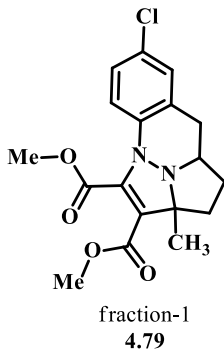
1.97 – 1.91 (m, 1H), 1.58 – 1.45 (m, 4H). ^{13}C NMR (126 MHz, CDCl_3) δ 164.8, 162.7, 145.4, 137.3, 130.8, 129.4, 128.9, 127.4, 125.2, 112.8, 70.9, 61.2, 53.0, 51.4, 36.1, 34.1, 27.5, 24.9, 18.0. MS (ESI) calcd for $[\text{C}_{19}\text{H}_{22}\text{N}_2\text{O}_4\text{H}]^+$: 343.1658, found: 343.1655.

Dimethyl 2a,9-dimethyl-3,4,4a,5-tetrahydro-2aH-2a¹,9b-diazapentaleno[1,6-



***ab*]naphthalene-1,2-dicarboxylate (4.78, fraction-2):** $R_f = 0.24$ in Hexane/EtOAc = 3:1. Yield 74% (45 mg). ^1H NMR (500 MHz, CDCl_3) δ 7.12 (t, $J = 7.5$ Hz, 1H), 7.09 – 7.05 (m, 1H), 6.98 (d, $J = 7.2$ Hz, 1H), 3.69 (s, 3H), 3.68 – 3.60 (m, 4H), 2.95 (dd, $J = 14.5, 5.5$ Hz, 1H), 2.81 (ddd, $J = 12.9, 7.0, 1.8$ Hz, 1H), 2.65 (dd, $J = 14.3, 11.4$ Hz, 1H), 2.32 (s, 3H), 2.24 – 2.14 (m, 1H), 2.06 – 1.95 (m, 1H), 1.66 (tdd, $J = 12.1, 9.2, 7.2$ Hz, 1H), 1.55 (s, 3H). ^{13}C NMR (126 MHz, CDCl_3) δ 164.0, 162.5, 149.8, 137.7, 136.7, 134.6, 128.9, 128.1, 124.7, 107.2, 75.2, 67.9, 52.8, 51.1, 36.0, 34.7, 34.1, 24.4, 16.9. MS (ESI) calcd for $[\text{C}_{19}\text{H}_{22}\text{N}_2\text{O}_4\text{H}]^+$: 343.1658, found: 343.1656.

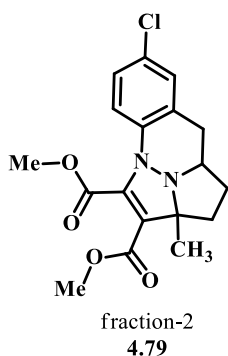
Dimethyl 7-chloro-2a-methyl-3,4,4a,5-tetrahydro-2aH-2a¹,9b-diazapentaleno[1,6-



***ab*]naphthalene-1,2-dicarboxylate (4.79, fraction-1):** $R_f = 0.45$ in Hexane/EtOAc = 3:1. Yield 60% (39 mg). ^1H NMR (500 MHz, CDCl_3) δ 7.15 (d, $J = 2.3$ Hz, 1H), 7.08 (dd, $J = 8.7, 2.4$ Hz, 1H), 6.90 (d, $J = 8.7$ Hz, 1H), 3.86 (s, 3H), 3.73 (s, 3H), 3.07 – 2.99 (m, 1H), 2.95 – 2.88 (m, 2H), 2.49 (ddd, $J = 13.4, 11.4, 8.4$ Hz, 1H), 2.11 (dd, $J = 13.5, 8.3$ Hz, 1H), 1.97 (ddd, $J = 12.3, 8.2, 4.5$ Hz, 1H), 1.62 – 1.50 (m, 1H), 1.42 (s, 3H). ^{13}C NMR (126 MHz, CDCl_3) δ 164.5, 162.8, 145.1, 136.9, 130.0, 129.7, 129.5, 126.9, 120.3, 111.2, 71.1, 62.1, 53.3, 51.5, 37.5, 33.9, 27.6, 26.0. MS (ESI) calcd for $[\text{C}_{18}\text{H}_{19}\text{ClN}_2\text{O}_4\text{H}]^+$: 363.1112, found: 363.1105.

Dimethyl 7-chloro-2a-methyl-3,4,4a,5-tetrahydro-2aH-2a¹,9b-diazapentaleno[1,6-

***ab*]naphthalene-1,2-dicarboxylate (4.79, fraction-2):** $R_f = 0.27$ in Hexane/EtOAc = 3:1. Yield 37% (24 mg). ^1H NMR (500 MHz, CDCl_3) δ 7.15 (s, 1H), 7.10 (ddd, $J = 8.5, 2.3,$

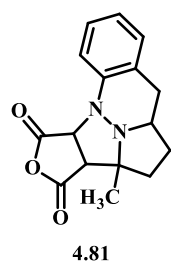


0.7 Hz, 1H), 6.98 (d, $J = 8.5$ Hz, 1H), 3.84 (s, 3H), 3.75 – 3.68 (m, 4H), 3.16 (dd, $J = 16.4, 7.7$ Hz, 1H), 2.68 (dd, $J = 16.3, 6.3$ Hz, 1H), 2.47 (ddd, $J = 13.0, 7.1, 2.4$ Hz, 1H), 2.18 – 2.09 (m, 1H), 1.91 (ddd, $J = 13.0, 11.2, 6.5$ Hz, 1H), 1.71 (dtd, $J = 18.3, 11.0, 7.2$ Hz, 1H), 1.59 (s, 3H). ^{13}C NMR (126 MHz, CDCl_3) δ 164.2, 162.5, 143.8, 136.0, 131.6, 131.0, 128.3, 126.9, 120.6, 10.3, 76.1, 65.0, 53.3, 51.1,

39.4, 32.8, 30.6, 27.0. MS (ESI) calcd for $[\text{C}_{18}\text{H}_{19}\text{ClN}_2\text{O}_4\text{H}]^+$: 363.1112, found:

363.1106.

3b-methyl-3b,4,5,5a,6,10c-hexahydro-1H-2-oxa-3b¹,10b-

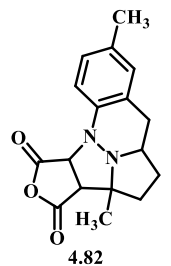


diazacyclopenta[2,3]pentaleno[1,6-*ab*]naphthalene-1,3(3*aH*)-dione

(4.81): Yield 99% (50 mg). ^1H NMR (500 MHz, CDCl_3) δ 7.62 (dd, $J = 8.1, 0.8$ Hz, 1H), 7.27 – 7.22 (m, 1H), 7.10 (d, $J = 7.6$ Hz, 1H), 7.03 (td, $J = 7.5, 1.1$ Hz, 1H), 4.68 (d, $J = 10.0$ Hz, 1H), 3.79 (d, $J = 10.0$ Hz, 1H),

2.92 (dd, $J = 15.4, 3.2$ Hz, 1H), 2.81 (dd, $J = 15.3, 10.8$ Hz, 1H), 2.57 (tdd, $J = 11.0, 5.5, 3.3$ Hz, 1H), 2.38 (dt, $J = 13.8, 9.3$ Hz, 1H), 2.27 – 2.19 (m, 1H), 2.11 – 2.03 (m, 1H), 1.76 – 1.65 (m, 1H), 1.47 (s, 3H). ^{13}C NMR (126 MHz, CDCl_3) δ 170.2, 168.5, 145.2, 129.4, 127.3, 125.0, 123.5, 121.4, 71.7, 70.9, 57.4, 56.0, 35.7, 34.7, 28.3, 22.5. MS (ESI) calcd for $[\text{C}_{16}\text{H}_{16}\text{N}_2\text{O}_3\text{H}]^+$: 285.1239, found: 285.1226.

3b,8-dimethyl-3b,4,5,5a,6,10c-hexahydro-1H-2-oxa-3b¹,10b-

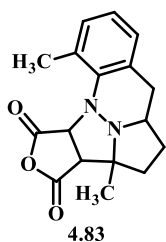


diazacyclopenta[2,3]pentaleno[1,6-*ab*]naphthalene-1,3(3*aH*)-dione

(4.82): Yield 99% (53 mg). ^1H NMR (500 MHz, DMSO) δ 7.31 (d, $J = 8.2$ Hz, 1H), 7.02 (d, $J = 8.2$ Hz, 1H), 6.93 (s, 1H), 4.76 (d, $J = 9.7$ Hz, 1H), 4.14 (d, $J = 9.8$ Hz, 1H), 2.82 (d, $J = 12.7$ Hz, 1H), 2.62 (ddt, $J = 31.1,$

25.3, 6.7 Hz, 2H), 2.34 (dt, $J = 13.3, 9.2$ Hz, 1H), 2.23 (s, 3H), 2.13 (ddd, $J = 10.5, 9.3, 5.6$ Hz, 1H), 1.87 (dd, $J = 12.2, 10.3$ Hz, 1H), 1.51 (dt, $J = 21.2, 10.6$ Hz, 1H), 1.25 (s, 3H). ^{13}C NMR (126 MHz, DMSO) δ 172.0, 169.9, 143.5, 131.4, 129.7, 127.4, 125.1, 120.2, 71.9, 70.3, 57.3, 54.8, 34.8, 34.1, 27.9, 22.3, 20.2. MS (ESI) calcd for $[\text{C}_{17}\text{H}_{18}\text{N}_2\text{O}_3\text{H}]^+$: 299.1396, found: 299.1397.

3b,10-dimethyl-3b,4,5,5a,6,10c-hexahydro-1H-2-oxa-3b¹,10b-



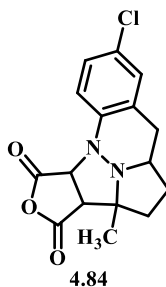
diazacyclopenta[2,3]pentaleno[1,6-*ab*]naphthalene-1,3(3aH)-dione

(4.83): Yield 53% (28 mg). ^1H NMR (500 MHz, CDCl_3) δ = 7.10 – 7.05 (m, 1H), 7.03 – 6.92 (m, 2H), 5.04 (d, $J=9.0$, 1H), 3.56 (d, $J=9.0$, 1H), 2.94 (dd, $J=15.6, 3.5$, 1H), 2.75 (dt, $J=14.7, 9.3$, 2H), 2.48 (tdd, $J=10.9,$

5.5, 3.6, 1H), 2.37 (s, 3H), 2.14 – 2.06 (m, 1H), 1.97 (ddd, $J=14.3, 10.6, 1.8$, 1H), 1.67 – 1.56 (m, 1H), 1.54 (s, 3H). ^{13}C NMR (126 MHz, CDCl_3) δ 170.6, 168.1, 139.5, 130.1, 128.8, 127.5, 126.1, 124.0, 72.0, 63.7, 57.3, 56.6, 35.0, 29.8, 29.6, 28.3, 19.1. MS (ESI) calcd for $[\text{C}_{17}\text{H}_{18}\text{N}_2\text{O}_3\text{H}]^+$: 299.1396, found: 299.1403.

8-chloro-3b-methyl-3b,4,5,5a,6,10c-hexahydro-1H-2-oxa-3b¹,10b-

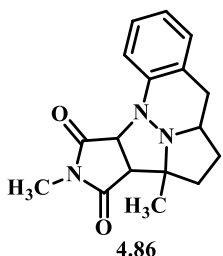
diazacyclopenta[2,3]pentaleno[1,6-*ab*]naphthalene-1,3(3aH)-dione (4.84): Yield 99%



(56 mg). ^1H NMR (500 MHz, DMSO) δ 7.41 (d, $J = 8.7$ Hz, 1H), 7.29 (dd, $J = 8.7, 2.4$ Hz, 1H), 7.22 (d, $J = 2.4$ Hz, 1H), 4.86 (d, $J = 9.8$ Hz, 1H), 4.17 (d, $J = 9.8$ Hz, 1H), 2.95 – 2.85 (m, 1H), 2.67 – 2.57 (m, 2H), 2.36 (dt, $J = 13.2, 9.3$ Hz, 1H), 2.19 – 2.09 (m, 1H), 1.89 (dd, $J = 12.3,$

10.5 Hz, 1H), 1.57 – 1.45 (m, 1H), 1.25 (s, 3H). ^{13}C NMR (126 MHz, DMSO) δ 171.9, 169.6, 144.7, 128.9, 127.6, 126.7, 126.4, 121.7, 71.8, 70.3, 57.3, 54.6, 34.9, 34.0, 27.9, 22.3. MS (ESI) calcd for $[\text{C}_{16}\text{H}_{15}\text{ClN}_2\text{O}_3\text{H}]^+$: 319.0849, found: 319.0859.

2,3b-dimethyl-3b,4,5,5a,6,10c-hexahydro-2,3b¹,10b-



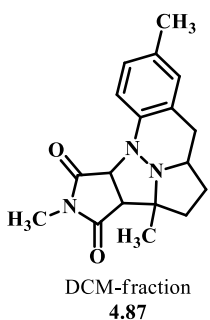
triazacyclopenta[2,3]pentaleno[1,6-*ab*]naphthalene-1,3(2*H*,3*aH*)-

dione (4.86): $R_f = 0.59$ in Hexane/EtOAc = 1:1. Yield 80% (43 mg).

Mixture of two diastereoisomers. ^1H NMR (500 MHz, CDCl_3) δ 7.81 (dd, $J = 8.2, 0.9$ Hz, 1H), 7.27 – 7.15 (m, 3H), 7.08 (t, $J = 6.6$ Hz,

2H), 7.01 – 6.88 (m, 2H), 4.90 (d, $J = 8.2$ Hz, 1H), 4.45 (d, $J = 9.4$ Hz, 1H), 3.60 (d, $J = 9.4$ Hz, 1H), 3.34 (d, $J = 8.2$ Hz, 1H), 3.05 (s, 3H), 2.90 (dd, $J = 15.2, 3.2$ Hz, 1H), 2.84 – 2.76 (m, 5H), 2.75 – 2.64 (m, 2H), 2.64 – 2.56 (m, 1H), 2.42 – 2.31 (m, 2H), 2.24 – 2.16 (m, 1H), 2.06 – 1.97 (m, 2H), 1.91 (ddd, $J = 14.1, 9.7, 1.1$ Hz, 1H), 1.72 – 1.62 (m, 1H), 1.61 – 1.50 (m, 4H), 1.33 (s, 3H). ^{13}C NMR (126 MHz, CDCl_3) δ 176.4, 175.6, 174.9, 174.9, 146.1, 142.0, 129.9, 129.4, 127.2, 126.0, 125.3, 125.1, 122.9, 122.5, 122.0, 72.9, 70.5, 70.4, 70.2, 66.6, 57.6, 57.2, 56.6, 55.7, 36.3, 35.3, 35.1, 31.1, 30.8, 28.9, 28.6, 25.1, 24.9, 22.1. MS (ESI) calcd for $[\text{C}_{17}\text{H}_{19}\text{N}_3\text{O}_2\text{H}]^+$: 298.1556, found: 298.1549.

2,3b,8-trimethyl-3b,4,5,5a,6,10c-hexahydro-2,3b¹,10b-



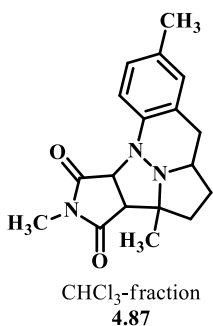
triazacyclopenta[2,3]pentaleno[1,6-*ab*]naphthalene-1,3(2*H*,3*aH*)-

dione (4.87, DCM- fraction): Yield 38% (21 mg). ^1H NMR (500 MHz,

CD_2Cl_2) δ 7.62 (d, $J = 8.2$ Hz, 1H), 7.02 (d, $J = 8.2$ Hz, 1H), 6.91 (s, 1H), 4.37 (d, $J = 9.4$ Hz, 1H), 3.60 (d, $J = 9.4$ Hz, 1H), 2.99 (s, 3H), 2.84 (d, $J = 12.3$ Hz, 1H), 2.78 – 2.56 (m, 2H), 2.34 (dt, $J = 13.4, 9.3$

Hz, 1H), 2.27 (s, 3H), 2.19 (dd, $J = 15.3, 6.8$ Hz, 1H), 1.99 (t, $J = 11.9$ Hz, 1H), 1.69 – 1.56 (m, 1H), 1.27 (s, 3H). ^{13}C NMR (126 MHz, CD_2Cl_2) δ 176.1, 175.1, 144.3, 132.5, 130.1, 128.0, 125.6, 121.8, 71.0, 70.4, 57.5, 55.9, 36.5, 35.3, 28.8, 24.9, 22.1, 20.7. MS (ESI) calcd for $[\text{C}_{18}\text{H}_{21}\text{N}_3\text{O}_2\text{H}]^+$: 312.1712, found: 312.1711.

2,3b,8-trimethyl-3b,4,5,5a,6,10c-hexahydro-2,3b¹,10b-



triazacyclopenta[2,3]pentaleno[1,6-*ab*]naphthalene-1,3(2*H*,3*aH*)-

dione (4.87, CHCl₃- fraction): *R*_f = 0.66 in Hexane/EtOAc = 1:1. Yield

34% (19 mg). ¹H NMR (500 MHz, CDCl₃) δ 7.12 (d, *J* = 8.2 Hz, 1H),

7.00 (dd, *J* = 8.3, 1.6 Hz, 1H), 6.88 (s, 1H), 4.86 (d, *J* = 8.2 Hz, 1H),

3.32 (d, *J* = 8.2 Hz, 1H), 2.82 (s, 3H), 2.77 (dd, *J* = 15.4, 3.4 Hz, 1H),

2.70 – 2.54 (m, 2H), 2.38 – 2.28 (m, 1H), 2.27 (s, *J* = 8.0 Hz, 3H), 2.05 – 1.94 (m, 1H),

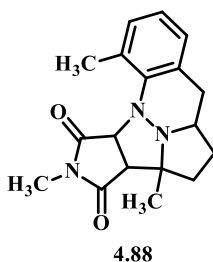
1.90 (ddd, *J* = 14.1, 9.7, 1.2 Hz, 1H), 1.61 – 1.53 (m, 1H), 1.52 (s, 3H). ¹³C NMR (126

MHz, CDCl₃) δ 176.6, 175.1, 139.5, 131.8, 130.2, 127.0, 125.0, 121.8, 70.5, 66.7, 57.7,

56.7, 35.2, 31.1, 30.8, 28.9, 25.1, 21.0. MS (ESI) calcd for [C₁₈H₂₁N₃O₂H]⁺: 312.1712,

found: 312.1702.

2,3b,10-trimethyl-3b,4,5,5a,6,10c-hexahydro-2,3b¹,10b-



triazacyclopenta[2,3]pentaleno[1,6-*ab*]naphthalene-1,3(2*H*,3*aH*)-

dione (4.88): *R*_f = 0.26 in Hexane/EtOAc = 3:1. Yield 78% (43 mg).

¹H NMR (500 MHz, CDCl₃) δ = 7.09 – 7.01 (m, 1H), 6.99 – 6.85 (m,

2H), 4.88 (d, *J* = 8.4, 1H), 3.32 (d, *J* = 8.4, 1H), 2.87 (dd, *J* = 15.5, 3.5,

1H), 2.80 (s, 3H), 2.79 – 2.64 (m, 2H), 2.40 (s, 3H), 2.38 – 2.25 (m, 1H), 2.07 – 1.94 (m,

1H), 1.90 (ddd, *J* = 14.0, 10.3, 1.5, 1H), 1.62 – 1.49 (m, 4H). ¹³C NMR (126 MHz, CDCl₃)

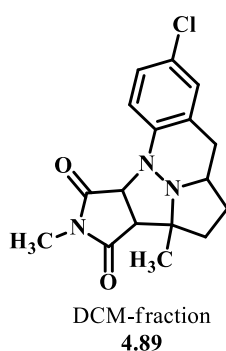
δ 176.8, 174.7, 140.5, 130.2, 128.4, 127.3, 125.8, 123.2, 69.9, 63.9, 57.1, 56.7, 35.4, 30.1,

29.8, 28.6, 25.1, 19.5. MS (ESI) calcd for [C₁₈H₂₁N₃O₂H]⁺: 312.1712, found: 312.1712.

8-chloro-2,3b-dimethyl-3b,4,5,5a,6,10c-hexahydro-2,3b¹,10b-

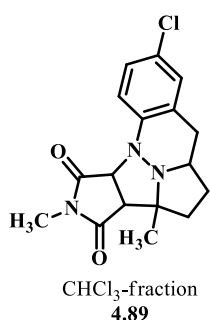
triazacyclopenta[2,3]pentaleno[1,6-*ab*]naphthalene-1,3(2*H*,3*aH*)-dione (4.89, DCM-

fraction): Yield 52% (31 mg). ¹H NMR (500 MHz, CD₂Cl₂) δ 7.73 (d, *J* = 8.8 Hz, 1H),



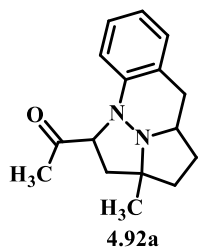
7.18 (d, $J = 8.7$ Hz, 1H), 7.09 (s, 1H), 4.41 (d, $J = 9.4$ Hz, 1H), 3.62 (d, $J = 9.4$ Hz, 1H), 3.00 (s, 3H), 2.90 – 2.81 (m, 1H), 2.78 – 2.69 (m, 1H), 2.68 – 2.59 (m, 1H), 2.36 (dt, $J = 13.3, 9.3$ Hz, 1H), 2.20 (t, $J = 13.0$ Hz, 1H), 2.00 (dd, $J = 21.5, 9.3$ Hz, 1H), 1.69 – 1.57 (m, 1H), 1.27 (s, 3H). ^{13}C NMR (126 MHz, CD_2Cl_2) δ 175.9, 174.8, 145.4, 129.3, 127.9, 127.7, 127.3, 123.2, 70.8, 70.5, 57.5, 55.6, 36.6, 35.3, 28.7, 25.0, 22.1. MS (ESI) calcd for $[\text{C}_{17}\text{H}_{18}\text{ClN}_3\text{O}_2\text{H}]^+$: 332.1166, found: 332.1167.

8-chloro-2,3b-dimethyl-3b,4,5,5a,6,10c-hexahydro-2,3b¹,10b-



triazacyclopenta[2,3]pentaleno[1,6-*ab*]naphthalene-1,3(2*H*,3*aH*)-dione (4.89, CHCl_3 -fraction): $R_f = 0.50$ in Hexane/EtOAc = 1:1. Yield 44% (26 mg). ^1H NMR (500 MHz, CDCl_3) δ 7.16 (s, 2H), 7.06 (s, 1H), 4.87 (d, $J = 8.2$ Hz, 1H), 3.34 (d, $J = 8.3$ Hz, 1H), 2.83 (s, 3H), 2.79 (dd, $J = 15.6, 3.3$ Hz, 1H), 2.73 – 2.57 (m, 2H), 2.34 – 2.26 (m, 1H), 2.06 – 1.97 (m, 1H), 1.92 (dd, $J = 14.2, 9.7$ Hz, 1H), 1.62 – 1.53 (m, 1H), 1.52 (s, 3H). ^{13}C NMR (126 MHz, CDCl_3) δ 176.2, 174.7, 140.7, 129.5, 127.5, 127.0, 126.3, 123.1, 70.5, 66.5, 57.6, 56.4, 35.2, 31.1, 30.8, 28.8, 25.2. MS (ESI) calcd for $[\text{C}_{17}\text{H}_{18}\text{ClN}_3\text{O}_2\text{H}]^+$: 332.1166, found: 332.1159.

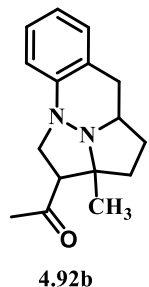
1-(2a-methyl-2,2a,3,4,4a,5-hexahydro-1*H*-2a¹,9b-diazapentaleno[1,6-*ab*]naphthalen-



1-yl)ethenone (4.92a): $R_f = 0.44$ in Hexane/EtOAc/ Et_3N = 70:30:1. Yield 55% (25 mg). ^1H NMR (500 MHz, CDCl_3) δ = 7.12 (t, $J = 7.7$ Hz, 1H), 7.05 (d, $J = 7.5$ Hz, 1H), 6.88 – 6.80 (m, 2H), 4.39 (dd, $J = 8.6, 7.1$ Hz, 1H), 3.45 (dt, $J = 18.8, 10.1$ Hz, 2H), 2.89 – 2.76 (m, 2H), 2.72 – 2.65 (m, 1H), 2.42 (dt, $J = 13.2, 9.3$ Hz, 1H), 2.25 (s, 3H), 2.22 (ddd, $J = 12.7, 5.9, 3.2$

Hz, 1H), 2.07 – 2.01 (m, 1H), 1.77 – 1.67 (m, 1H), 1.25 (s, 3H). ¹³C NMR (126 MHz, CDCl₃) δ = 205.1, 147.2, 129.6, 126.6, 123.74, 120.4, 119.2, 70.15, 61.3, 55.4, 54.7, 36.0, 35.2, 30.6, 29.0, 23.2. MS (ESI) calcd for [C₁₆H₂₀N₂OH]⁺: 257.1654, found: 257.1651.

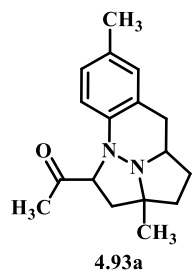
1-(2a-methyl-2,2a,3,4,4a,5-hexahydro-1*H*-2a¹,9b-diazapentaleno[1,6-*ab*]naphthalen-



2-yl)ethenone (4.92b): R_f = 0.44 in Hexane/EtOAc/Et₃N = 70:30:1. Yield 43% (20 mg). ¹H NMR (500 MHz, CDCl₃) δ = 7.12 – 7.03 (m, 2H), 6.95 (d, *J*=7.8, 1H), 6.91 – 6.86 (m, 1H), 3.70 (dt, *J*=17.8, 9.9, 2H), 3.41 (dd, *J*=10.4, 8.0, 1H), 2.90 (ddd, *J*=11.3, 8.9, 4.5, 1H), 2.80 – 2.74 (m, 2H), 2.22 (s, 3H), 1.98 (ddd, *J*=12.9, 7.5, 4.1, 1H), 1.82 – 1.75 (m, 2H), 1.63 (s, 3H), 1.61 – 1.50 (m, 1H).

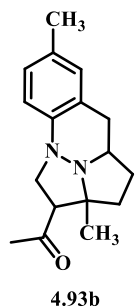
¹³C NMR (126 MHz, CDCl₃) δ 206.7, 146.6, 129.7, 126.1, 125.9, 121.5, 121.0, 68.8, 64.8, 55.0, 52.0, 34.8, 34.0, 31.8, 31.3, 28.3. MS (ESI) calcd for [C₁₆H₂₀N₂OH]⁺: 257.1654, found: 257.1656.

1-(2a,7-dimethyl-2,2a,3,4,4a,5-hexahydro-1*H*-2a¹,9b-diazapentaleno[1,6-



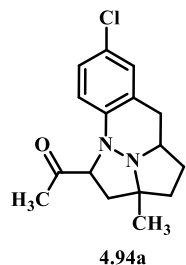
***ab*]naphthalen-1-yl)ethenone (4.93a):** R_f = 0.30 in Hexane/EtOAc/Et₃N = 80:20:1. Yield 52% (25 mg). ¹H NMR (500 MHz, CDCl₃) δ = 6.94 (d, *J*=8.0, 1H), 6.86 (s, 1H), 6.78 (d, *J*=8.1, 1H), 4.38 – 4.26 (m, 1H), 3.46 (dd, *J*=16.4, 6.6, 1H), 3.35 (t, *J*=9.9, 1H), 2.85 – 2.61 (m, 3H), 2.40 (dt, *J*=13.1, 9.3, 1H), 2.27 – 2.12 (m, 7H), 2.04 (dd, *J*=22.8, 11.3, 1H), 1.70 (dt, *J*=21.3, 10.5, 1H), 1.25 (s, 3H). ¹³C NMR (126 MHz, CDCl₃) δ = 205.3, 144.9, 129.95, 129.9, 127.4, 123.8, 119.4, 70.2, 61.5, 55.6, 54.4, 35.9, 35.1, 30.6, 28.9, 23.2, 20.6. MS (ESI) calcd for [C₁₇H₂₂N₂OH]⁺: 271.1810, found: 271.1801.

1-(2a,7-dimethyl-2,2a,3,4,4a,5-hexahydro-1*H*-2a¹,9b-diazapentaleno[1,6-



ab]naphthalen-2-yl)ethenone (4.93b): $R_f = 0.31$ in Hexane/EtOAc/Et₃N = 80:20:1. Yield 31% (15 mg). ¹H NMR (500 MHz, CDCl₃) δ = 6.93 – 6.86 (m, 2H), 6.84 (d, J = 8.1 Hz, 1H), 3.64 (dt, J = 17.8, 9.9 Hz, 2H), 3.38 (dd, J = 10.4, 8.0 Hz, 1H), 2.94 – 2.86 (m, 1H), 2.72 (d, J = 6.3 Hz, 2H), 2.25 (s, 3H), 2.20 (s, 3H), 1.96 (ddd, J = 12.5, 6.1, 1.9 Hz, 1H), 1.80 – 1.74 (m, 2H), 1.61 (s, 3H), 1.58 – 1.48 (m, 1H). ¹³C NMR (126 MHz, CDCl₃) δ = 207.2, 144.4, 131.2, 130.3, 127.1, 126.3, 121.2, 69.1, 65.3, 55.4, 52.2, 34.9, 34.3, 32.1, 31.7, 28.6, 20.8. MS (ESI) calcd for [C₁₇H₂₂N₂OH]⁺: 271.1810, found: 271.1811.

1-(7-chloro-2a-methyl-2,2a,3,4,4a,5-hexahydro-1*H*-2a¹,9b-diazapentaleno[1,6-

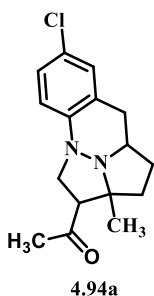


ab]naphthalen-1-yl)ethenone (4.94a): $R_f = 0.38$ in Hexane/EtOAc/Et₃N = 80:20:1. Yield 29% (15 mg). ¹H NMR (500 MHz, CDCl₃) δ = 7.08 (dd, J = 8.6, 2.3 Hz, 1H), 7.02 (d, J = 2.2 Hz, 1H), 6.77 (d, J = 8.6 Hz, 1H), 4.36 (dd, J = 9.5, 8.1 Hz, 1H), 3.46 (dd, J = 10.0, 8.2 Hz, 1H), 3.37 (t, J = 9.9 Hz, 1H), 2.79 (ddd, J = 25.3, 15.2, 6.8 Hz, 1H), 2.69 – 2.59 (m, 1H), 2.42 (dt, J = 13.2, 9.3 Hz, 1H), 2.28 – 2.18 (m, 4H), 2.09 – 2.00 (m, 1H), 1.75 – 1.65 (m, 1H), 1.25 (d, J = 7.8 Hz, 4H). ¹³C NMR (126 MHz, CDCl₃) δ = 204.8, 145.8, 129.1, 126.7, 125.5, 125.3, 120.2, 70.2, 61.2, 55.7, 54.4, 35.9, 35.1, 30.6, 28.90, 23.1. MS (ESI) calcd for [C₁₆H₁₉ClN₂OH]⁺: 291.1264, found: 291.1259.

1-(7-chloro-2a-methyl-2,2a,3,4,4a,5-hexahydro-1*H*-2a¹,9b-diazapentaleno[1,6-

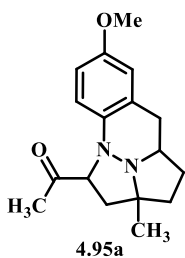
ab]naphthalen-2-yl)ethenone (4.94b): $R_f = 0.32$ in Hexane/EtOAc/Et₃N = 80:20:1.

Yield 48% (25 mg). ¹H NMR (500 MHz, CDCl₃) δ = 7.06 (dd, J = 4.2, 1.9 Hz, 2H), 6.88 – 6.85 (m, 1H), 3.71 – 3.62 (m, 2H), 3.40 (dd, J = 10.3, 8.1 Hz, 1H), 2.86 (ddd, J = 11.3,



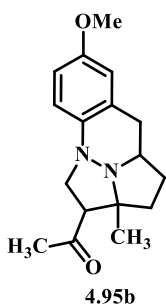
9.5, 4.8 Hz, 1H), 2.77 – 2.73 (m, 2H), 2.22 (s, 3H), 2.03 – 1.95 (m, 1H), 1.84 – 1.74 (m, 2H), 1.62 (s, 3H), 1.30 – 1.24 (m, 1H). ^{13}C NMR (126 MHz, CDCl_3) δ = 206.9, 145.5, 129.5, 128.2, 126.4, 122.4, 113.0, 69.2, 65.1, 55.3, 52.0, 34.9, 34.2, 32.0, 31.6, 28.4. MS (ESI) calcd for $[\text{C}_{16}\text{H}_{19}\text{ClN}_2\text{OH}]^+$: 291.1264, found: 291.1262.

1-(7-methoxy-2a-methyl-2,2a,3,4,4a,5-hexahydro-1H-2a1,9b-diazapentaleno[1,6-



ab]naphthalen-1-yl)ethenone (4.95a): R_f = 0.47 in Hexane/EtOH/Et₃N = 70:30:1. Yield 39% (20 mg). ^1H NMR (500 MHz, CDCl_3) δ = 6.84 (d, J = 8.8 Hz, 1H), 6.76 – 6.71 (m, 1H), 6.63 – 6.59 (m, 1H), 4.30 (dd, J = 9.7, 7.4 Hz, 1H), 3.77 – 3.71 (m, 5H), 3.47 (dd, J = 10.3, 7.4 Hz, 1H), 3.30 (t, J = 10.0 Hz, 1H), 2.86 – 2.68 (m, 3H), 2.47 – 2.36 (m, 1H), 2.25 (s, 3H), 2.09 – 2.00 (m, 1H), 1.25 (s, 3H). ^{13}C NMR (126 MHz, CDCl_3) δ = 205.3, 154.1, 141.1, 125.3, 120.9, 114.2, 112.9, 70.3, 61.8, 55.6, 55.4, 53.7, 36.1, 35.3, 30.6, 28.8, 23.2. MS (ESI) calcd for $[\text{C}_{17}\text{H}_{22}\text{N}_2\text{O}_2\text{H}]^+$: 287.1760, found: 287.1751.

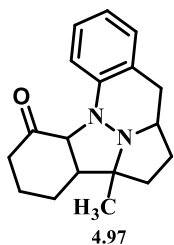
1-(7-methoxy-2a-methyl-2,2a,3,4,4a,5-hexahydro-1H-2a1,9b-diazapentaleno[1,6-



ab]naphthalen-2-yl)ethenone (4.95b): R_f = 0.39 in Hexane/EtOH/Et₃N = 70:30:1. Yield 49% (25 mg). ^1H NMR (500 MHz, CDCl_3) δ = 6.87 (d, J = 8.8 Hz, 1H), 6.69 (dd, J = 8.8, 2.8 Hz, 1H), 6.60 (d, J = 2.8 Hz, 1H), 3.73 (s, 3H), 3.60 (dt, J = 17.7, 9.9 Hz, 2H), 3.36 (dd, J = 10.4, 7.9 Hz, 1H), 2.96 – 2.88 (m, 1H), 2.73 (d, J = 6.4 Hz, 2H), 2.19 (s, 3H), 1.98 – 1.92 (m, 1H), 1.80 – 1.72 (m, 2H), 1.60 (s, 3H), 1.52 (qd, J = 11.2, 8.6 Hz, 1H). ^{13}C NMR (126 MHz, CDCl_3) δ = 207.3, 154.8, 140.2, 127.5, 122.4, 114.2, 112.9, 69.2, 65.3, 55.6, 55.5,

51.8, 35.1, 34.2, 32.1, 31.7, 28.5. MS (ESI) calcd for $[C_{17}H_{22}N_2O_2H]^+$: 287.1760, found: 287.1761

4b-methyl-2,3,4,4a,4b,5,6,6a,7,11c-decahydro-1H-4b¹,11b-



diazabenzocyclopenta[*lm*]fluoren-1-one (4.97): R_f = 0.45 in

Hexane/EtOAc/Et₃N = 80:20:1. Yield 50% (25 mg). ¹H NMR (500 MHz,

CDCl₃) δ = 7.11 (t, J = 7.6 Hz, 1H), 7.05 (dd, J = 16.4, 7.6 Hz, 2H), 6.90
– 6.84 (m, 1H), 3.85 (td, J = 10.7, 6.8 Hz, 1H), 3.17 (d, J = 10.6 Hz, 1H),

2.85 (dd, J = 15.1, 3.1 Hz, 1H), 2.76 (dd, J = 15.0, 10.7 Hz, 1H), 2.62 (tdd, J = 10.9, 5.4,

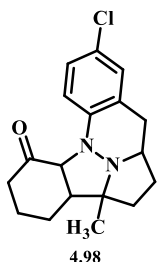
3.2 Hz, 1H), 2.54 – 2.44 (m, 3H), 2.29 – 2.19 (m, 1H), 2.17 – 1.92 (m, 3H), 1.86 – 1.78

(m, 1H), 1.71 – 1.57 (m, 2H), 1.36 (s, 3H). ¹³C NMR (126 MHz, CDCl₃) δ = 212.2, 146.9,

129.9, 126.5, 124.7, 121.2, 118.8, 71.4, 67.3, 59.4, 56.2, 41.3, 35.8, 35.4, 33.73, 28.5,

24.5, 20.9. MS (ESI) calcd for $[C_{18}H_{22}N_2OH]^+$: 283.1810, found: 283.1809.

9-chloro-4b-methyl-2,3,4,4a,4b,5,6,6a,7,11c-decahydro-1H-4b¹,11b-



diazabenzocyclopenta[*lm*]fluoren-1-one (4.98): R_f = 0.45 in

Hexane/EtOAc/Et₃N = 80:20:1. Yield 53% (30 mg). ¹H NMR (500 MHz,

CDCl₃) δ = 7.09 – 7.04 (m, 2H), 6.96 (d, J = 8.5 Hz, 1H), 3.82 (td, J =
10.7, 6.9 Hz, 1H), 3.18 (d, J = 10.7 Hz, 1H), 2.83 (dd, J = 15.2, 3.2 Hz,

1H), 2.78 – 2.70 (m, 1H), 2.64 – 2.41 (m, 4H), 2.25 (ddd, J = 17.6, 13.3, 5.8 Hz, 1H),

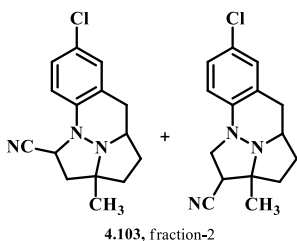
2.18 – 2.02 (m, 2H), 1.97 (tdd, J = 13.6, 10.9, 3.0 Hz, 1H), 1.87 – 1.80 (m, 1H), 1.72 –

1.58 (m, 2H), 1.35 (s, 3H). ¹³C NMR (126 MHz, CDCl₃) δ = 211.9, 145.5, 129.5, 126.6,

126.7, 126.2, 119.9, 71.5, 67.6, 59.4, 55.9, 41.2, 35.9, 35.3, 33.6, 28.4, 24.4, 20.8. MS

(ESI) calcd for $[C_{18}H_{21}ClN_2OH]^+$: 317.1421, found: 317.1417.

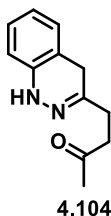
7-chloro-2a-methyl-2,2a,3,4,4a,5-hexahydro-1H-2a¹,9b-diazapentaleno[1,6-*ab*]naphthalene-1-carbonitrile or, **7-chloro-2a-methyl-2,2a,3,4,4a,5-hexahydro-1H-2a¹,9b-diazapentaleno[1,6-*ab*]naphthalene-2-carbonitrile (4.103, fraction-2):** $R_f =$



0.35 in Hexane/EtOAc = 3:1. Yield 4% (2 mg). ¹H NMR (500 MHz, CDCl₃) δ = 7.16 – 7.07 (m, 2H), 6.75 – 6.63 (m, 1H), 4.17 (dd, $J=9.3, 5.4$, 1H), 3.75 – 3.60 (m, 1H), 3.26 (dd, $J=17.1, 8.2$, 1H), 2.79 – 2.70 (m, 1H), 2.70 – 2.69 (m, 1H), 2.61 (ddd,

$J=22.1, 12.8, 7.4$, 2H), 2.21 – 2.12 (m, 1H), 2.11 – 1.95 (m, 2H), 1.83 (ddd, $J=12.8, 8.9, 7.3$, 1H), 1.28 (s, 3H). ¹³C NMR (126 MHz, CDCl₃) δ 142.8, 128.6, 126.5, 126.0, 125.7, 118.1, 113.2, 70.1, 60.2, 46.3, 44.1, 38.2, 31.4, 29.4, 26.3. MS (ESI) calcd for [C₁₅H₁₆ClN₃H]⁺: 274.1111, found: 2574.1102.

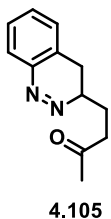
4-(1,4-dihydrocinnolin-3-yl)butan-2-one (4.104): $R_f = 0.47$ in Hexane/EtOAc = 1:1.



Yield 34% (12 mg). ¹H NMR (500 MHz, CDCl₃) δ = 7.22 (s, 1H), 7.11 (td, $J=7.9, 1.3$, 1H), 7.01 (d, $J=7.5$, 1H), 6.92 (td, $J=7.4, 1.1$, 1H), 6.67 (d, $J=7.9$, 1H), 3.27 (s, 2H), 2.76 (t, $J=7.0$, 2H), 2.58 (t, $J=7.1$, 2H), 2.19 (s, 3H). ¹³C NMR (126 MHz, CDCl₃) δ 207.9, 145.2, 140.1, 127.5, 127.0, 122.1, 116.1,

111.7, 77.1, 39.1, 30.1, 30.0. MS (ESI) calcd for [C₁₂H₁₄N₂OH]⁺: 203.1184, found: 203.1182.

4-(3,4-dihydrocinnolin-3-yl)butan-2-one (4.105): $R_f = 0.26$ in Hexane/EtOAc = 1:1.



Yield 17% (6 mg). ¹H NMR (500 MHz, CDCl₃) δ = 8.14 (d, $J=8.1$, 1H), 7.50 (td, $J=7.5, 1.2$, 1H), 7.42 (t, $J=7.8$, 1H), 7.26 (d, $J=8.9$, 1H), 3.83 (ddt, $J=14.1, 9.7, 4.3$, 1H), 2.92 – 2.79 (m, 3H), 2.78 – 2.64 (m, 1H), 2.20 – 2.10 (m, 4H), 2.01 (ddt, $J=14.0, 9.9, 6.4$, 1H). ¹³C NMR (126 MHz, CDCl₃) δ 208.1, 140.3, 132.7,

131.4, 128.2, 127.3, 122.3, 59.1, 39.2, 30.1, 27.9, 27.7. MS (ESI) calcd for
[C₁₂H₁₄N₂OH]⁺: 203.1184, found: 203.1172.

COMPREHENSIVE BIBLIOGRAPHY

- (1) Abraham, E. P. *Biochem. J.* **1956**, 62, 651.
- (2) Al-Bataineh, N. Q.; Brewer, M. *Tetrahedron Lett.* **2012**, 53, 5411.
- (3) Al-Bataineh, N.; Houk, K. N.; Brewer, M.; Hong, X. *J. Org. Chem.* **2017**, 82, 4001.
- (4) Alderson, J. M.; Phelps, A. M.; Scamp, R. J.; Dolan, N. S.; Schomaker, J. M. *J. Am. Chem. Soc.* **2014**, 136, 16720.
- (5) Al-Masoudi, N.; Hassan, N. A.; Al-Soud, Y. A.; Schmidt, P.; Gaafar, A. E-D. M.; Weng, M.; Marino, S.; Schoch, A.; Amer, A.; Jochims, J. *J. Chem. Soc., Perkin Trans. I* **1998**, 947.
- (6) Al-Soud, Y. A.; Al-Masoudi, N. A. *Heteroatom Chemistry* **2003**, 14, 298.
- (7) Al-Soud, Y. A.; Shrestha-Dawadi, P. B.; Winkler, M.; Wirschun, W.; Jochims, J. C. *J. Chem. Soc., Perkin Trans.* **1998**, 1, 3759.
- (8) Al-Soud, Y. A.; Wirschun, W.; Hassan, N. A.; Maier, G. M.; Jochims, J. C. *Synthesis* **1998**, 721
- (9) Al-Soud, Y. A.; Wirschun, W.; Hassan, N. A.; Maier, G. M.; Jochims, J. C. *Synthesis* **1998**, 721.
- (10) Arrieta, A.; Carrillo, J. R.; Cossío, F. P.; Díaz-Ortiz, A.; Gómez-Escalonilla, M. J.; de la Hoz, A.; Langa, F.; Moreno, A. *Tetrahedron* **1998**, 54, 13167.
- (11) Badiei, Y. M.; Dinescu, A.; Dai, X.; Palomino, R. M.; Heinemann, F. W.; Cundari, T. R.; Warren, T. H. *Angew. Chem. Int. Ed.* **2008**, 47, 9961.
- (12) Baumann, S. O.; Bendova, M.; Puchberger, M.; Schubert, U. *Eur. J. Inorg. Chem.* **2011**, 573.
- (13) Becke, A. D. *J. Chem. Phys.* **1993**, 98, 5648.
- (14) Belskaya, N.P.; Bakulev, V.A.; Fan, Z. *Chem. Heterocycl. Comp.* **2016**, 52, 627.
- (15) Bercovici, D. A.; Brewer, M. *J. Am. Chem. Soc.* **2012**, 134, 9890.
- (16) Bercovici, D. A.; Ogilvie, J. M.; Tsvetkov, N.; Brewer, M. *Angew. Chem., Int. Ed.* **2013**, 52, 13338.
- (17) Bergman, R. G. *Nature* **2007**, 446, 391.
- (18) Breslow, R.; Gellman, S. H. *J. Am. Chem. Soc.* **1983**, 105, 6728.

- (19) Brewer, M. *Tetrahedron Lett.* **2006**, 47, 7731.
- (20) Bur, S. K.; Padwa, A. *Chem. Rev.* **2004**, 104, 2401.
- (21) Butler, R. N. *Chem. Rev.* **1984**, 84, 249.
- (22) Davies, H. M. L.; Beckwith, R. E. J. *Chem. Rev.* **2003**, 103, 2861.
- (23) Davies, H. M. L.; Manning, J. *Nature* **2008**, 451, 417.
- (24) Davis, H. M. L. *Angew. Chem. Int. Ed.* **2006**, 45, 6422.
- (25) Dhakal, R. C.; Brewer, M. *Tetrahedron* **2016**, 72, 3718.
- (26) Dorn, H.; Otto, A. *Angew. Chem. Int. Ed.* **1968**, 7, 214.
- (27) El-Gazzar, A-R. B. A.; Scholten, K.; Guo, Y.; Weibenbach, K.; Hitzler, M.; Roth, G.; Fischer, H.; Jochims, J. C. *J. Chem. Soc., Perkin Trans. 1* **1999**, 1999.
- (28) Ellman, J. A. *Science* **2007**, 316, 1131.
- (29) Fiori, K. W.; Espino, C. G.; Brodsky, B. H.; Du Bois, J. *Tetrahedron* **2009**, 65, 3042.
- (30) Fleet, G. W.; Son, J. C.; Derome, A. E. *Tetrahedron*, **1988**, 44, 625.
- (31) Fountain, K. R.; White, R. D.; Patel K. D.; New, D. G.; Xu, Y.; Cassely A. J. *J. Org. Chem.* **1996**, 61, 9434.
- (32) Frank, E.; Kardos, Z.; Wölfling, J.; Schneider, G. *Synlet*, **2007**, 1311.
- (33) Frisch, M. J.; Trucks, G. W.; Schlegel, H. B.; Scuseria, G. E.; Robb, M. A.; Cheeseman, J. R.; Scalmani, G.; Barone, V.; Mennucci, B.; Petersson, G. A.; Nakatsuji, H.; Caricato, M.; Li, X.; Hratchian, H. P.; Izmaylov, A. F.; Bloino, J.; Zheng, G.; Sonnenberg, J. L.; Hada, M.; Ehara, M.; Toyota, K.; Fukuda, R.; Hasegawa, J.; Ishida, M.; Nakajima, T.; Honda, Y.; Kitao, O.; Nakai, H.; Vreven, T.; Montgomery, J. A., Jr.; Peralta, J. E.; Ogliaro, F.; Bearpark, M.; Heyd, J. J.; Brothers, E.; Kudin, K. N.; Staroverov, V. N.; Kobayashi, R.; Normand, J.; Raghavachari, K.; Rendell, A.; Burant, J. C.; Iyengar, S. S.; Tomasi, J.; Cossi, M.; Rega, N.; Millam, J. M.; Klene, M.; Knox, J. E.; Cross, J. B.; Bakken, V.; Adamo, C.; Jaramillo, J.; Gomperts, R.; Stratmann, R. E.; Yazyev, O.; Austin, A. J.; Cammi, R.; Pomelli, C.; Ochterski, J. W.; Martin, R. L.; Morokuma, K.; Zakrzewski, V. G.; Voth, G. A.; Salvador, P.; Dannenberg, J. J.; Dapprich, S.; Daniels, A. D.; Farkas, O.; Foresman, J. B.; Ortiz, J. V.; Cioslowski, J.; Fox, D. J. Gaussian 09, revision D.01; Gaussian, Inc.: Wallingford, CT, **2013**.
- (34) Gamba, D.; Pisoni, D. S.; da Costa, J. S.; Petzhhold, C. L.; Borges, A. C. A.; Ceschi, M. A. *J. Braz. Chem. Soc.* **2008**, 19, 1270.

- (35) Gaonkar, S. L.; Rai, K. M. L. *Tetrahedron Lett.* **2005**, *46*, 5969.
- (36) Ghose, A. K.; Viswanadhan, V. N.; Wendoloski, J. J. *J. Combi. Chem.* **1999**, *1*, 55.
- (37) Ghosh, A. K.; Schiltz, G.; Perali, R. S.; Leshchenko, S.; Kay, S.; Walters, D. E.; Koh, Y.; Maeda, K.; Mitsuya, H. *Bioorg. Med. Chem. Lett.* **2006**, *16*, 1869.
- (38) Godula, K.; Sames, D. *Science* **2006**, *312*, 67.
- (39) Gómez-Gallego, M.; Sierra, M. A. *Chem. Rev.* **2011**, *111*, 4857.
- (40) Grigg, R.; Kemp, J.; Thompson, N. *Tetrahedron Lett.* **1978**, *19*, 2827.
- (41) Gunic, E.; Tabakovic, I. *J. Org. Chem.* **1988**, *53*, 5081.
- (42) Guo, Y. P.; Wang, Q., R.; Jochims, J. C. *Synth.* **1996**, 274.
- (43) Hammerich, O.; Paker, V. D. *J. Chem. Soc., Perkin Trans. 1* **1997**, *2*, 1781.
- (44) Harvey, M. E.; Musaev, D. G.; Du Bois, J. *J. Am. Chem. Soc.* **2011**, *133*, 17207.
- (45) Hashimoto, T.; Kimura, H.; Kawamata, Y.; Maruoka, K. *Nat. Chem.* **2011**, *3*, 642.
- (46) Hashimoto, T.; Maeda, Y.; Omote, M.; Nakatsu, H.; Maruoka, K. *J. Am. Chem. Soc.* **2010**, *132*, 4076.
- (47) Hashimoto, T.; Omote, M.; Maruoka, K. *Angew. Chem. Int. Ed.* **2011**, *50*, 8952.
- (48) Hassan, N. A.; Mohamed, T. K.; Abdel Hafez, O. M.; Lutz, M.; Karl, C. C.; Wirschun, W.; Al-Soud, Y. A.; Jochims, J. *J. Prakt. Chem.* **1998**, *340*, 151.
- (49) Hegarty, A. F.; Kearney J. A. *J. Org. Chem.* **1975**, *40*, 3529.
- (50) Hehre, W. J.; Radom, L.; Schleyer, P. V. R.; Pople, J. A. *Ab Initio Molecular Orbital Theory*, Wiley: New York, 1986.
- (51) Hendrickson, J.; Hussoin, M. S. *J. Org. Chem.* **1987**, *52*, 4139.
- (52) Hinman, A.; Du Bois, J. *J. Am. Chem. Soc.* **2003**, *125*, 11510.
- (53) Hong, L.; Kai, M.; Wu, C.; Sun, W.; Zhu, G.; Li, G.; Yao, X.; Wang, R. *Chem. Commun.* **2013**, *49*, 6713.
- (54) Hong, X.; Bercovici, D.; Yang, Z.; Al-Bataineh, N.; Srinivasan, R.; Dhakal, R.; Houk, K. N.; Brewer, M. *J. Am. Chem. Soc.* **2015**, *137*, 9100.
- (55) Hong, X.; Liang, Y.; Brewer, M.; Houk, K. N. *Org. Lett.* **2014**, *16*, 4260.

- (56) Hu, X.-Q.; Chen, J.-R.; Gao, S.; Feng, B.; Lu, L.-Q.; Xiao, W.-J. *Chem. Commun.* **2013**, 49, 7905.
- (57) Huisgen, R.; Koch, H.-J, *Justus Liebigs Ann. Chem.* **1955**, 591, 200.
- (58) Hunt, A. D.; Dion, I.; das Neves, N.; Taing, S.; Beauchemin, A. M. *J. Org. Chem.* **2013**, 78, 8847.
- (59) Javed, M. I., Brewer, M. *Org Lett.* **2007**, 9, 1789.
- (60) Javed, M. I., Brewer, M. *Org. Lett.* **2007**, 9, 1789.
- (61) Javed, M. I.; Wyman, J. M.; Brewer, M. *Org. Lett.* **2009**, 11, 2189.
- (62) Jia, Q.; Chen, L.; Yang, G.; Wang, J.; Wei, J.; Du, Z. *Tetrahedron Lett.* **2015**, 56, 7150.
- (63) Jones, R. C. F.; Hollis, S. J.; Iley, J. N. *ARKIVOC*, **2007**, 152.
- (64) Jones, W. D. *Acc. Chem. Res.* **2003**, 36, 140.
- (65) King, S. M.; Herzon, S. *J. Org. Chem.* **2014**, 97, 8937.
- (66) Lee, C.; Yang, W.; Parr, R. G. *Phys. Rev. B* **1988**, 37, 785.
- (67) Lewgowd, W.; Stanczak, A. *Arch. Pharm.* **2007**, 340, 65.
- (68) Loewenthal, H. J. E. *Tetrahedron*, **1959**, 6, 269.
- (69) Lutz, K. E.; Thomson, R. J. *Angew. Chem. Int. Ed.* **2011**, 50, 4437.
- (70) MacCross, M.; Baillie, T. *Science* **2004**, 303, 1810.
- (71) Marenich, A. V.; Cramer, C. J.; Truhlar, D. G. *J. Phys. Chem. B* **2009**, 113, 6378.
- (72) Meng, W.; Zhao, H.-T.; Mie, J.; Zheng, Y.; Fu, A.; Ma, J.-A. *Chem. Sci.* **2012**, 3, 3053.
- (73) Mitsuya, H.; Yarchoan, R.; Broder, S. *Science*, **1990**, 249, 1553.
- (74) Moon, M. W. *J. Org. Chem.* **1972**, 37, 2005.
- (75) Moon, M. W. *J. Org. Chem.* **1972**, 37, 383.
- (76) Moon, M. W. *J. Org. Chem.* **1972**, 37, 386.
- (77) Mundal, D. A.; Lutz, K. E.; Thomson, R. J. *Org. Lett.* **2008**, 11, 465.

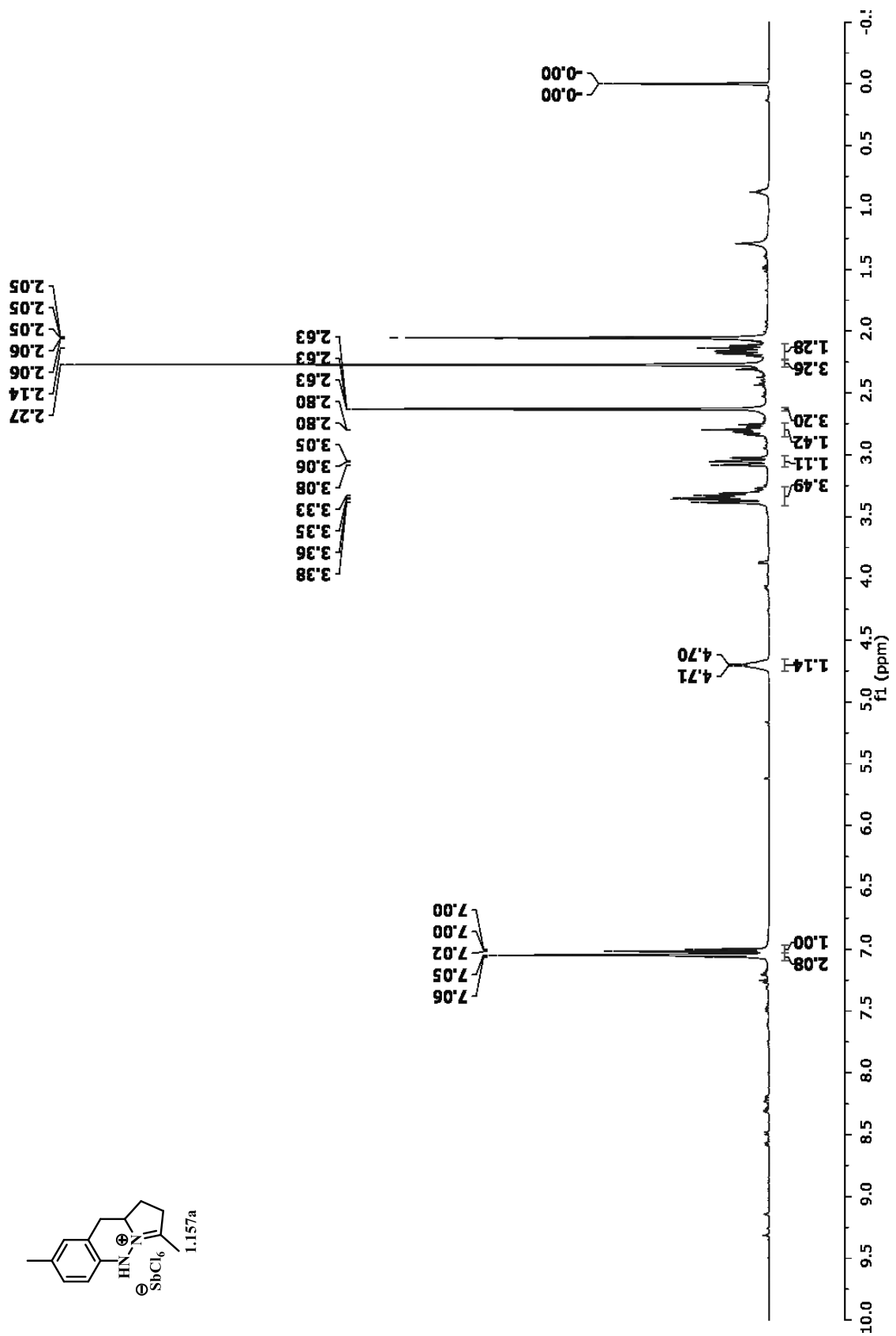
- (78) Na, R.; Jing, C.; Xu, Q.; Jiang, H.; Wu, X.; Shi, J.; Zhong, J.; Wang, M.; Benitez, D.; Tkatchouk, E.; Goddard, III, W. A.; Guo, H.; Kwon, O. *J. Am. Chem. Soc.* **2011**, *133*, 13337.
- (79) Nägeli, I.; Baud, C.; Bernardinelli, G.; Jacquier, Y.; Moran, M.; Muller, P. *Helv. Chim. Acta* **1997**, *80*, 1087.
- (80) Nájera, C.; Sansano, J. M.; Yus, M. *Org. Biomol. Chem.* **2015**, *13*, 8596.
- (81) Nikolov, A.; Danielsson, B. *Enzyme Microb. Technol.* **1994**, *16*, 1037.
- (82) Ochi, M.; Kawasaki, K.; Kataoka, H.; Uchio, Y.; Nishi, H. *Biochem. Biophys. Res. Commun.* **2001**, *283*, 1118.
- (83) Okimoto, M.; Chiba, T. *J. Org. Chem.* **1990**, *55*, 1070.
- (84) Omura, K.; Swern, D. *Tetrahedron* **1978**, *34*, 1651.
- (85) Omura, K.; Swern, D. *Tetrahedron* **1978**, *34*, 1651. Wang, Q. R.; Jochims, J. C.; Kohlbrandt, S.; Dahlenburg, L.; Altalib, M.; Hamed, A.; Ismail, A. E. H. *Synthesis* **1992**, 710.
- (86) Perreault, C.; Goudreau, S. R.; Zimmer, L. E.; Charette, A. B. *Org. Lett.* **2008**, *10*, 689.
- (87) Perronnet, J.; Girault, P.; Demoute, J. P. *J. Heterocycl. Chem.* **1980**, *17*, 727.
- (88) Pezdirc, L.; Jovanovski, V.; Bevk, D.; Jakše, R.; Pirc, S.; Meden, A.; Stanovnik, B.; Svete, J. *Tetrahedron*, **2005**, *61*, 3977.
- (89) Roullier, C.; Chollet-Krugler, M.; Weghe, P.; Devehat, F. L.; Boustie, J. *Bioorg. Med. Chem. Lett.* **2010**, *20*, 4582.
- (90) Sibi, M. P.; Rane, D.; Stanley, L. M.; Soeta, T. *Org. Lett.* **2008**, *10*, 2971.
- (91) Simmons, E. M.; Hartwig, J. F. *Angew. Chem. Int. Ed.* **2012**, *51*, 3066.
- (92) Smolinsky, G.; Feuer, B. I. *J. Am. Chem.* **1984**, *86*, 3085.
- (93) Soeta, T.; Tamura, K.; Ukaji, Y. *Org. Lett.* **2012**, *14*, 1226.
- (94) Sun, C. L.; Li, H.; Yu, D. G.; Yu, M.; Zhou, X.; Lu, X. Y.; Huang, K.; Zheng, S.; Li, B. J.; Shi, Z. *J. Nat. Chem.* **2010**, *2*, 1046.
- (95) Szychowski, J.; Truchon, J-F.; Bennani, Y. L. *J. Med. Chem.* **2014**, *57*, 9292.
- (96) Thi Tong, T. M.; Soeta, T.; Suga, T.; Kawamoto, K.; Hayashi, Y.; Ukaji, Y. *J. Org. Chem.* **2017**, *82*, 1969.

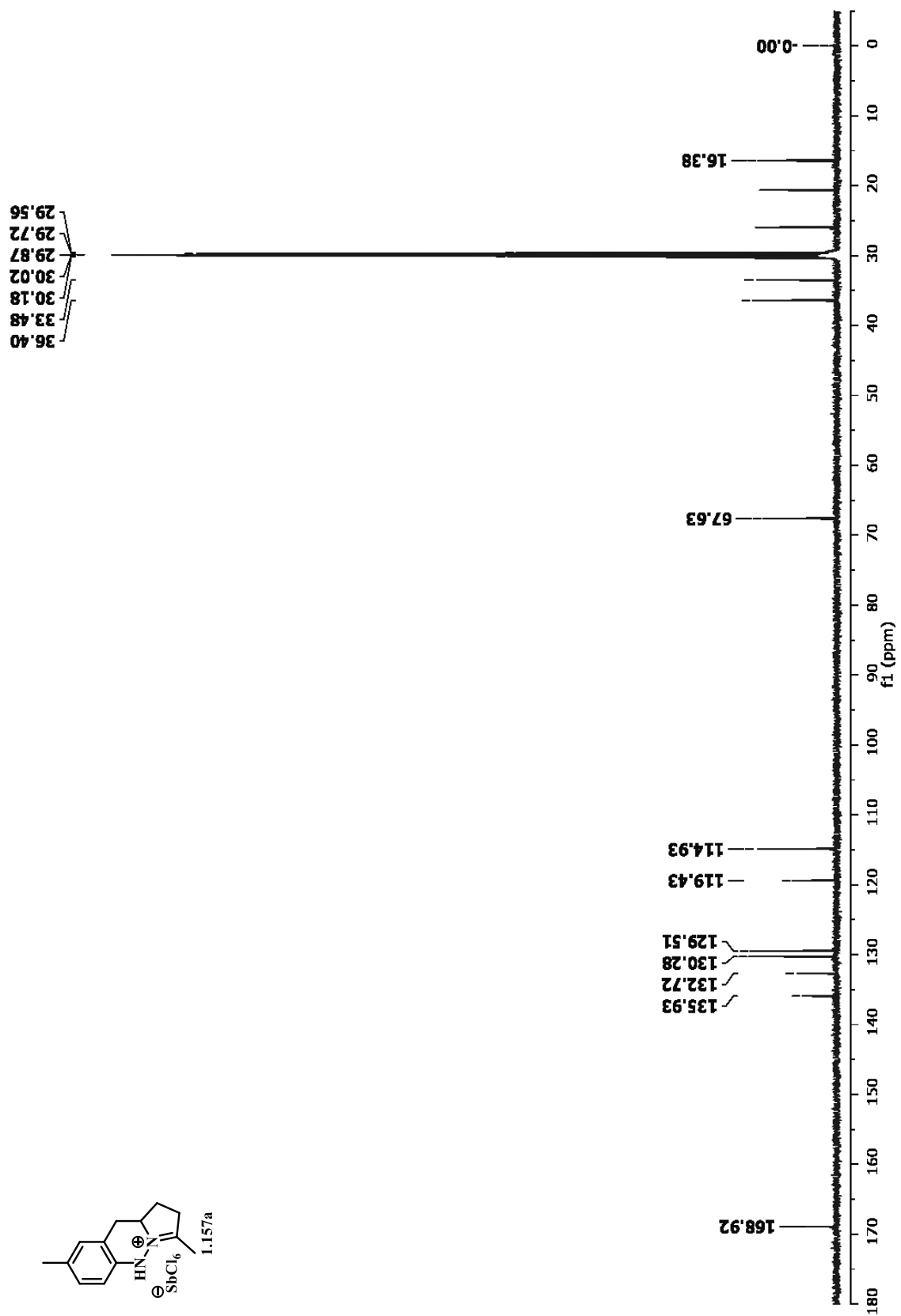
- (97) Tong, M.-C.; Chen, X.; Tao, H.-Y.; Wang, C.-J. *Angew. Chem. Int. Ed.* **2013**, *52*, 12377.
- (98) Turk, C.; Svete, J.; Stanovnik, B.; Golič, L.; Golič-Grdadolnik, S.; Golobič, A.; Selič, L.; *Helv. Chim. Acta* **2001**, *84*, 146.
- (99) Visnick, M.; Battiste, M. *J. Chem. Soc. Chem. Commun.* **1985**, 1621.
- (100) Wang, J-m.; Li, Z-m.; Wang, Q-R.; Tao, F-g. *J. Mol. Model* **2013**, *19*, 83.
- (101) Wang, Q. R.; Amer, A.; Mohr, S.; Ertel, E.; Jochims, J. C. *Tetrahedron* **1993**, *49*, 9973.
- (102) Wang, Q. R.; Amer, A.; Troll, C.; Fischer, H.; Jochims, J. C. *Chem. Ber.* **1993**, *126*, 2519.
- (103) Wang, Q. R.; Jochims, J. C.; Kohlbrandt, S.; Dahlenburg, L.; Altalib, M.; Hamed, A.; Ismail, A. E. H. *Synthesis* **1992**, 710.
- (104) Wang, Q. R.; Jochims, J. C.; Kohlbrandt, S.; Dahlenburg, L.; Altalib, M.; Hamed, A.; Ismail, A. E. H. *Synthesis* **1992**, 710.
- (105) Wang, Q.; Al-Talib, M.; Jochims, J. C. *Chem. Ber.* **1994**, *127*, 541.
- (106) Wang, Q.; Mohr, S.; Jochims, J. C. *Chem. Ber.* **1994**, *127*, 947.
- (107) Wang, X.; Wu, L.; Yang, P.; Song, X.-J.; Ren, H.-X; Peng, L.; Wang, L. *Org. Lett.* **2017**, *19*, 3051.
- (108) Wang, X-N.; Shao, P-L.; Lv, H.; Ye, S. *Org. Lett.* **2009**, *11*, 4029.
- (109) Warkentin, J. *Synthesis* **1970**, 279.
- (110) Wehn, P. M.; DuBois, J. *J. Am. Chem. Soc.* **2002**, *124*, 12950.
- (111) Wei, M-J.; Fang, D-C.; Liu, R-Z. *Eur. J. Org. Chem.* **2004**, 4070.
- (112) Winkler, J. *Chem. Rev.* **1996**, *96*, 167.
- (113) Winterton, S. E.; Ready, J. M. *Org. Lett.* **2016**, *18*, 2608.
- (114) Wirschun, W. G.; Al-Soud, Y. A.; Nusser, K. A.; Orama, O.; Mailer, G-M.; Jochims, J. *J. Chem. Soc., Perkin Trans. 1* **2000**, 4356.
- (115) Wirschun, W.; Jochims, J. *Synthesis* **1997**, 233.
- (116) Wyman, J. M.; Jochum, S.; Brewer, M. *Synth. Comm.* **2008**, *38*, 3623.

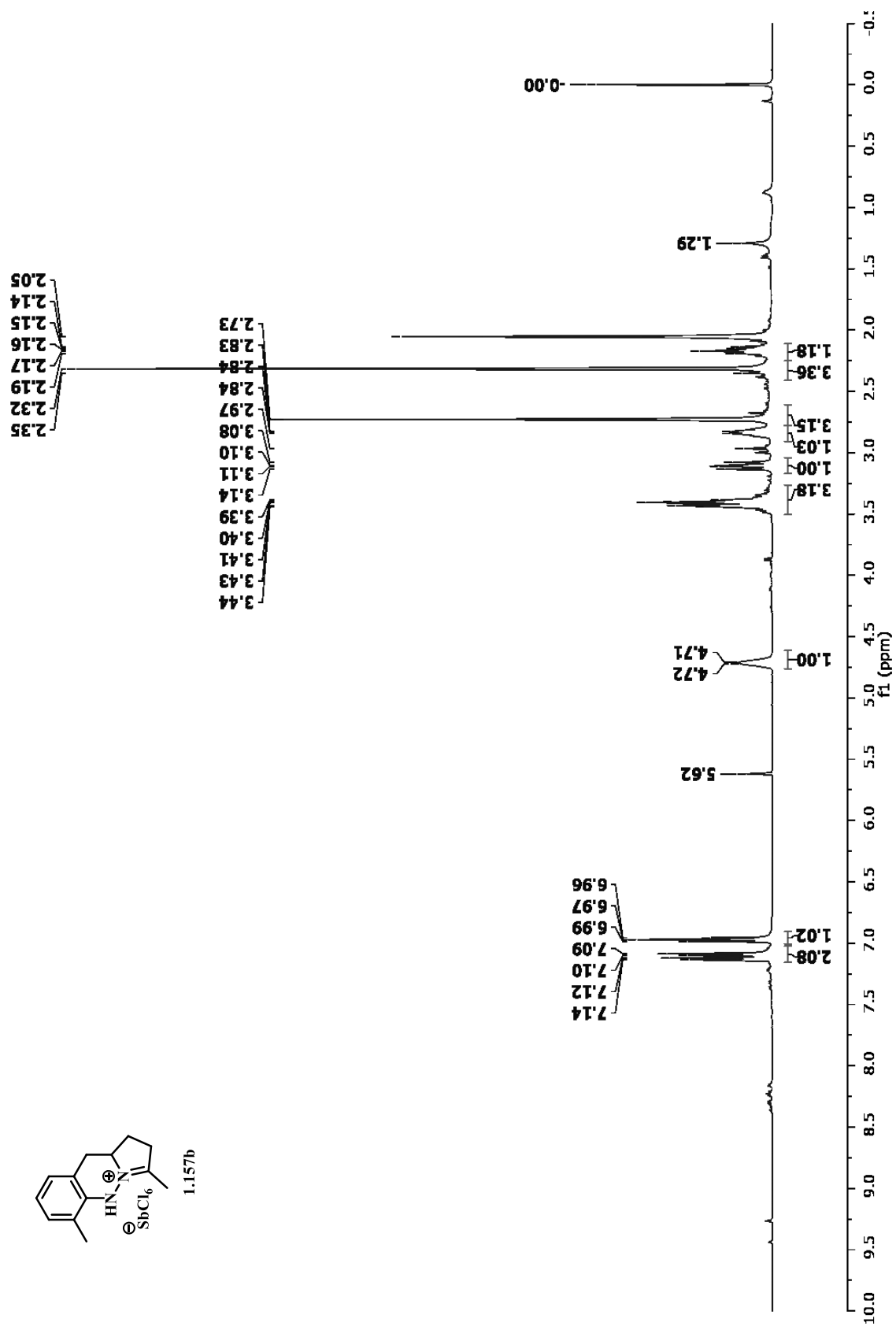
- (117) Wyman, J.; Javed, M. I.; Al-Bataineh, N.; Brewer, M. *J. Org. Chem.* **2010**, *75*, 8078.
- (118) Yuvaraj, P.; Reddy, B. S. R. *Tetrahedron Lett.* **2014**, *55*, 806.
- (119) Zhao, Y.; Truhlar, D. G. *Acc. Chem. Res.* **2008**, *41*, 157.
- (120) Zhao, Y.; Truhlar, D. *Theor. Chem. Acc.* **2008**, *120*, 215.
- (121) Zhou, Y.-Y.; Li, J.; Ling, L.; Liao, S.-H.; Sun, X.-L.; Li, Y.-X.; Wang, L.-J.; Tang, Y. *Angew. Chem. Int. Ed.* **2013**, *52*, 1452.
- (122) Zhu, G.; Sun, W.; Wu, C.; Li, G.; Hong, L.; Wang, R.; *Org. Lett.* **2013**, *15*, 4988.

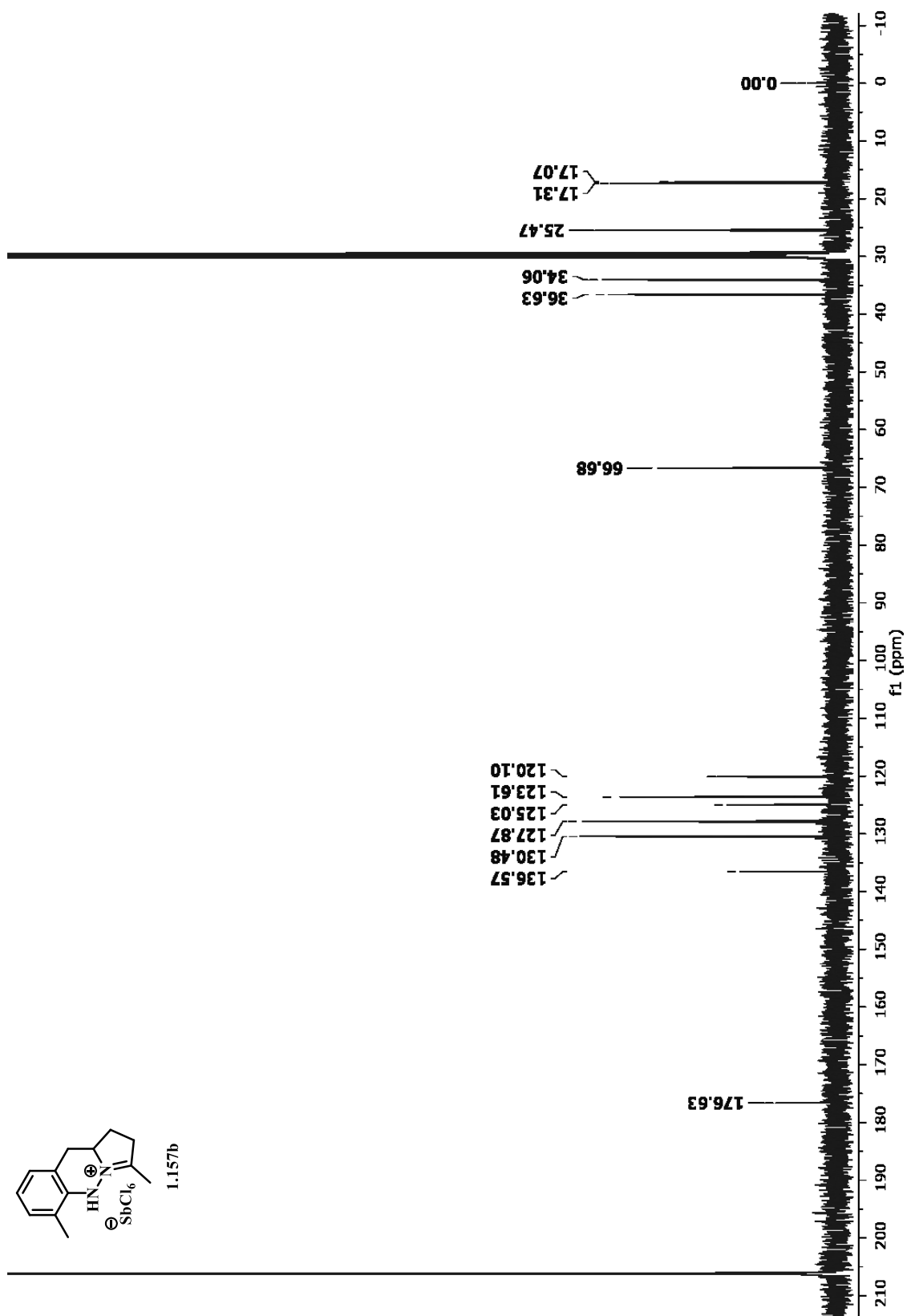
APPENDIX

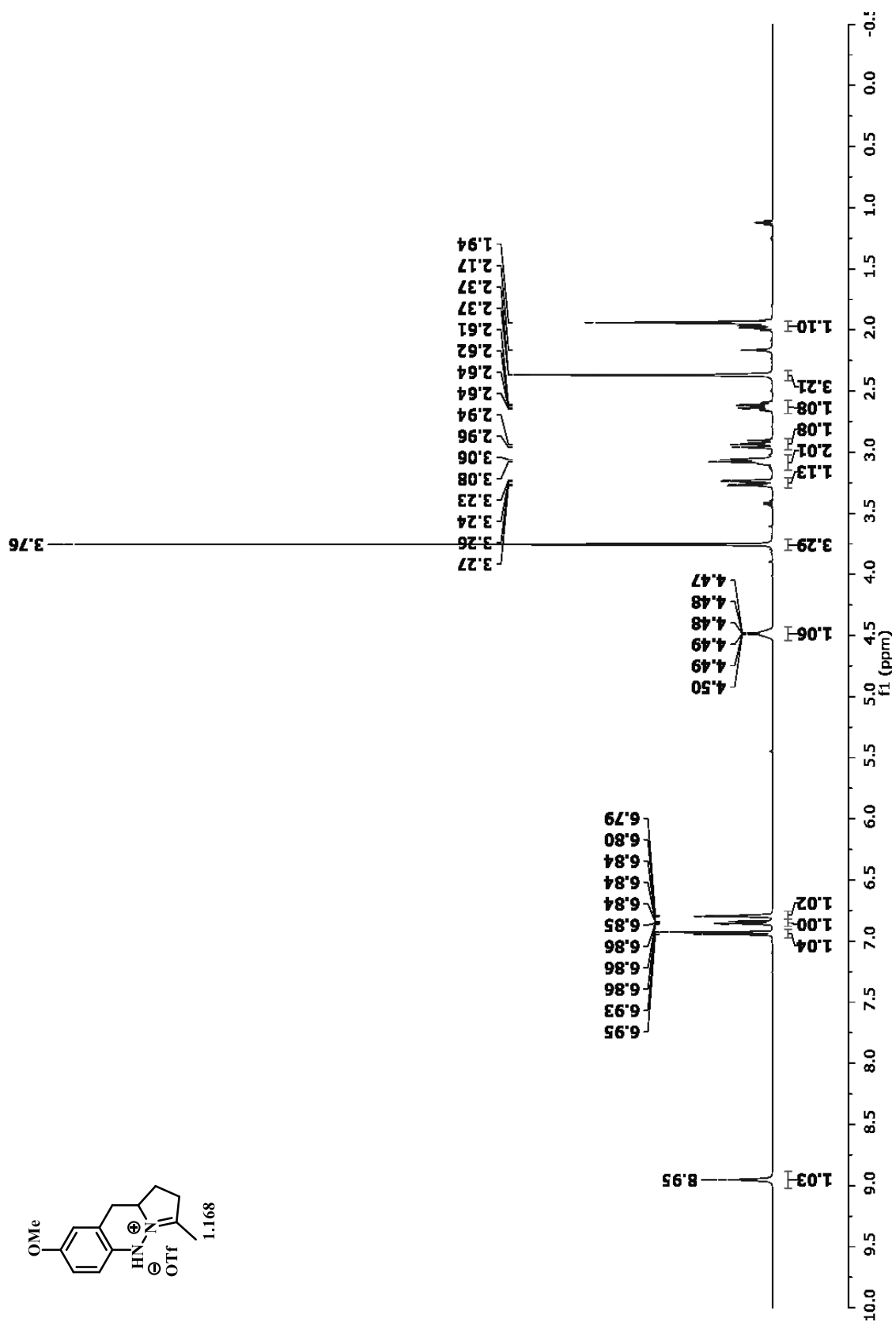
Spectroscopic Data

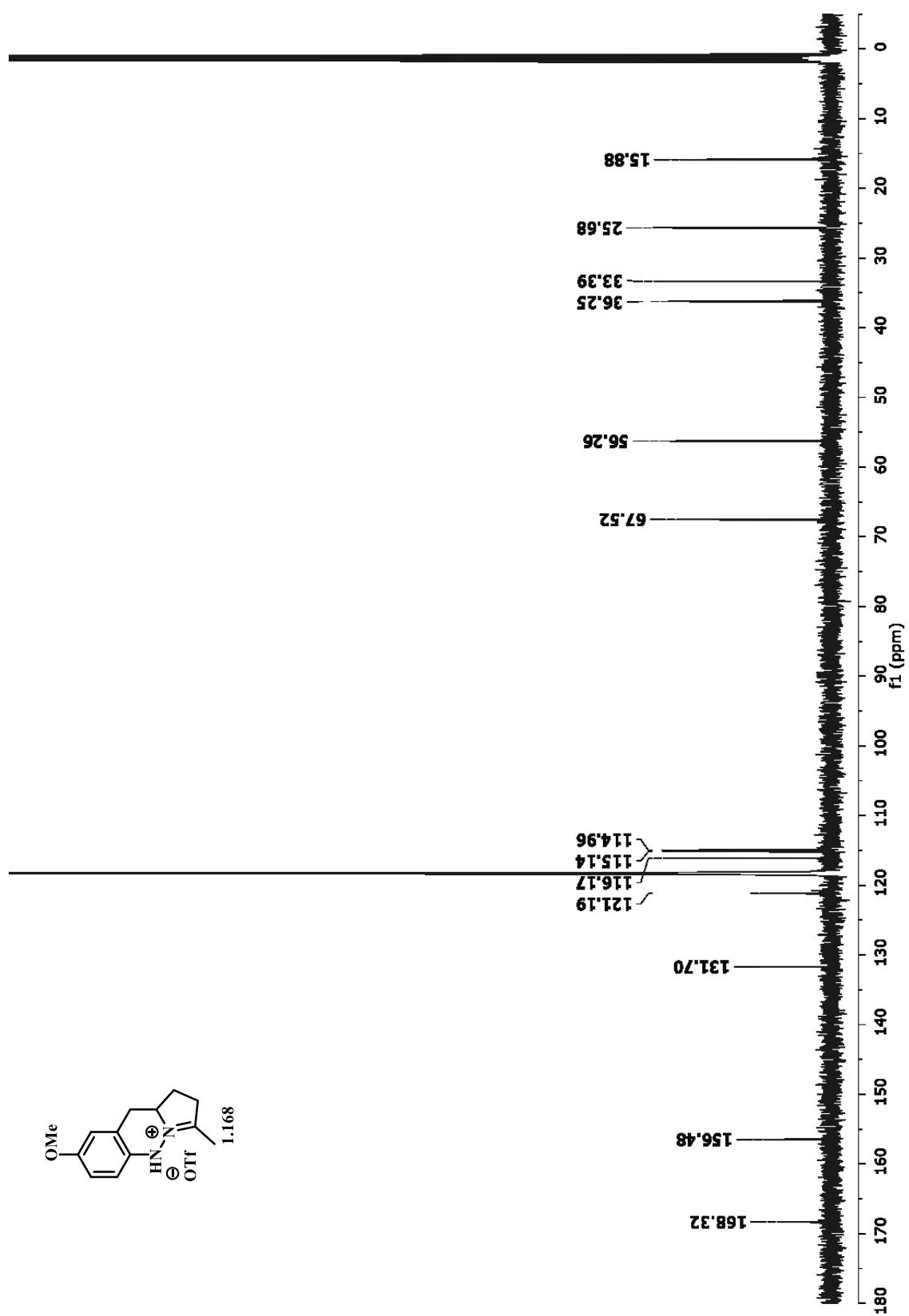


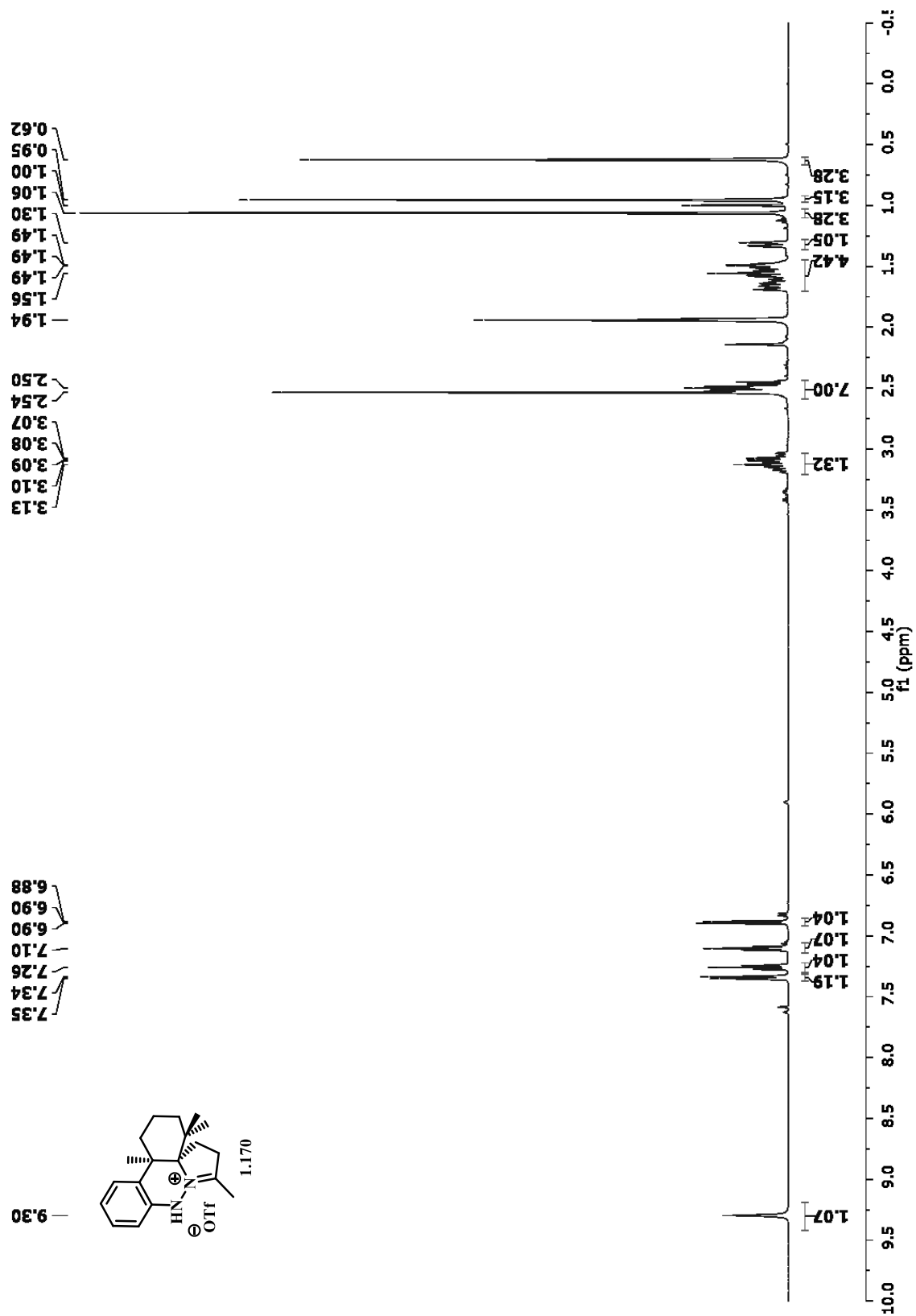


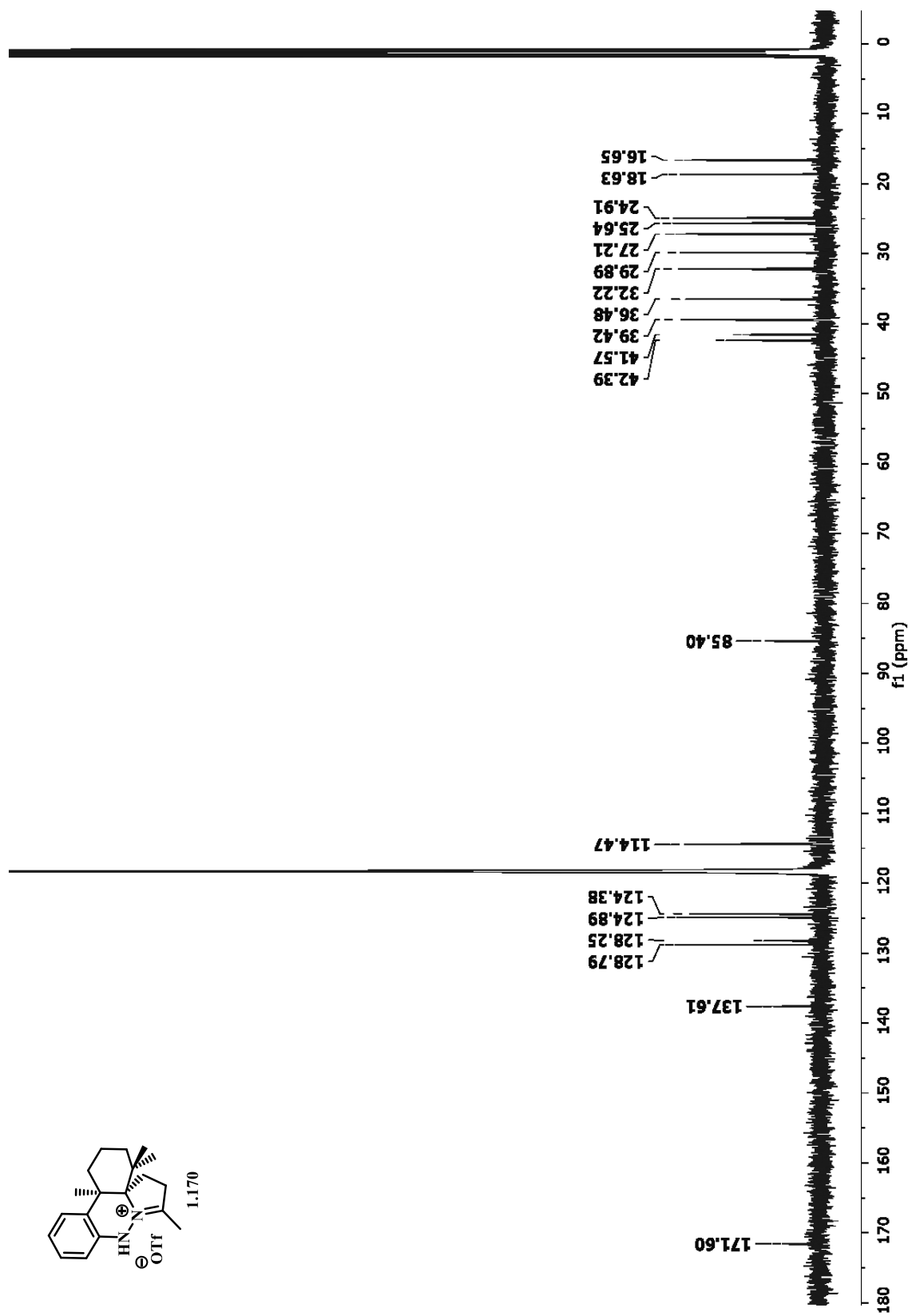


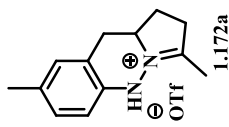


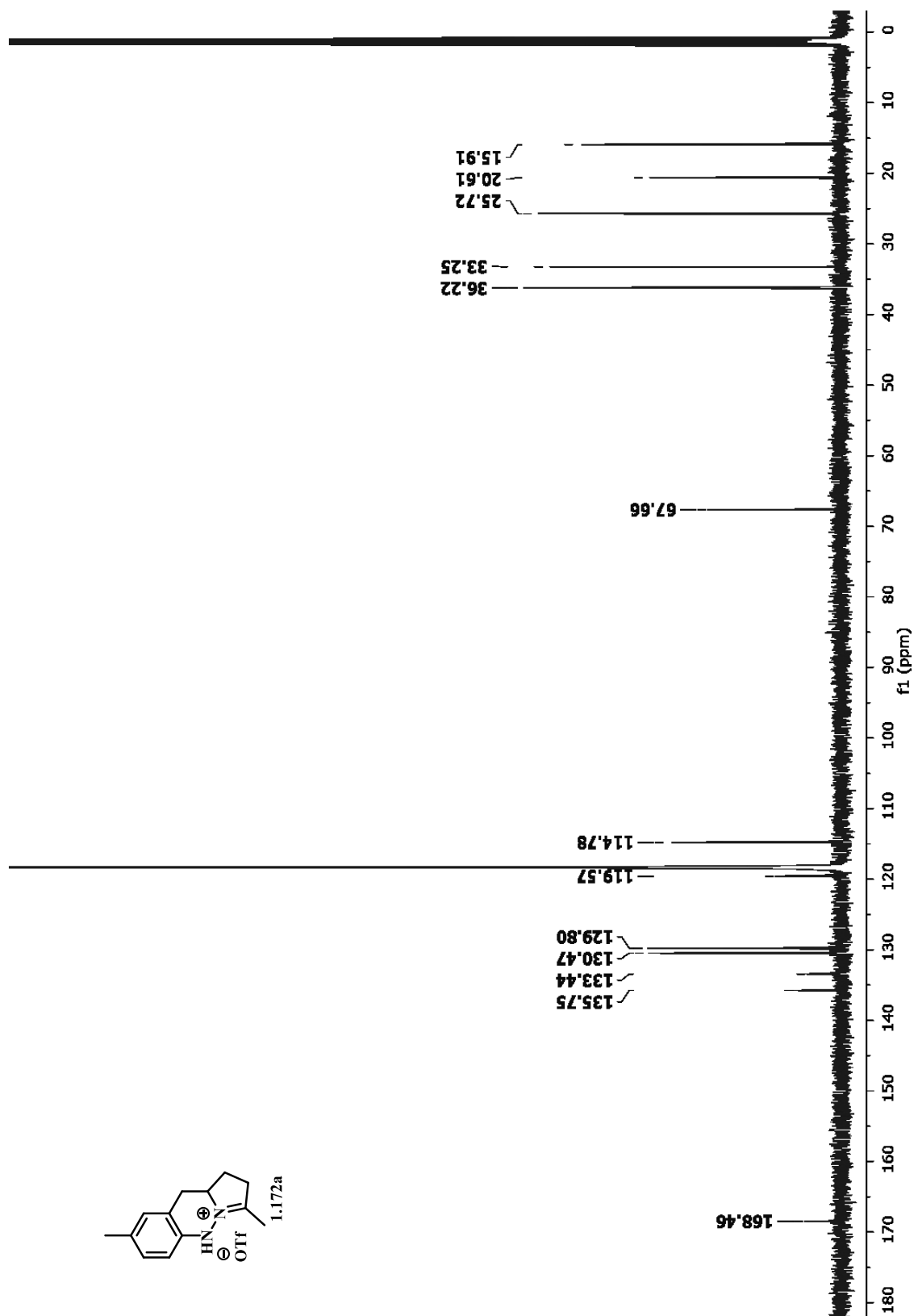


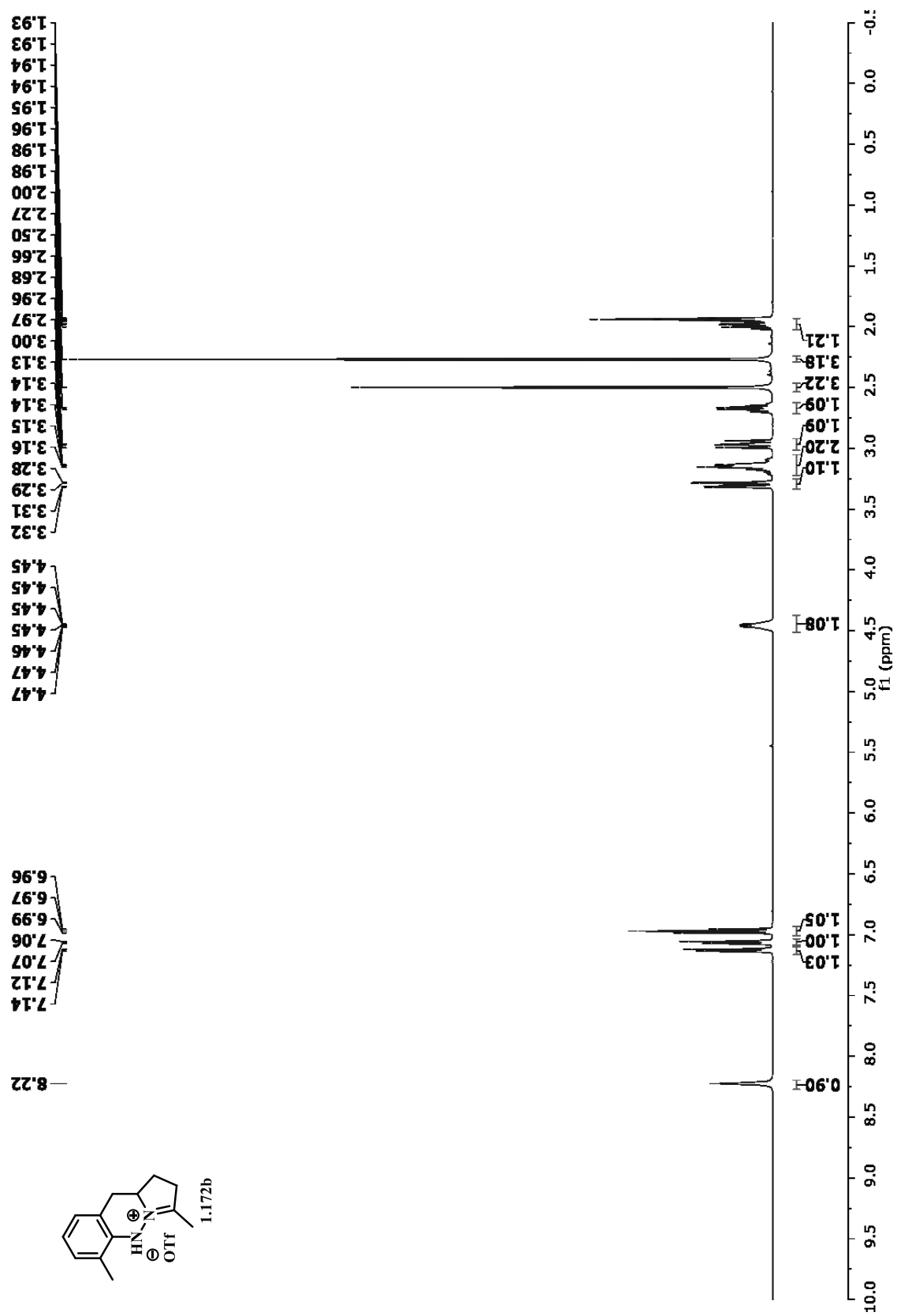


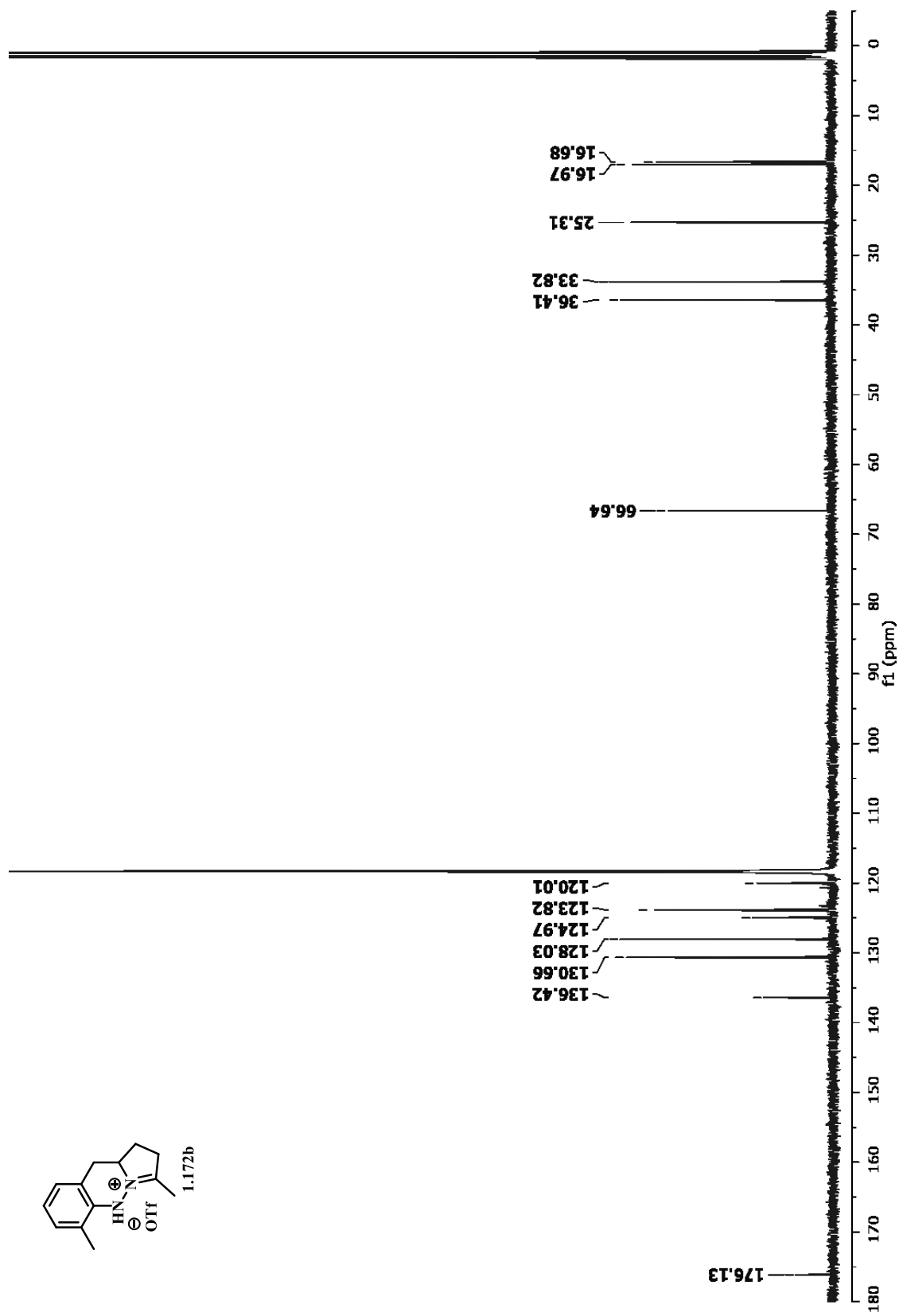


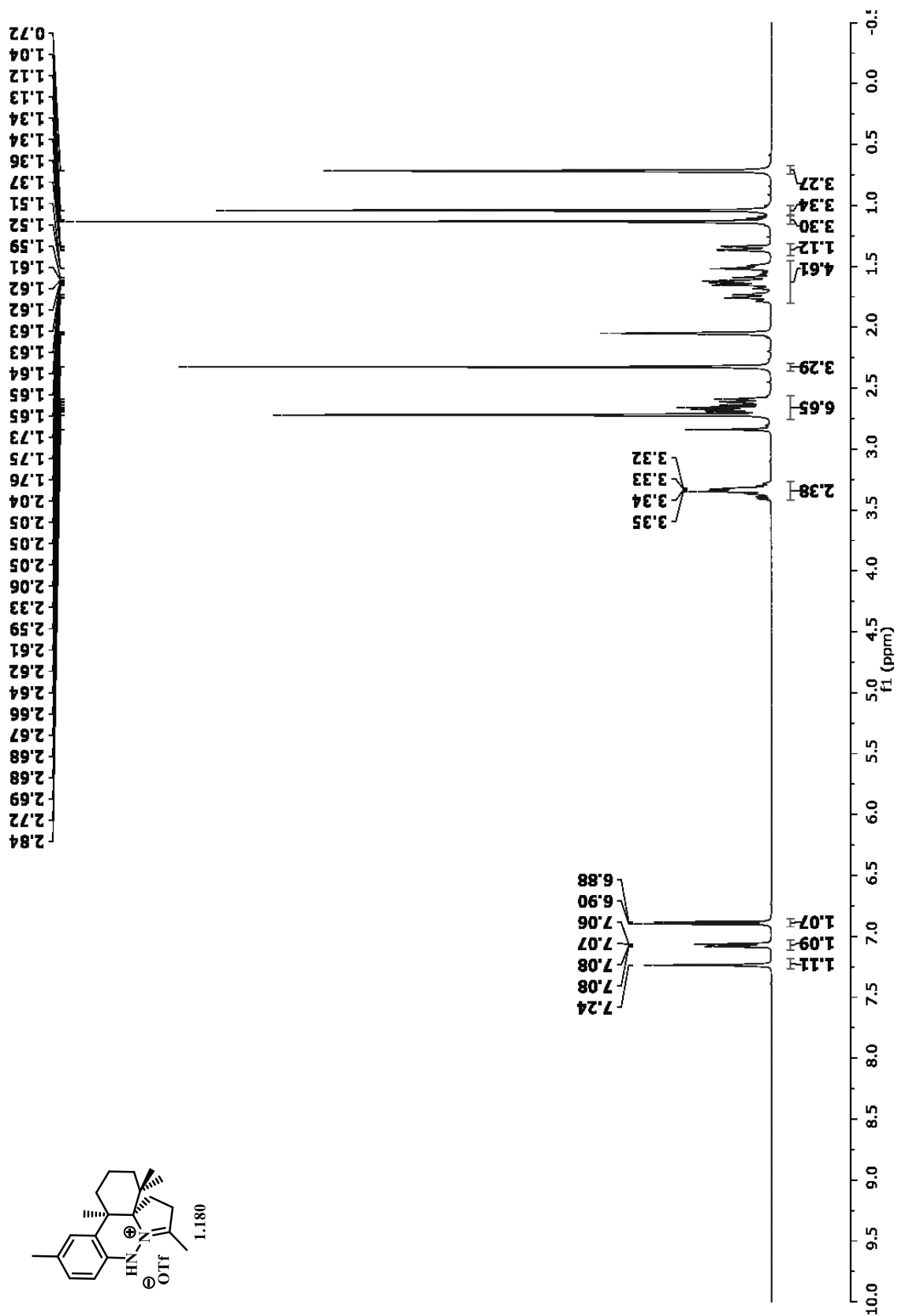


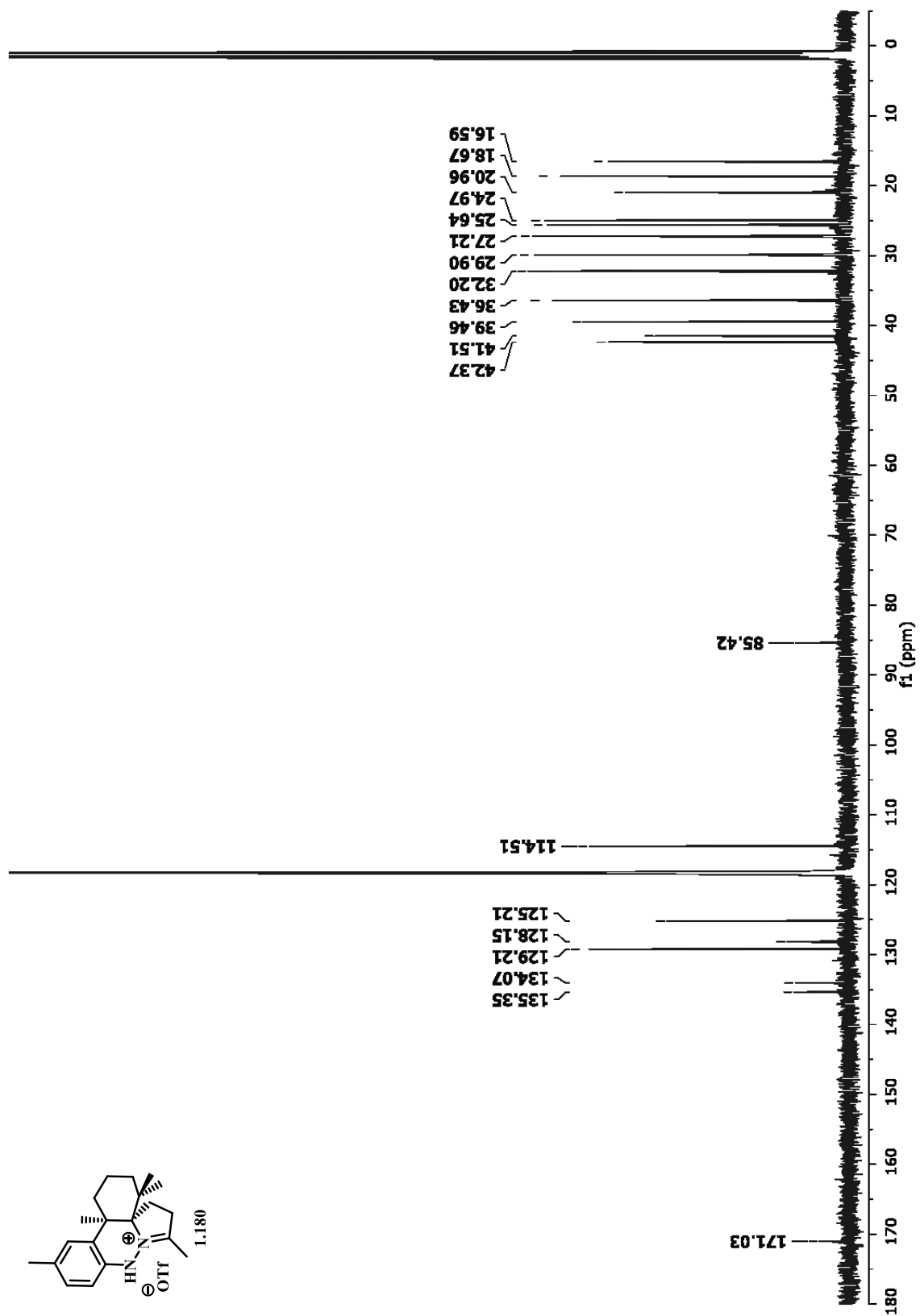


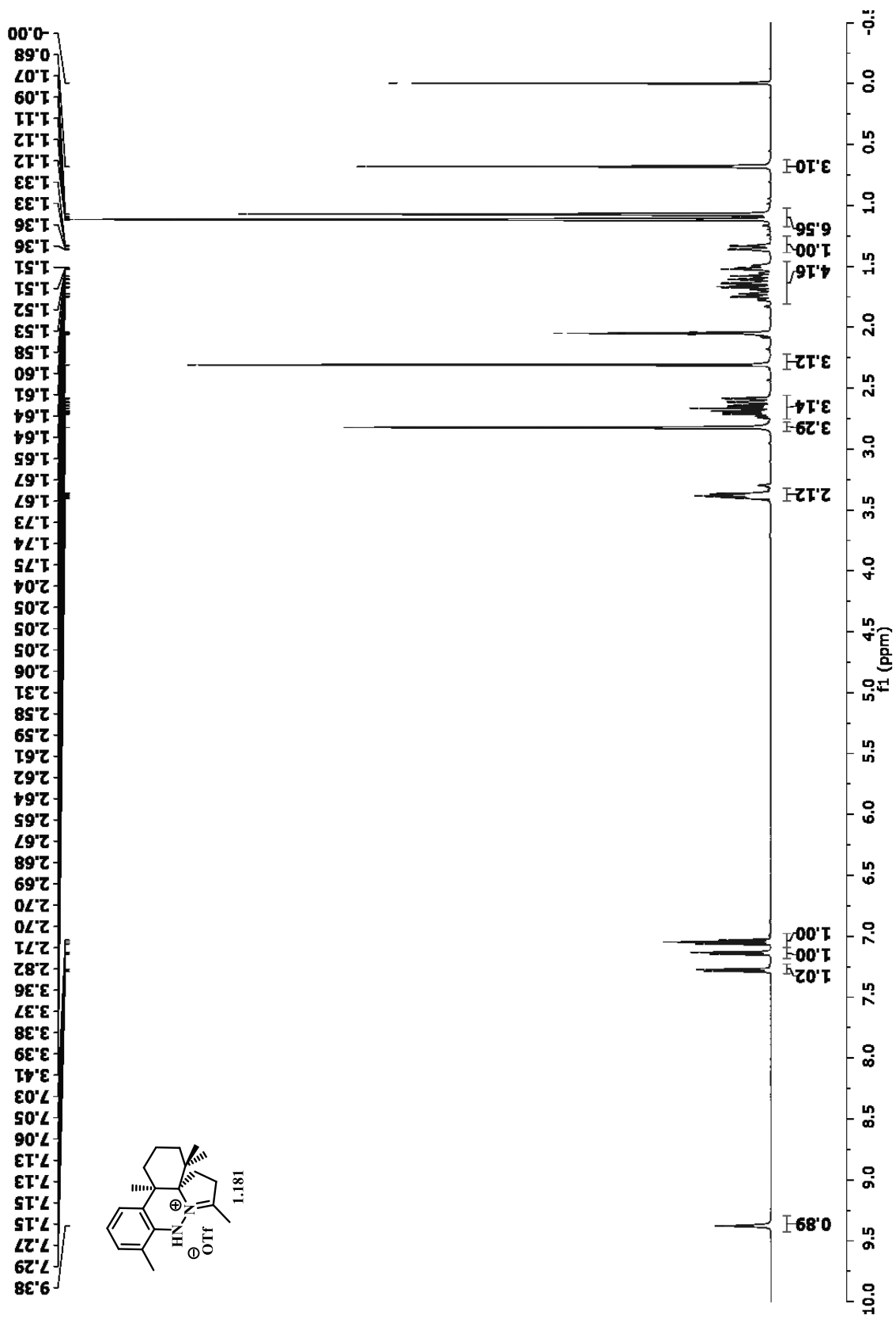


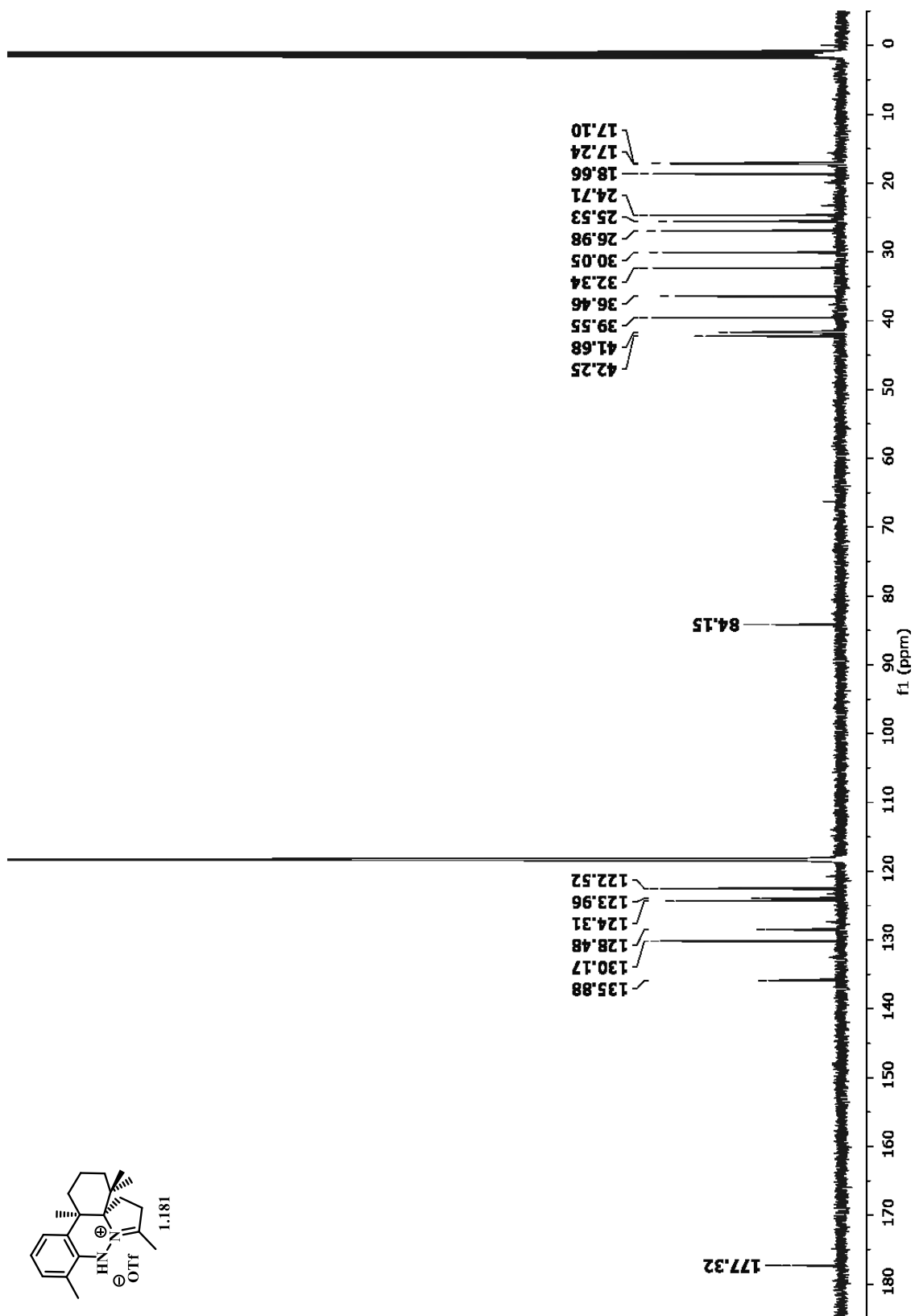


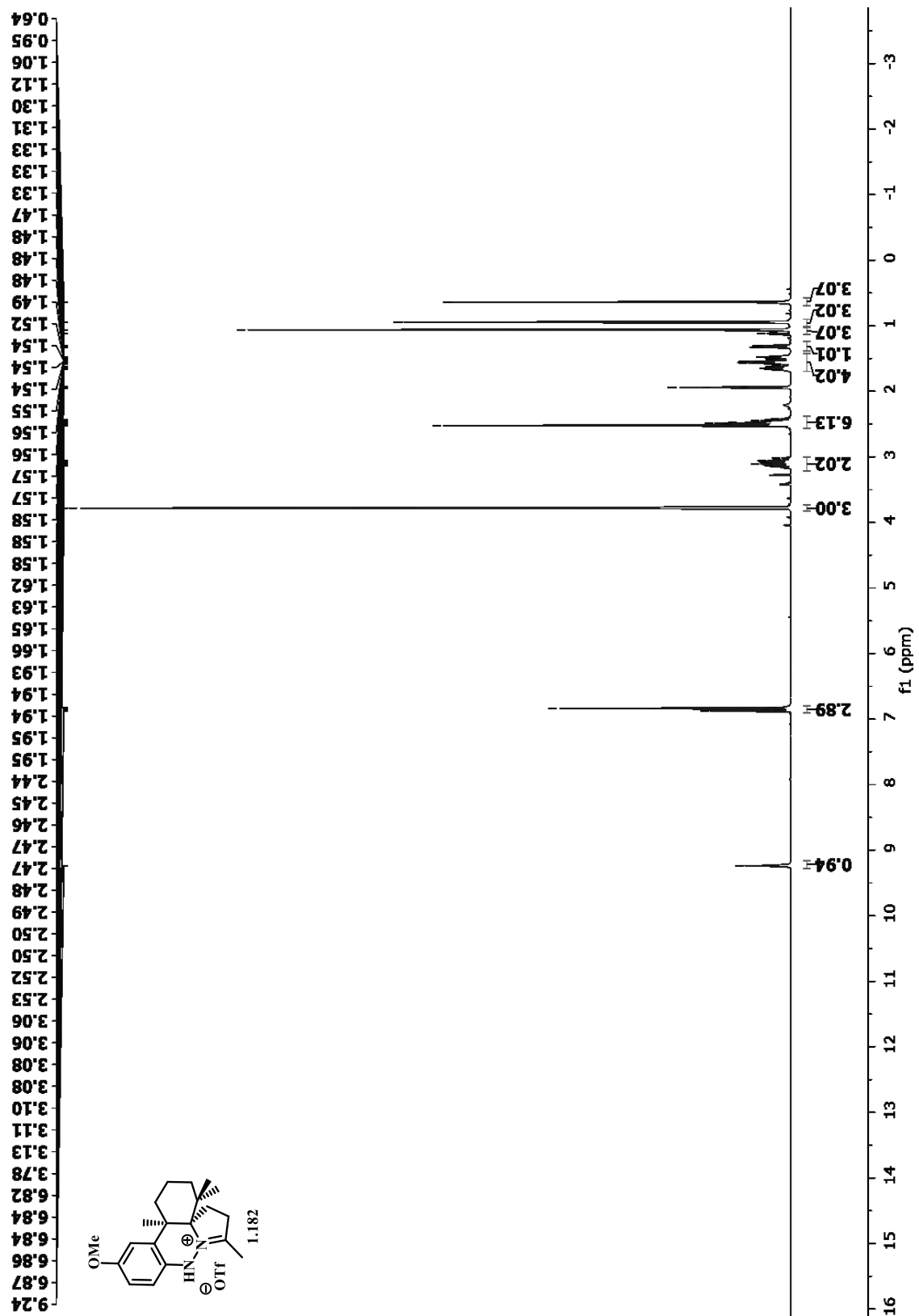


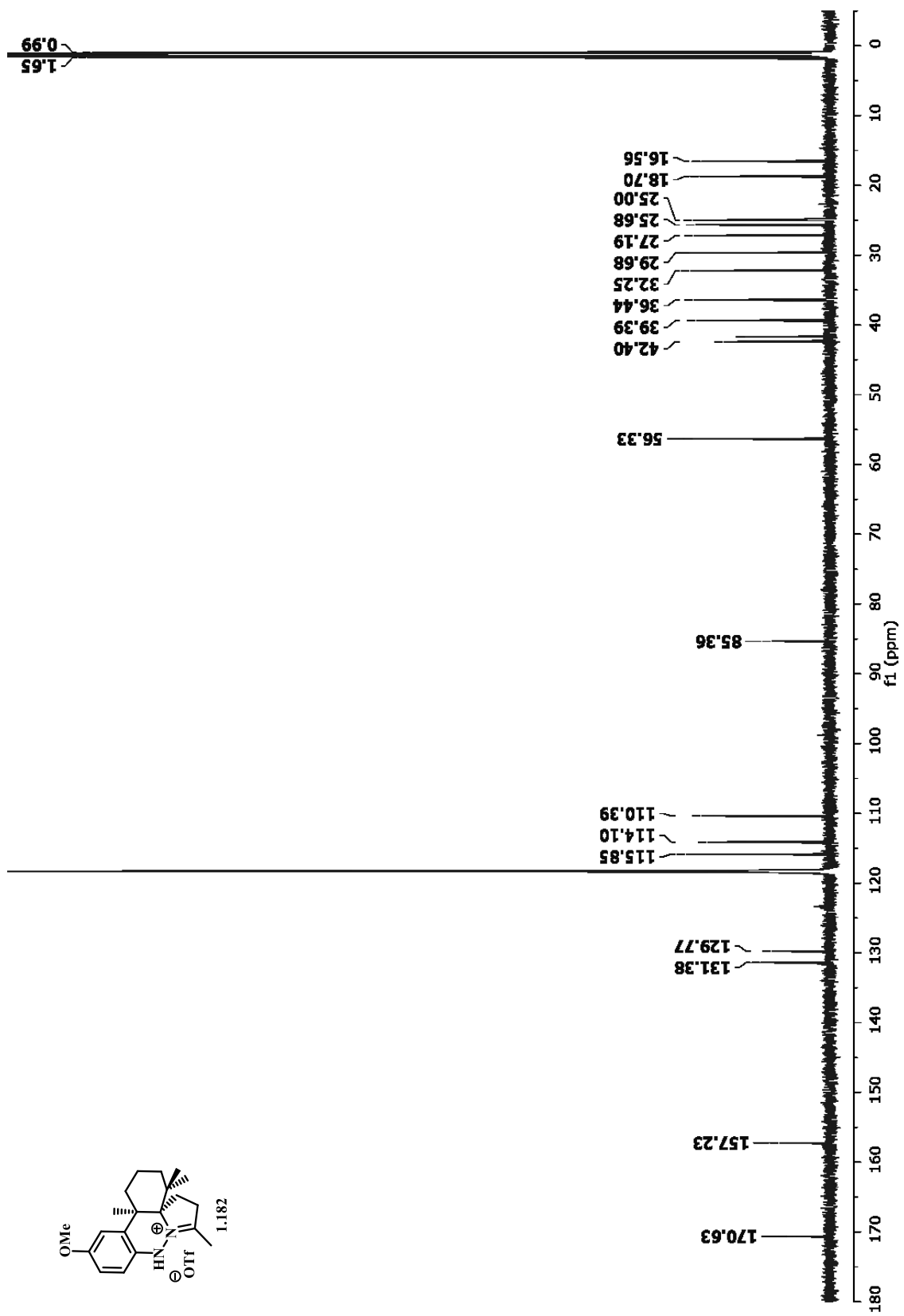


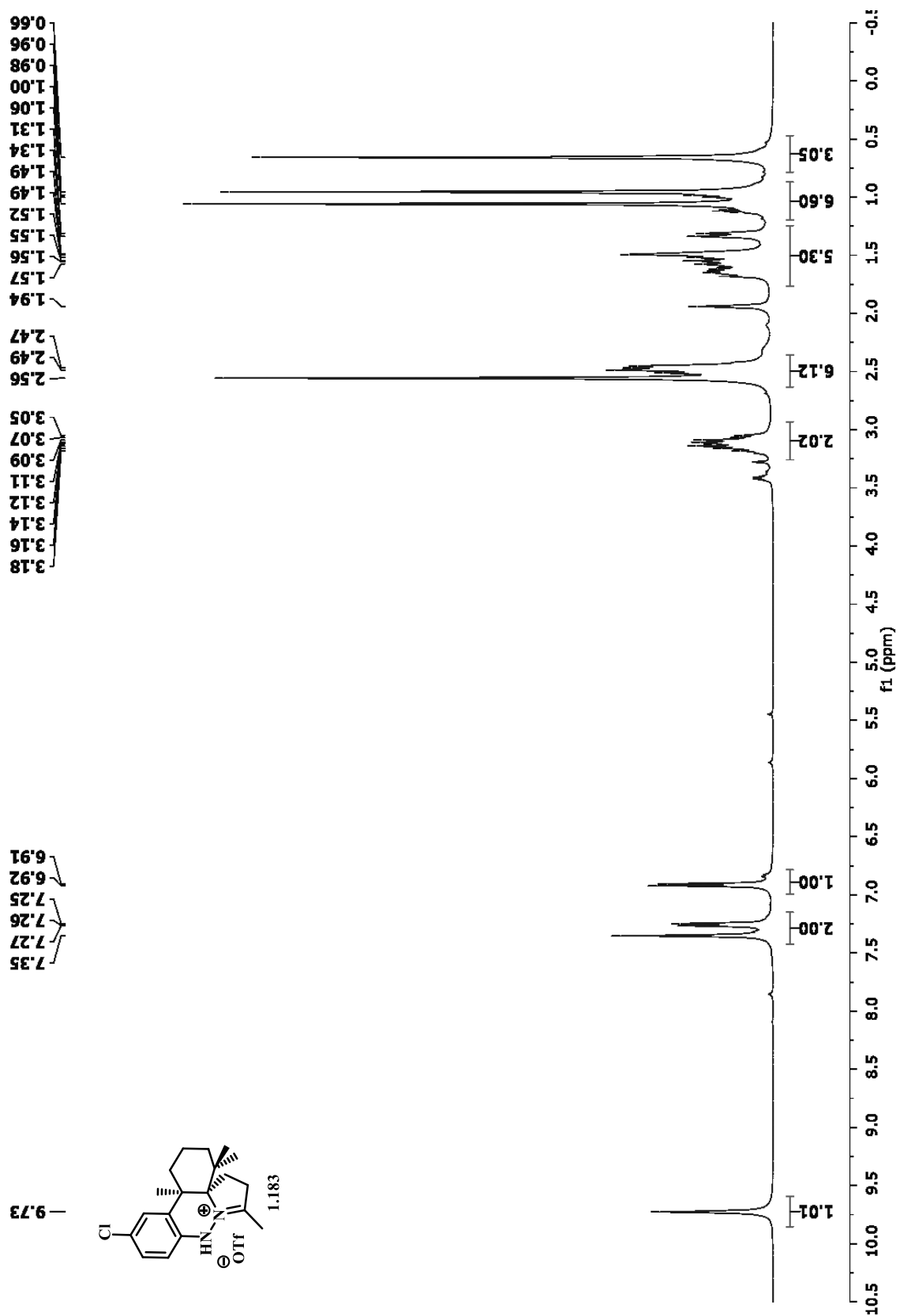


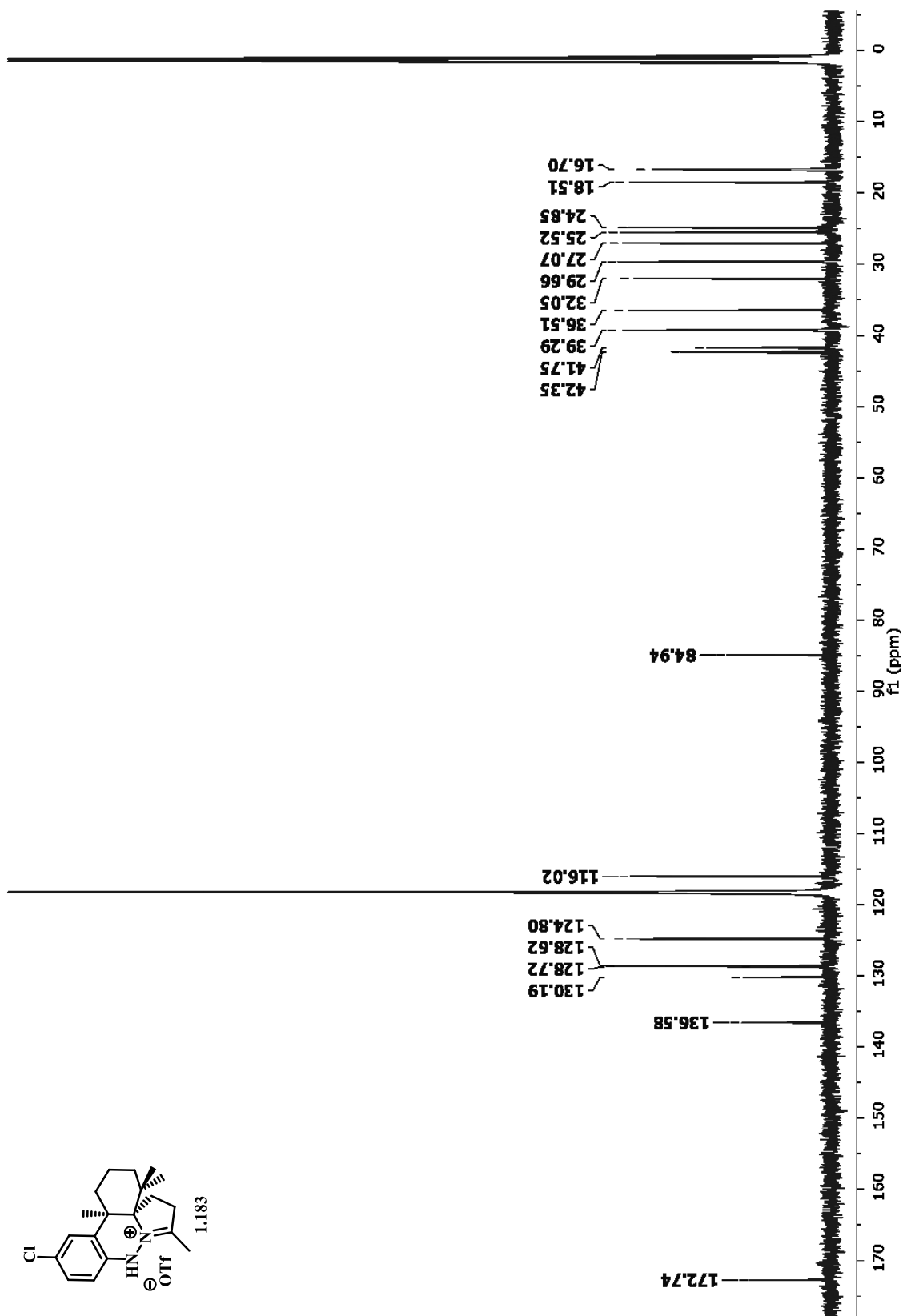


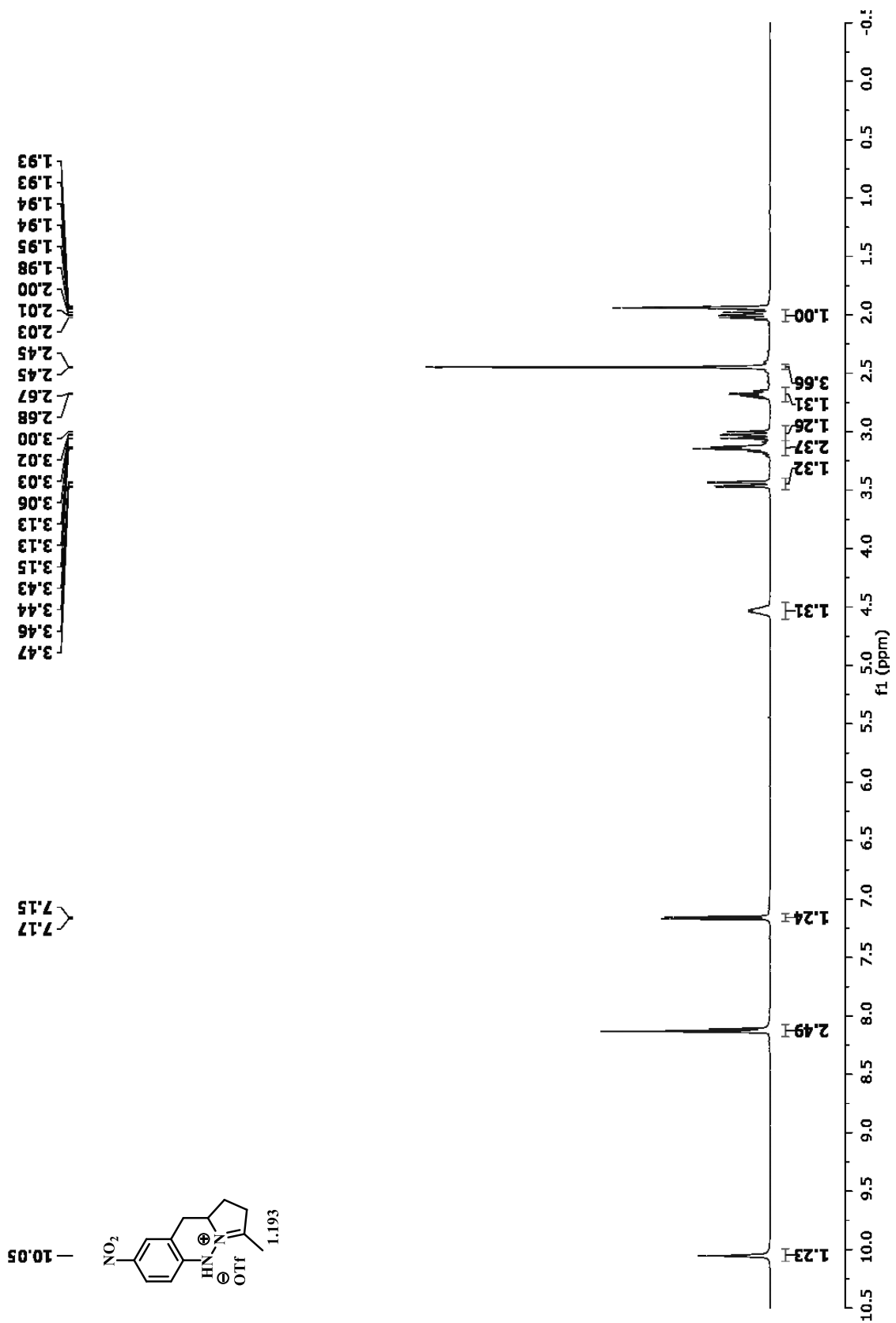


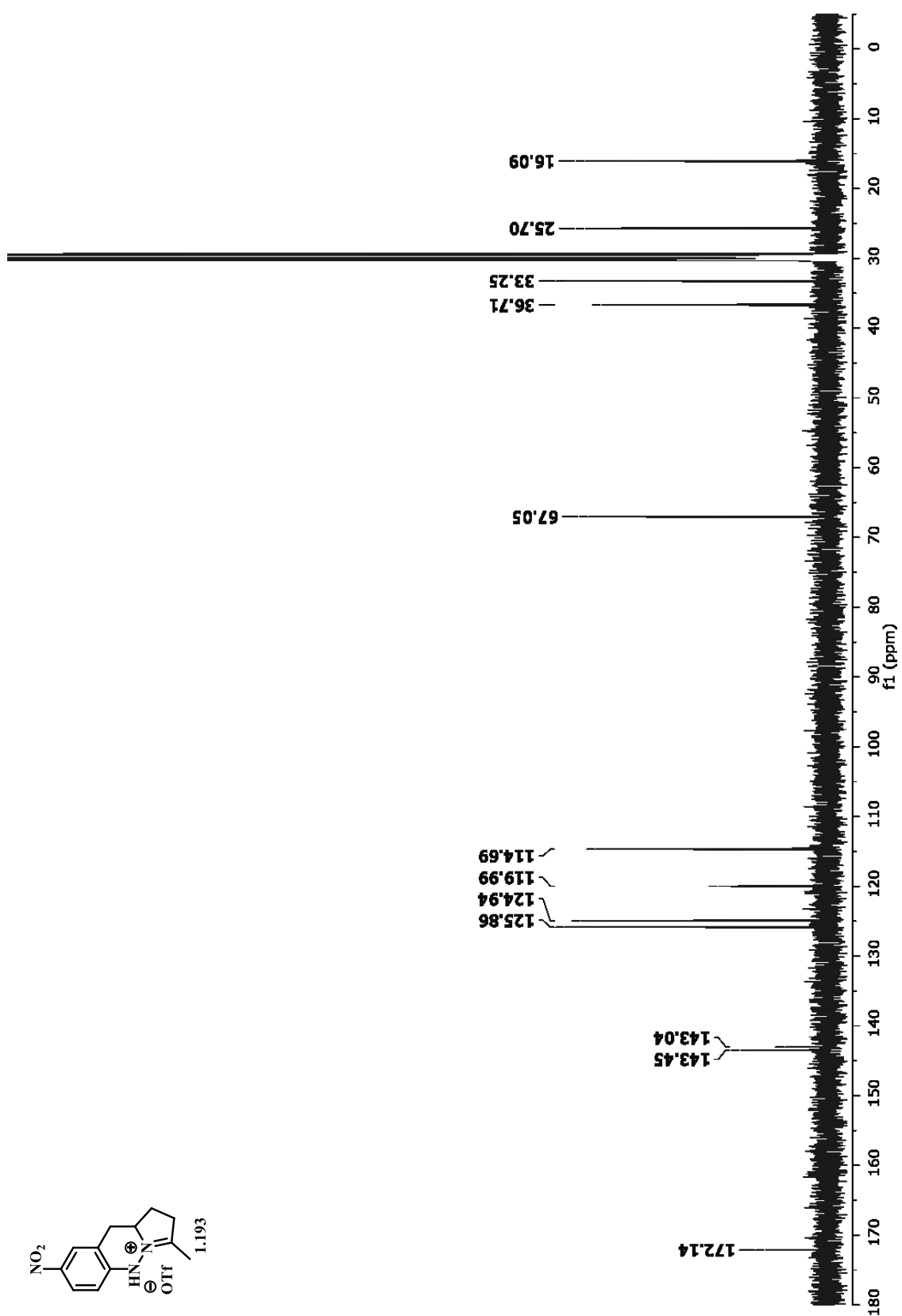


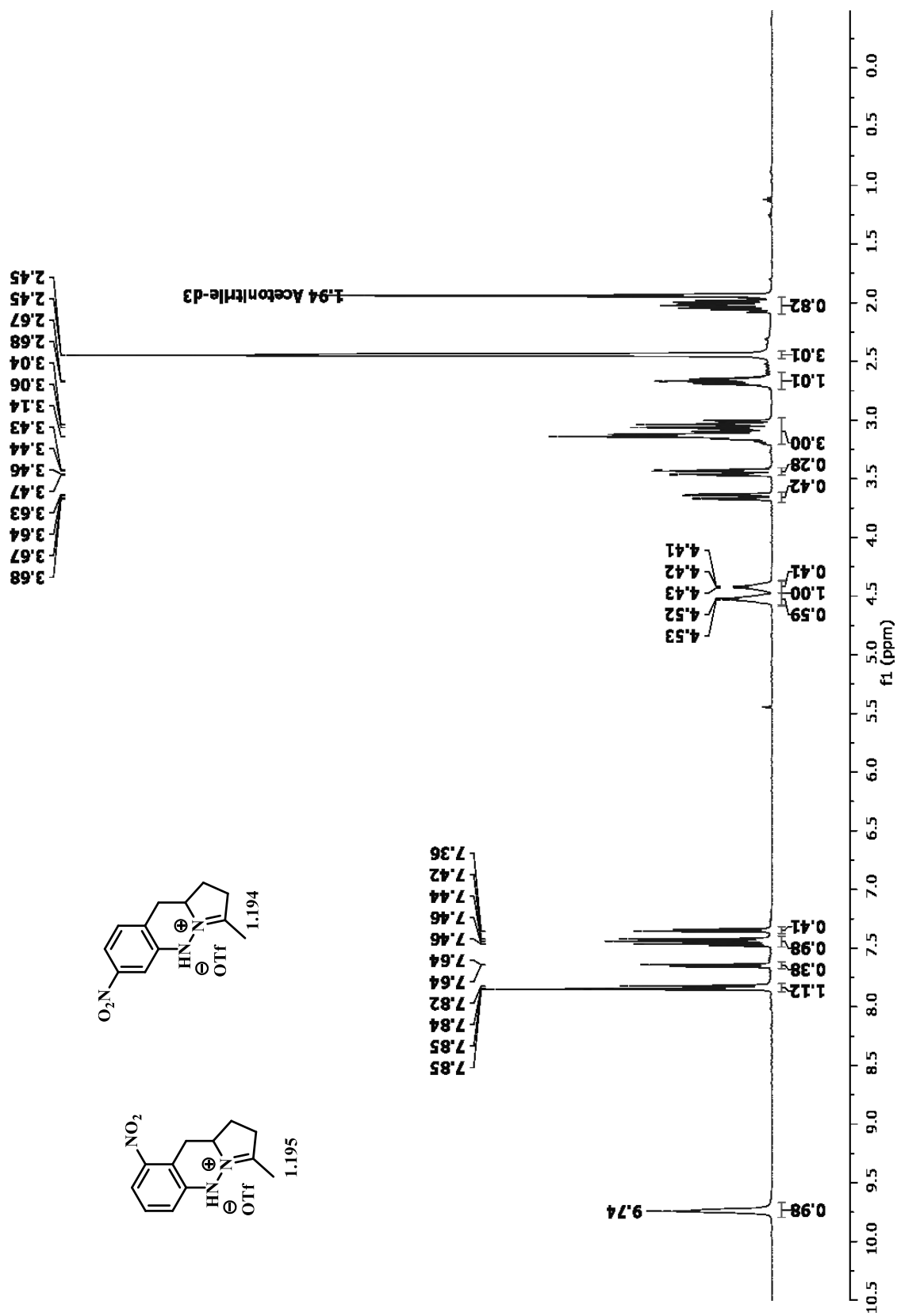


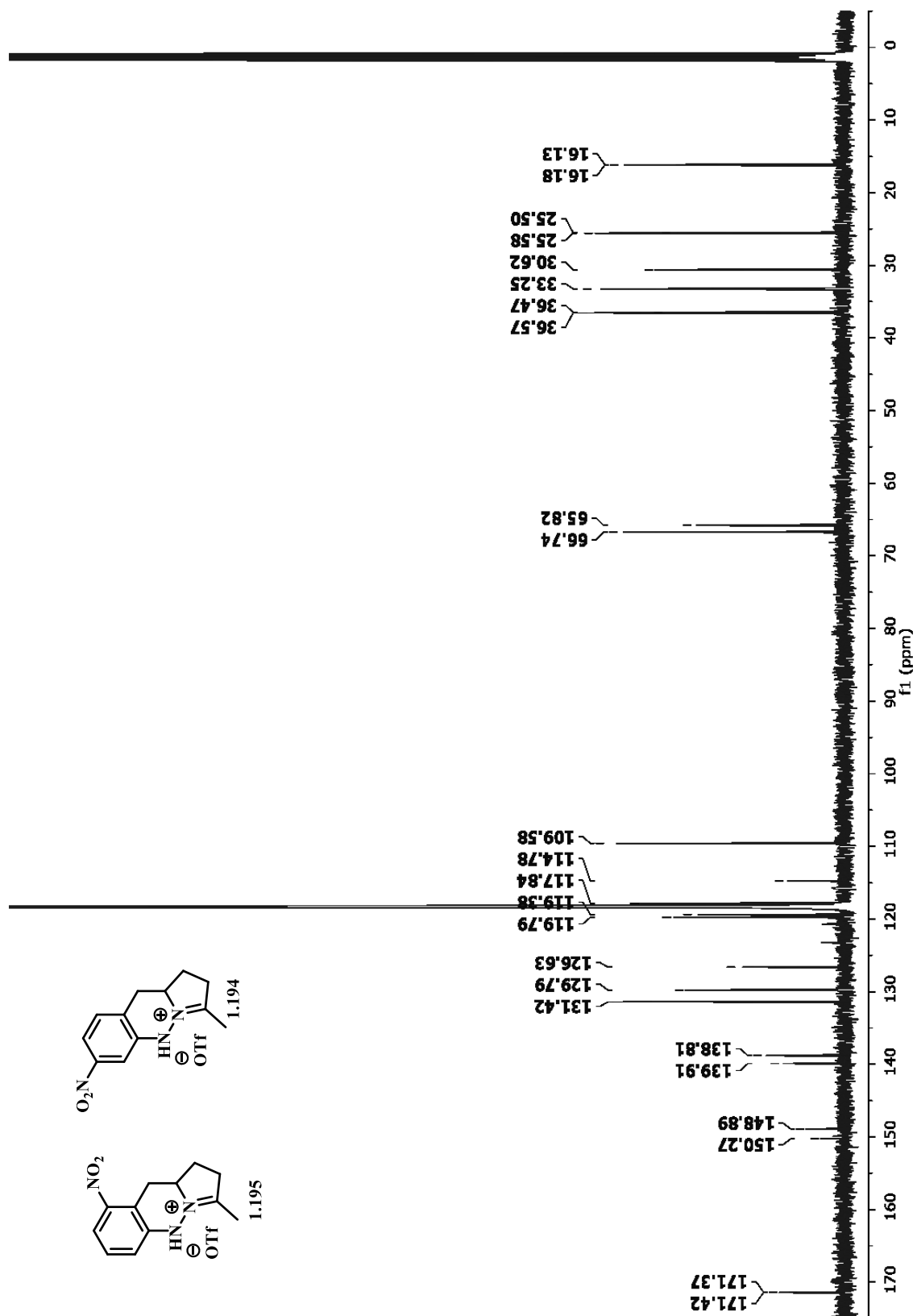


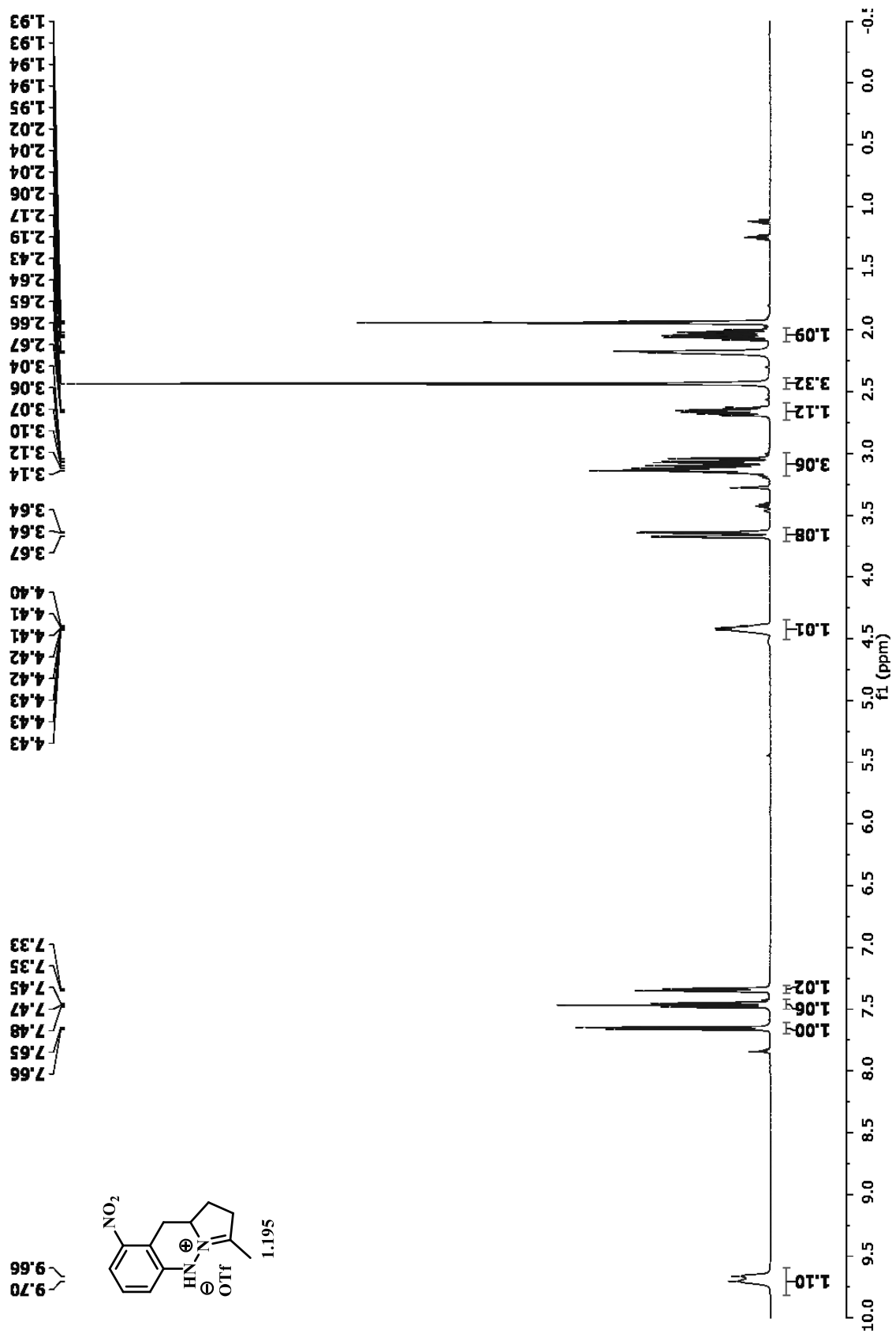


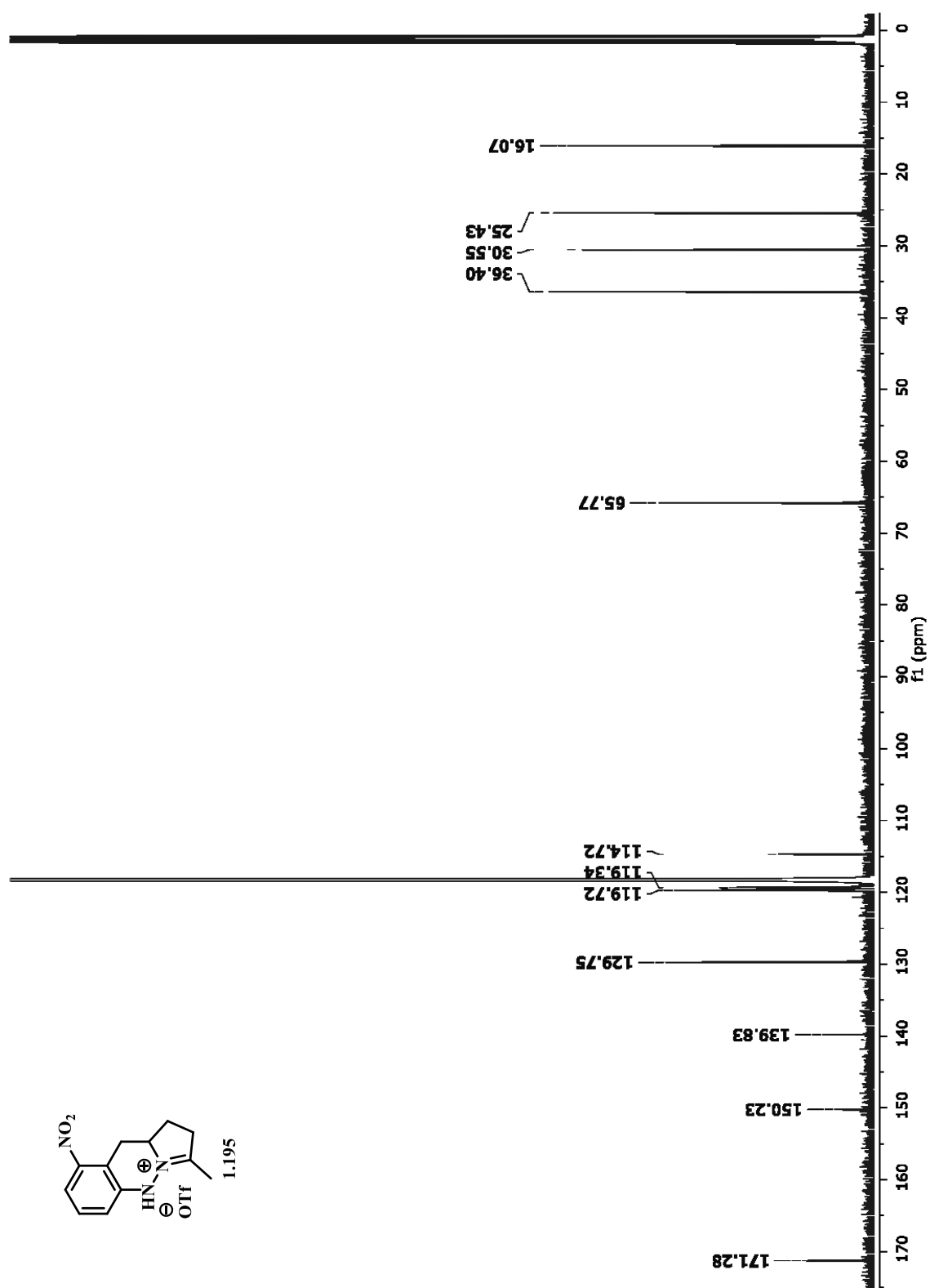


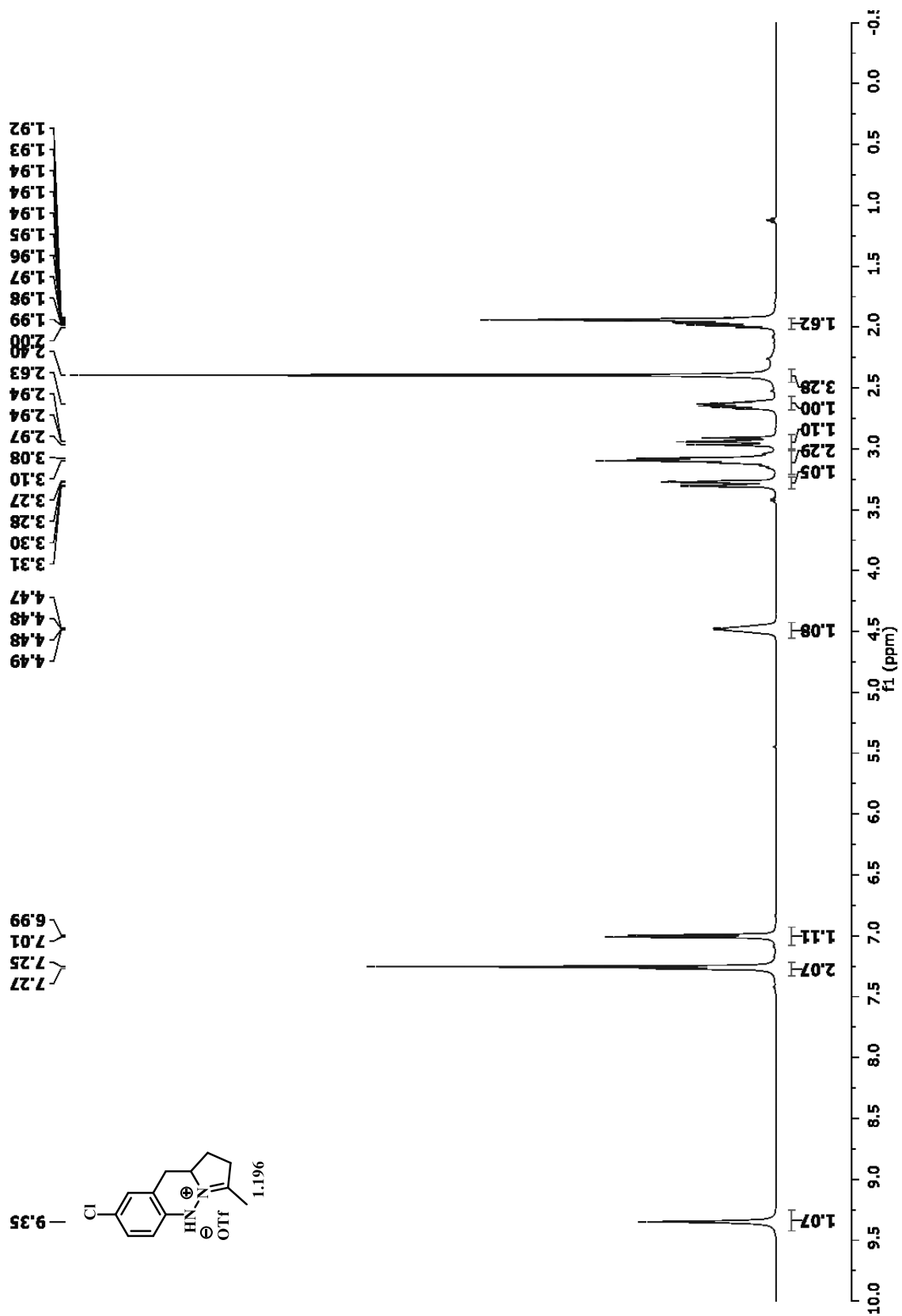


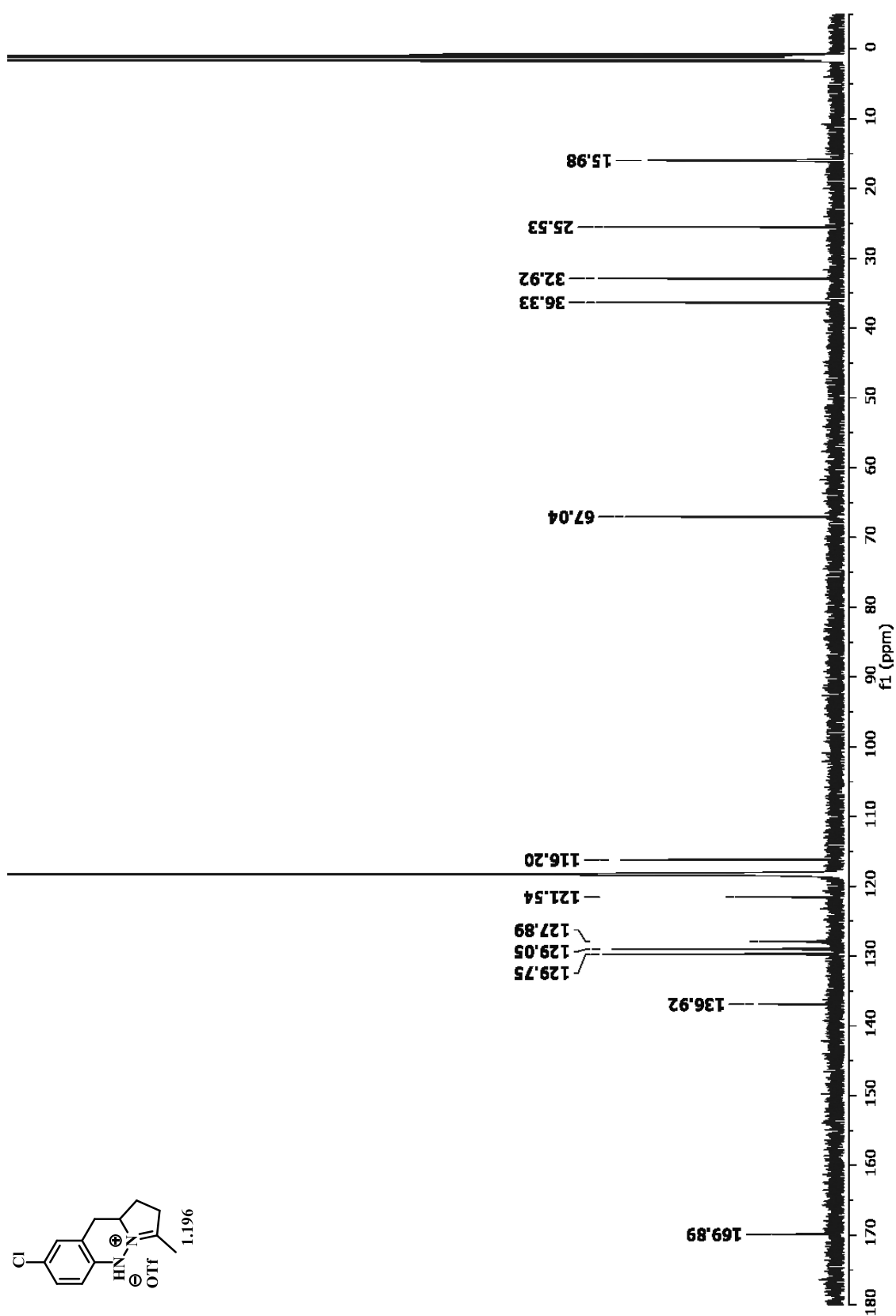


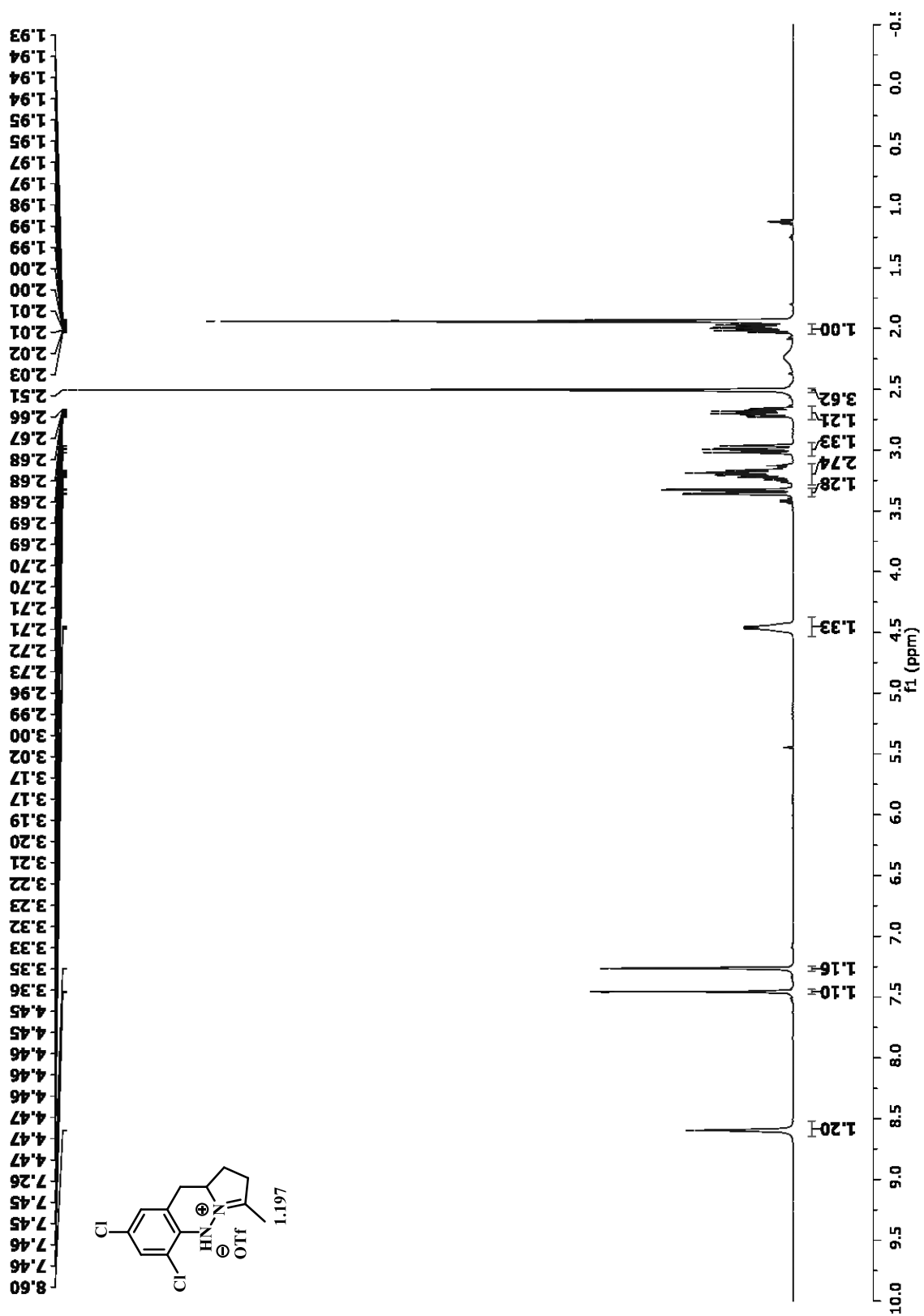


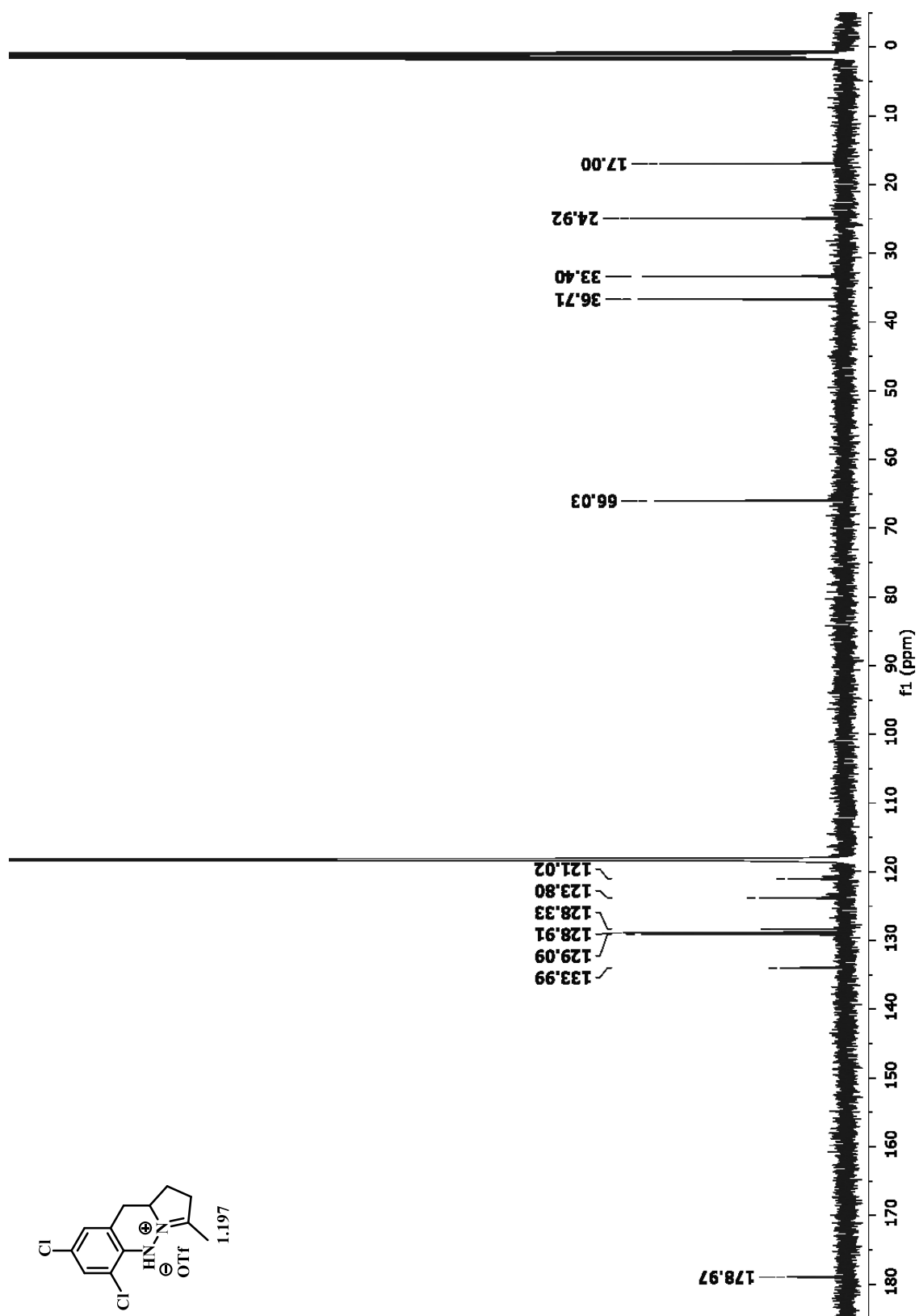


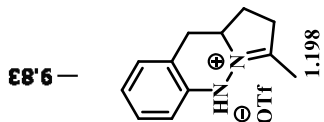


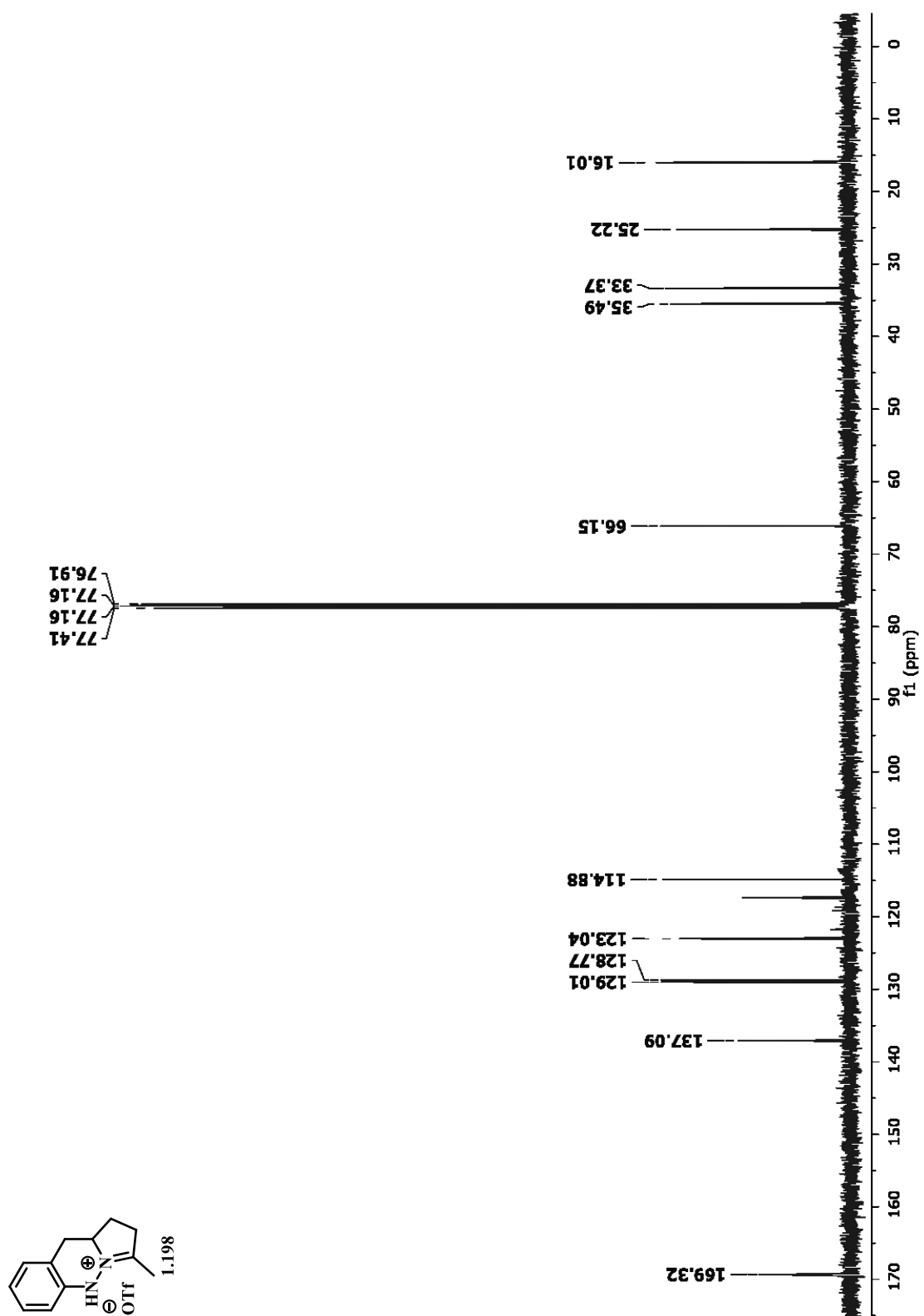


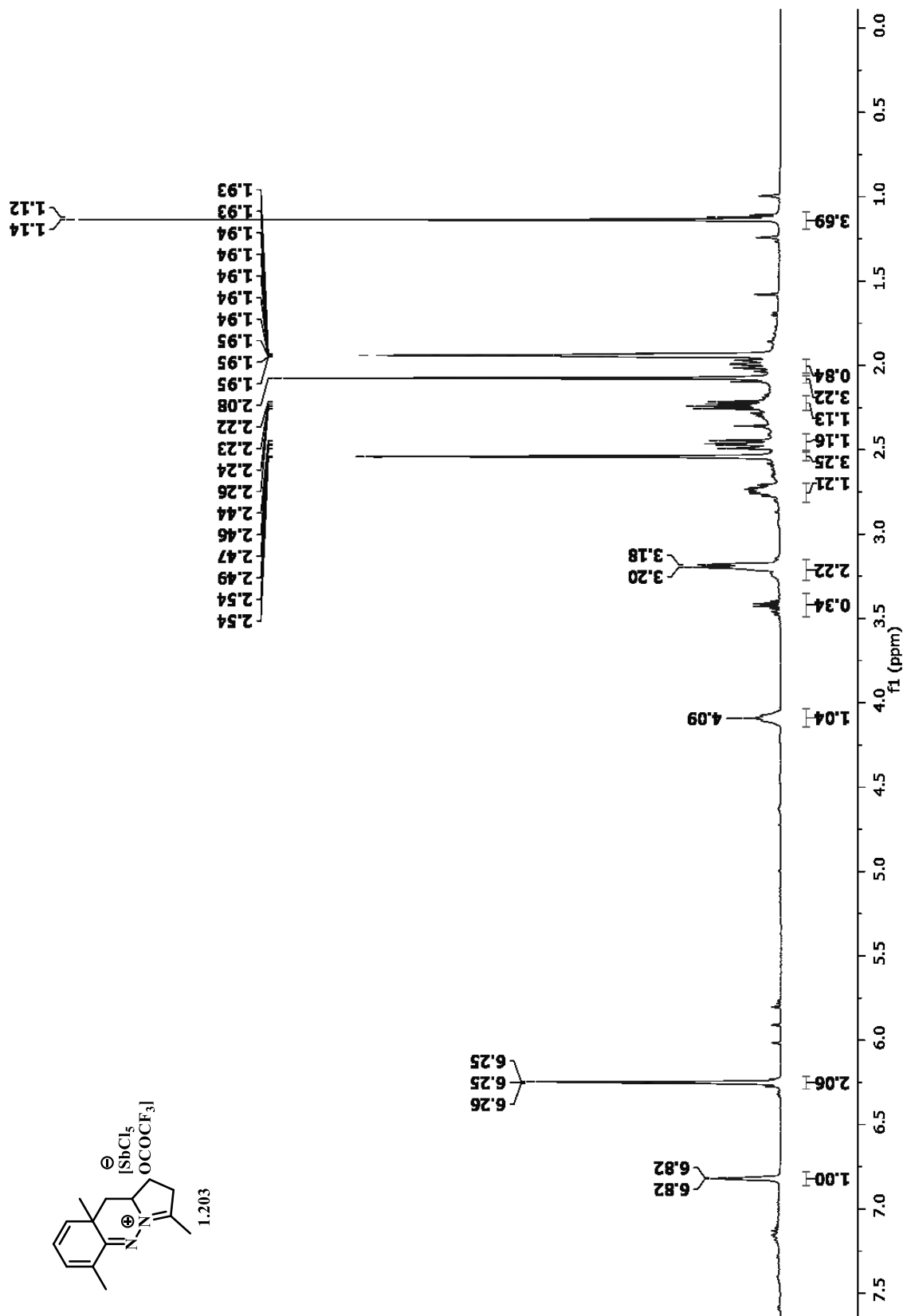


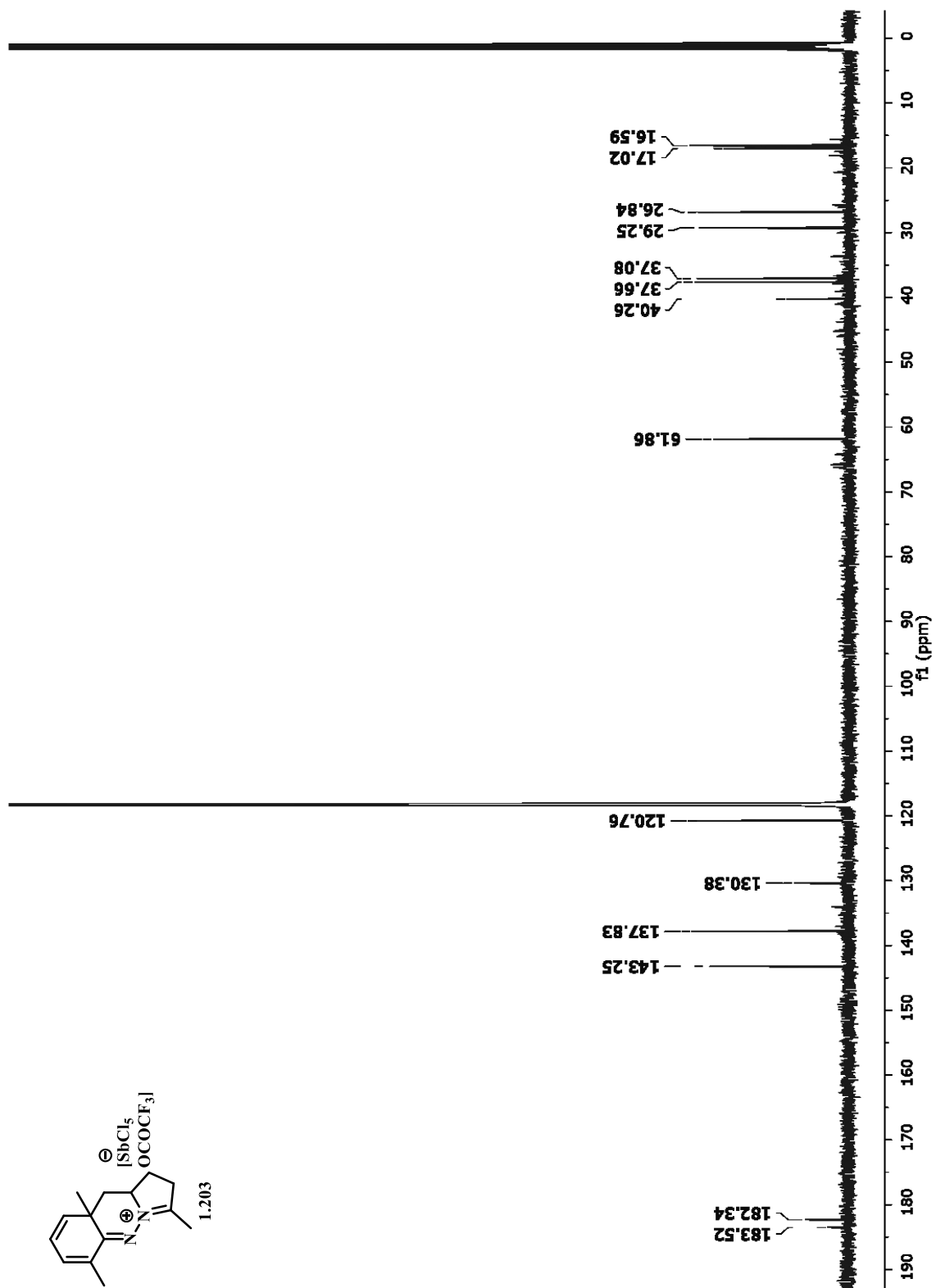


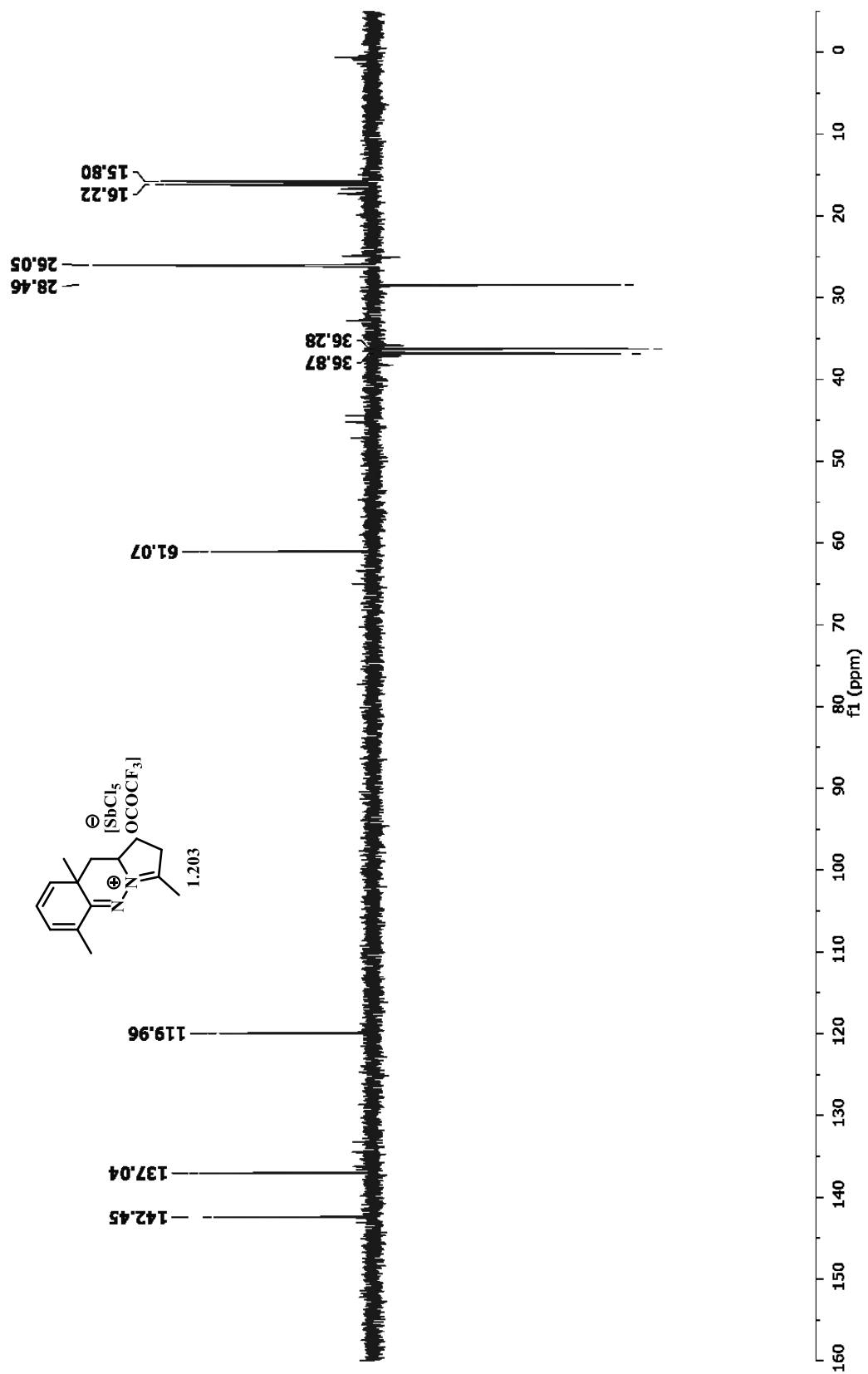


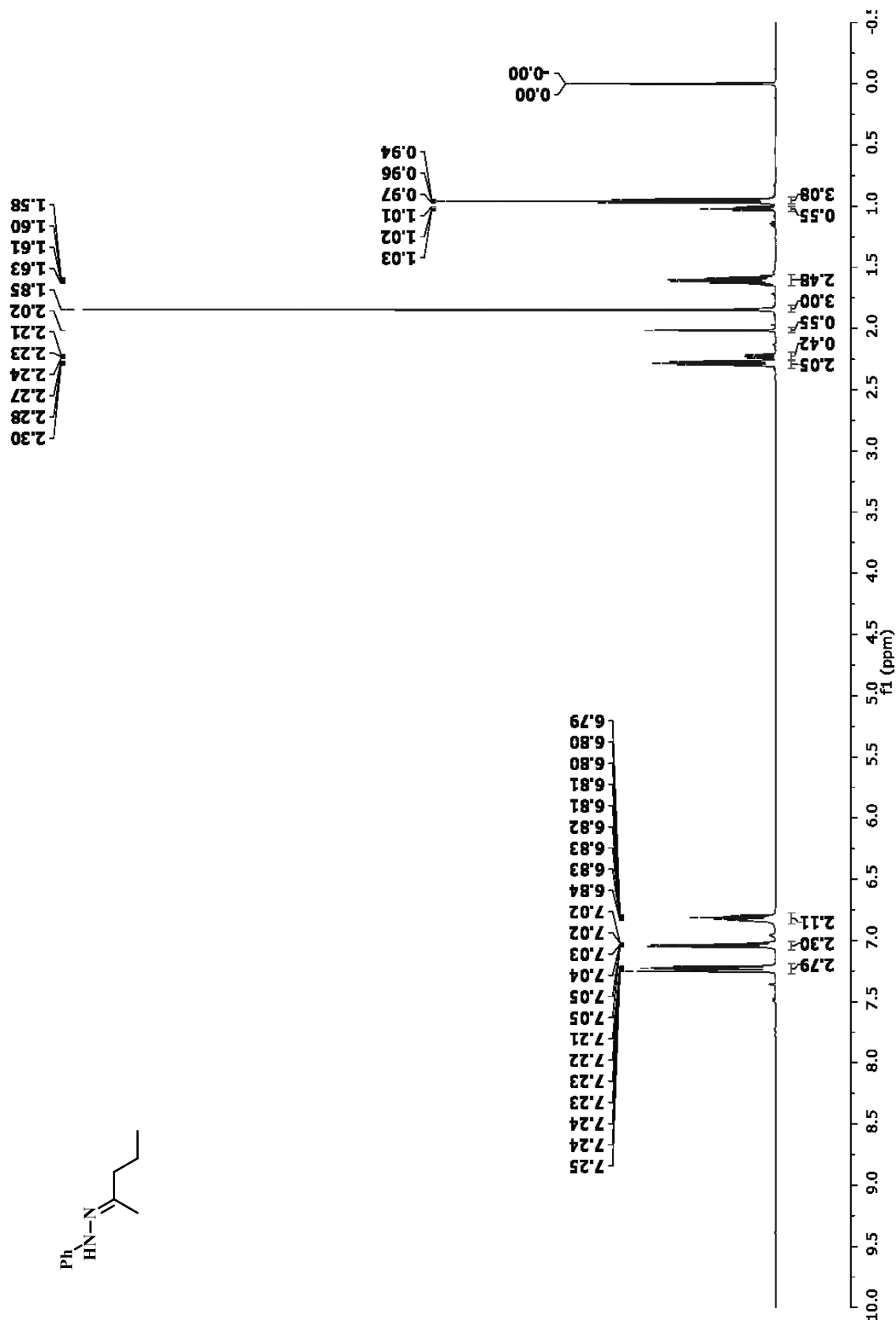


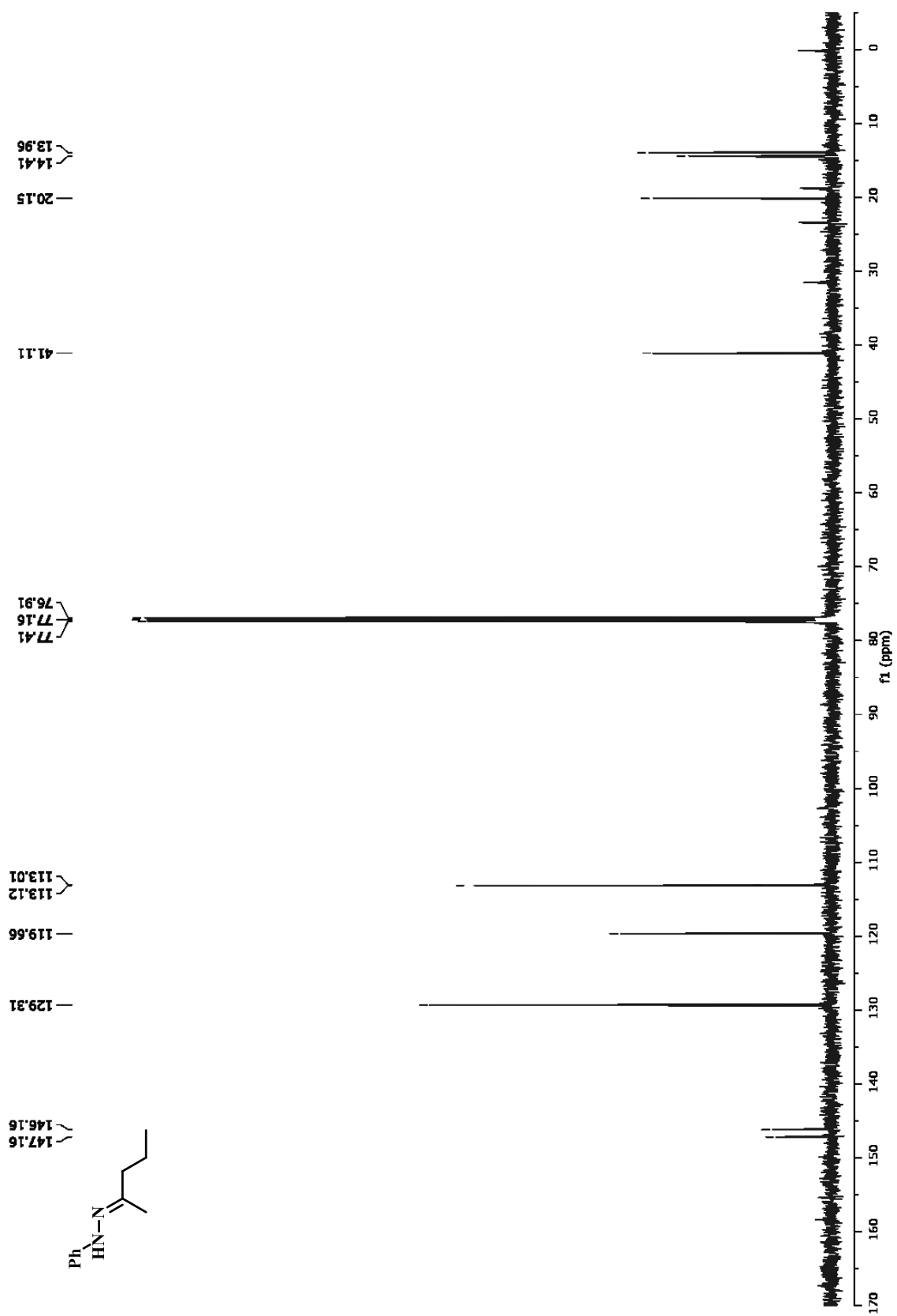


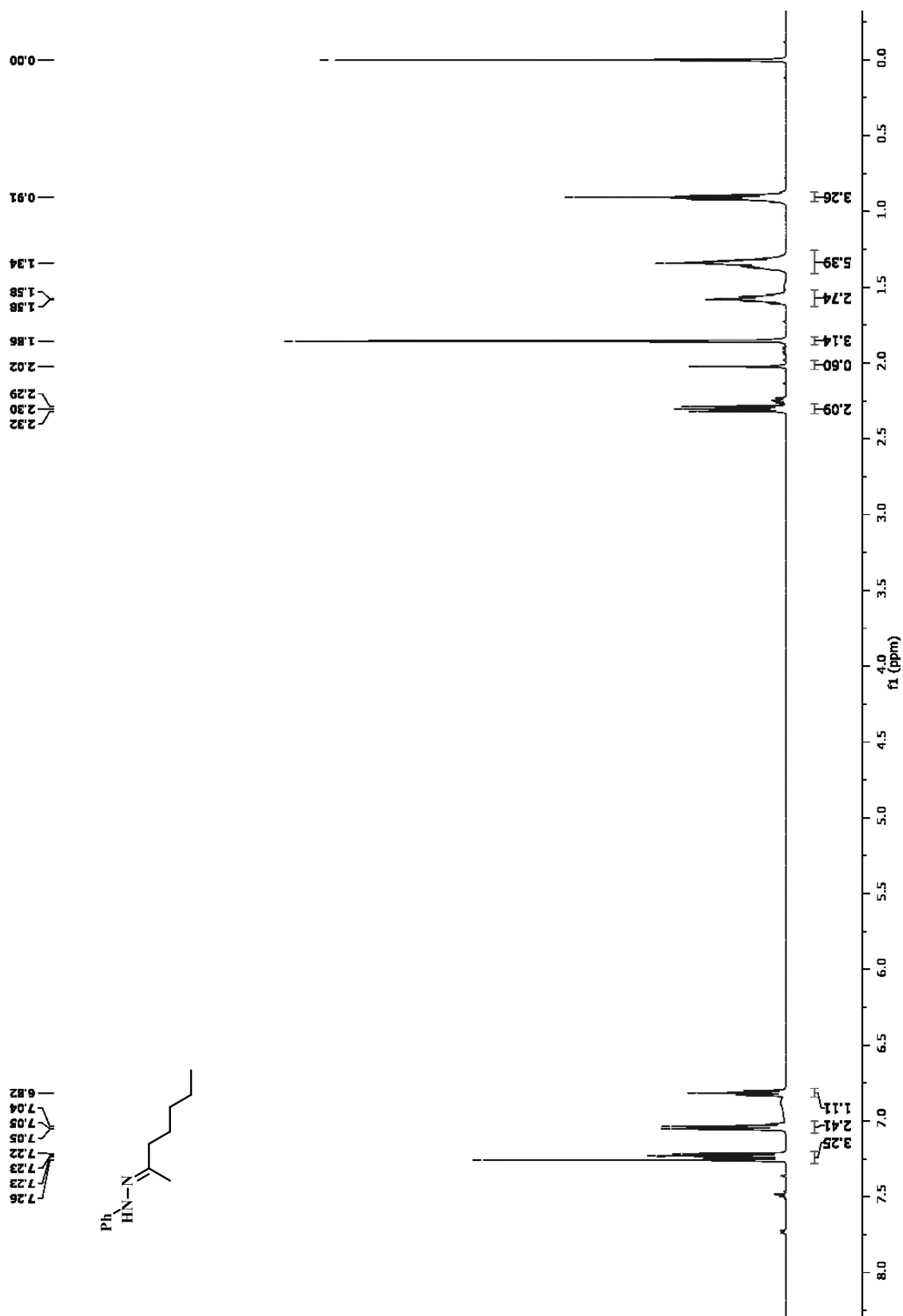


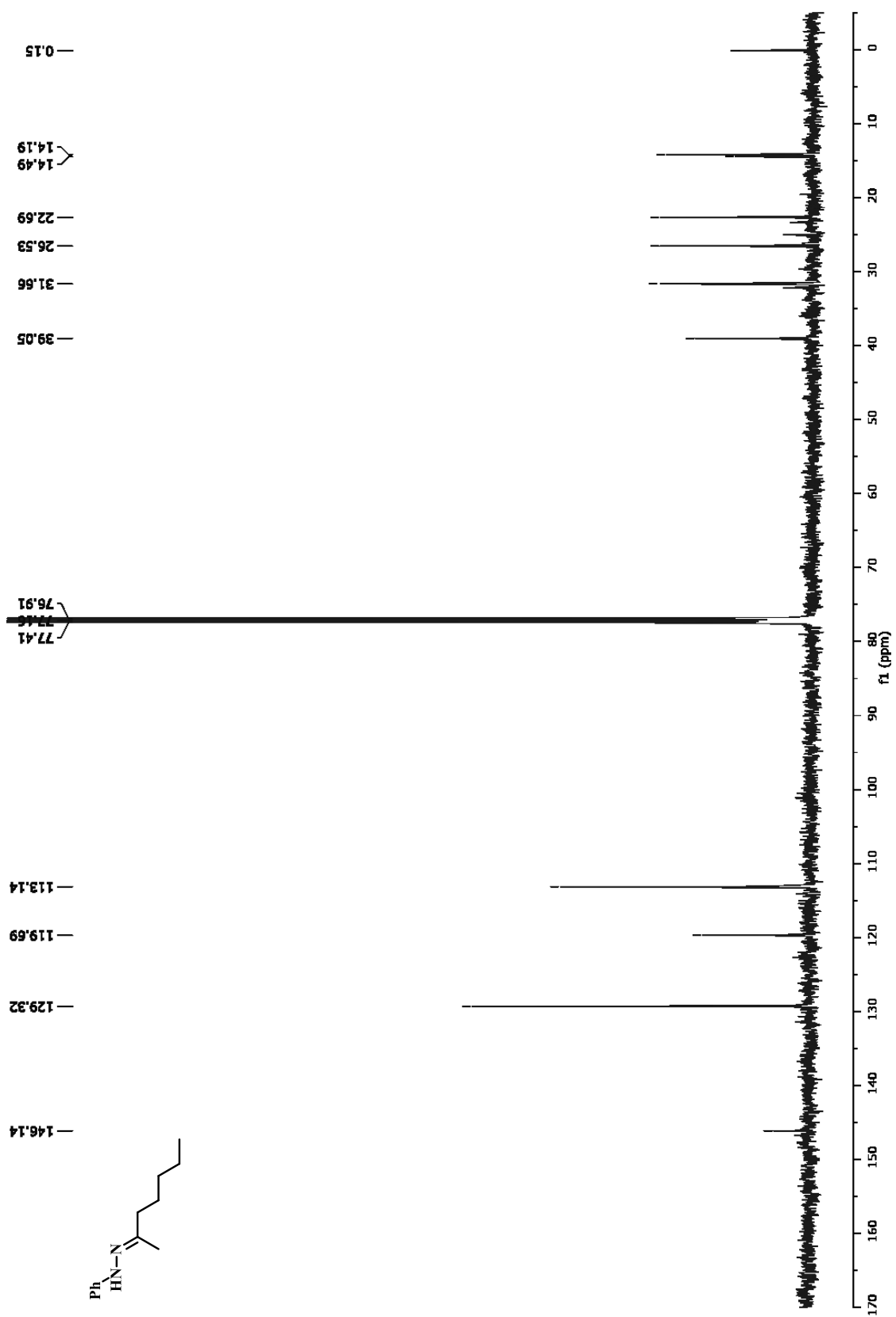


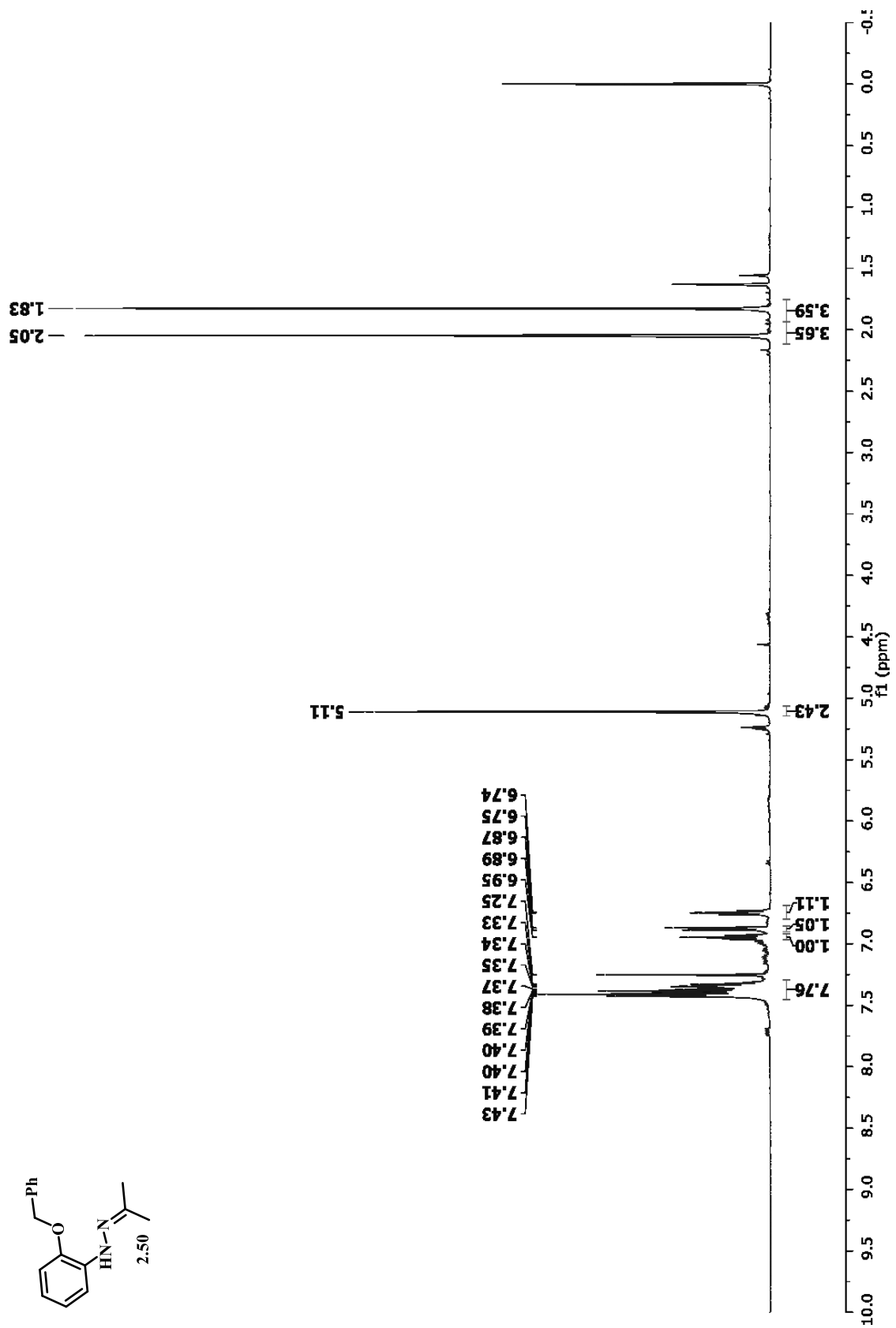


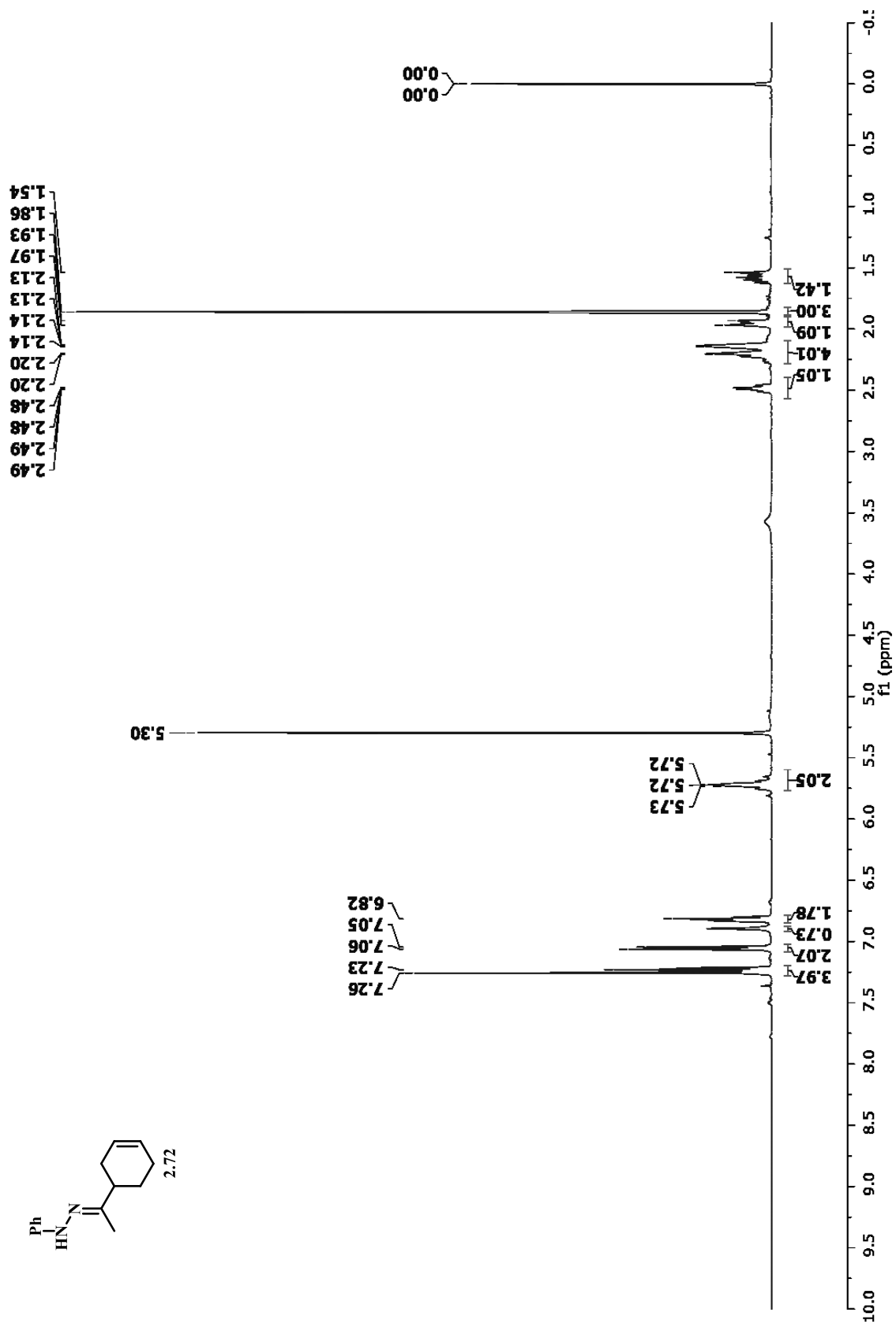


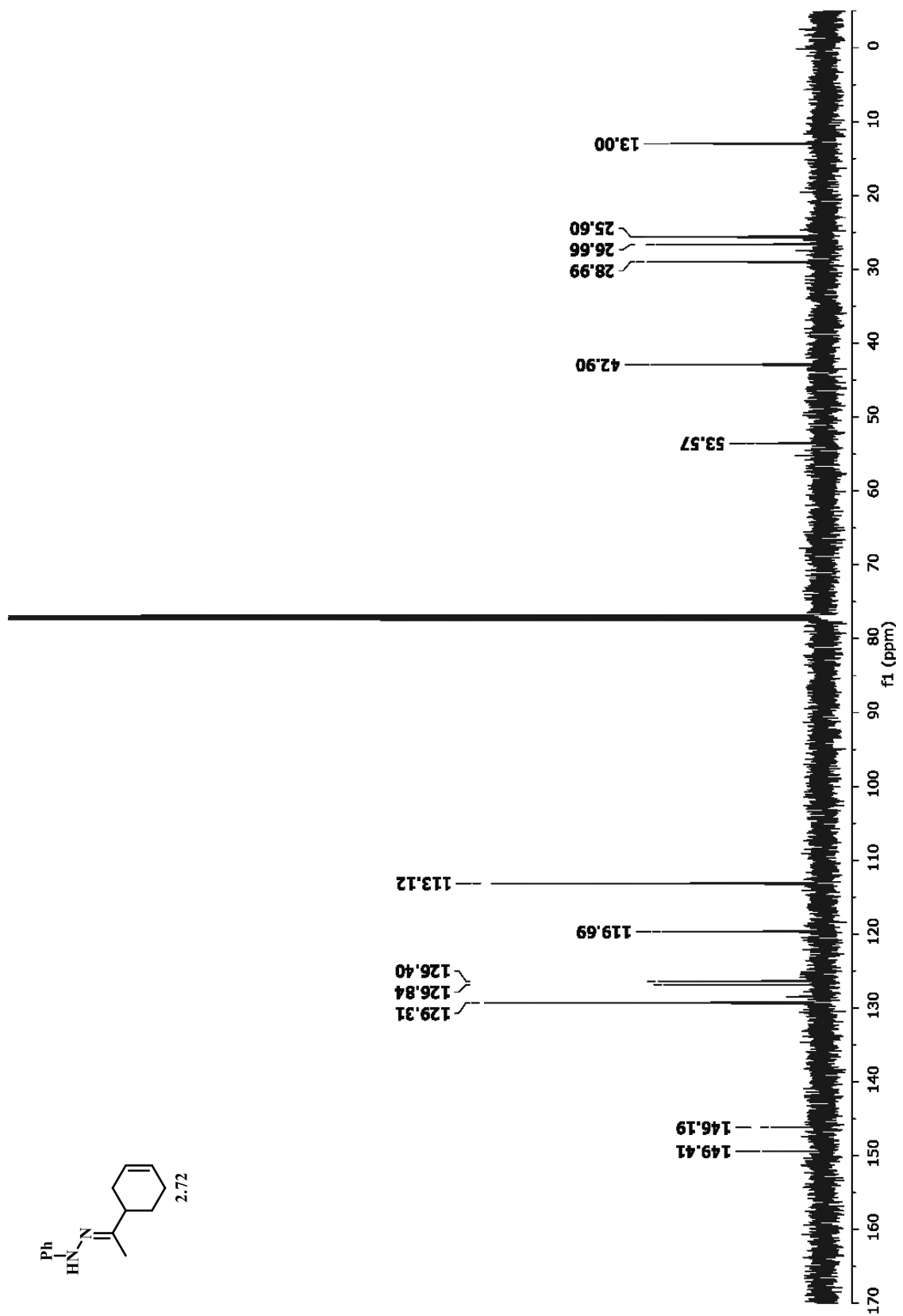


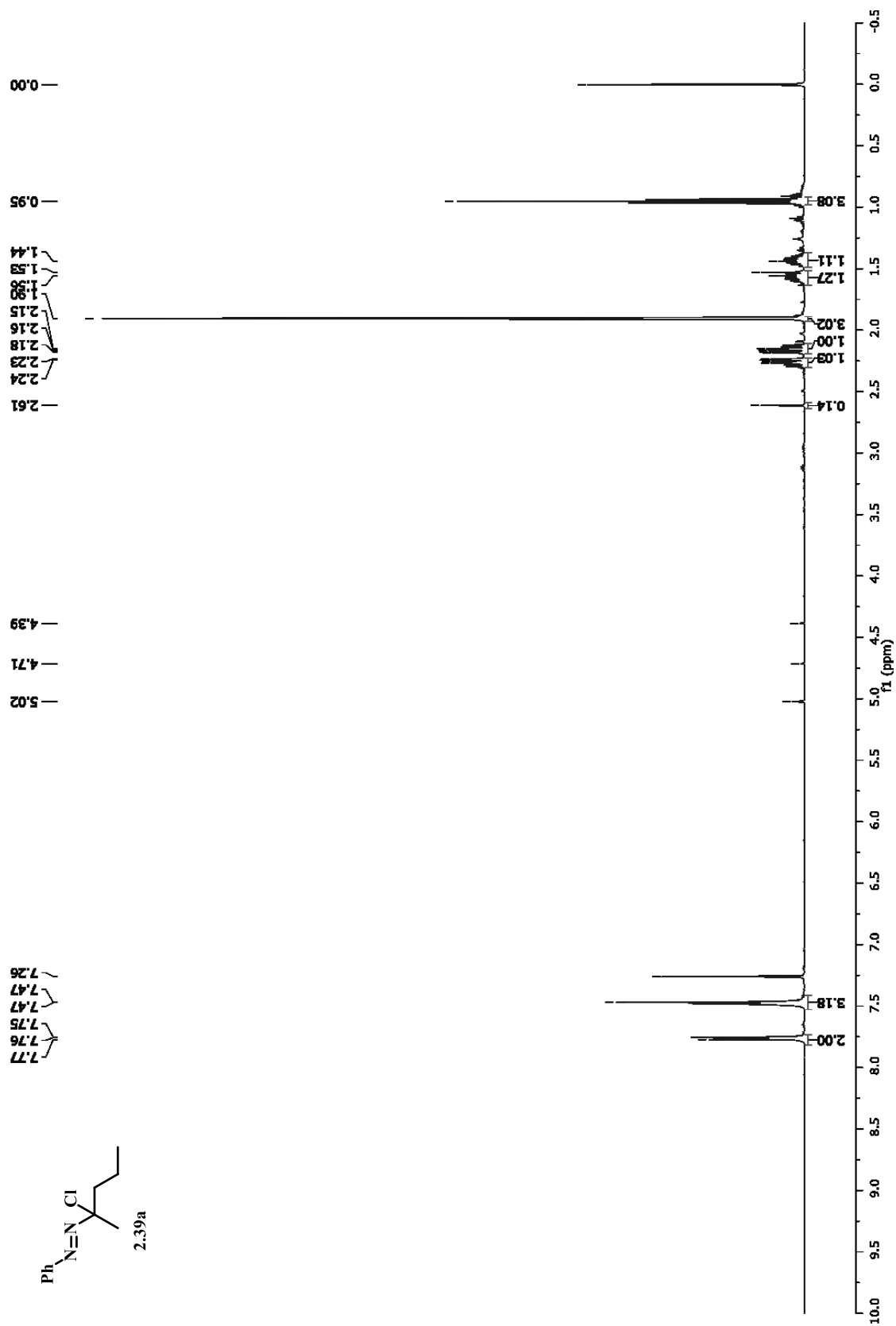


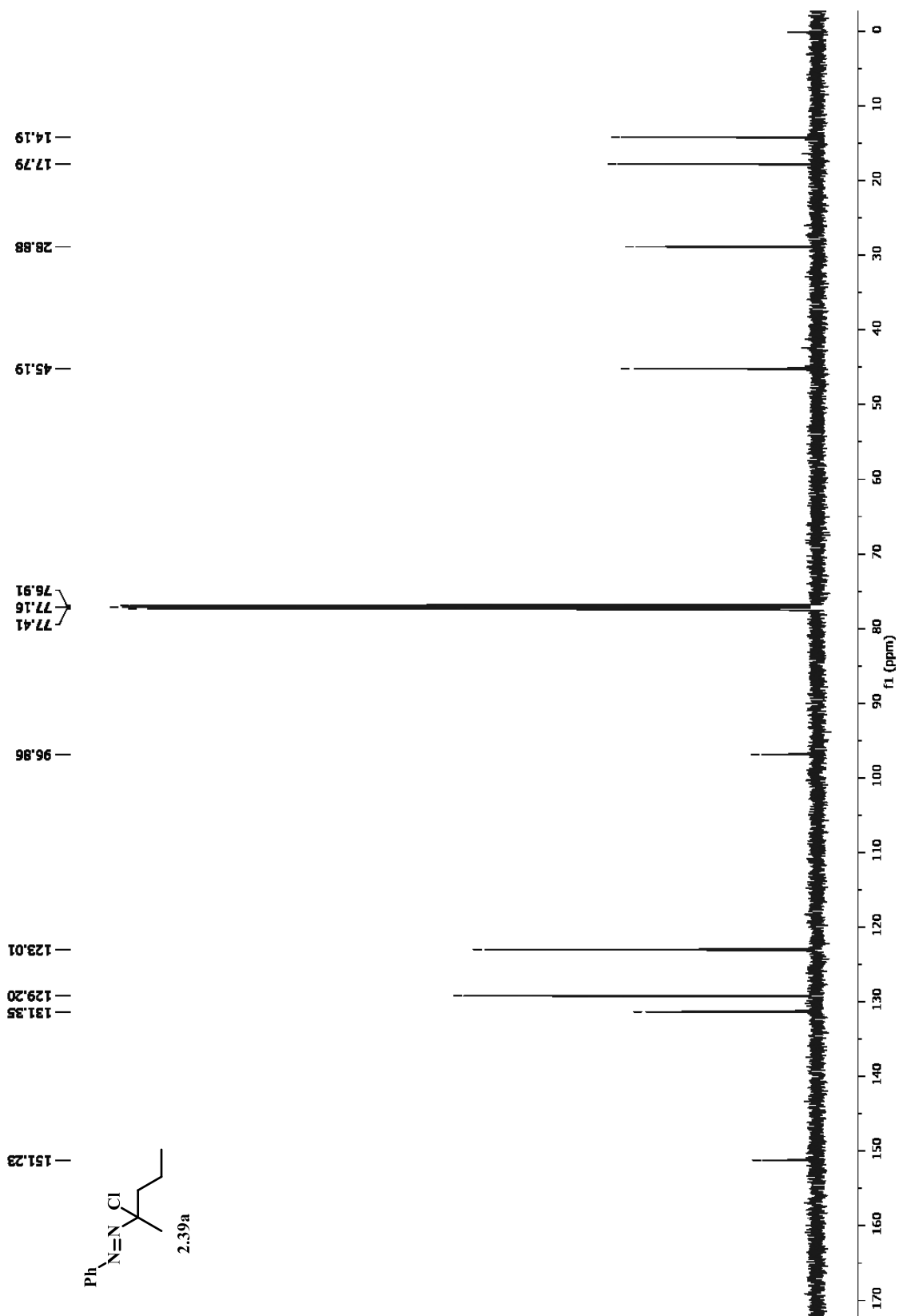


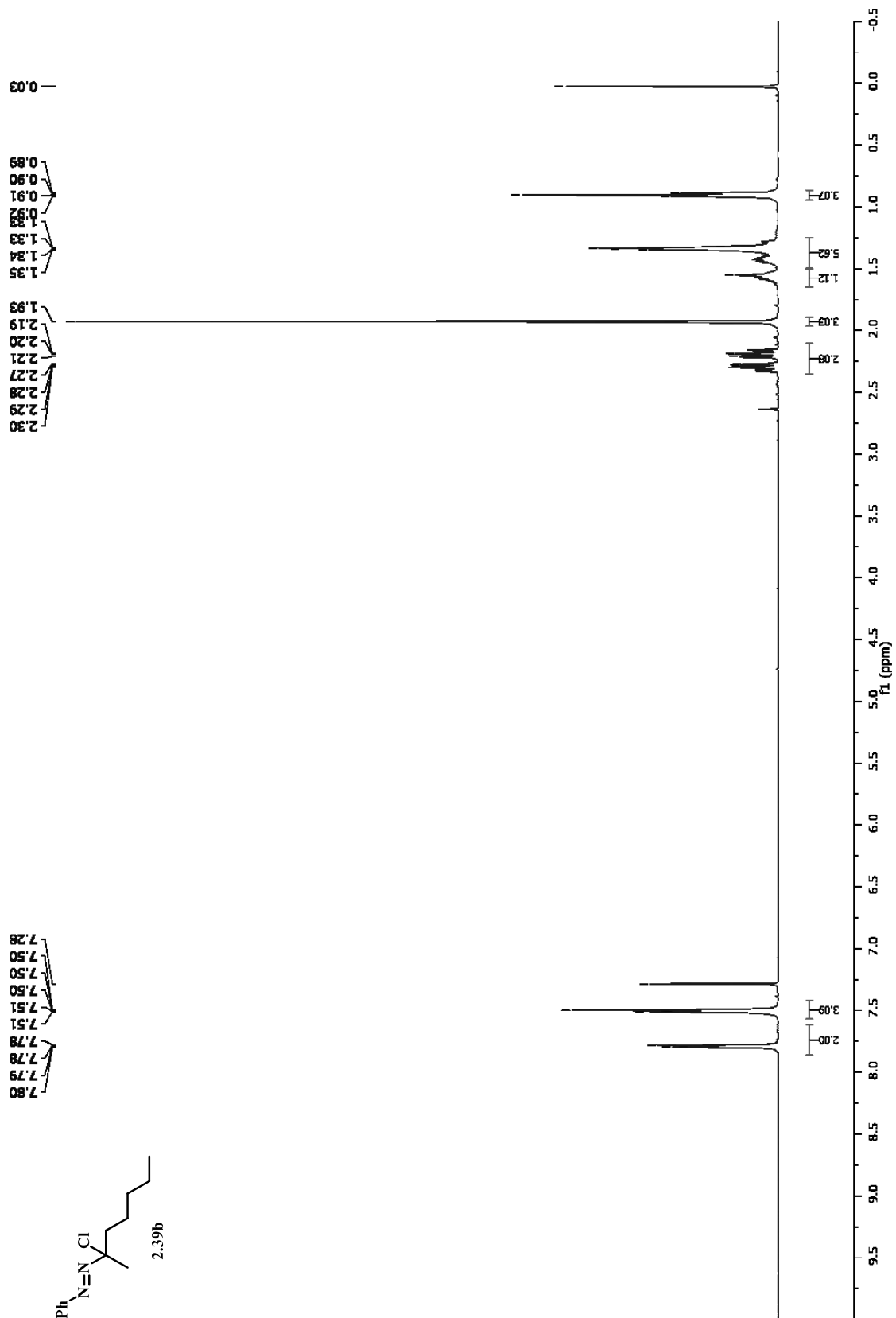


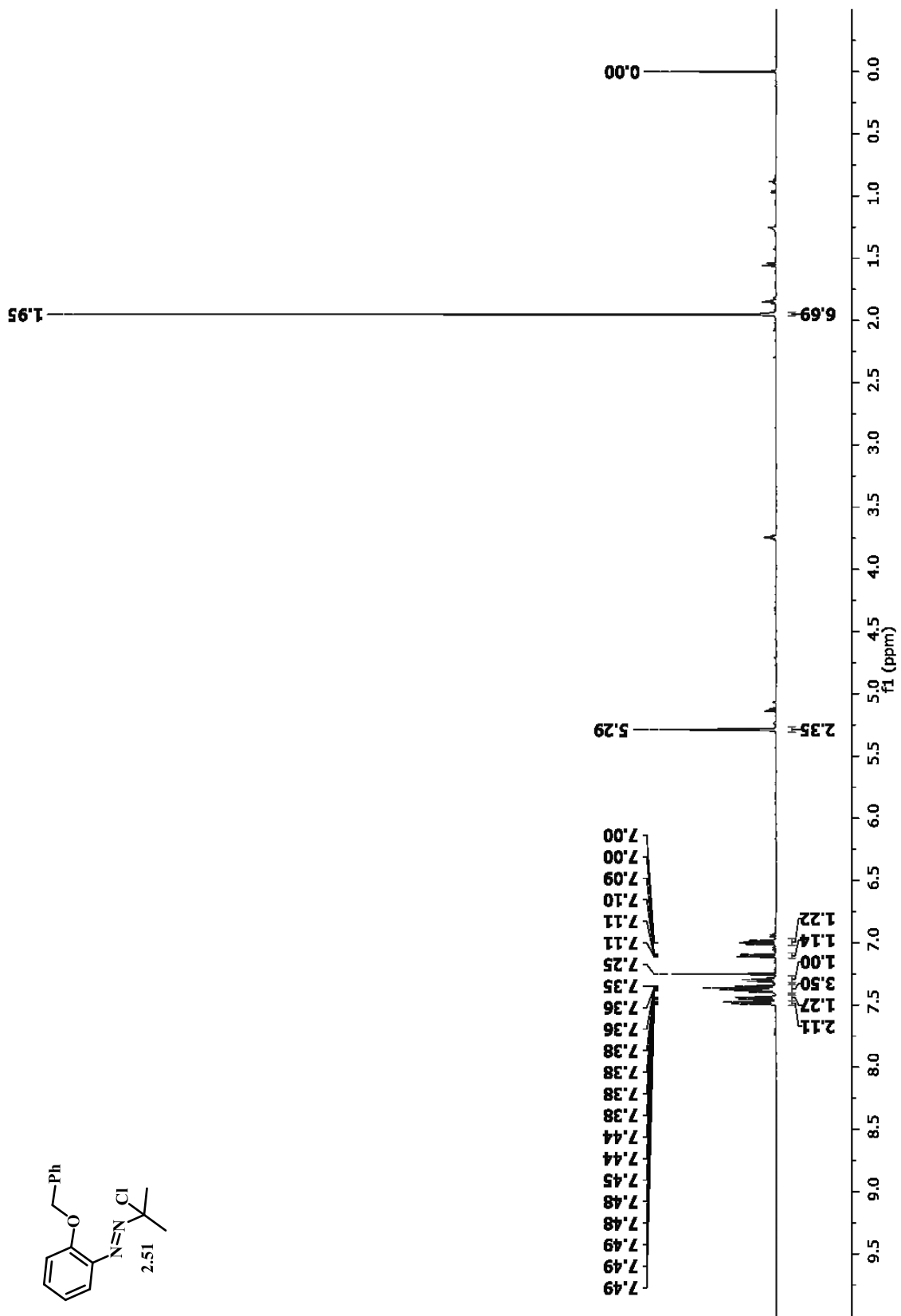


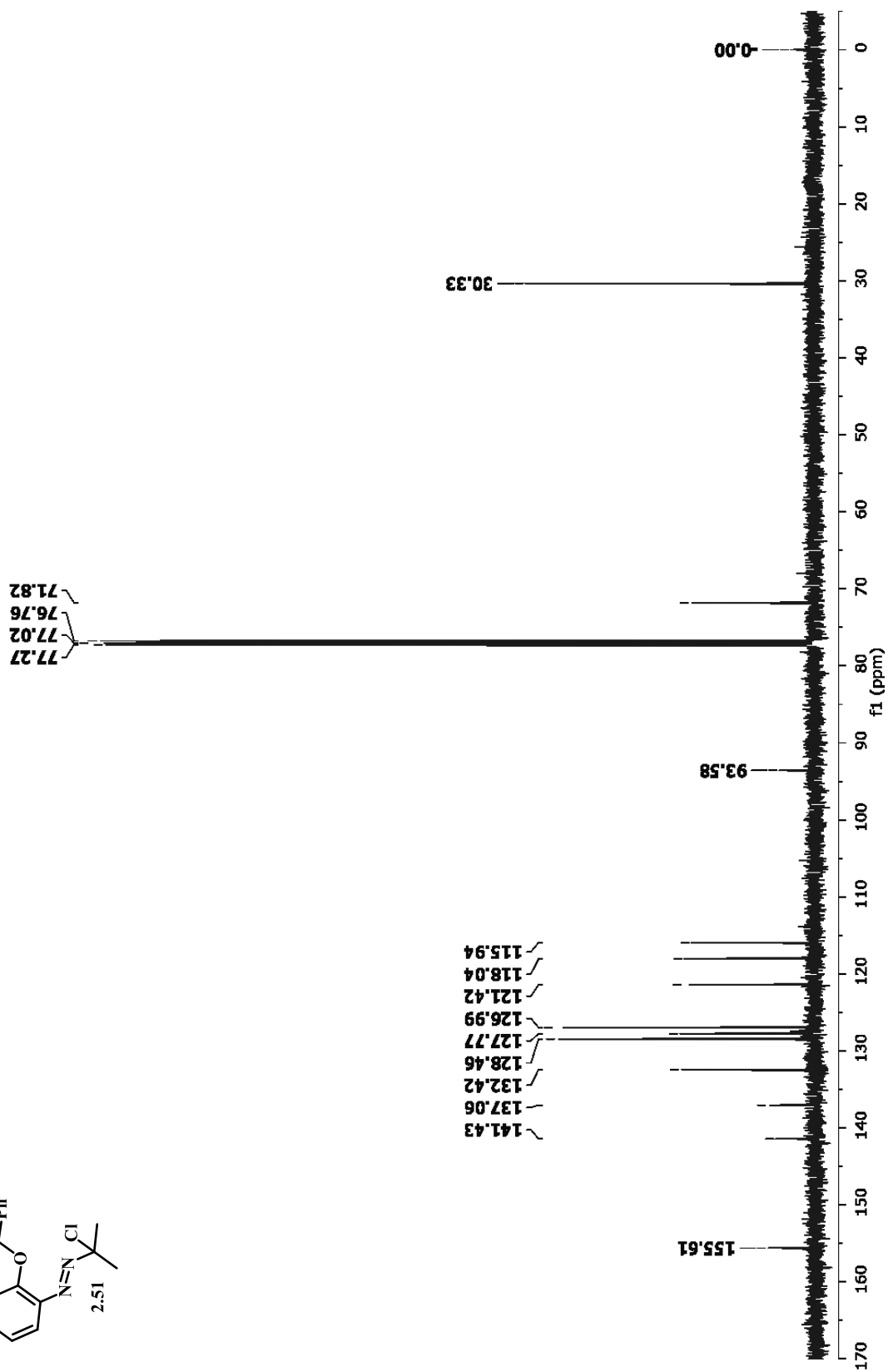
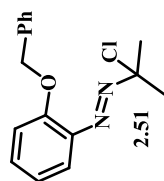


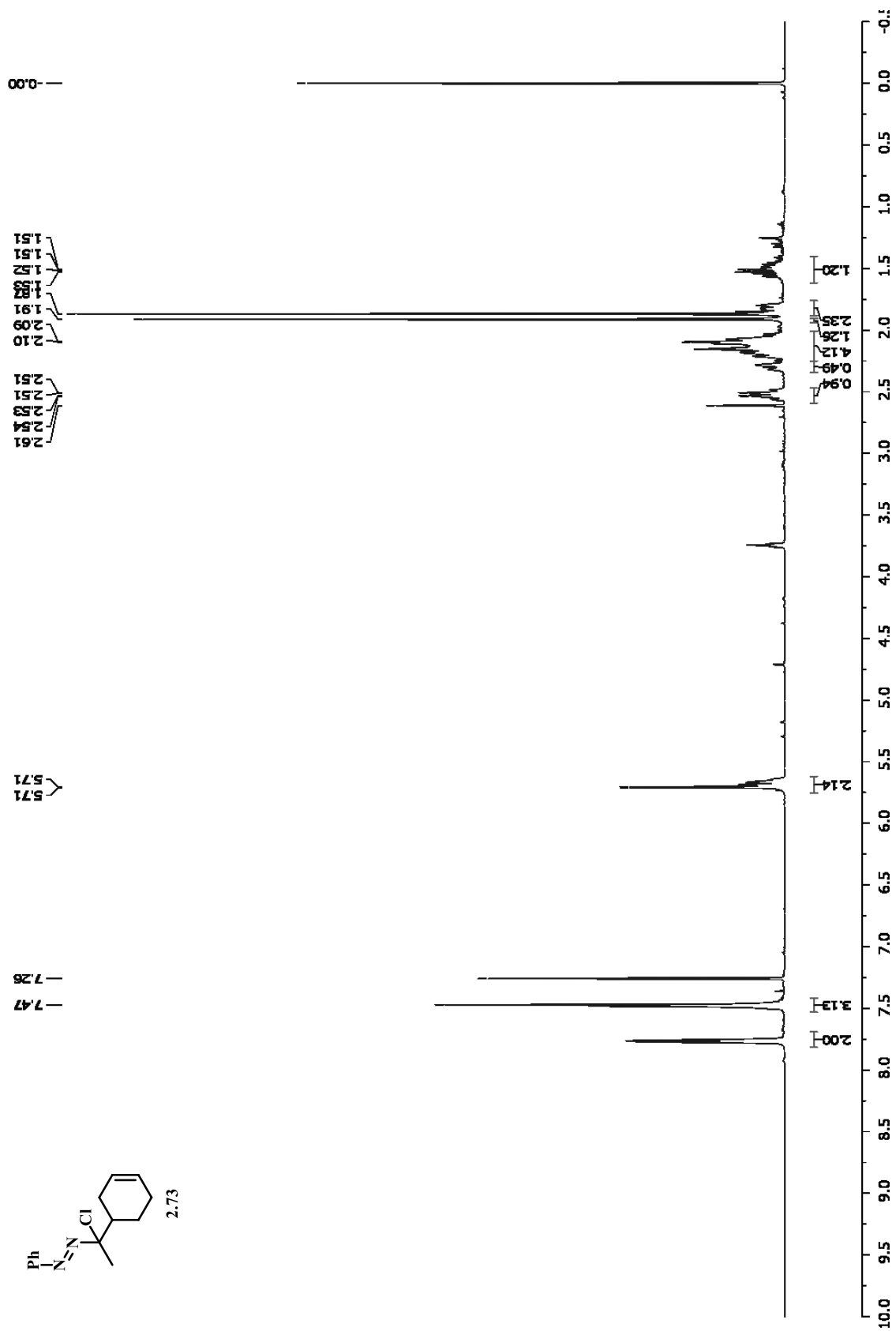


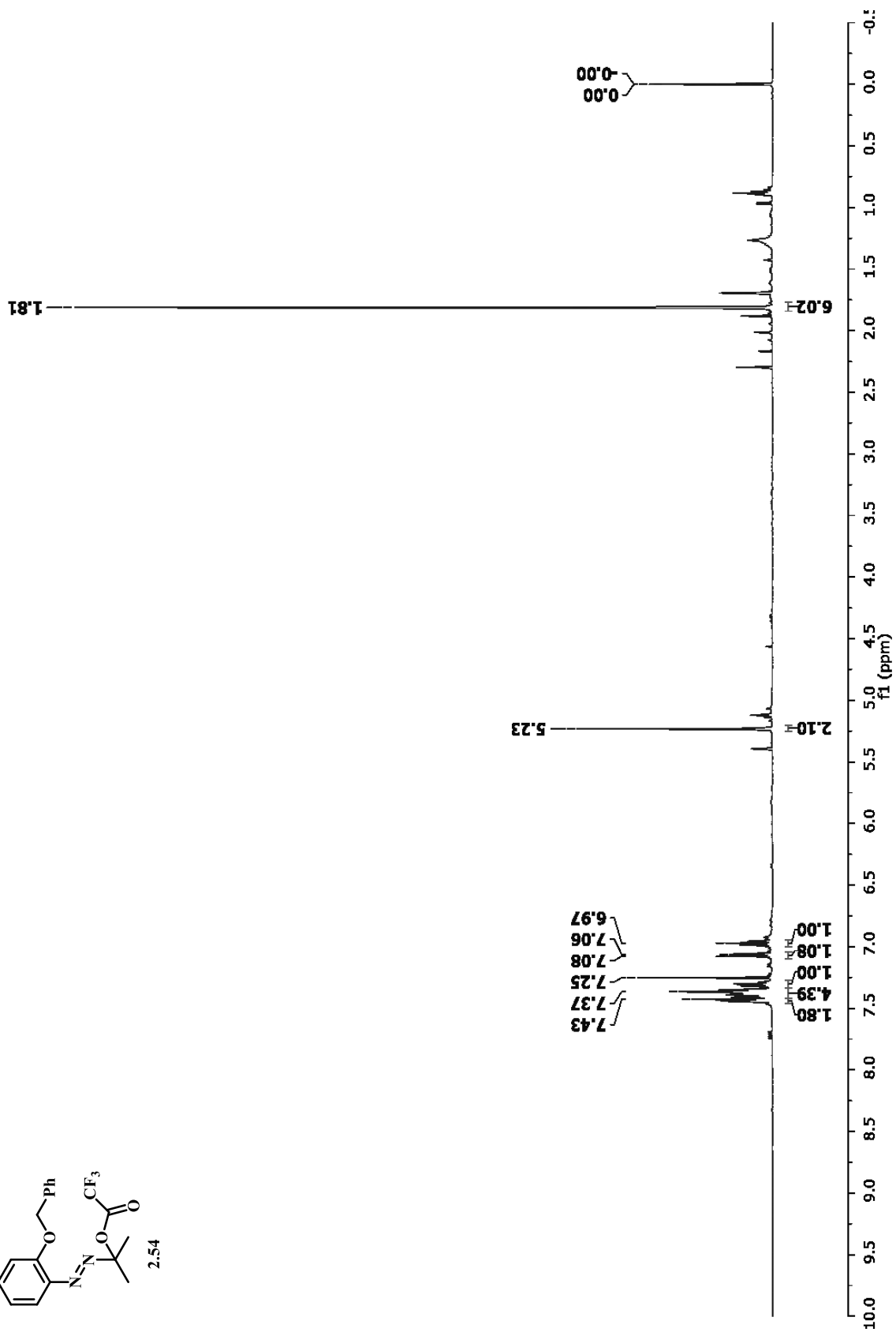
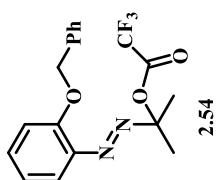




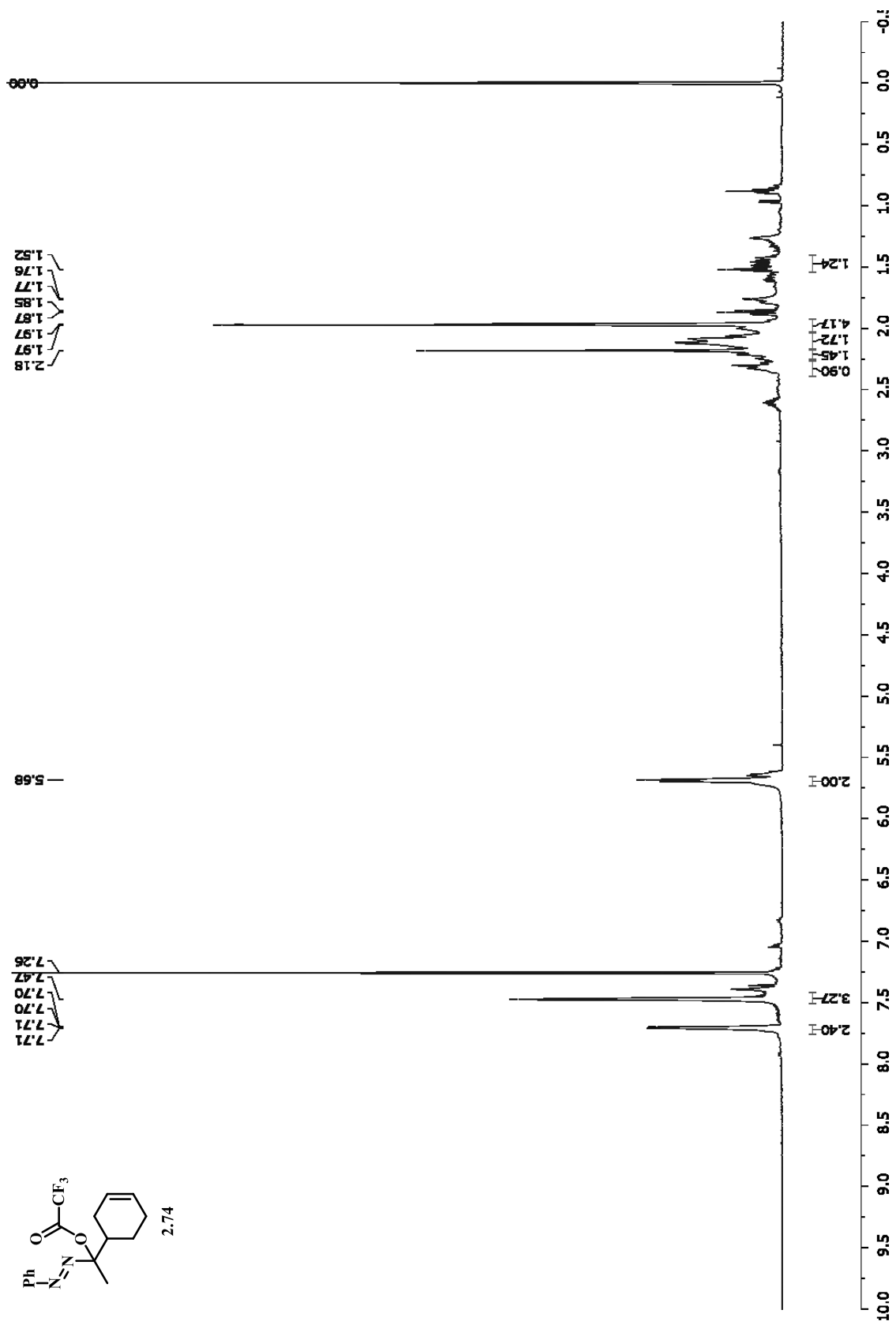




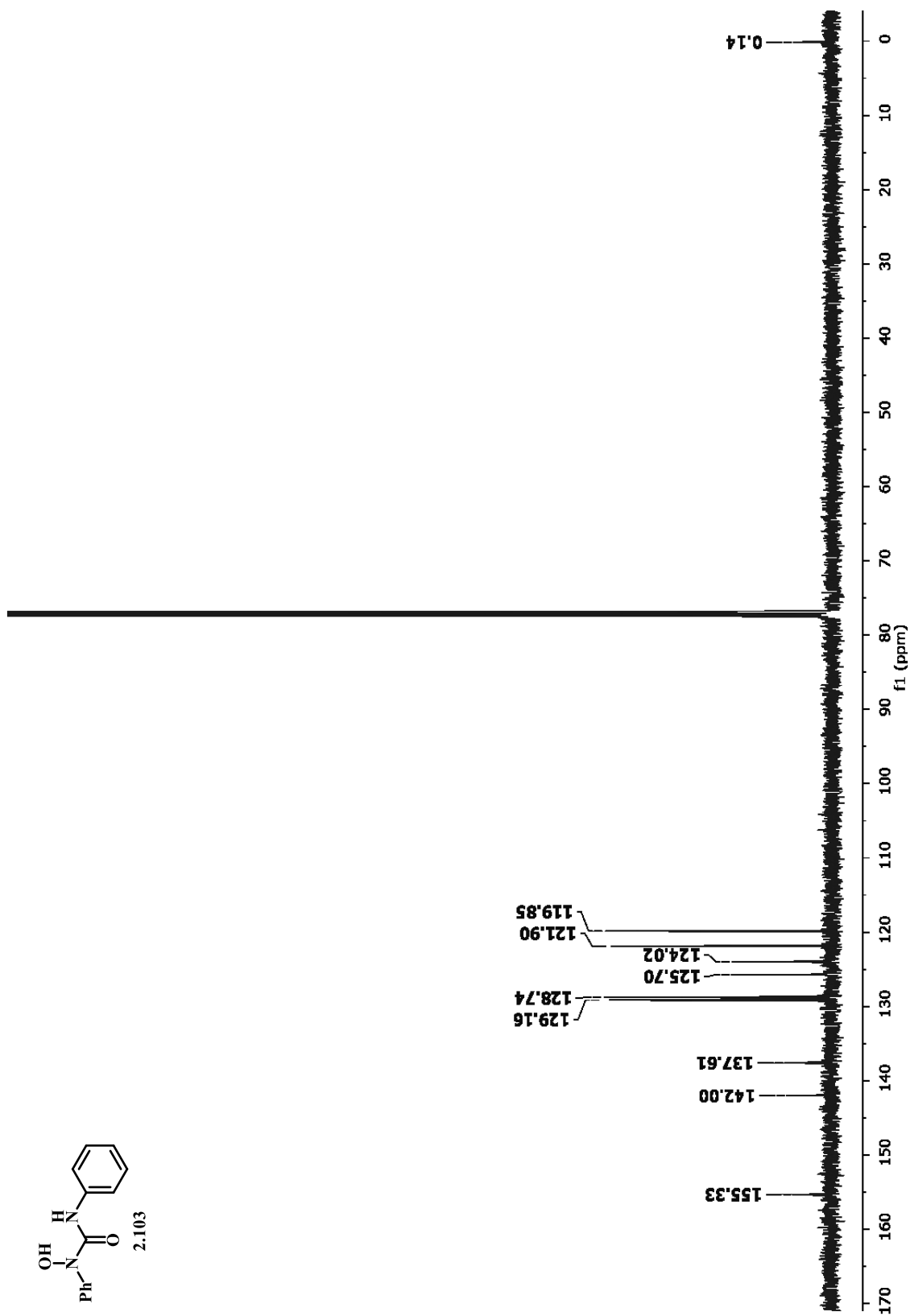


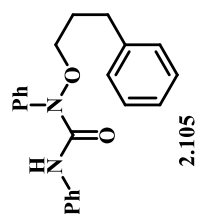
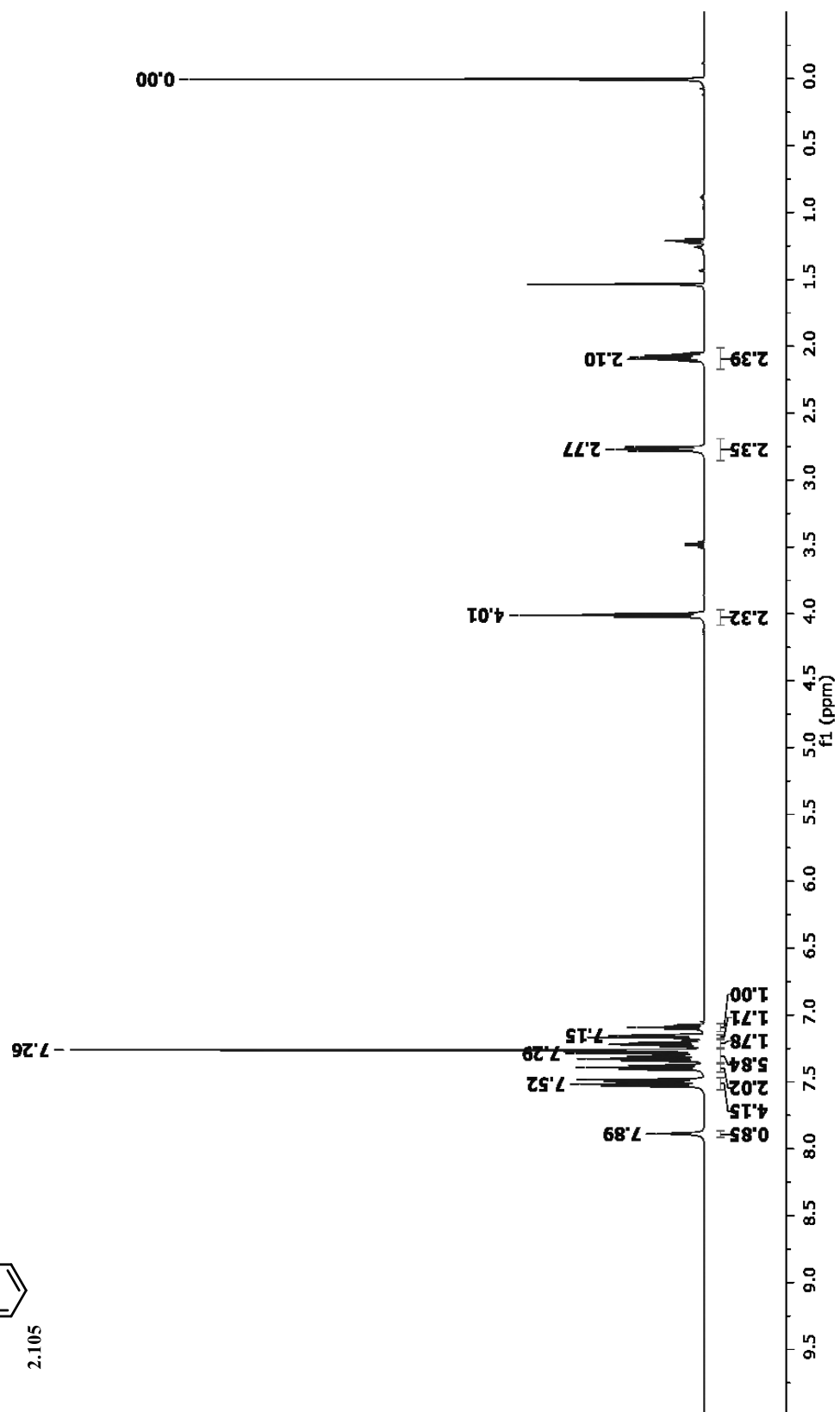


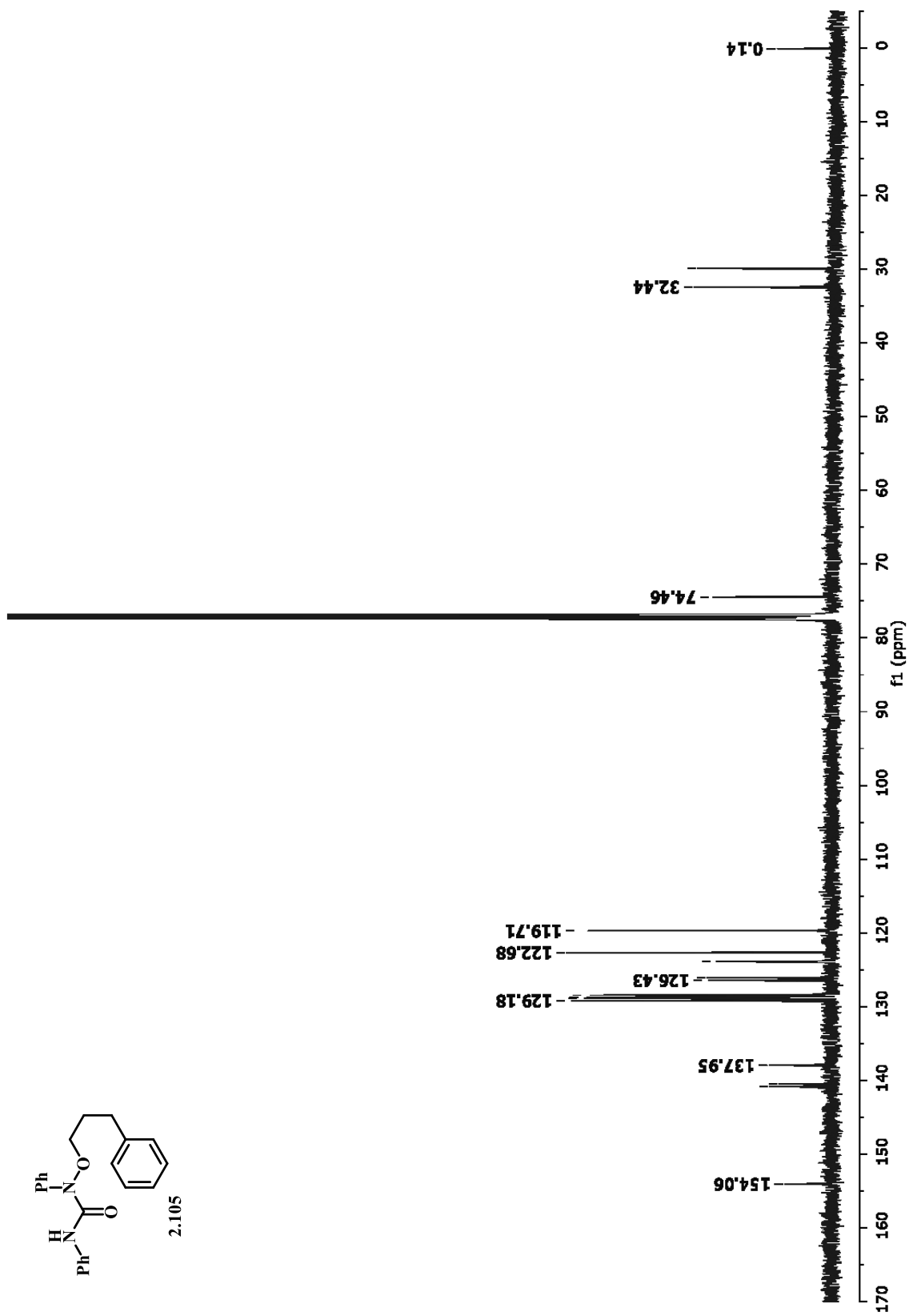


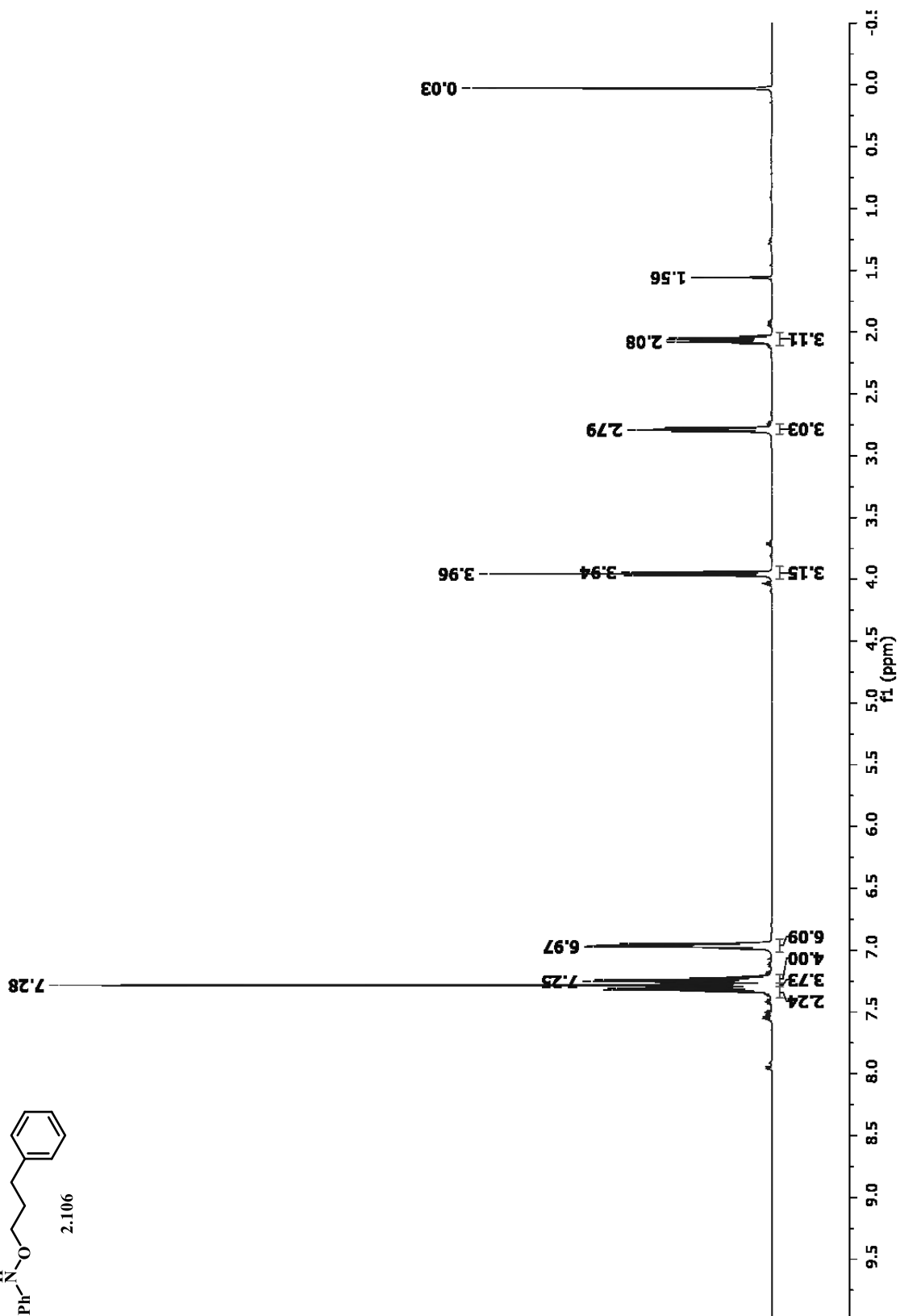
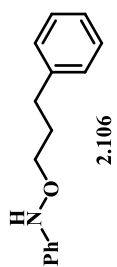


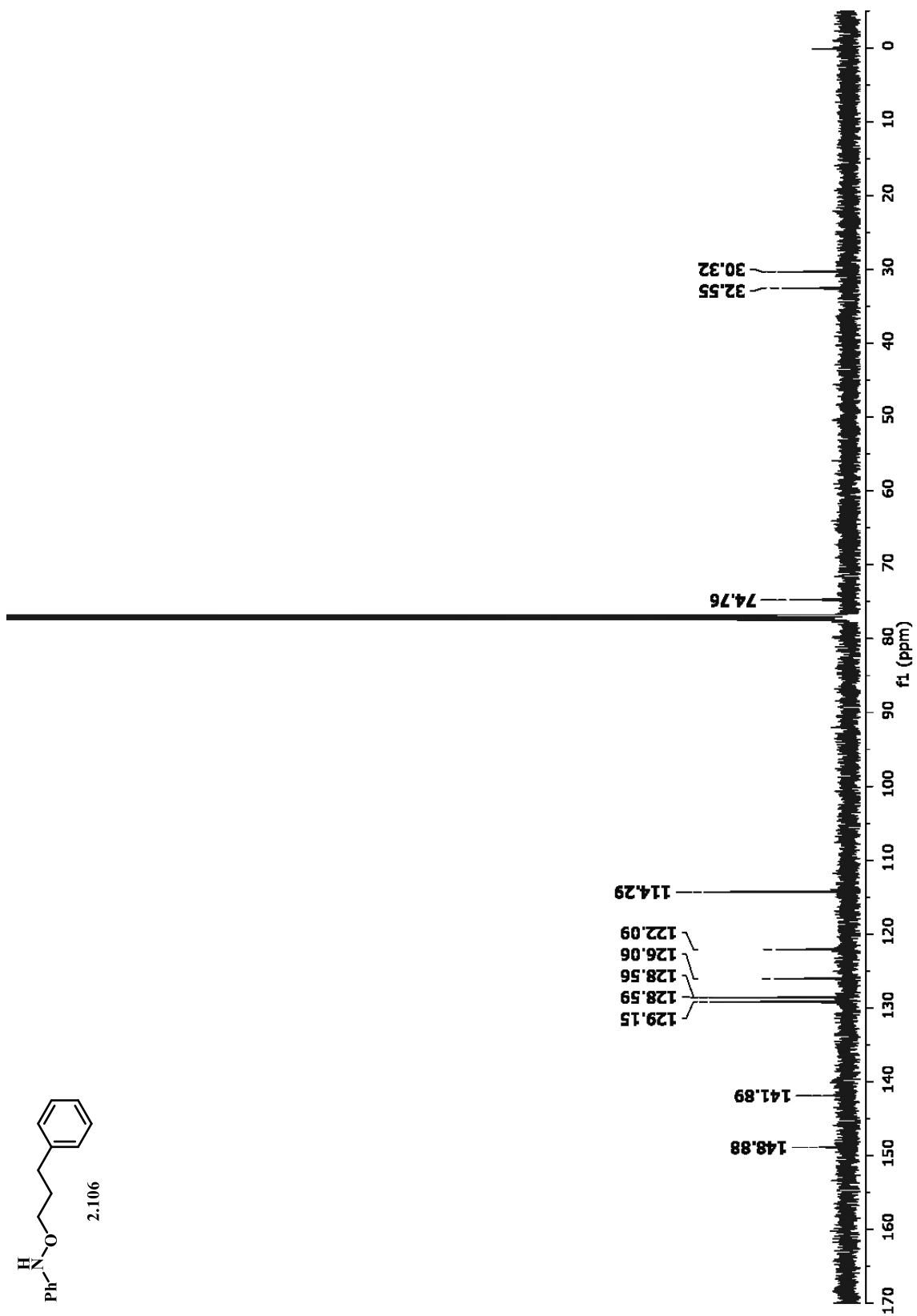


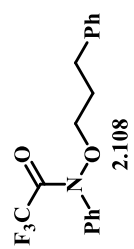












7.48
7.47
7.26
7.25
7.25
7.18
7.12

10.51
10.50

3.96
3.94
3.93

2.70
2.69

2.01
2.00
1.98

-0.00
-0.00

1.00

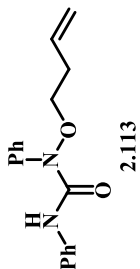
4.44
4.61

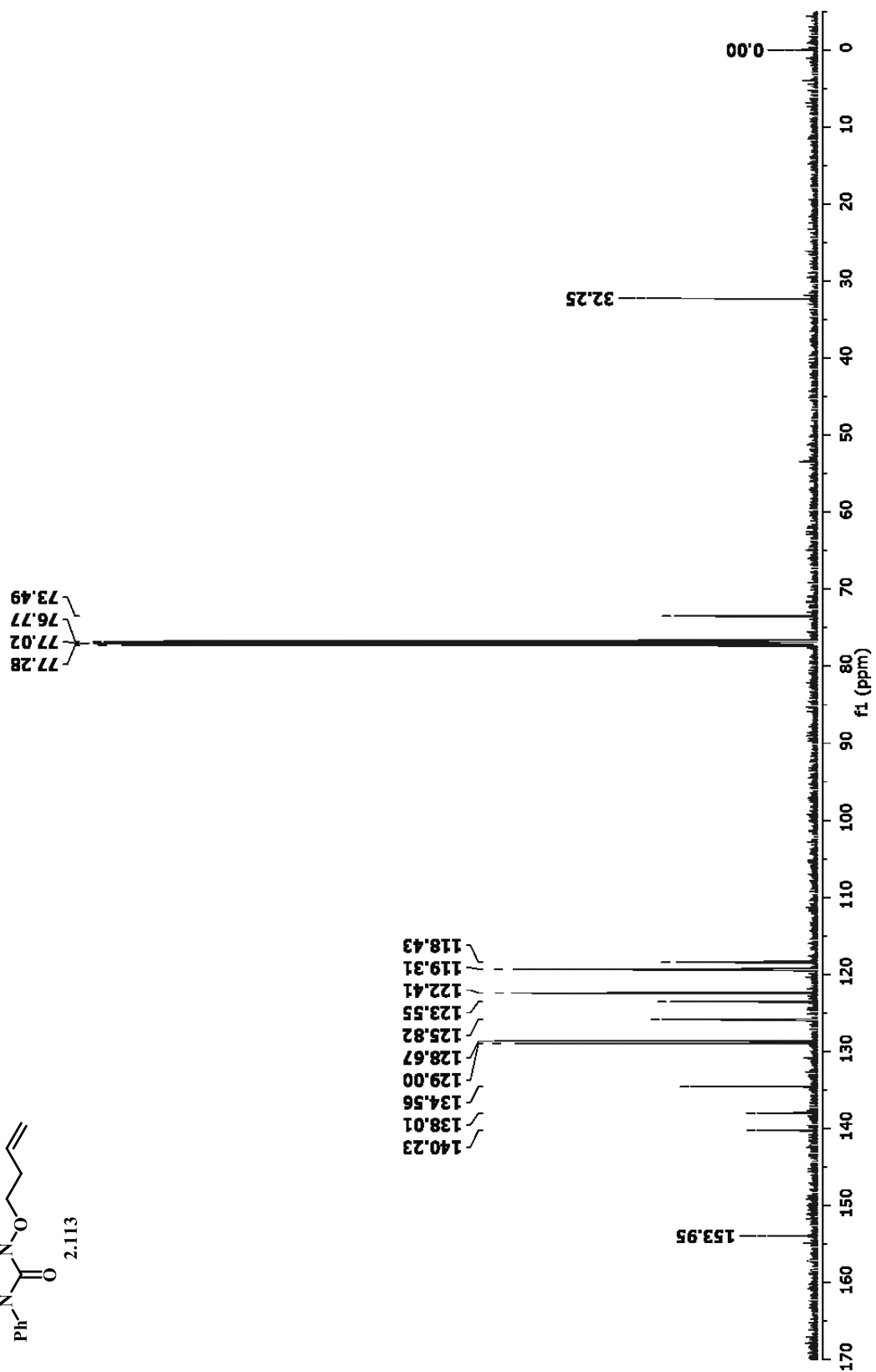
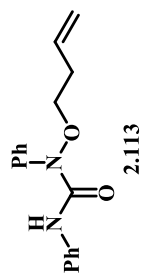
2.16
2.15

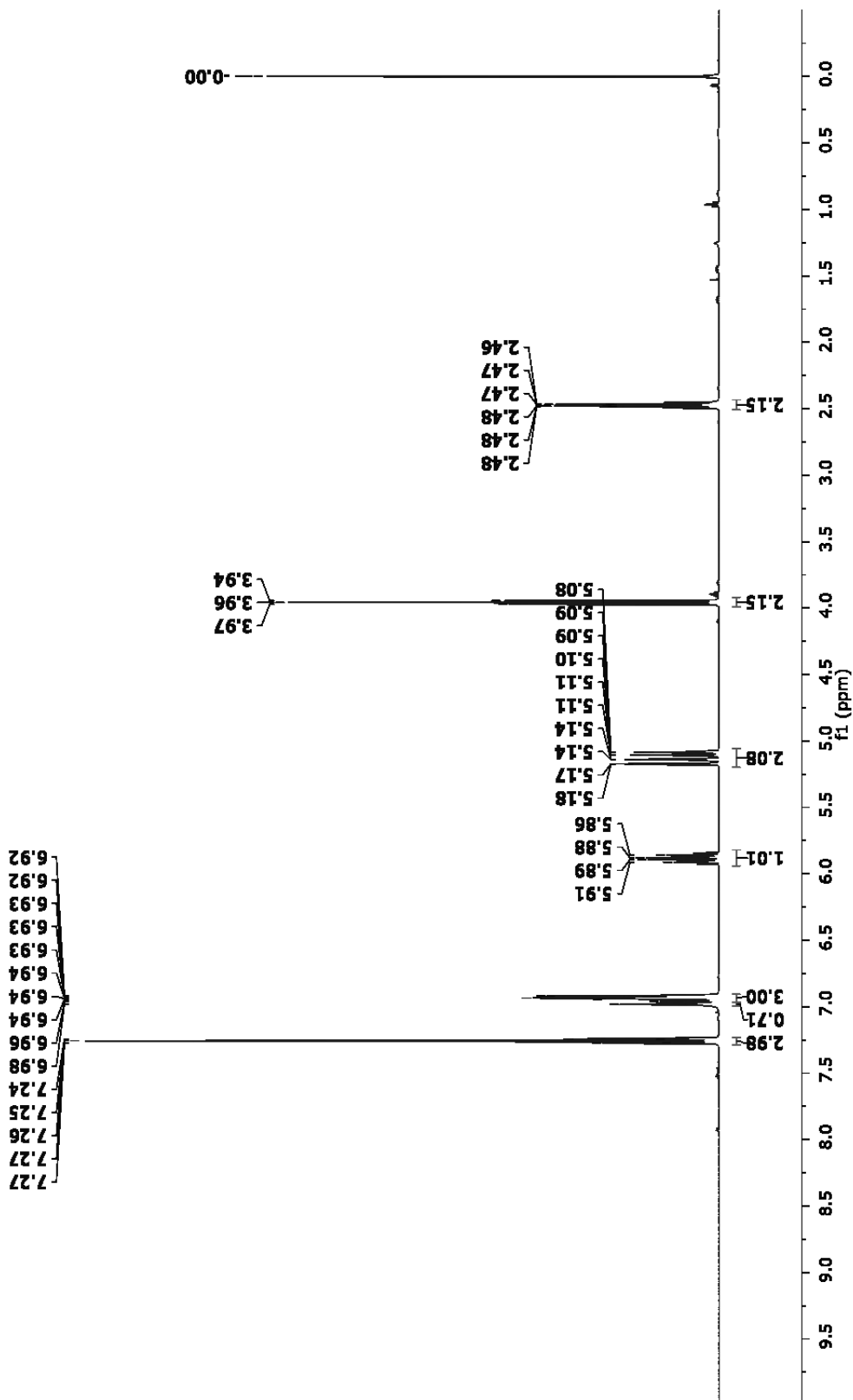
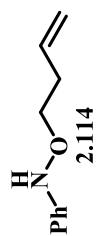
2.20

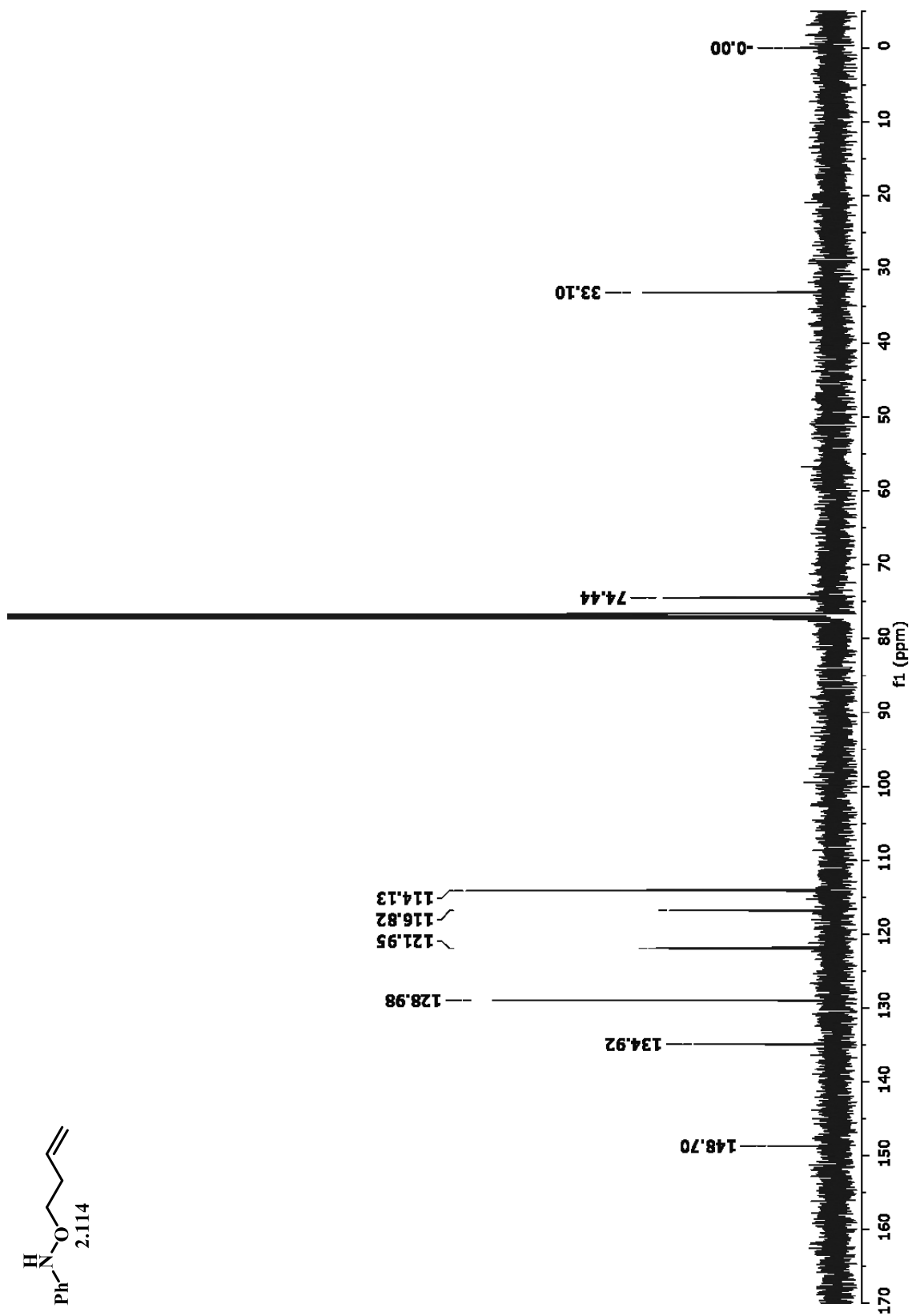
11.0 10.5 10.0 9.5 9.0 8.5 8.0 7.5 7.0 6.5 6.0 5.5 5.0 4.5 4.0 3.5 3.0 2.5 2.0 1.5 1.0 0.5 0.0 -0.5

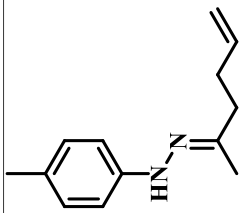
δ (ppm)

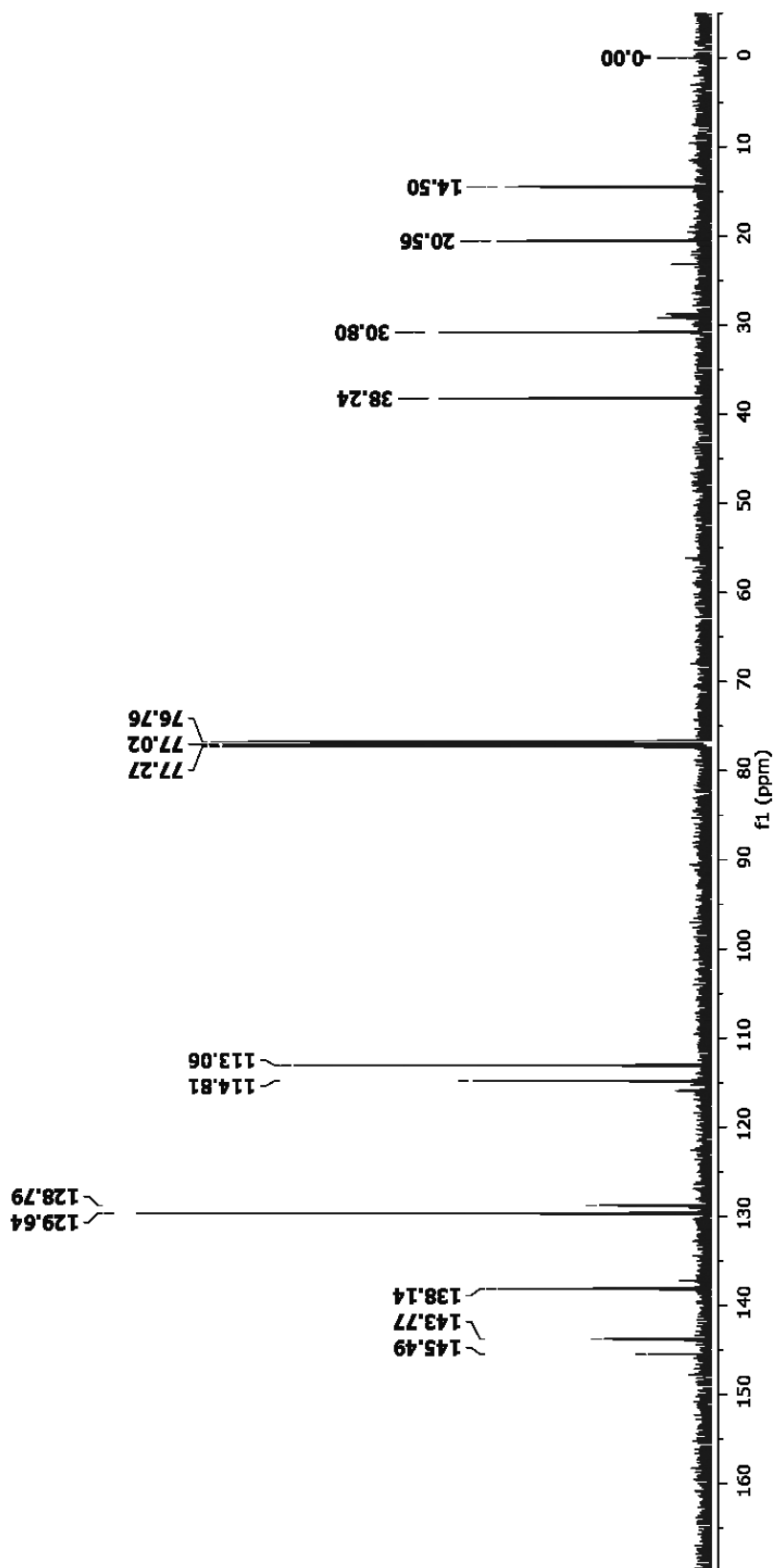
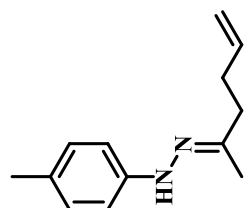


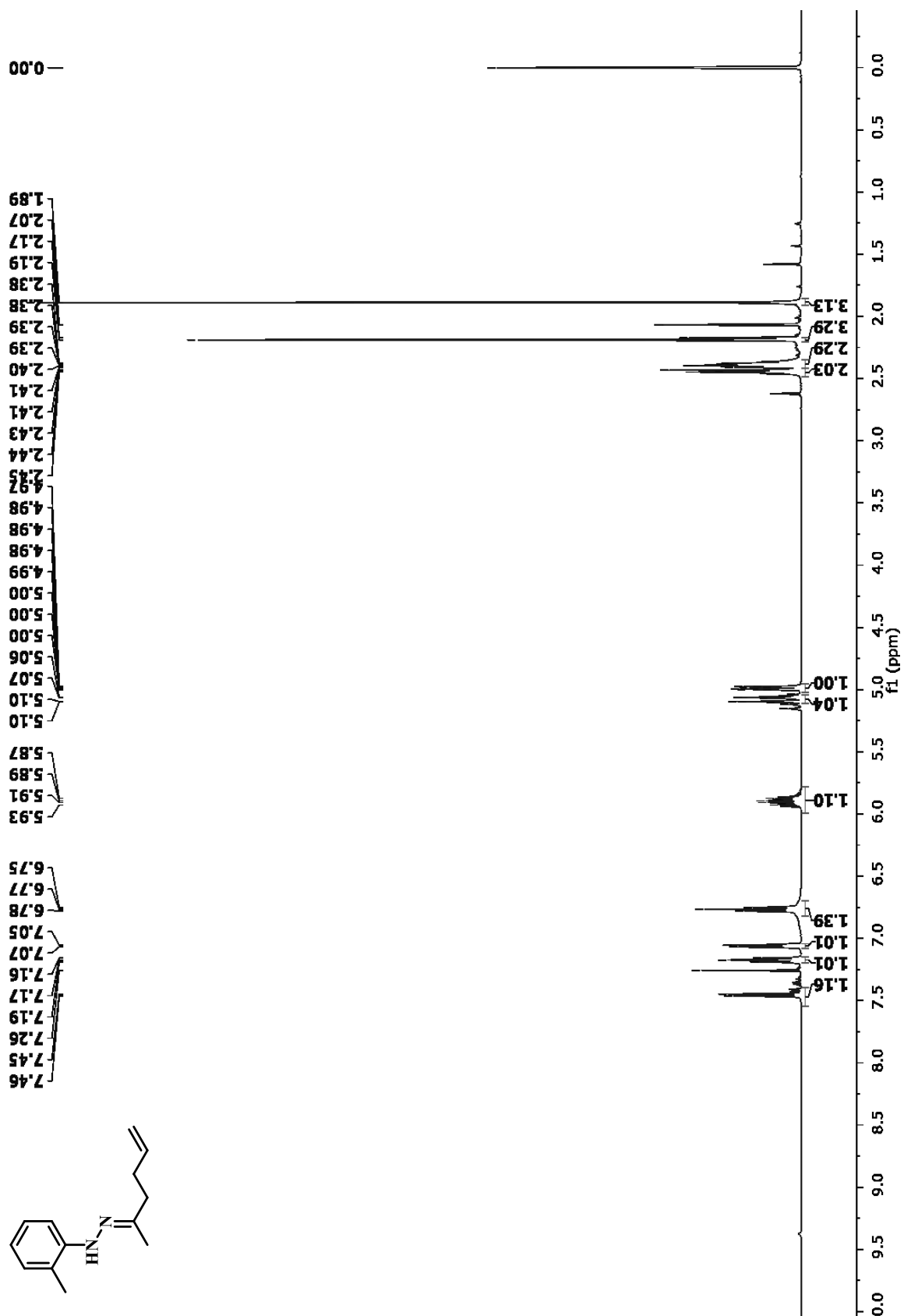


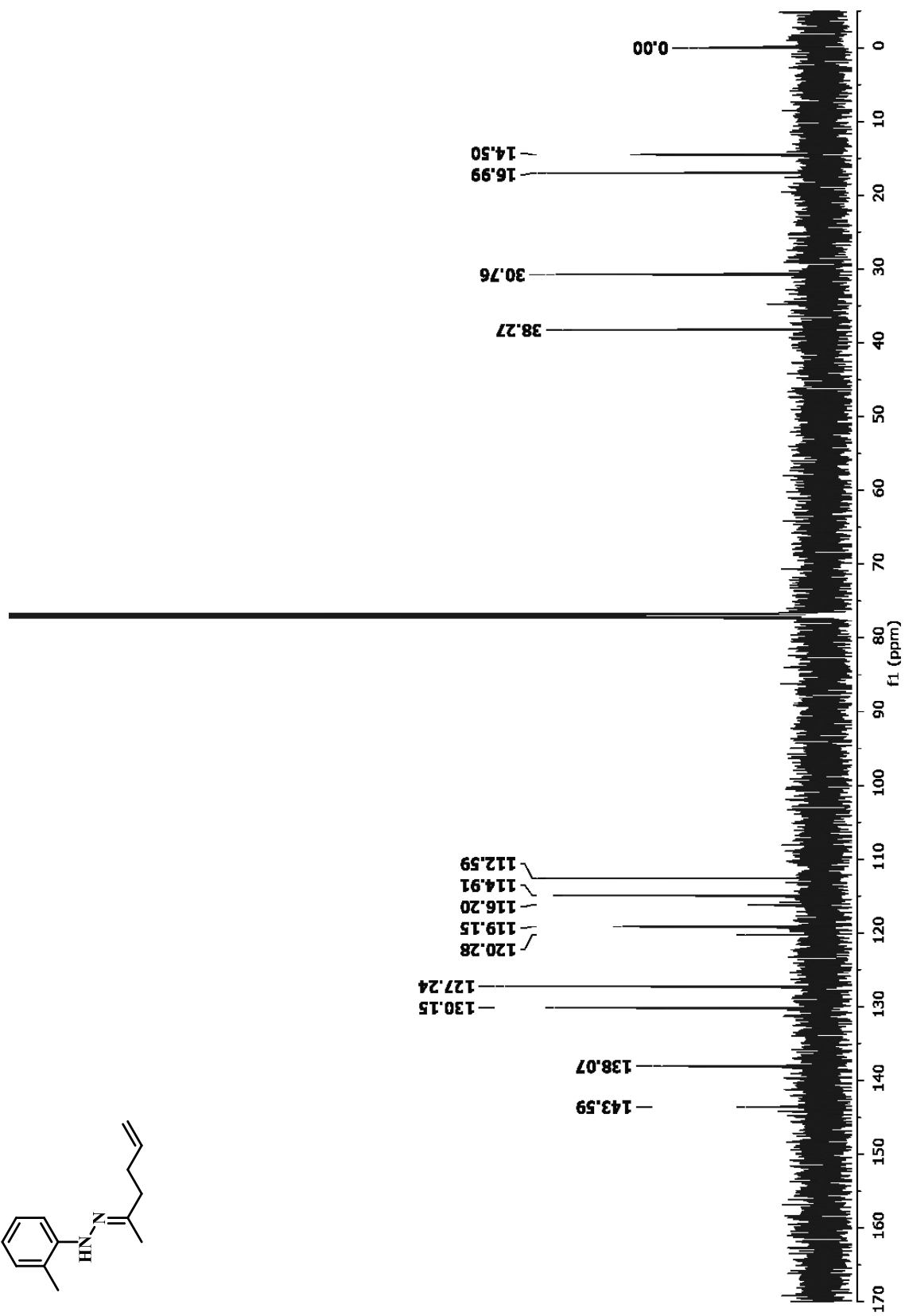
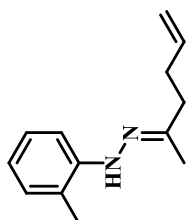


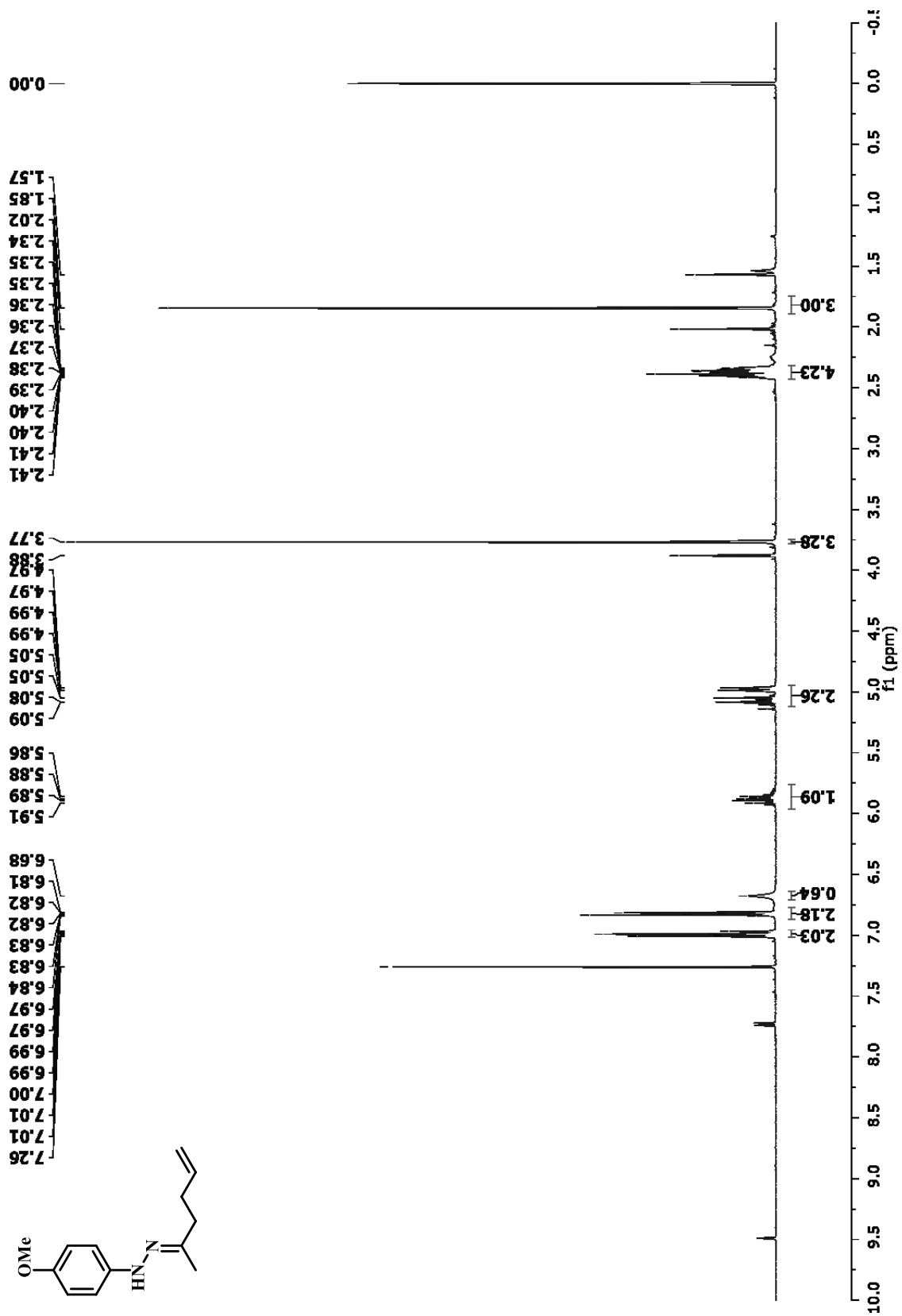


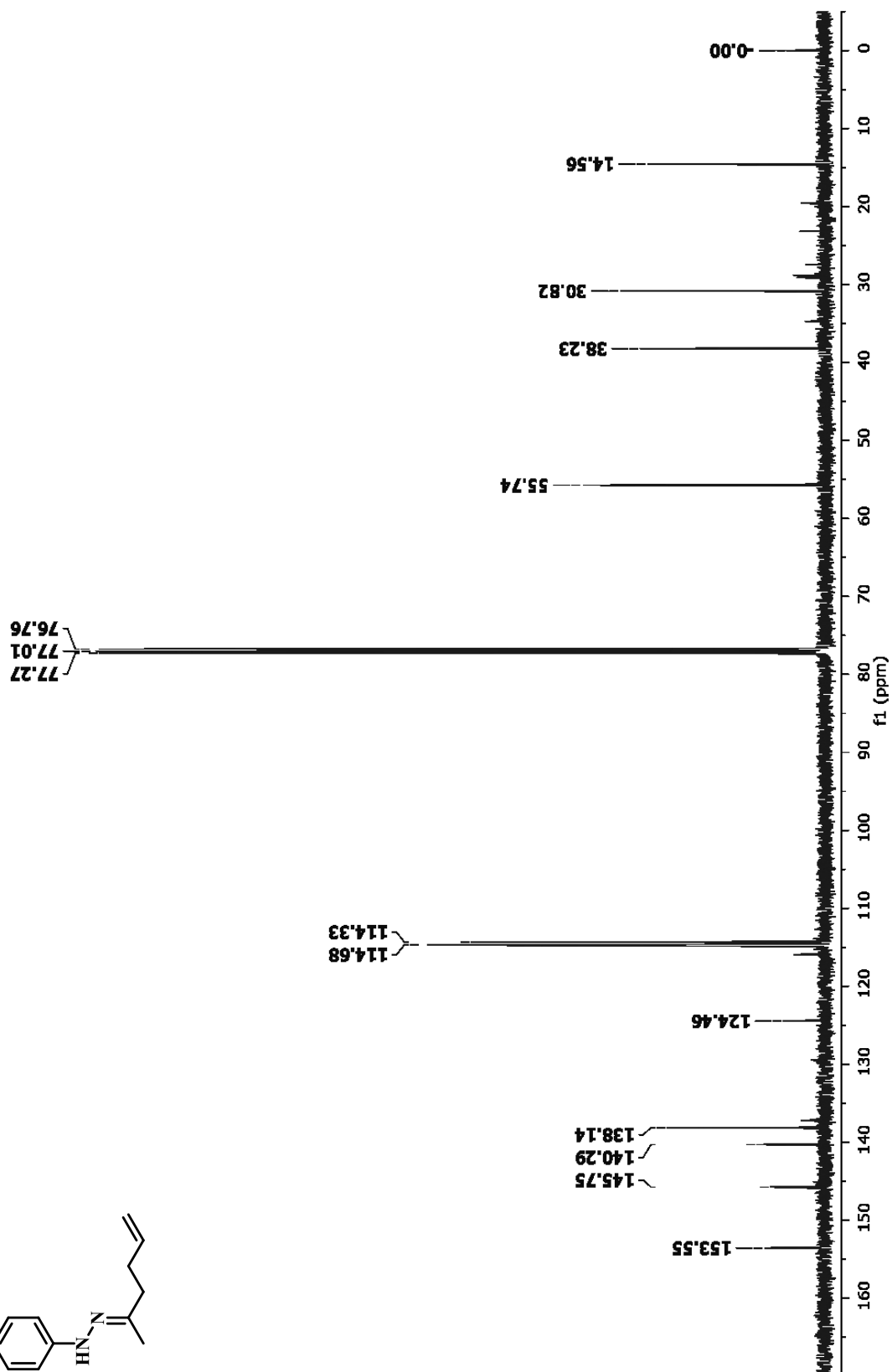
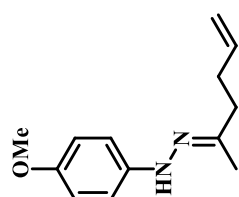


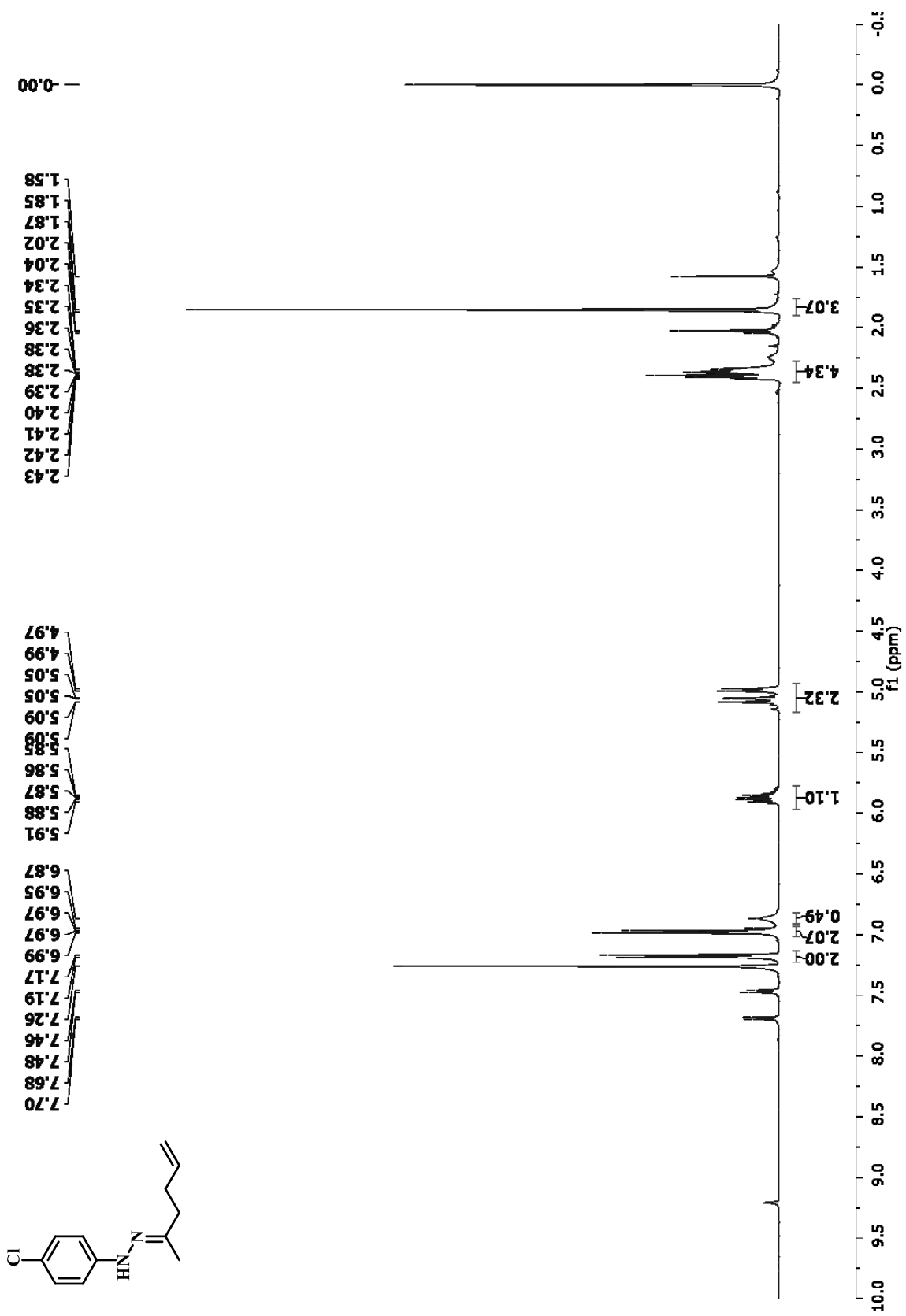


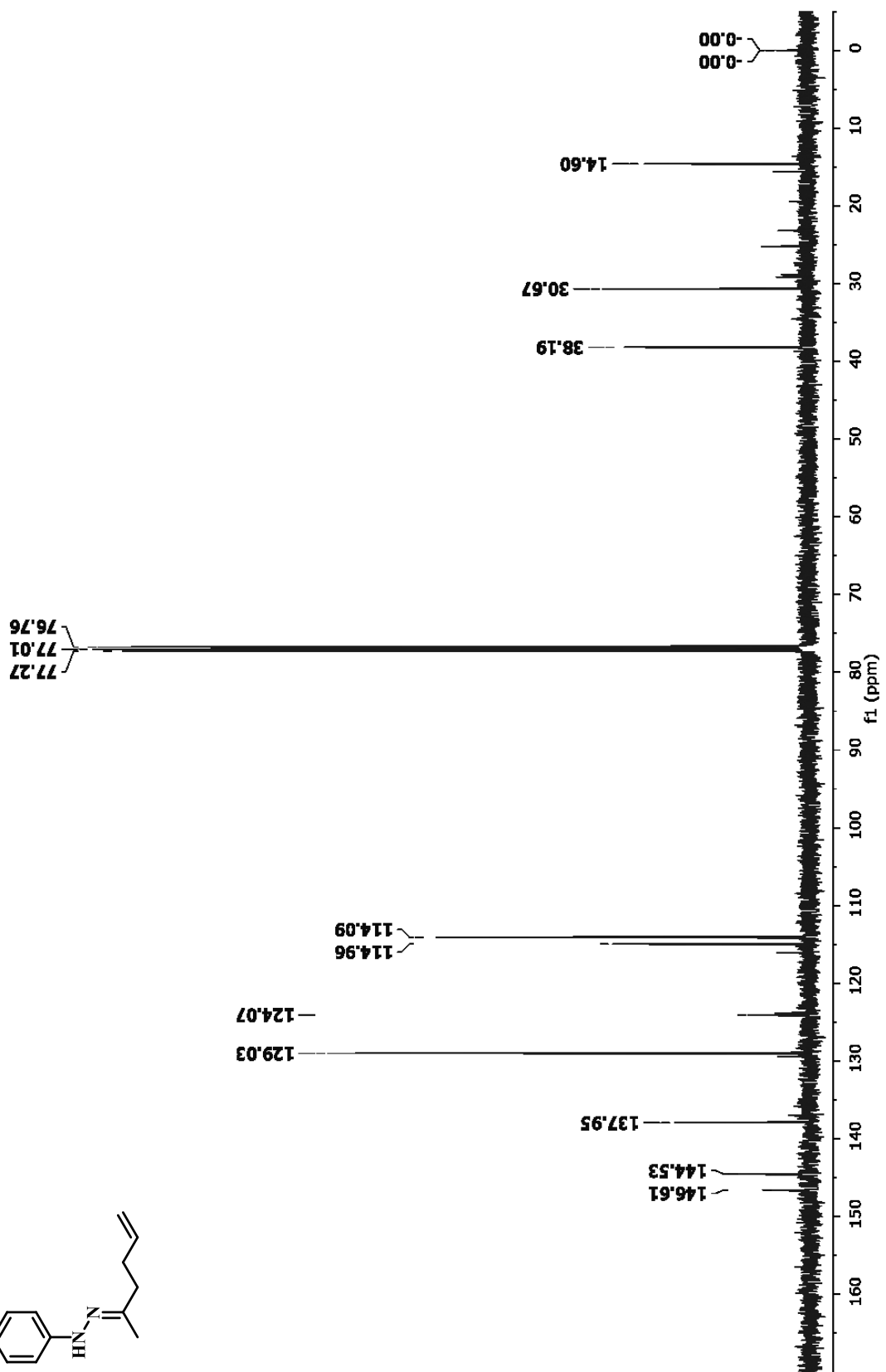
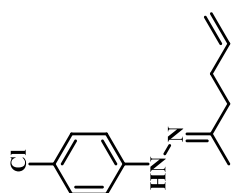


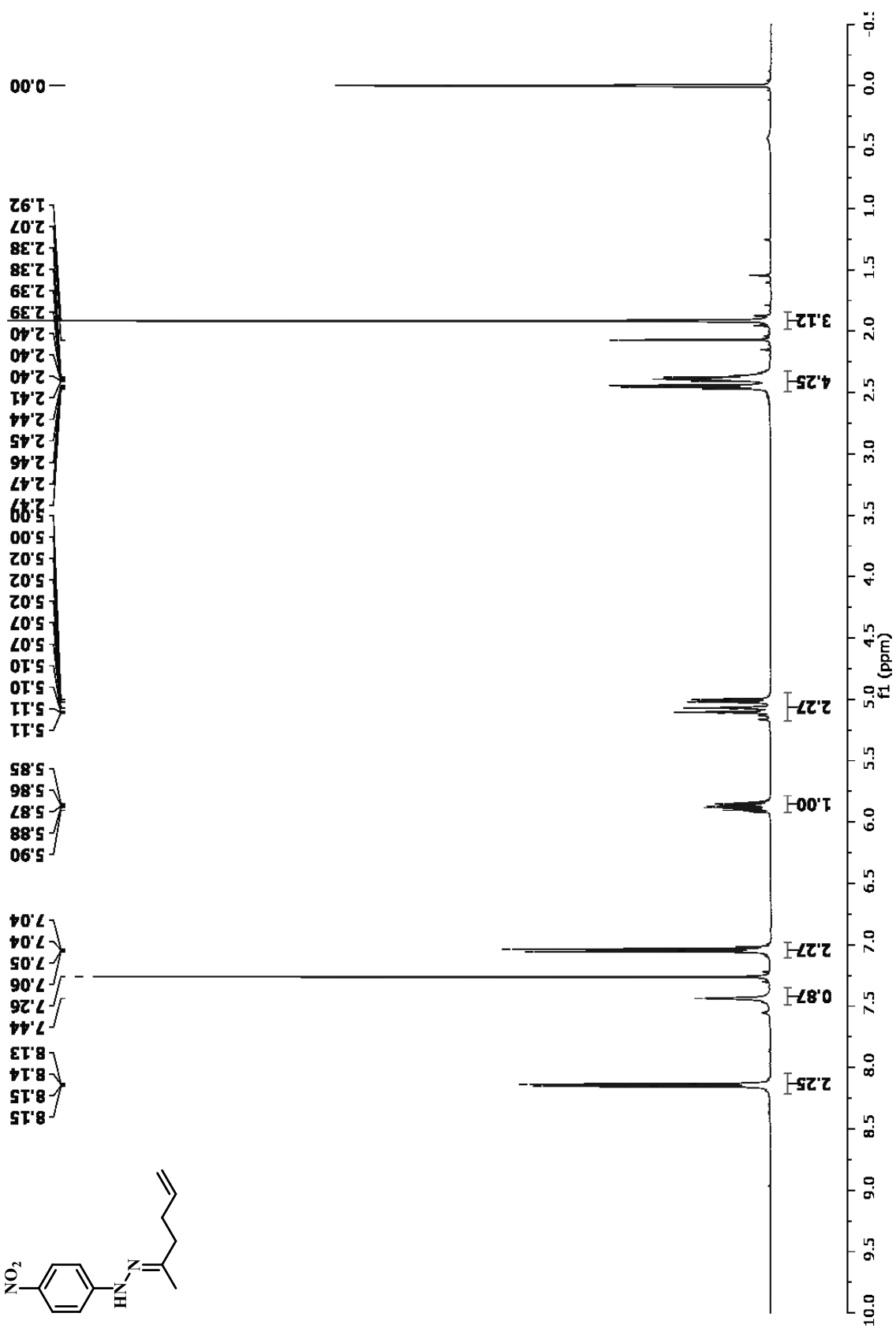
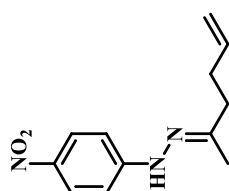


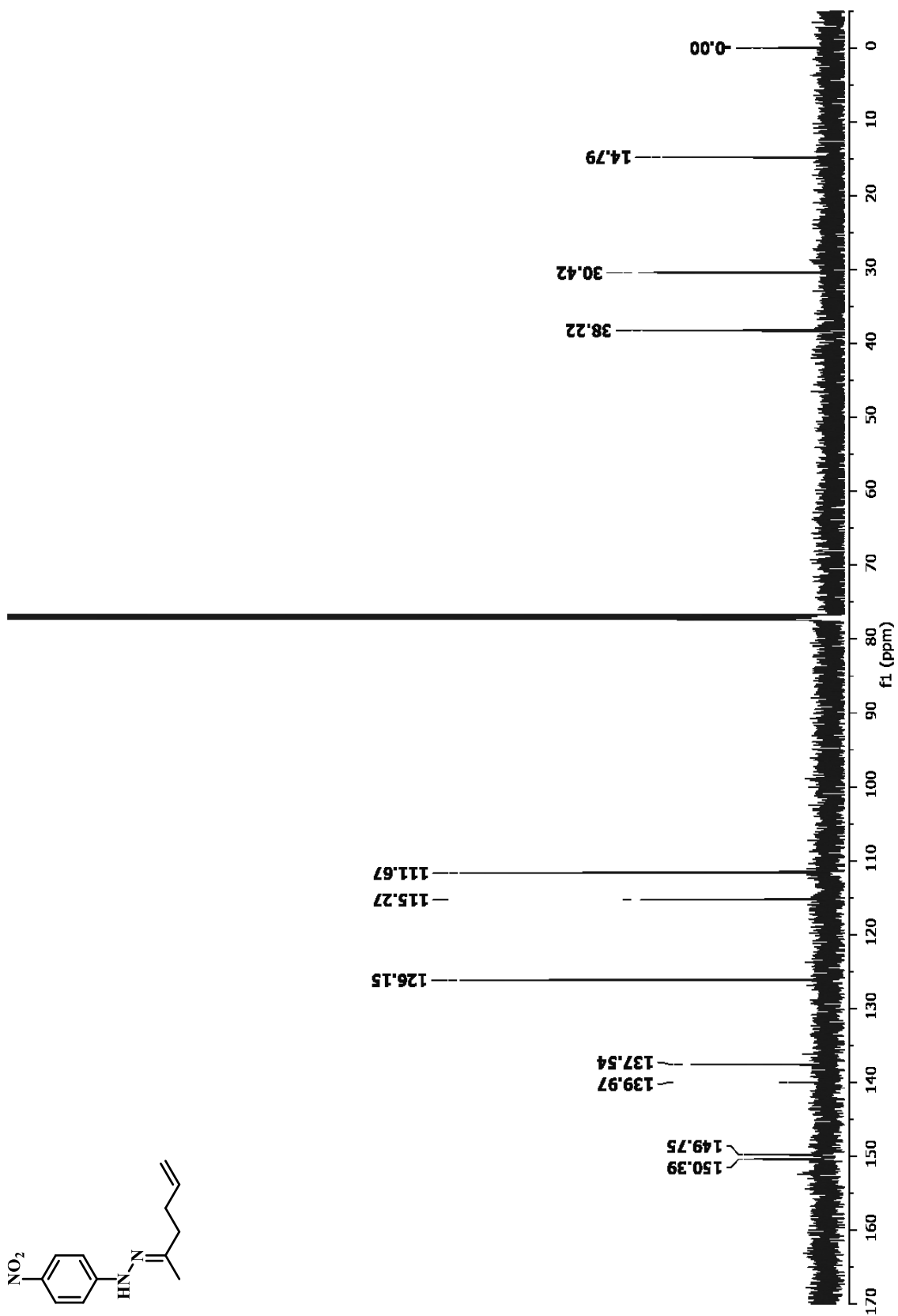


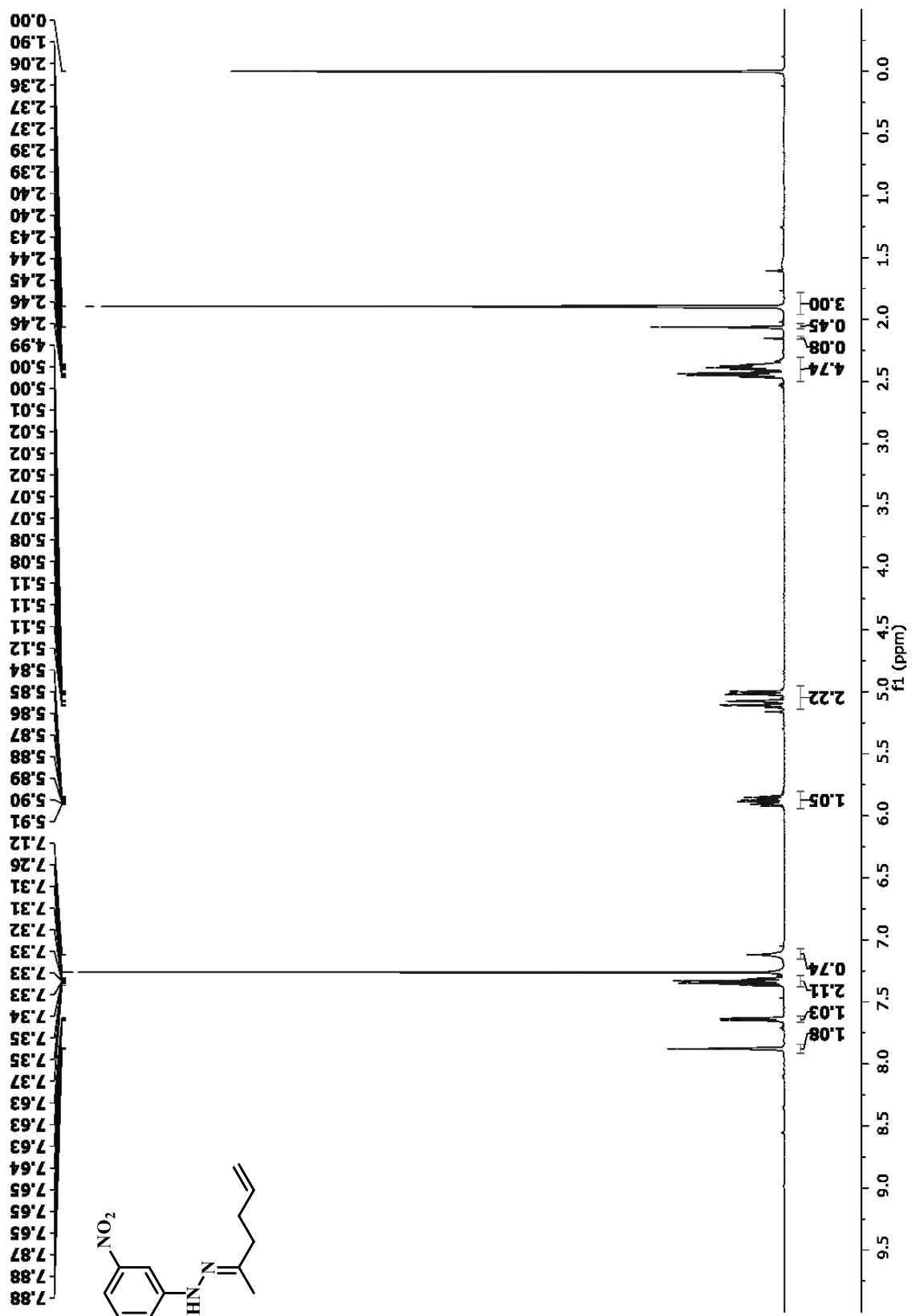


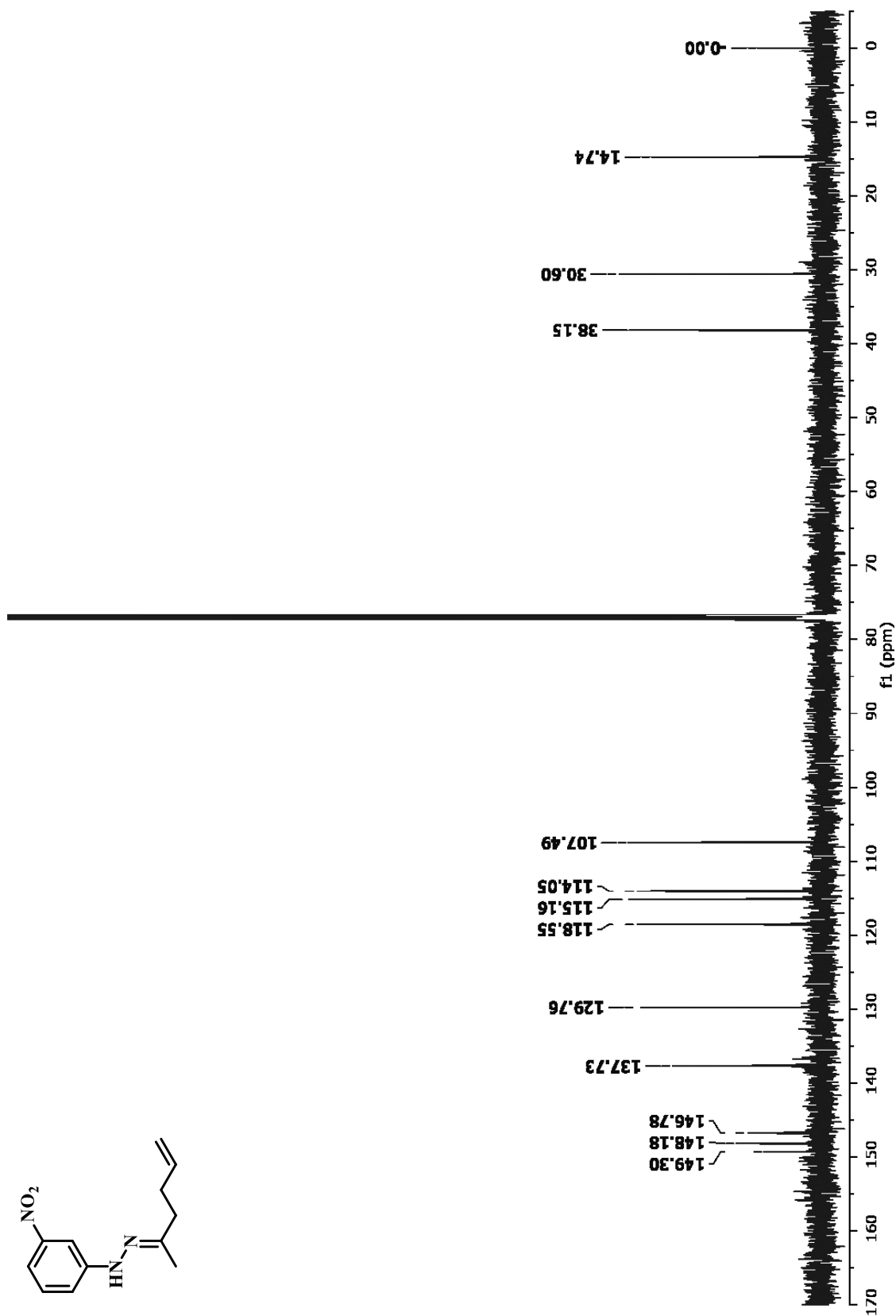


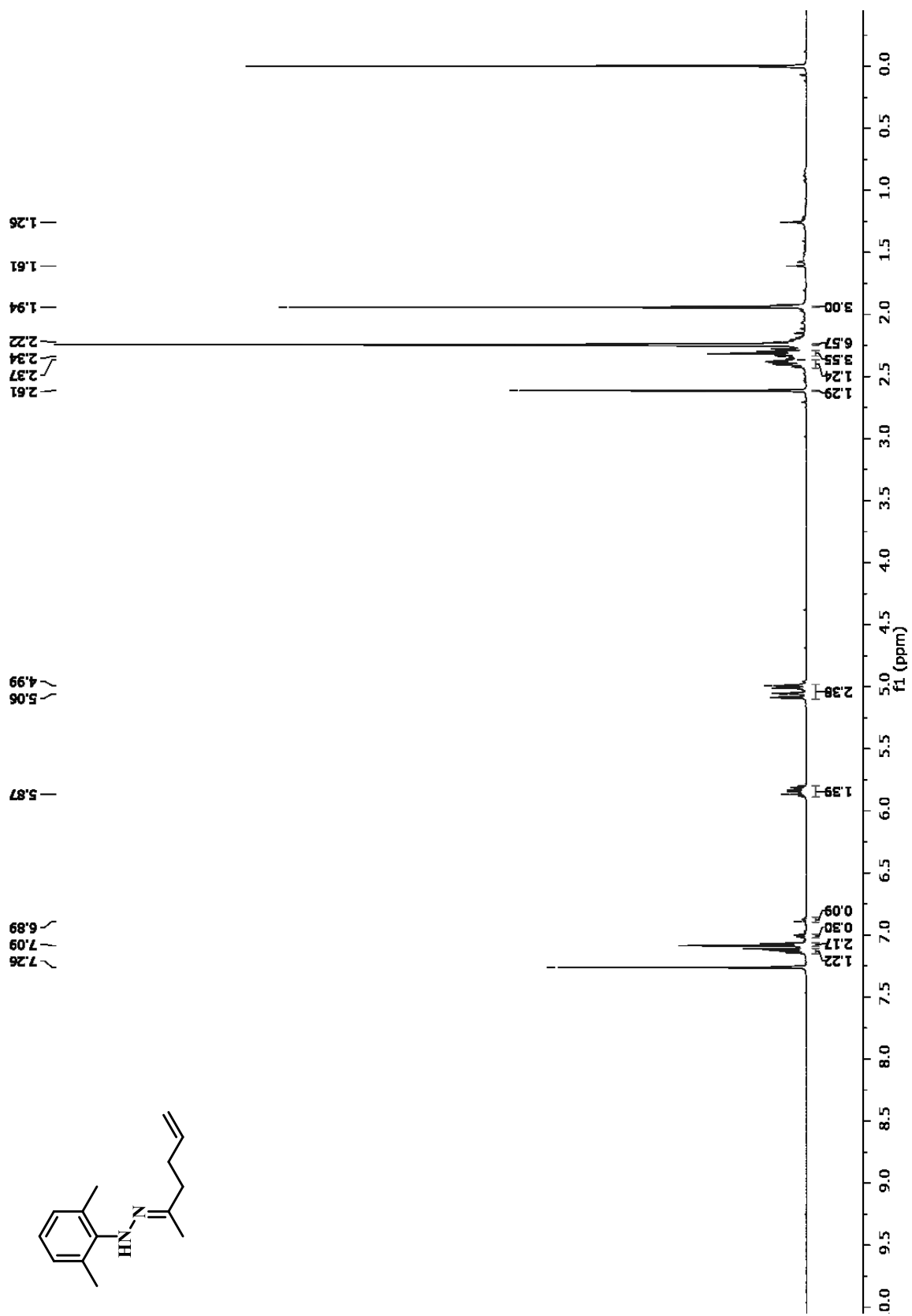


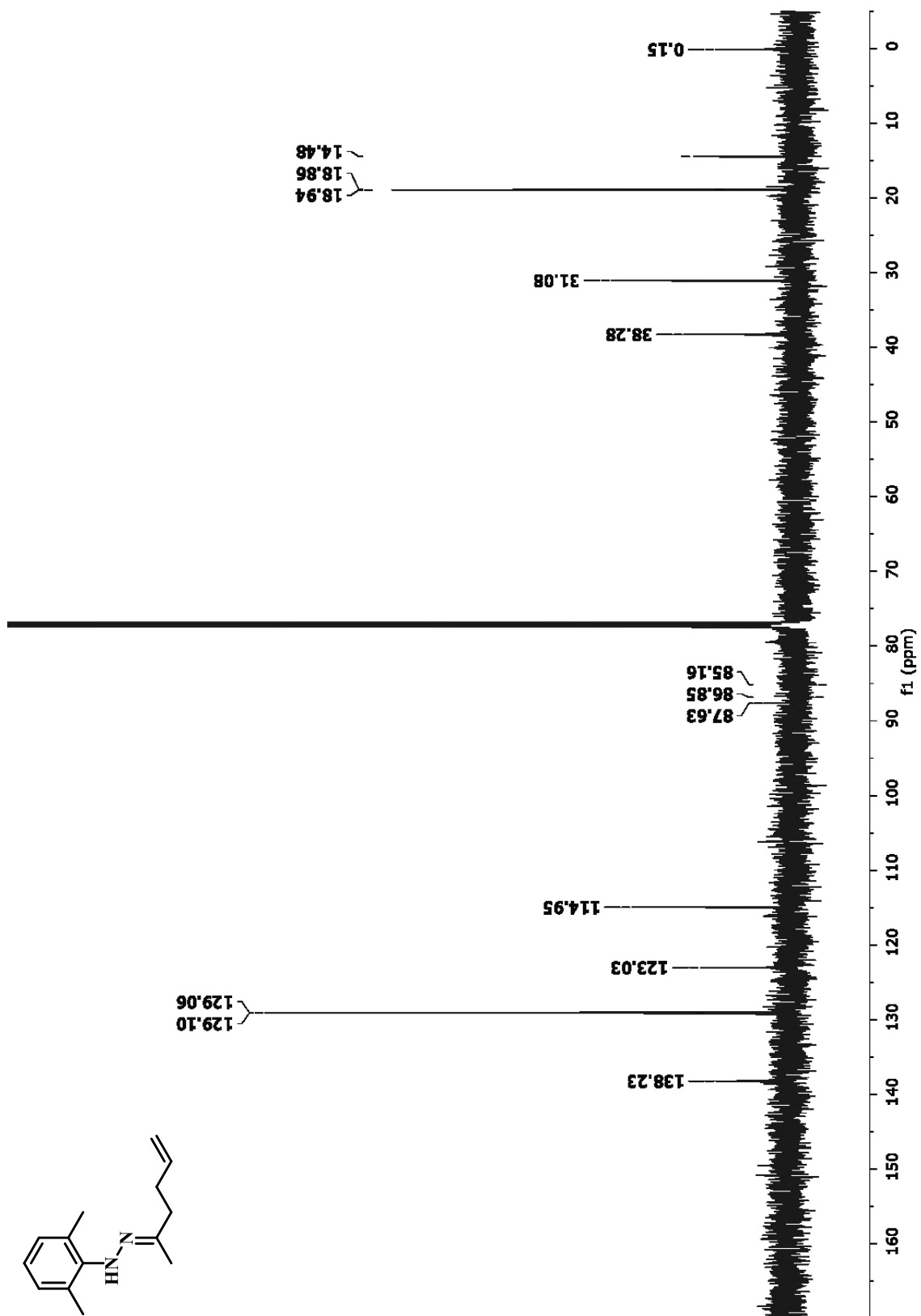


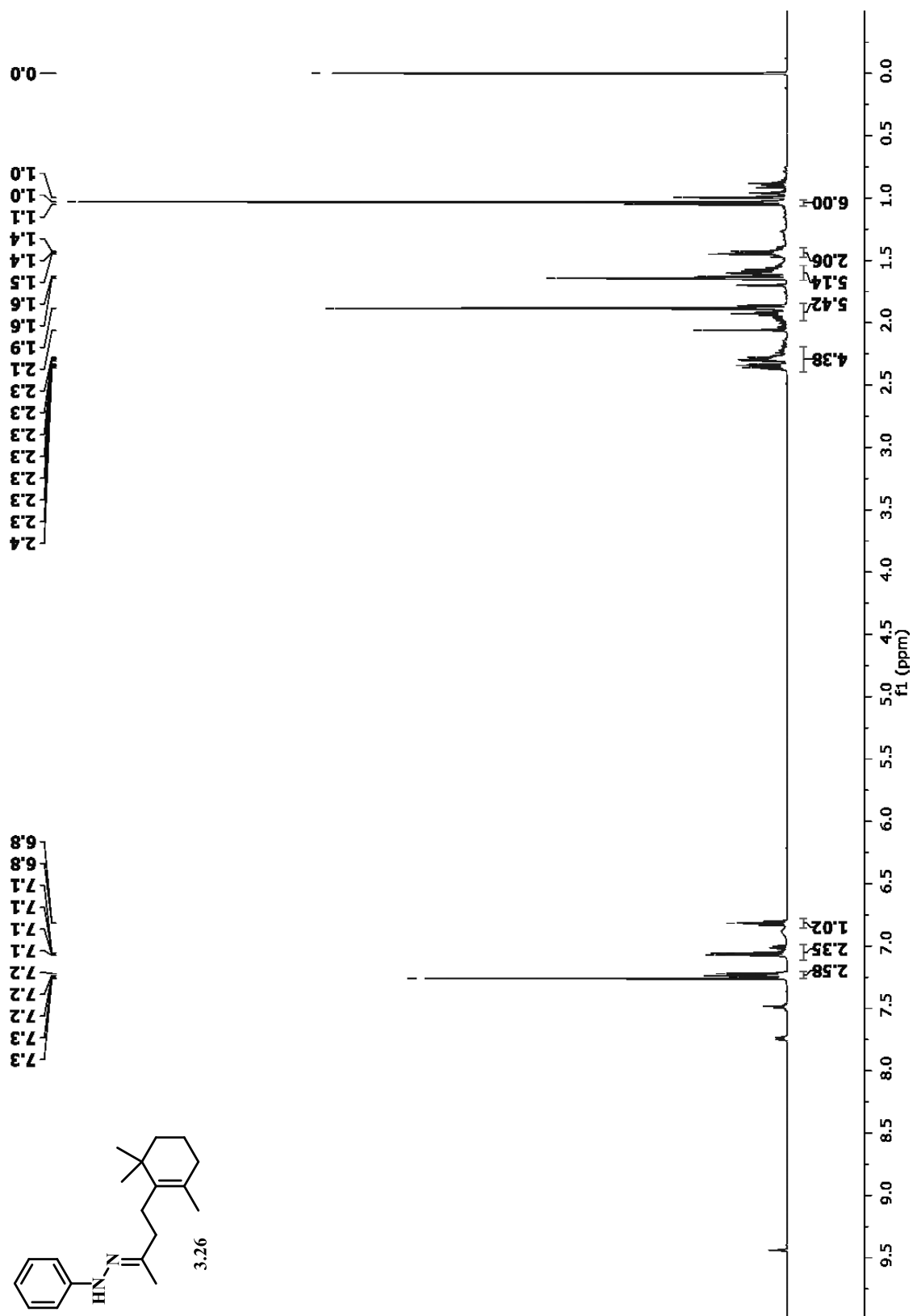


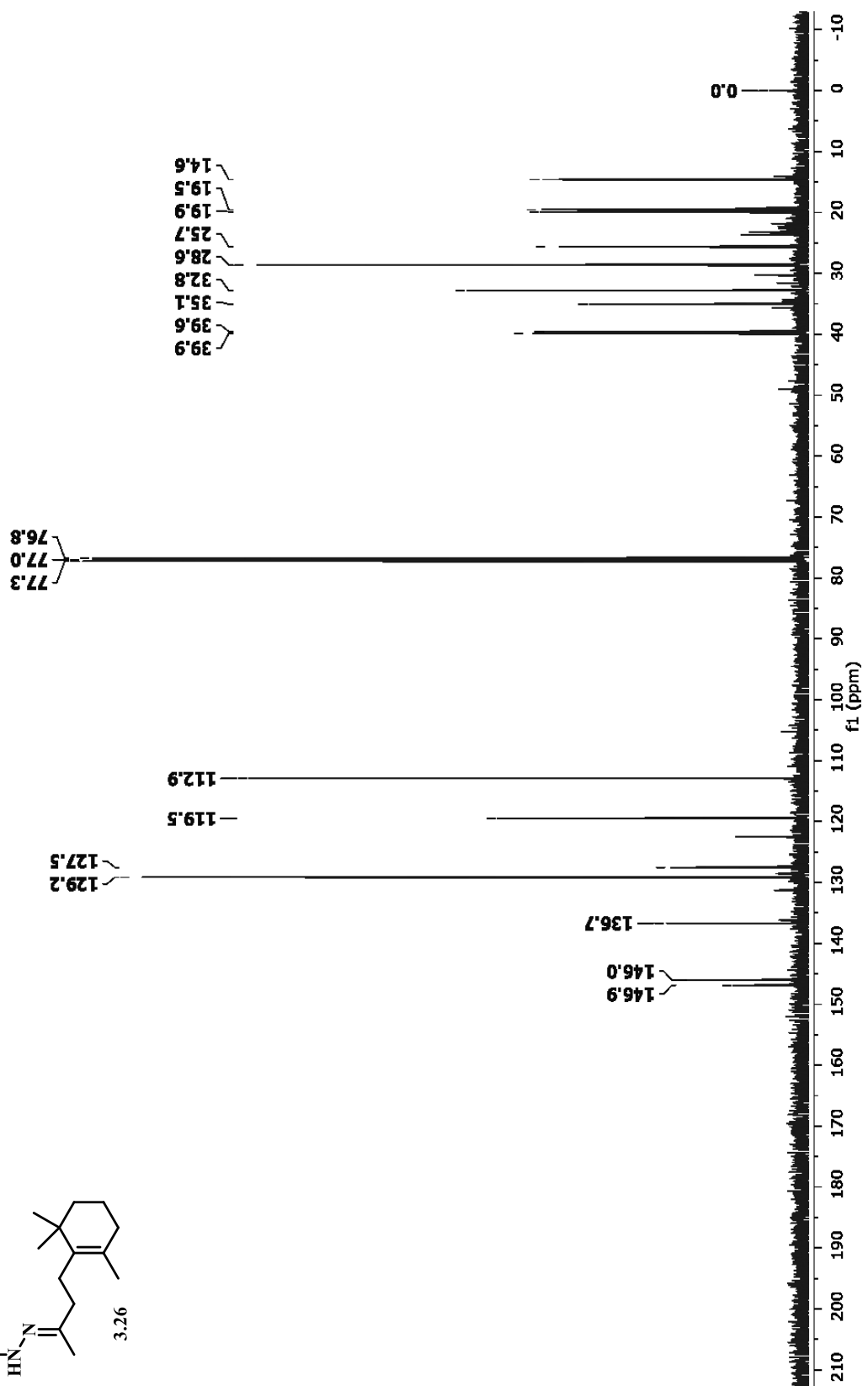
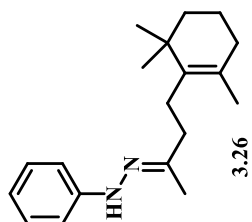


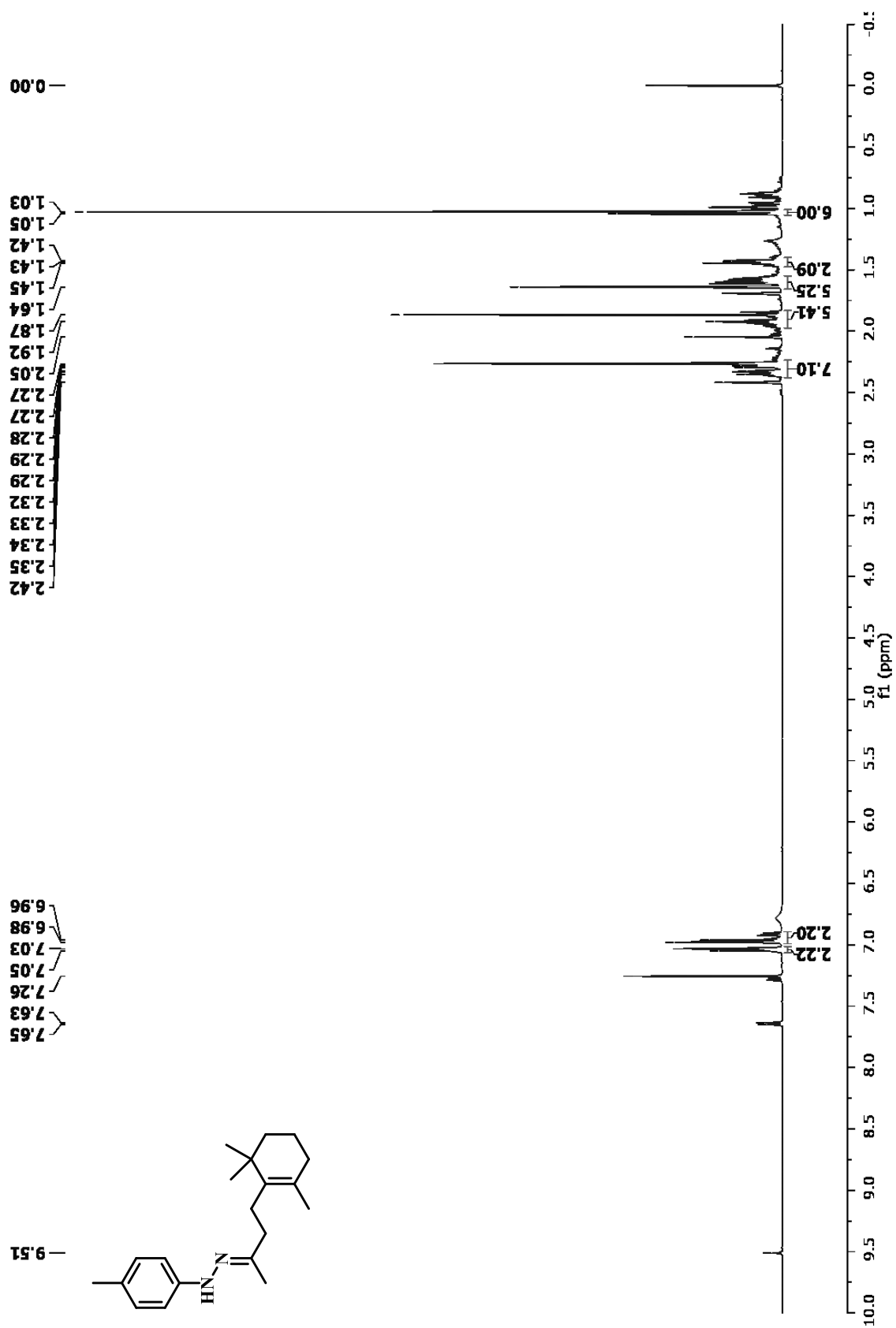


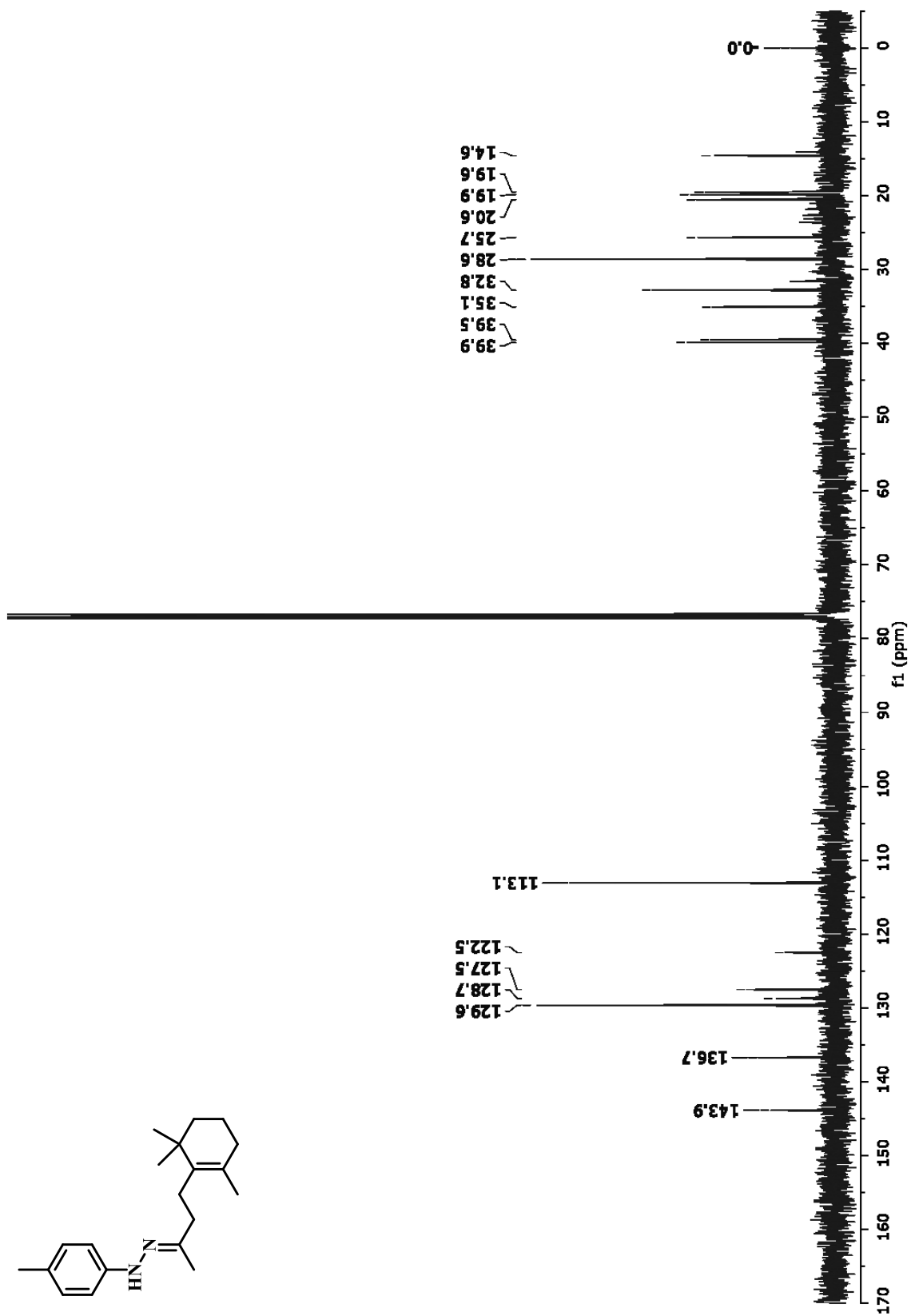


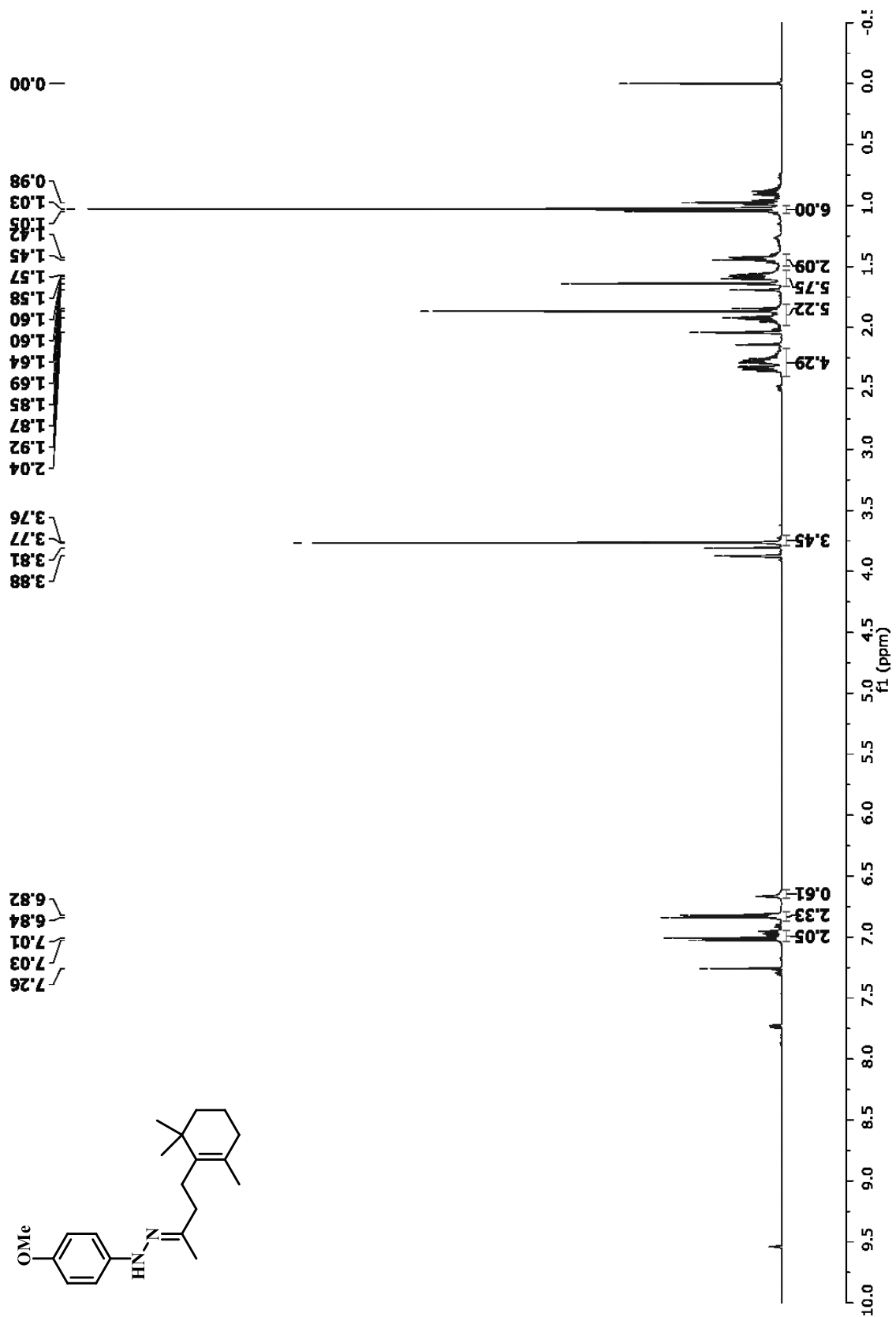


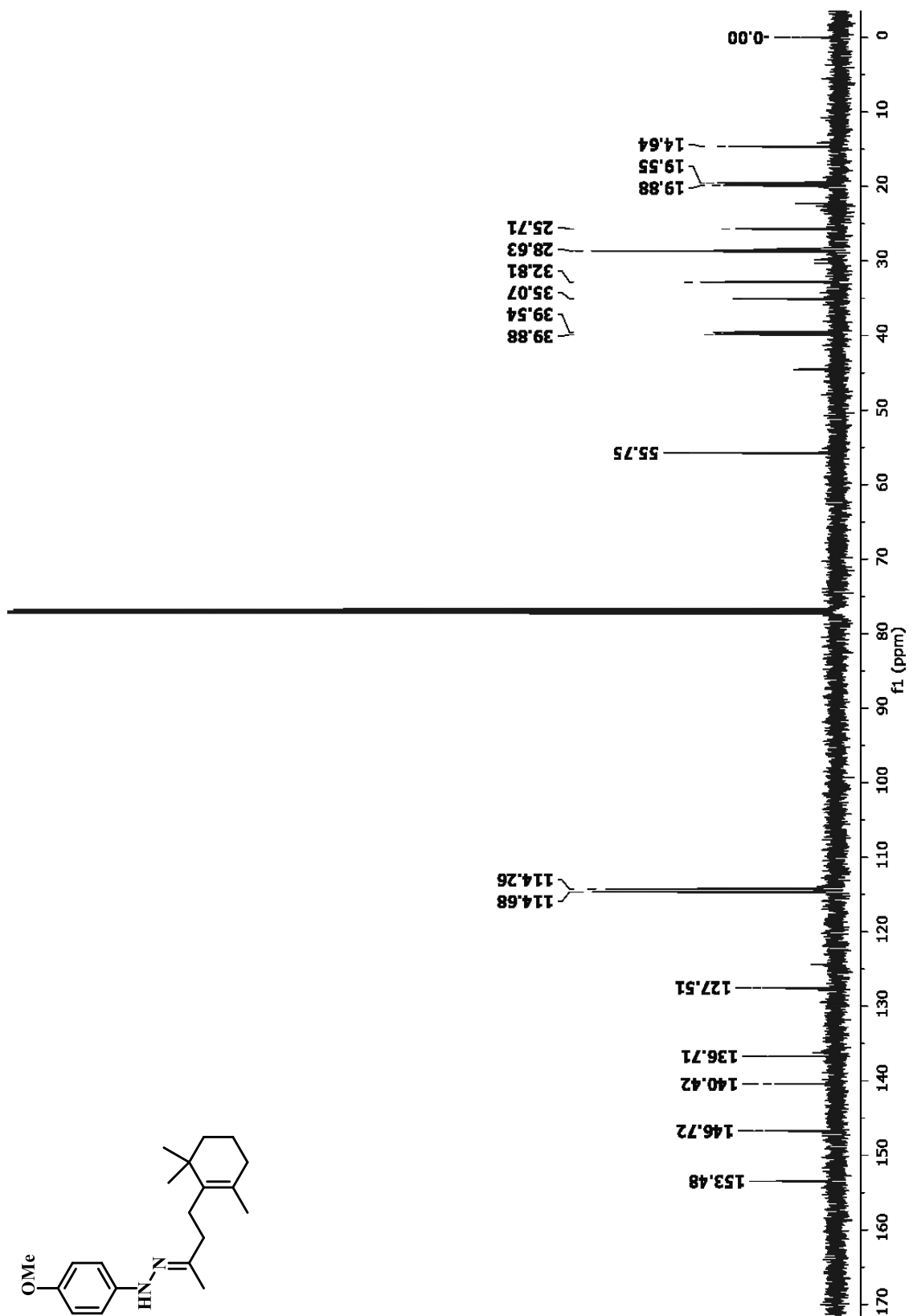


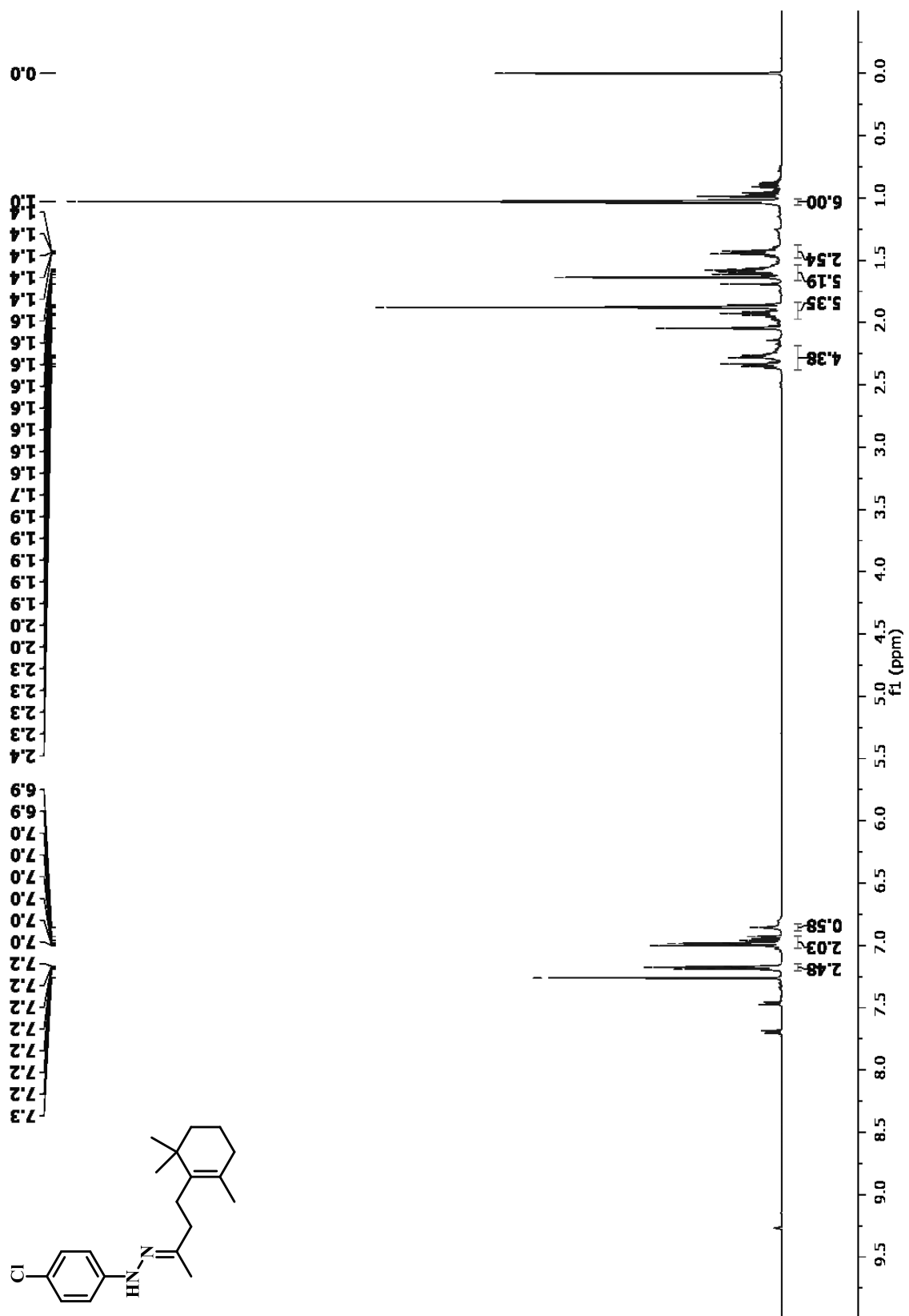


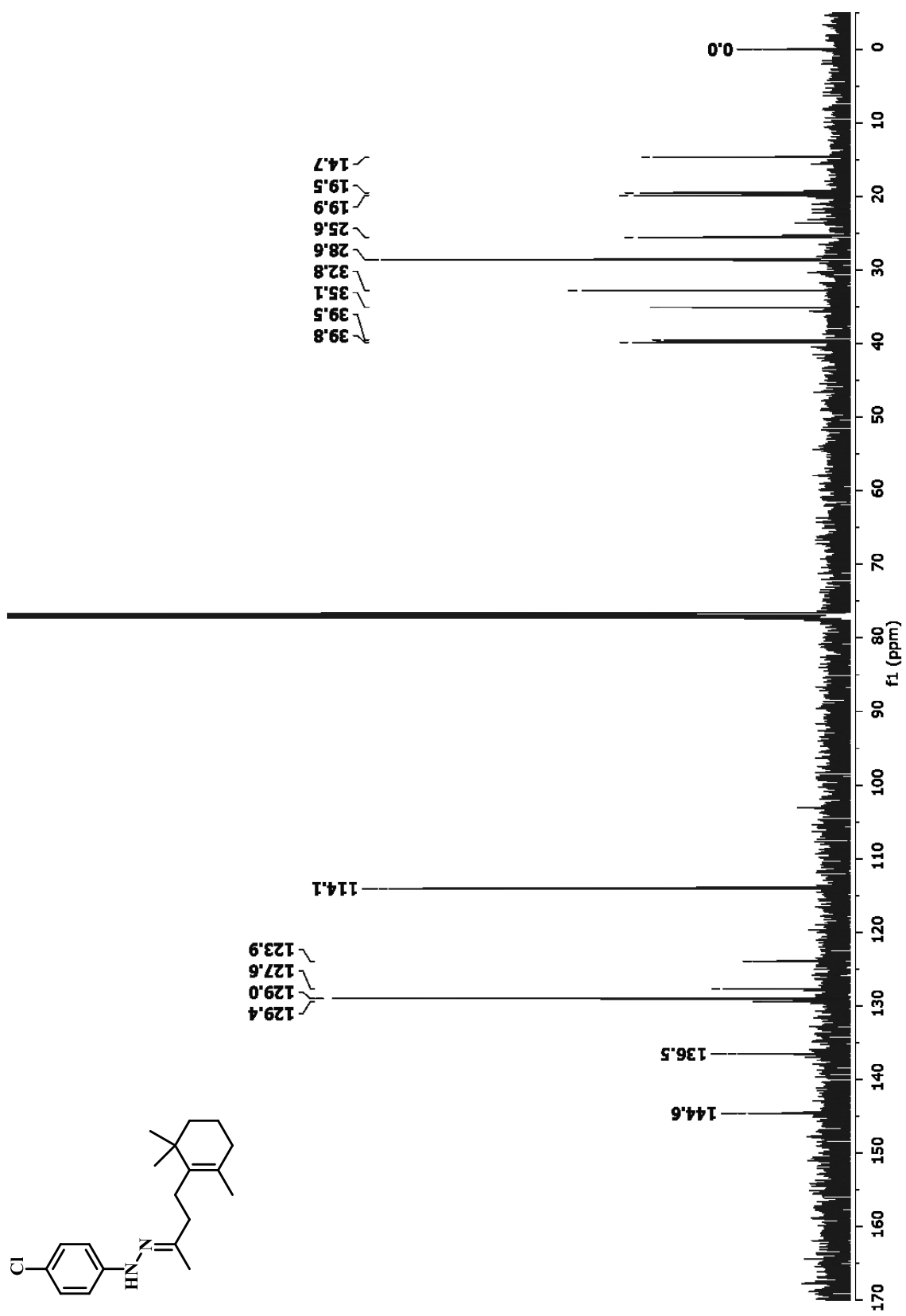


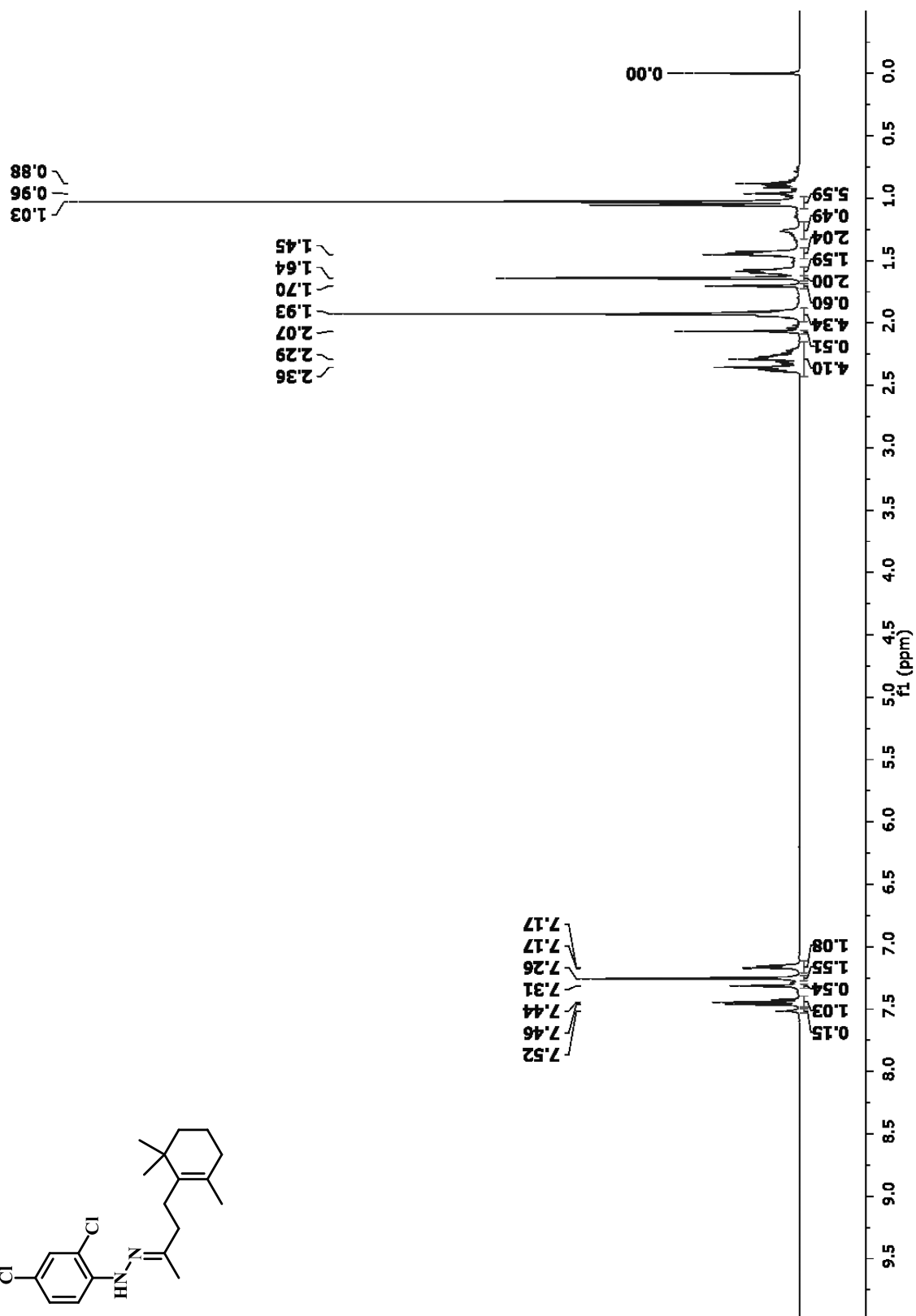
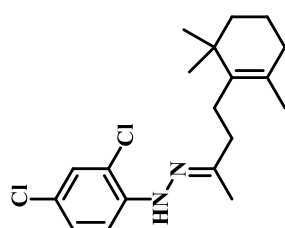


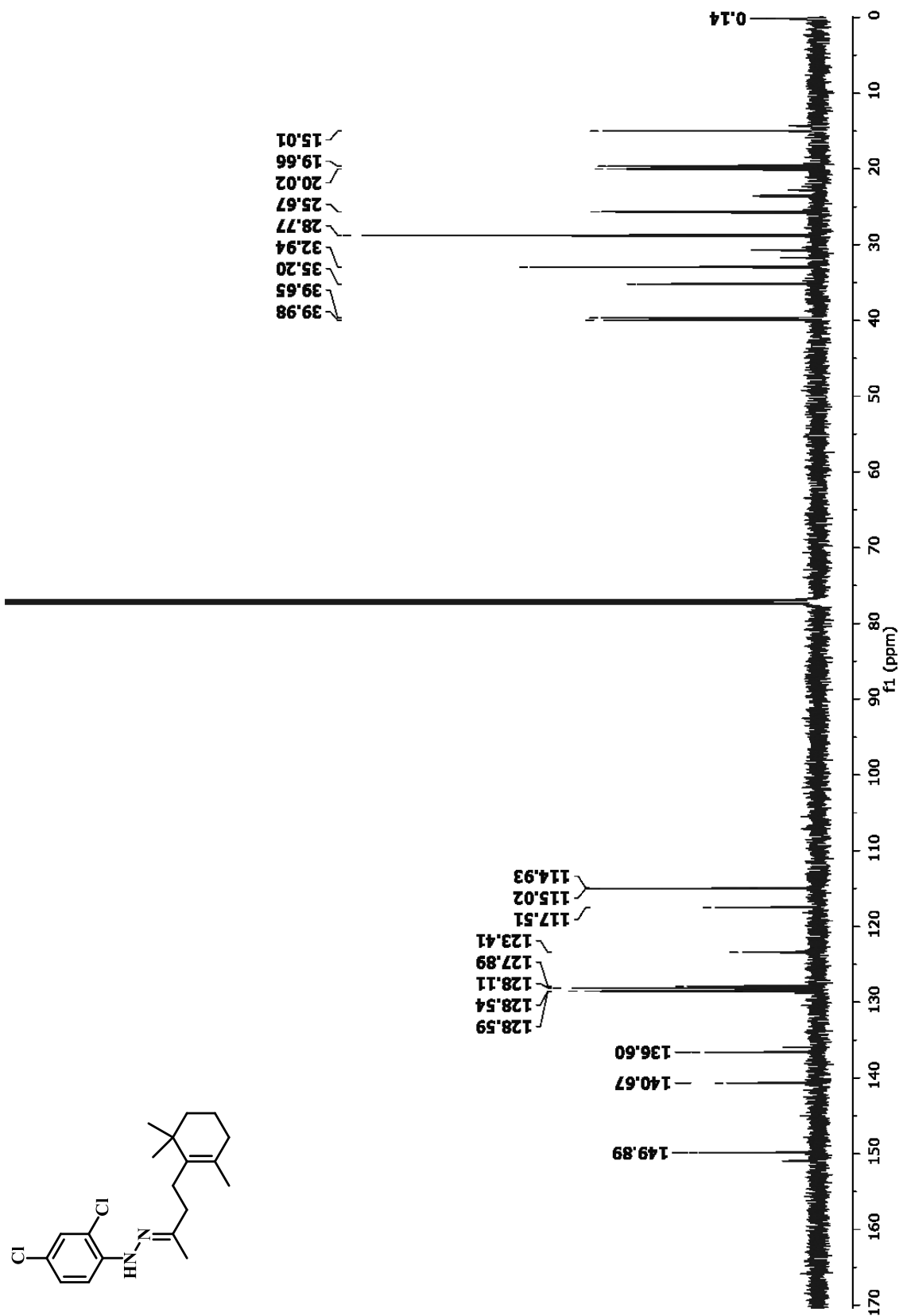


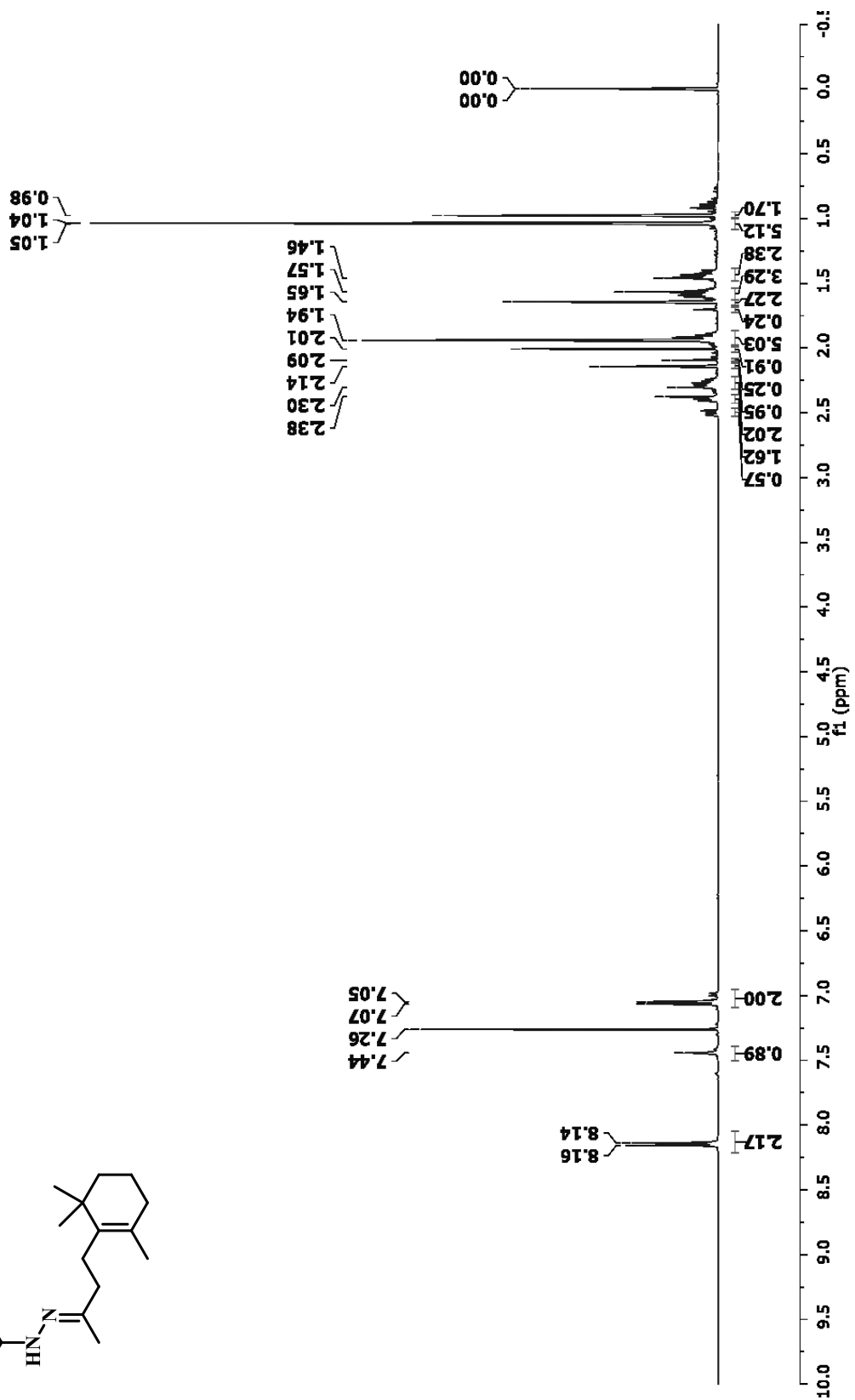
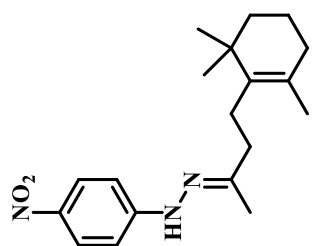


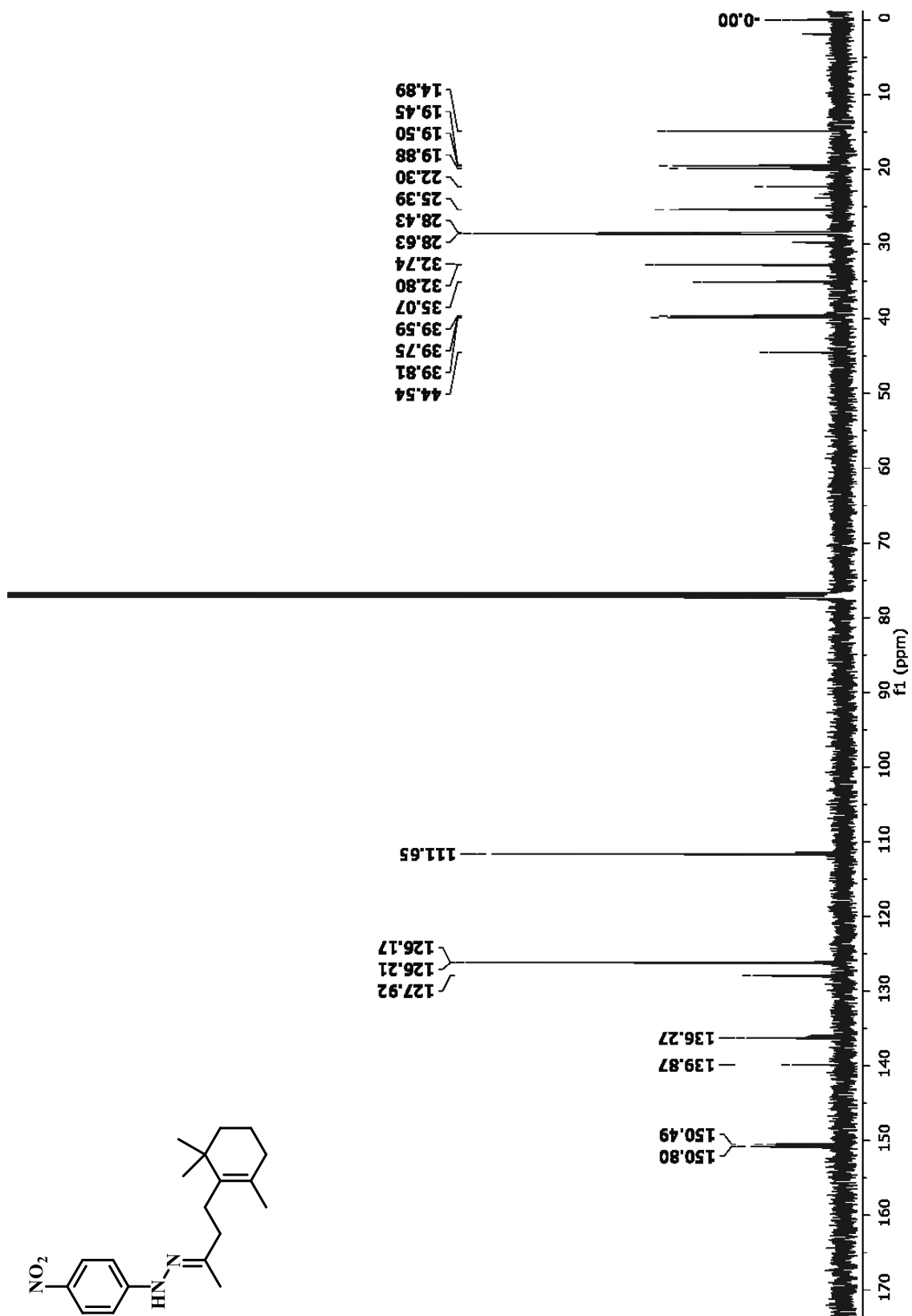


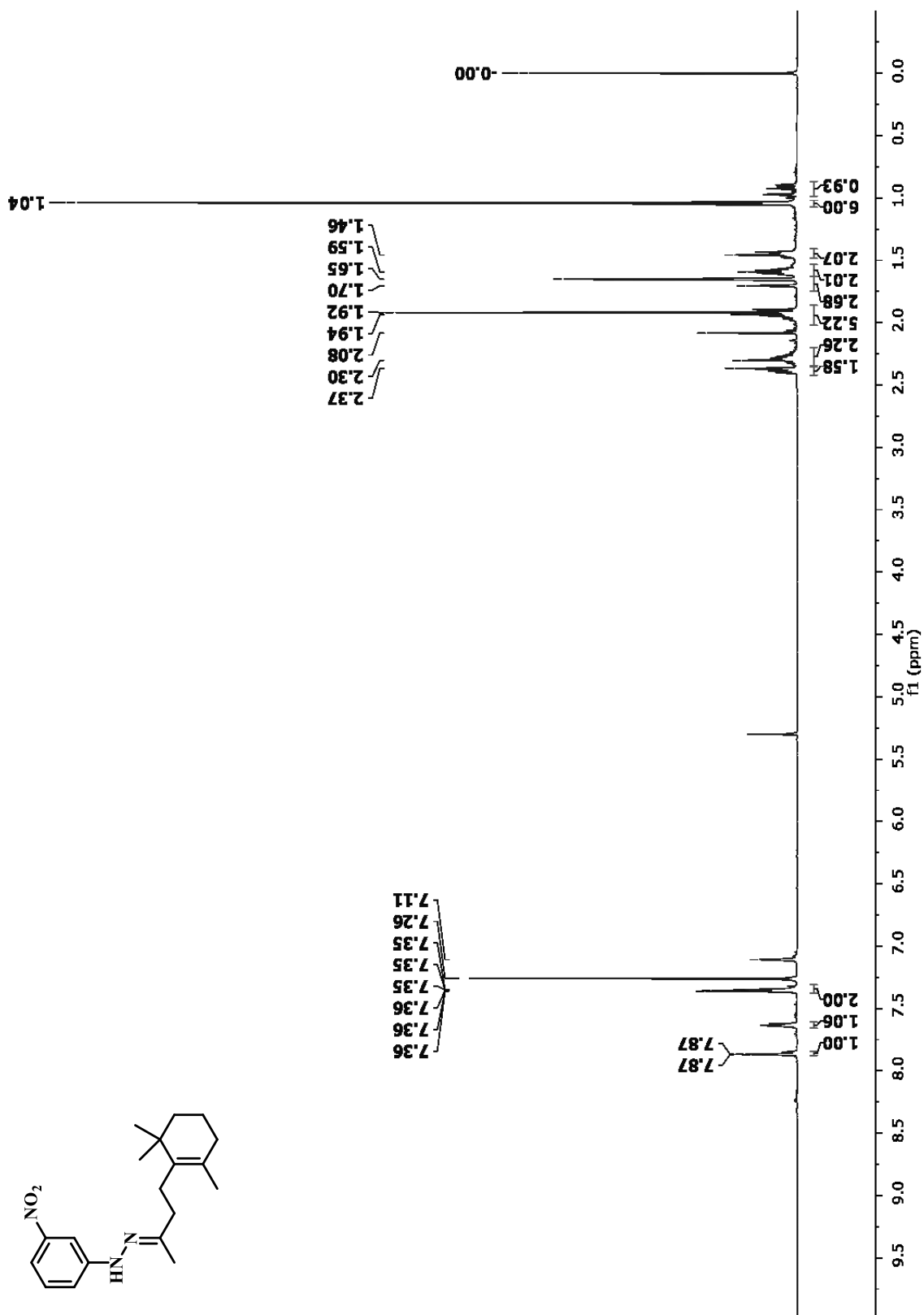


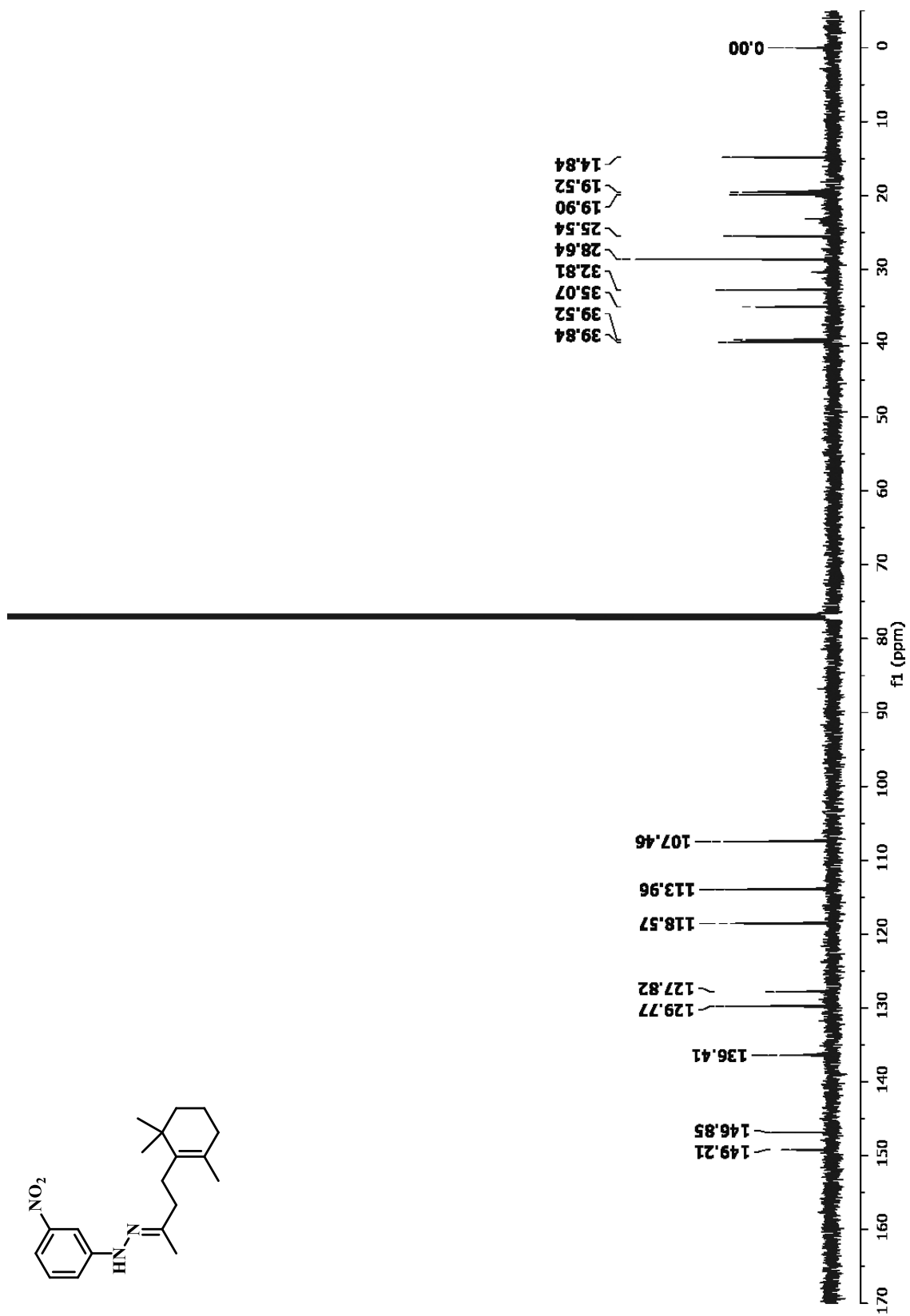


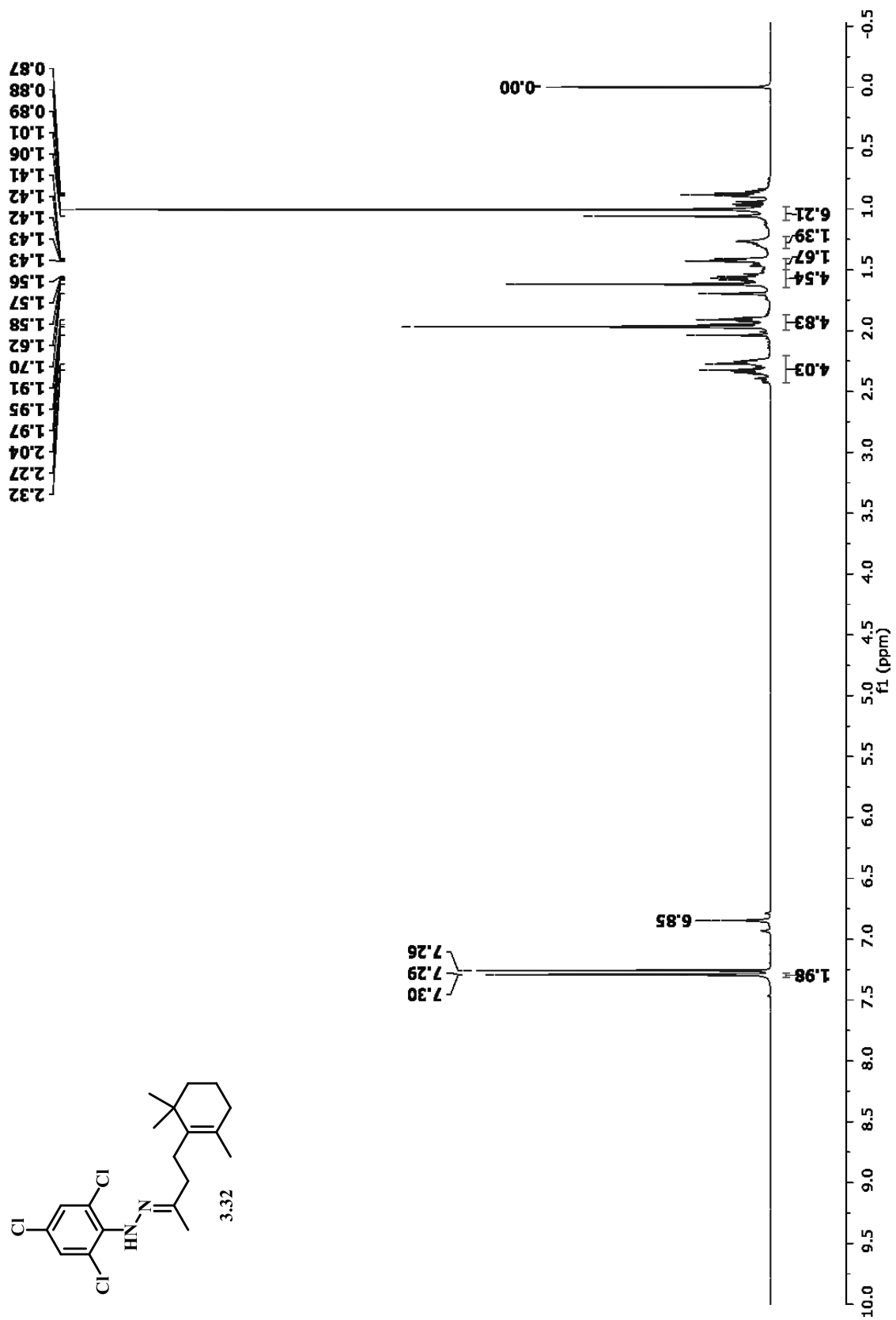
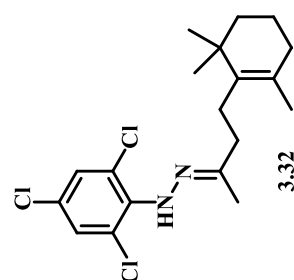


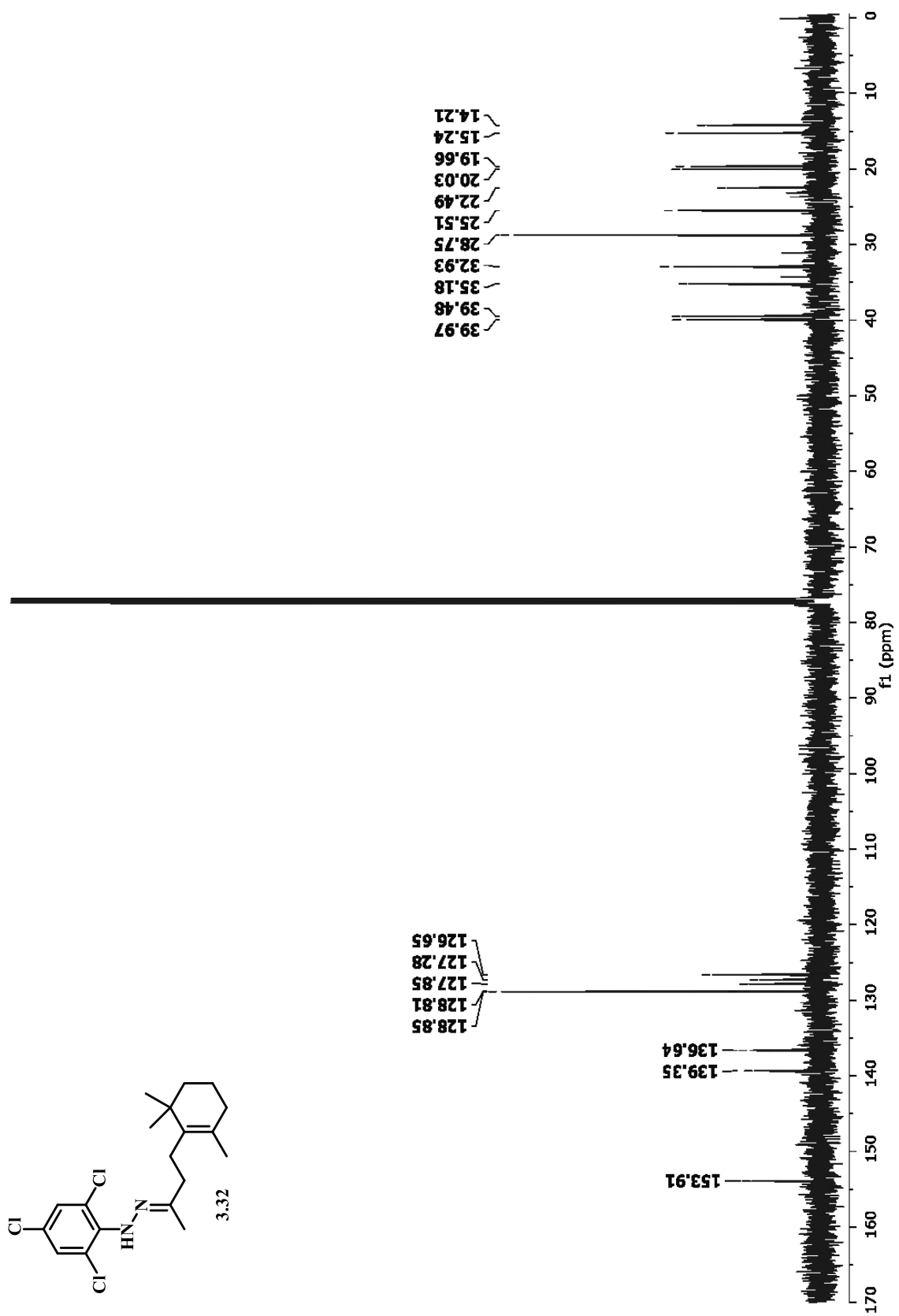


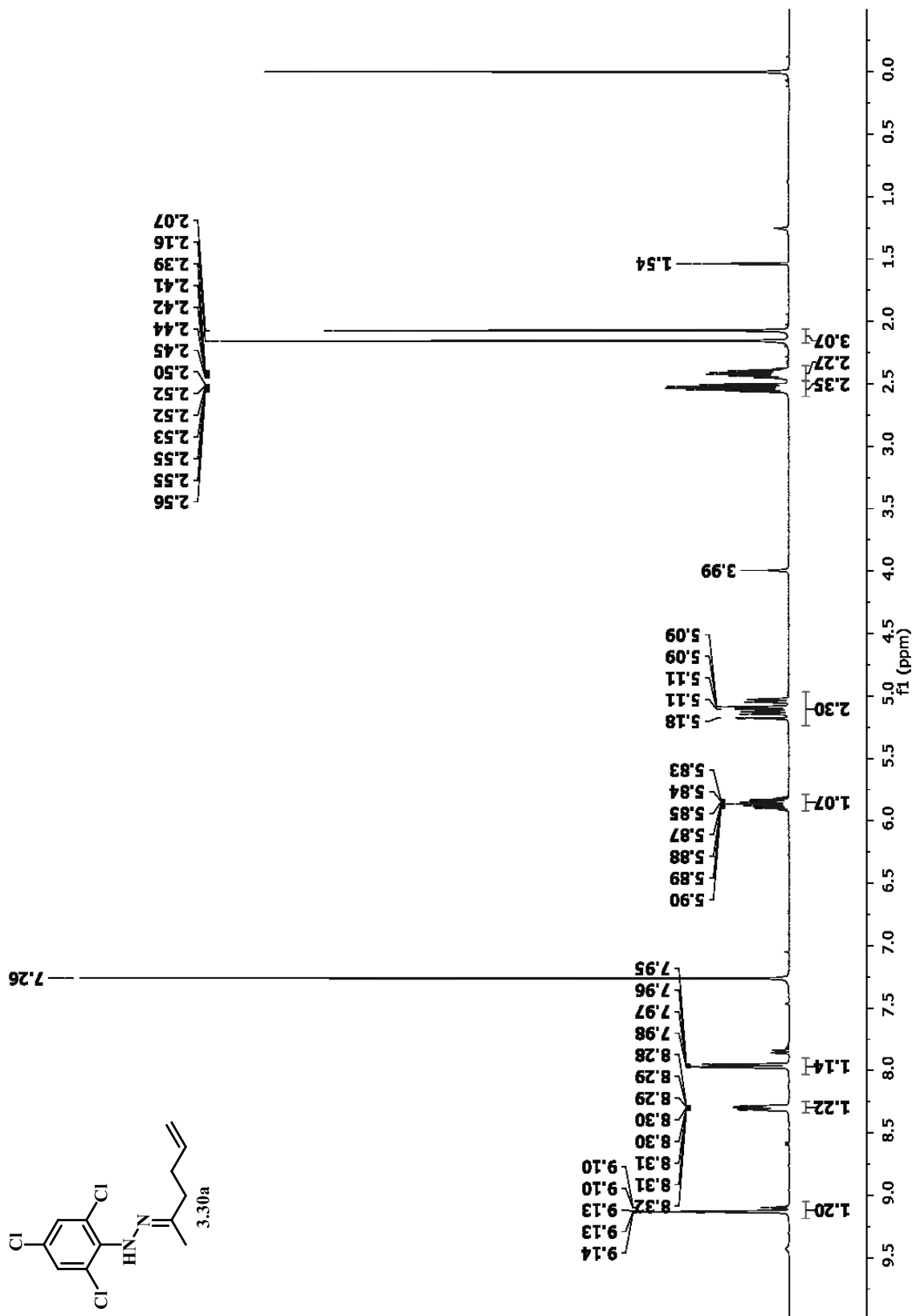


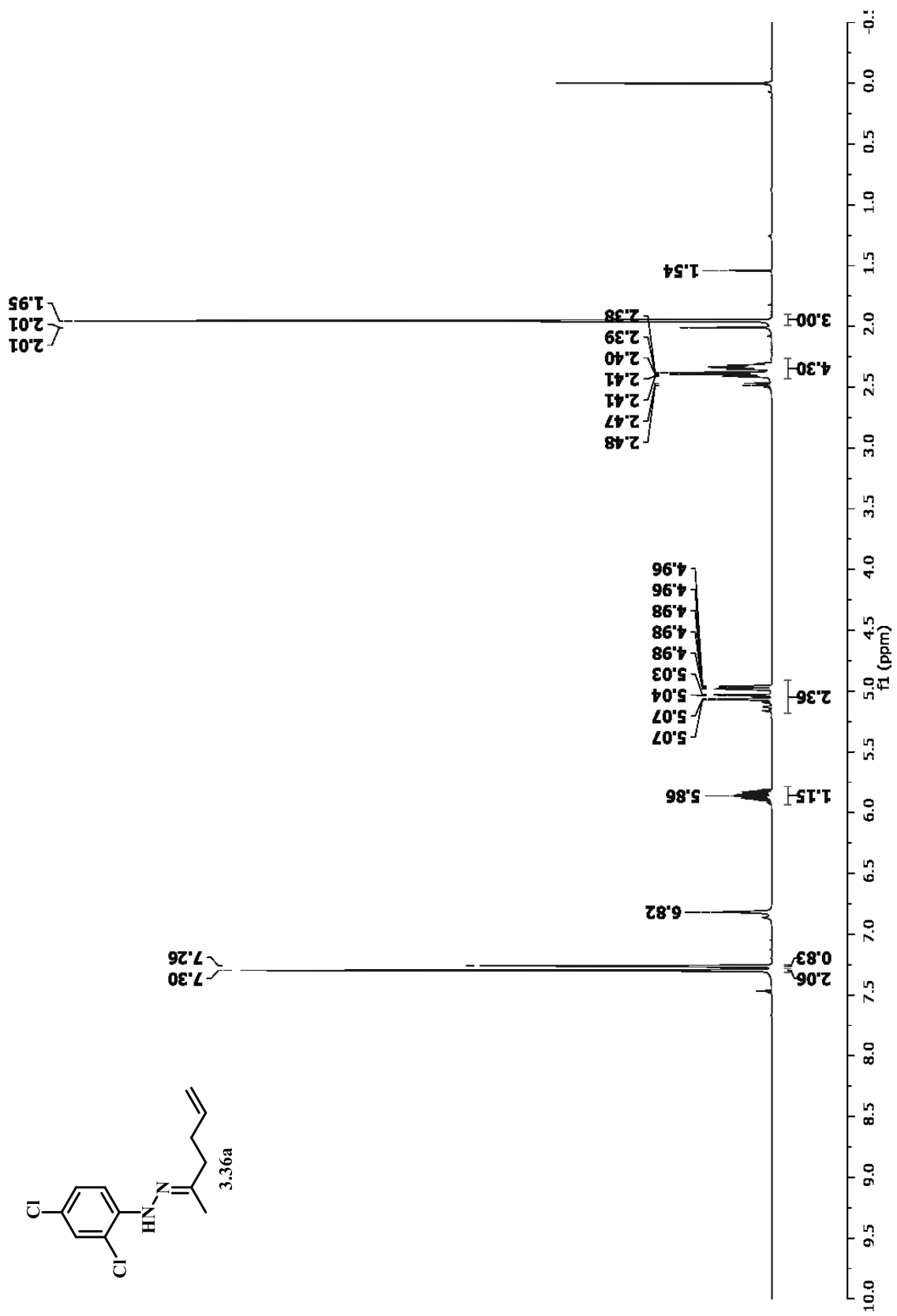


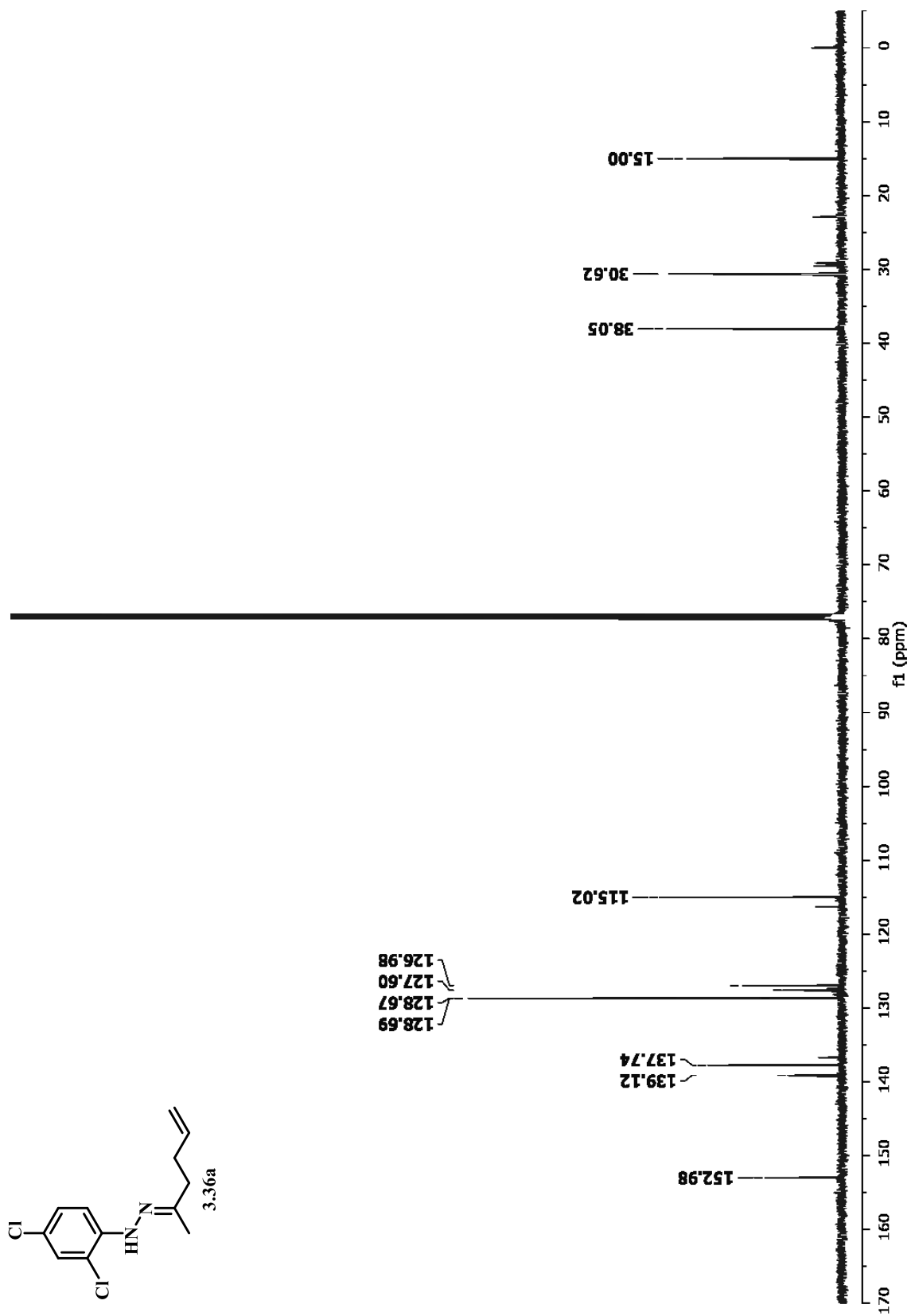


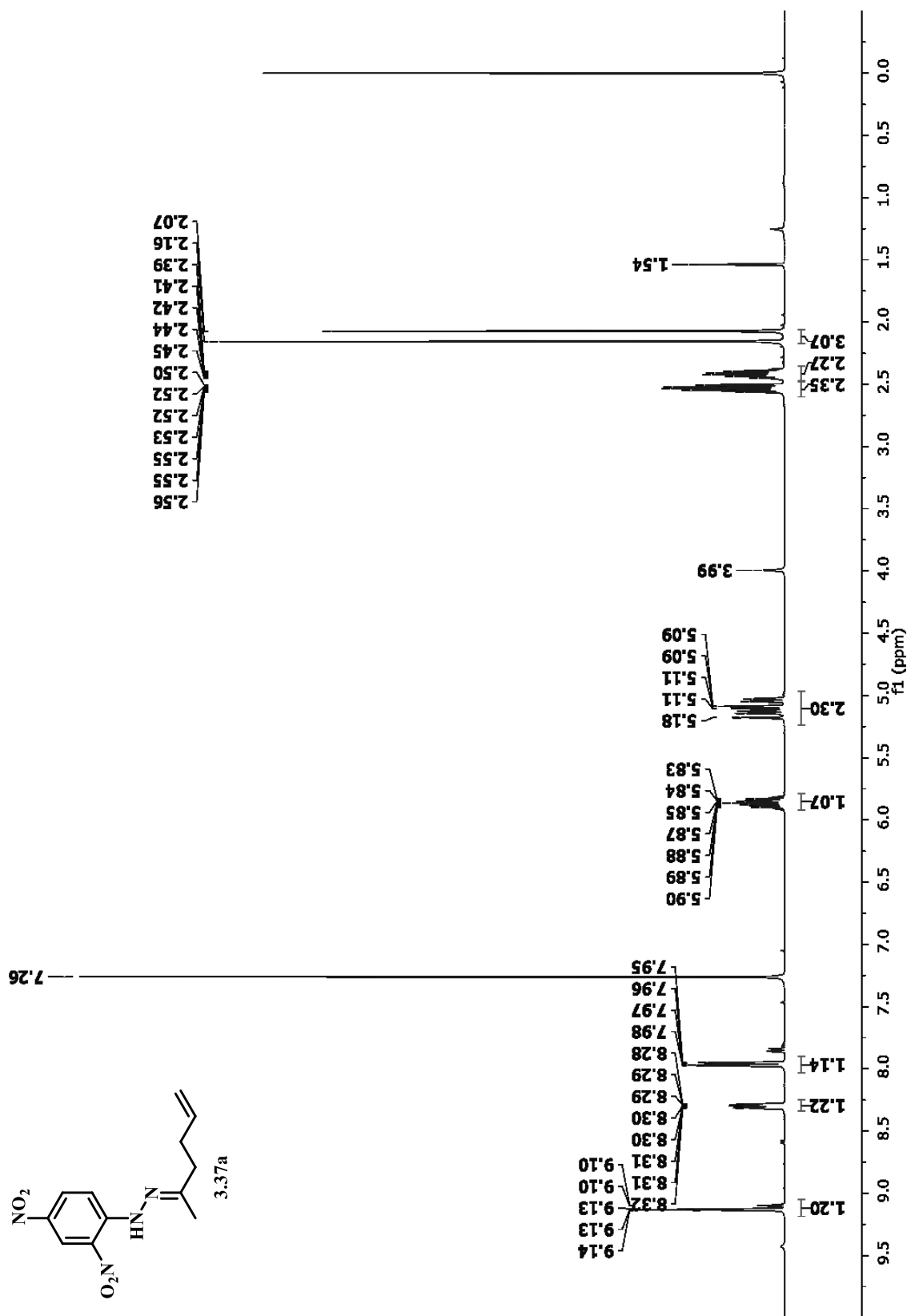


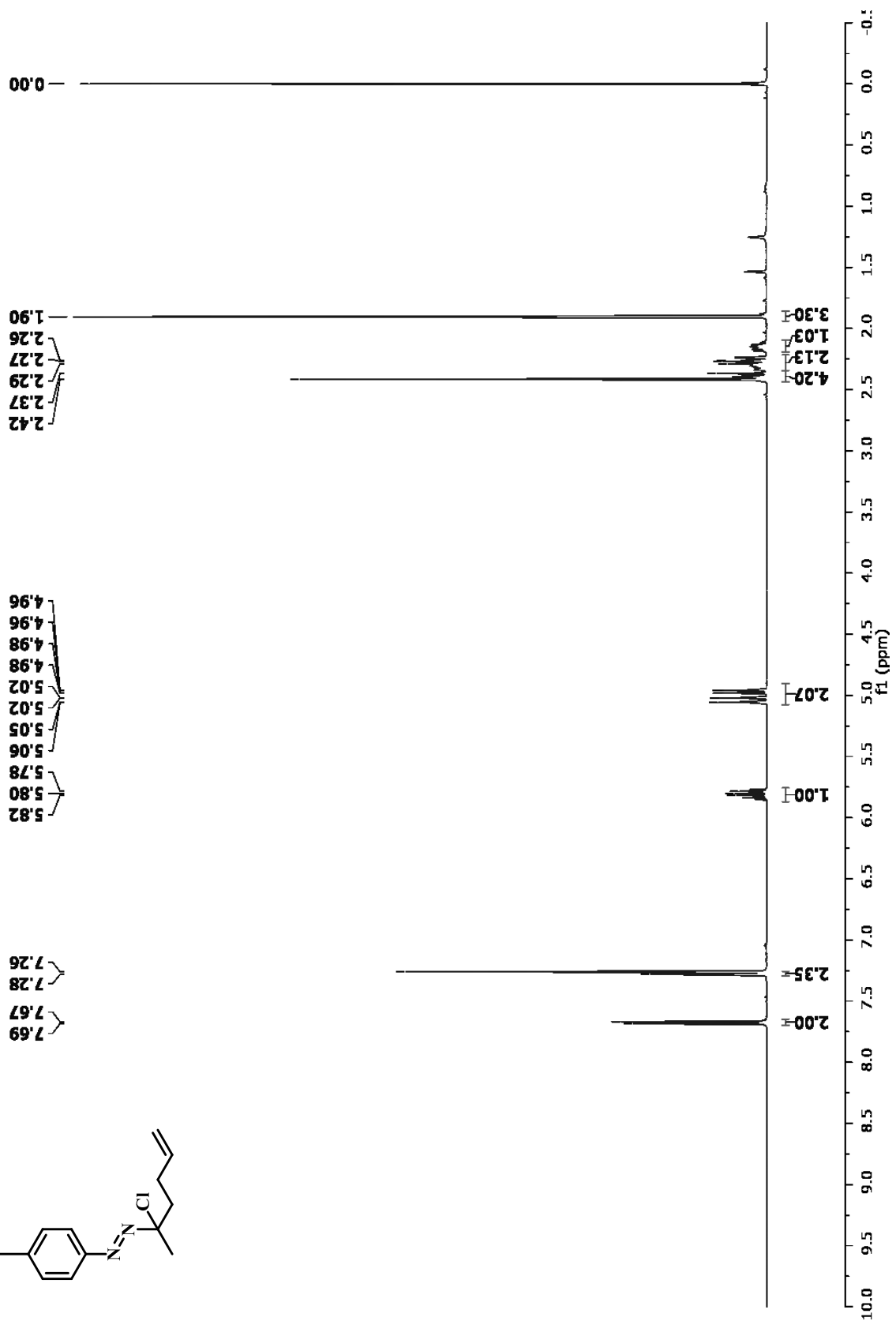
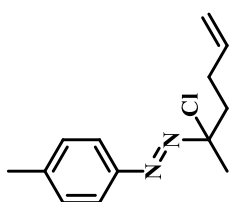


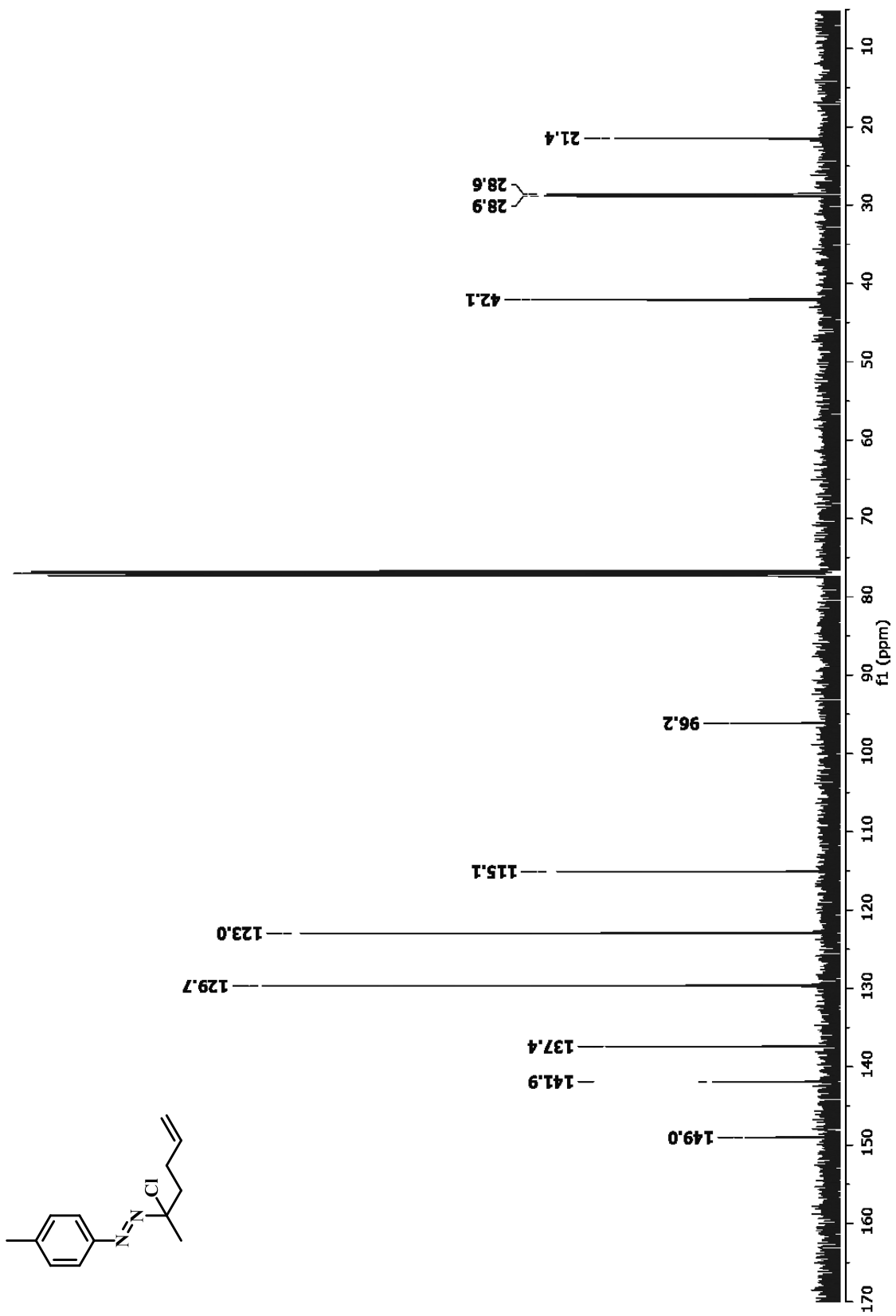


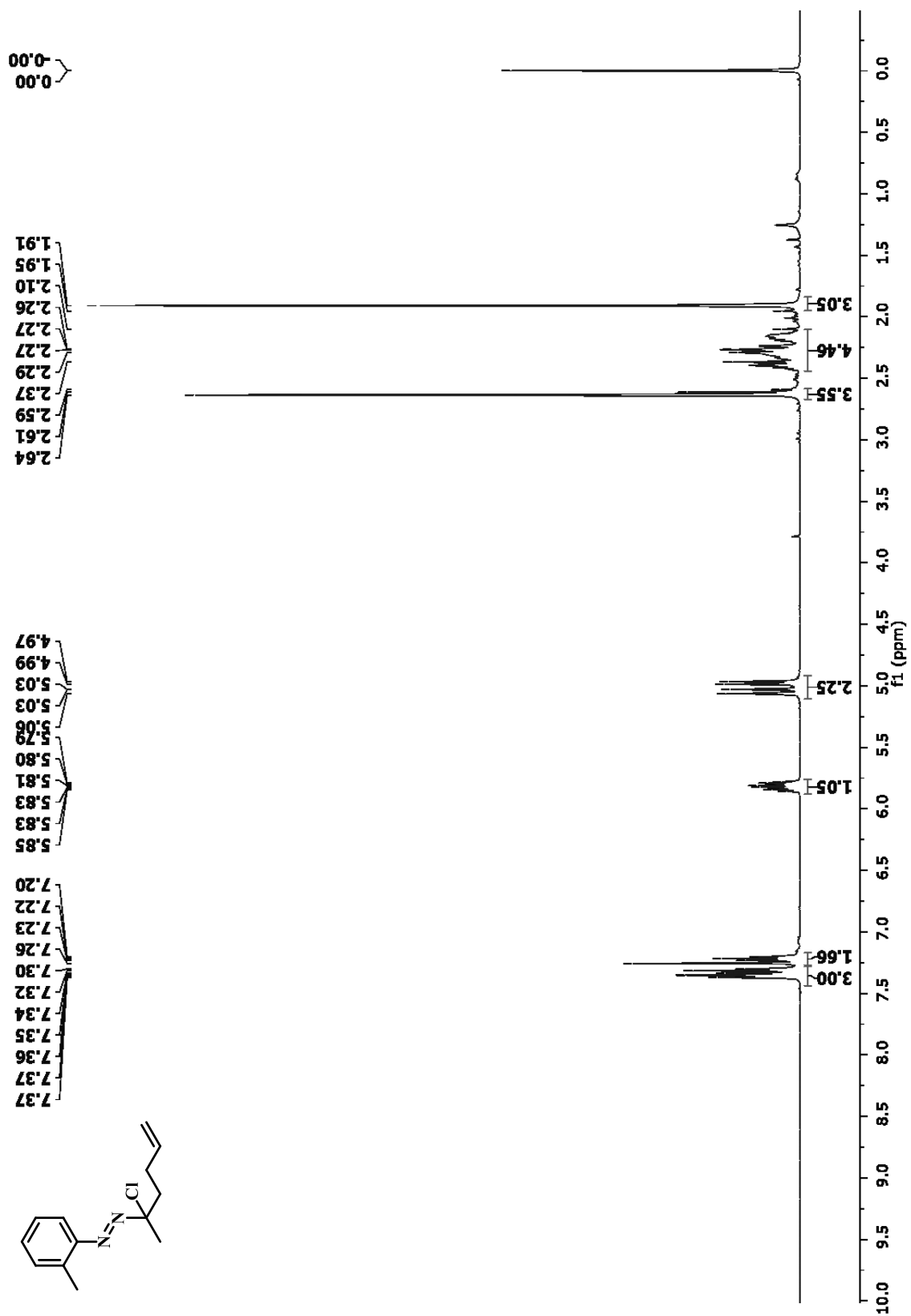


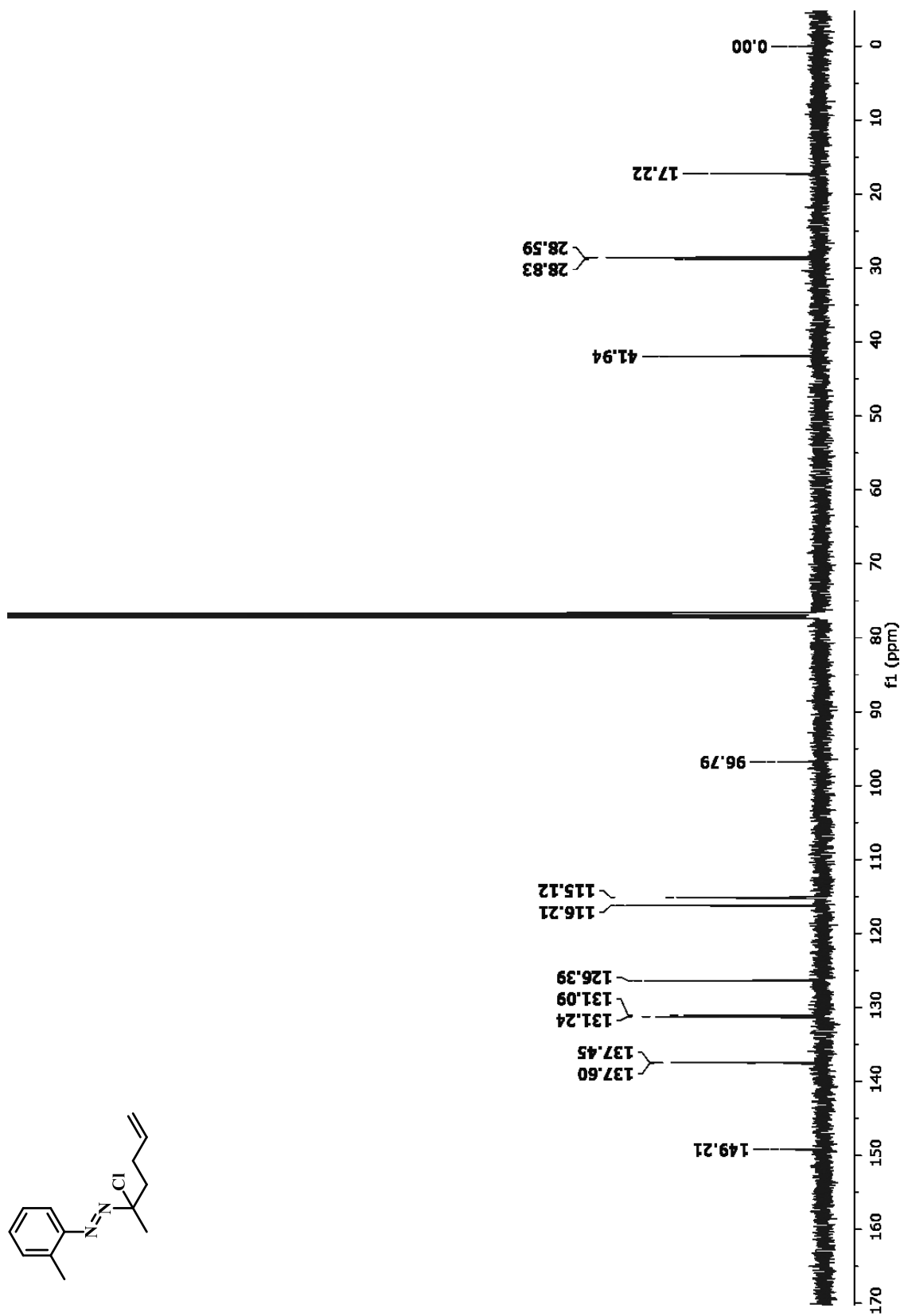


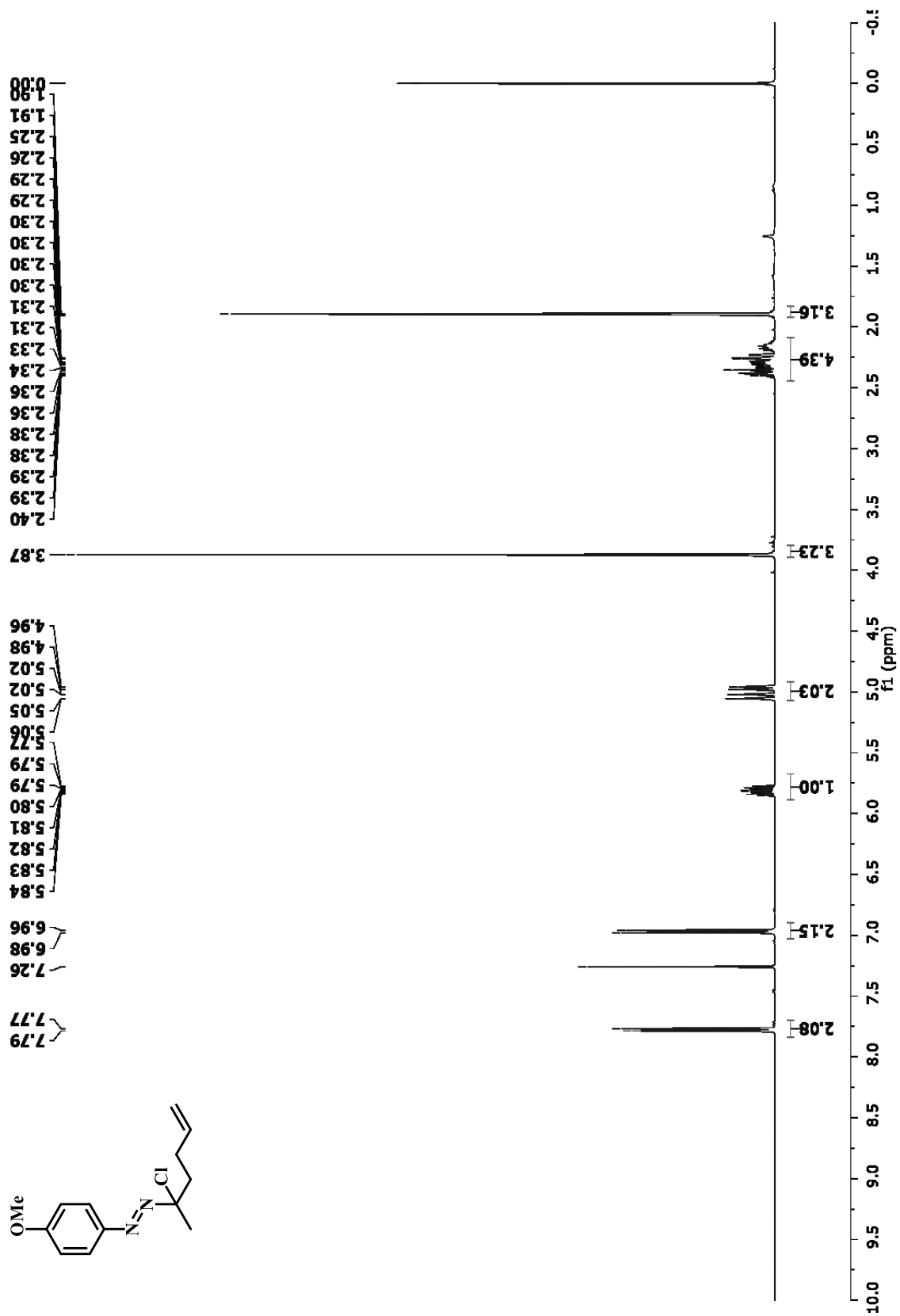


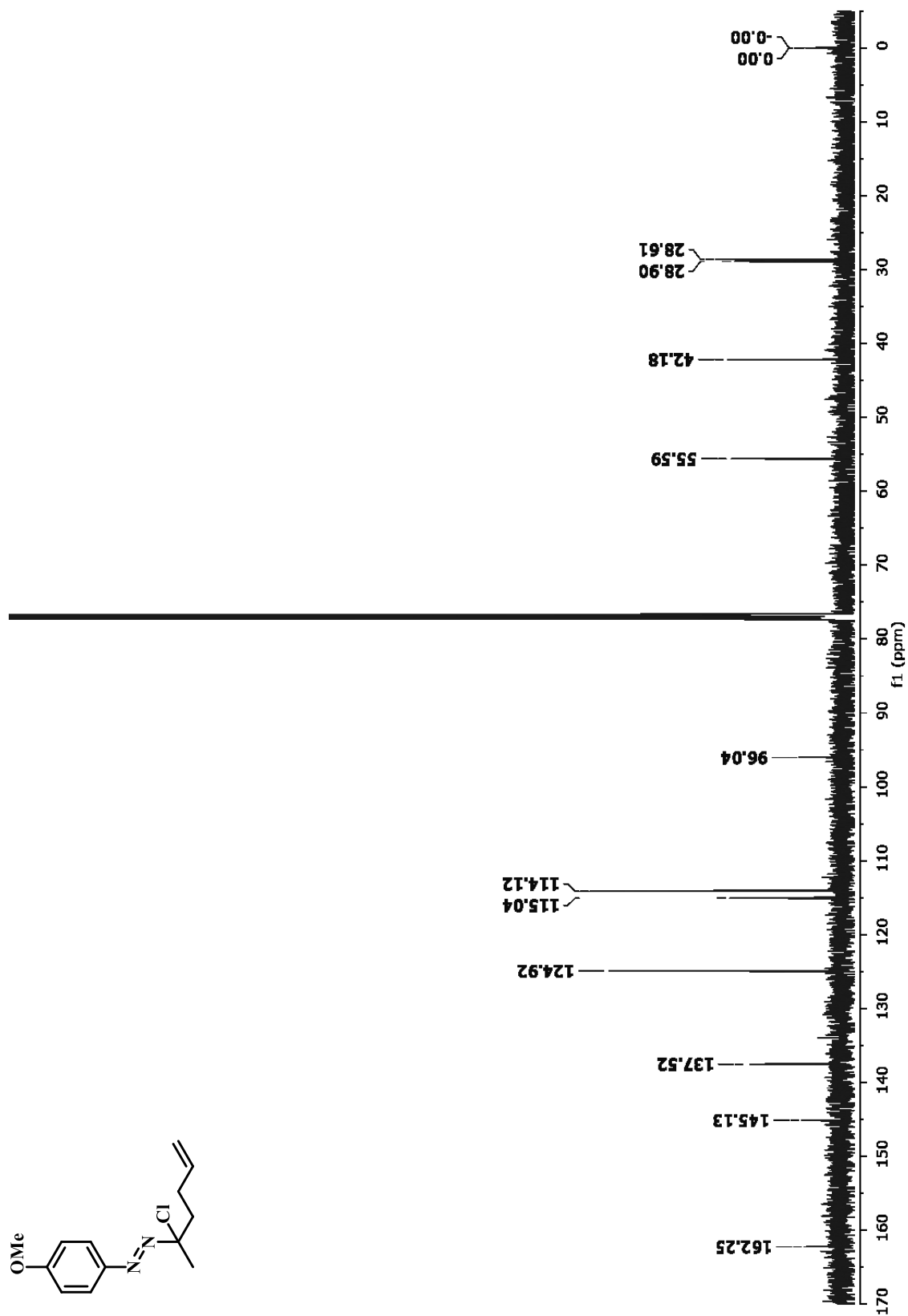
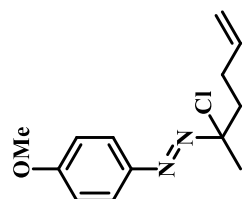


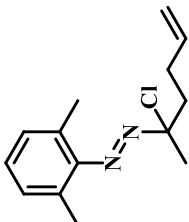


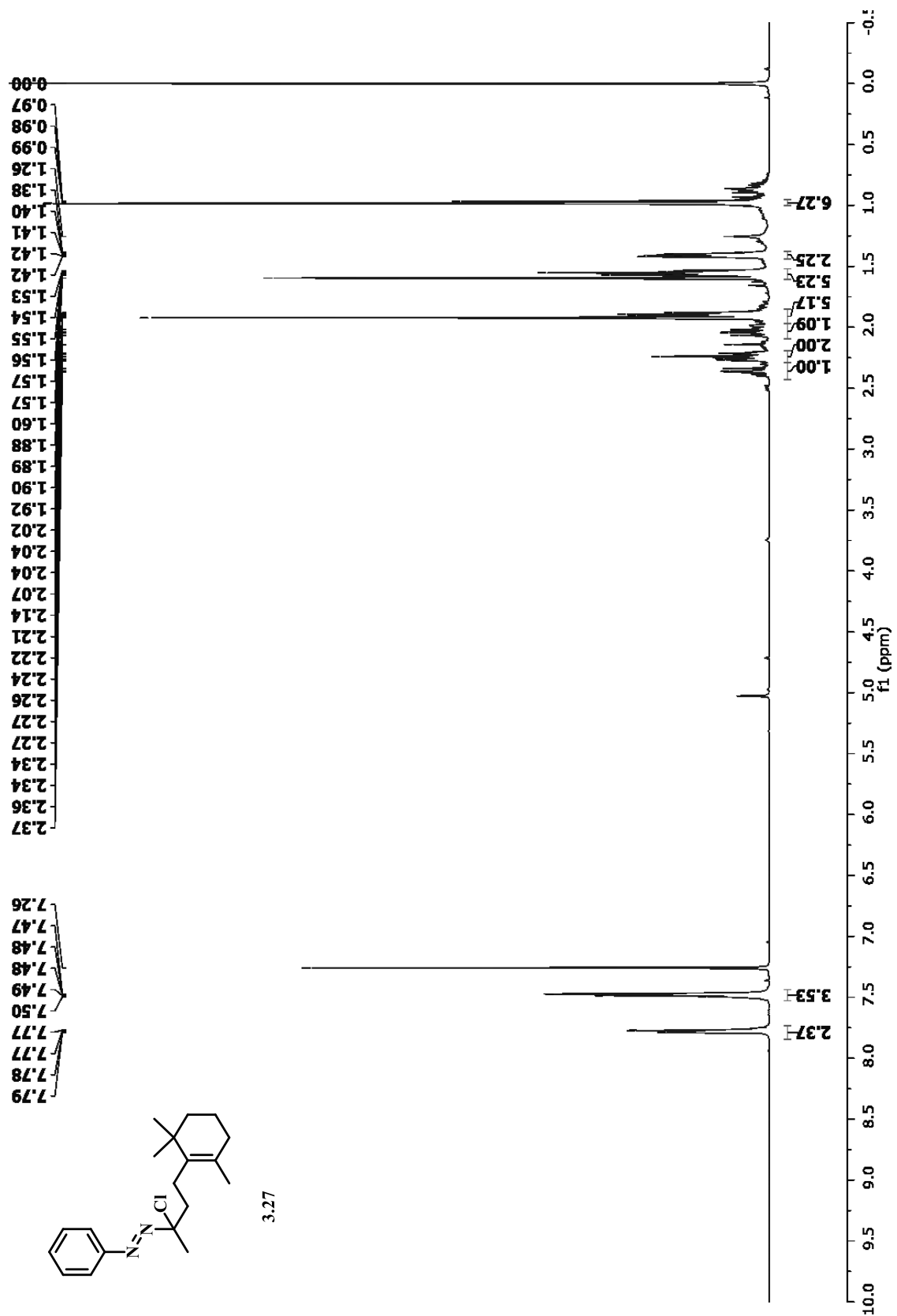


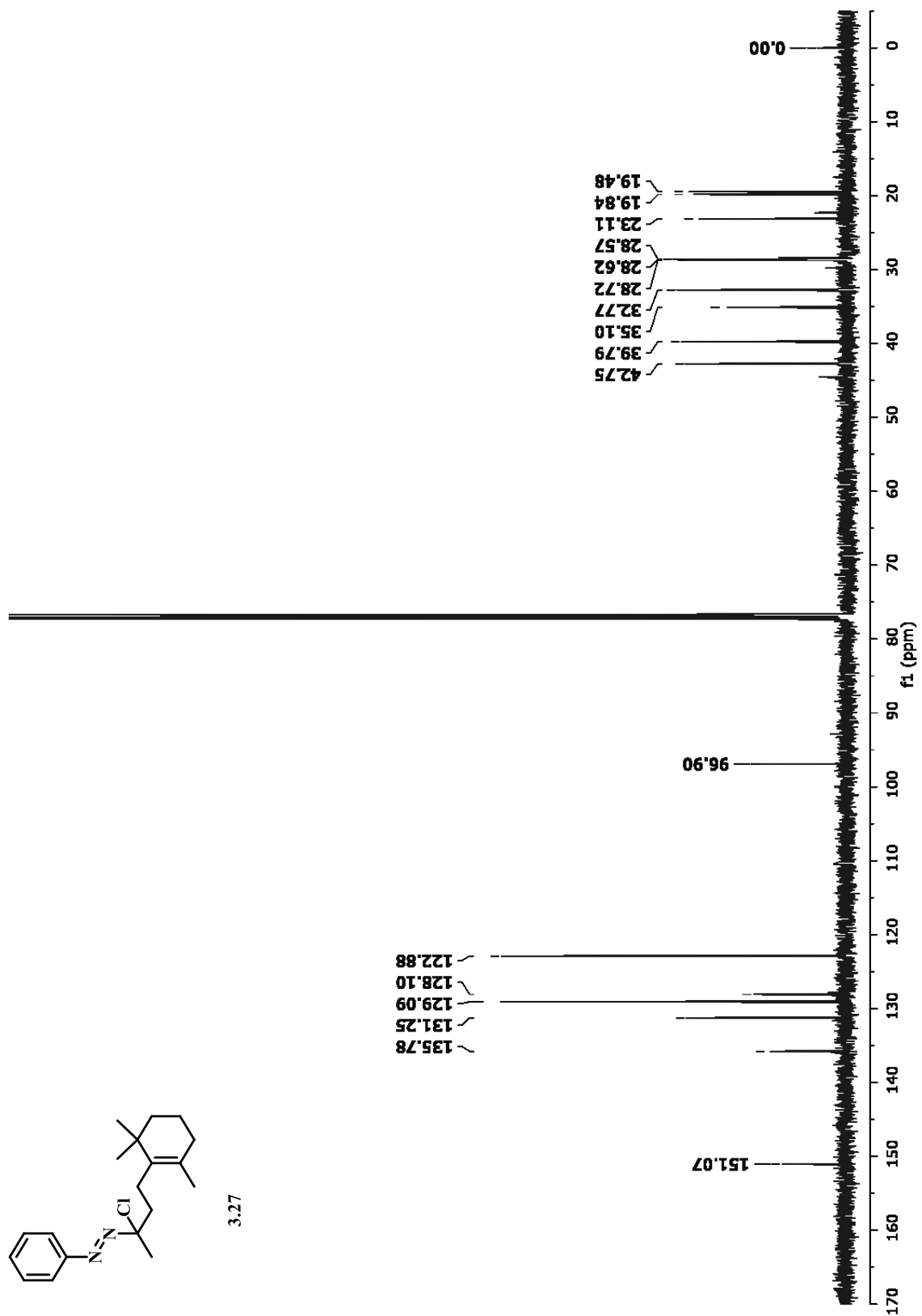


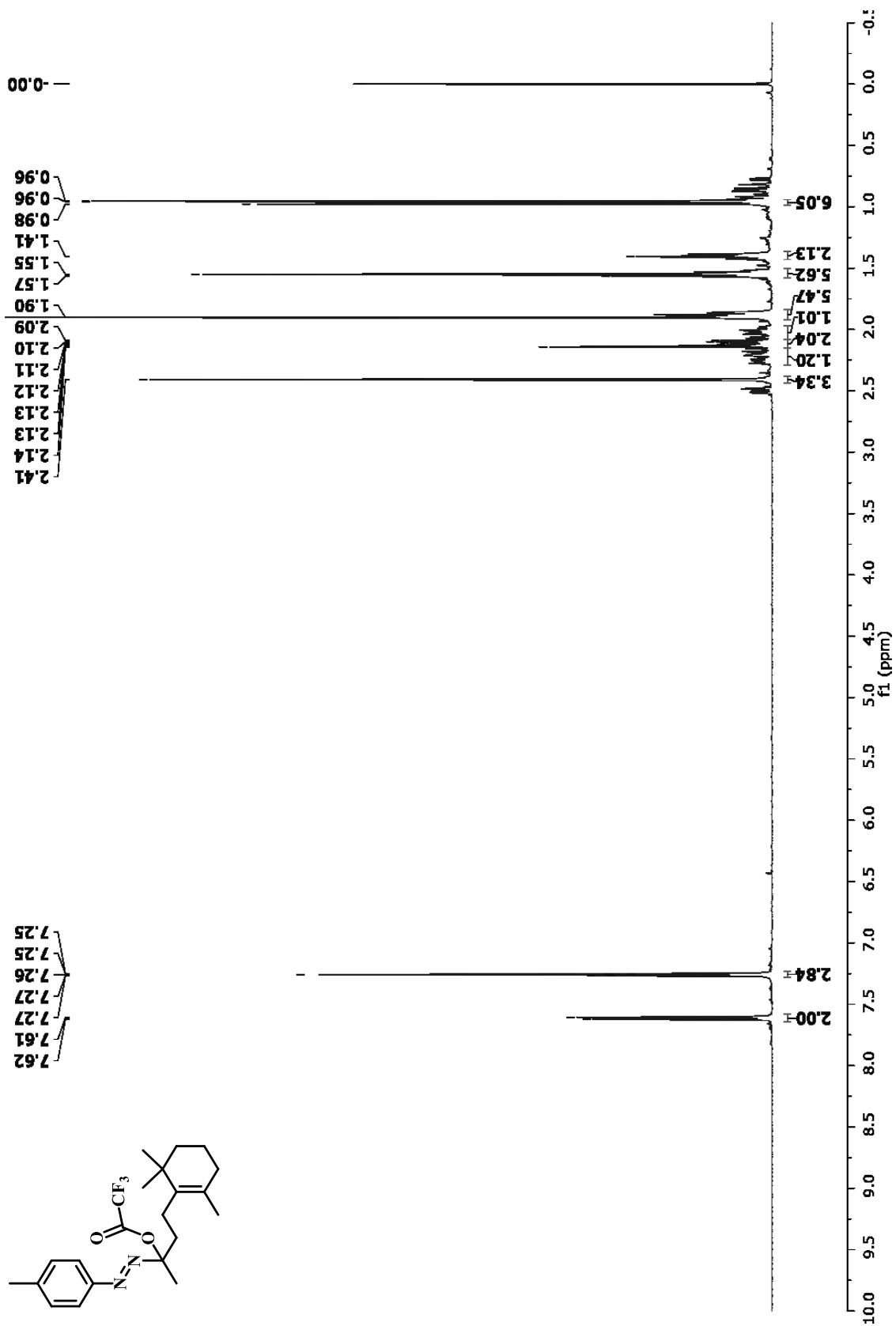


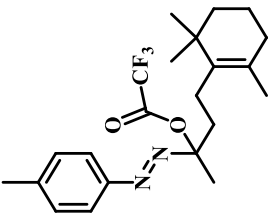


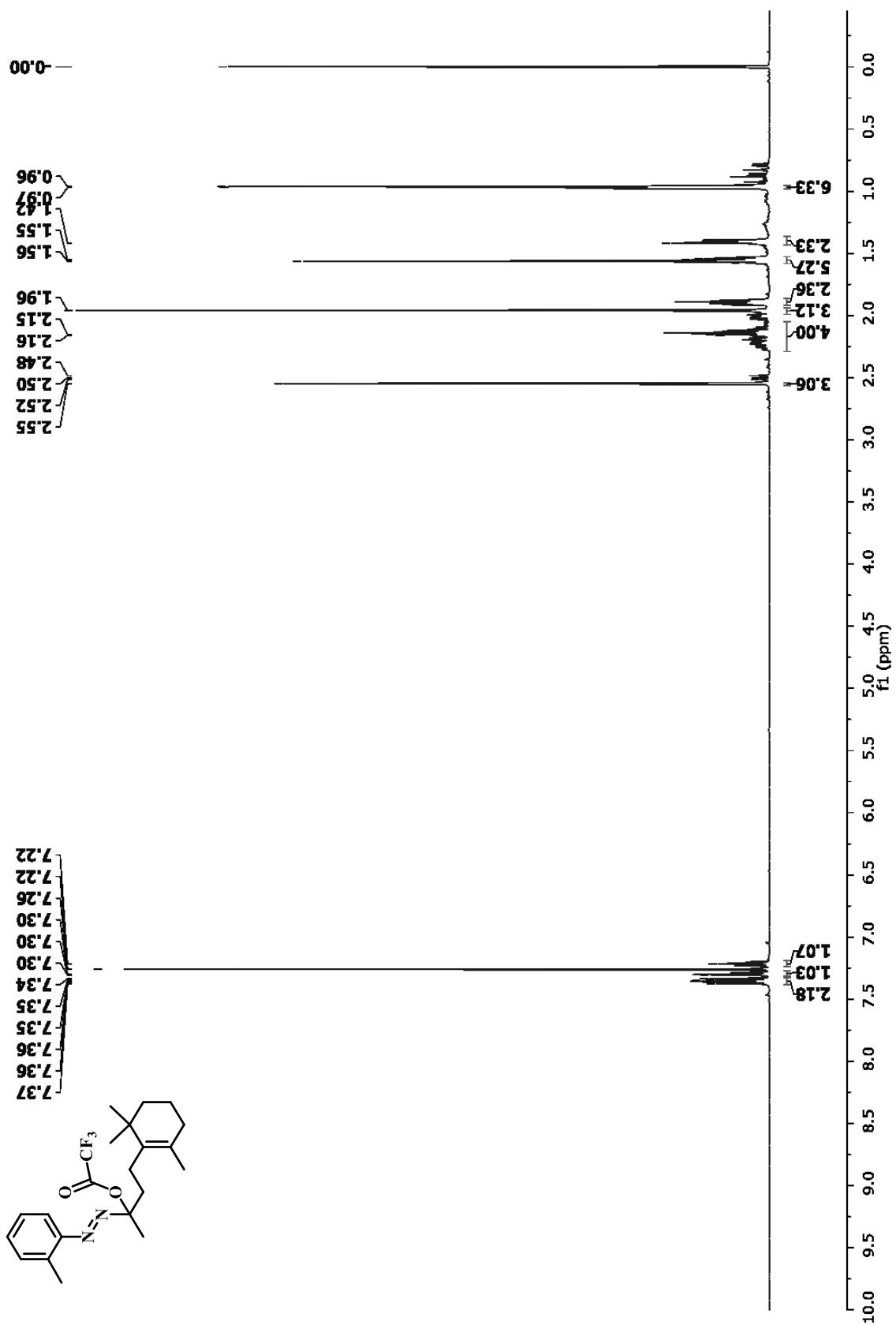


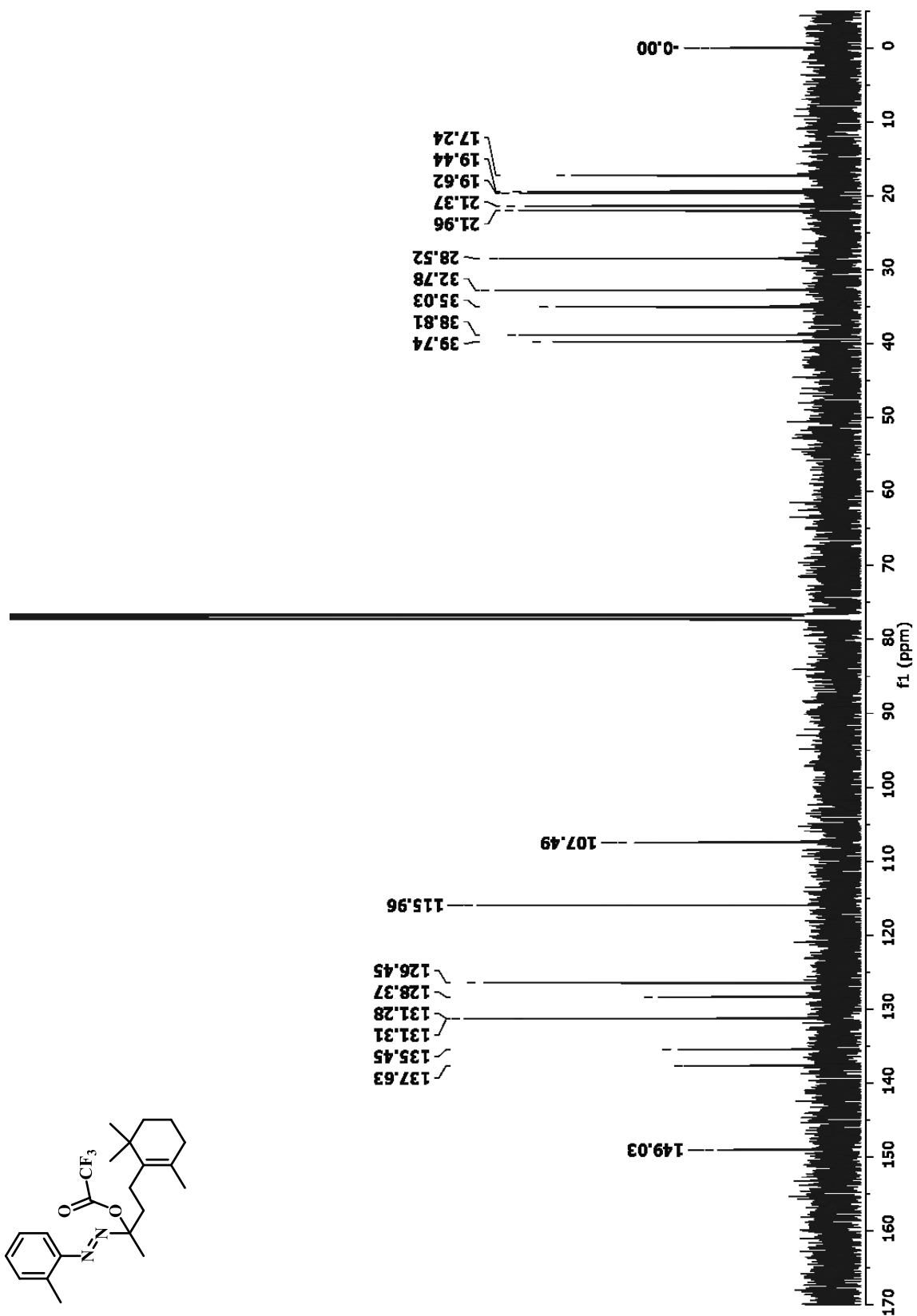


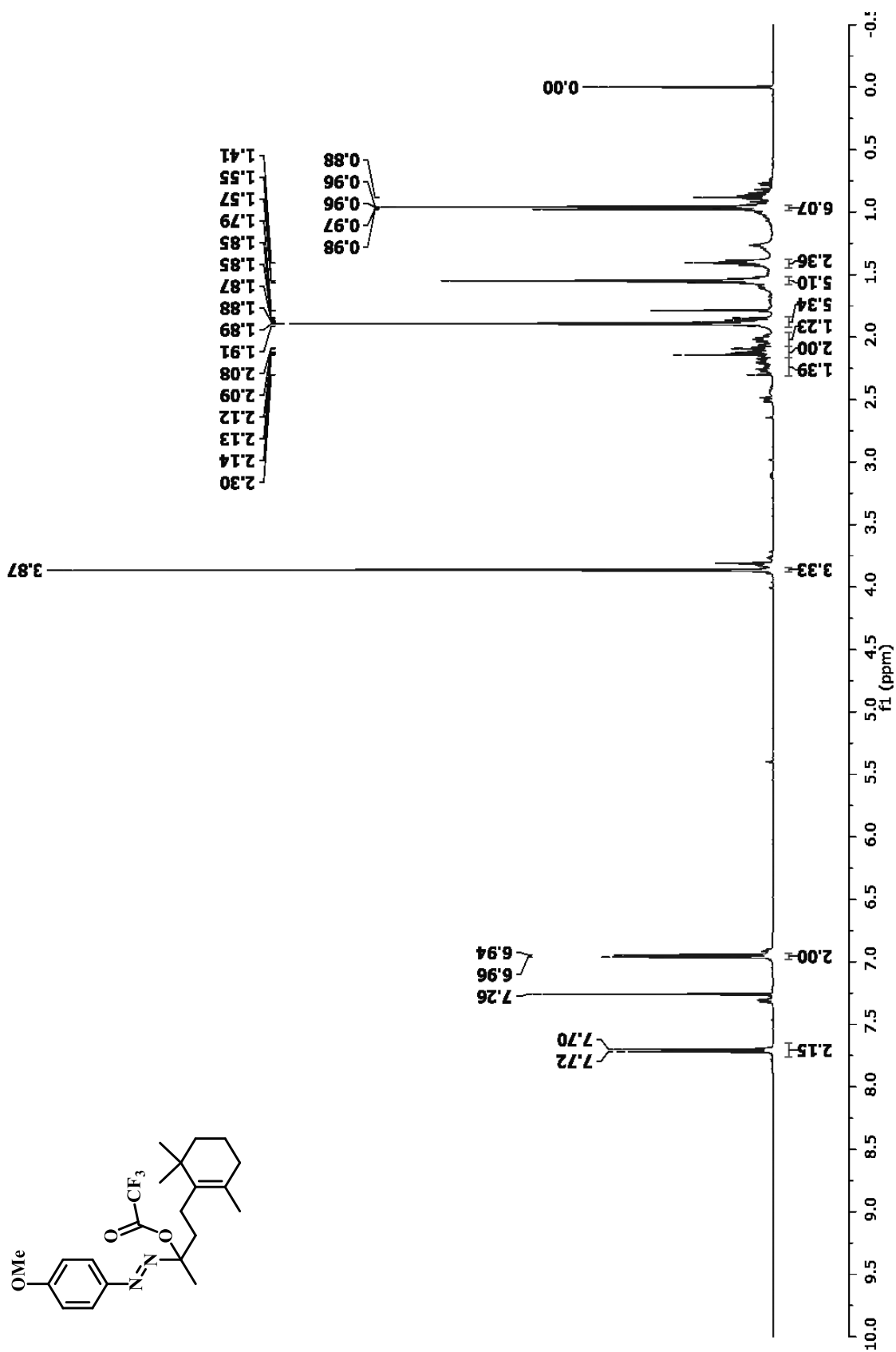
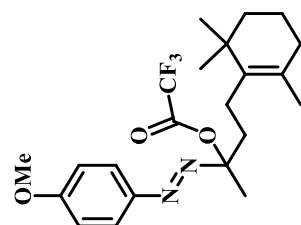


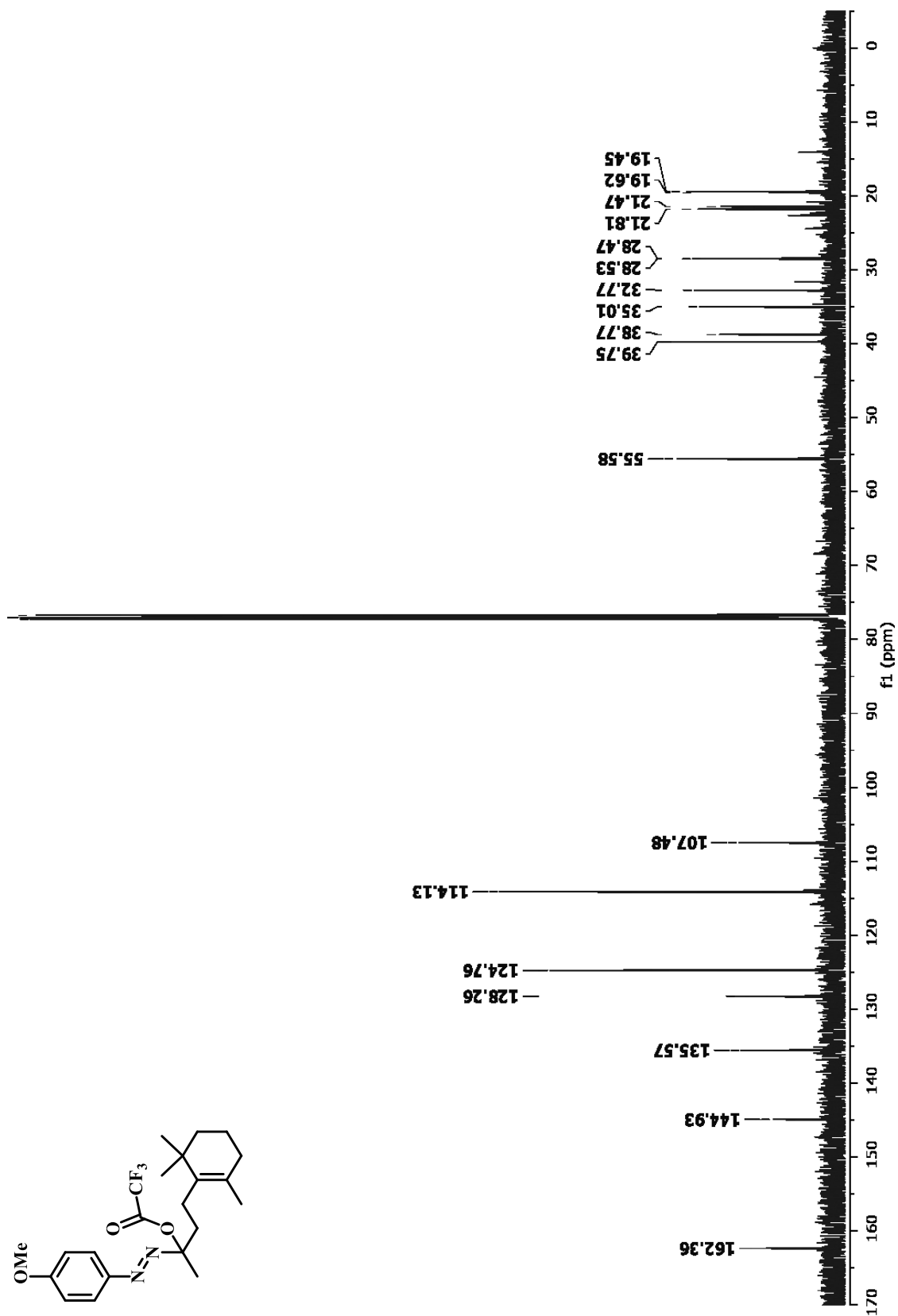


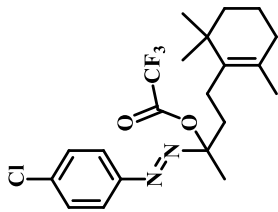


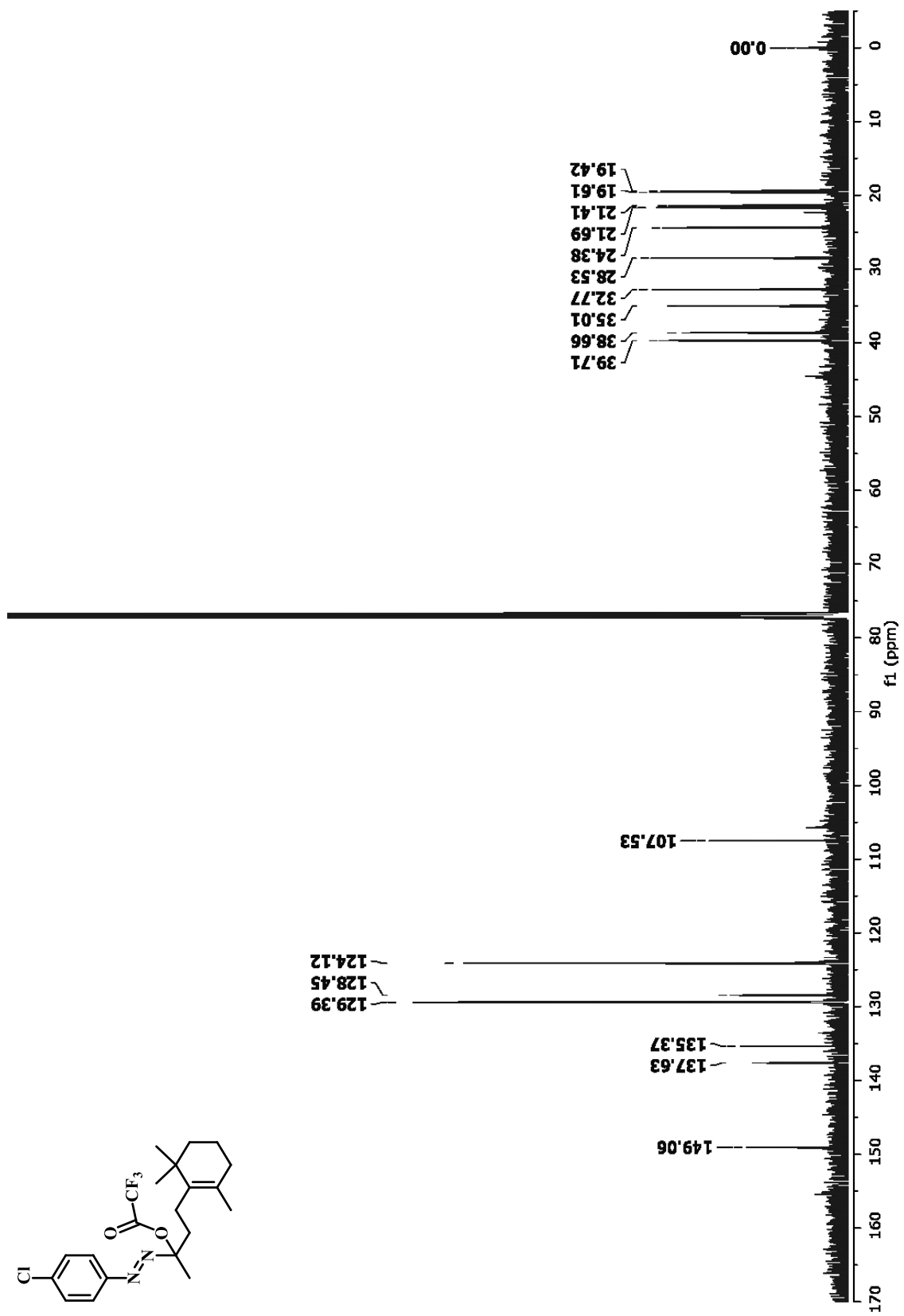


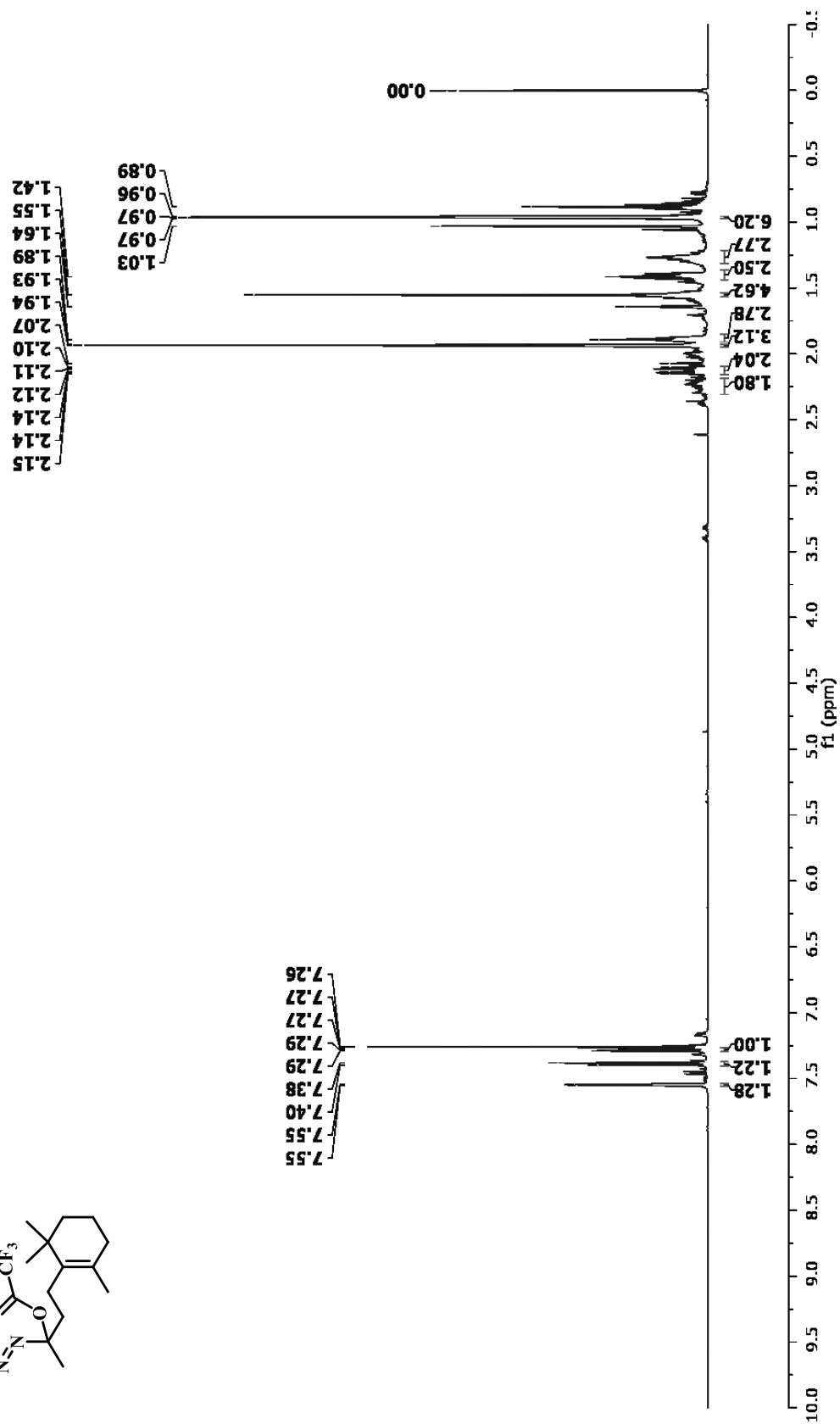
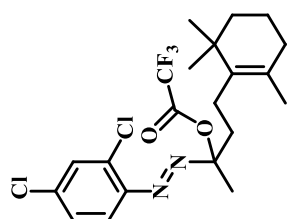


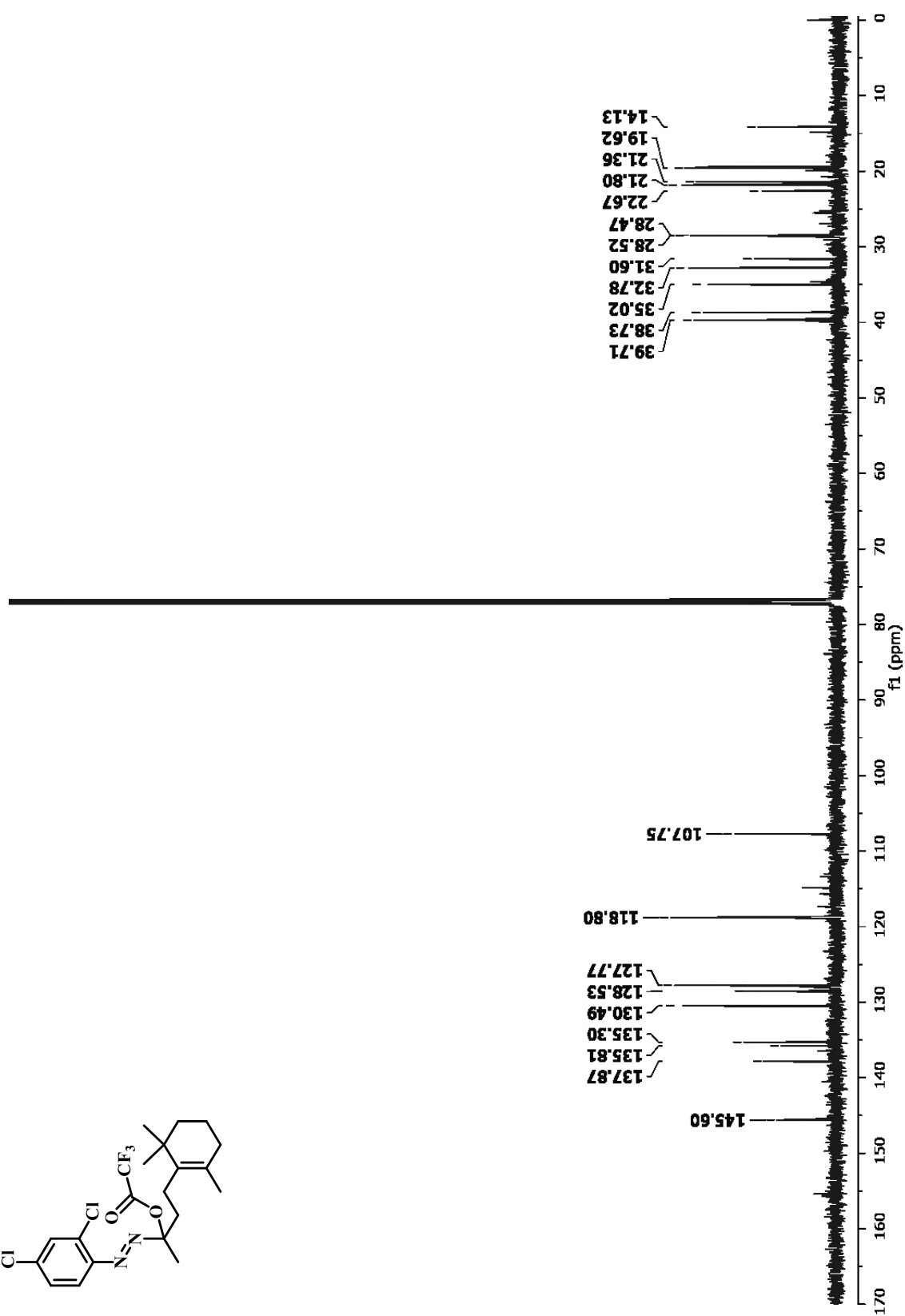
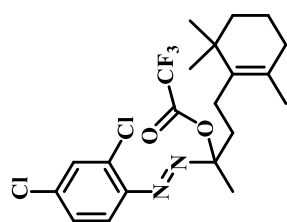


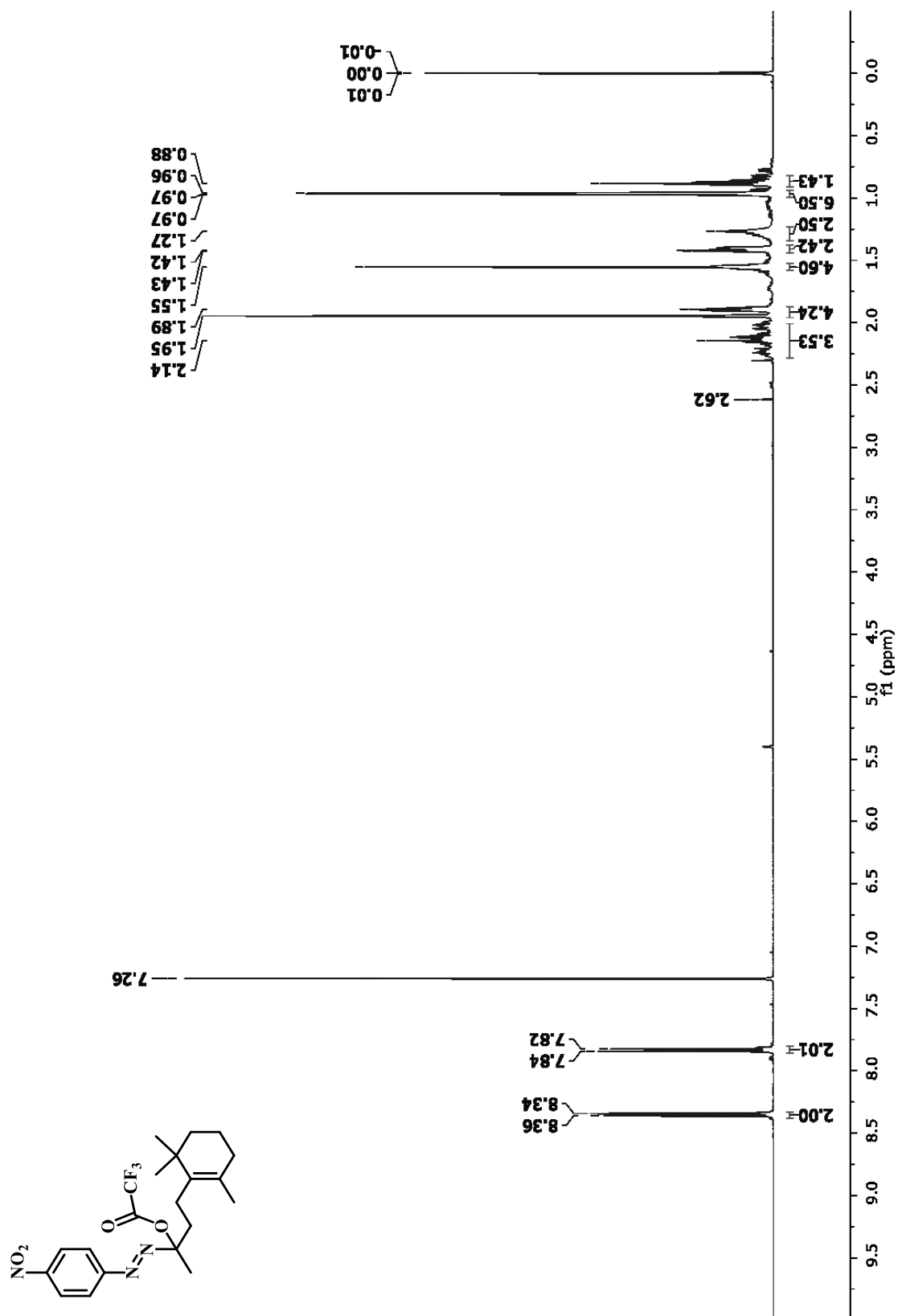


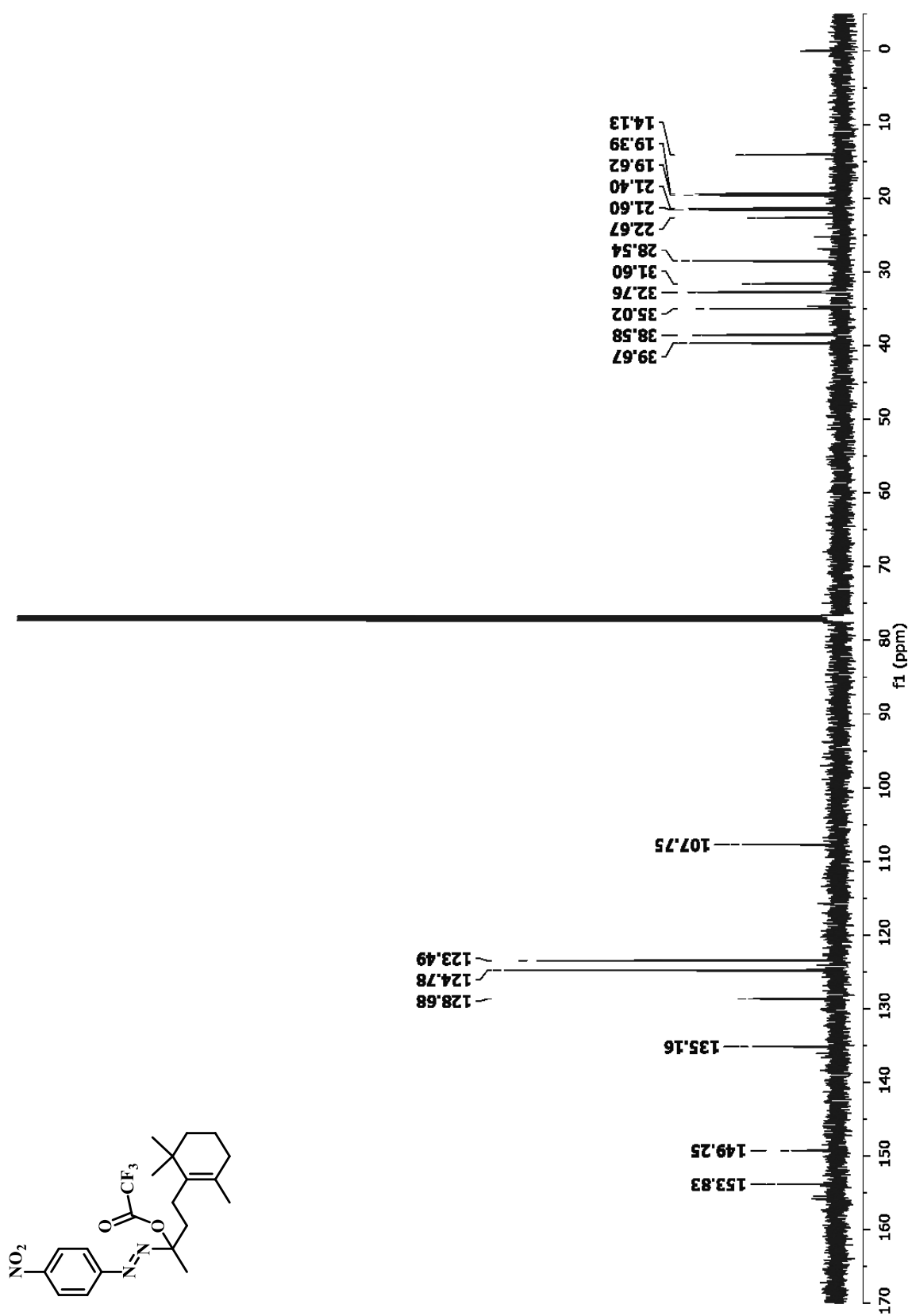


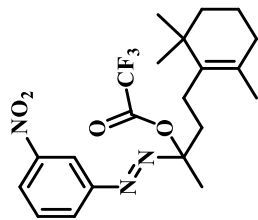


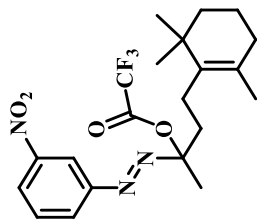


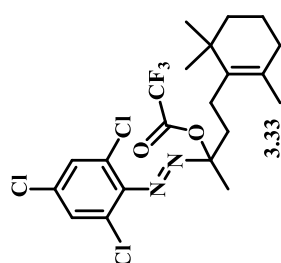




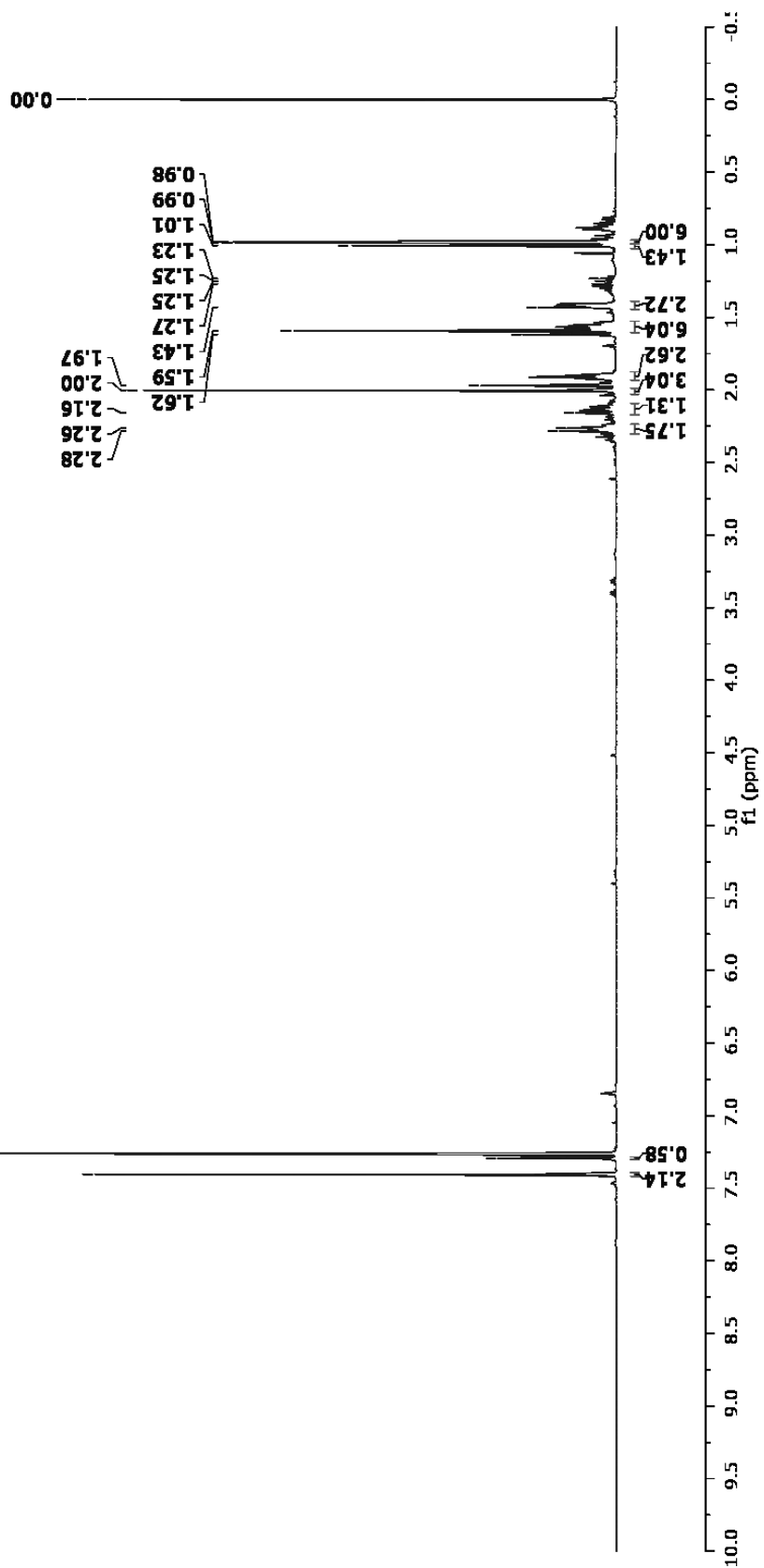


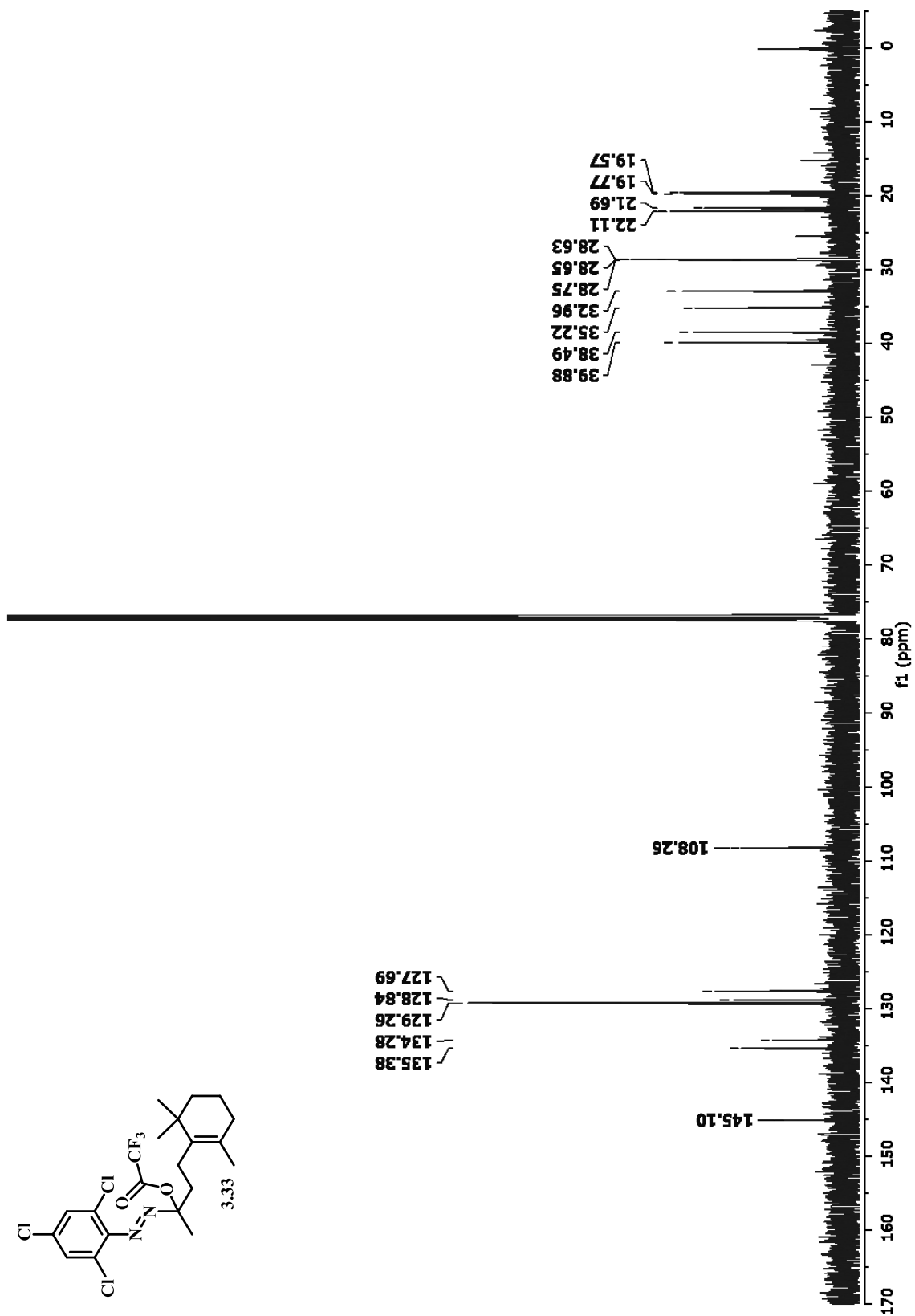


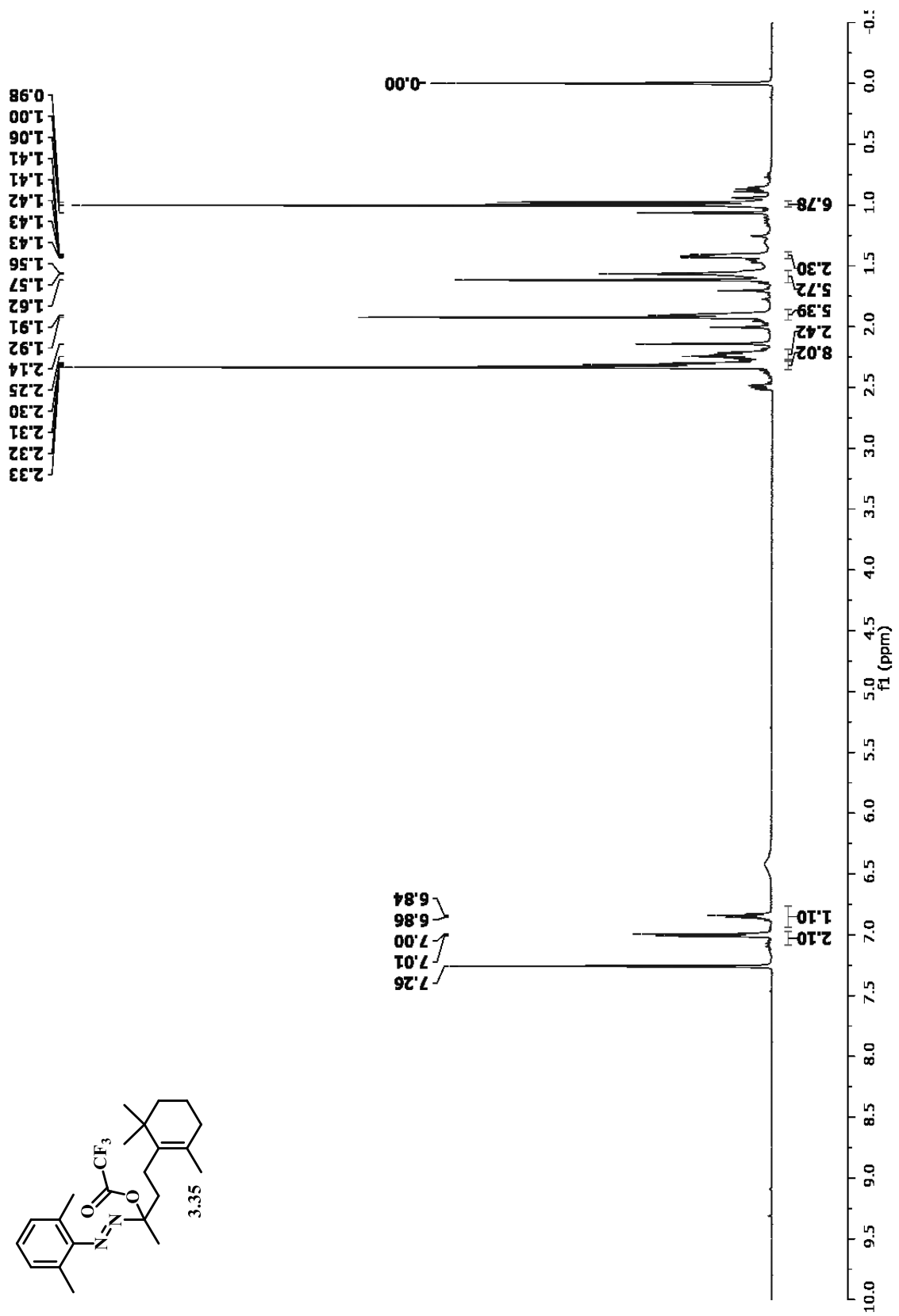


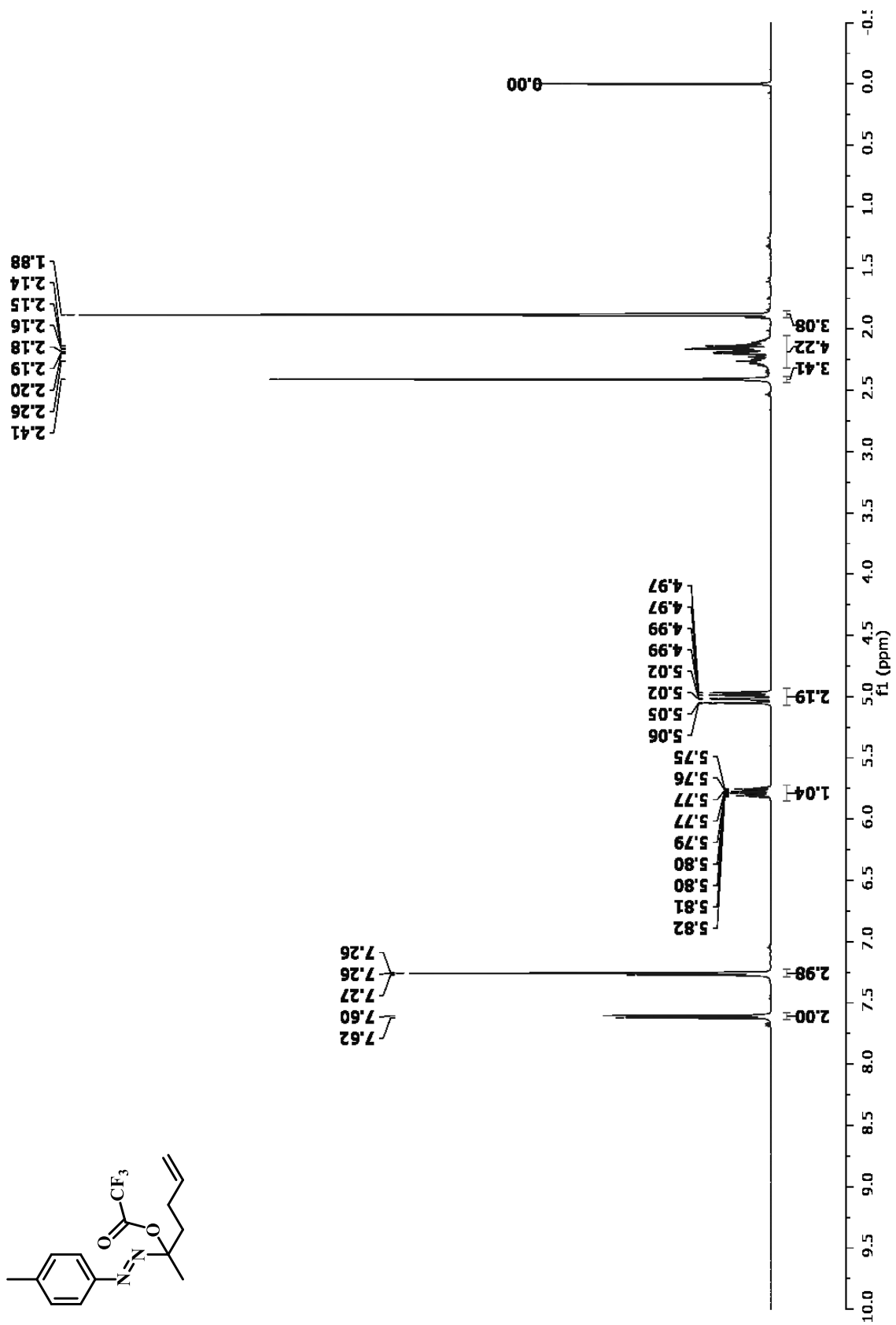
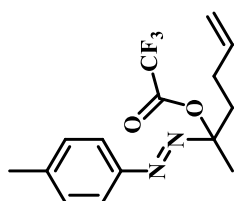


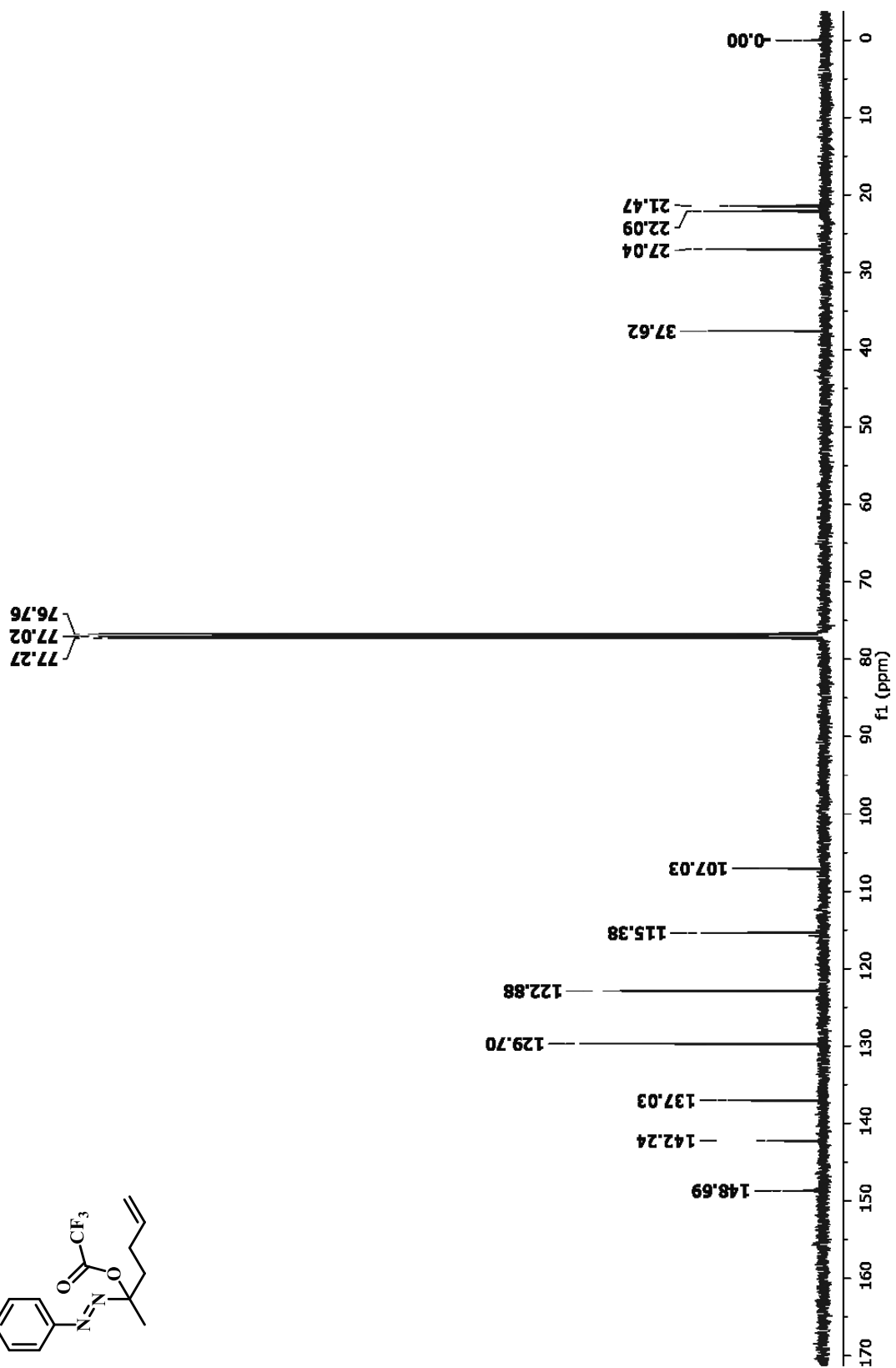
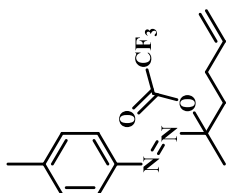
7.40
7.29
7.26

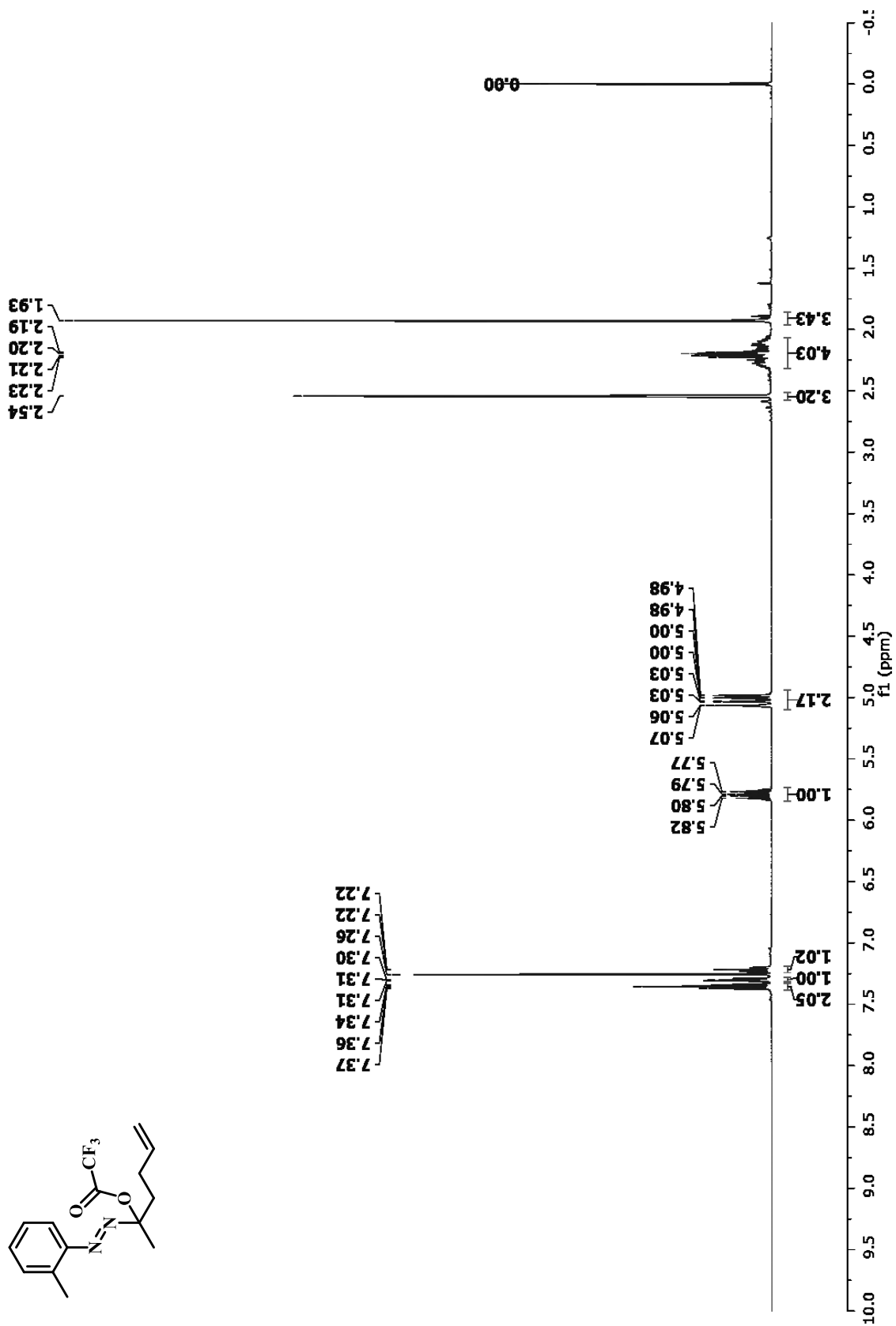
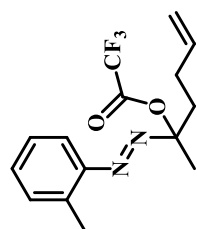


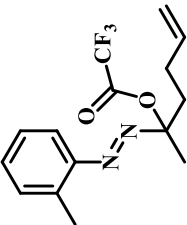


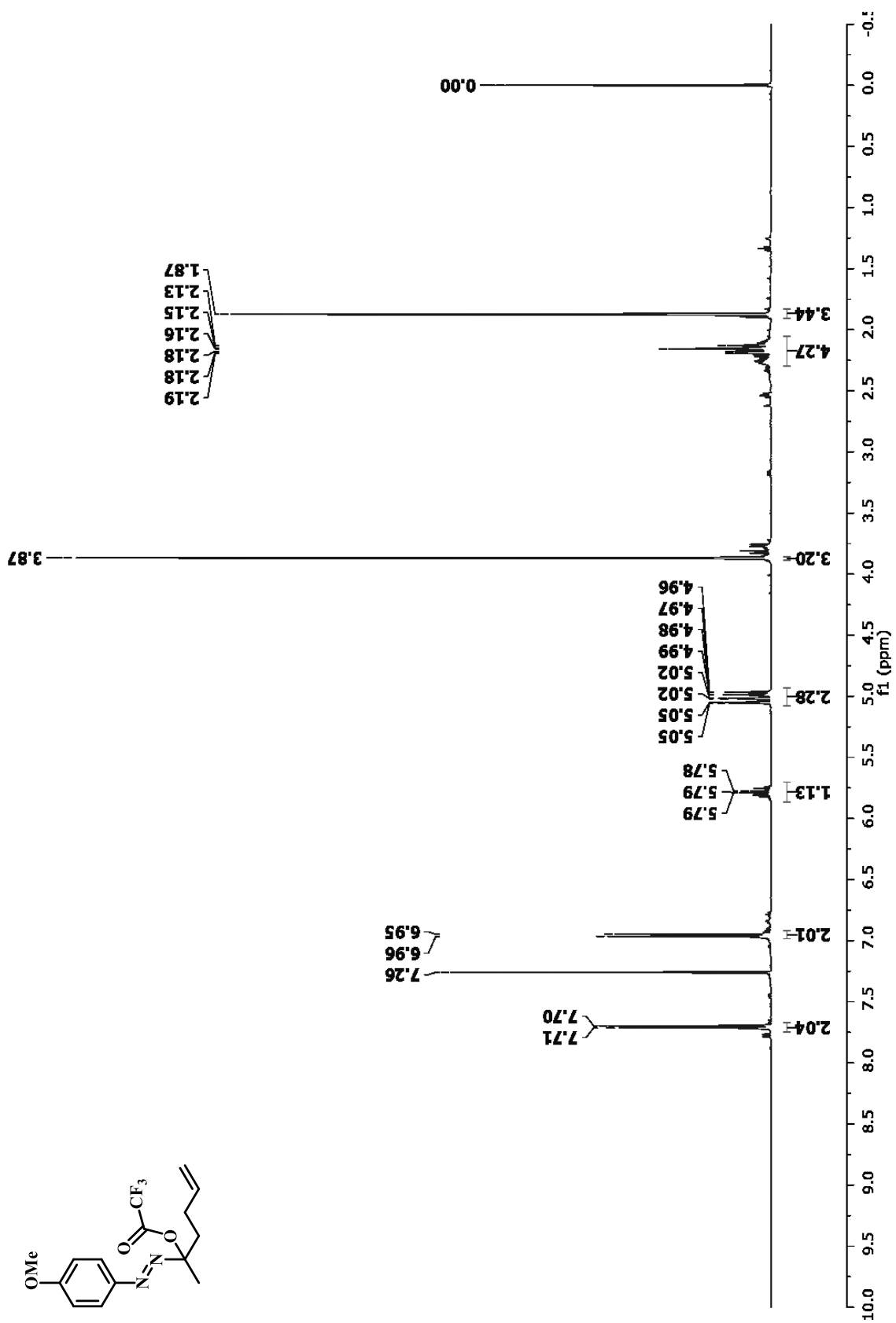


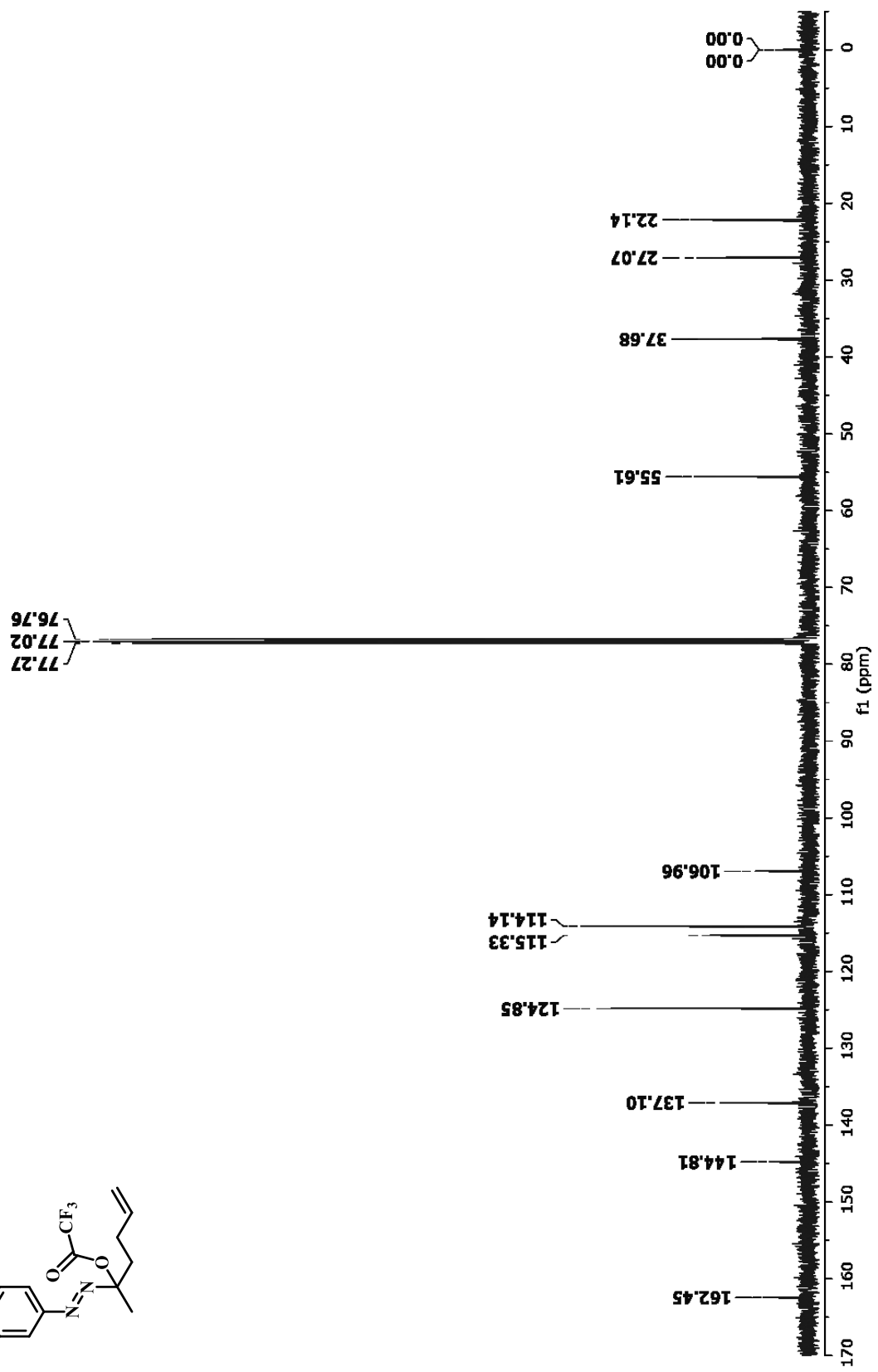
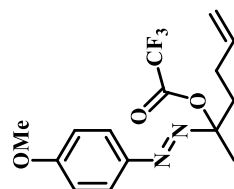


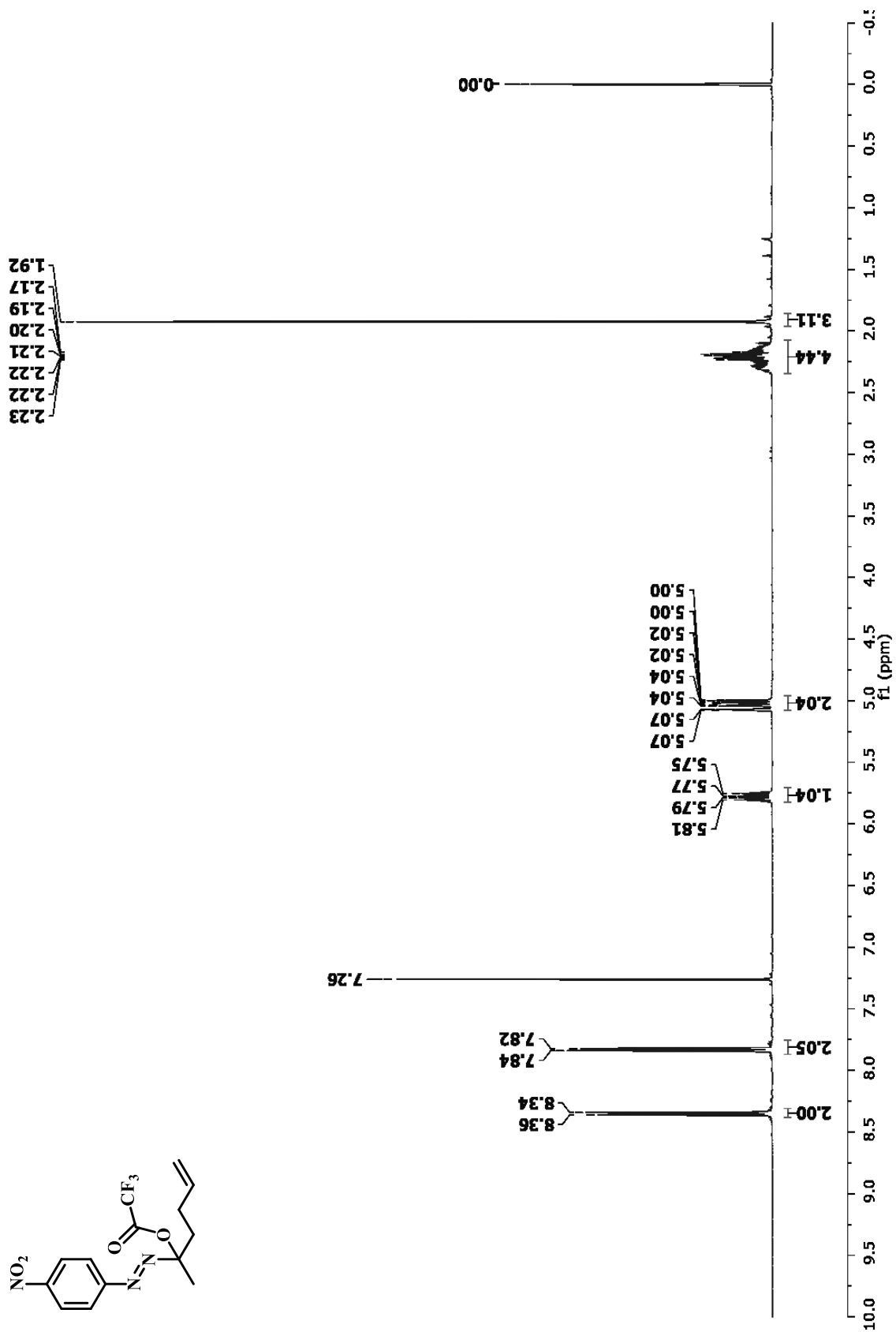
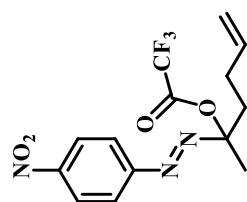


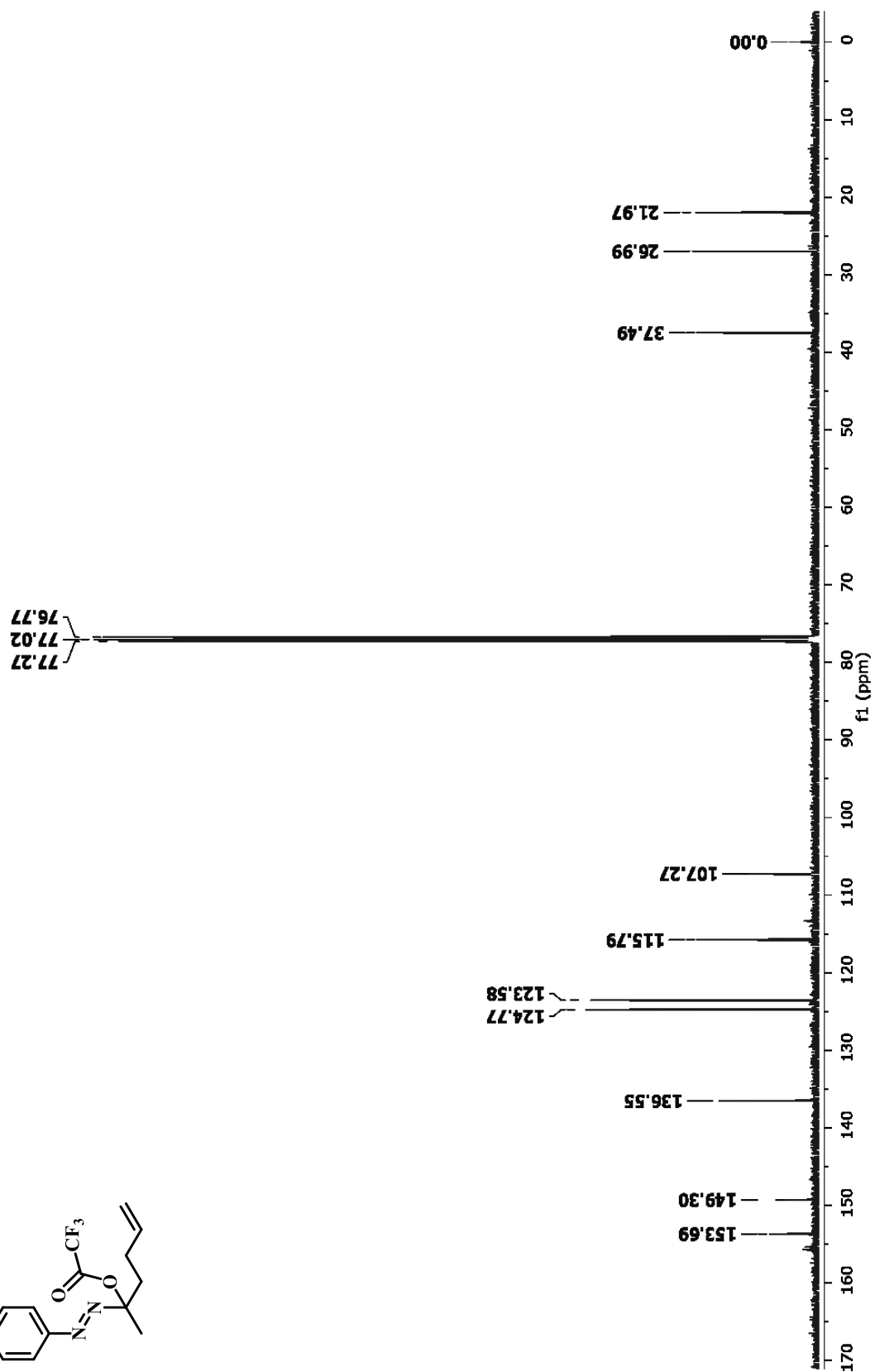
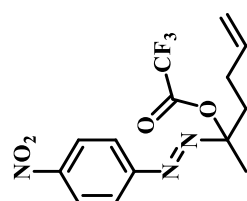


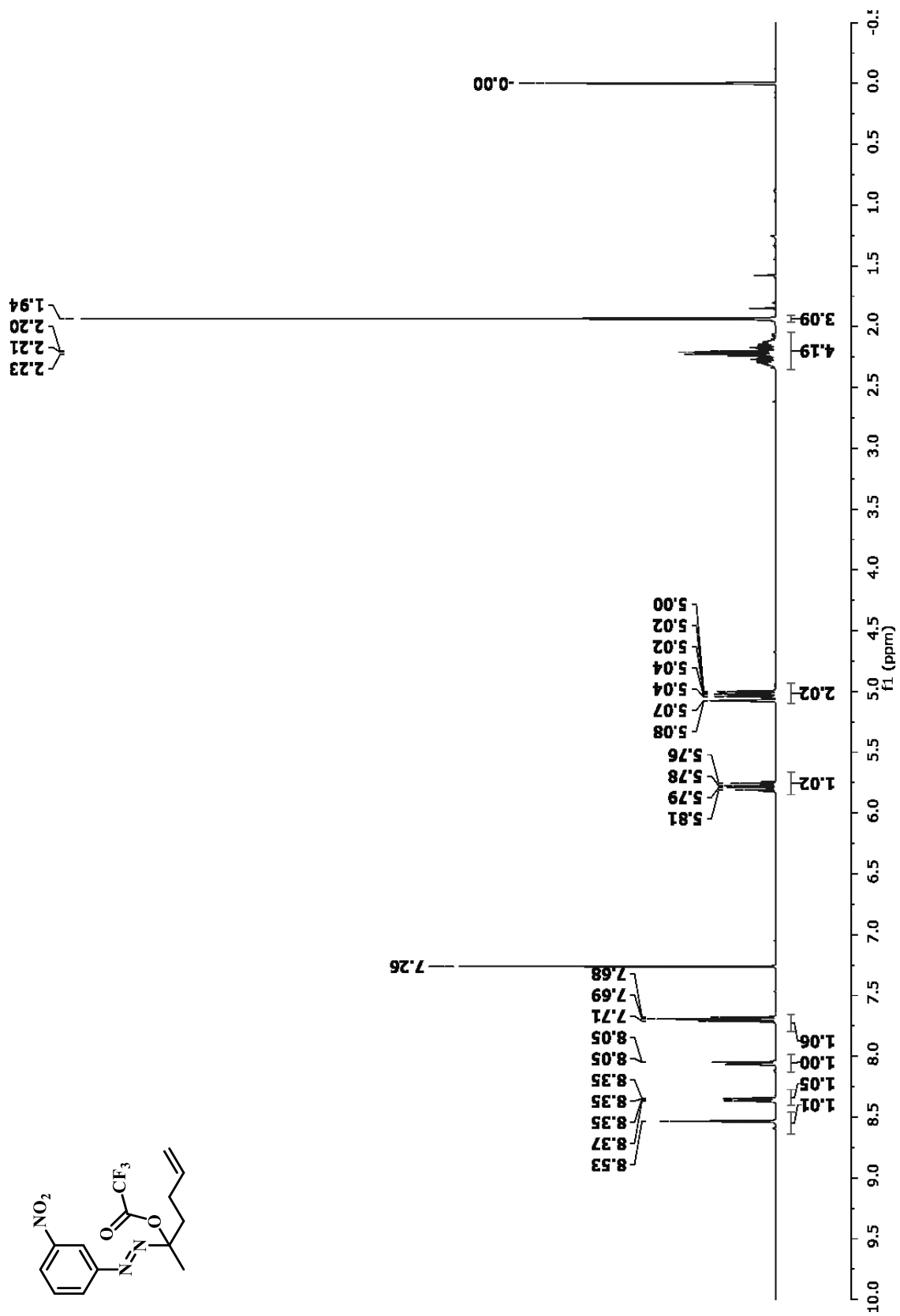


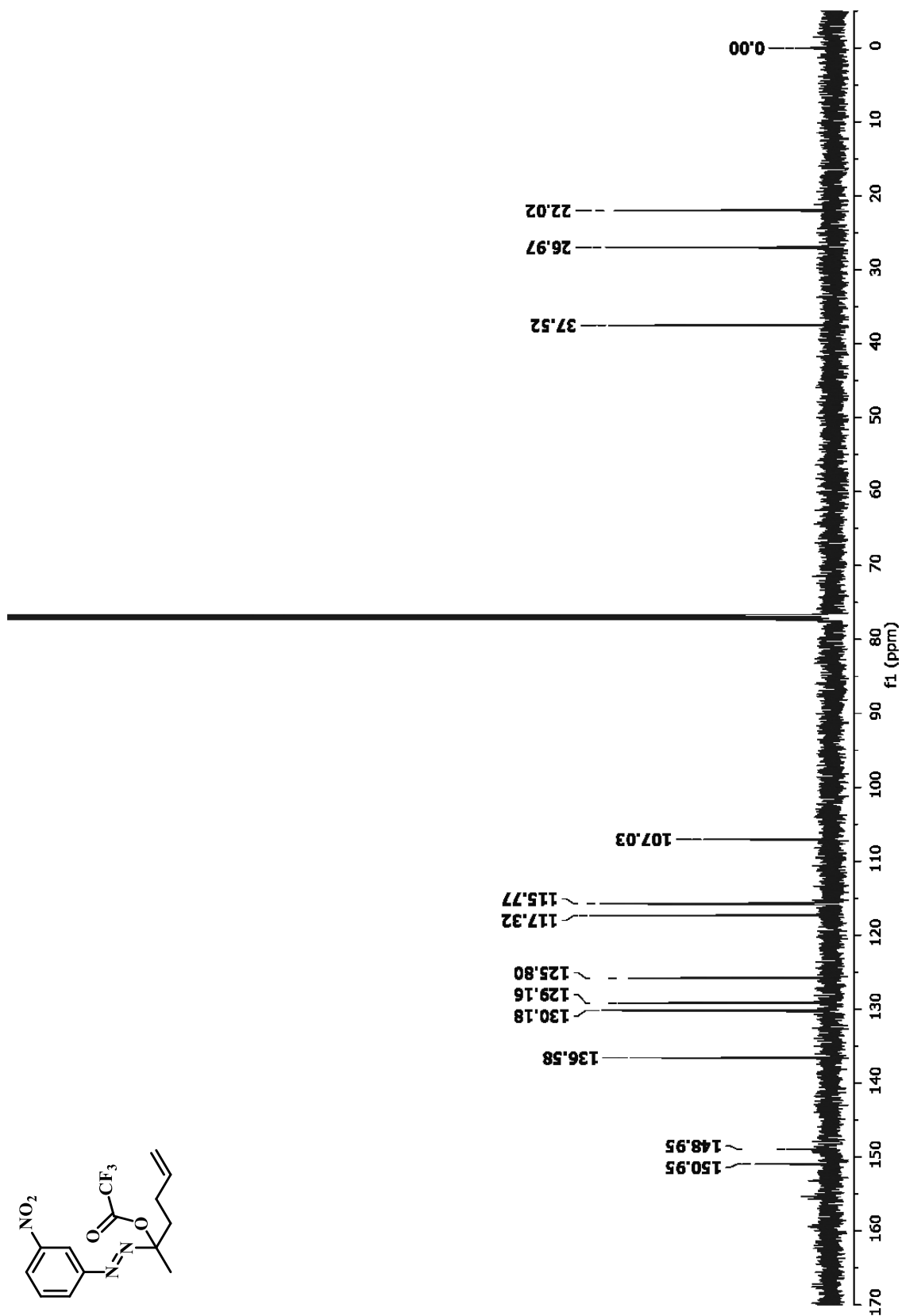


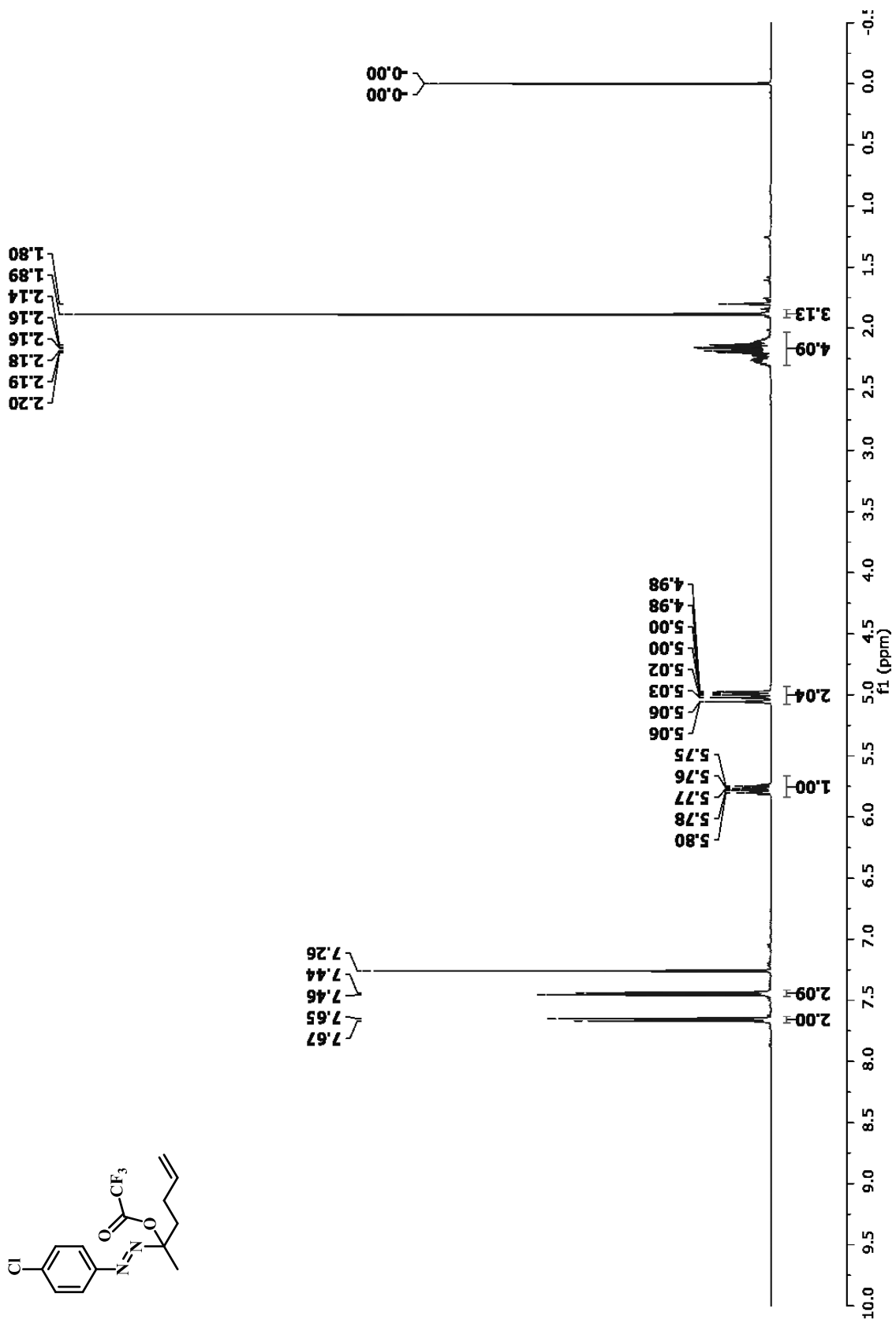
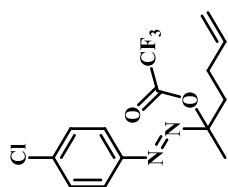


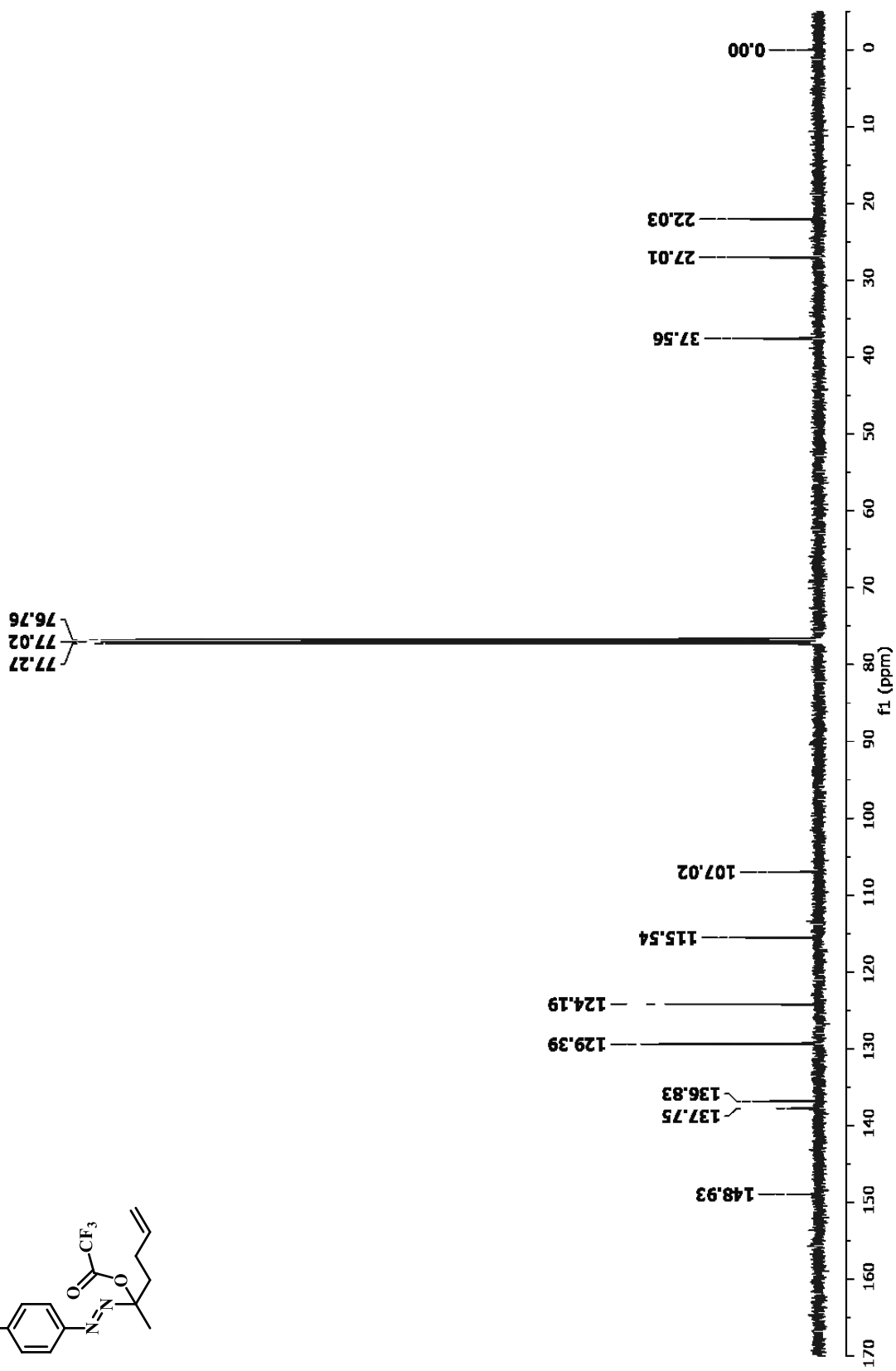
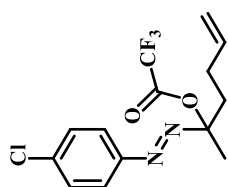


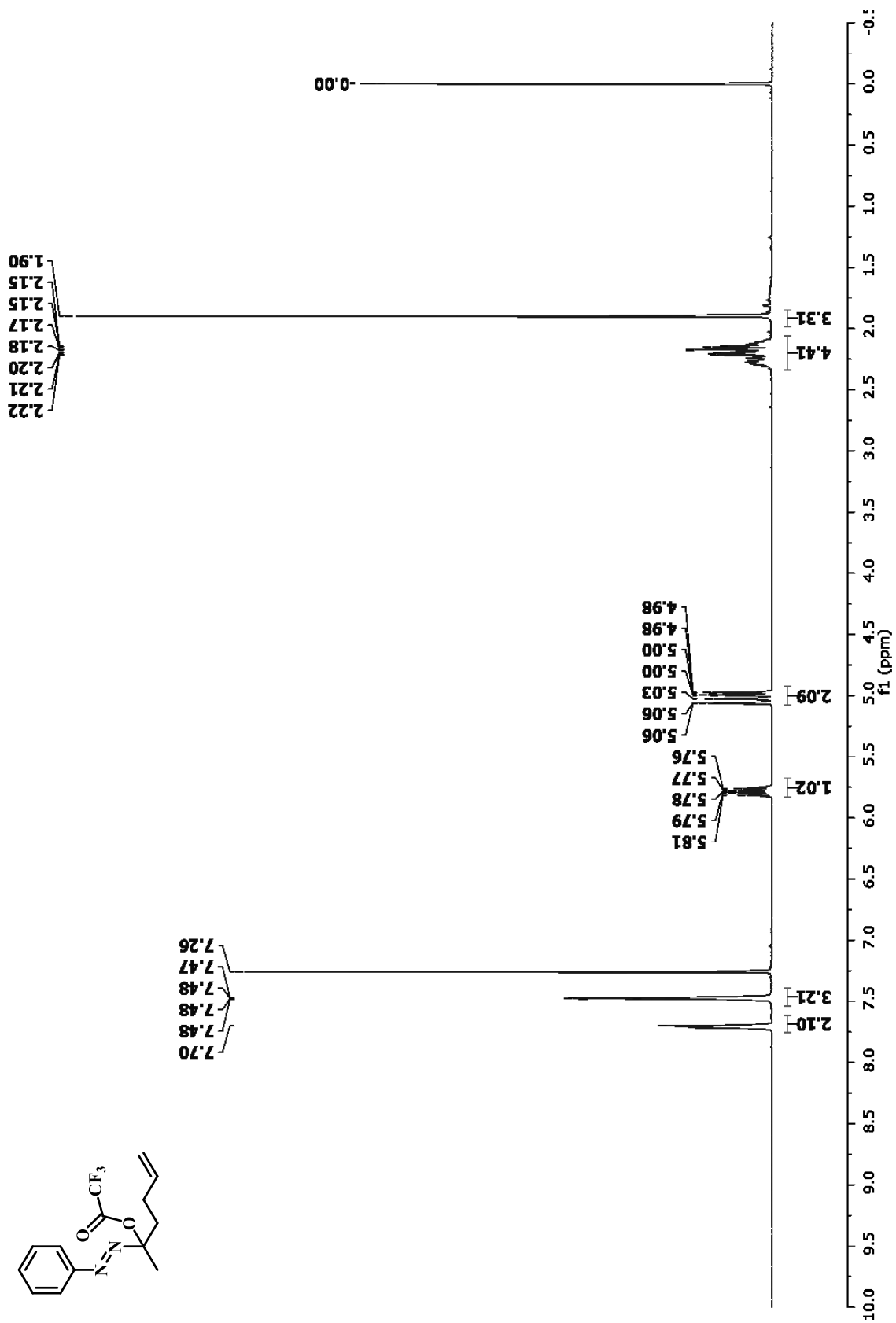
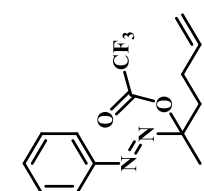


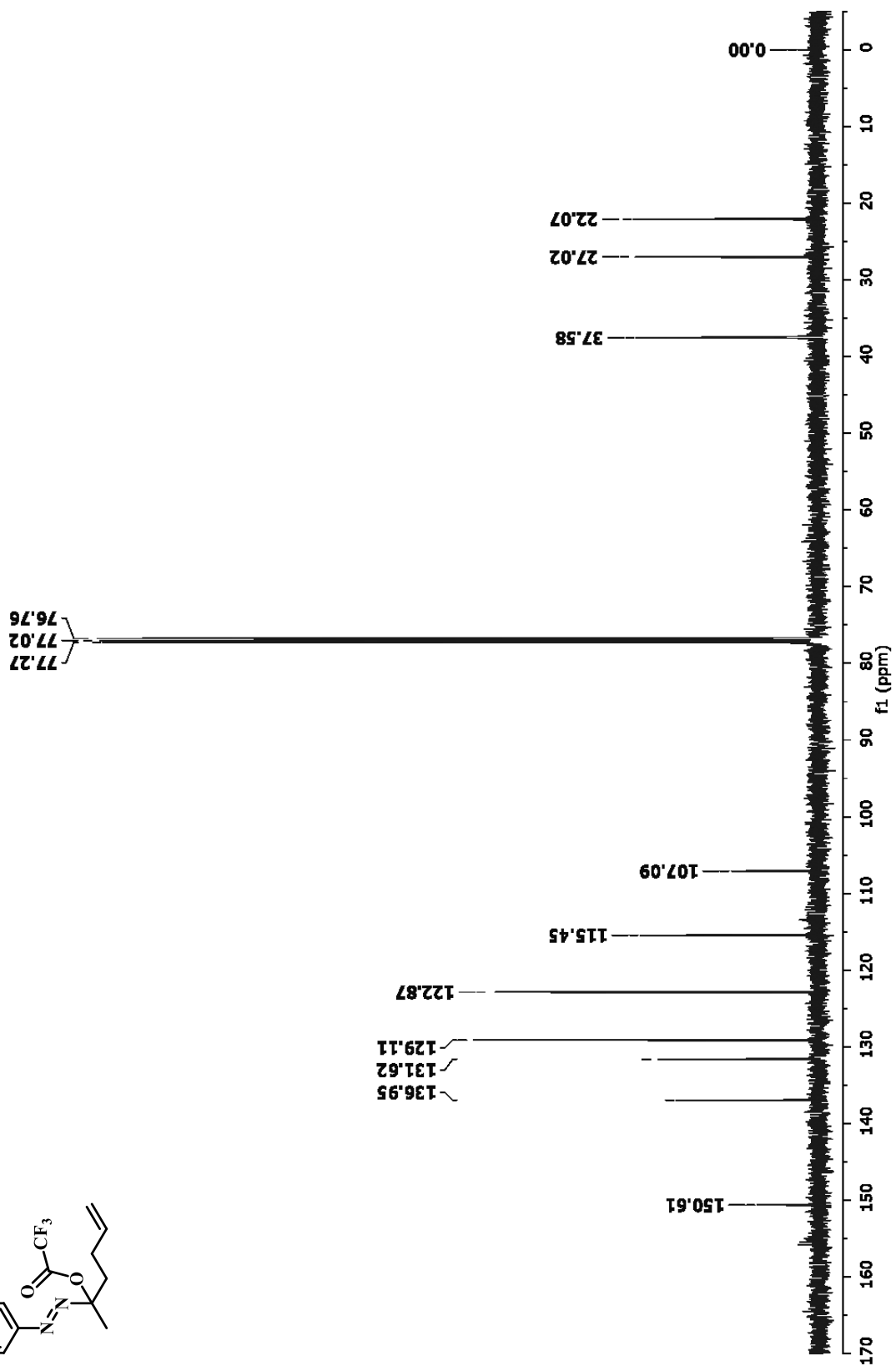
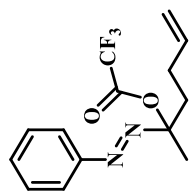


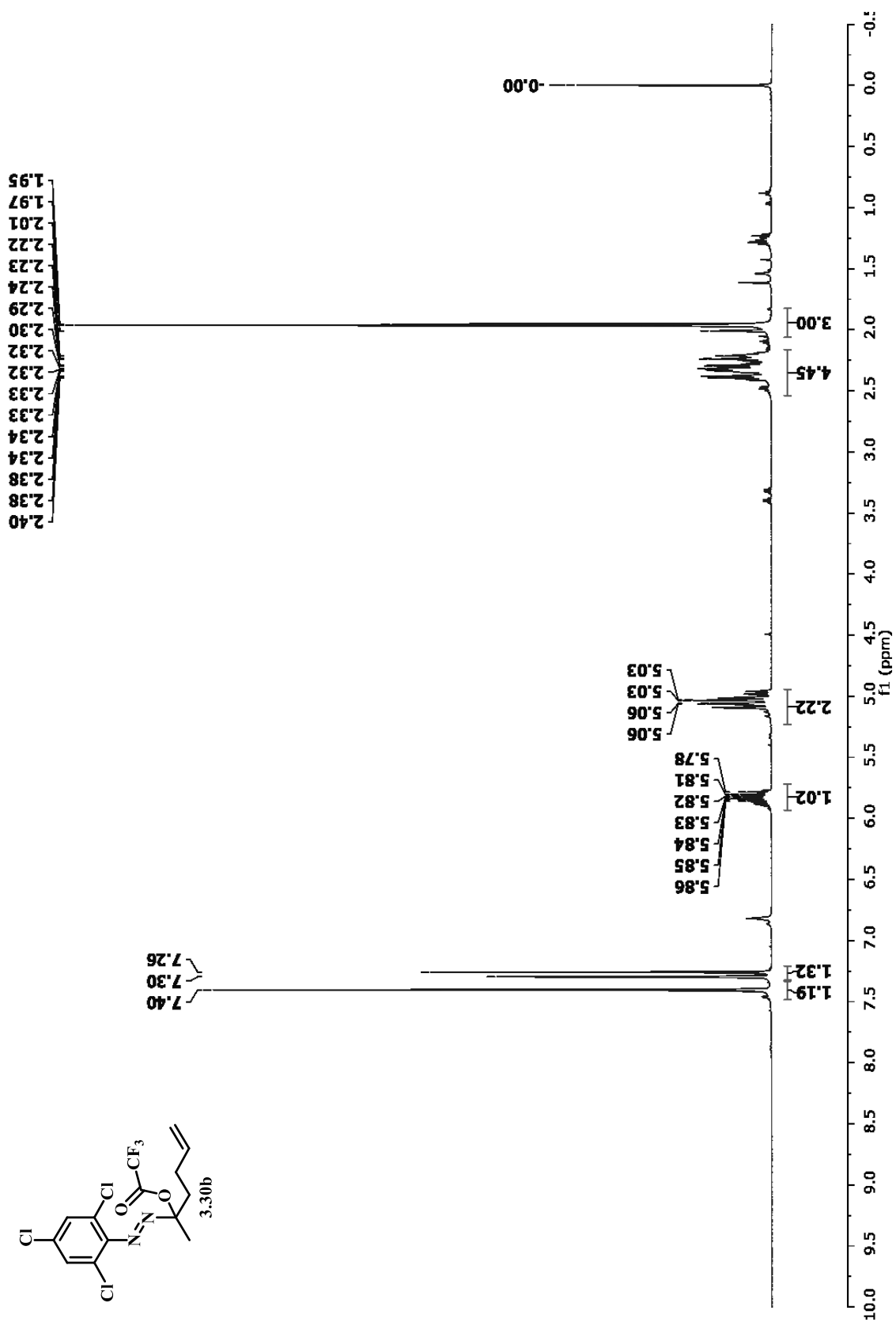


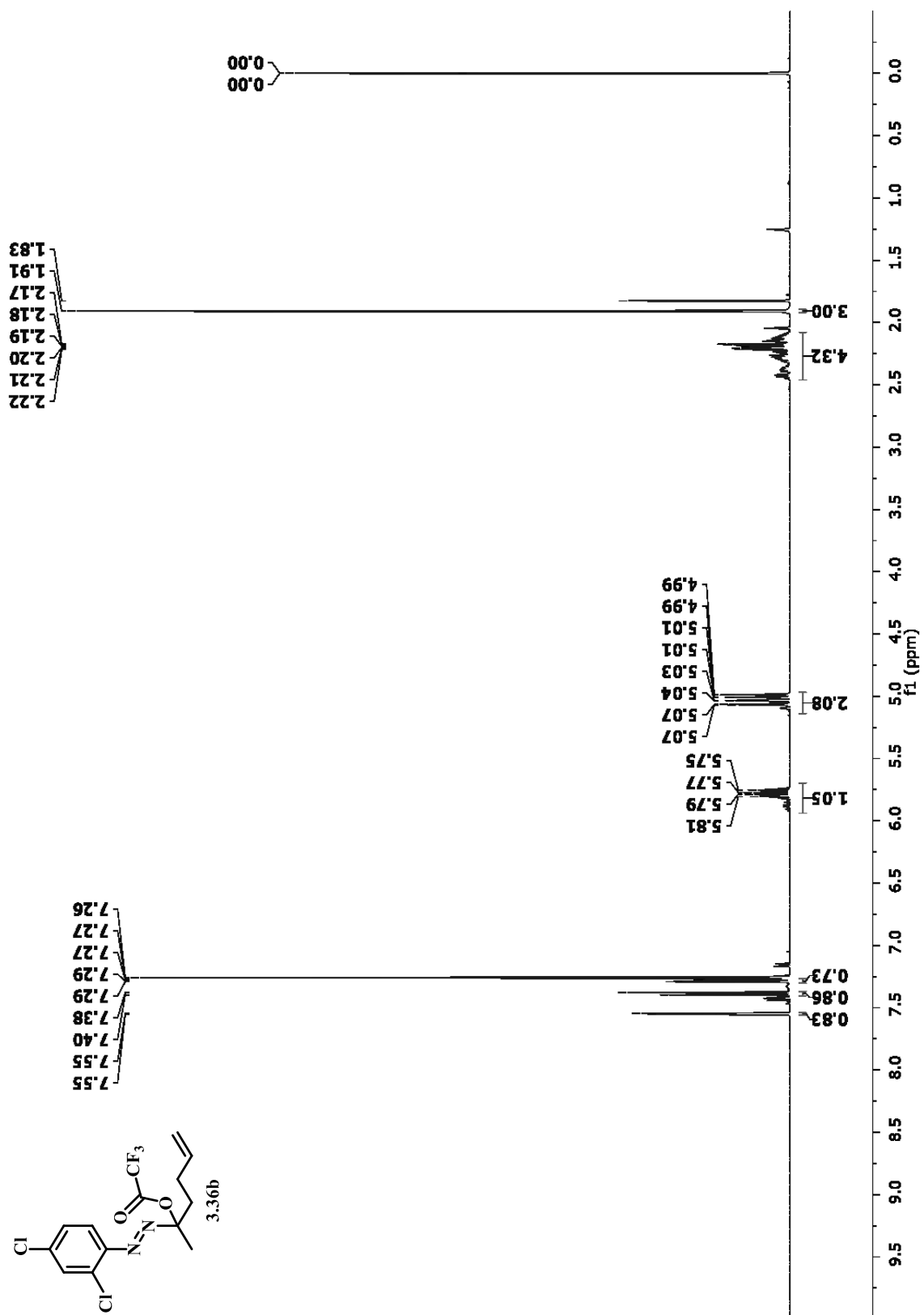


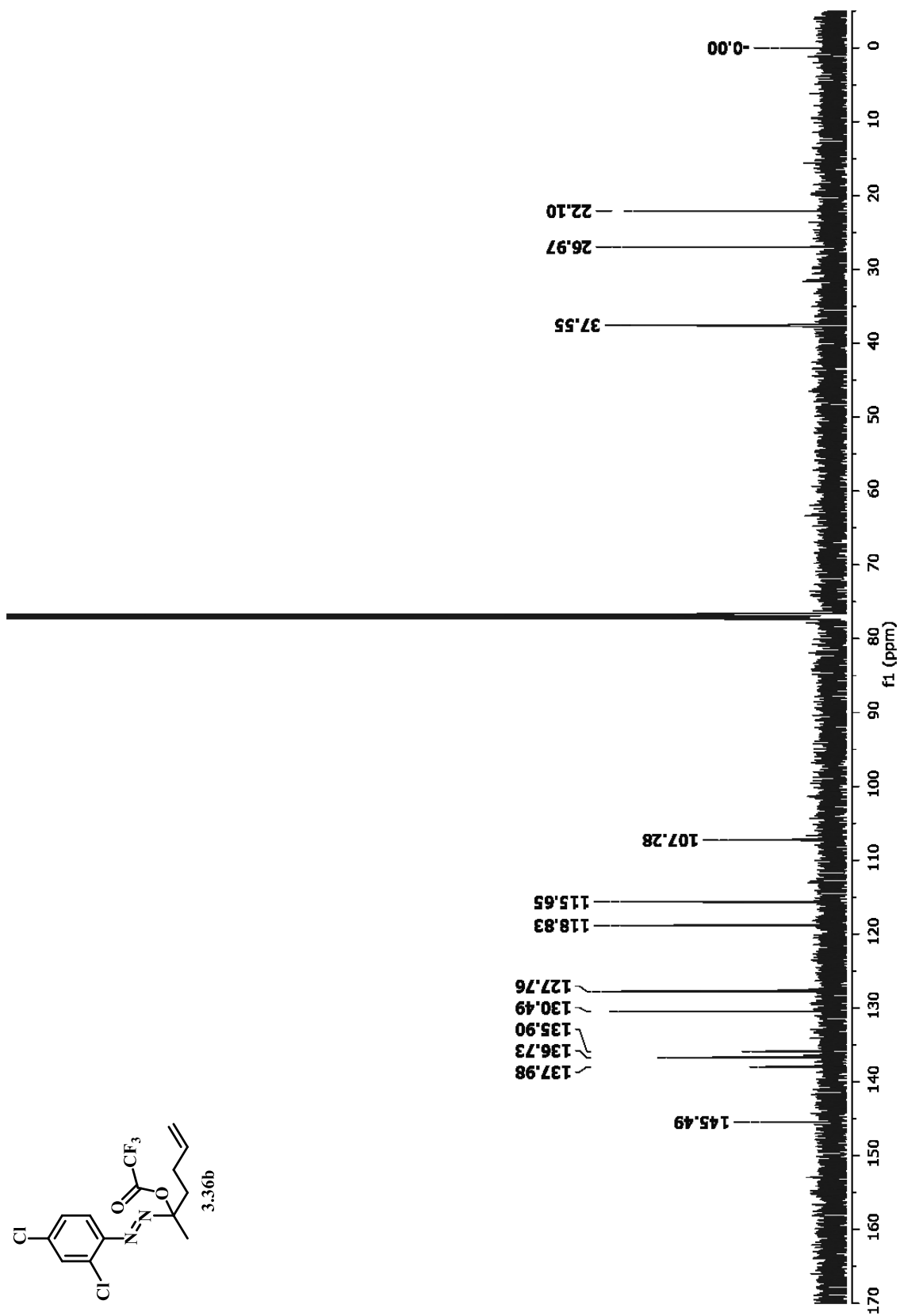


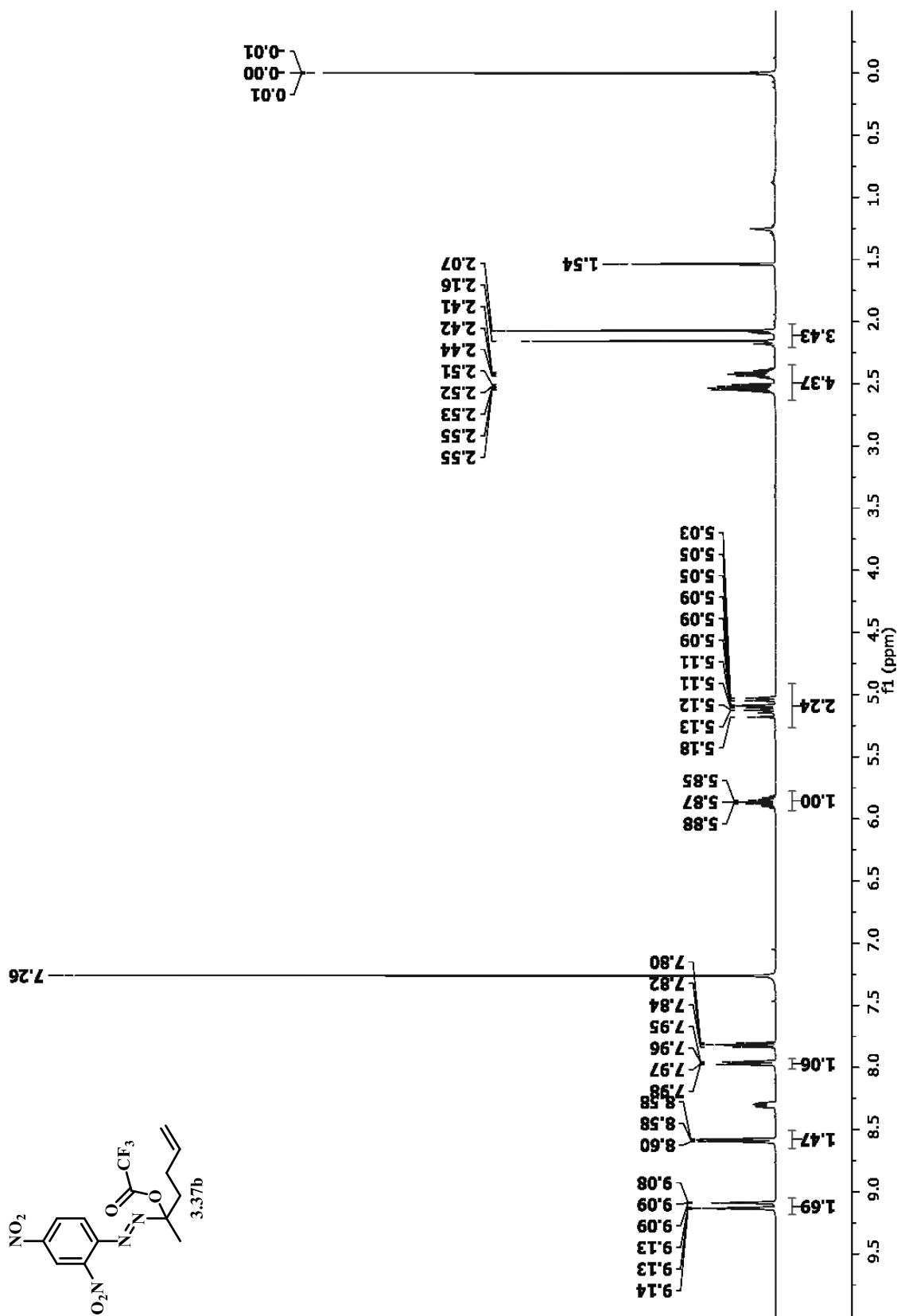


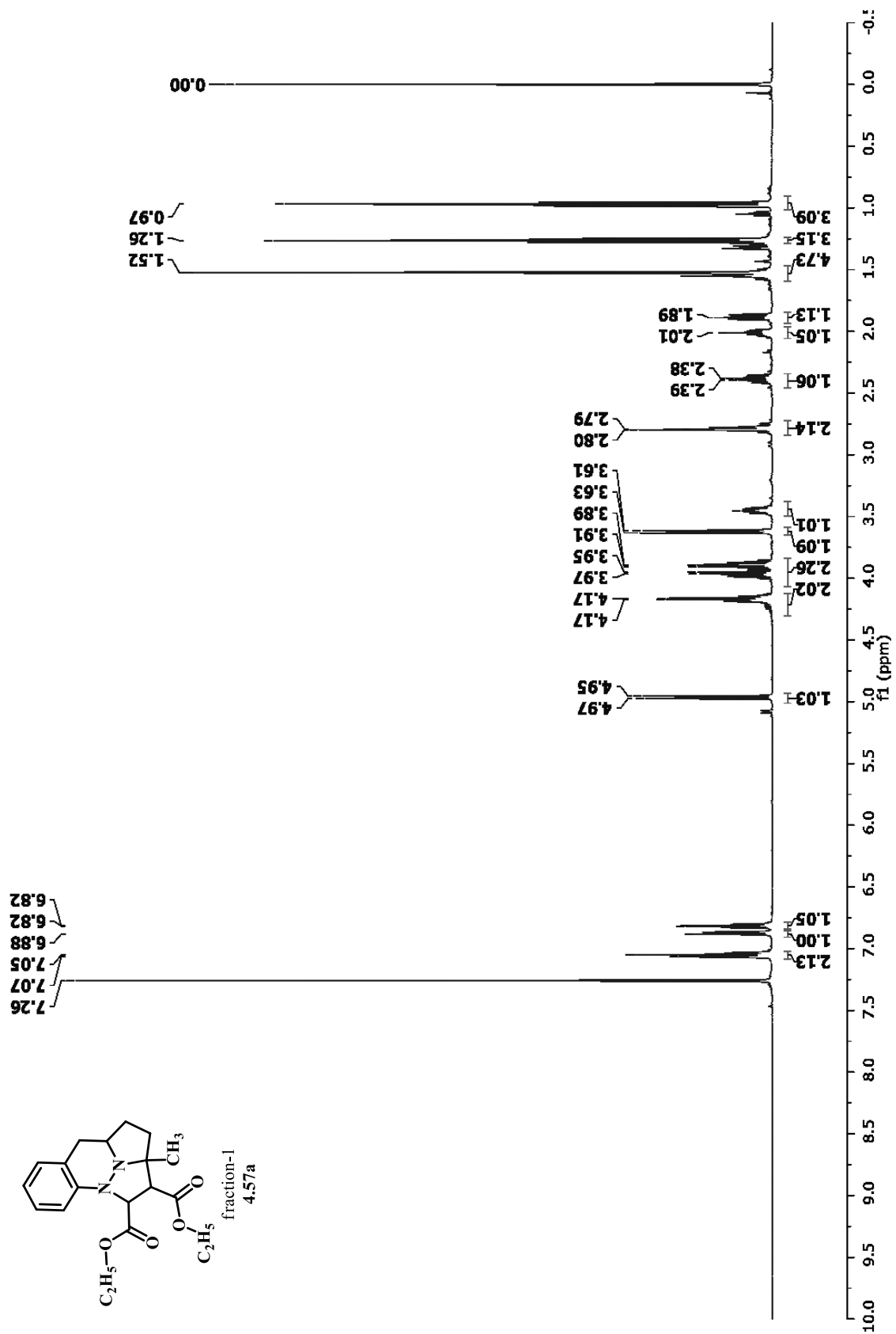


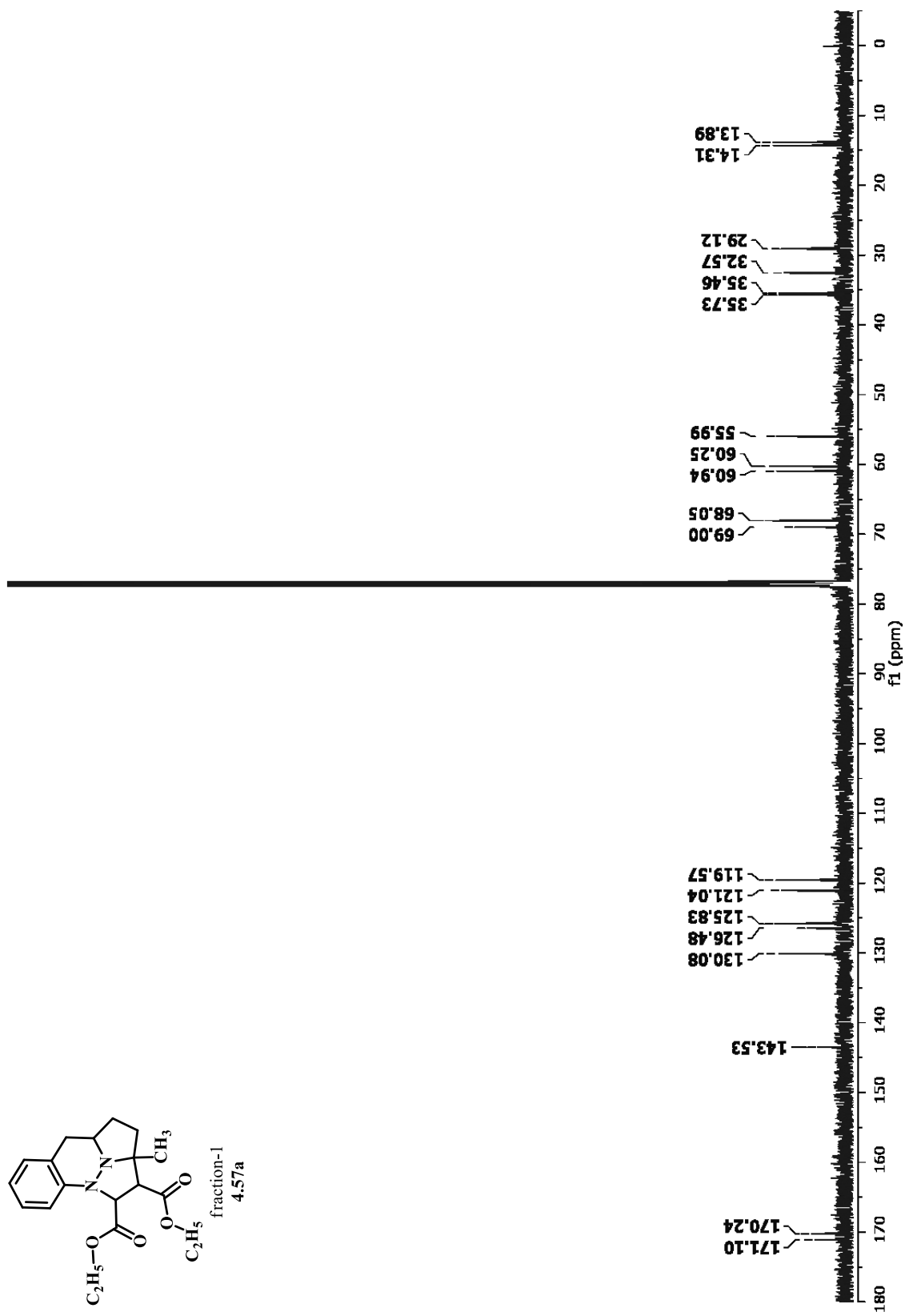


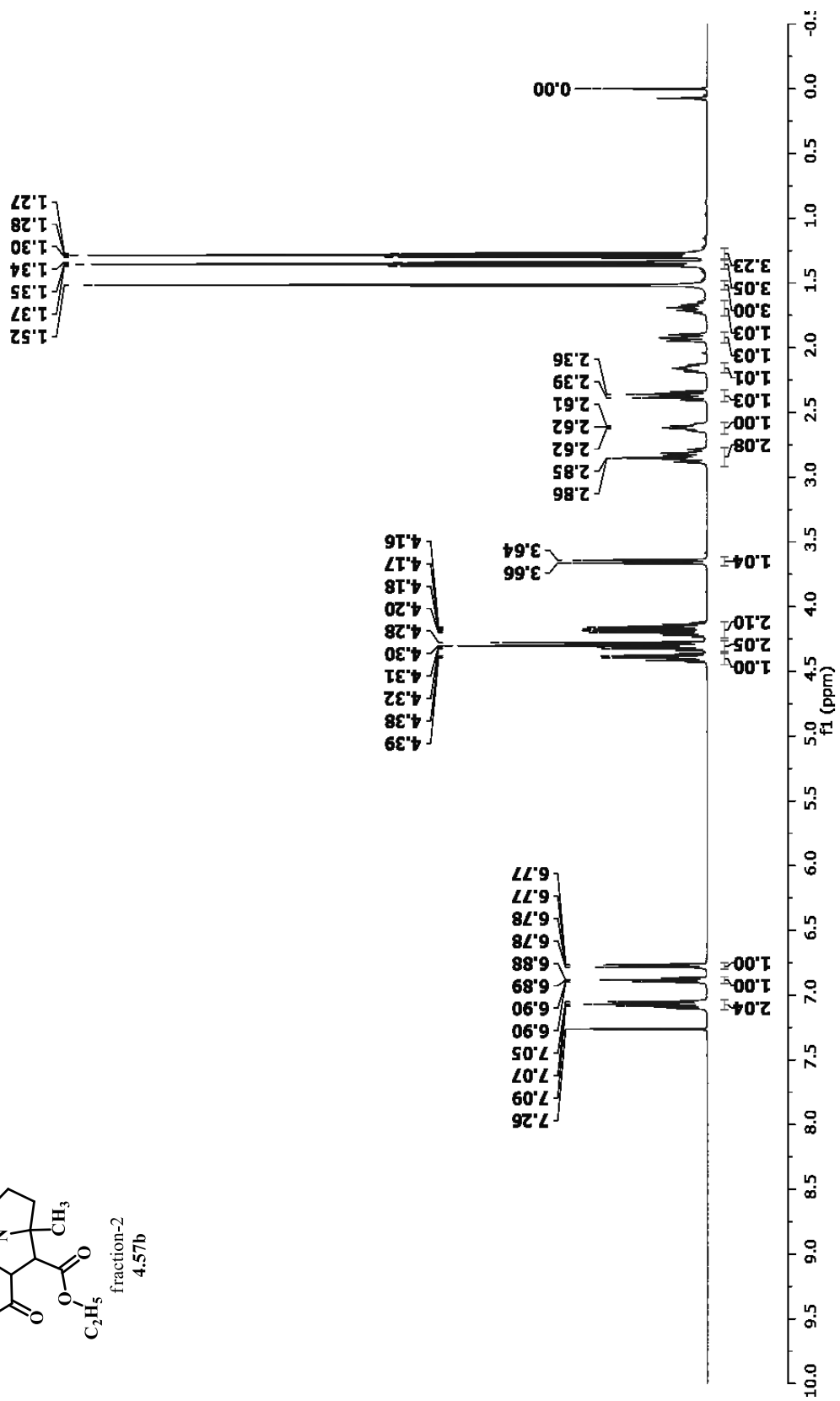
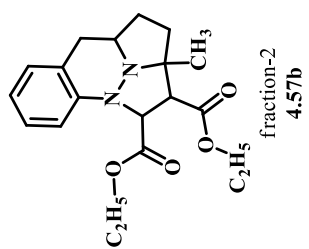


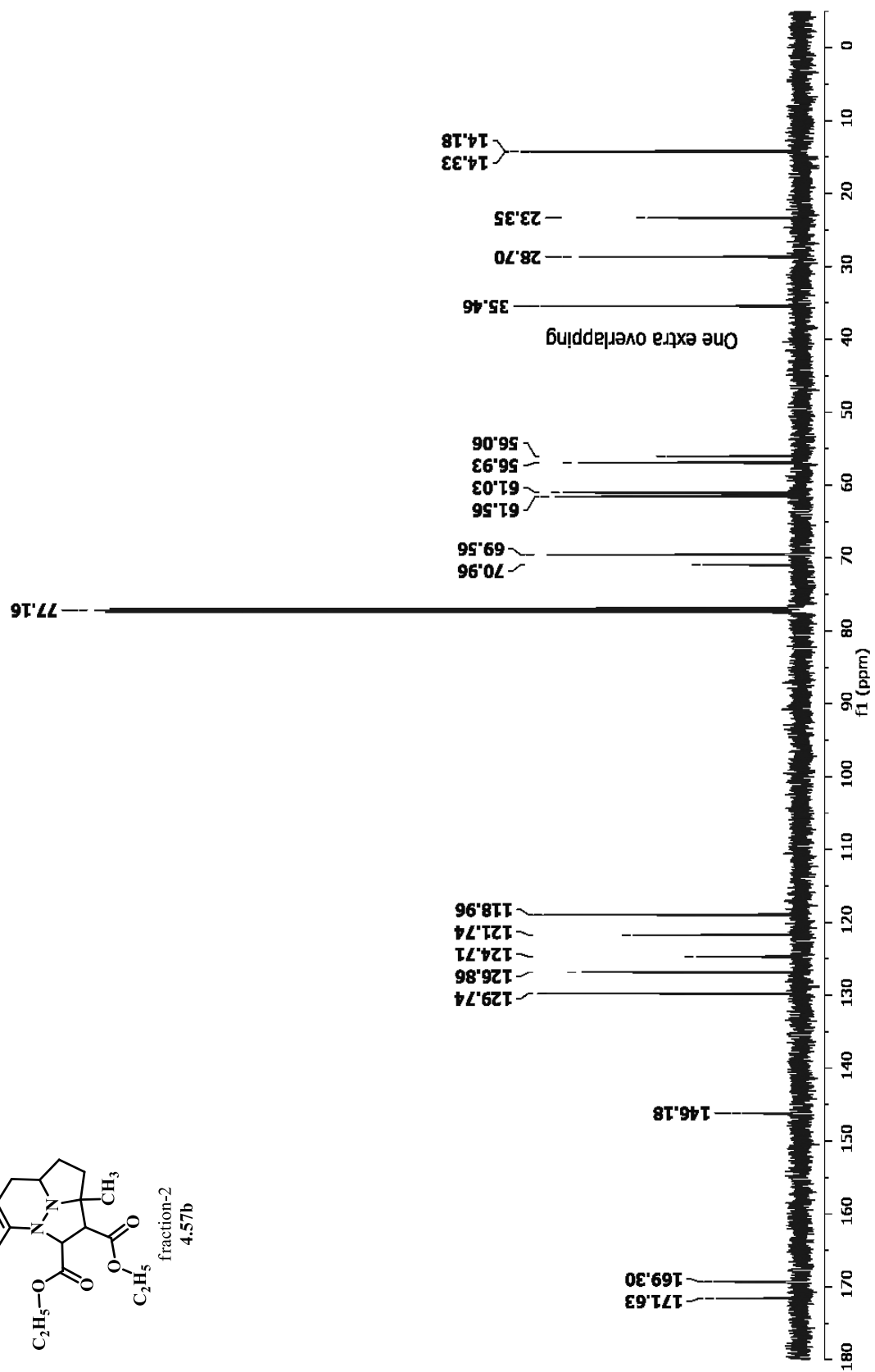
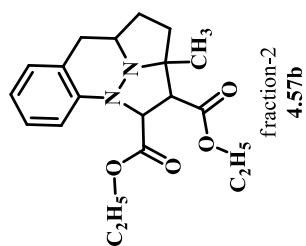


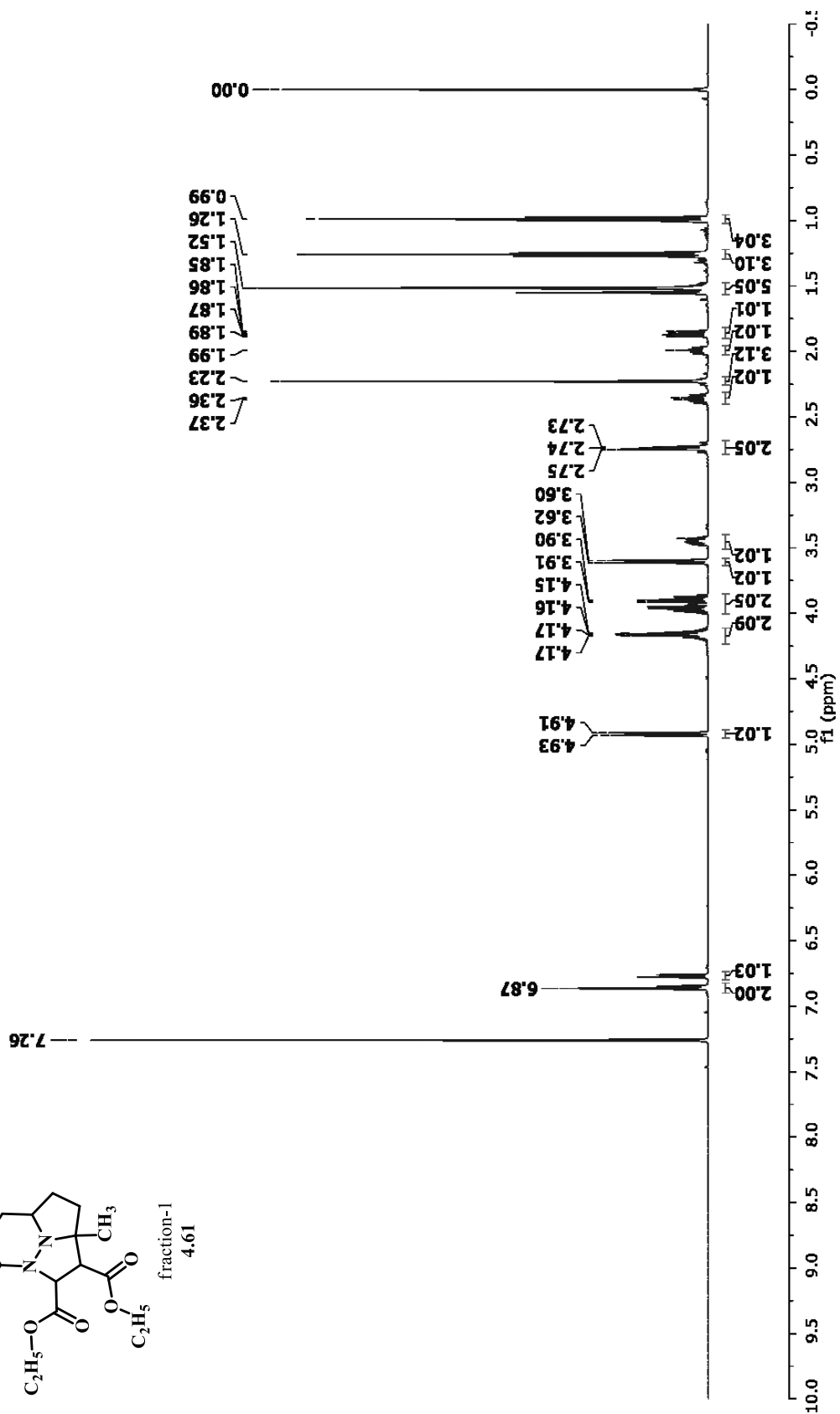
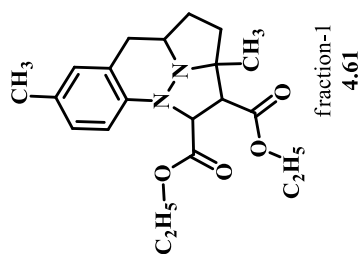


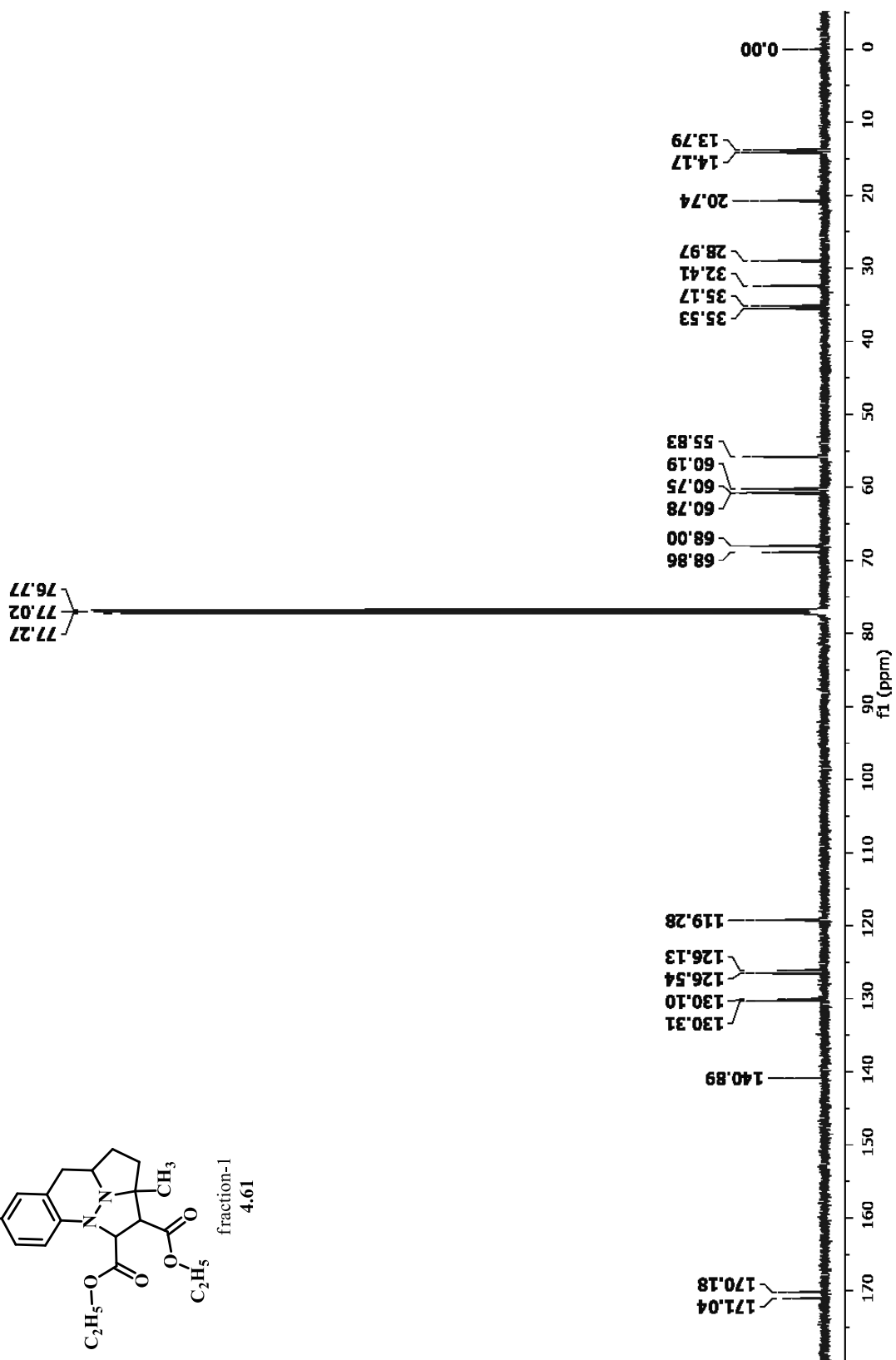
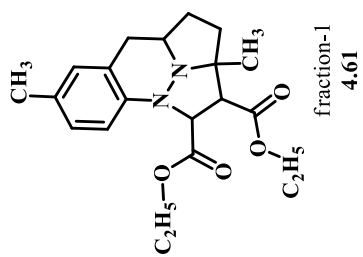


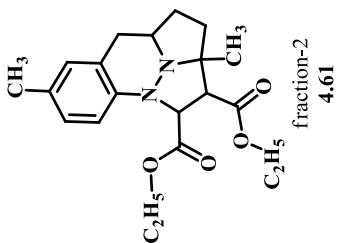


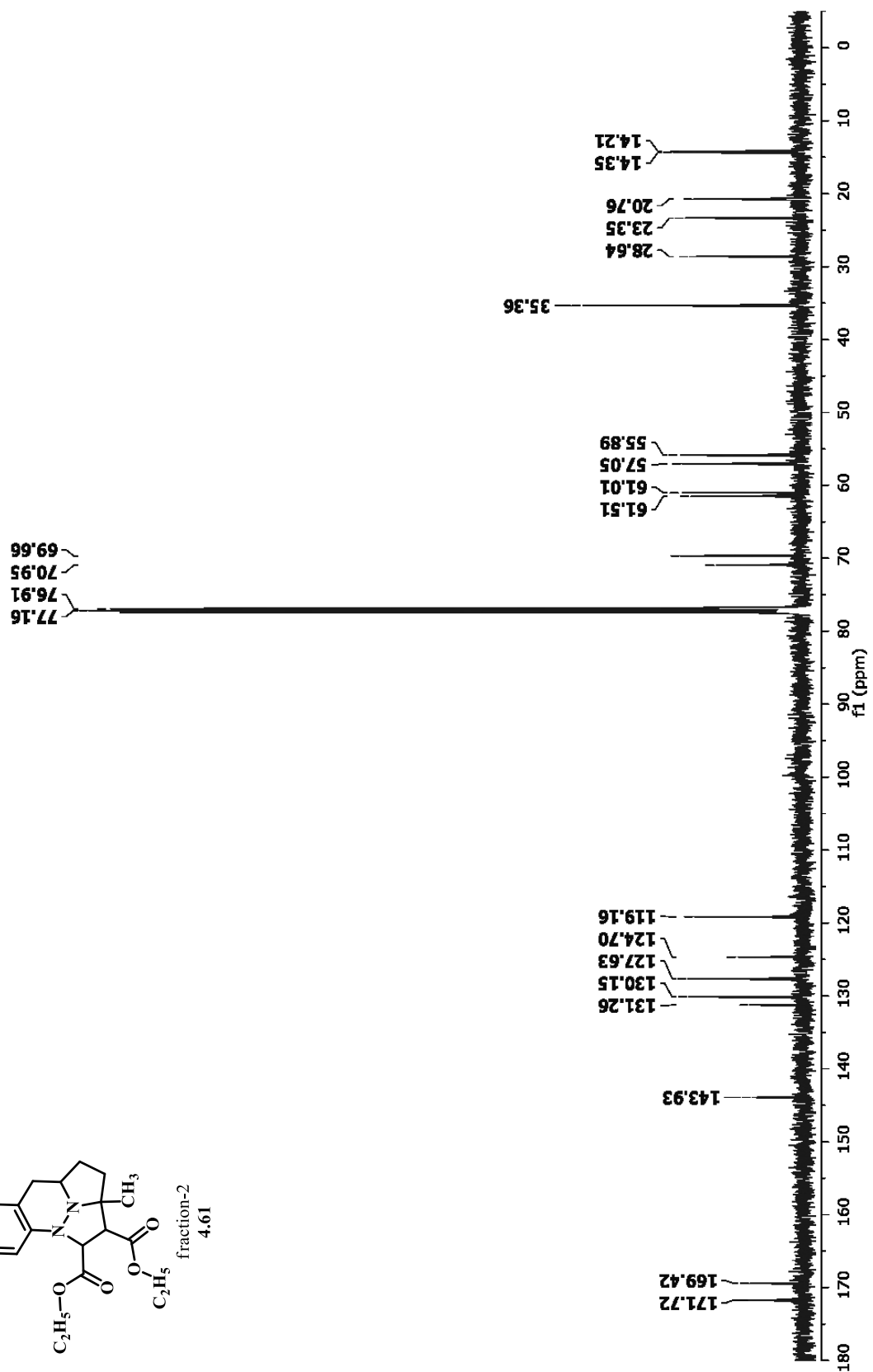
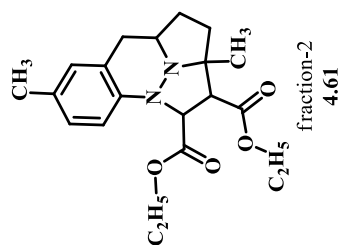


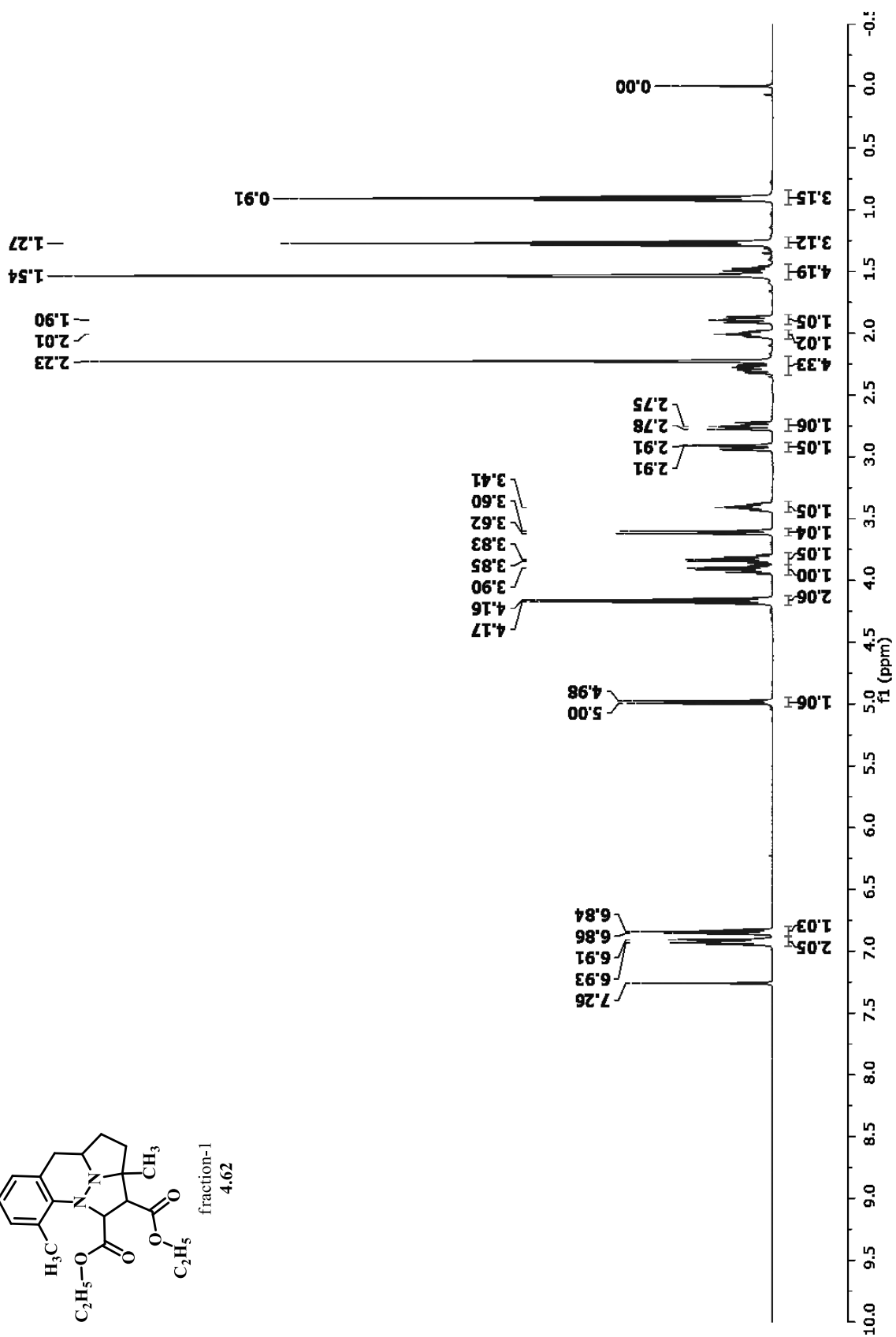
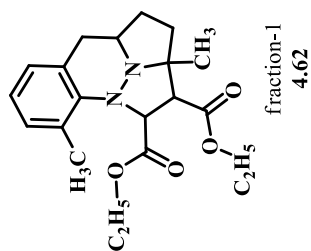


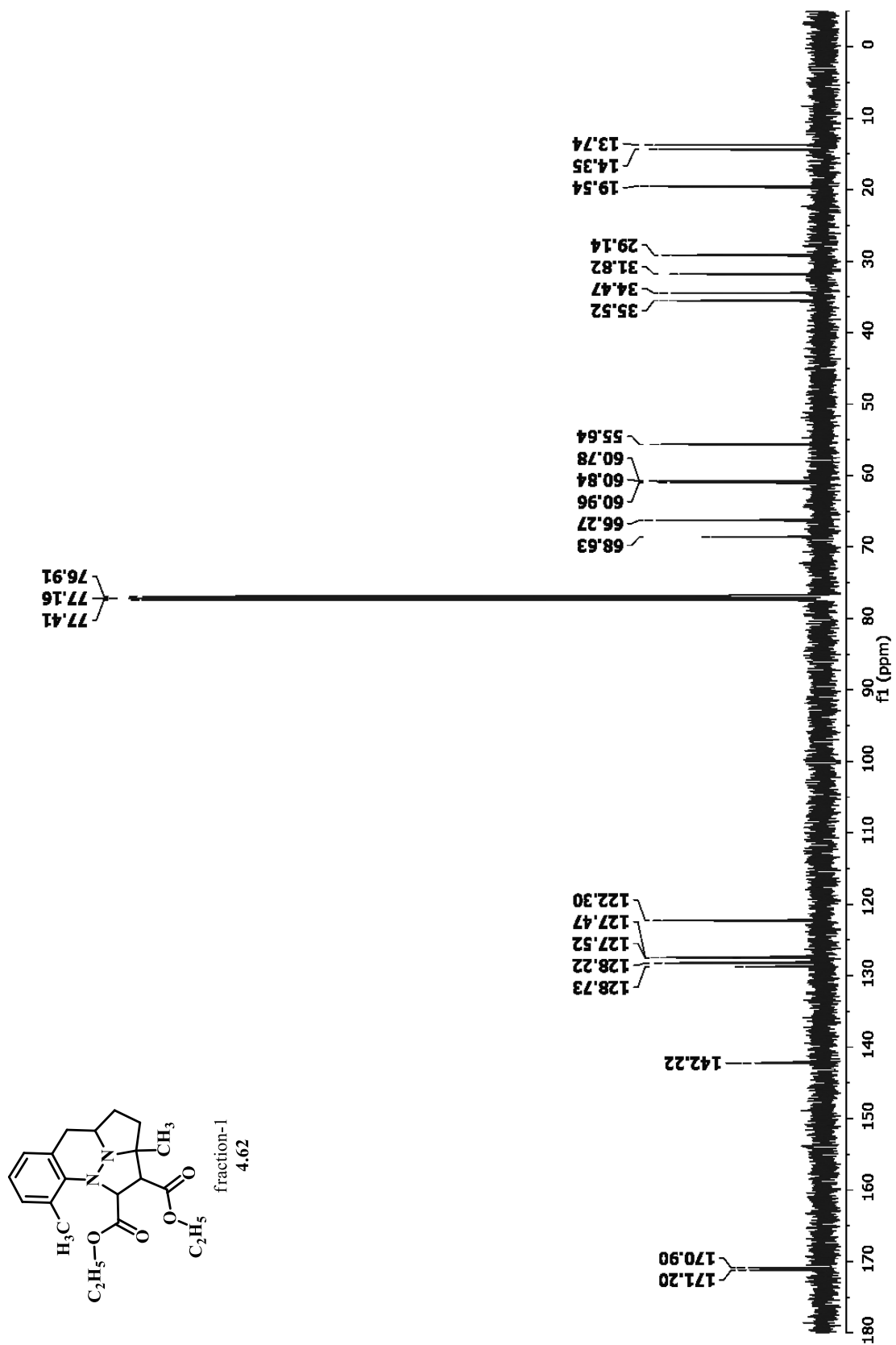


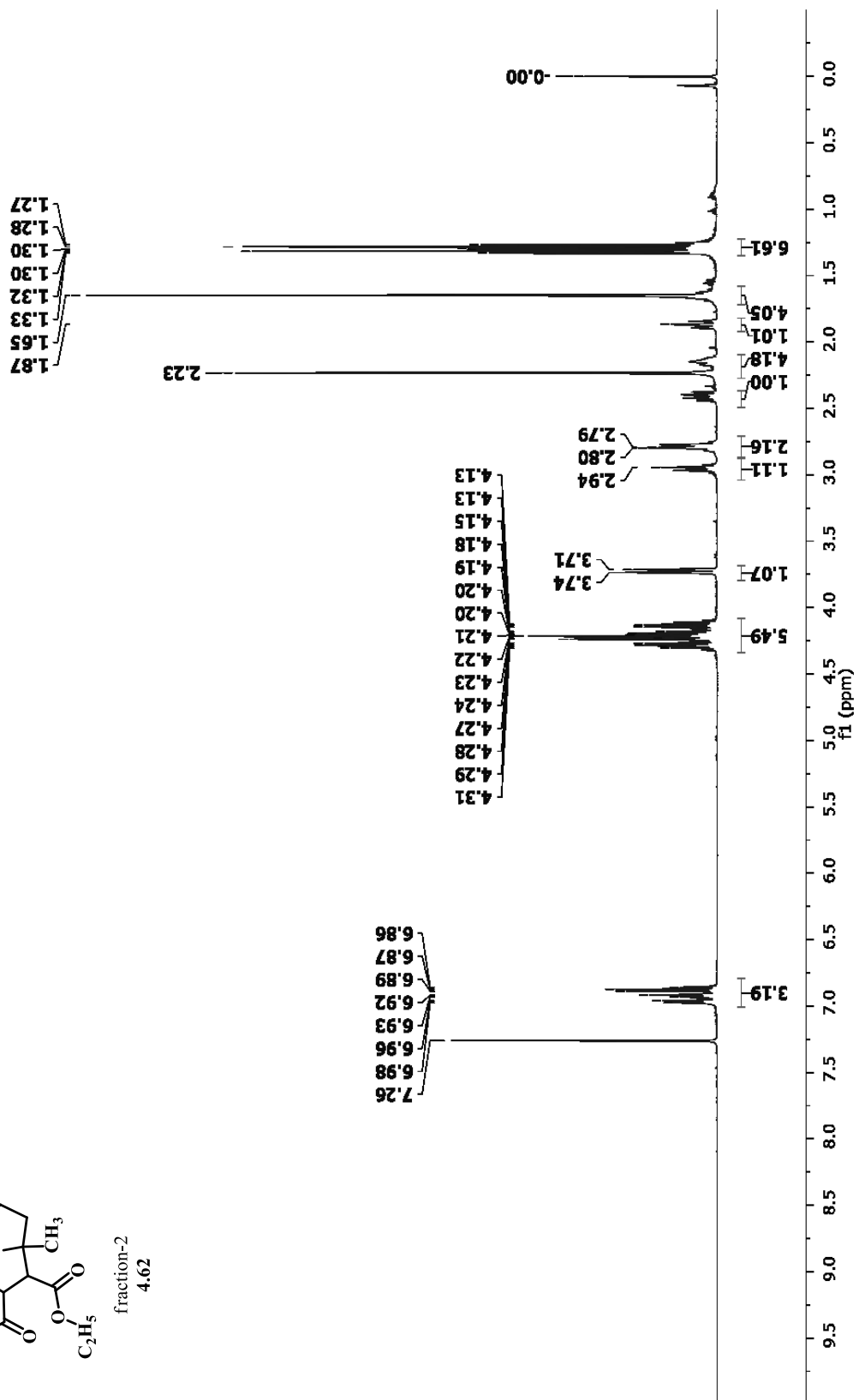
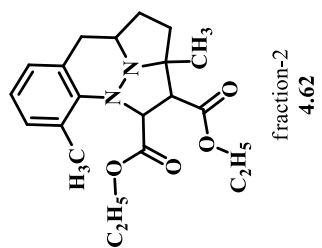


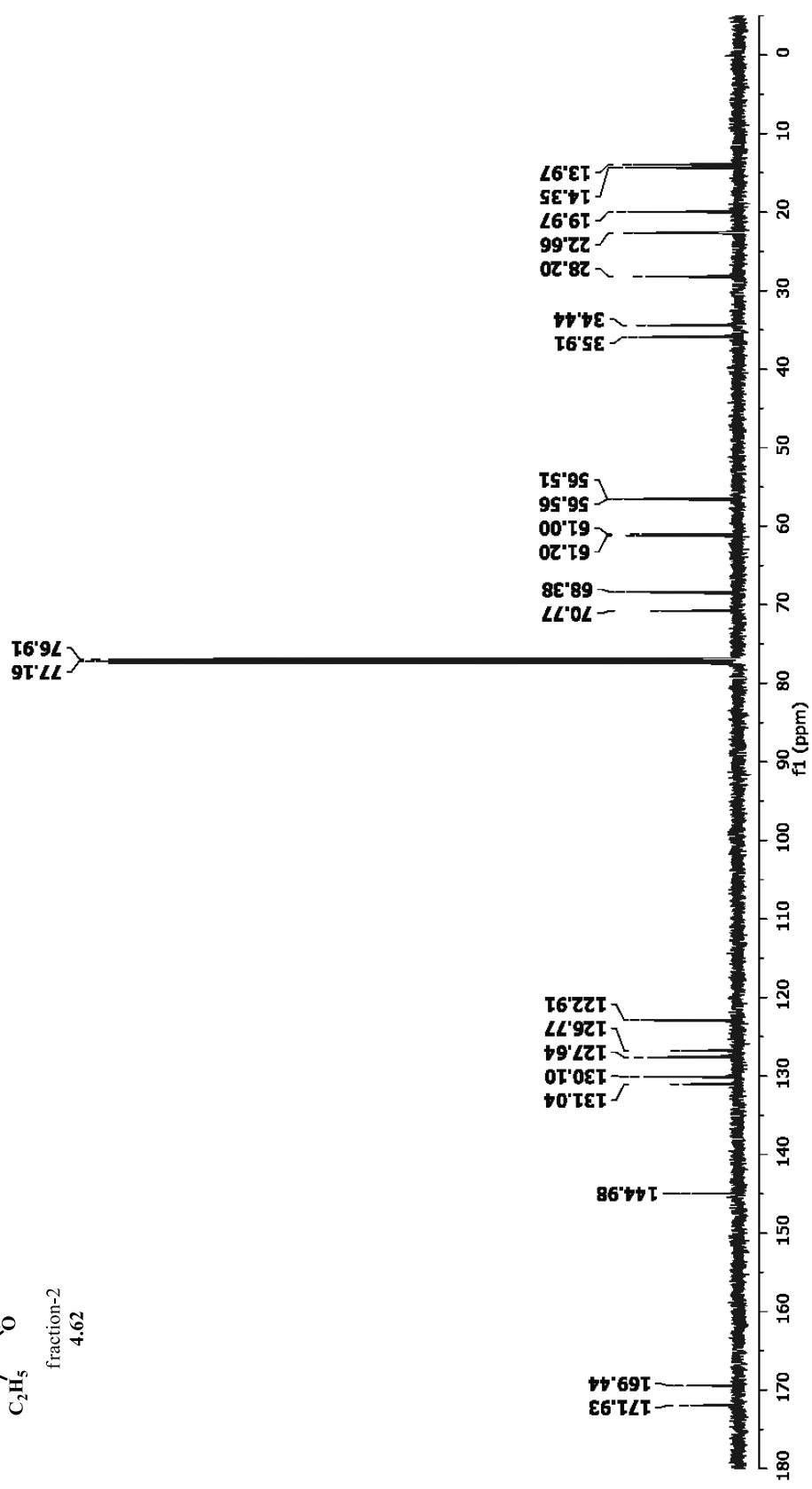
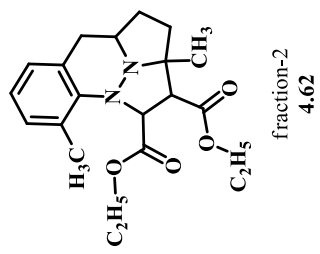


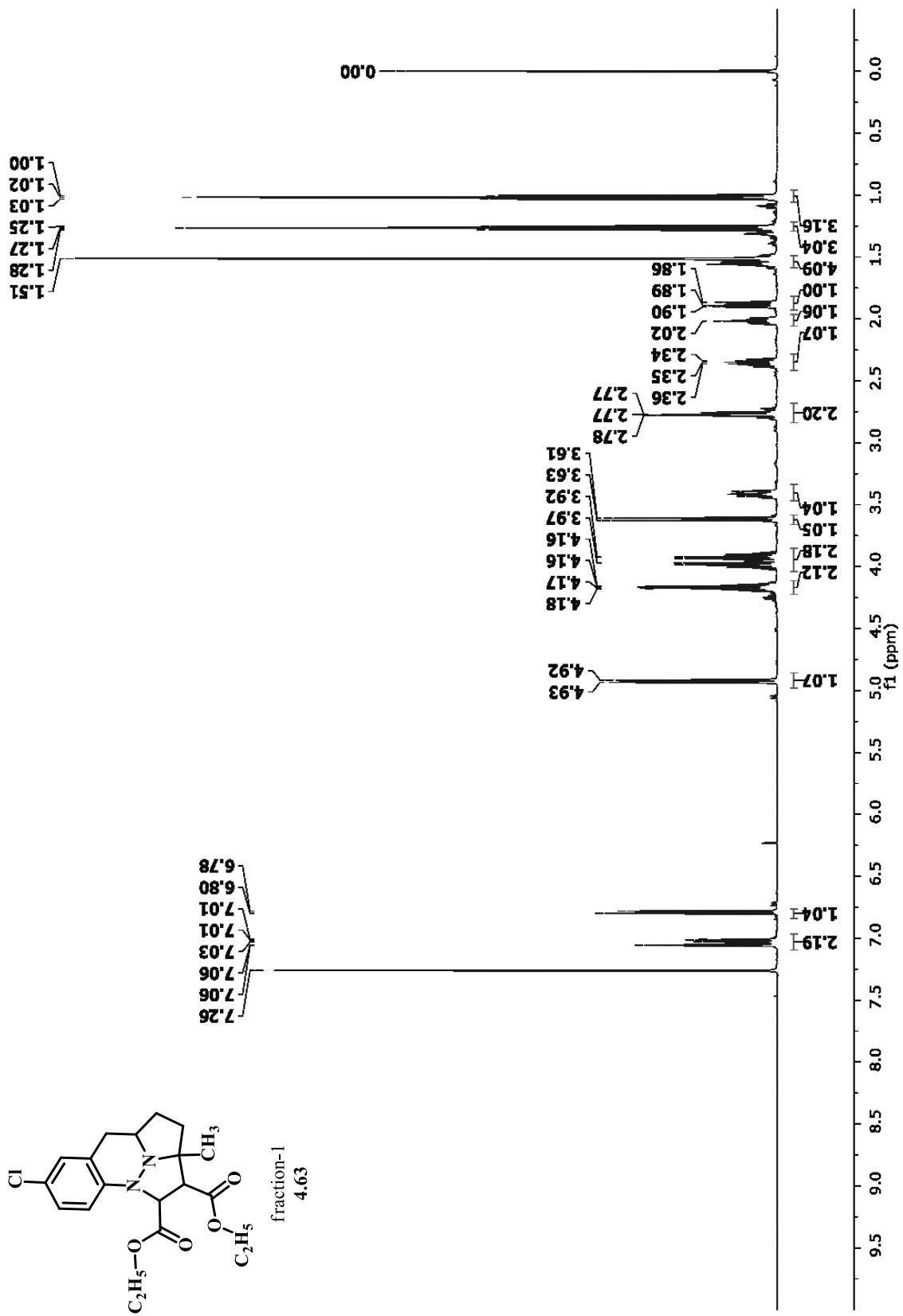


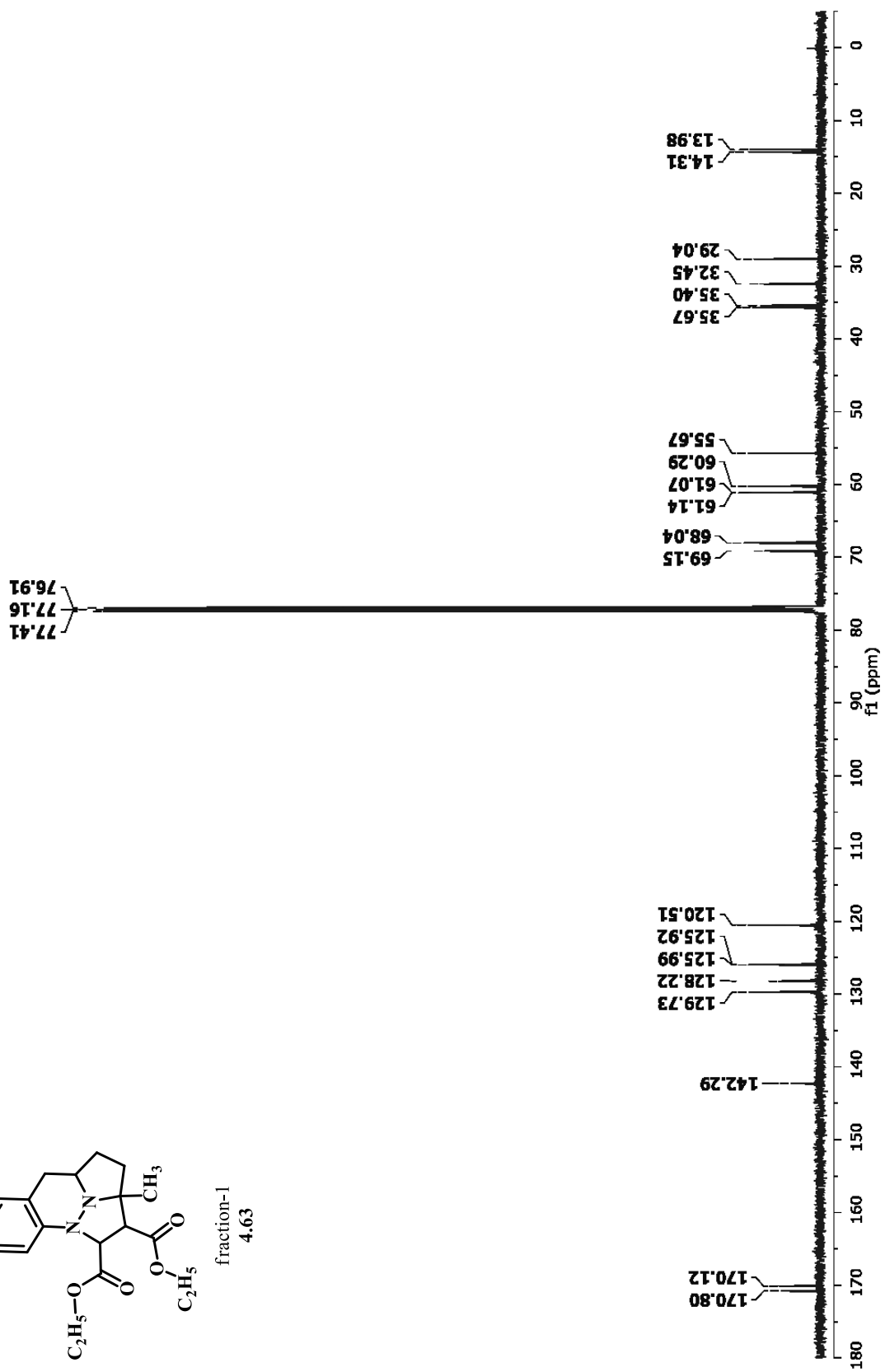
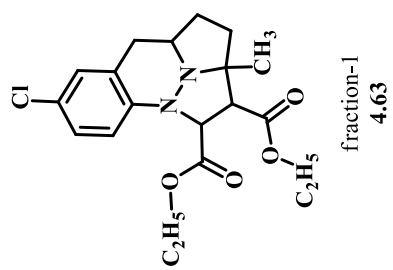


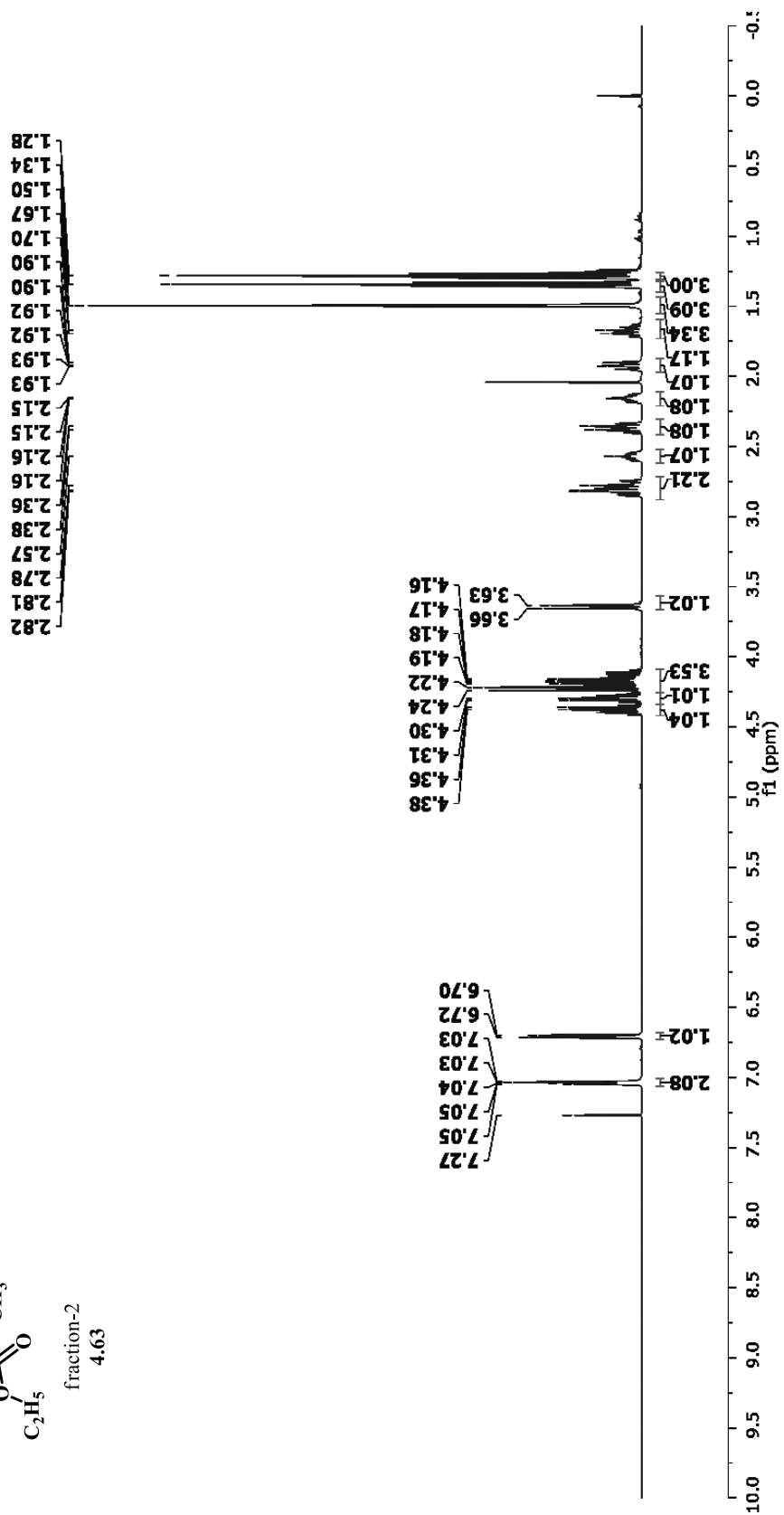
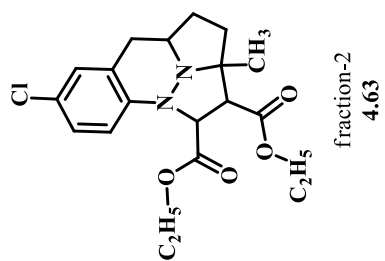


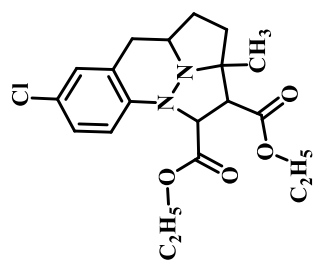












fraction-2
4.63

